

Global Environmental Impact Assessment of the Selected Engineered Nanomaterials and
Development of Characterization Factors

By

Sila Temizel Sekeryan

A dissertation submitted in partial fulfillment of
the requirements for the degree of

Doctor of Philosophy
(Civil and Environmental Engineering)

at the
UNIVERSITY OF WISCONSIN-MADISON

2020

Date of final oral examination: 12/1/2020

The dissertation is approved by the following members of the Final Oral Committee:

Andrea L. Hicks, Assistant Professor, Civil and Environmental Engineering

Bu Wang, Assistant Professor, Civil and Environmental Engineering

Joel A. Pedersen, Professor, Soil Science

Matthew Ginder-Vogel, Associate Professor, Civil and Environmental Engineering

Robert Anex, Professor, Biological Systems Engineering

Global Environmental Impact Assessment of the Selected Engineered Nanomaterials and
Development of Characterization Factors

By

Sila Temizel Sekeryan

Under the supervision of Dr. Andrea L. Hicks, assistant professor of Civil and Environmental
Engineering at the University of Wisconsin-Madison

Abstract

Engineered nanomaterials have been incorporated into a large number of conventional products in order to solve problems that the world has been facing. However, the current research in this area often overlooks the fact that not only using the end product but also producing it might have significant impacts on the environment and human health. Therefore, systems thinking and applying a holistic approach to assess the sustainability performance of these products is critical for decision-making. Global production and consumption of engineered nanomaterials is forecasted to increase significantly due to their applications in modern technologies, which raises concerns regarding their environmental implications. One way to analyze the environmental impacts of engineered nanomaterials is through life cycle assessment (LCA). This work investigates the cradle-to-grave environmental costs of silver nanoparticles (nAg) and global cradle-to-gate environmental costs of carbon nanotubes (CNTs) using LCA and multiple midpoint environmental impact categories in order to provide a holistic assessment. For

the nAg case study, environmental performances of thirteen different synthesis routes are evaluated with cradle-to-gate boundaries and a mass based functional unit, and the results are presented in a disaggregated format based on industrial uses of nAg in a global scale. Similarly, for CNTs, the environmental impacts of eight single-walled and seven multi-walled CNTs synthesis processes are evaluated and global scale impacts of manufacturing (including raw materials) CNTs are modeled. Similar to nAg, results are segregated and presented based on industries that use CNTs the most. Results showed that as some synthesis processes are more environmentally impactful than others, and industries prefer specific processes to synthesize their nanomaterials, industry-based impacts are not exactly proportional with the industrial shares for nAg and CNTs. Following the cradle-to-gate analysis, in order to incorporate direct (or nano-specific) impacts resulting from nAg release, a physicochemical property-based characterization factor is developed using published mesocosm studies. Lastly, these findings are combined as a case study for silver enabled textiles to evaluate the necessity of nano-specific characterization factors for nAg. The case study results suggested that, calculating nano-specific impacts and incorporating them into the overall LCA results do not make a significant difference for ecotoxicity impact category unless there is a very large quantity of initial silver loading per textile. However, human health related impacts may require more attention because the release phase showed a significant sensitivity for human health LCA impacts. These results suggest the need for developing nAg specific characterization factors for human health (carcinogenics and non-carcinogenics) impact categories to be incorporated into LCA results for more thorough evaluation. While there is a need for further research, this work fills the gap in the body of knowledge surrounding environmental performances of two of the most utilized engineered nanomaterials in consumer products.

Dedication

I would like to dedicate this work to the memory of my grandmother Janet Monos and grandfather Bogos Monos. I love you *yaya* and *dede*.

Acknowledgements

First and foremost, I would like to thank my advisor, Dr. Andrea Hicks for her continuous guidance, support and care. I am very grateful for having the opportunity to work with her. I would also like to thank my committee members Dr. Bu Wang, Dr. Joel A. Pedersen, Dr. Matthew Ginder-Vogel and Dr. Robert Anex for their time and guidance.

I owe great thanks to my colleagues, the past and present members of the Sustainability and Emerging Technology Research Group, especially Monica Rodriguez Morris, Ramin Ghamkhar, Maddie Sena and Wissam Kontar for their friendship, support and constructive feedbacks throughout my PhD process. It was a pleasure working with you all.

I am grateful for the Global Health Institute and the Nelson Institute for Environmental Studies for the Planetary Health Scholarship Award and their support. I would like to thank Wisconsin Alumni Research Foundation (WARF) and the United States Department of Agriculture (USDA) National Institute of Food and Agriculture (NIFA) grant 2017-67003-26055 for funding my research and studies. I also would like to acknowledge the support from the Armenian International Women's Association and Vahan Adjemian Scholarship Fund of Tibrevank Alumni.

My deepest gratitude to my husband, Ari Sekeryan, for his love, trust and guidance. Ari, thank you for encouraging me to pursue my studies further and always believing in me. Your endless support made all of this possible. Additionally, I owe great thanks to my family, Hilda-Arman Temizel, Teni-Arno Inciduzen and Ararat Sekeryan, whose encouragements throughout my studies have enabled me to reach my goals. Special thanks to my precious nieces, Nora and Mira Inciduzen, for always cheering me up and make me smile. Being far away from you was the most challenging part in this journey, but your love guided me all the way. I love you all.

I owe a great deal to my friends Sibil Arsenyan, Yolanda Kaplan, Hena-Bernar Tasci and Lerna Untur for always being there when I need. Finally, I would like to thank my previous advisor at Lamar University, Dr. Liv Haselbach, for her encouragement, and friends Nara Almeida, Adarsh Bafana, Shishir Kumar and Sailee Gawande for their friendship.

Table of Contents

Abstract.....	i
Dedication	iii
Acknowledgements	iv
List of Figures.....	xiii
List of Tables	xix
List of Symbols/Abbreviations.....	xx
1. Introduction.....	1
<i>1.1. Research Summary and Goals.....</i>	<i>1</i>
<i>1.2. Research Objectives and Questions.....</i>	<i>2</i>
<i>1.3. Nanomaterials Industry</i>	<i>4</i>
<i>1.4. Life Cycle Assessment.....</i>	<i>7</i>
1.4.1. Goal and Scope Definition.....	7
1.4.2. Inventory Analysis	8
1.4.3. Impact Assessment.....	9
1.4.3.1. Ozone Depletion	9
1.4.3.2. Global Warming.....	9
1.4.3.3. Smog	10
1.4.3.4. Acidification	10
1.4.3.5. Eutrophication.....	10
1.4.3.6. Carcinogenics and Non-carcinogenics.....	11
1.4.3.7. Respiratory Effects.....	11
1.4.3.8. Ecotoxicity	12

1.4.3.9. Fossil Fuel Depletion	12
1.4.4. Interpretation.....	12
<i>1.5. Characterization Factors and the USEtox Model</i>	<i>13</i>
2. Global environmental impacts of silver nanoparticle production methods supported by life cycle assessment	15
2.1. Abstract.....	16
2.2. Introduction.....	17
2.3. Materials and methods.....	23
2.3.1. Goal and scope definition	23
2.3.2. Synthesis procedures.....	25
2.3.3. Industrial scale production.....	27
2.3.4. Prediction of sectoral emissions.....	28
2.4. Results and discussion	31
2.4.1 Life cycle impact assessment comparison.....	31
2.4.2. Implications of scaling up.....	34
2.4.3. Sectoral environmental impacts.....	37
2.5. Conclusions.....	40
2.6. Acknowledgements.....	41
3. Global scale life cycle environmental impacts of single- and multi-walled carbon nanotube synthesis processes	42
3.1. Abstract.....	43
3.1.1. Purpose.....	43
3.1.2. Methods.....	43

3.1.3. Results and discussion	43
3.1.4. Conclusions.....	44
3.2. <i>Introduction</i>	45
3.3. <i>Materials and methods</i>	49
3.3.1. Goal and scope definition	49
3.3.2. Synthesis procedures.....	51
3.3.3. Impact projections for large scale manufacturing.....	55
3.3.4. Projecting sectoral emissions	57
3.4. <i>Results and discussion</i>	60
3.4.1. Impact assessment and comparison of synthesis processes	60
3.4.1.1. Alternative scenarios for electricity source.....	63
3.4.2. Implications of large scale manufacturing.....	66
3.4.3. Sectoral environmental impacts	69
3.5. <i>Conclusions</i>	71
3.6. <i>Acknowledgements</i>	73
4. Calculating size- and coating- dependent effect factors for silver nanoparticles to inform characterization factor development for usage in life cycle assessment	74
4.1. <i>Abstract</i>	75
4.2. <i>Introduction</i>	76
4.3. <i>Review of ecotoxicity literature and methods for EF calculation</i>	80
4.3.1. Considerations on USEtox and EF calculation.....	80
4.3.2. Ecotoxicity literature.....	83
4.3.3. Selection criteria	84

4.3.4. Previous research on nAg-EF	85
<i>4.4. Results and discussion</i>	86
4.4.1. Ecotoxicity literature on nAg.....	86
4.4.1.1. Crustaceans	90
4.4.1.2. Algae	93
4.4.1.3. Fish.....	95
4.4.1.4. Protozoa	97
4.4.2. Ecotoxicity literature on ionic silver.....	98
4.4.3. Effect factor calculation.....	100
4.4.4. Discussion and implications	104
<i>4.5. Conclusion</i>	106
<i>4.6. Acknowledgements</i>	107
5. Developing physicochemical property-based ecotoxicity characterization factors for silver nanoparticles under mesocosm conditions for use in life cycle assessment.....	108
5.1. <i>Abstract</i>	109
5.2. <i>Introduction</i>	110
5.3. <i>Background information for characterization factors</i>	112
5.3.1. Effect Factor (EF)	113
5.3.2. Fate Factor (FF)	113
5.3.2.1. Current understanding of fate descriptors.....	115
5.3.3. Exposure Factor (XF)	116
5.3.4. Review of characterization factor literature for nAg	117
5.4. <i>Materials and Methods</i>	119

5.4.1. Effect Factor (EF) Calculation.....	119
5.4.2. Fate Factor (FF) Calculation.....	121
5.4.2.1. Dissolution.....	122
5.4.2.2. Hetero-aggregation	124
5.4.2.3. Sedimentation	125
5.4.2.4. Advection.....	126
5.4.3. Exposure Factor (XF) Calculation	127
5.4.4. Sensitivity Analysis	127
5.5. <i>Results and Discussions</i>	128
5.5.1. Fate Factor	128
5.5.2. Characterization Factor.....	131
5.5.3. Sensitivity Analysis	134
5.5.4. Limitations	136
5.5.5. Implications for LCA.....	137
5.6. <i>Conclusions</i>	138
5.7. <i>Acknowledgements</i>	139
6. Cradle-to-grave environmental impact assessment of silver enabled t-shirts: Do direct impacts exceed the indirect emissions?	140
6.1. <i>Abstract</i>	141
6.2. <i>Introduction</i>	142
6.3. <i>Materials and Methods</i>	145
6.3.1. Goal and scope definition	145
6.3.2. Considerations for developing life cycle inventory informed by the literature	146

6.3.2.1. Raw materials acquisition and manufacturing	147
6.3.2.2. Use	148
6.3.2.3. End-of-life	149
6.3.3. Ecotoxicity characterization factors for nAg	152
6.3.4. Sensitivity and uncertainty analyses	152
<i>6.4. Results</i>	<i>153</i>
6.4.1. Life cycle impact assessment	153
6.4.2. Sensitivity analysis	155
<i>6.5. Discussion</i>	<i>158</i>
6.5.1. Environmental significance	158
<i>6.6. Acknowledgements</i>	<i>161</i>
7. Conclusions and Future Work	162
7.1. <i>Summary and Contributions</i>	162
7.2. <i>Future Work</i>	164
References	165
Appendix A	195
Appendix B	238
Appendix C	329
Appendix D	391
Appendix E	407
Appendix F	457
Appendix G	500
Appendix H	555

Curriculum Vitae (CV)	611
Permissions	617

List of Figures

Figure 1. Nanomaterials market value in USD \$ Billion/year, compiled from the literature [7] and commercial reports [6, 8–11].	5
Figure 2. The number of applications of the selected ENMs in different development stages [1].6	
Figure 3. Simplified LCA inventory framework and representations of different system boundaries (adapted from [17]).	8
Figure 4. Global market (tons) for silver nanoparticles (AgNPs) where diamond markers indicate skeptical estimations, circle markers indicate single estimations and triangle markers indicate optimistic estimations [1, 41–49].	18
Figure 5. System boundaries considered in the current study (included life cycle stages are represented by green box). (For interpretation of the references to color in this figure legend, the reader is referred to the web version of this article).	24
Figure 6. Industry-based estimations for AgNPs-enabled consumer products compiled from the literature [5, 40, 44, 84–87].	29
Figure 7. Environmental impacts of multiple synthesis routes for 1 kg AgNPs, using multiple impact categories as A) ODP, B) GWP, C) SP, D) AP, E) EP, F) HHCP, G) HHNCP, H) RP, I) ETP, J) FFP and K) CED.	33
Figure 8. Global annual environmental impacts using different scale-up factors (2, 4 and 6) as well as laboratory scale results for A) GWP (tons CO ₂ -eq./year) with skeptical B) GWP (tons CO ₂ -eq./year) with optimistic C) FFP (MJ surplus energy/year) with skeptical, D) FFP (MJ surplus energy/year) with optimistic production volumes. Error bars represent 95% confidence intervals for the uncertainties modeled by Monte Carlo simulations.	36

- Figure 9.** Sankey diagrams for industry-based emissions in 2018 A) GWP with skeptical estimations and laboratory scale, B) GWP with optimistic estimations and laboratory scale, C) GWP with skeptical estimations and SF = 6, D) GWP with optimistic estimations and SF = 6, E) FFP with skeptical estimations and laboratory scale, F) FFP with optimistic estimations and laboratory scale, G) FFP with skeptical estimations and SF = 6, and H) FFP with optimistic estimations and SF = 6. 39
- Figure 10.** Global market (in tons) for carbon nanotubes (CNTs) where diamond markers indicate pessimistic estimations, circle markers indicate single estimations, triangle markers indicate optimistic estimations and error bars indicate the potential range for the respective estimation [1, 45, 100–106]. 46
- Figure 11.** System boundaries considered in the current study. 50
- Figure 12.** Industry-based estimations for CNTs-enabled consumer products compiled from the literature (Other includes materials, textile, food, personal care, military and other miscellaneous sectors) [1, 5, 40, 44, 85, 145–148]. 58
- Figure 13.** Environmental impacts of multiple synthesis routes for 1 kg CNTs (S- and M-) in logarithmic scale, using multiple impact categories as A) OD, B) GW, C) PS, D) AC, E) EU, F) HHC, G) HHNC, H) RE, I) EC, J) FF and K) CED (*large scale inventories are marked with an asterisk). 61
- Figure 14.** Different electricity scenarios and their corresponding impacts for A) SWCNTs-GW, B) SWCNTs-EU, C) MWCNTs-GW, and D) MWCNTs-EU (*large scale inventories are marked with an asterisk). 64
- Figure 15.** Projected global GW (tons CO₂-eq./year) for A) SWCNTs with pessimistic production volumes B) SWCNTs with optimistic production volumes, C) MWCNTs with

pessimistic production volumes D) MWCNTs with optimistic production volumes, E) CNTs with pessimistic production volumes F) CNTs with optimistic production volumes. Error bars represent 95% confidence intervals for the uncertainties modeled by Monte Carlo simulations. 68

Figure 16. Sankey diagrams for industry-based GW for the year 2019 using A) pessimistic estimations-laboratory scale, B) optimistic estimations-laboratory scale, C) pessimistic estimations-S1, D) optimistic estimations-S1..... 70

Figure 17. Flowchart of selection criteria for EF calculation applied in this study..... 84

Figure 18. Number of toxicity data disaggregated by the test medium, nAg size and coating for A) crustaceans, B) algae, C) fish and D) protozoa. 88

Figure 19. Toxicity data points for crustaceans grouped based on coating and size in A) water, B) mineral medium, C) complex medium, and D) regardless of test medium (upper bound indicates the maximum $L(E)C_{50}$, the marker indicates the median $L(E)C_{50}$ and the lower bound indicates the minimum $L(E)C_{50}$ level for the representative set of data; toxicity ranking based on US EPA is as following: very high: $L(E)C_{50} < 1 \text{ mg L}^{-1}$, high: $1 \text{ mg L}^{-1} < L(E)C_{50} < 10 \text{ mg L}^{-1}$, moderate: $10 \text{ mg L}^{-1} < L(E)C_{50} < 100 \text{ mg L}^{-1}$, and low: $L(E)C_{50} > 100 \text{ mg L}^{-1}$)..... 91

Figure 20. Toxicity data points for algae grouped based on coating and size in A) water, B) mineral medium, C) complex medium, and D) regardless of test medium (upper bound indicates the maximum $L(E)C_{50}$, the marker indicates the median $L(E)C_{50}$ and the lower bound indicates the minimum $L(E)C_{50}$ level for the representative set of data; toxicity ranking based on US EPA is as following: very high: $L(E)C_{50} < 1 \text{ mg L}^{-1}$, high: $1 \text{ mg L}^{-1} < L(E)C_{50} < 10 \text{ mg L}^{-1}$, moderate: $10 \text{ mg L}^{-1} < L(E)C_{50} < 100 \text{ mg L}^{-1}$, and low: $L(E)C_{50} > 100 \text{ mg L}^{-1}$)..... 93

Figure 21. Toxicity data points for fish grouped based on coating and size in A) water, B) mineral medium, C) complex medium, and D) regardless of test medium (upper bound indicates

the maximum $L(E)C_{50}$, the marker indicates the median $L(E)C_{50}$ and the lower bound indicates the minimum $L(E)C_{50}$ level for the representative set of data; toxicity ranking based on US EPA is as following: very high: $L(E)C_{50} < 1 \text{ mg L}^{-1}$, high: $1 \text{ mg L}^{-1} < L(E)C_{50} < 10 \text{ mg L}^{-1}$, moderate: $10 \text{ mg L}^{-1} < L(E)C_{50} < 100 \text{ mg L}^{-1}$, and low: $L(E)C_{50} > 100 \text{ mg L}^{-1}$)..... 95

Figure 22. Toxicity data points for protozoa grouped based on coating and size in A) water, B) mineral medium, C) complex medium, and D) regardless of test medium (upper bound indicates the maximum $L(E)C_{50}$, the marker indicates the median $L(E)C_{50}$ and the lower bound indicates the minimum $L(E)C_{50}$ level for the representative set of data; toxicity ranking based on US EPA is as following: very high: $L(E)C_{50} < 1 \text{ mg L}^{-1}$, high: $1 \text{ mg L}^{-1} < L(E)C_{50} < 10 \text{ mg L}^{-1}$, moderate: $10 \text{ mg L}^{-1} < L(E)C_{50} < 100 \text{ mg L}^{-1}$, and low: $L(E)C_{50} > 100 \text{ mg L}^{-1}$)..... 97

Figure 23. Toxicity data points for ionic silver on the aquatic organisms in water, mineral medium, complex medium, and regardless of test medium (upper bound indicates the maximum $L(E)C_{50}$, the marker indicates the median $L(E)C_{50}$ and the lower bound indicates the minimum $L(E)C_{50}$ level for the representative set of data; toxicity ranking based on US EPA is as following: very high: $L(E)C_{50} < 1 \text{ mg L}^{-1}$, high: $1 \text{ mg L}^{-1} < L(E)C_{50} < 10 \text{ mg L}^{-1}$, moderate: $10 \text{ mg L}^{-1} < L(E)C_{50} < 100 \text{ mg L}^{-1}$, and low: $L(E)C_{50} > 100 \text{ mg L}^{-1}$)..... 99

Figure 24. Effect factors for freshwater ecotoxicity impact category under different scenarios A) citrate coated, B) PVP coated, C) uncoated, D) coated with other agents, E) all coatings, F) all coatings and all test mediums but disaggregated based on size..... 102

Figure 25. A) Potential environmental pathways for nanomaterials and physicochemical characteristics of ENMs that affect fate factors [23, 25, 129, 155, 174] B) Relative importance of potential transformation processes in modeling environmental fate of nAg (darker shades indicate higher importance) [129, 249]..... 114

Figure 26. Processes relevant to ENMs in aquatic environments (adapted from [261, 263, 268]).	121
Figure 27. Comparison of characterization factors calculated in the current study with the literature values where Group A shows literature values, Group B shows CF values obtained in the current study using EFs regardless of size and coating (compatible with the literature), and Group C shows CF values obtained in the current study using EFs for PVP coated nAg regardless of size (S1: scenario 1, S2: scenario 2, O: optimistic, S: skeptical).	132
Figure 28. Sensitivity factors (SFs) of the selected inputs on the rate constants for A) Scenario 1 and B) Scenario 2.....	134
Figure 29. A) The range of the initial silver content in silver-enabled textiles (n indicates the number of data points used to draw the boxplots, initial silver > 500 mg Ag/kg textile are excluded); B) percentage of silver released from textiles due to laundering and exposure to artificial sweat (triangle markers show that initial silver source in textiles were conventional, circle markers indicate that initial silver source in textiles were nano, color scheme illustrates different number of washing cycles) [80, 82, 83, 296–311] (the points that indicate >100% of initial Ag release is due to the Ag/nAg not uniformly distributed in experimental samples). ...	144
Figure 30. System boundaries considered in the current study along with flows for each life cycle phase. Processes/flows with dashed outlines are not included in the LCA. Green arrows indicate inputs and red arrows represent outputs.....	146
Figure 31. Environmental impacts of various silver enabled textiles under different laundering scenarios A) GW, B) EC, C) HHNC and D) EU (x axis reads product code_type of washer/type of dryer, e.g. T_HE/LN means product T with high efficiency washer and line drying).....	154

Figure 32. Sensitivity factors of each input/output parameter to environmental impact categories under HE/LN scenario for A) product T, B) product E, C) product A and D) product C. 156

List of Tables

Table 1. Summary of background information for chemical and physical methods.	19
Table 2. Summary of synthesis procedures used in the current study.	26
Table 3. Summary of SWCNTs (S-) synthesis processes used in the current study.....	53
Table 4. Summary of MWCNTs (M-) synthesis processes used in the current study.	54
Table 5. Summary of the literature on developing nAg specific freshwater ecotoxicity CFs. ..	117

List of Symbols/Abbreviations

ACR	acute-to-chronic ratio
$A_{\text{freshwater}}$	area of freshwater
Ag/S or Ag ₂ S	silver sulfide
Ag ⁺	ionic silver
AgCl	silver chloride
AM	arc method
AP	arc plasma
AP-MNL	arc plasma by Metal Nanopowders Ltd., United Kingdom
AP-UDE ₁	arc plasma #1 by University of Duisburg- Essen, Germany
AP-UDE ₂	arc plasma #2 by University of Duisburg- Essen, Germany
AP-UDE ₃	arc plasma #3 by University of Duisburg- Essen, Germany
AP or AC	acidification
Ar	argon
A_{soil}	area of soil
BAF	bioaccumulation factor in biota
BIO _{mass}	concentration of biota in water
C	carbon
C ₀	initial concentration
C ₂ H ₂	acetylene
C ₆ H ₆	benzene
CCS	cumulative case scenario
CE	conventional efficiency

CED	cumulative energy demand
CeO ₂	cerium(IV) oxide
CF(s)	characterization factor(s)
CFC	chlorofluorocarbon
CFC-11-eq.	chlorofluorocarbon 11 equivalent
CH ₄	methane
CML	University of Leiden Institute of Environmental Sciences
CNT(s)	carbon nanotube(s)
Co	cobalt
CO	carbon monoxide
Co-Mo	cobalt-molybdenum
CO ₂	carbon dioxide
CO ₂ -eq.	carbon dioxide equivalent
CoMoCat	cobalt-molybdenum catalytic method
CR	chemical reduction
CR-EG	chemical reduction, reducing agent: ethylene glycol
CR-SB	chemical reduction, reducing agent: sodium borohydride
CR-starch	chemical reduction, reducing agent: starch
CR-TSC	chemical reduction, reducing agent: trisodium citrate
C _{spm}	suspended particulate matter concentration
C _t	concentration at time t
CTUe	comparative toxic units for ecosystems
CTUe-eq.	comparative toxic units for ecosystems equivalent

CTUh	comparative toxic units for humans
CTUh-eq.	comparative toxic units for humans equivalent
CuO	copper oxide
CVD	chemical vapor deposition
DNA	deoxyribonucleic acid
d_{nAg}	diameter of suspended nanosilver
DOC	dissolved organic carbon
d_{SPM}	diameter of suspended particulate matter
EC ₅₀	effective concentration
EF	effect factor
ELCD	European reference Life Cycle Database
ENM(s)	engineered nanomaterial(s)
EP or EU	eutrophication
EPS	Environmental Priority Strategies
Eqn	equation
ETP or EC	ecotoxicity
Fe	iron
Fe(CO) ₅	iron pentacarbonyl
Fe ₂ O ₃ /Fe ₃ O ₄	ferrous oxides
FF	fate factor
FFP or FF	fossil fuel depletion
FSP-MS	flame spray pyrolysis by melt spun incorporation
FUn	functional unit

g	gram
GHG	greenhouse gas emissions
GI	global environmental impact
GO	graphene oxide
GWP/GW	global warming
h	hours
H ₂	hydrogen
HC ₅₀	hazardous concentration
HE	high efficiency
HFC	hydrofluorocarbon
HH	human health
HHCP or HHC	human health carcinogenics
HHNCP or HHNC	human health non carcinogenics
HiPCO	high-pressure carbon monoxide reaction
h _w	depth of water compartment
IC	impact category
IC ₅₀	inhibitory concentration
IEA	International Energy Agency
IF	intake factor
IPCC	International Panel on Climate Change
IS	impact score
ISO	International Organization for Standardization
k ^{nAg} _{sed}	sedimentation rate constant for nAg

k_{adv}	advection rate constant
k_{coll}	collion rate
k_{diss}	dissolution rate constant
K_{DOC}	partitioning coefficient between dissolved carbon and water
kg	kilogram
$k_{het-agg}$	hetero-aggregation rate constant
K_p	partitioning coefficient
$k_{precipitation}$	precipitation rate
K_{pss}	partitioning coefficient between water and suspended solids
k_{sed} or k_{sed}'	sedimentation rate constant for nAg
$k_{w,w}$	removal rate constant for freshwater
L	liter
$LaCoO_3$	lanthanum cobaltite
LC_{50}	lethal concentration
LCA	life cycle assessment
LCI	life cycle inventory
LN	line drying
LV	laser vaporization
m^2	square meter
m^3	cubic meter
mg	miligram
Mg	magnesium
MgO	magnesium oxide

MJ	megajoule
mm	millimeter
MW	microwave
MW-	multi walled-
MWCNT(s)	multi walled carbon nanotube(s)
M	mass
N	nitrogen
N-eq.	nitrogen equivalent
N/A	not available or not stated
nAg or AgNP	silver nanoparticle
NH ₄ ⁺	ammonium
Ni	nickel
NIFA	National Institute of Food and Agriculture
nm	nanometer
NREL	National Renewable Energy Laboratory
O ₃	ozone
O ₃ -eq.	ozone equivalent
°C	degree Celsius
ODP or OD	ozone depletion
OECD	Organization for Economic Co-operation and Development
PAF	potentially affected fraction
PEG	polyethylene glycol
PES	polyester

PET	polyethylene terephthalate
PM2.5	particulate matter that has a diameter of less than 2.5 micrometers
PM2.5-eq.	particulate matter that has a diameter of less than 2.5 micrometers equivalent
PVP	polyvinylpyrrolidone
RA	rural air
RCS	Regular case scenario
RMS-Ar-N	reactive magnetron sputtering
RP or RE	respiratory effects
s	second
S1	scenario 1
S2	scenario 2
S3	scenario 3
SB4N	Simple Box 4 Nano
SETAC	Society for Environmental Toxicology and Chemistry
SF	sensitivity factor
SF(s)	scaling up factor(s)
SO ₂	sulfur dioxide
SO ₂ -eq.	sulfur dioxide equivalent
SP or PS	smog (photochemical smog)
Spark-TUD	spark system by Delft University of Technology, the Netherlands
SPL	species level
SPM	suspended particulate matter

SS	suspended solids
SW-	single walled-
SWCNT(s)	single walled carbon nanotube(s)
TCLP	toxicity characteristic leaching protocol
TiO ₂	titanium dioxide
TPL	trophic level
TRACI	tool for reduction and assessment of chemicals and other environmental impacts
UNEP	United Nations Environment Program
US EPA	United States Environmental Protection Agency
USD	United States Dollars
USDA	United States Department of Agriculture
USEtox	the UNEP-SETAC toxicity model
USLCI	United States Life Cycle Inventory
USPTO	United States Patent and Trademark Office
v_{set}^{nAg}	settling velocity
V _w	volume of freshwater
WARF	Wisconsin Alumni Research Foundation
WWTP	wastewater treatment plant
XF	exposure factor
Y	yttrium
ZnO	zinc oxide
μg	microgram

ρ	density
φ	water run-off fraction
%	percentage
$\alpha_{\text{het-agg}}$	hetero-aggregation/attachment efficiency

1. Introduction

1.1. Research Summary and Goals

If one thinks from a non-expert perspective, nanoparticles would not seem harmful to the environment because they are so tiny, only one billionth of a meter or about half the width of a single strand of human DNA. They also comprise a very small portion by mass of total elemental flows (e.g. nano fraction of ore production for silver nanoparticles is 0.5%) [1]. This would also make consumers think that the production of nanomaterials has a low to neutral impact on the resource depletion problem, which is an indicator for unsustainable consumption of material and energy supplies (e.g. water, fossil fuels, mines). However, thinking from a scientific perspective, the field of nanotechnology may have significant impacts on the environment while providing advantages by improving the functions of conventional products. Nanotechnology is a rapidly growing industry, and its products have already started taking part in our everyday lives. As engineered nanomaterials have remarkable properties, they are used in various industries. Being widely incorporated in consumer products raises environmental and human health related concerns; therefore, research on evaluating performances of engineered nanomaterials (ENMs) and nano-enabled consumer products is critical.

The main goal of this research is to investigate the environmental impacts of manufacturing and using the selected ENMs. Case studies are constructed for silver nanoparticles (nAg) and carbon nanotubes (CNTs), two representative classes of ENMs that are utilized in various consumer products. Life cycle assessment (LCA) and USEtox methodologies are used to analyze the environmental costs.

1.2. Research Objectives and Questions

Existing literature mostly considers calculating environmental impacts of particular nano-enabled consumer products with varying scopes, and system boundaries as well as environmental impact categories. Studies also showed that incorporating ENMs may have greater impacts on the overall environmental impact of nano-enabled products. Thinking from a global perspective, the growing nanomaterials industry requires significant amounts of materials and energy inputs in order to meet the market demand. Another critical point is that each sector requires different synthesis routes in order to produce ENMs with certain morphologies, which affects the overall environmental impact of that specific industry/sector. Incorporating industrial shares as well as impacts from particular synthesis processes may help modeling disaggregated impacts and further examine cradle-to-grave life cycle impacts of the nanomaterials industry.

Furthermore, impacts resulting from the potential nanomaterial release to the environment (e.g. water, soil, air) as a result of the manufacturing, use, and end-of-life phases have been largely disregarded among the existing LCA literature. Besides the conventional life cycle assessment results, nano-specific impacts should also be incorporated to provide a holistic assessment. In order to achieve this goal, a handful of studies derived characterization factors (CF) for different ENMs; however, the method used to develop CFs are not consistent, which result in significantly different CFs for the same type of ENM. These considerations shaped the framework of this research and resulted in asking the research questions presented below.

Q1. What are the global environmental impacts of manufacturing the selected ENMs? What are the hotspots for each synthesis process? How can the cradle-to-gate impacts be disaggregated by industry/sectoral applications where the selected ENMs are used the most? (Chapters 2 and 3)

Q2. How are the freshwater ecotoxicity effect factors influenced by the different properties of nAg and the receiving medium? Should specific effect factors be developed based on the physiochemical properties of nAg and the release media, or would a general effect factor be useful for modeling nano-specific impacts in any aquatic environment? (Chapter 4)

Q3. What is the nano-specific characterization factor of nAg? Which framework should be used to model the fate and exposure of nAg? What factors influence the particle-specific characterization factor the most? (Chapter 5)

Q4. How do nano-specific characterization factors help researchers model the cradle-to-grave environmental impacts of nAg enabled textiles? Does modeling released nAg as ionic silver cause an overestimation or an underestimation? Is it worth the resources required to calculate characterization factors for ecotoxicity and human health impacts? (Chapter 6)

In order to address the research questions presented above, research objectives are defined as follows.

O1. Conduct LCAs for different industrially preferred synthesis processes on a mass based functional unit, define process hotspots and model environmental impacts per industry/sector where the selected ENMs used the most.

O2. Explore the trends of freshwater ecotoxicity effect factors for nAg based on their physicochemical properties (size, coating) as well as various release mediums (complex, mineral) using nanotoxicology literature.

O3. Calculate physicochemical property based freshwater ecotoxicity characterization factors for nAg by extracting relevant information from aquatic mesocosms, using USEtox methodology and principles of colloidal science.

O4. Model the cradle-to-grave (both indirect and direct) environmental impacts of a nAg enabled consumer product using currently developed characterization factors (textile case study) to determine the necessity of calculating nanospecific factors.

1.3. Nanomaterials Industry

Nanomaterials are characterized as having at least one external dimension in the nanoscale. More specifically, ENMs are materials having a size of 1-100 nanometers (nm) [2]. Due to their size dependent properties, ENMs perform either enhanced or different functions compared with their bulk counterparts and have been used in a wide variety of sectors including electronics, medical, cosmetics, coatings, and packaging [3–5]. As presented in Figure 1, market reports show that the nanomaterials industry is constantly growing and the market value is expected to reach \$92 billion by 2028 [6].

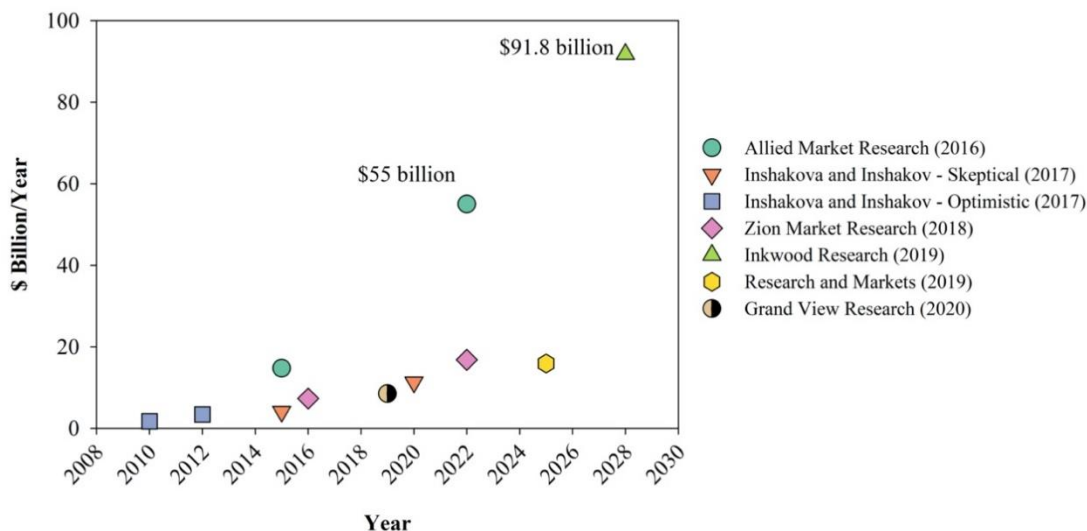


Figure 1. Nanomaterials market value in USD \$ Billion/year, compiled from the literature [7] and commercial reports [6, 8–11].

ENMs are categorized in four main classes as metals (e.g. silver, iron, gold), metal oxides (e.g. titanium dioxide, aluminum oxide, zinc oxide), metal chalcogens (e.g. cadmium sulfide) and carbon-based (e.g. carbon nanotubes, fullerenes) materials [12]. Jankovic and Plata classified ENMs according to their level of maturity (i.e. *technology readiness*) [1]. They found that CNTs are the most commercialized ENMs with a great number of sectoral applications already in operation as well as numerous final prototypes. They added that commercial applications of ENMs that are in metal group are more limited in number. For the current research, in addition to CNTs, nAg are selected to represent a different class as well as a different level of maturity. Although, the *technology readiness level* for nAg is reported as low-to-mid due to the low number of applications used for different purposes, they account for more than 50% of the global nanomaterial consumer products [1, 7]. Figure 2 shows the status of the selected ENMs represented by the number of applications in different levels [1].

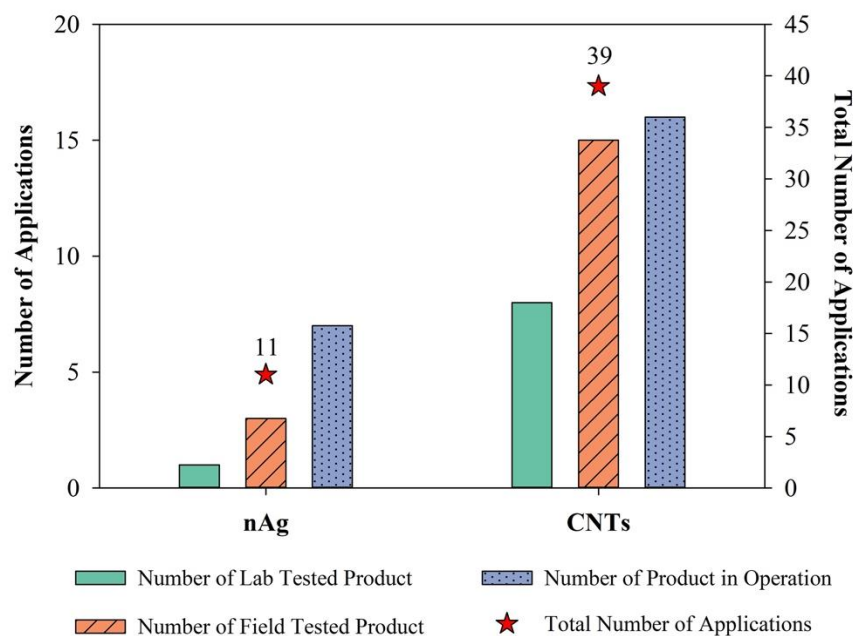


Figure 2. The number of applications of the selected ENMs in different development stages [1].

Given that the ENMs are incorporated into various products and they are used by numerous industries for diverse purposes, their production is continuously increasing. This situation raises questions on their environmental implications. Environmental impact assessment of any product or process by using LCA provides results in a broad category of impacts (e.g. global warming, eutrophication, toxicity, etc.), which are quantifications of the unit release of chemicals to the environment, in other words, their corresponding effect on the environment. LCA can be utilized to identify hotspots and to improve the environmental performances of the product/process. In the nanomaterials industry, applying LCA to ENMs provides impact projections on several different potential environmental impact categories. These may be grouped as “non-nanoscale emissions to the environment” and do not include nano-specific emissions to soil, air and water [13]. Non-nanoscale emissions represent indirect impacts due to the nanomaterial production, whereas nano-specific emissions denote direct impacts resulting

from the nanomaterial release as a function of size and shape. Existing literature on the LCA of ENMs typically develop impact projections based on point-value estimates by converting masses emitted into the potential impacts they cause [14]. In order to calculate nano-specific emissions, defining CFs is critical. Fundamentals of LCA and CF calculation are explained in the following subsections.

1.4. Life Cycle Assessment

LCA is a tool to evaluate environmental impact of a product, service or process throughout its entire life cycle (i.e. from raw material acquisition to end-of-life including manufacturing and use phase) [15, 16]. This methodology is governed by the International Organization for Standardization (ISO) and can be used for wide variety of applications ranging from sustainable product development to comparative environmental assessment. LCA has four stages as goal and scope definition, inventory analysis, impact assessment and interpretation. As per ISO 14040, LCA has both mandatory (selection of impact categories, classification, and characterization) and optional elements (normalization, grouping, and weighting). In the following subsections, brief definitions of each LCA phase are provided.

1.4.1. Goal and Scope Definition

This first stage of an LCA requires a clear declaration of the overall aim of the project. Functional unit(s) and scenario(s) should be developed, and system boundaries should be defined prior to analysis. The functional unit is an important component of an LCA study, which is outlined as “quantified performance of a product system for use as a reference unit” by ISO 14040 [15]. Similarly, schematizing system boundaries is crucial to make effective decisions at

the end of the study. To outline system boundaries, four stages of a product life cycle should be defined. Raw materials acquisition, manufacturing, use, and end-of-life are the four stages of a product life cycle and system boundaries may be developed by taking into account different combinations. For instance, cradle-to-gate system boundaries includes only the first two phases (raw materials acquisition and manufacturing), whereas cradle-to-grave includes all four stages. A holistic LCA requires cradle-to-grave system boundaries, but the selection is optional depending on the scope of the project [17].

1.4.2. Inventory Analysis

In this phase, the necessary life cycle inventory data is collected from literature and industry. This involves gathering quantitative data on the material and energy inputs, as well as the waste and emission outputs for the selected system boundaries. Figure 3 is a simplified inventory data framework illustrating the required information for a unit process as well as different system boundaries.

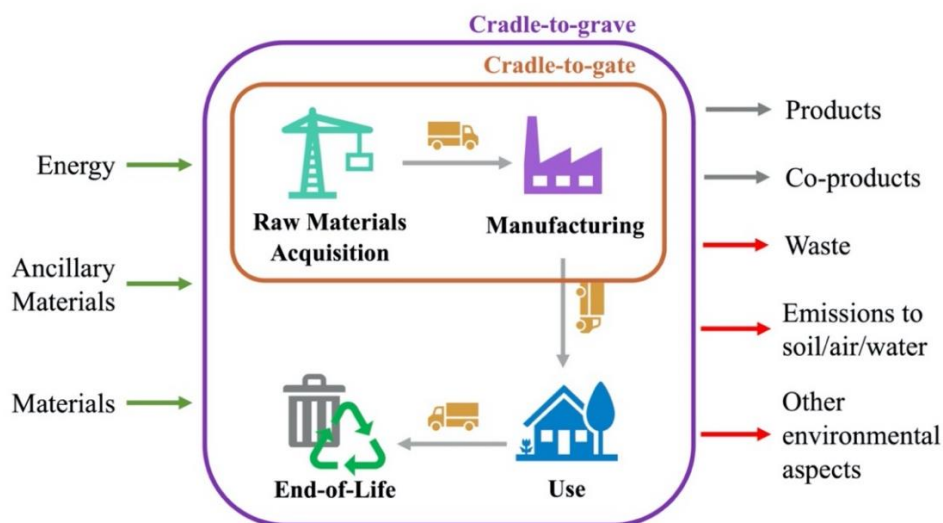


Figure 3. Simplified LCA inventory framework and representations of different system boundaries (adapted from [17]).

1.4.3. Impact Assessment

The life cycle impact assessment step helps classifying and characterizing the inputs (i.e. material and energy) and outputs (i.e. waste and emissions) from modeled processes into various impact categories, depending on the selected method. For instance, US EPA's Tool for Reduction and Assessment of Chemicals and Other Environmental Impacts (TRACI) models impacts in ozone depletion, global warming, smog, acidification, eutrophication, carcinogenics, non carcinogenics, respiratory effects, ecotoxicity, and fossil fuel depletion [18]. Another example may be CML impact assessment method, which lists impacts in abiotic depletion, global warming, ozone layer depletion, human toxicity, fresh water aquatic ecotoxicity, marine aquatic ecotoxicity, terrestrial ecotoxicity, photochemical oxidation, acidification and eutrophication [19]. Given that TRACI 2.1. impact assessment methodology is used in this research, a short description of each impact category is provided in the subsequent subsections.

1.4.3.1. Ozone Depletion

Ozone depletion (to air) occurs due to the increasing concentration of substances that are classified as chemicals that contribute to decreasing the stratospheric ozone levels such as chlorofluorocarbons (CFC), halons and hydrofluorocarbons (HFC) [4, 18]. This category affects both human health and the environment. TRACI provides ozone depletion results as kilogram (kg) CFC-11-eq. per functional unit [18].

1.4.3.2. Global Warming

Global warming (to air) occurs due to the increasing greenhouse gas (GHG) emissions which results in an increase in the temperature of the atmosphere [18]. GHG emissions include

naturally occurring or human induced carbon dioxide, methane and nitrous oxides [4]. TRACI uses indicators from the International Panel on Climate Change (IPCC) and provides global warming (in some sources it refers to as climate change) results as kg CO₂-eq. per functional unit [18].

1.4.3.3. Smog

Smog (to air) occurs due to the increasing concentrations of nitrous oxides, volatile organic compounds, carbon monoxide, methane and other ozone forming molecules in the troposphere [4]. This category affects both human health and the environment, and in some sources refers to as photochemical smog formation [18]. TRACI provides smog results as kg O₃-eq. per functional unit [18].

1.4.3.4. Acidification

Acidification (to air and water) occurs due to the increasing concentration of hydrogen ion in an environmental compartment [4, 18]. The acidity of the environment may increase as a result of several chemical reactions, biological activities or natural circumstances. According to the US EPA, sulfur dioxides and nitrogen oxides are the largest contributors of this category. Results are modeled regardless of site-specific characteristics as each site may show different sensitivities. TRACI provides acidification results as kg SO₂-eq. per functional unit [18].

1.4.3.5. Eutrophication

Eutrophication (to air and water) occurs due to the increasing concentration of nitrates and phosphates which contribute to an undesirable biological productivity such as algal growth

[4, 18]. According to US EPA, for freshwater lakes and streams, phosphorus is more impactful than nitrogen; and nitrogen mostly affects coastal environments [18]. TRACI provides eutrophication results as kg N-eq. per functional unit [18].

1.4.3.6. Carcinogenics and Non-carcinogenics

In order to calculate carcinogenics and non-carcinogenics impacts (to urban air, non-urban air, freshwater, seawater, natural soil, agricultural soil), TRACI incorporates the USEtox methodology, which is the consensus model developed by the UNEP/SETAC initiative as described in Section 1.5 [18, 20]. These are calculated listing the mass of emissions inhaled or ingested by humans [20]. USEtox uses cancer and non-cancer potentials of substances from databases that provide experimental results, and TRACI provides carcinogenics and non-carcinogenics as CTUh per functional unit [18].

1.4.3.7. Respiratory Effects

Respiratory effects (to air) occur due to the increasing levels of ambient particulate matter. This category quantifies the particulate matter and precursors of these particulates (e.g. sulfur dioxide and nitrogen oxides) in order to calculate negative human health effects [18]. This category can be named human health particulate or human health criteria pollutants category, and combines effects resulting from inhalable coarse particles (2.5-10 μm in diameter) as well as fine particles ($\leq 2.5 \mu\text{m}$ in diameter). TRACI provides respiratory effects results as kg PM_{2.5}-eq. per functional unit [18].

1.4.3.8. Ecotoxicity

Similar to human health carcinogenics and non-carcinogenics, in order to calculate ecotoxicity (to urban air, non-urban air, freshwater, seawater, natural soil, agricultural soil), TRACI uses models from the USEtox methodology [18, 20]. Ecotoxicity is calculated by the chronic toxicity of any substance to an ecosystem using its bioavailable fraction [20]. TRACI provides ecotoxicity as CTUe per functional unit [18].

1.4.3.9. Fossil Fuel Depletion

The fossil fuel depletion category calculates the surplus energy needed to produce fossil fuel in the future. TRACI provides non-site specific results as MJ surplus energy per functional unit [4, 18].

1.4.4. Interpretation

Interpretation is the last stage for an LCA, where the impact assessment results are carefully evaluated. ISO 14044 suggests three evaluation methods to be implemented including (1) completeness check, (2) sensitivity check, and (3) consistency check [16]. These methods help to evaluate the LCA data to make sure that it is complete, how sensitive the analysis was with different input sources, and the overall study to ensure that the analysis is internally consistent [17]. Since uncertainty exists with novel technologies, application of these methods is critical within the context of this dissertation.

1.5. Characterization Factors and the USEtox Model

In LCA, the environmental impact of a product or process is calculated during the impact assessment step, which covers the characterization stage. CFs are used to quantify the impact of any product or process in different categories. In other words, they indicate how much a single unit of mass contributes to an impact category, e.g. 1 kg methane release contributes as 25 kg of carbon dioxide to global warming [21]. This is called the impact score (IS) of a substance and can be calculated as eqn (1.1), where $CF_{x,i}$ is the characterization factor for the respective impact of substance x released to the compartment i (e.g. in cases/kg emitted); and $M_{x,i}$ is the mass of the emission of substance x to compartment i (in kg emitted) [20].

$$IS = \sum_i \sum_x CF_{x,i} * M_{x,i} \quad (1.1)$$

Regarding nanomaterials related impact assessment studies, general practice among the literature is based on quantifying the upstream or embodied impacts due to nanomaterial production, while direct impacts resulting from the nanomaterial release are not well documented [13]. In order to develop nano-specific CFs, incorporation of fate factor (FF), exposure factor (XF) and effect factor (EF) is needed for a systematic modeling. USEtox model is the common methodology used among the LCA literature to develop specific CFs for several chemicals [22]. It is a scientific model which provides a framework for characterizing toxicity impacts with a set of factors and linking different indicators to characterize human toxicity and freshwater ecotoxicity [20]. In other words, it helps to derive the CFs for any substance to be incorporated into the impact score calculations.

$$CF = FF * XF * EF \quad (1.2)$$

Eqn (1.2) shows a calculation framework for CF [20], expressed in $PAF.m^3.day/kg$ emitted or $CTUe$ (comparative toxic units for ecosystems) for freshwater ecotoxicity, and in

cases/kg emitted or *CTUh* (comparative toxic units for humans) for human toxicity. *FF* represents the duration that an ENM resides in a specific environmental compartment such as air, water or soil. The *FF* is typically presented in *days* and it is the same for ecotoxicity and human toxicity categories [20, 23, 24]. *XF* represents dissolved and bioavailable fraction (i.e. probability) of an ENM that an organism will be exposed to [23, 24]. For freshwater ecotoxicity, impacts on biota may occur through invertebrate uptake, plant uptake and bioaccumulation, and microbial interactions. *XF* for freshwater ecotoxicity is dimensionless, and represents only the fraction of the ENM that is dissolved in water [20, 25]. For human toxicity, intake route may be through inhalation, ingestion and dermal contact from an environmental compartment (e.g. water, air, soil). *XF* for human toxicity is presented with a unit of $days^{-1}$ or kg_{intake}/day per $kg_{in\ compartment}$ and is calculated for both direct and indirect pathways [20, 22, 25]. *EF* relies on the toxicological data and represents the impact of ENMs on the ecosystem. For freshwater ecotoxicity, it is the slope of the concentration – response plot when the potentially affected fraction is 0.5 (i.e. 50% of the population is affected) [26]. *EF* has two different units, representing different impact categories. For human toxicity category, *EF* is in *cases/kg* and for freshwater ecotoxicity category, *EF* is in $PAF.m^3/kg$ [20].

2. Global environmental impacts of silver nanoparticle production methods supported by life cycle assessment

The following chapter is a reproduction of an article published in the Resources, Conservation and Recycling, with the citation:

Temizel-Sekeryan, S.; Hicks, A.L. (2020) Global environmental impacts of silver nanoparticle production methods supported by life cycle assessment, *Resources, Conservation and Recycling*, Vol. 156, 104676.

The article appears as published, although style and formatting modifications have been made.

Authorship contribution statement

Sila Temizel-Sekeryan: Designed Research, Performed Research, Analyzed Data, Wrote the Paper.

Andrea L. Hicks: Designed Research, Wrote the Paper.

2.1. Abstract

Considering their antimicrobial, electrical and optical properties, silver nanoparticles (AgNPs) are the most common type of engineered nanomaterials found in consumer products. AgNPs may be synthesized through multiple methods, including chemical, biological and physical techniques; however, literature suggests that the manufacturers prefer to use physical and chemical methods (85%) rather than biological. This work presents cradle-to-gate life cycle impact assessments in order to evaluate global environmental impacts of six different AgNPs synthesis routes (two chemical and four physical) along with thirteen different inventories and a mass based functional unit of 1 kg of AgNPs. Results are then combined with the annual global AgNPs production estimates, and global environmental impact calculations are performed based on both optimistic and skeptical estimations. Since AgNPs production volumes are forecasted to increase drastically, industrial scale AgNPs syntheses are modeled and future life cycle impacts are projected using three different scale-up factors. Furthermore, given that each industry has specific preferences for properties of AgNPs (i.e. size, surface area) and those are dependent on the synthesis methods, industry based environmental impact projections are developed for industries where the majority of AgNPs are used such as textiles; coatings, paints and pigments; consumer electronics and optics; cosmetics; medical and packaging. Results show that scaling up may reduce the environmental emissions up to 90% globally, and up to 83% per industrial sector which suggest that the global environmental impact of AgNPs may vary significantly as a function of the synthesis method, scale, and desired product application.

2.2. Introduction

Silver nanoparticles (AgNPs) are well known for their antimicrobial, electrical and optical properties. Their sizes range from 1 nanometer (nm) to 100 nm, with the small size influencing their characteristics [27, 28]. Different synthesis methods are appropriate for particular desired applications and properties (such as a specific sized particle). Inshakova and Inshakov suggest that AgNPs are the most commercialized engineered nanomaterials (ENMs), and account for more than 50% of global nanomaterial consumer products [7]. They are listed in the Organization for Economic Co-operation and Development's (OECD) list of thirteen manufactured nanomaterials that are currently available for commercial use [29]. Beneficial properties of AgNPs include antibacterial, antimicrobial, antifungal and antifouling activity; deodorization; non-allergenic; stain resistance; electrical conductivity; self-cleaning and antiseptic [30–39]. According to the Nanotechnology Products Database, AgNPs have been used in 278 different product types, 34 countries and 15 industries (i.e. medical, textile, electronics, cosmetics, packaging, coatings) with diverse properties and applications [40].

Due to their diverse applications, the total quantity of AgNPs produced annually is subject to some debate, although many estimates have been generated. Pulit-Prociak and Banach reported a skeptical (i.e. minimum, low or pessimistic estimation) global production volume of AgNPs at 210 tons/year, and an optimistic (i.e. maximum, high or promising estimation) global production volume at 530 tons/year for the year 2018 [41]. Figure 4 presents the global market (tons) for AgNPs, collected from multiple studies [1, 41–48] and commercial reports [49]. Although the estimates differ to some degree, the overall trend is indicated to increase. In addition to mass based global production estimations, change in the global AgNPs market size is an indicator of increased use. In 2015, the global AgNPs market was valued at approximately \$1

billion, and it is estimated to reach \$3 billion by 2024 [50]. In terms of sectoral breakdown, medical applications (i.e. healthcare and life sciences) are expected to be valued over \$1 billion, while textile applications are anticipated to surpass \$750 million, and food and beverages applications are projected to exceed \$300 million by 2024 [50].

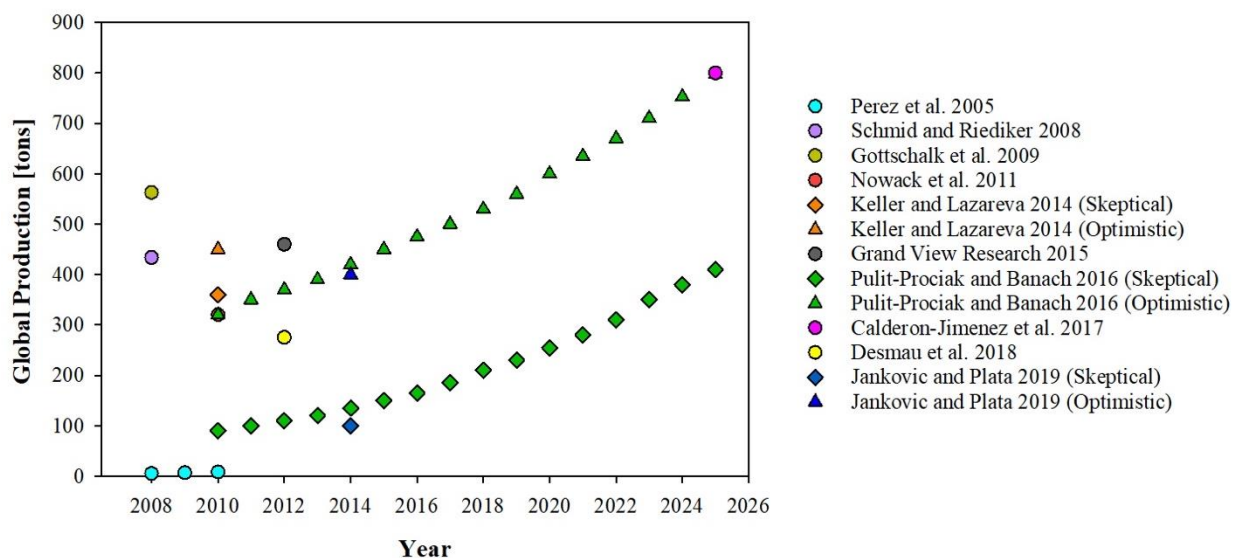


Figure 4. Global market (tons) for silver nanoparticles (AgNPs) where diamond markers indicate skeptical estimations, circle markers indicate single estimations and triangle markers indicate optimistic estimations [1, 41–49].

AgNPs can be synthesized using a wide variety of techniques which may be grouped as chemical (wet chemistry), physical (dry chemistry) and biological (using microorganisms and plants) methods. According to Charitidis et al., physical and chemical methods constitute 85% of the overall production of inorganic nanoparticles [51]. Since these techniques are preferred among industries, environmental implications of physical and chemical methods are evaluated in

the current study. Table 1 shows a summary on AgNPs synthesis methods along with their properties and some relevant examples.

Table 1. Summary of background information for chemical and physical methods.

	Process	Properties	Examples
Chemical methods	Use solvents or liquid reagents as reducing agents (i.e. sodium citrate, sodium borohydride, ethylene glycol) to reduce the monovalent ionic silver (Ag^+) to metallic silver (Ag^0), then produce nanoparticles by chemical coprecipitation [52, 53]	<ul style="list-style-type: none"> • Easy to apply, have low cost and high yield, but often involve the use of hazardous chemicals that are harmful to living organisms [54] • Desired shape and size of the AgNPs may be achieved by controlling the type and concentration of reducing or stabilizing agent, the addition of complexing agents to decrease particle size and the addition of co-reducers [42, 55] 	<ul style="list-style-type: none"> • Precipitation [56] • Sol-gel [56] • Chemical reduction [36] • Microwave [28] • Liquid-phase reduction [52]
Physical methods	Do not use any solvents for reducing Ag^+ , however consume a sizable quantity of energy since they produce AgNPs using furnaces or tubes with high temperature and pressure [57]	<ul style="list-style-type: none"> • Fast and generally no hazardous chemicals are involved in the synthesis, but they require high energy, have low synthesis yield and product uniformity [54] • The shape of the AgNPs may be controlled by changing the experimental conditions such as the thermal conditions, power, and arc discharge [51, 55] 	<ul style="list-style-type: none"> • Reactive magnetron sputtering [38] • Flame spray pyrolysis [36, 58] • Plasma arcing [36, 58, 59] • Grinding [52] • Laser ablation [52] • Vapor deposition [52]

The environmental impacts of AgNPs enabled consumer products as well as manufacturing AgNPs have been previously investigated using life cycle assessment (LCA). LCA is a tool to evaluate environmental performances of products and services through their life cycle, from raw materials acquisition to end-of-life including manufacturing, transportation, distribution, use and disposal stages [17]. Depending on the scope of the project, system boundaries may be drawn either cradle-to-gate or cradle-to-grave. According to Pourzahedi et al., conducting cradle-to-grave LCAs for nano-enabled products is challenging since these

products provide added values due to technological advantages which are unique and challenging to compare with the conventional products [37]. For example, AgNPs enabled textiles offer the potential for less frequent laundering, bandages help eliminate the conventional ointment use and provide better wound healing, and food storage containers contribute to reducing the amount of food loss [60]. Although it is challenging to quantify and incorporate these product specific properties (i.e. benefits) in LCA analysis, in order to make a holistic comparison between conventional and nano-enabled products that are used for the same purpose (e.g. clothing), considering cradle-to-grave boundaries is preferable. In this regard, Hicks and Temizel-Sekeryan reviewed cradle-to-grave LCA literature of AgNPs enabled consumer products and presented a framework to quantify the benefits and detriments of nanoenabling along with break-even points [60].

A substantial number of LCAs have been performed for the AgNP textile industry (e.g. antibacterial t-shirts, socks, household textiles) with varying scopes and bounds; cradle-to-gate [37] or cradle-to-grave [30, 56, 58, 61, 62]. Additionally, there are studies where manufacturing and incorporation of AgNPs are excluded from cradle-to-grave boundaries (where the raw materials were considered, but not the synthesis processes themselves) [32, 63] or screening level LCA is conducted [36]. LCAs implemented for AgNPs enabled food storage containers are also popular among literature where mostly cradle-to-grave results are presented [39, 64, 65]. Other examples include LCAs with various system boundaries on AgNPs enabled packaging materials [66], coatings [67], medical gowns [31, 37], wound dressings [37, 38], environmental applications [68], and products for children [37]. Aside from product-based studies, there are LCAs conducted only for producing AgNPs with different impact assessment methodologies. While there are comparative LCA studies in order to understand the environmental advantages

and tradeoffs of several manufacturing methods [53, 59, 69], evaluations of single technique are also studied [28]. Since the results of the aforementioned LCA studies are not standardized (i.e. they have different system boundaries, or they use different impact assessment methodologies), direct comparisons cannot be carried out.

As the global production estimations show, the popularity of AgNPs is increasing due to their use in different modern technological applications. Considering the environmental impacts of, AgNP synthesis, silver acquisition in particular has been found to be the main contributor of the total environmental impact due to the environmental intensity of mining and refining the silver [53, 63]. Taking into account all inputs and outputs (e.g. raw materials, energy, water, heat, emissions etc.) for each synthesis method, additional factors such as the amount of energy used, have significant contributions on the overall potential environmental impacts, especially when an equal amount of silver is utilized among multiple techniques. Therefore, it is critical to evaluate the environmental impacts of different AgNP production methods and their contributions to global environmental impacts to identify the most efficient synthesis route in terms of environmental sustainability.

LCA results based on laboratory scale inventories help identify hotspots of the system as well as comparing the alternatives used for the same application; however, they are not optimized in terms of resource efficiency [70]. Therefore, laboratory scale LCA results are not representative for large scale synthesis as there will likely be changes in the process yield, material, and energy inputs. Industrial processes are often connected as a continuous flow rather than being independent or isolated, which result in more realistic impacts [71, 72]. As Gao et al. discussed, with industrial scale manufacturing and utilization of efficient equipment, the resource and energy consumption needed to produce the same amount of ENM is expected to be lower

than laboratory scale production [73]. On the contrary, Arvidsson and Molander modeled large scale production for epitaxial graphene, where they experienced increased environmental impacts due to the necessary use of an advanced material (e.g. silicon carbide wafers) [74]. Piccinno et al. argued that in order to evaluate the benefits and detriments resulting from large scale manufacturing, using a simple scaling up factor may not be sufficient [75]. However, due to the lack of inventory for industrial scale production (i.e. systematically collected empirical data), environmental impacts of large scale ENMs manufacturing have rarely been studied [76]. This acknowledges the utilization of theoretical scaling up factors and the practice of linear extrapolation as a current strategy among literature [71, 72, 75, 77].

The goal of this study is to project the cradle-to-gate global environmental impacts of manufacturing AgNPs by including various industrially preferred synthesis methods and using global AgNPs production estimates (tons/year). Given the improvement in ENMs sector, presenting results for large scale production would be more realistic. Therefore, environmental impacts as a result of industrial scale production are also envisaged by using scaling up factors to address the potential savings in the materials and energy consumption. Additionally, this work seeks to quantify sectoral environmental impacts resulting from manufacturing AgNPs by using industry-based estimations. The results are intended to provide a quantification of the current and potential future environmental impacts due to the manufacturing of AgNPs at a global scale, as a function of raw materials and manufacturing methods.

2.3. Materials and methods

2.3.1. Goal and scope definition

In the current study, six different AgNPs synthesis procedures along with thirteen different inventories are evaluated using LCA methodology with a cradle-to-gate approach. Potential environmental impacts are modeled using the SimaPro 8.5.2 software with Ecoinvent 3, USLCI (U.S. Life Cycle Inventory) and ELCD (European reference Life Cycle Database) databases. TRACI 2.1 (tool for the reduction and assessment of chemical and other environmental impacts) and Cumulative Energy Demand (CED) are used as impact assessment methodologies. Selected potential environmental impact categories, along with their units and abbreviations based on TRACI 2.1 are ozone depletion (ODP in kg CFC11-eq.), global warming (GWP in kg CO₂-eq.), smog (SP in kg O₃-eq.), acidification (AP in kg SO₂-eq.), eutrophication (EP in kg N-eq.), carcinogenics (HHCP in CTUh), non-carcinogenics (HHNCP in CTUh), respiratory effects (RP in kg PM_{2.5}-eq.), ecotoxicity (ETP in CTUe), and fossil fuel depletion (FFP in MJ surplus energy) potentials. A mass based functional unit (FUn) is selected as 1 kilogram (kg) of AgNPs for compatibility with the global production estimates, as they are presented mass based (tons/year) in the literature. System boundaries considered in this study are presented in Figure 5.

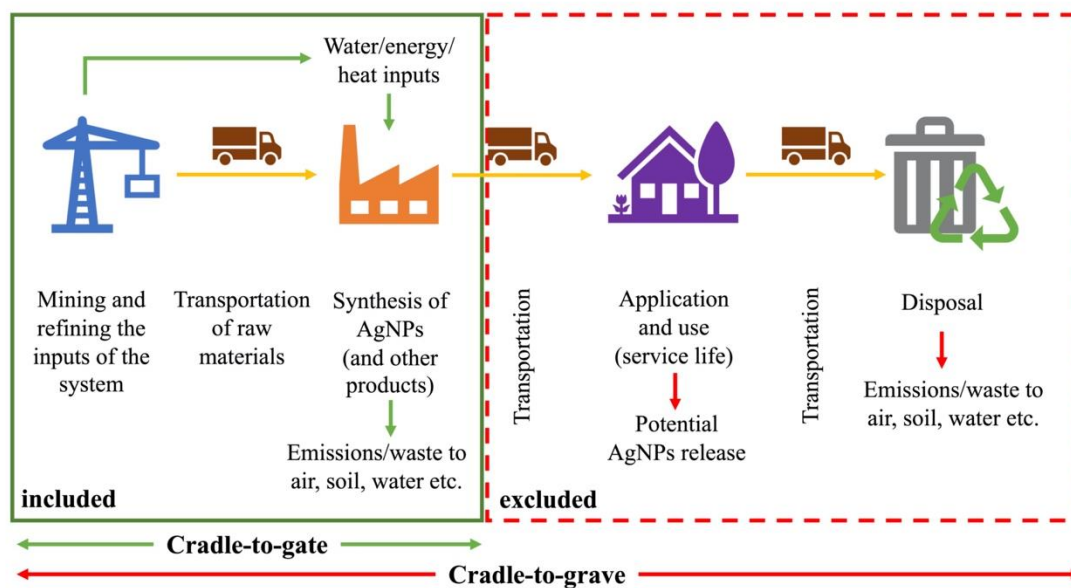


Figure 5. System boundaries considered in the current study (included life cycle stages are represented by green box). (For interpretation of the references to color in this figure legend, the reader is referred to the web version of this article).

Use and disposal phases are excluded from the selected system boundaries because there are not any specific uses assigned for the synthesized AgNPs in the current study. Although enabling AgNPs offer advanced properties to conventional products, added benefits are strictly dependent on the use phase, which is a product specific consideration [78]. Numerous studies have examined the AgNPs release by providing ranges for the mass of initial silver content and release as Ag⁺, because details of nano-specific particle characterizations are lacking [60]. For instance, Adam et al. developed material flow analysis for AgNPs where they probabilistically modeled the AgNPs release to wastewater, air, soil and surface water based on peer-reviewed literature [79]. They presented the forms of released nanomaterials as dissolved, transformed, pristine and matrix-embedded without distinguishing the particle formation and silver speciation due to lack of data. As Mitrano et al. argued, silver released after the use and end of life phases

can undergo various transformations including Ag^0 , AgCl , Ag_2S or Ag^+ [80], which is dependent on the characteristics of the receiving location as well as the chemical structure of AgNPs [81–83]. Given that there are high variability and uncertainties in the reported data, a generalized interpretation of their use and disposal could not be provided.

2.3.2. Synthesis procedures

In order to compile different inventories for AgNPs synthesis methods, a literature survey is conducted by using an academic search engine, Web of Science Core Collection, by searching combinations of key terms including nanosilver, life cycle assessment, silver nanoparticles, sustainability, environmental impact assessment and nanosilver-enabled. From this search, 4 studies were selected for inclusion in the current study because they provided the laboratory scale inventories for AgNPs synthesis. Table 2 is a summary of the selected methods, where life cycle inventories (LCI) and methodologies are also included. Detailed explanations for these methods can be found in the Appendix A.

Table 2. Summary of synthesis procedures used in the current study.

	Method	Abbreviation	Materials and Energy (LCI)	Methodology (M) Software (S)	Reference
Chemical Methods	Microwave (Table A1)	MW	glucose (reducing agent), food grade corn starch (stabilizing agent), AgNO ₃ (silver source), electricity, deionized water	M: TRACI v2.1 S: GaBi 6.0	[28]
	Chemical Reduction (Table A2-A5)	CR-TSC	trisodium citrate (reducing agent), AgNO ₃ (silver source), deionized water, heat	M: TRACI v2.1 S: SimaPro 8.1	[53]
		CR-SB	NaBH ₄ (reducing agent), AgNO ₃ (silver source), deionized water, heat	M: TRACI v2.1 S: SimaPro 8.1	[53]
		CR-EG	ethylene glycol (reducing agent), poly n-vinylpyrrolidone (stabilizing agent), AgNO ₃ (silver source), deionized water	M: TRACI v2.1 S: SimaPro 8.1	[53]
		CR-starch	soluble starch (reducing agent), AgNO ₃ (silver source), deionized water, heat	M: TRACI v2.1 S: SimaPro 8.1	[53]
Physical Methods	Flame Spray Pyrolysis (Table A6-A8)	FSP-MS	oxygen, methane, water, silver-octanoate (silver source), 2-ethylhexanoic acid (C ₈ H ₁₆ O ₂), xylene, electricity	M: ReCiPe, CED S: Simple Treat 3.0	[58]
	Arc Plasma (Table A9-A13)	AP	argon, Ag _(s) (silver source), electricity	M: TRACI v2.1 S: SimaPro 8.1	[53]
		AP-UDE ₁	nitrogen, Ag _(s) (silver source), electricity	M: IMPACT 2002+ S: SimaPro 7.3	[59]
		AP-UDE ₂	nitrogen, Ag _(s) (silver source), electricity	M: IMPACT 2002+ S: SimaPro 7.3	[59]
		AP-UDE ₃	nitrogen, Ag _(s) (silver source), electricity	M: IMPACT 2002+ S: SimaPro 7.3	[59]
		AP-MNL	nitrogen, Ag _(s) (silver source), electricity	M: IMPACT 2002+ S: SimaPro 7.3	[59]
	Spark system (Table A14)	Spark-TUD	argon, Ag _(s) (silver source), electricity	M: IMPACT 2002+ S: SimaPro 7.3	[59]
Reactive Magnetron Sputtering (Table A16)	RMS-Ar-N	argon, nitrogen gas, Ag _(s) (silver source), electricity	M: TRACI v2.1 S: SimaPro 8.1	[53]	

Even though there are more LCA studies on AgNPs enabled products found as a result of the literature survey, either the inventories or the conditions of manufacturing AgNPs were not detailed [30, 31, 36, 56]. Therefore, they are excluded from the scope of this study which resulted in evaluation of six different AgNPs synthesis procedures overall. As presented in Table 2, Bafana et al. [28] and Pourzahedi and Eckelman [53] used TRACI 2.1, Walser et al. [58] used ReCiPe, and Slotte and Zevenhoven [59] used IMPACT 2002+ methodology to report LCA results for manufacturing 1 kg AgNPs with different synthesis methods (for reference, impact categories of each methodology are presented in Table A17). Due to these inconsistencies among reporting schemes, cradle-to-gate LCAs for six different methods (with thirteen different approaches) are performed in the current study in order to report LCA results on the same basis.

2.3.3. Industrial scale production

Due to the lack of inventories for large scale ENMs production, predicting potential environmental impacts for industrial scale manufacturing currently relies on theoretical frameworks such as translation of laboratory methods to large scale processes (e.g. switching from heating plates to batch reactors) [70]. Since there is not any advanced material use among the considered inventories in the present study, scaling up for AgNPs production is assumed to contribute to a reduction of the environmental impacts. Piccinno et al. indicated that savings on material and energy by a factor of up to 6.5 per one kg of ENM can be achieved via industrial scale manufacturing [75]. Wu et al. used simplified scaling up factors (SF) in accordance with Piccinno et al. as 2, 4 and 6 [72, 75]. Given that the level of impact reduction due to industrial scale manufacturing (i.e. increased resource efficiency and lower energy consumption compared to laboratory scale synthesis) is not clearly known, using several scaling up factors to project the

potential environmental impacts is helpful. Therefore, the approach applied by Wu et al. is used herein and the results are computed to model the future environmental impacts of manufacturing AgNPs [72]. Additionally, uncertainty analysis for each of the thirteen-synthesis method is conducted using Monte Carlo simulations in SimaPro 8.5.2 in order to estimate the highest and the lowest bounds of environmental impacts. For this evaluation, 95% confidence interval is selected, and analysis is run for 1000 times (Table A18).

As previously mentioned, physical methods are preferred by 43% and chemical methods are preferred by 42% of manufacturers for synthesizing metallic nanoparticles in large scales [51]. Taking into account these percentages and highest and lowest bounds of impacts for each synthesis method, different combinations are created to derive an industry technology mix, and potential environmental impacts of manufacturing AgNPs are projected accordingly.

$$\frac{\text{AgNPs production}}{\text{year}} * \frac{\sum \left[\left(\frac{IC_{min_i} + IC_{med_i} + IC_{max_i}}{3} * 0.42 \right) + \left(\frac{IC_{min_j} + IC_{med_j} + IC_{max_j}}{3} * 0.43 \right) \right]}{\text{number of combinations generated}} \quad (2.1)$$

Eqn (2.1) is used to calculate different combinations of technology mixes for laboratory scale results, where i represents the type of chemical method (five in total), j represents the type of physical method (eight in total) and IC_{min} , IC_{med} and IC_{max} indicate potential environmental impact category results obtained from Monte Carlo simulations. This equation is used for all TRACI 2.1. and CED impact categories. Furthermore, scaling up is performed by dividing the characterization results by the selected factors, and plugging into eqn (2.1). Details on calculations are included in the Appendix A (Table A19-A21).

2.3.4. Prediction of sectoral emissions

In order to predict sectoral emissions due to manufacturing AgNPs, industries where the majority of AgNPs are used are identified. Figure 6 is a compilation of various studies where

disaggregated global AgNPs production per industries are presented. Although the proportions of sectors are not consistent among literature, AgNPs market is still emerging and their utilization may differ between geographies, which make these variations reasonable.

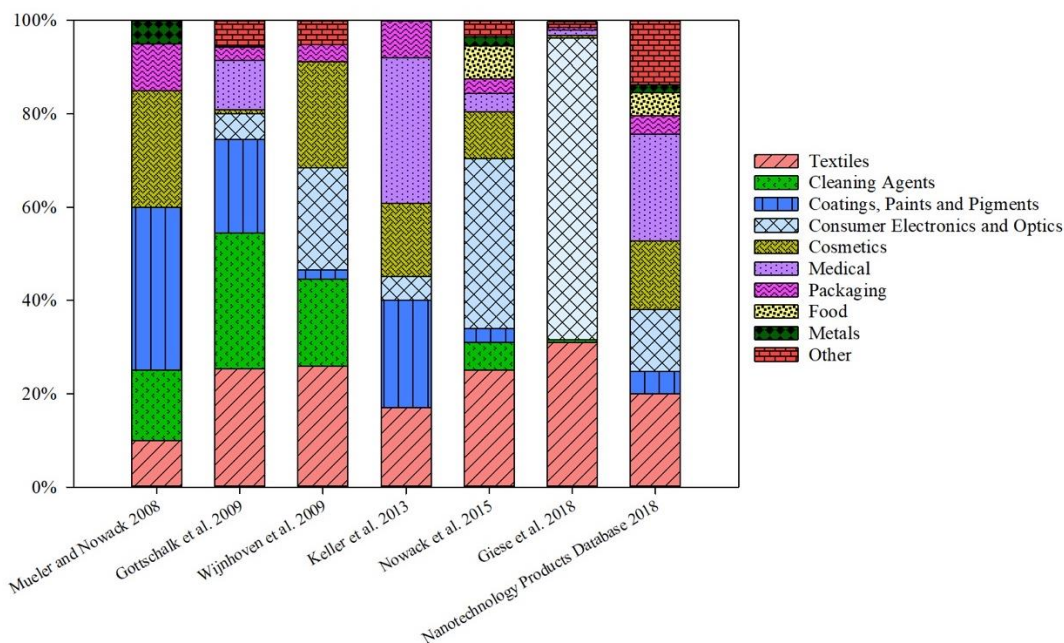


Figure 6. Industry-based estimations for AgNPs-enabled consumer products compiled from the literature [5, 40, 44, 84–87].

Keller et al. provided a global framework by distributing the total annual production of AgNPs among their largest consumers as medical (31%); coating, paints and pigments (23%); textiles (17%); cosmetics (16%); packaging (8%) and consumer electronics and optics (5%) industries [5]. Other references cited in Figure 6 used surveys [84], simulations [44, 85] or commercial reports [40, 86, 87] to provide industrial shares. Since Keller et al. categorized industries assuming maximum AgNPs production by mass (e.g. 141 tons of AgNPs used for the medical industry when the total AgNPs production was 452 tons) rather than the number of

commercial products in the market, further calculations on industry-based projections are created based on this reference [5].

Each industry may require different synthesis methods in order to have certain morphologies or surface chemistries of AgNPs to be incorporated to their products. The synthesis methods considered in this study and their industrial uses are tabulated along with synthesis yield, size range and surface area of the AgNPs synthesized, known applications and references in Table A22. In summary, the textile industry mostly uses CR, FSP-MS, AP and Spark; electronics and optics industry uses AP and RMS-Ar-N; cosmetics industry uses MW and medical industry uses MW, CR and RMS-Ar-N methods to make AgNPs in order to be incorporated to their products. There are not any designated AgNPs synthesis methods found for coatings, paints and pigments and packaging industries. Eqn (2.2) gives industry-based annual GWP for skeptical production estimations in tons CO₂-eq./year, where industrial proportions are extracted from Keller et al. [5], *i* represents the respective AgNPs synthesis method used for that industry and *n* represents the number of methods applied for that industry. This equation is used for calculating impacts of all TRACI 2.1 potential environmental impact categories with skeptical and optimistic estimations.

$$\sum_i^n \frac{\text{industrial proportions} * \frac{\text{skeptical AgNPs production}}{\text{year}}}{n} * GWP_i \left(\text{in } \frac{\text{kg CO}_2 - \text{eq.}}{\text{kg AgNPs}} \right) \quad (2.2)$$

If there are not any specific methods reported per industrial use, all of the thirteen methods are included in the analysis, which is the case for coatings, paints and pigments and packaging industries only. AgNPs synthesis methods are considered as equally preferable and estimated global impacts are calculated by using Laplace criterion. Laplace criterion is a method that treats different options as equally likely, if the likelihoods of these options are not known

[88]. Besides calculating the global impact projections based on LCA results obtained in the current study, large scale global impacts per sectors are also calculated by using the aforementioned scaling up approach.

2.4. Results and discussion

2.4.1 Life cycle impact assessment comparison

Evaluation of the different synthesis routes is performed, and characterization results are presented in Figure 7, by involving the impact categories from TRACI 2.1 and CED (results are provided in Tables A23-A24). Given that CR and AP methods are included along with different inventories (e.g. CR-TSC, CR-SB; AP-UDE, AP-MNL etc.) in the present study, average results are presented for each general technique, which result in the assessment of six different groups. Error bars on both CR and AP represent standard deviations of impacts resulting from the inclusion of different inventories. Since there are single inventories considered for MW, FSP-MS, Spark and RMS-Ar-N methods, they do not have error bars. Based on a mass-based functional unit, the environmental impacts of synthesis methods follow the general trend of $\text{RMS-Ar-N} < \text{MW} < \text{AP} < \text{CR} < \text{Spark} < \text{FSP-MS}$ with some exceptions discussed herein (Table A28).

Considering the wet chemistry methods, microwave synthesis does not express higher impacts in any of the potential environmental impact categories except ODP and AP, compared to CR. The higher impacts in these two categories are mainly due to the electricity consumption during microwave utilization. Since chemical reduction methods require several chemicals as reducing and stabilizing agents, they increase life cycle environmental impacts of manufacturing. Among CR methods, CR-SB is found to be the least environmentally impactful route due to

showing the lowest impacts for all impact categories considered. Furthermore, CR-starch has the highest impacts across AP, EP, HHNCP and ETP. According to Pourzahedi and Eckelman the reason that this method has the greatest contribution in these categories is the use of trichloromethane in pesticides and the use of fertilizers for potatoes to manufacture starch [38]. In terms of GWP and ODP, CR-TSC has the largest impact since the synthesis is performed at high temperatures for heating which results in higher emissions. With regard to FFP, SP, HHCP, RP and CED, CR-EG performs the highest impact due to the use of a fossil-fuel based raw materials [53]. Midpoint LCA results for AgNPs production with wet chemistry methods are presented in Figure A1 in order to provide details on process contributions.

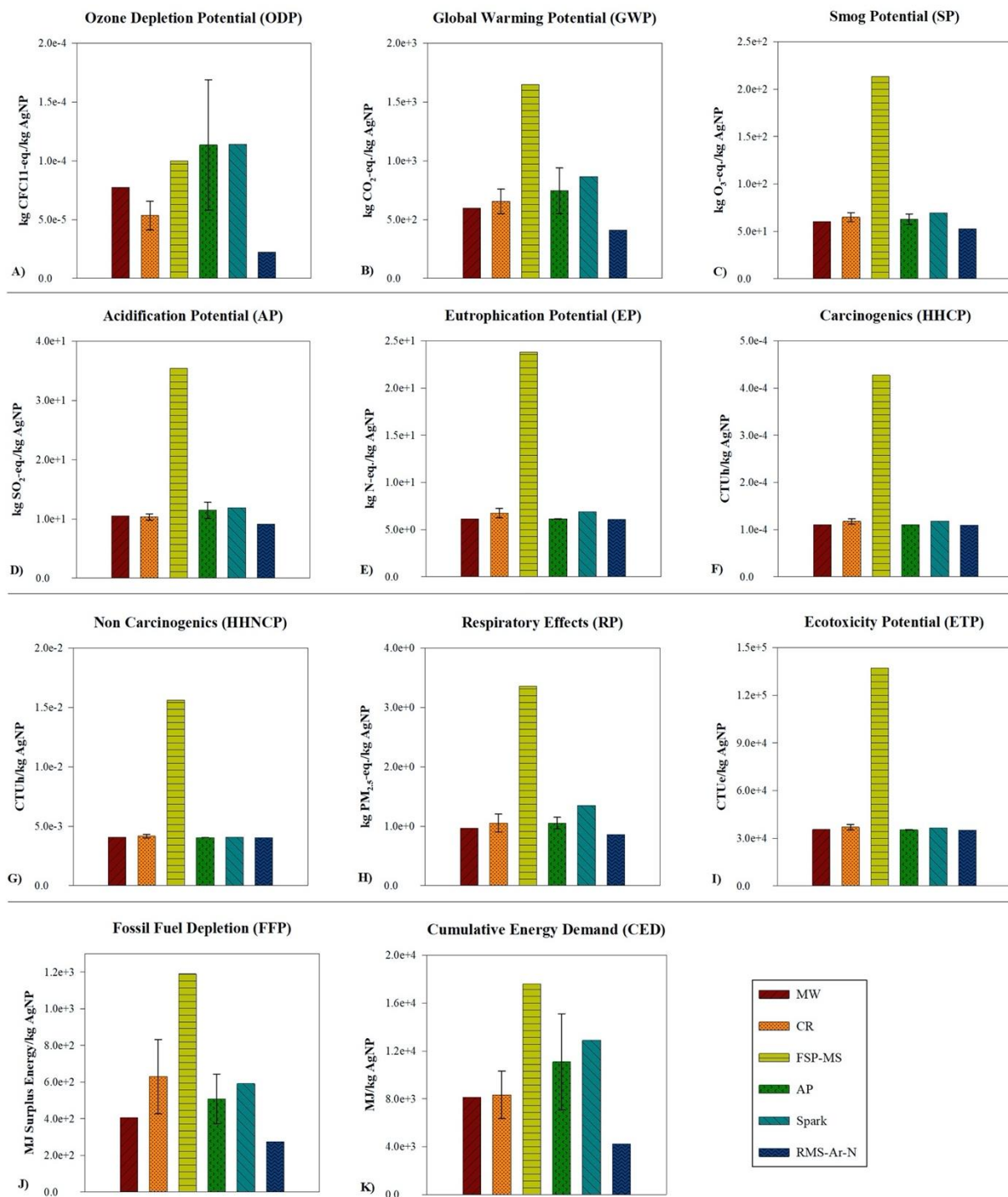


Figure 7. Environmental impacts of multiple synthesis routes for 1 kg AgNPs, using multiple impact categories as A) ODP, B) GWP, C) SP, D) AP, E) EP, F) HHCP, G) HHNCP, H) RP, I) ETP, J) FFP and K) CED.

Taking into account the physical chemistry methods, RMS-Ar-N has the lowest environmental impact across all impact categories due to low amount of chemicals and electricity inputs associated with synthesis. While material and energy inputs of AP and Spark methods are similar, their life cycle impacts differ due to varied energy delivery techniques. In general, AP performs lower environmental performance than spark method. Spark method does not express the highest impact in any category except ODP, which may be attributed to its relatively low material requirement. The higher impact in ODP is due to the high amount of electricity need to supply the energy with varying frequencies to the spark system. Among AP methods, while AP-UDE3 has the highest environmental impacts in all categories except ETP and HHCP resulting from the silver acquisition process, AP is found to be the least environmentally impactful method by having least impacts on every impact category. Finally, FSP-MS has the highest impacts across all potential environmental impact categories with the exception of ODP. These relatively high impacts are largely due to the use of silver-octanoate as a precursor because 1.7 kg of silver is needed to produce 1 kg of silver-octanoate. Details on process contributions to produce 1 kg of AgNPs with physical chemistry methods are presented in Figure A2.

2.4.2. Implications of scaling up

Considering the skeptical and optimistic AgNPs production estimations from 2018 to 2025 and using eqn (2.1), annual environmental impacts based on TRACI 2.1. and CED are projected. Global overall predicted CO₂-eq. emissions due to AgNPs manufacturing in 2018 is calculated as $1.20\text{E}+05 \pm 2.88\text{E}+04$ tons CO₂-eq. for skeptical estimations, and $3.03\text{E}+05 \pm 7.26\text{E}+04$ tons CO₂-eq. for optimistic estimations, before implementing scale-up approach.

Literature suggest that scaling up the manufacturing process from laboratory scale to industrial scale helps to save considerable amount of materials and energy, and therefore contributes to sustainable production and resource conservation concepts [72, 73, 75, 89, 90]. With the assumed scaling up factors, $1.52\text{E}+04 - 7.44\text{E}+04$ tons of $\text{CO}_2\text{-eq.}$ is emitted as a result of AgNPs production in 2018, and these are projected to increase more than 2.5 times until 2025. According to Gilbertson et al., primary life cycle impact indicators of interest due to raw materials acquisition and manufacturing phases of AgNPs are GWP and FFP [12]. Therefore, only GWP (tons $\text{CO}_2\text{-eq./year}$) and FFP (MJ surplus energy/year) are presented in Figure 8, while projected impact results for all impact categories are included in the Appendix A (Figures A3-A13 and Tables A29-A39).

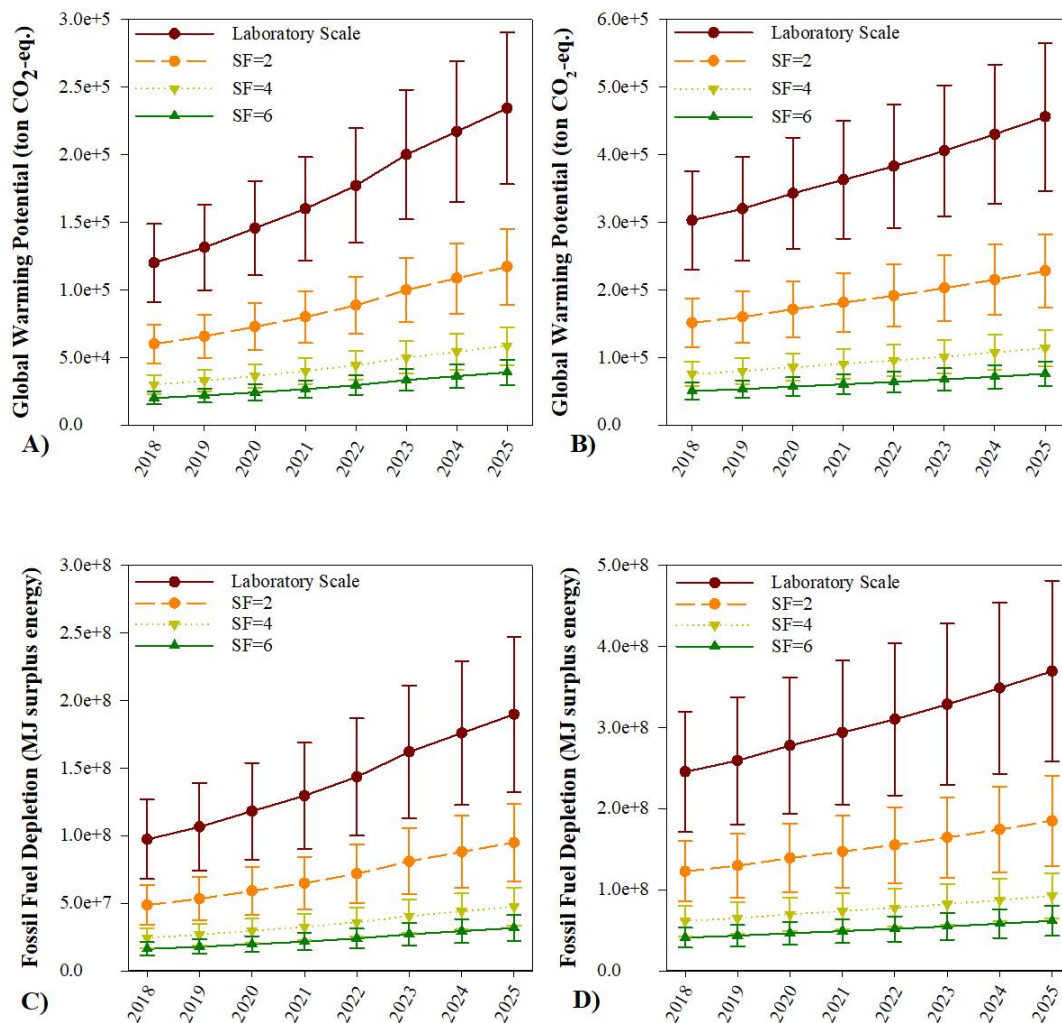


Figure 8. Global annual environmental impacts using different scale-up factors (2, 4 and 6) as well as laboratory scale results for A) GWP (tons CO₂-eq./year) with skeptical B) GWP (tons CO₂-eq./year) with optimistic C) FFP (MJ surplus energy/year) with skeptical, D) FFP (MJ surplus energy/year) with optimistic production volumes. Error bars represent 95% confidence intervals for the uncertainties modeled by Monte Carlo simulations.

In order to compare these numbers with industrial analogies, aluminum production industry is selected. According to the US Greenhouse Gas Inventory, the US aluminum

production industry emitted $1.30\text{E}+06$ of tons of CO₂-eq. emissions in 2016 [91]. With respect to AgNPs, the CO₂-eq. emissions of laboratory scale synthesis for optimistic estimations accounts for 29% of the emissions resulting from the US aluminum production industry. Despite industrial scale processes offering lower materials and energy consumption, the amount of emissions generated is still significant and needs further optimization.

2.4.3. Sectoral environmental impacts

In order to project the environmental performance of the sectors where AgNPs are used the most, Sankey diagrams are developed for each impact category to better illustrate the follows of impact. Figure 9 shows sectoral GWP (in tons CO₂-eq.) and FFP (in MJ surplus energy) per laboratory scale (Figure 9A, B, E, F) and large-scale manufacturing (Figure 9C, D, G, H) of AgNPs. SF = 6 is included in the figure as it shows the highest factor considered and thus resulting in the lowest environmental impact. Sankey diagrams for the remainder of the environmental impact categories are included in the Appendix A (Figures A14-A24) along with example calculations and additional explanations.

As some synthesis methods are more environmentally impactful than others, industry-based impacts are not exactly proportional with the industrial shares and each environmental impact category has a different trend. Accordingly, the proportions of impacts are different for each industry. As presented in Figure 9, although the industrial proportions of medical and coating industries vary 8%, their GWPs differ 5% and FFPs differ 10%. One interesting finding was that ODP resulting from the medical industry is 13% lower than the coating industry, even though the share of medical industry is higher than the coating industry. Furthermore, although textiles and cosmetics have similar industrial shares (i.e. the difference is 1%), the difference

between their GWPs is 41%, and FFP is 46%. The variation of the potential environmental impacts of textiles and cosmetics industries is ranging from 32 to 39% for all impact categories except HHCP, which is found as 11%. A drastic change is observed between packaging and electronics and optics industries. There is a 3% difference in the shares of these two sectors; however, GWP resulting from packaging industry is 94% higher than electronics and optics industry, and the rest of the impact categories differ by 29–66%.

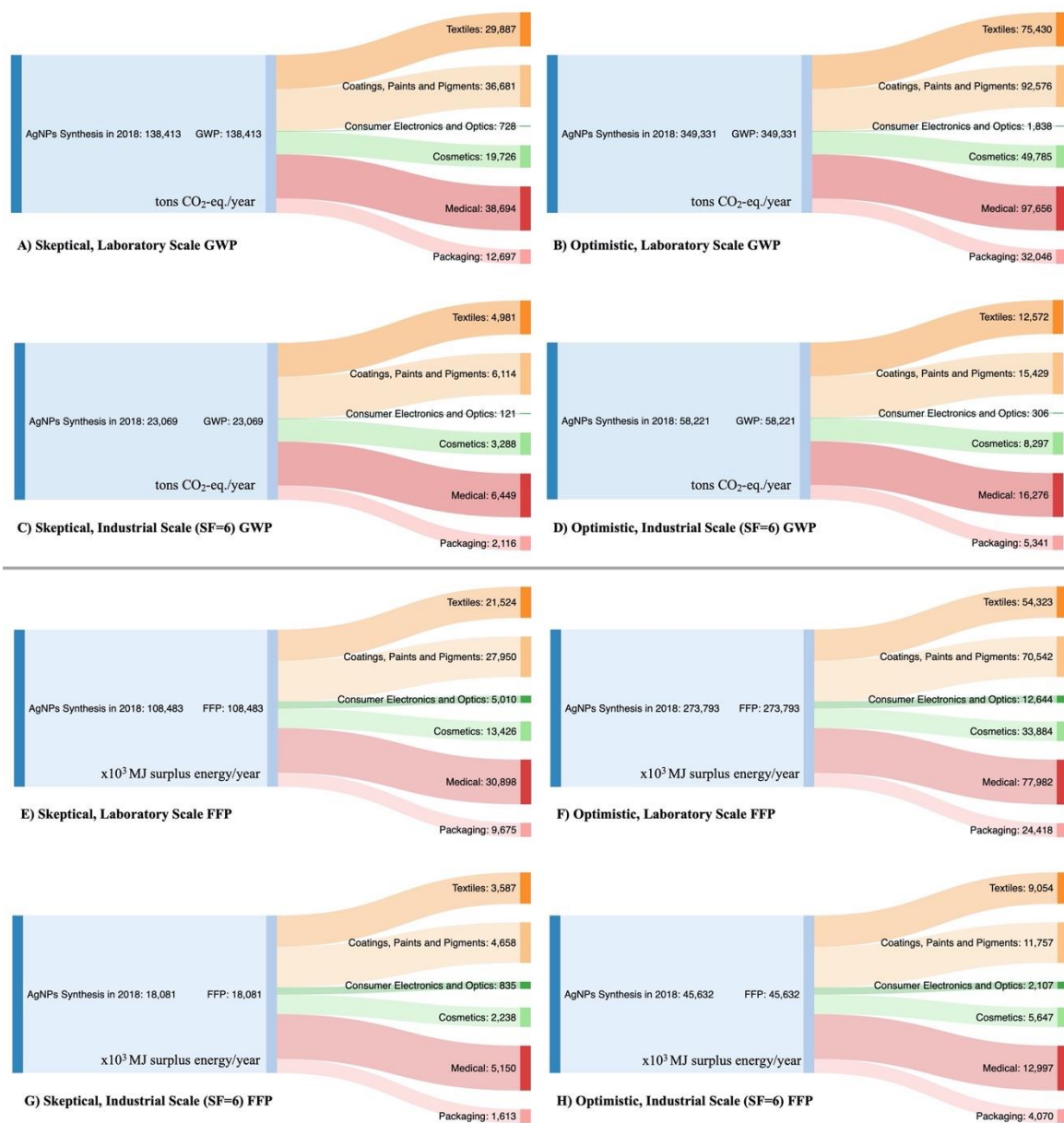


Figure 9. Sankey diagrams for industry-based emissions in 2018 A) GWP with skeptical estimations and laboratory scale, B) GWP with optimistic estimations and laboratory scale, C) GWP with skeptical estimations and SF = 6, D) GWP with optimistic estimations and SF = 6, E) FFP with skeptical estimations and laboratory scale, F) FFP with optimistic estimations and laboratory scale, G) FFP with skeptical estimations and SF = 6, and H) FFP with optimistic estimations and SF = 6.

Currently, there is not a clear consensus on the AgNPs synthesis methods for specific industries [92, 93]. Meanwhile, it was shown that synthesis methods of AgNPs directly affect the environmental implications of nano-enabled products [36, 38]. The results from the current study suggest that the life cycle impacts of ENMs manufacturing is a factor of desired product application. These diagrams may be used as initial models which quantify and disaggregate the cradle-to-gate environmental impacts associated with the manufacturing of AgNPs for different industries. Moreover, they contribute to monitoring industrial emissions of AgNPs, which then may be combined with the release patterns to present cradle-to-grave environmental impacts and create broader evaluations.

2.5. Conclusions

As supported by commercial market reports and scientific literature, AgNP production is forecasted to increase in the coming decades. On a mass basis, FSP-MS is found to be the most environmentally impactful method, while RMS-Ar-N is found to be the least impactful route. This work suggests that the synthesis method utilized for the AgNP has potentially to greatly influence the global environmental impact of the future production of this ENM. Besides laboratory scale LCA results, the environmental impact of industrial scale manufacturing is projected by using simplified scale-up factors. Results showed that scaling up approach helps reducing up to 90% of environmental emissions. Although a significant decrease in the environmental impact is identified by large scale synthesis, several other factors such as the cost, product quality, required equipment etc. are also needed to be considered for a holistic sustainability assessment and process optimization. Additionally, disaggregated global projections are created based on different industrial applications. It is found that industry-based

impacts are not exactly proportional with their popularities since industries prefer to use different method combinations to achieve desired AgNPs characteristics. ENMs also confer additional benefits depending on the properties, such as less frequent laundering of textiles due to their antibacterial properties or rapid wound healing due to bandages. Future work should investigate the environmental and health benefits of AgNPs in different applications and provide guidance as to the anticipated environmental tradeoffs of new AgNPs incorporated consumer products. Finally, it is important to note that, although LCAs can pinpoint the hotspots for the overall system, most of the literature excluded the nano-specific impacts from the release and exposure phases of nano-enabled products. This is mainly due to the lack of ENMs specific characterization factors as well as various ENMs speciation and particle formation patterns. In order to improve future LCAs and model cradle-to-grave impacts, development of nano-specific characterization factors is critical.

2.6. Acknowledgements

This work is supported by the Wisconsin Alumni Research Foundation (WARF). We would like to thank the anonymous reviewers for their time and insightful comments. This work has not been formally reviewed by the WARF, and the findings of the authors are their own.

3. Global scale life cycle environmental impacts of single- and multi-walled carbon nanotube synthesis processes

The following chapter has been submitted for consideration for publication with the citation:

Temizel-Sekeryan, S.; Wu, F.; Hicks, A.L., Global scale life cycle environmental impacts of single- and multi-walled carbon nanotube synthesis processes.

The article appears as submitted, although style and formatting modifications have been made.

Authorship contribution statement

Sila Temizel-Sekeryan: Designed Research, Performed Research, Analyzed Data, Wrote the Paper.

Fan Wu: Contributed Reagents or Analytical Tools.

Andrea L. Hicks: Designed Research, Wrote the Paper.

3.1. Abstract

3.1.1. Purpose

Carbon nanotubes (CNTs) are well known for their mechanical resistance, durability and flexibility, which make them preferable for a wide variety of applications. The global production volume of CNTs is expected to reach 7,000 tons by 2025. This work performs cradle-to-gate life cycle assessments (LCAs) of industrially preferred single- and multi-walled CNTs synthesis processes. The aim is to evaluate global environmental impacts associated with raw materials acquisition and manufacturing and identify hotspots in CNTs production.

3.1.2. Methods

Eight single-walled and seven multi-walled CNTs synthesis processes are evaluated using LCA. A mass based functional unit is selected as 1 kilogram of CNTs produced, and LCAs are conducted using SimaPro 8.5.2 Software with Tool for Reduction and Assessment of Chemicals and Other Environmental Impacts (TRACI 2.1) and Cumulative Energy Demand (CED) impact categories. It is expected that industrial scale production provides significant material and energy savings as well as reduces environmental impacts per unit mass of the product, due to the use of efficient equipment and recycling of reagents. Therefore, hypothetical scaling up scenarios are applied in order to estimate associated impacts. Lastly, industry-based impact projections are developed for industries where the majority of CNTs are used using the Laplace criterion.

3.1.3. Results and discussion

The results showed that chemical vapor deposition is the most impactful route for manufacturing single- and multi-walled CNTs. Whereas, high pressure carbon monoxide route

for producing single-walled CNTs, and arc discharge route for manufacturing multi-walled CNTs are found to be the least environmentally impactful techniques among different processes considered. Results indicate that the preference of synthesis process dominates the overall environmental cost of the CNTs as well as CNTs-enabled products. Additionally, using different scaling up scenarios, it is projected that the environmental emissions associated with producing CNTs may be reduced up to 88% globally. As industries use particular routes to synthesize the CNTs to be embedded in their products, it is found that the sectoral environmental impacts are not proportional with the industrial shares.

3.1.4. Conclusions

CNTs offer technological advances to conventional products (i.e. heated jacket). However, thinking from a global scale, manufacturing CNTs has significant environmental impacts. This study provides segmented impact projections for industries, which then may be used to inform sectoral cradle-to-grave environmental impacts as a function of manufacturing processes. Based on the desired characteristics of produced CNTs (e.g. diameter, surface area), manufacturing CNTs with environmentally responsible production routes may help decreasing global environmental impacts significantly.

3.2. Introduction

Carbon nanotubes (CNTs) are one of the top produced engineered nanomaterials (ENM) with more than a 26% market share of the overall nanomaterials industry [11]. CNTs are strong, light, efficient, flexible, wearable; and have high thermal and electronic conductivity, high density and large surface area [94–97]. Due to their electrical, thermal and mechanical properties, CNTs are used in the supercapacitors, photovoltaic devices, transparent and electrical electrodes, lithium ion batteries, computer and memory chips, conducting composites/films, organic light-emitting diodes, food packaging materials, drug delivery systems, energy and hydrogen storage, scanning probes and different types of sensors, among other applications [5, 94, 97–99]. Figure 10 presents the forecasted global CNT production volumes and potential demand in tons, based on multiple studies [1, 45, 100–103] and commercial reports [104–106]. Although there is a great diversity among the estimations, the production volume is indicated to increase overall. This growing trend is supported by different market reports as well, where the market size of CNTs industry was valued \$1 billion in 2014, \$3.95 billion in 2017, \$4.55 billion in 2018 and it is expected to reach \$9.84 billion by 2023 and \$15.02 billion by 2026 [107–110]. Besides the global mass production, the number of patents issued by the United States Patent and Trademark Office (USPTO) may be a good indicator for the growth rate of CNTs. Figure B1 in Appendix B presents both the number of patents issued per year and a cumulative number of patents issued until 2019. The first patent was issued in 1999 and the number of patents has been increasing drastically since then (cumulative number was 2,957 in 2019) [111].

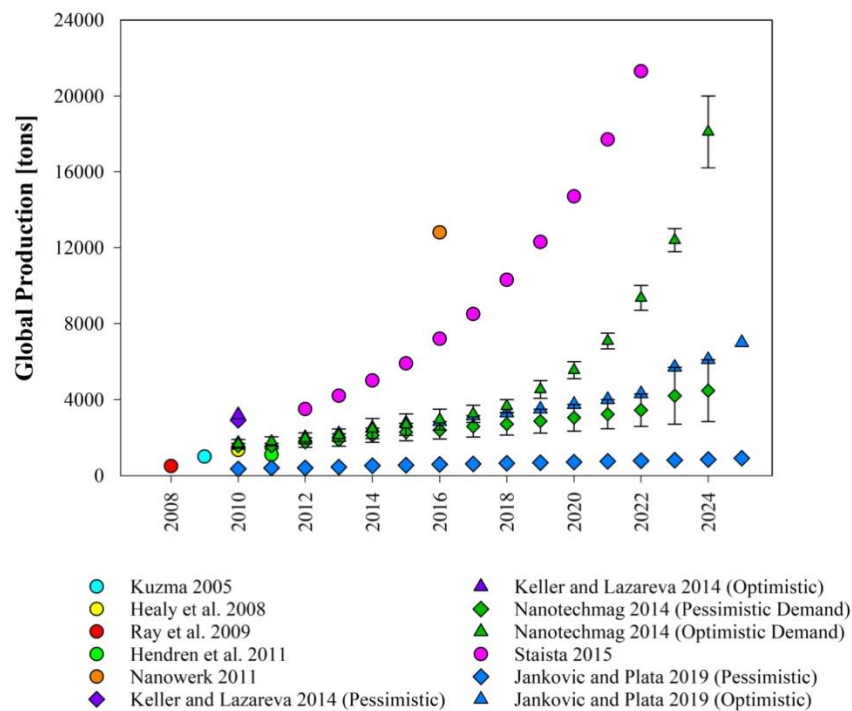


Figure 10. Global market (in tons) for carbon nanotubes (CNTs) where diamond markers indicate pessimistic estimations, circle markers indicate single estimations, triangle markers indicate optimistic estimations and error bars indicate the potential range for the respective estimation [1, 45, 100–106].

Although production quantities of CNTs is given on a mass basis without a distinction between single-walled (SW-) or multi-walled (MW-) in Figure 10, Borm et al. predicted the proportion as 20% SWCNTs and 80% MWCNTs [112]. Findings from Pulidindi and Pandey [113] and Ghaffarzadeh [114] also support this share by indicating that MWCNTs are the dominant form in the market.

MWCNTs and SWCNTs can be synthesized using a wide variety of vapor phase techniques including chemical vapor deposition (CVD), arc process (AP), laser vaporization (LV), high-pressure carbon monoxide reaction (HiPCO), cobalt-molybdenum catalytic process

(CoMoCat) and flame synthesis among others [51, 115–117]. It should be noted that manufacturing of SWCNTs is more difficult, environmentally impactful and expensive compared to MWCNTs due to requiring an additional purification step in order to achieve high yields [96, 114, 115, 118]. There are several routes for purification such as oxidation, acid treatment, annealing, sonication and filtering chemical functionalization [94]. For reference, Roes et al. found that the energy used to produce MWCNTs are approximately 10% of the energy used to produce SWCNTs [119].

The environmental impacts of CNTs-enabled products as well as manufacturing CNTs have been previously investigated using life cycle assessment (LCA). LCA is a tool to evaluate environmental performances of products throughout their life cycle by quantifying all inputs, outputs and associated wastes for the four stages of life including raw materials acquisition, manufacturing, use and end of life [15]. Various scopes, system boundaries and methods have been used among the LCA literature, which challenges having a standardized information to interpret and compare the impact assessment results. As a result of the preliminary literature review on previously applied LCAs for CNTs enabled products and/or manufacturing CNTs, 28 studies are identified in total, in which the majority of them involved SWCNTs (16 out of 28). It is also found that various impact assessment methods were used including CED, CML 2001, EPS 2000, Eco Indicator 99, TRACI, ReCiPe, IPCC and NREL. The system boundaries considered dominantly consisted of cradle-to-gate scopes (20 out of 28). Finally, in terms of scale, 22 studies were based on laboratory scale research, 1 was based on small-scale production, 2 were based on pilot-scale production and 3 were based on large-scale production. A comprehensive table that includes detailed information may be found in Appendix B as Table B1.

Rapid development of the CNTs sector has encouraged industries to scale up current production to achieve more efficient results such as lower costs, lower impacts on the environment and higher synthesis yields [103, 120–122]. Laboratory scale LCA results may help comparing different alternatives used for the same purpose and also identifying the energy and material intensive processes [123]. However, they may not be representative for large scale synthesis because laboratory scale experiments are not in a form of continuous flow and are independent [70, 71, 124]. For instance, Gavankar et al. stated that scaling up the manufacturing process of SWCNTs from small scale to large scale could reduce up to 94% of the cradle-to-gate impacts due to the profitability of recycled feedstock [77]. Another study suggested that, scaling up the production process from grams/kilograms to tons may decrease the energy consumption by 1-2 orders of magnitude [125]. Research argued that, due to the lack of actual empirical data to create inventories for industrial scale production, utilization of theoretical scaling up factors and linearly extrapolating the results is the current strategy among literature [71, 72, 126].

The goal of this study is to project the cradle-to-gate global environmental impacts of producing CNTs (both for SWCNT and MWCNT) with multiple synthesis processes using LCA. Detailed environmental assessments of different synthesis processes are presented in order to investigate the trends of impacts and to identify hotspots. Given the forecasted increase in CNTs mass production, analyzing environmental impacts resulting from the large scale manufacturing would be more appropriate. Therefore, global environmental impacts of large scale production are also projected using different scaling up scenarios, and environmental impact savings are calculated accordingly. Finally, by using industry-based estimations, sectoral global environmental impacts resulting from industries that use CNTs are also projected. The results

help to quantify the future environmental impacts associated with manufacturing CNTs (with a disaggregation of SWCNTs and MWCNTs) at a global scale.

3.3. Materials and methods

3.3.1. Goal and scope definition

In the current study, eight different SWCNTs and seven different MWCNTs synthesis processes are evaluated using attributional LCA with a cradle-to-gate system boundary. Environmental impacts are modeled using the SimaPro 8.5.2 software with Ecoinvent 3 and USLCI (U.S. Life Cycle Inventory) databases. TRACI 2.1 (tool for the reduction and assessment of chemical and other environmental impacts) and Cumulative Energy Demand (CED) are used as impact assessment methods. Impact categories, along with their units and abbreviations based on TRACI 2.1 are ozone depletion (OD in kg CFC11-eq.), global warming (GW in kg CO₂-eq.), smog (PS in kg O₃-eq.), acidification (AC in kg SO₂-eq.), eutrophication (EU in kg N-eq.), carcinogenics (HHC in CTUh), non-carcinogenics (HHNC in CTUh), respiratory effects (RE in kg PM_{2.5}-eq.), ecotoxicity (EC in CTUe), and fossil fuel depletion (FF in MJ surplus energy). The functional unit, in other words a reference unit which helps quantifying performance of a system, is selected as 1 kilogram (kg) of CNT (single-walled or multi-walled) produced. The selected functional unit is compatible with the global production estimates and will be used to project future global environmental impacts of manufacturing CNTs. System boundaries considered in this study are presented in Figure 11, where solid lines indicate included processes and dashed lines indicate excluded processes.

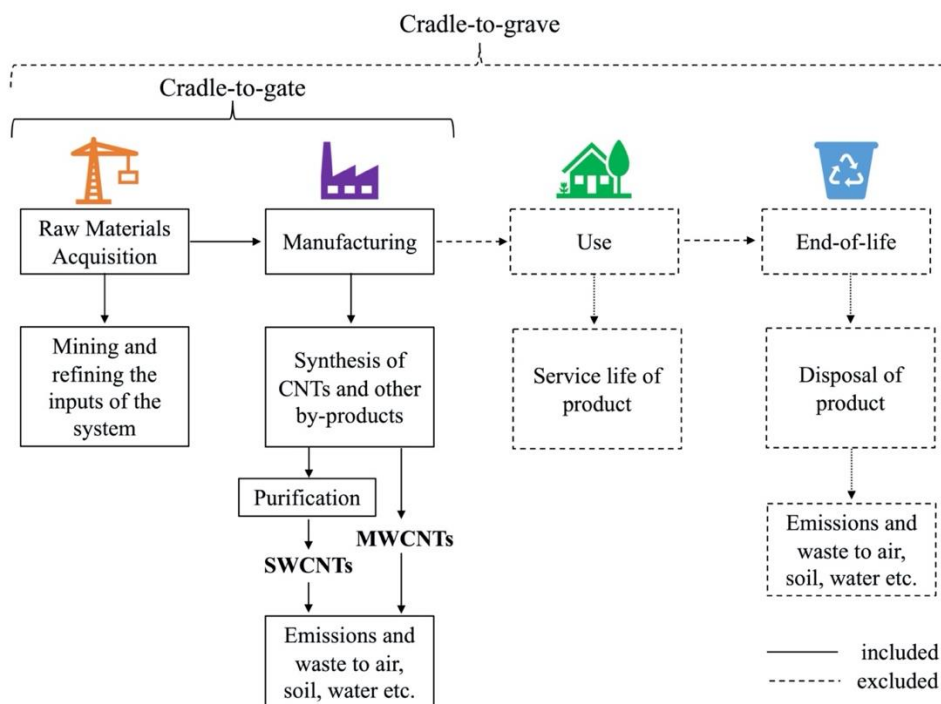


Figure 11. System boundaries considered in the current study.

According to Upadhyayula et al., there are several uncertainties regarding the use and end-of-life phases of CNT incorporated products [99]. These include unknown environmental burdens and potential consequences of exposure and toxicity, and unclear fate and transport patterns. In order to quantify direct (i.e. nano-specific) impacts resulting from CNTs release, several studies calculated ecotoxicity and human health characterization factors (CF). For freshwater ecotoxicity impacts, Eckelman et al. found a CF range of $3.7 \times 10^3 - 2.9 \times 10^4$ CTUe/kg SWCNT [127]; Rodriguez-Garcia et al. shared CFs of 1.2×10^{-1} CTUe/kg SWCNT and 7.4×10^2 CTUe/kg MWCNT [128]; Deng et al. calculated a CF of 6.78×10^4 CTUe/kg CNT [26]; and Garvey et al. reported a CF range of $2.6 \times 10^3 - 4.1 \times 10^4$ CTUe/kg SWCNT [69]. For human health non-cancer impacts, Rodriguez-Garcia et al. found CFs of 2.4×10^{-4} CTUh/kg SWCNT and 1.67×10^{-3} CTUh/kg MWCNT [128]. Eckelman et al. further suggested that the ecotoxicity

impacts of producing CNTs are significantly higher than the impacts resulting from their release [127]. CNTs also have very low solubility and they rapidly reach to the sediment phase after release, which decreases the exposure time for freshwater organisms [129, 130]. Therefore, during the use and end-of-life, their impacts on the environment are probably relatively low compared to raw materials acquisition and production stages. With regard to cradle-to-grave impacts of CNTs-enabled products, Parsons et al. conducted a contribution analysis where the percentage contribution of CNT synthesis on the total impact of a product was reported as more than 92% in all environmental impact categories [131]. Moreover, cradle-to-gate studies are useful to investigate hotspots of the production processes and can be used in LCAs that are conducted for specific products containing the CNTs [132]. These considerations make the system boundaries selected in the current study acceptable. Further discussion about direct and indirect impacts are included in the subsequent sections.

3.3.2. Synthesis procedures

In order to collect different inventories for CNTs production processes, a comprehensive literature survey is conducted by using an academic search engine, Web of Science Core Collection, by searching combinations of key terms including carbon nanotube, CNTs, SWCNTs, MWCNTs, sustainability, life cycle assessment, environmental impact assessment and CNTs-enabled. From this search, eleven studies were selected for inclusion in the current study because they either provided the inventories in different scales or disclosed the synthesis conditions for producing SWCNTs/MWCNTs. Table 3 (for SWCNTs) and Table 4 (for MWCNTs) provide summaries of the considered processes, where scale, input parameters, reactor type, batch size, purity and yield information are specified for each in order to distinguish

different inventories of the same route. Inventories for these processes can be found in the Appendix B (Tables B2-B17).

As mentioned, only studies that shared their inventories and process conditions to synthesize CNTs are considered, which resulted evaluation of five different processes including CVD, HiPCO, CoMoCat, AP and LV. Due to the utilization of varying impact methods (e.g. ReCiPe, TRACI, CML, CED) by the previously published LCAs as presented in Table 3 and Table 4, the environmental impact categories of these studies are inconsistent (for reference, impact categories of each method are presented in Table B18). In order to report the results on the same basis, data from these five studies were used to conduct five cradle-to-gate LCAs (with fifteen separate routes) in the current study.

Table 3. Summary of SWCNTs (S-) synthesis processes used in the current study.

Process	Abbreviation	Scale	LCA Method	Input parameters	Reactor Type	Batch size	Purity ^a / Yield ^b	LCI source
Chemical Vapor Deposition	S-CVD1 (Table B2)	Laboratory	N/A	Feedstock: CH ₄ Catalysts: NH ₄ ⁺ , Mg, Co, citric acid Carrier gas: H ₂ , Ar Temperature: 1000°C	two furnaces with a quartz tube passing through them	8 mg/h	Purity: 90% Yield: 2.95% (optimized 20%)	[100]
	S-CVD2 (Table B3)	Laboratory	CED and CML 2001	Feedstock: C ₂ H ₂ Catalysts: Ni Carrier gas: H ₂ , Ar Temperature: 400-600°C	thermal reactor (CNTs are directly produced on a substrate surface with three metal layers)	N/A	Purity: N/A Yield: 20%	[98, 133]
High-Pressure Carbon Monoxide Reaction	S-HiPCO1 (Table B4)	Laboratory	N/A	Feedstock: CO Catalysts: Fe(CO) ₅ , CO Carrier gas: Ar Temperature: 900-1100°C	customized vessel (quartz tube in an aluminum cylinder surrounded by an electrical heating element)	0.45 g/h	Purity: 90% Yield: 0.08% (optimized 46%)	[100]
	S-HiPCO2* (Table B5)	Large	TRACI (unspecified version)	Feedstock: CO Catalysts: Fe(CO) ₅ , CO Carrier gas: - Temperature: 1000-1200°C	high pressure plug-flow reactor	595 kg/h	Purity: 97% Yield: 90%	[133, 134]
Cobalt-Molybdenum Catalytic Process	S-CoMoCat1 (Table B6)	Laboratory	TRACI 2.1	Feedstock: CO Catalysts: Co-Mo Carrier gas: - Temperature: 700-950°C	fluidized bed catalytic reactor	N/A	Purity: <i>sufficient</i> Yield: 28%	[135]
	S-CoMoCat2* (Table B7)	Large	TRACI (unspecified version)	Feedstock: CO Catalysts: Co-Mo Carrier gas: - Temperature: 700-950°C	fluidized bed catalytic reactor	595 kg/h	Purity: 97% Yield: 80%	[133, 134]
Arc Process	S-AP (Table B8)	Laboratory	N/A	Feedstock: graphite Catalysts: Fe, Y, S, C powder Carrier gas: He Temperature: N/A	water cooled cylindrical stainless-steel chamber with graphite rods	34 mg/h	Purity: 70% Yield: 4.5% (optimized 20%)	[100]
Laser Vaporization	S-LV (Table B9)	Laboratory	CED	Feedstock: graphite Catalysts: Co, Ni Carrier gas: Ar Temperature: 1150°C	one zone high temperature furnace	100 mg/h	Purity: 30% Yield: N/A	[136]

^a Purity represents the percentage of SWCNTs extracted from the final product as a result of synthesis process.

^b Yield represents the ratio of the final product to the total amount of carbon entering the process (i.e. feedstock).

N/A: not specified.

Table 4. Summary of MWCNTs (M-) synthesis processes used in the current study.

Process	Abbreviation	Scale	LCA Method	Input parameters	Reactor Type	Batch size	Purity ^a / Yield ^b	LCI source
Chemical Vapor Deposition	M-CVD1 (Table B10)	Laboratory	synthesis paper, not an LCA study	Feedstock: C ₂ H ₂ Catalysts: LaCoO ₃ Carrier gas: N ₂ Temperature: 675-700°C	fluidized bed catalytic reactor	22 g/h	Purity: 96% Yield: N/A	[137]
	M-CVD2 (Table B11)	Laboratory	synthesis paper, not an LCA study	Feedstock: C ₂ H ₂ Catalysts: Fe ₂ O ₃ /MgO Carrier gas: Ar Temperature: 500-650°C	fluidized bed (quartz glass tube and vertical furnace)	62.5 mg/h	Purity: N/A Yield: up to 35%	[138]
	M-CVD3 (Table B13)	Laboratory	ReCiPe (unspecified version)	Feedstock: Toluene Catalysts: Ferrocene Carrier gas: Ar Temperature: 790°C	horizontal three zone tube furnace	20 mg/h	Purity: 99% Yield: 50%	[139]
	M-CVD4 (Table B14)	Laboratory	ReCiPe (H)	Feedstock: Camphor Catalysts: Ferrocene Carrier gas: N ₂ Temperature: 850°C	thermal reactor (horizontal quartz tube housed in a three-zone cylindrical furnace)	0.625 g/h	Purity: 87.6% Yield: 5-7%	[140]
	M-CVD5 (Table B15)	Laboratory	ReCiPe (H)	Feedstock: C ₂ H ₂ Catalysts: Fe ₂ O ₃ /zeolite Carrier gas: N ₂ Temperature: 700°C	thermal reactor (horizontal quartz tube housed in a three-zone cylindrical furnace)	0.9 g/h	Purity: 92.8% Yield: >50%	[140]
	M-CVD6 [*] (Table B16)	Large	synthesis paper, not an LCA study	Feedstock: C ₆ H ₆ Catalysts: Ferrocene Carrier gas: H ₂ Temperature: 1200°C	horizontal tubular reactor made of quartz tube	20 g/h	Purity: N/A Yield: 86%	[141]
Arc Process	M-AP (Table B17)	Laboratory	synthesis paper, not an LCA study	Feedstock: graphite Catalysts: - Carrier gas: N ₂ Temperature: N/A	liquid-nitrogen reaction chamber	82 g/h	Purity: <i>high</i> Yield: <i>high</i>	[142]

^a Purity represents the percentage of SWCNTs extracted from the final product as a result of synthesis process.

^b Yield represents the ratio of the final product to the total amount of carbon entering the process (i.e. feedstock).

N/A: not specified.

3.3.3. Impact projections for large scale manufacturing

Full market scale production data on emerging technologies (e.g. CNTs), because of being fairly new, are not widely available [143]. Shibasaki et al. indicated that developing a large scale production plant starts with laboratory scale experiments and involves creating scenarios for pilot scale, which is the highest level of development phase [90]. Given that the level of environmental impact reduction cannot be known without conducting an LCA using actual empirical data for large scale production, in the current study, three different scaling up scenarios are implemented to project a potential range of impacts. Authors recognize that modeling each synthesis route based on its technical parameters would be more robust; however, it requires technology expertise from the actual manufacturers [144]. Therefore, hypothetical scale-up scenarios are evaluated herein. Scenarios are developed using assumptions from Gavankar et al. (S1) [77], Teah et al. (S2) [125] and Piccinno et al. (S3) [75]. In S1, potential reductions presented in Gavankar et al. are implemented for each synthesis process, where authors worked with a manufacturer to collect details on process design and engineering estimates for the scaled-up operation [77]. They provided potential changes in the input, output, and asset (e.g. additional machinery) requirements for large scale production. According to Gavankar et al., decrease in feedstock requirement can be by 96%, carrier gas by 62%, hydrogen by 96%, catalysts and deionized water by 50% and electricity requirement by 87%. In terms of outputs, same proportions of direct emissions and releases between small scale and mass production were assumed [77]. In S2, the electricity, carrier gas and carbon feedstock flows are modified as per the recommendations presented in Teah et al., where authors suggested that the electricity demand for large scale CNTs production process can be reduced to less than 11%, and consumption of the carrier gas can be reduced to 1/10 if the feedstock input is increased by 10

times [125]. Using the modifications proposed by Gavankar et al. (S1) [77] and Teah et al. (S2) [125], inputs and outputs for each of the production route are adjusted to model large scale production and LCAs are conducted accordingly (i.e. separate LCAs for S1 and S2). Finally, in S3, the suggestion from Piccinno et al. is used, where authors indicated that scaling up from the laboratory to a commercialized scale production, environmental impact per kg of produced ENM can be reduced by a factor of 6.5 [75]. Considering this reference, a scaling up factor of 6.5 is used to linearly extrapolate the LCA results [75]. Furthermore, uncertainty analysis for each process is conducted using Monte Carlo simulations in SimaPro 8.5.2 Software in order to estimate the maximum and the minimum boundaries of environmental impacts (confidence interval: 95% and sample size: 1000). Median, lower and upper bounds of TRACI 2.1 impact categories and CED are determined for each synthesis process for both laboratory and large scales, and are tabulated in Tables B19-B26. Using results obtained from Monte Carlo simulations, environmental impacts of producing CNTs are projected for both laboratory and large scale scenarios. The information on CNTs production volumes per year is extracted from Janković and Plata, where authors provided both optimistic (i.e. high production estimate) and pessimistic (i.e. low production estimate) production estimations [1]. For instance, for the year 2025, Janković and Plata estimated that 915 (as pessimistic) to 7000 (as optimistic) tons CNTs/year will be produced [1]. For individual global mass productions, it is assumed that CNTs are comprised of 20% SWCNTs and 80% MWCNTs [112, 113].

$$\begin{aligned}
 GI(\text{year}) = & \left\{ \frac{\left(\frac{\text{SWCNTs production}}{\text{year}} * \sum_{i=1}^n \left[\left(\frac{IC_{\min_i} + IC_{\text{med}_i} + IC_{\max_i}}{3} \right) \right] \right)}{n} \right\} \\
 & + \left\{ \frac{\left(\frac{\text{MWCNTs production}}{\text{year}} * \sum_{j=1}^m \left[\left(\frac{IC_{\min_j} + IC_{\text{med}_j} + IC_{\max_j}}{3} \right) \right] \right)}{m} \right\}
 \end{aligned} \tag{3.1}$$

Eqn (3.1), modified from Temizel-Sekeryan and Hicks, is used to calculate global environmental impacts (GI) of producing CNTs for the respective year, where i is the type of process for SWCNTs, n is the number of different synthesis processes considered for SWCNTs ($n=8$), j is the type of process for MWCNTs, m is the number of different synthesis processes considered for MWCNTs ($m=7$), and IC_{\min} , IC_{med} and IC_{\max} indicate impact category results obtained from Monte Carlo simulations [126]. All impacts based on TRACI 2.1 and CED are calculated using eqn (3.1). Regionality is neglected in the current study due to the limited knowledge about future production sites for CNTs. For reference, Keller and Lazareva provided estimated distribution of ENM production by regions as 53% for North America, 24% for Asia, 19% for Europe and 4% for the rest of the world; however, there were not any distinction for specific types of ENMs [45]. Therefore, in this work, TRACI 2.1. and CED are used for global impact calculations, but impact assessment results using different methods (CML (baseline), ReCiPe (Midpoint) and IMPACT 2002+) are also conducted and presented for laboratory scale results in Tables B27-B29 for future reference.

3.3.4. Projecting sectoral emissions

In order to project sectoral emissions regarding CNTs production, industries where the majority of CNTs are used are surveyed. Figure 12 is a summary of the existing literature, which presents disaggregated utilization of CNTs per industry. Keller et al. categorized industries using mass-based shares instead of the total number of commercial products in the market [5]. For instance, they suggested that 25% of produced CNTs were consumed by composites industry, which corresponds to 800 tons/year. Remaining industries from the same study were listed as electronics and optics; energy and environment; coatings, paints and pigments; automotive;

aerospace and sensors with shares of 24%, 23%, 10%, 10%, 5% and 3% respectively. Other references cited in Figure 12 used surveys [145], simulations [44, 85], total number of available products in the market [40, 146, 147] or a combination of those [1, 148] to provide shares on market demand. Since they categorized industries assuming maximum CNTs production by mass (e.g. 768 tons of CNTs used for electronics and optics industry when the total CNTs production was 3200 tons) rather than the number of CNTs-enabled products on the market, industry-based global environmental impact projections are developed using sectoral proportions published by Keller et al. [5].

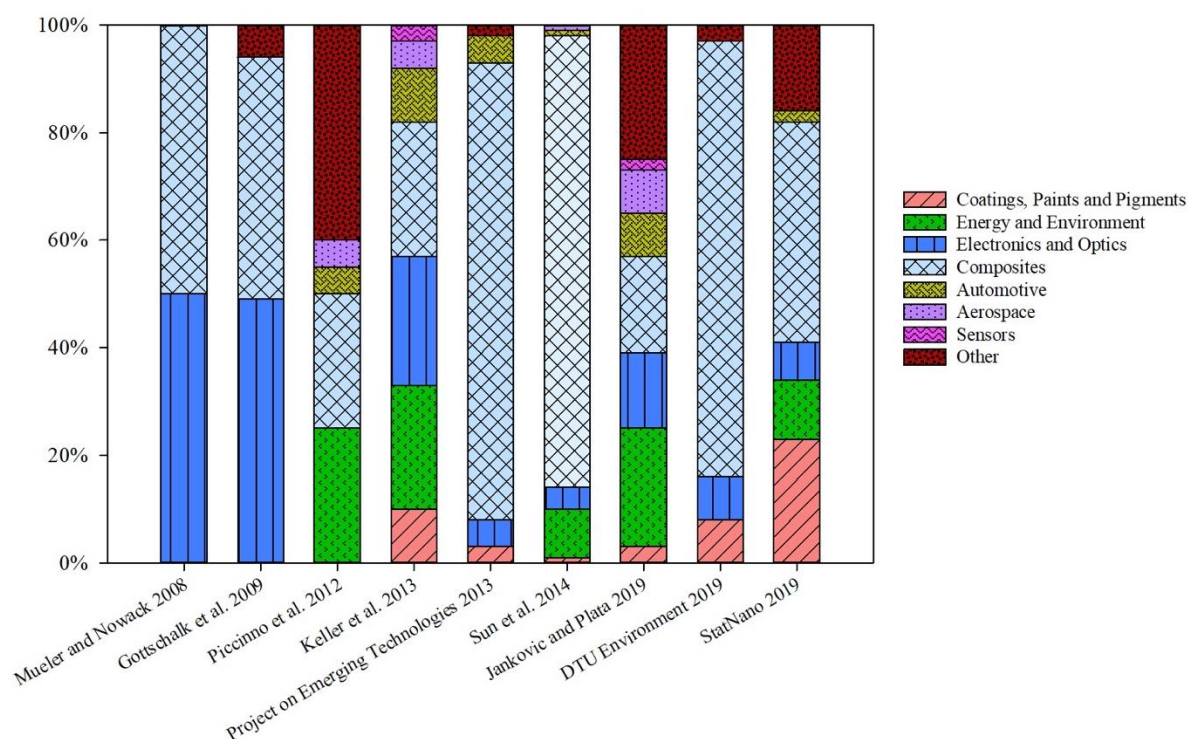


Figure 12. Industry-based estimations for CNTs-enabled consumer products compiled from the literature (Other includes materials, textile, food, personal care, military and other miscellaneous sectors) [1, 5, 40, 44, 85, 145–148].

Industries prefer using particular processes to synthesize the CNTs, as each process produces materials with specific morphology and surface chemistry. Currently, there is no explicit information in the published body of the literature that shed light on the product-process pairs, therefore a literature review is conducted in order to develop an understanding. Table B30 (for SWCNTs) and Table B31 (for MWCNTs) show applications of CNTs in different industries and respective synthesis processes to be used to construct product-based impact projections. It is found that SWCNTs for electronics and optics industry are mostly synthesized via HiPCO, CVD, CoMoCat and AP; for composites and sensors industries are synthesized via CVD; for energy and environment industry are synthesized via CVD, LV and AP; and for automotive industry are synthesized via CVD and LV. MWCNTs for electronics, optics, energy and environment industries are synthesized via AP and CVD; and for composites, sensors and automotive industries are synthesized via CVD. In terms of the processes to manufacture SWCNTs and MWCNTs for aerospace and coatings, paints and pigments industries, no information was available in the literature. Since current breakdown of production by synthesis is unclear, all CNTs synthesis processes are considered as equally preferable and estimated global impacts are calculated by using the Laplace criterion [88].

$$GGW_{sector}(year) = \sum_i^n \frac{\text{industrial proportions} * \frac{\text{skeptical SWCNTs production}}{\text{year}}}{n} * GW_i \left(\text{in } \frac{\text{kg } CO_2 - \text{eq.}}{\text{kg SWCNTs}} \right) + \sum_j^n \frac{\text{industrial proportions} * \frac{\text{skeptical MWCNTs production}}{\text{year}}}{n} * GW_j \left(\text{in } \frac{\text{kg } CO_2 - \text{eq.}}{\text{kg MWCNTs}} \right) \quad (3.2)$$

Eqn (3.2), which is an example for global sectoral GW calculation (i.e. GGW_{sector}) per year, is used to estimate the sectoral annual environmental impacts considering pessimistic production forecasts. Industrial proportions are extracted from Keller et al., i and j represent the

respective CNTs (SW- and MW- respectively) synthesis processes used for that industry and n represents the number of processes applied for that particular industry [5, 126].

3.4. Results and discussion

3.4.1. Impact assessment and comparison of synthesis processes

Different synthesis processes are assessed, and characterization results for 1 kg of CNTs (SW- and MW-) are presented in Figure 13, by including the impact categories from TRACI 2.1 (Table B32) and CED (Table B33). The line in the middle separates the results for SWCNTs (left) from MWCNTs (right). As multiple inventories are included for CVD route to synthesize SWCNTs (e.g. S-CVD1, S-CVD2) as well as MWCNTs (e.g. M-CVD1, M-CVD2, M-CVD3, M-CVD4, M-CVD5), average results are presented for each route. Error bars represent standard deviations of environmental impacts. Results from large scale inventories are presented separately and marked with an asterisk. On a mass-based functional unit, the environmental impacts of synthesis processes generally follow the trend of S-HiPCO2* < S-CoMoCat2* < S-HiPCO1 < S-LV < S-AP < S-CoMoCat1 < S-CVD1 < S-CVD2 for SWCNTs; and M-AP < M-CVD1 < M-CVD5 < M-CVD6* < M-CVD4 < M-CVD2 < M-CVD3 for MWCNTs. The authors recognize that although functional comparisons would require more detailed assessment (e.g. by taking into account the size, purity or surface area), the current study presents a baseline to cross compare the environmental impacts of commercially important synthesis routes for manufacturing both SWCNTs and MWCNTs on a mass basis functional unit. Results indicate that the preference of synthesis process dominates the overall environmental cost of the ENM.

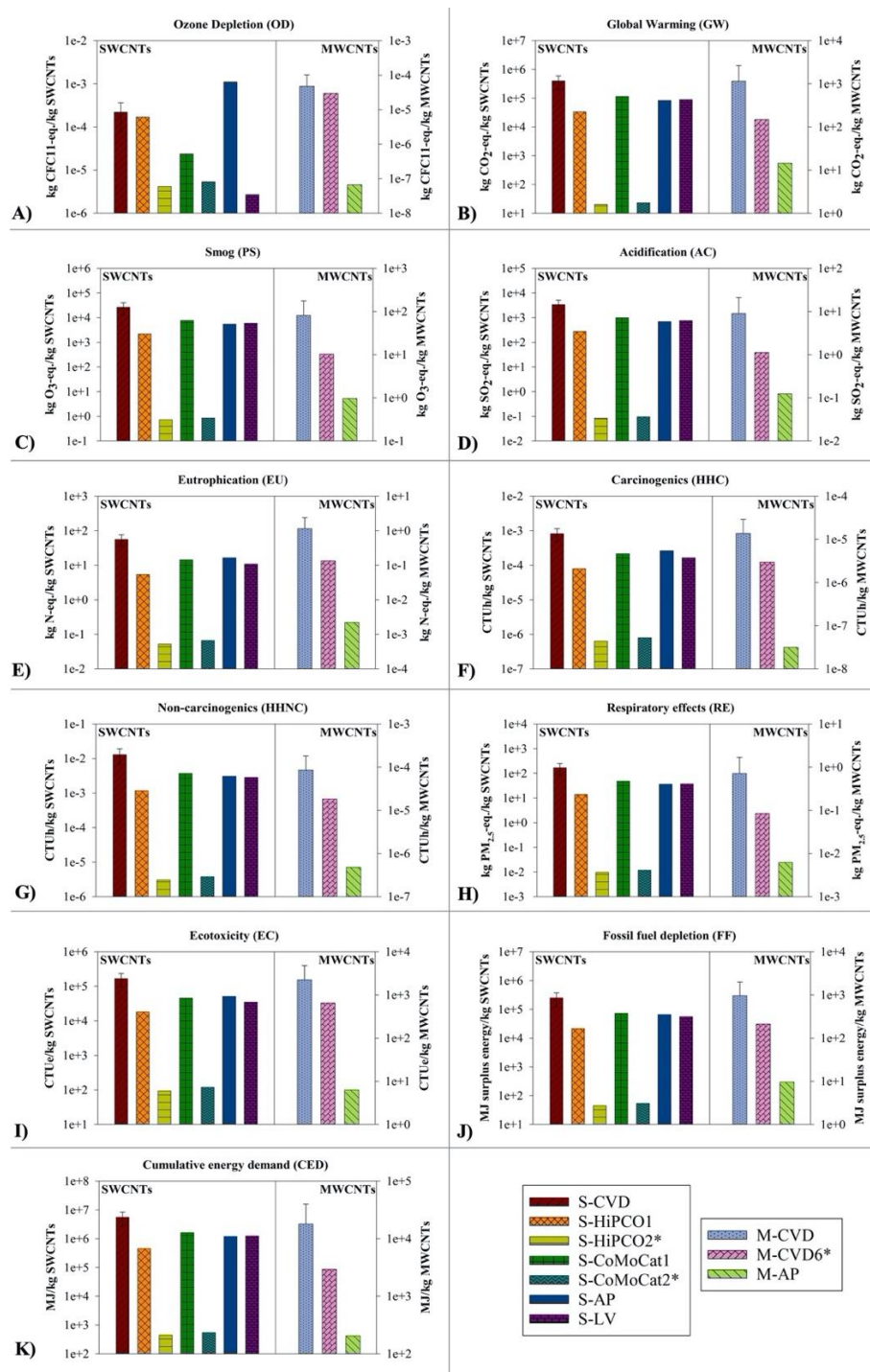


Figure 13. Environmental impacts of multiple synthesis routes for 1 kg CNTs (S- and M-) in logarithmic scale, using multiple impact categories as A) OD, B) GW, C) PS, D) AC, E) EU, F) HHC, G) HHNC, H) RE, I) EC, J) FF and K) CED (*large scale inventories are marked with an asterisk).

Regarding manufacturing SWCNTs, CVD route has the highest impact across all environmental impact categories except OD. This is mainly due to the significant amount of electricity consumption during the syntheses. This finding matches with the interpretation from Bauer et al., since it was also mentioned that the large impact is almost entirely due to the energy used for the CVD process [98]. The environmental impacts resulting from synthesizing SWCNTs with S-CoMoCat1 and S-AP/S-LV follow CVD, respectively. In terms of AC, GW, RE, PS, HHNC, FF and CED impact categories, S-AP/S-LV performs better than S-CoMoCat1. However, due to the helium, carbon and nitric acid inputs required for the S-AP process, it performs worse than S-CoMoCat1 and S-LV in categories including EC, EU, HHC and OD, with OD being the largest among all synthesis routes considered. Environmental impacts resulting from the S-LV process has lower impacts than S-AP in OD, EU, HHC, HHNC, EC and FF. Impacts resulting from S-HiPCO1 process performed lower impacts than the previously analyzed routes except OD due the consumption of nitric acid for purification step. These findings slightly differ from Promentilla et al. where they identified the environmental impact ranking as HiPCO < CVD < LV < AP using multi criteria decision analysis [149]. Two processes which have large scale inventories (S-HiPCO2* and S-CoMoCat2*) are also included in the current evaluation. As expected, they perform the least environmentally impactful results comparing to other routes, due to the optimized process conditions. Between these two routes, S-HiPCO2* has slightly lower impacts than S-CoMoCat2* in all environmental impact categories, because it requires lower amount of inputs, e.g. lesser carbon monoxide as a carbon source and energy for the reactor. Midpoint LCA results of producing SWCNTs with the considered pathways are presented in Figures B2-B9 in order to provide details on process contributions.

In terms of manufacturing MWCNTs, M-CVD3 process has the highest impact across all environmental impact categories. This is mainly due to the use of significant amount of argon as a carrier gas and grid electricity as an energy source. The second most impactful route is M-CVD2 (except GW, PS, AC, and RE) where the impacts are resulting from the use of hydrochloric acid and ethanol as precursor. Impact of M-CVD4 route follows M-CVD2, which uses camphor as an eco-friendly carbon precursor. However, M-CVD4 includes silicon wafer as a substrate, and it has a significant impact contribution to all categories. Therefore, it is ranked as the third most impactful route. Interestingly, despite being a large scale synthesis route, M-CVD6* is not the one which has the least environmental impact in any category. This is due to the use of argon, hydrochloric acid and benzene as inputs for the synthesis process. M-CVD5 and M-CVD1 follow M-CVD6* and show moderate impacts across all environmental impact categories. Finally, M-AP is found to be the least environmentally impactful route for all categories. Details on process contributions to produce 1 kg of MWCNTs by the selected routes are presented in Figures B10-B16. Besides, Table B34 shows impact rankings (lowest, medium and highest) grouped by wall number (SWCNTs or MWCNTs) for TRACI 2.1 and CED impact categories.

3.4.1.1. Alternative scenarios for electricity source

As presented by contribution analyses in Appendix B (Figures B2-B16), electricity is identified as the main contributor of environmental impacts in the majority of synthesis routes considered. The electricity process that is used in the impact assessment represents grid electricity, which is reported as the mix of fuels used for utility electricity generation including coal, fuel oil, nuclear, hydroelectric, solar, wind and geothermal [150]. In order to evaluate

potential impact changes due to the utilization of different sources of energy, various scenarios are developed herein. According to the International Energy Agency (IEA), oil, coal, natural gas, nuclear, hydro, wind and solar are being used as sources of energy supply in the world [151]. Accordingly, in addition to the grid electricity, seven different scenarios are computed for each synthesis route using the aforementioned energy sources in order to project potential changes in environmental impacts.

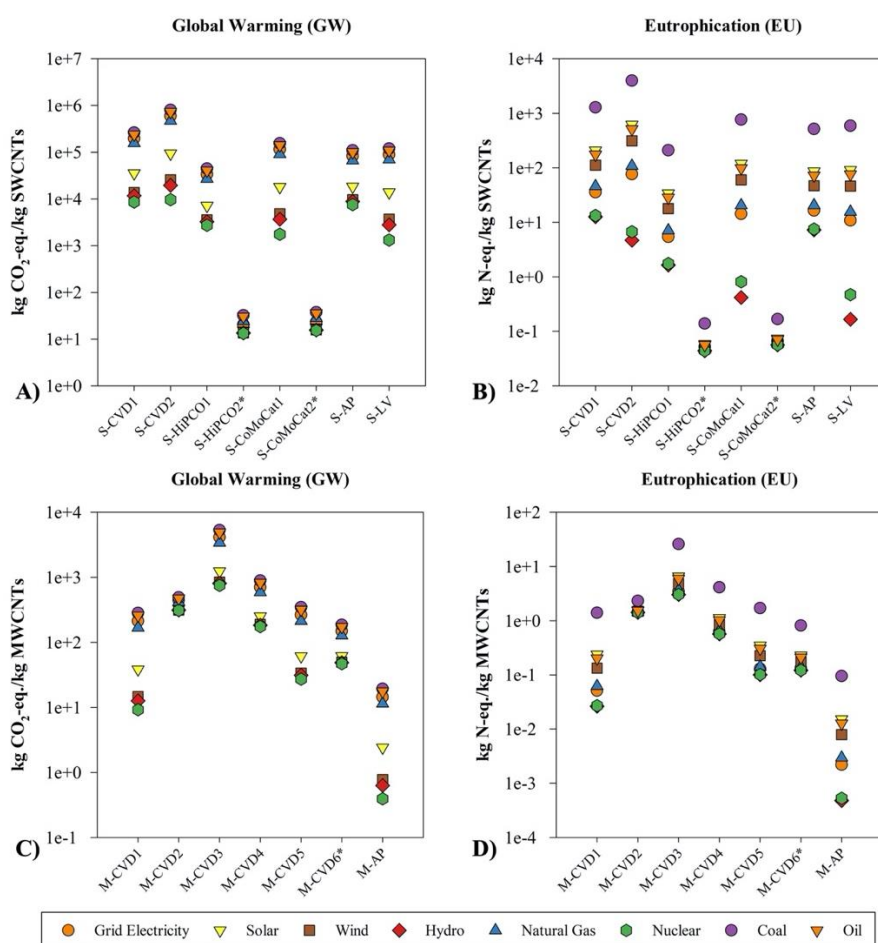


Figure 14. Different electricity scenarios and their corresponding impacts for A) SWCNTs-GW, B) SWCNTs-EU, C) MWCNTs-GW, and D) MWCNTs-EU (*large scale inventories are marked with an asterisk).

GW and EU are illustrated as example impact categories in Figure 14, where total impacts are presented per functional unit. For SWCNTs (Figure 14A-B), the trend for all synthesis routes for GW is found as nuclear < hydro < wind < solar < natural gas < grid electricity < oil < coal except for S-HiPCO₂* and S-CoMoCat₂*. The reason that natural gas performed slightly impactful than grid electricity in these two processes is that, they require heat input which was previously modeled as steam from chemical industry. The largest difference is identified to be associated with the S-CVD₂ route, where switching from grid electricity to nuclear would save 5.86×10^5 kg CO₂-eq./kg SWCNTs. Differently, switching from grid electricity to coal for S-CVD₂ would create 2.05×10^5 kg CO₂-eq. more emissions per 1 kg of SWCNTs production. The trend for EU in all synthesis routes is found as hydro < nuclear < grid electricity < natural gas < wind < oil < solar < coal except for S-HiPCO₂* and S-CoMoCat₂*, due to their heat requirements as discussed previously. The largest difference is identified to be associated with the S-CVD₂ route, where switching from grid electricity to hydro would save 7.17×10^1 kg N-eq./kg SWCNTs, and from grid electricity to coal would create 3.88×10^3 kg N-eq./kg SWCNTs more emissions. For MWCNTs (Figure 14C-D), the trend for all synthesis routes for both GW and EU showed the same pattern as SWCNTs without any exceptions. The largest difference is found to be linked with the M-CVD₃ route, where switching from grid electricity to nuclear would save 3.38×10^3 kg CO₂-eq./kg MWCNTs, and from grid electricity to coal would add 1.18×10^3 kg CO₂-eq./kg MWCNTs. In terms of EU, again associated with the M-CVD₃ route, switching from grid electricity to hydro would save 4.14×10^{-1} kg N-eq./kg MWCNTs, and from grid electricity to coal would create 2.24×10^1 kg N-eq./kg MWCNTs more emissions. Different electricity scenarios and their corresponding environmental impacts for CNTs production are presented in Table B35 (SWCNTs) and Table B36 (MWCNTs).

3.4.2. Implications of large scale manufacturing

Based on the CNTs production forecasts (in both low/pessimistic and high/optimistic levels) [1] and eqn (3.1), global environmental impacts are projected from 2018 to 2025. As being an historically utilized single category reporting method, GW is selected for discussion as a representative impact category [152]. Considering laboratory scale inventories, global CO₂-eq. emissions for 2019 are estimated as $1.96 \times 10^7 \pm 1.07 \times 10^5$ tons CO₂-eq. for pessimistic estimations, and $9.98 \times 10^7 \pm 5.50 \times 10^5$ tons CO₂-eq. for optimistic estimations. However, given that large scale production has a potential to increase materials and energy efficiency as well as recycling rates of reagents, it helps decreasing the environmental impacts per unit mass of the product synthesized [89, 90]. Thus, it may not be practical to calculate global impacts by using laboratory scale LCA results since economies of scale are at play [72, 153]. Although industrial CNTs production is currently operated at large scale, there is a lack of inventory data from a commercial scale manufacturing. In order to estimate global production impacts, different scenarios are computed to rescale the LCA results from a laboratory into large scale. Considering S1, GW is projected as $2.65 \times 10^6 \pm 4.65 \times 10^4$ tons CO₂-eq. for pessimistic estimations, and $1.35 \times 10^7 \pm 2.37 \times 10^5$ tons CO₂-eq. for optimistic estimations for the year 2019. Assuming production as modeled based on S2, GW performed slightly higher than S1 as $2.73 \times 10^6 \pm 9.03 \times 10^4$ tons CO₂-eq. for pessimistic estimations, and $1.40 \times 10^7 \pm 4.61 \times 10^5$ tons CO₂-eq. for optimistic estimations in 2019. Finally, considering S3, GW indicated the highest impact among large scale scenarios as $3.01 \times 10^6 \pm 1.69 \times 10^4$ tons CO₂-eq. for pessimistic estimations, and $1.54 \times 10^7 \pm 8.62 \times 10^4$ tons CO₂-eq. for optimistic estimations. Figure 15 shows the annual global GW (tons CO₂-eq.) using different scale-up scenarios as well as laboratory scale estimates for SWCNTs, MWCNTs and their combined CNTs industry. Projected impact results for all impact

categories are included in Appendix B (Tables B37-B58). It is also found that, the trends for large-scale scenarios differ from one impact category to another. For instance, while the ranking for EU is found as $S2 < S1 < S3$, it performed as $S1 < S3 < S2$ for FF. Table B59 provides an example heatmap, where all of the eleven impact category results are presented for pessimistic CNTs production in 2019. The trend is expected to be the same for all remaining years, as only the mass production is changing in the calculations.

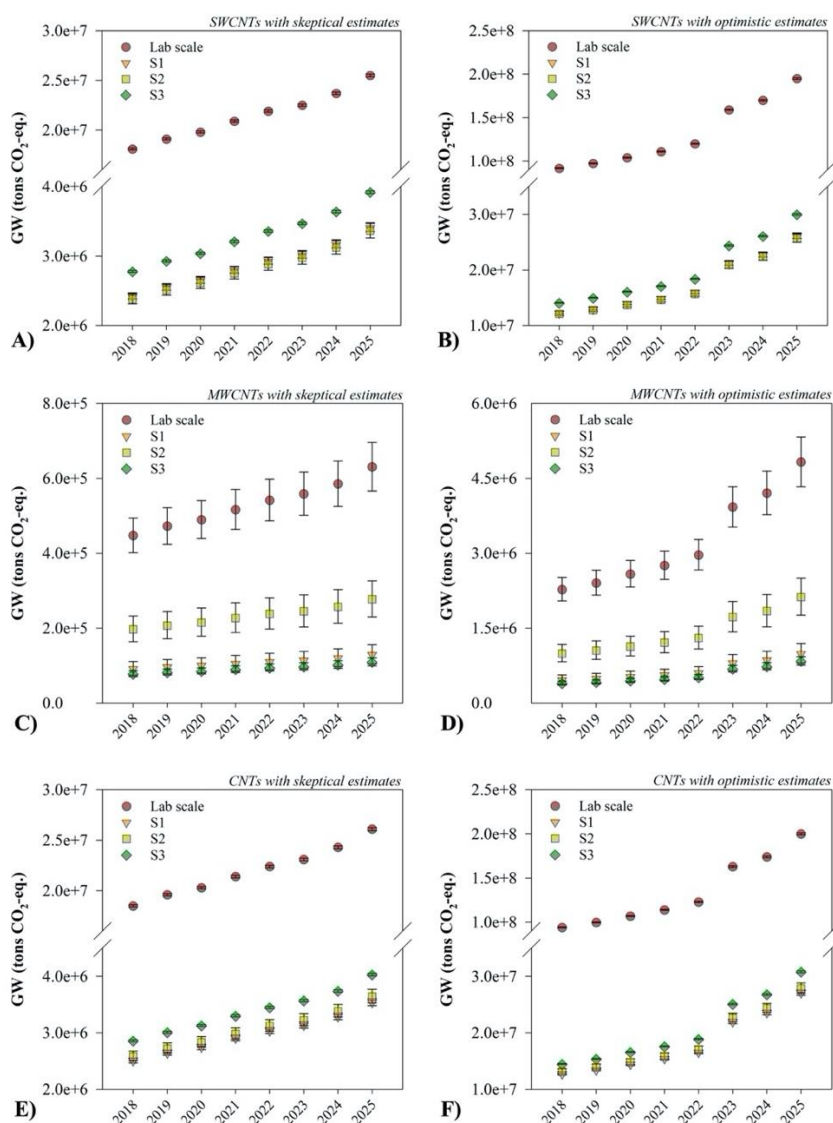


Figure 15. Projected global GW (tons CO₂-eq./year) for A) SWCNTs with pessimistic production volumes B) SWCNTs with optimistic production volumes, C) MWCNTs with pessimistic production volumes D) MWCNTs with optimistic production volumes, E) CNTs with pessimistic production volumes F) CNTs with optimistic production volumes. Error bars represent 95% confidence intervals for the uncertainties modeled by Monte Carlo simulations.

Like other ENMs, CNTs are embedded into nano-enabled products at relatively low concentrations. For reference, Gilbertson et al. studied a chemical gas sensor with 7 mg SWCNT per chip, which was equivalent to 0.17% of the total mass of nano-enabled product [154]. Another example may be given from Celik et al., where 0.1 g CNT was used in 1 m² photovoltaic cell [135]. There are not any data on the proportion of industrially manufactured CNTs versus CNTs that are produced in laboratory scales in the published body of the literature. Therefore, projecting environmental impacts resulting from both scales enables a better understanding of possible environmental impact ranges associated with CNTs manufacturing. In terms of evaluating the extent of direct impacts, results obtained from the current study are compared with the previous studies that developed CFs. Considering laboratory scale LCA results, production-based EC for SWCNTs (6.21×10^4 CTUe/kg) and MWCNTs (1.95×10^3 CTUe/kg) are larger than the CFs calculated by the previous literature (i.e. up to 2.9×10^4 CTUe/kg SWCNTs and 7.4×10^2 CTUe/kg SWCNTs), which supports the finding from Eckelman et al. [127]. The production-based HHNC for SWCNTs (4.66×10^{-3} CTUh/kg) are found to be higher than the direct impacts considering CF developed by Rodriguez-Garcia et al. (2.4×10^{-4} CTUh/kg) [128]. However, for the case of MWCNTs, production-based HHNC (7.92×10^{-5} CTUh/kg) are found two orders of magnitude lower than the direct impacts (1.67×10^{-3} CTUh/kg)

extracted from the same reference [128], indicating that release of MWCNTs may pose risks for human health. Although these comparisons can show potential consequences, the fate and behavior of ENMs depend on various considerations such as the physicochemical properties of ENMs and the environmental conditions that they are released into [155]. Therefore, using CFs that are presented by the literature may not be representative and serves as a limitation.

In order to highlight the significance of the environmental impacts associated with CNTs, the global CO₂-eq. emissions resulting from synthesizing CNTs are compared with global CO₂ emissions of transportation and buildings sectors. According to IEA, transportation sector emitted 8.26×10^9 tons of CO₂ and buildings sector produced 2.88×10^9 tons of CO₂ in 2018, globally [156]. The GW predicted for large scale CNTs manufacturing in 2019 is found as equivalent up to 0.2% of the CO₂ emissions resulting from the global transportation sector, and up to 0.54% of the CO₂ emissions resulting from the global buildings sector.

3.4.3. Sectoral environmental impacts

Sankey diagrams are developed for each of the impact category to depict the environmental performances of the sectors where CNTs are used the most. Figure 16 presents sectoral GW projections for both pessimistic and optimistic production volumes forecasted for 2019. As being the least impactful scenario in terms of GW, projections based on S1 are included in Figure 16 along with laboratory scale projections to present a range for potential extent of impact. Detailed sectoral impacts for the remaining environmental impact categories are presented in Tables B60-B70.

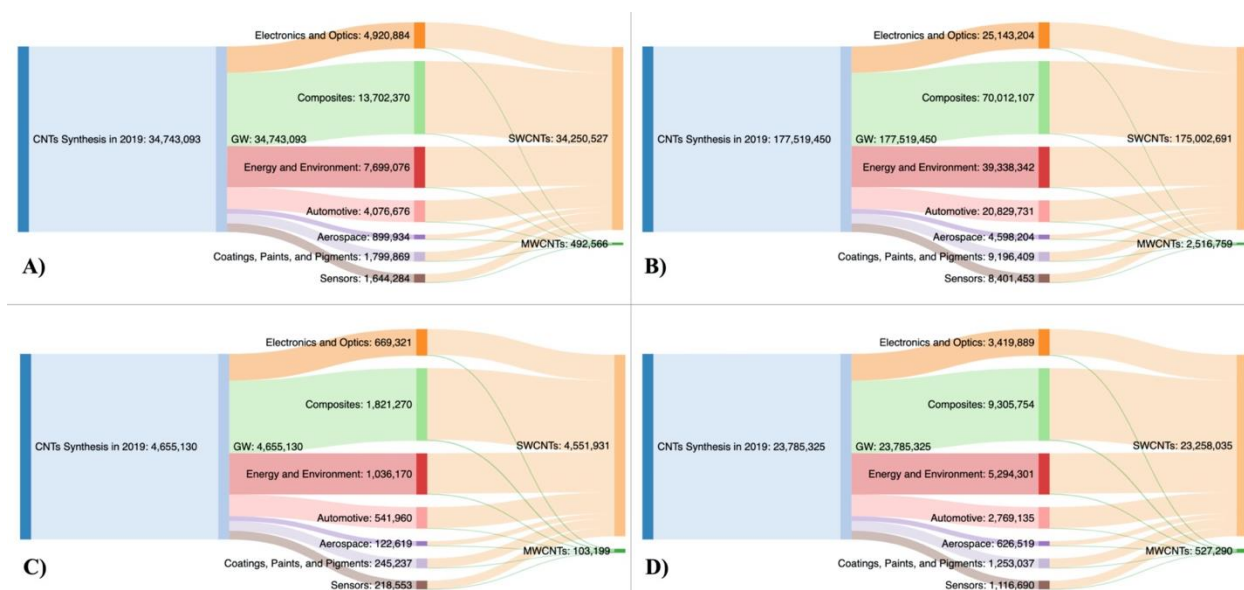


Figure 16. Sankey diagrams for industry-based GW for the year 2019 using A) pessimistic estimations-laboratory scale, B) optimistic estimations-laboratory scale, C) pessimistic estimations-S1, D) optimistic estimations-S1.

As presented in Section 3.4.1, each process has different environmental impacts, which are varying more than one order of magnitude per 1 kg of CNTs synthesized. Due to this difference, industry-based impacts are not proportional with the industrial shares. For instance, although the share of composites (25%) and electronics and optics (24%) industries are very close, the difference between their environmental impacts range from 87-94%, with composites having higher impacts in all categories. Only OD performed similar for both industries with a 3% of difference. Similarly, when comparing composites (25%) and energy and environment (23%) industries, it is observed that the variances in environmental impacts differ by 51-56%, except OD. OD resulting from the composites industry is found as 21% lower than the energy and environment industry, even though it has a higher industrial share. Another example may be given from automotive and coatings, paints and pigments industries. While they have the same

sectoral shares (10%), automotive industry has drastically higher environmental impacts (>69%) comparing to coatings, paints and pigments industry in all categories except OD. One interesting finding was that, all of the considered environmental impacts resulting from the energy and environment industry are 24-45% higher than the electronics and optics industry, even though the share of electronics and optics industry is higher than the energy and environment industry. It should be highlighted that, besides presenting the disaggregated sectoral environmental costs, Figure 16 illustrates the drastic difference between the environmental impacts of manufacturing SWCNTs and MWCNTs. As aforementioned, manufacturing SWCNTs is more environmentally impactful than producing MWCNTs, which can be observed from the right end sides of the Sankey diagrams in Figure 16. As these disaggregated projections represent cradle-to-gate impacts, they may be combined with the release patterns to model cradle-to-grave impacts for specific industries. These then may be used to monitor and calculate industrial emissions in different scales, e.g. global, regional, local. It should be noted that, a minor change in precursor, catalyst and growth mechanism significantly affect the properties of the CNTs. Research suggested that the selection of these parameters is directly linked with the physical, chemical, electronic, optical and magnetic properties of the final product [51]. Therefore, specific processes are needed to synthesize CNTs to be used for particular applications, as properties differ with the employed route [117, 157].

3.5. Conclusions

Production of CNTs are anticipated to increase due to a numerous uses and applications in the modern technology. Therefore, in order to create a basis for understanding the environmental hotspots of manufacturing CNTs, conducting an LCA is helpful. This work

investigates and compares the industrially preferred synthesis processes for SWCNTs and MWCNTs and draws a global framework to emphasize the environmental impacts resulting from manufacturing these novel materials. As a result of multiple attributional LCAs, CVD is found as the most impactful route for manufacturing SWCNTs and MWCNTs; and HiPCO for SWCNTs and AP for MWCNTs are identified as the least impactful routes, among others. Process contribution analysis showed that, grid electricity is the largest contributor for all of the environmental impacts, except OD. Scenarios for different energy sources are computed to project potential changes (either reduction or increase) associated with switching from grid electricity to more/less impactful energy supply. Although the trend was varying among impact categories, for GW, electricity obtained from nuclear is found as the most environmentally benign source and coal as the worst. It is known that industrial scale production provides savings for both environmental and economic considerations per unit mass of the product synthesized. Therefore, in addition to laboratory scale impact evaluations, scenarios for scaled up production are developed to project future impacts associated with CNTs manufacturing. Results indicated that up to 88% global impact reduction may be achieved with large scale production. Aside from comparing synthesis processes, segmented global environmental impact projections are developed using different industrial applications and their preference on the use of either SWCNTs or MWCNTs. The biggest consumer of CNTs, composites industry performed as the largest impactful industry, followed by energy and environment, electronics and optics, automotive, coatings, sensors and aerospace industries, respectively. It is also found that the sectoral environmental impacts are not commensurate with the industrial shares as industries use certain processes to synthesize the CNTs to be embedded in their products. Although estimating non-nanoscale emissions (i.e. impacts due to ENMs production) is essential, future work should

demystify nano-specific emissions (i.e. direct impacts resulting from the nanomaterial release from manufacturing, use and disposal phases). This can be achieved by developing nano-specific characterization factors and elucidating ENMs transformation patterns as a function of nano-enabled product and characteristics of the receiving location.

3.6. Acknowledgements

The authors acknowledge the support of Wisconsin Alumni Research Foundation (WARF). This work has not been formally reviewed by the WARF, and the findings of the authors are their own.

4. Calculating size- and coating- dependent effect factors for silver nanoparticles to inform characterization factor development for usage in life cycle assessment

The following chapter is a reproduction of an article published in the Environmental Science: Nano, with the citation:

Temizel-Sekeryan, S.; Hicks, A.L. (2020) Emerging investigator series: Calculating size- and coating- dependent effect factors for silver nanoparticles to inform characterization factor development for usage in life cycle assessment, *Environmental Science: Nano*, Vol. 7, Issue. 9, pp. 2436-2453.

The article appears as published, although style and formatting modifications have been made.

Authorship contribution statement

Sila Temizel-Sekeryan: Designed Research, Performed Research, Analyzed Data, Wrote the Paper.

Andrea L. Hicks: Designed Research, Wrote the Paper.

4.1. Abstract

Concerns about the environmental and human health implications of engineered nanomaterials (ENMs) are growing with the increased use in consumer and industrial products. Numerous studies have applied life cycle assessments (LCAs) to model the potential environmental and human health impacts of ENMs. Most of them have not included nano-specific emissions (i.e. impacts due to ENM release) and evaluated only non-nanoscale emissions (i.e. impacts due to ENM production). However, both considerations need to be included for more thorough evaluation of the environmental implications of these ENMs. One solution to calculate nano-specific emissions is to derive characterization factors (CF), which are comprised of information on fate, exposure, and effect factors for ENMs. This paper seeks to provide size, coating, and test medium dependent effect factors (EF) for silver nanoparticles (nAg), one of the most commercialized ENMs, using the USEtox model. A comprehensive literature review is performed, and 366 toxicity data points are used to derive physicochemical property based EFs. EFs are modeled based on different scenarios including species and trophic level HC_{50} calculations under regular (using EC_{50} values only) and cumulative (using LC_{50} , EC_{50} and IC_{50} values) cases. Different EFs are calculated based on varying size, coating, and testing medium combinations and presented in the form of matrices. Results suggest that larger nAg have lower EF, and coating is an important consideration in toxicity assessment. Regardless of specific properties, an EF range is proposed as 8,035–14,675 PAF $m^3 kg^{-1}$. Future work should combine fate and exposure factors to calculate CF for further application to LCA.

4.2. Introduction

Engineered nanomaterials (ENMs) have at least one dimension in the nanoscale (1–100 nanometers) and are used in various industries for diverse purposes [2, 3]. Market reports show that the nanomaterials industry is constantly growing, and the market value is expected to reach up to \$98 billion by 2025 from \$11.3 billion in 2020 [7, 158]. Silver nanoparticles (nAg) are the most commercialized ENMs with a share of >50% of the global nanomaterial consumer products [7]. It is expected that the global nAg production will reach to 753 tons per year and the market value will be worth \$3 billion by 2024 [1, 50].

Monovalent ionic silver (Ag^+) is well known for its antimicrobial properties as it slows down the pathogenic microbial activity for both Gram-negative (e.g. *Escherichia*, *Pseudomonas* and *Salmonella*) and Gram-positive (e.g. *Staphylococcus*, *Streptococcus* and *Listeria*) bacteria, some viruses (e.g. HIV-1 and influenza) and some fungi (e.g. *Aspergillus* and *Saccharomyces*), which is why it has been utilized at the bulk scale since antiquity, particularly in the medical sector [41, 60, 159]. With the evolving research on nanotechnology, nAg have been developed to serve for various purposes besides medical applications such as electronics (e.g. nanoscale sensors), optics (e.g. electroluminescent displays), textiles (e.g. anti-stink gear), packaging (e.g. food storage containers) and coatings (e.g. façade paints) among others [5, 32, 33, 35, 39, 66, 67, 126]. Being widely incorporated in consumer products raises environmental and human health related concerns, since at the end of their useful lifetimes (and also sometimes during their lifetimes), nAg will ultimately be released to the environment [45, 60]. Therefore, research on evaluating the environmental performance of nAg is critical to determine the extent of such an impact.

Environmental impact assessment of any product or process using life cycle assessment (LCA) methodology provides results in often a broad category of impacts (e.g. global warming, eutrophication, toxicity etc.), which are quantifications of the impact of unit release of chemicals to the environment [14]. LCA can be utilized to identify hotspots and to improve the comparative environmental performances of products or processes. In the nanomaterial industry, applying LCA to ENMs provides impact projections on several different potential environmental impact categories, which may be grouped as “non-nanoscale emissions to the environment” and do not include nano-specific emissions to soil, air and water [13]. Numerous LCA studies on ENMs have already been published with various scopes. Salieri et al. provided a comprehensive review of previously published LCAs and identified gaps, in which one of the gaps was investigating the nano-specific emissions for ENMs [22]. For instance, considering nAg, due to the lack of nano-specific characterization, the majority of the LCA studies model the release of Ag as Ag⁺ without particular speciation (e.g. Ag⁺, Ag/S, AgCl etc.) [30–32, 39, 60, 64, 65, 80]. Non-nanoscale emissions represent indirect impacts due to the nanomaterial production (such as the raw materials and manufacturing), whereas nano-specific emissions denote direct impacts resulting from the nanomaterial release as a function of size and shape [4]. In order to calculate nano-specific emissions, defining characterization factors (CF) is critical.

Life cycle impact assessment is one of the four phases of LCA, in which quantification of the potential environmental impact of a product or process is evaluated [15, 16]. Eqn (4.1) is used to calculate the potential impact (i.e. impact score),

$$I^i = \sum_{xm} CF_{xm}^i * M_{xm} \quad (4.1)$$

where x is the substance of interest, i is the impact category of concern, m is the media, I^i is the potential impact of x for i , CF_{xm}^i is the characterization factor for x emitted to m for i , and M_{xm} is

the mass of x emitted to m [18, 160]. The USEtox multimedia fate and exposure model is recommended for quantifying potential ecotoxicity and human toxicity for chemicals for usage in LCAs [23, 161]. The USEtox calculates CF using eqn (4.2),

$$CF = EF * FF * XF \quad (4.2)$$

where EF represents the effect factor, FF represents the fate factor and XF represents the exposure factor. XF is dissolved and bioavailable fraction of an ENM that an organism will be exposed to [23, 24]. FF is the duration (days) that an ENM resides in a specific environmental compartment such as air, water or soil [20, 23, 24]. Lastly, EF is the impact of ENMs on the ecosystem which relies on the toxicological data. For freshwater ecotoxicity, EF needs to be calculated using chronic effective concentrations for aquatic organisms. Whereas for human toxicity, EF is calculated using lethal or effective doses reported for animals (e.g. guinea pig, mouse, rabbit) [20, 23, 24]. It is important to note that XF and FF depend on physicochemical properties of ENMs as well as the environmental conditions (i.e. release media), which affect fate and transport kinetics [127, 155, 162]. Examples for potential environmental pathways include hetero- or homo-aggregation, agglomeration, sedimentation, dissolution and transformation [155]. Therefore, XF and FF should be calculated specifically for each environmental scenario of interest. In the present study, special focus is given on the calculating EFs only for freshwater ecotoxicity.

It should be acknowledged that a substantial research effort has been made to investigate the toxicity of ENMs to freshwater and saltwater organisms, which are used to inform EF and CF development practices. Several review articles on the toxicity and risk assessment of ENMs have been published previously [163–174]. For instance, Bondarenko et al. reviewed toxicities of nAg, copper oxide (CuO) and zinc oxide (ZnO) nanoparticles as well as ions on target (bacteria,

yeast/fungi and algae) and non-target (crustaceans, fish, *vibrio fischeri*, protozoa, nematode and mammalian cells *in vitro*) organisms. Although they listed the lethal, effective and/or inhibitory concentrations (LC, EC and/or IC) along with details on ENMs size, coating and test medium, they categorized toxic or non-toxic concentrations of the ENMs regardless of these properties [163]. Similarly, Juganson et al. developed a comprehensive database for the most studied ENMs for the year of the publication (i.e. CNTs, fullerenes, titanium dioxide (TiO₂), iron oxide (Fe₂O₃/Fe₃O₄), cerium dioxide (CeO₂), Ag, ZnO and CuO nanoparticles) including details on ENMs, characteristics of the test environment and toxicity testing [168]. Besides these reviews, Hund-Rinke et al. proposed a concept to skip the step of toxicity testing for ENMs in order to save time and money, by applying grouping and read-across strategies. However, they excluded surface modifications (e.g. coating) which greatly influence the range of ecotoxicity results. They concluded that the impact of coating on ecotoxicity has to be investigated in depth for a more thorough analysis [166]. Given that the physicochemical properties have significant impacts on the toxicity of nAg, it is critical to incorporate them in EF calculation to further evaluate the potential ecotoxicity of these ENMs on aquatic organisms.

To the best of the authors' knowledge, this is the first study that comprehensively investigates size- and coating-dependent EFs for nAg in various environmental mediums (i.e. mineral, complex). Results are intended to inform future research in this area, particularly evaluating impacts of nAg that have different physicochemical characteristics, which eventually affect their toxicity on aquatic organisms. Assessments will advise researchers as to the need of categorized (i.e. based on size/coating/medium) EF calculation to develop CF for nAg, with the goal of future incorporation into life cycle impact assessments.

4.3. Review of ecotoxicity literature and methods for EF calculation

4.3.1. Considerations on USEtox and EF calculation

As included in the introduction section, the USEtox model is commonly used in the LCA literature to develop specific CFs for chemical substances [22]. It is a consensus model which provides a framework for characterizing human toxicity (cancer and non-cancer) and freshwater ecotoxicity impacts of chemicals [20]. In other words, it helps to derive the CFs for any chemical substance to be incorporated into the impact calculations. As mentioned previously, the focus of the current study is calculating EFs for freshwater ecotoxicity to inform CF development.

The EF for freshwater ecotoxicity is the slope of the concentration–response plot when potentially affected fraction (PAF) is 0.5 (i.e. 50% of the population is affected), and its unit is $\text{PAF m}^3 \text{ kg}^{-1}$ [20, 26]. Eqn (4.3) and (4.4) are used to calculate the EF, where HC_{50} (hazardous concentration) is calculated by the geometric mean of species-specific experimental EC_{50} data, and EC_{50} is the concentration of a substance at which 50% of the population responds [26, 127].

$$EF = \frac{PAF}{HC_{50}} = \frac{0.5}{HC_{50}} \quad (4.3)$$

$$HC_{50} = \sqrt[n]{\prod_{i=1}^n EC_{50,i}} \Rightarrow \log HC_{50} = \frac{1}{n} \sum_{i=1}^n \log EC_{50,i} \quad (4.4)$$

According to USEtox, EC_{50} values that have mortality, immobilization, reproduction or other effects as endpoints should be used to calculate the hazardous concentration [20, 23].

Further, Larsen and Hauschild distinguished the endpoints for acute and chronic test results to be used in EF calculation. They recommended lethality (i.e. LC_{50}), growth inhibition (i.e. IC_{50}) and immobilization endpoints for acute, and inhibition of reproduction and reduced growth endpoints for chronic tests [175]. Miseljic and Olsen calculated a CF for nAg, and they derived the EF

considering only acute EC_{50} values using conversion factors [25]. Other studies included LC_{50} and/or IC_{50} values in addition to EC_{50} , in order to account for different toxicity endpoints [26, 69, 127, 176, 177]. One discrepancy that is identified in the literature was the $LC_{50}/IC_{50}/EC_{50}$ notations. For instance, studies provided toxicity values for growth inhibition endpoint for algae and reported them as EC_{50} rather than IC_{50} [178, 179]. Similarly, in some papers, lethal concentrations were reported as EC_{50} rather than LC_{50} [180, 181]. Considering the definition from USEtox, this notation is also acceptable as growth inhibition or lethality indicate effects (i.e. endpoints) [12, 20]. However, the USEtox did not explicitly acknowledged the use of the notations of LC_{50} and IC_{50} in HC_{50} calculation. Therefore, based on the notations provided by the papers, two different scenarios are studied in the current research as regular case (using EC_{50} values only) and cumulative case (using LC_{50} , EC_{50} and IC_{50} values). It should be noted that the toxicity data points that are used for calculating EF for human toxicity impact category include different endpoints, which is excluded herein as the focus of this work is freshwater ecotoxicity.

Another point identified in the literature was the debate on using either species- or trophic-level HC_{50} values. Salieri et al. argued that in order not to put weight on one trophic level that has notably more toxicity data than others, trophic-level HC_{50} should be used [175, 176]. For instance, Salieri et al. calculated EF for nano- TiO_2 , where they had unequal distribution of toxicity data points as 17 for crustaceans, 11 for algae and 2 for fish. Therefore, they assessed both scenarios and concluded that trophic-level HC_{50} calculation reduced the bias resulting from the varying number of toxicity values identified for test species and is more representative [176]. Figures defining the calculation frameworks are provided as Figures C1 and C2 in Appendix C.

USEtox suggests compiling toxicity data for at least three trophic levels including crustaceans, fish, and algae as well as a minimum of three toxicity values associated with each

trophic level [20, 22]. Additionally, USEtox recommends using chronic or sub-chronic species level EC_{50} values to quantify environmental impacts. However, given that acute toxicity values are more commonly studied throughout the literature, it is reported that chronic toxicity values can be estimated from acute values by using acute-to-chronic ratios (ACR) [20]. There are not currently any standardized ACRs developed specifically for ENMs, but current approach is using ACR of 10 for crustaceans, 20 for fish and 15 for all other trophic levels [20, 26, 182, 183]. For reference, Harmon et al. developed ACR of citrate coated nAg using one of the most studied crustacean species, *Ceriodaphnia dubia*, and found that ACRs range from 1.6 (for 20 nm) to 7.6 (for 100 nm) depending on the quantity of food crustaceans are fed. They also mentioned that the ACRs may differ depending on the water characteristics (i.e. having organic contamination) as well as the size and coating of ENMs [184].

USEtox shared duration requirements for toxicity tests to help researchers with the decision making on whether tests can be classified as chronic or acute unless specified [20]. According to the USEtox documentation, durations of chronic testing for invertebrates (e.g. crustaceans) have to be ≥ 21 days, for vertebrates (e.g. fish) ≥ 32 days and for algae ≥ 3 days. For acute toxicity testing, invertebrates and vertebrates have to be tested for less than 7 days and algae for less than 3 days [20]. The durations that fall between these frames are considered as sub-chronic (≥ 7 days, < 32 days for vertebrates; ≥ 7 days, < 21 days for invertebrates) and can be used in HC_{50} calculation without being converted using ACR [20].

In the current research, different scenarios are studied in order to evaluate the previously mentioned considerations applied throughout the literature. Firstly, all toxicity data points are grouped based on the nAg size, coating, and testing environment. As a regular case scenario (RCS), only EC_{50} values are used and species- (SPL) and trophic- (TPL) level HC_{50} s are

calculated for different size and coating pairs in water, mineral and complex media, separately. As a cumulative case scenario (CCS), LC₅₀, EC₅₀ and IC₅₀ values are included and calculations are conducted accordingly. Lastly, all HC₅₀ values are used to calculate size-, coating- and media-dependent EFs.

4.3.2. Ecotoxicity literature

As mentioned in section 4.3.1, USEtox suggests including more than three toxicity (preferably chronic) data for at least three aquatic organisms. Previous studies included three organisms while calculating EFs [25, 69]. In order to account for an additional consideration and fulfill the USEtox requirement, crustaceans, algae, fish and protozoa are included in the current study. In order to compile a dataset for the selected organisms, a comprehensive literature survey is conducted using an academic search engine (Web of Science Core Collection) and Nano E-Tox database [168] by searching combinations of key terms including toxicity, LC₅₀, EC₅₀, acute, chronic, nano silver (search queries can be found in Appendix C). Salieri et al. suggested that in order to collect high-quality toxicity values to calculate EF, well documented studies which report experimental conditions as well as the physicochemical properties of ENMs should be taken into account [22]. Considering this recommendation, toxicity studies that include procedures for standard aquatic toxicity organisms, state chemical composition of test medium and report EC₅₀, LC₅₀ and/or IC₅₀ values are included in the current study [22, 185–188]. Accordingly, data are collected along with details on exposure time and endpoint, nanomaterial size, test media (mineral, complex, etc.), coating (uncoated, citrate, polyvinylpyrrolidone, etc.) and testing method (OECD, EPA, ISO) when applicable. Additionally, toxicity values for ionic

silver are also included in the tables in order to provide information for further toxicity comparison, when provided by the examined papers.

4.3.3. Selection criteria

After identifying relevant studies resulting from the literature review detailed in section 4.3.2, selection criteria are applied to list the ones that are suitable for EF calculation. Figure 17 shows a flowchart that is applied in the current study.

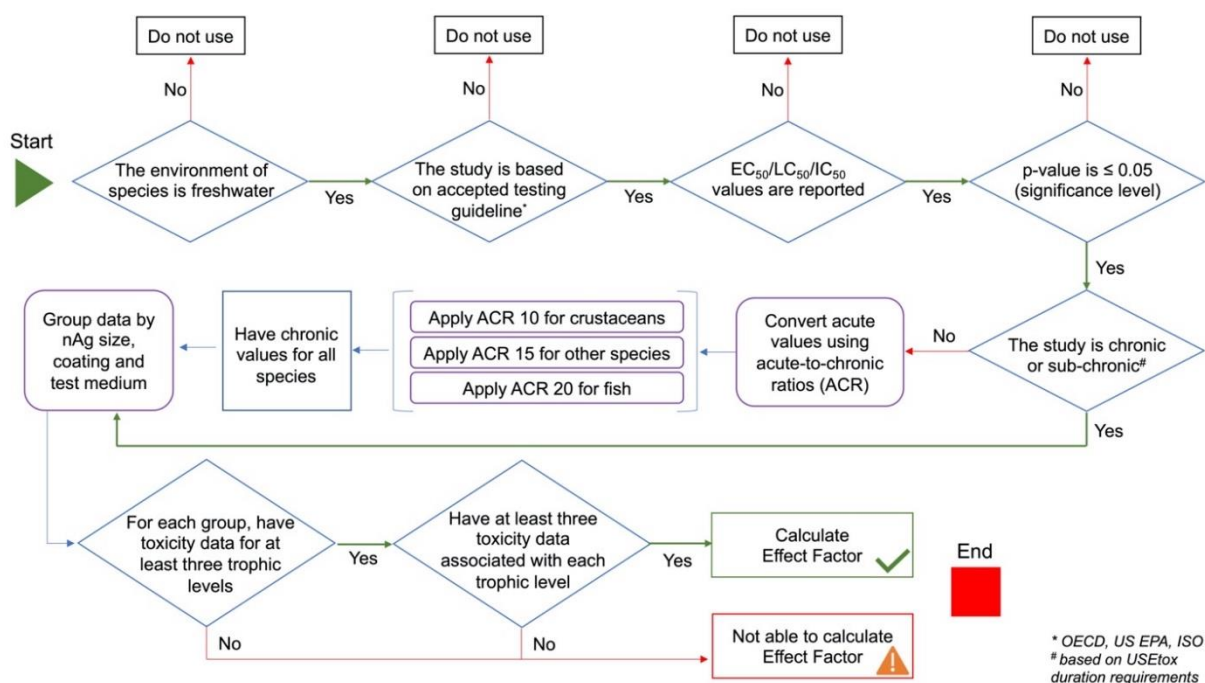


Figure 17. Flowchart of selection criteria for EF calculation applied in this study.

As a first step, the species are identified whether they are freshwater organisms or not. Following this, information on the testing method used in that study is collected when applicable. Toxicity data points ($EC_{50}/LC_{50}/IC_{50}$) and exposure durations are collected from the studies where the p-value was equal or less than the significance level of 0.05. Then, all toxicity data

points are sorted based on the duration of testing in order to distinguish their (sub)chronicity unless specified by the respective studies. Following this step, the toxicity data points that fall under acute group (based on previously specified USEtox durations) are converted to chronic using ACR of 10 for crustaceans, 20 for fish and 15 for all other trophic levels [20]. After having chronic toxicity values, all data points are grouped based on nAg size, coating and test medium. Once there are enough data points in each group (three trophic levels and three toxicity data for each level), EFs are calculated based on different scenarios. It should be noted that, for fish, only *in vivo* studies are considered for EF calculation.

4.3.4. Previous research on nAg-EF

Salieri et al. provided a comprehensive literature review of previously conducted CF research for ENMs [22]. Given that the focus of this work is to develop EF for nAg, only the studies related with nAg are explored in detail. From the survey conducted using Web of Science Core Collection academic search engine, three studies are identified where CFs are derived for nAg freshwater ecotoxicity. For EF calculation, Miseljic and Olsen compiled toxicity information for three trophic levels, in which eight different species were listed along with 21 EC₅₀ values [25]. Different from the recommendation by USEtox, Miseljic and Olsen used an ACR of 2 for all trophic levels. Another study by Garvey et al. included toxicity data points for four phyla along with 73 different toxicity data points including EC₅₀, IC₅₀ and LC₅₀ to calculate the EF [69]. They used an ACR of 10 for all trophic levels and worked on two different scenarios. Lastly, Pu provided EF for nAg using three trophic levels and 61 data points (EC₅₀ and LC₅₀) [189]. It should be highlighted that, these three studies did not account for different properties of nAg, such as size or coating. While the aforementioned studies calculated CFs for

freshwater ecotoxicity, Buist et al. and Salieri et al. developed health EFs (i.e. CFs for human toxicity), which is not the scope of this study and therefore excluded [190, 191].

4.4. Results and discussion

4.4.1. Ecotoxicity literature on nAg

This section provides a summary on the literature survey conducted as detailed in section 4.3.2 It should be noted that different statistical methods are used to calculate LC₅₀, EC₅₀ or IC₅₀ values among the reviewed literature, such as trimmed Spearman–Karber method [192, 193] and probit analysis [194–196]. Potential calculation differences due to the utilization of various statistical programs may slightly affect the final toxicity values. However, these are assumed as negligible and all data are treated as they are equivalently calculated.

As the majority of environmental risk assessment papers indicate, more detailed studies are needed to evaluate the toxicity of nAg; because their size, surface coating and the exposure conditions (i.e. testing environment) significantly influence their toxicity [197–201]. Numerous research suggested that smaller nAg induces a greater toxicity than their large counterparts, as the surface area to volume ratio increases with a decreasing size [202–204]. Moreover, different coatings affect the bioavailability of silver ions released from nAg and the fate and behavior of nAg, therefore the toxicity mechanisms are also affected [205, 206]. For instance, Schiavo et al. found that the coating agent itself was as toxic as the examined nAg on microalgae [207]. Another example may be given from Angel et al., where authors showed that the presence of an organic component (e.g. humic acid) affected the aggregation process and reduced toxicity of nAg on aquatic organisms [208]. As Kleiven et al. mentioned, there are numerous studies that show how ionic strength, organic matter or minerals that are present in the test medium influence

the fate and behavior of nAg. However, as these are studied under controlled laboratory environments, there are still uncertainties on toxicity mechanisms that occur in natural waters [209].

Taking into account all the factors discussed previously, collected data are illustrated based on the size range, type of coating, and test medium. As citrate and polyvinylpyrrolidone (PVP) are listed among the most used coatings in the review by Kalantzi et al., they are presented individually [170]. They also represent examples of anionic and non-ionic capping materials, respectively [210]. Besides citrate and PVP, nAg that are uncoated and coated with other capping agents (e.g. coffee, polyethyleneimine, sodium dodecylbenzene sulfonate, aminated silica, gelatin, lactate, protein etc.) are included in the current research. Figure 18 shows the number of retrieved toxicity data points disaggregated by the test medium, nAg size and coating for crustaceans, algae, fish and protozoa. X-Axis represents the test medium as water, mineral, complex and regardless, where regardless indicates all data independent from the medium (i.e. sum of all mediums).

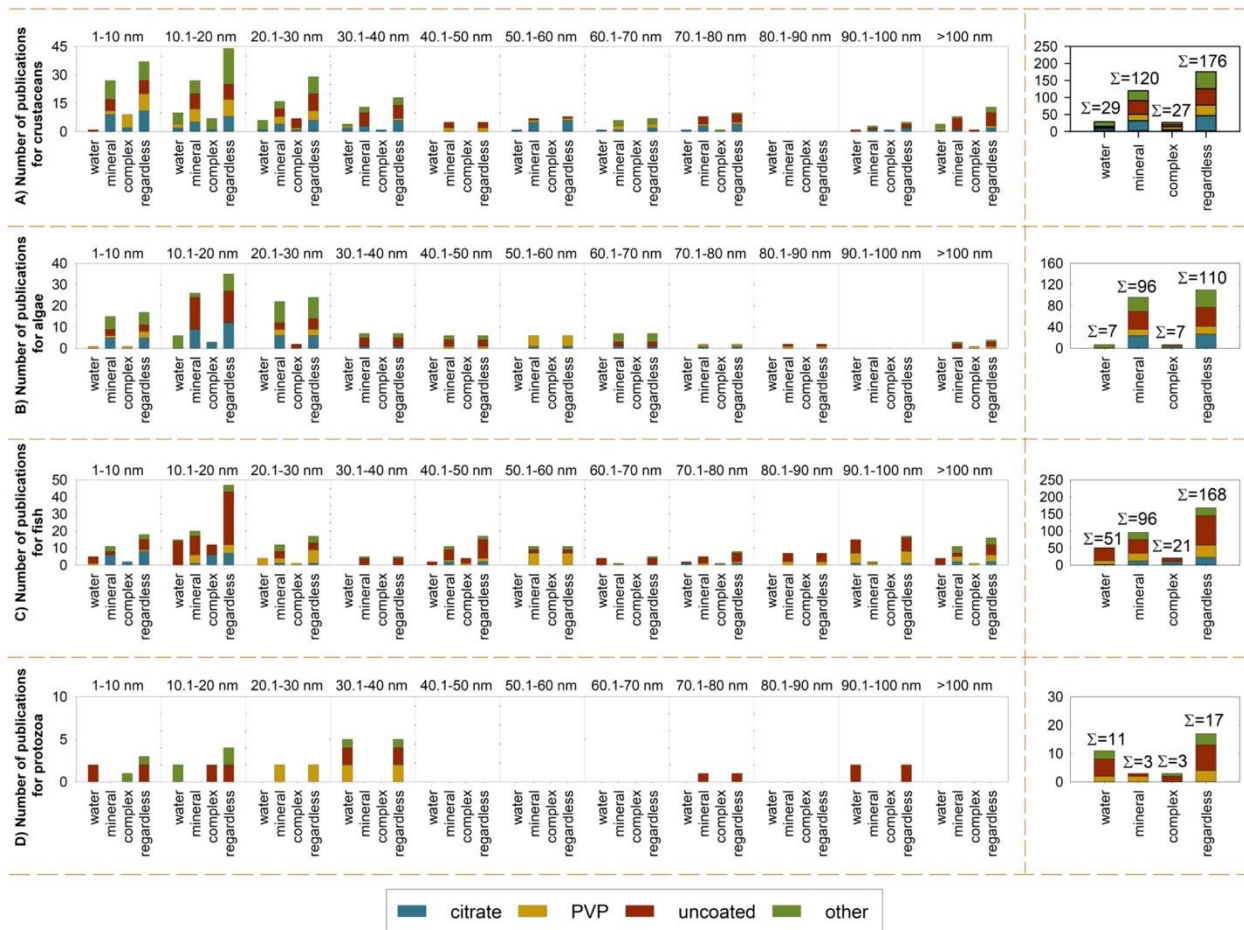


Figure 18. Number of toxicity data disaggregated by the test medium, nAg size and coating for A) crustaceans, B) algae, C) fish and D) protozoa.

At a first glance, it can be seen that the majority of the toxicity tests are conducted in mineral media, following by water and complex environments. As it can be seen from Figure 18A, for crustaceans, most of the studies are conducted for nAg with a size range of 1–40 nm in a mineral medium. Similarly, for algae (Figure 18B), the most studied size range is 1–30 nm and the testing environment is mineral. Considering fish species, most of the toxicity research is conducted for 1–20 nm nAg in water and mineral mediums. Lastly, for protozoa, the toxicity evaluations are conducted in water media for 1–40 nm size range. As Figure 18 shows, toxicity

of nAg that are larger than 40 nm are not well studied for the selected aquatic organisms. In addition, toxicity testing in water and complex mediums are not conducted as much as mineral medium. In terms of coatings, for crustaceans, algae and fish species, citrate, PVP and uncoated nAg are studied dominantly. For protozoa, PVP and uncoated nAg are evaluated mostly. The last column in Figure 18 shows the cumulative literature counts for each aquatic organism.

Regardless of coating, test medium and size, 176 studies for crustaceans, 110 studies for algae, 168 studies for fish and 17 studies for protozoa are identified under the scope of the current study. Additional information may be found on these figures such as the number of papers disaggregated based on test mediums but independent from the coating and nAg size (Figure C3, Table C1). The next subsections show analyses of retrieved toxicity data set for each aquatic organism.

Although 176 data points were identified for freshwater crustaceans from the literature review, selection criteria (based on Figure 17) is applied to specify the data points that are used in EF calculation. As a result of the filtering, 166 data points (143 acute, 17 chronic and 6 sub-chronic) are used in EF calculation for freshwater crustaceans (i.e. 10/176 did not meet the criteria). Similarly, among the 110 data points, only 70 were identified as suitable for inclusion in EF calculation for freshwater algae with 28 acute and 42 chronic toxicity data points (i.e. 40/110 did not meet the criteria). For fish, there were 113 studies (3 sub-chronic and 110 acute) out of 168 that are included for EF calculation as they represent *in vivo* experiments and meet the selection criteria (i.e. 55/168 did not meet the criteria). Lastly, for freshwater protozoa 17 data points were included in the calculation.

4.4.1.1. Crustaceans

From the literature review detailed in section 4.3.2, more than 180 toxicity values are identified for 15 different crustacean species (tabulated in Appendix C as Table C2). Crustaceans are classified according to their habitats (e.g. freshwater or marine) using the Animal Diversity Web and World Register of Marine Species [211, 212]. Figure 19 is a compilation of ecotoxicity values for freshwater crustaceans in a disaggregated format. Additionally, reference lines for toxicity classification are embedded in the figure [213]. These lines represent the criteria developed by US EPA to rank the aquatic toxicity hazards of chemical substances [213].

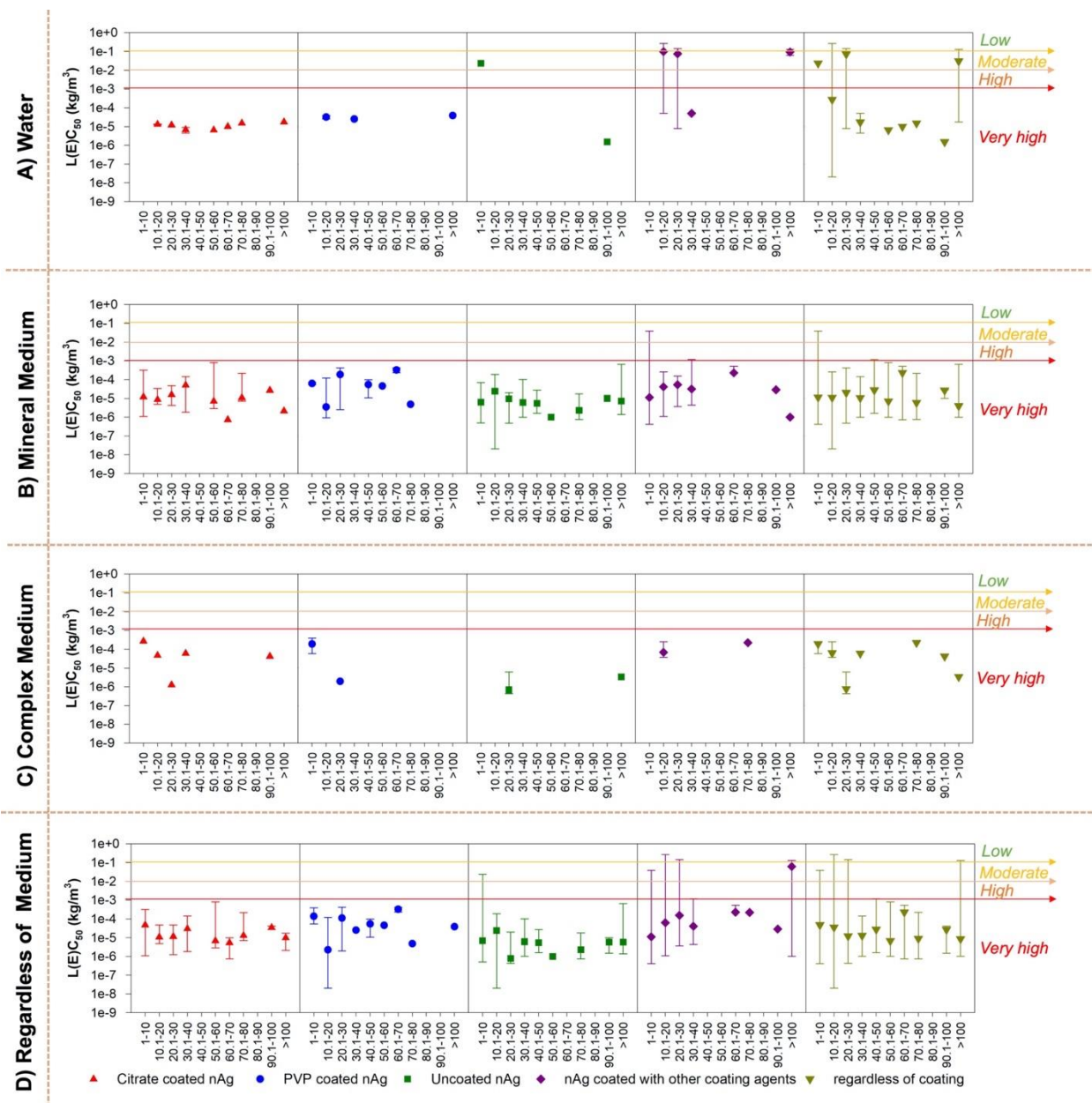


Figure 19. Toxicity data points for crustaceans grouped based on coating and size in A) water, B) mineral medium, C) complex medium, and D) regardless of test medium (upper bound indicates the maximum $L(E)C_{50}$, the marker indicates the median $L(E)C_{50}$ and the lower bound indicates the minimum $L(E)C_{50}$ level for the representative set of data; toxicity ranking based on US EPA is as following: very high: $L(E)C_{50} < 1 \text{ mg L}^{-1}$, high: $1 \text{ mg L}^{-1} < L(E)C_{50} < 10 \text{ mg L}^{-1}$, moderate: $10 \text{ mg L}^{-1} < L(E)C_{50} < 100 \text{ mg L}^{-1}$, and low: $L(E)C_{50} > 100 \text{ mg L}^{-1}$).

As presented in Figure 19, nAg in all size ranges, coatings and test media fall under very high toxic category. Some exceptions are observed, such as protein coated nAg (10–30 nm) which tested in water performed as moderately toxic for crustaceans. However, this does not change the overall trend for nAg as having very high toxicity on crustaceans, which is compatible with the finding by Bondarenko et al. where they found the median L(E)C₅₀ for crustaceans as 0.01 mg L⁻¹ [163]. Additionally, it was observed that the toxicity for uncoated nAg in the majority of size ranges (except 10.1–20 nm) are slightly higher (i.e. lower L(E)C₅₀) than the coated nAg, which corresponds with the finding by Asghari et al [214]. Although the number of toxicity testing in complex test media (i.e. where organic substance is present) is very low comparing to others, general trend in Figure 19C showed that having an organic component in the testing environment contributes to a decreased toxicity value of nAg for crustaceans [215]. As mentioned and illustrated in section 4.4.1, most of the toxicity studies on freshwater crustaceans are conducted in mineral media, which challenges making an overall conclusion on the test media-dependent aquatic toxicity. Despite the number of studies per test medium, median toxicity of nAg for freshwater crustaceans in water is found as 0.038 mg L⁻¹ (very high toxicity), in mineral media as 0.011 mg L⁻¹ (very high toxicity), in complex media as 0.06 mg L⁻¹ (very high toxicity) and overall as 0.018 mg L⁻¹ (very high toxicity), considering all sizes. Additionally, in order to evaluate the impact of size on the toxicity, a trendline is added for the last box of Figure 19D (regardless of test medium and coating). The trendline has a positive slope, meaning that increasing nAg size result in increased L(E)C₅₀ levels and therefore decreased toxicity for crustaceans (Figure C4), which is also suggested by the literature [202].

4.4.1.2. Algae

From the literature review detailed in section 4.3.2, more than 130 toxicity values are identified for 26 different algae species (tabulated in Appendix C as Table C3). Algae are classified according to their habitats (e.g. freshwater or marine) using AlgaeBase [216]. Figure 20 is a compilation of ecotoxicity values for freshwater algae in a disaggregated format.

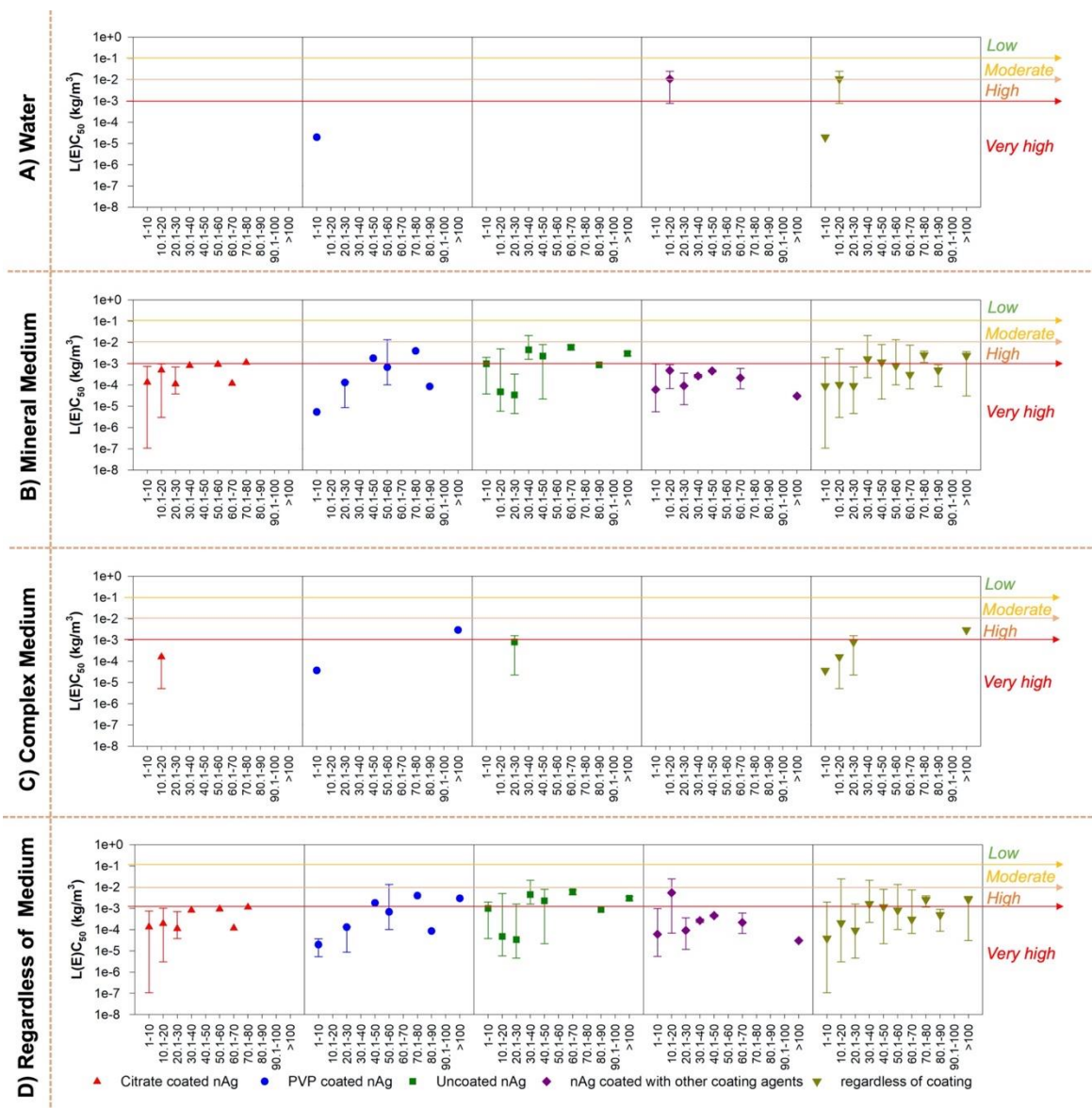


Figure 20. Toxicity data points for algae grouped based on coating and size in A) water, B) mineral medium, C) complex medium, and D) regardless of test medium (upper bound indicates

the maximum $L(E)C_{50}$, the marker indicates the median $L(E)C_{50}$ and the lower bound indicates the minimum $L(E)C_{50}$ level for the representative set of data; toxicity ranking based on US EPA is as following: very high: $L(E)C_{50} < 1 \text{ mg L}^{-1}$, high: $1 \text{ mg L}^{-1} < L(E)C_{50} < 10 \text{ mg L}^{-1}$, moderate: $10 \text{ mg L}^{-1} < L(E)C_{50} < 100 \text{ mg L}^{-1}$, and low: $L(E)C_{50} > 100 \text{ mg L}^{-1}$.

According to the aforementioned categorization scheme, toxicity of nAg for algae ranges from very high to high levels for all size ranges, coatings and test mediums with minor exceptions. For instance, 10–20 nm sized and protein coated nAg that was tested in water was found as moderately toxic for algae rather than being very toxic [206]. Bondarenko et al. included 17 toxicity studies in their review and concluded that nAg is very toxic to algae with a median $L(E)C_{50}$ of 0.36 mg L^{-1} [163]. Although there were not many toxicity data points for nAg in complex medium, it was observed that the toxicity in a medium where organic substances are present is slightly lower than the others. Similarly, research suggested that organic matter help decreasing the surface charge of nAg, which result in development of an electrostatic barrier and limit interactions between particles and algae cells [217]. Like crustaceans, making an overall conclusion based on test media is not possible due to the lack of toxicity studies performed in environments other than mineral. Considering all size ranges and coating types, median toxicity of nAg for freshwater algae in water is found as 10 mg L^{-1} (high toxicity), in mineral media as 0.18 mg L^{-1} (very high toxicity), in complex media as 0.16 mg L^{-1} (very high toxicity) and overall as 0.195 mg L^{-1} (very high toxicity). Additionally, in order to interpret the impact of nAg size on the toxicity, a trendline is added for the data points that are independent from coating and test medium. The trendline gives a positive slope, meaning that increasing nAg size result in decreased toxicity for algae (Figure C5).

4.4.1.3. Fish

From the literature review detailed in section 4.3.2, more than 170 toxicity values are identified for 20 different fish species (tabulated in Appendix C as Table C4). Fish are classified according to their habitats (e.g. freshwater or marine) using FishBase [218]. Figure 21 is a compilation of ecotoxicity values for freshwater fish in a disaggregated format.

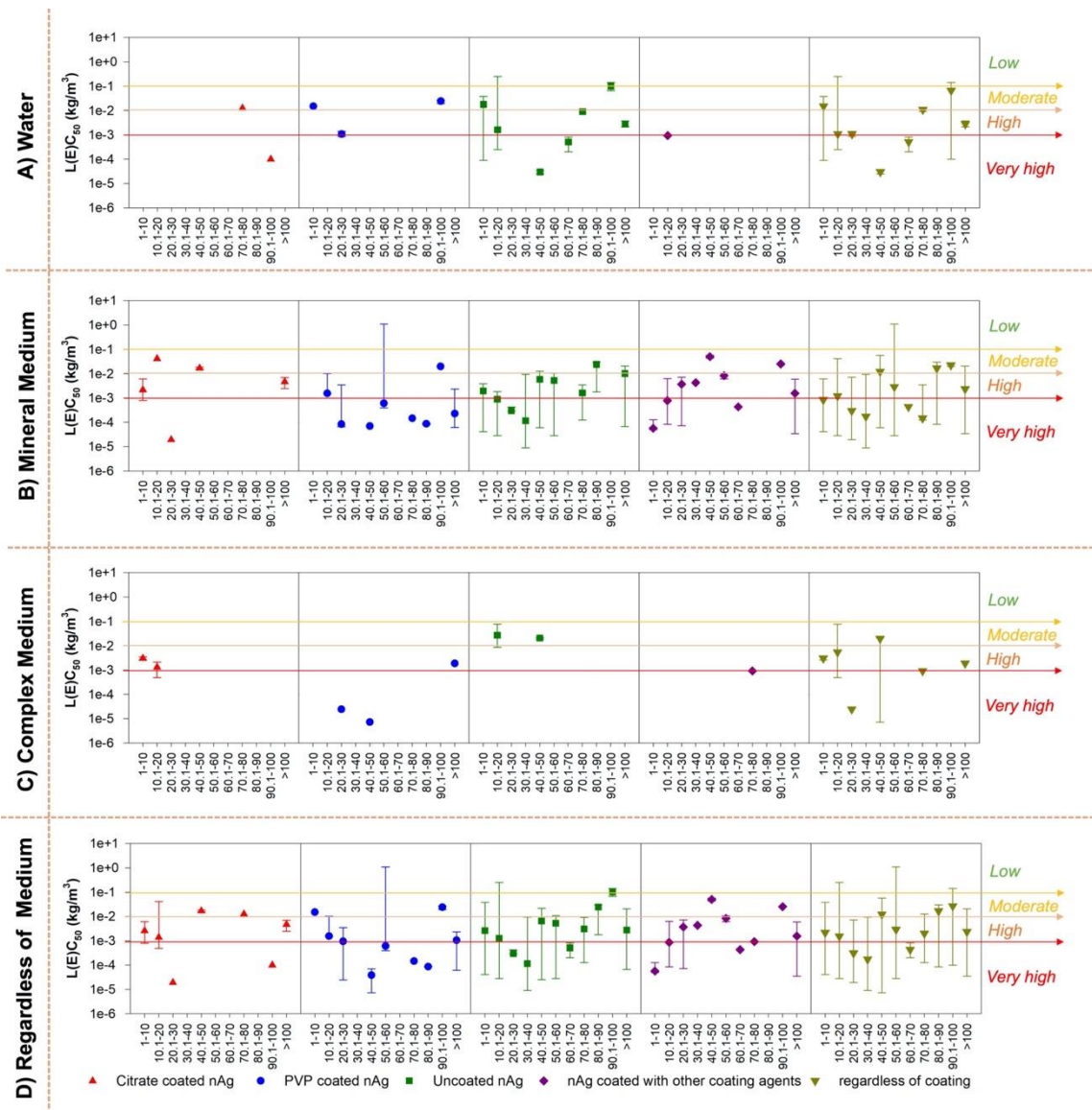


Figure 21. Toxicity data points for fish grouped based on coating and size in A) water, B) mineral medium, C) complex medium, and D) regardless of test medium (upper bound indicates

the maximum $L(E)C_{50}$, the marker indicates the median $L(E)C_{50}$ and the lower bound indicates the minimum $L(E)C_{50}$ level for the representative set of data; toxicity ranking based on US EPA is as following: very high: $L(E)C_{50} < 1 \text{ mg L}^{-1}$, high: $1 \text{ mg L}^{-1} < L(E)C_{50} < 10 \text{ mg L}^{-1}$, moderate: $10 \text{ mg L}^{-1} < L(E)C_{50} < 100 \text{ mg L}^{-1}$, and low: $L(E)C_{50} > 100 \text{ mg L}^{-1}$.

As can be observed from Figure 21, nAg toxicity on freshwater fish ranges from very high to high toxic levels, with the majority of data points being under high toxic category. This finding is compatible with the analysis conducted by Bondarenko et al. where they found the median $L(E)C_{50}$ for fish as 1.36 mg L^{-1} [163]. It is found that the toxicity of nAg on fish is affected by the presence of other contaminants in environment (e.g. organic matter have impacts on the stability and bioavailability of nAg) [217, 219, 220]. The type of fish species is another consideration that needs to be accounted when evaluating the aquatic toxicity. As the majority of nAg in the aquatic environment tend to be present in the sediment, bottom feeding fish might be more susceptible to nAg [44, 219, 221]. However, in Figure 21, toxicity results for all the 20 fish species are plotted equally to present a general framework on the nAg toxicity. Using an aggregated information and including all size ranges and coating types, the median toxicity of nAg for freshwater fish in water is found as 2.75 mg L^{-1} (high toxicity), in mineral media as 1.40 mg L^{-1} (high toxicity), in complex media as 2.6 mg L^{-1} (high toxicity) and overall as 1.8 mg L^{-1} (high toxicity). Similar to the previous aquatic organisms, the impact of nAg size on the fish toxicity is investigated. Figure C6 shows the trendline that has a positive slope, indicating a relationship between size and toxicity that is inversely proportional.

4.4.1.4. Protozoa

From the literature review detailed in section 4.3.2, 18 toxicity values are identified for 6 protozoa species (tabulated in Appendix C as Table C5). Figure 22 is a compilation of ecotoxicity values for freshwater protozoa in a disaggregated format.

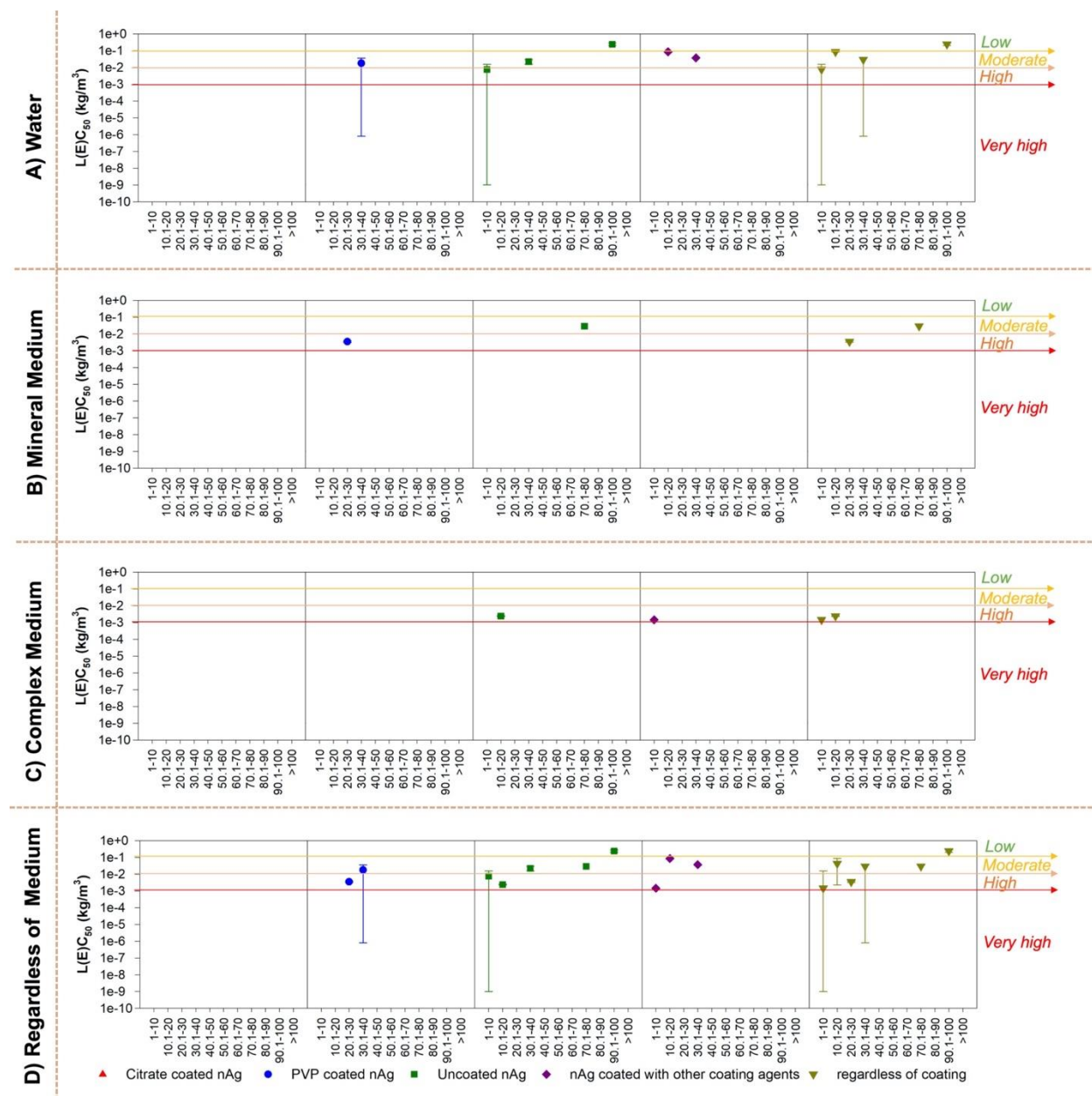


Figure 22. Toxicity data points for protozoa grouped based on coating and size in A) water, B) mineral medium, C) complex medium, and D) regardless of test medium (upper bound indicates

the maximum L(E)C₅₀, the marker indicates the median L(E)C₅₀ and the lower bound indicates the minimum L(E)C₅₀ level for the representative set of data; toxicity ranking based on US EPA is as following: very high: L(E)C₅₀ < 1 mg L⁻¹, high: 1 mg L⁻¹ < L(E)C₅₀ < 10 mg L⁻¹, moderate: 10 mg L⁻¹ < L(E)C₅₀ < 100 mg L⁻¹, and low: L(E)C₅₀ > 100 mg L⁻¹.

Protozoan is one of the key organisms that act as a trophic link in aquatic food chain, i.e. it is consumed by crustaceans and crustaceans are consumed by fish [222]. Although the number of toxicity tests for protozoa is much lower comparing to the previously examined aquatic organisms, they are included in the current research for effect factor calculation. As Figure 22 shows, the majority of nAg toxicity values are either under high or moderately toxic category for protozoa. Despite the lower number of studies, median toxicity of nAg for freshwater protozoa in water is found as 36 mg L⁻¹ (moderate toxicity), in mineral media as 3.9 mg L⁻¹ (high toxicity), in complex media as 2.34 mg L⁻¹ (high toxicity) and overall as 16 mg L⁻¹ (moderate toxicity), considering all sizes and coatings. Bondarenko et al. found slightly different value than the current work. The median L(E)C₅₀ for protozoa on compound basis was reported as 38 mg L⁻¹ considering 7 data points [163]. Similar to previous trophic levels, size dependent nAg toxicity is evaluated by drawing a trendline on median toxicity data (Figure C7), which also showed an inverse proportion between size and toxicity levels.

4.4.2. Ecotoxicity literature on ionic silver

In the majority of toxicity literature, it is suggested that ionic silver (Ag⁺) is more toxic than nAg [69, 163, 167, 202, 223, 224]. In order to investigate whether the testing environment has any impact on this finding or not, toxicity data points for Ag⁺ are also included in the current study. Figure 23 shows L(E)C₅₀ values for Ag⁺ for crustaceans, algae, fish and protozoa. Given

that the toxicity values for Ag^+ are developed using silver nitrate, size and coating are not considered as physicochemical parameters in this case. However, data are presented in a disaggregated format using different test mediums. Similar to previous figures, ‘regardless’ category includes all of the data for the respective aquatic organism independent from the test media (i.e. all of the collected $L(E)C_{50}$ values) and reference lines for toxicity classification are embedded in the figure [213].

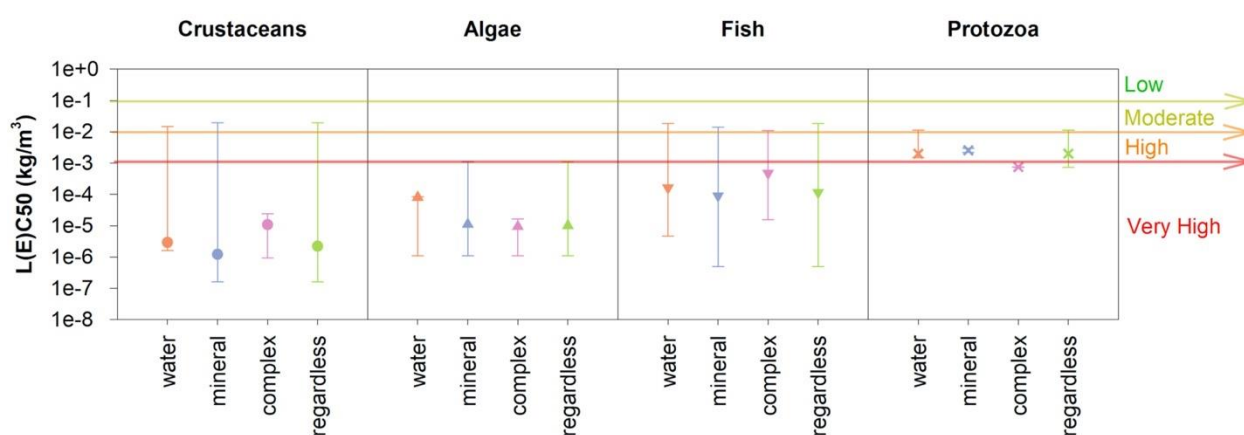


Figure 23. Toxicity data points for ionic silver on the aquatic organisms in water, mineral medium, complex medium, and regardless of test medium (upper bound indicates the maximum $L(E)C_{50}$, the marker indicates the median $L(E)C_{50}$ and the lower bound indicates the minimum $L(E)C_{50}$ level for the representative set of data; toxicity ranking based on US EPA is as following: very high: $L(E)C_{50} < 1 \text{ mg L}^{-1}$, high: $1 \text{ mg L}^{-1} < L(E)C_{50} < 10 \text{ mg L}^{-1}$, moderate: $10 \text{ mg L}^{-1} < L(E)C_{50} < 100 \text{ mg L}^{-1}$, and low: $L(E)C_{50} > 100 \text{ mg L}^{-1}$).

Median toxicity of Ag^+ for freshwater crustaceans in water is found as 0.003 mg L^{-1} (very high toxicity), in mineral media as 0.001 mg L^{-1} (very high toxicity), in complex media as 0.011 mg L^{-1} (very high toxicity) and overall as 0.002 mg L^{-1} (very high toxicity). Similarly, for

algae, the L(E)C₅₀ levels fall under extremely toxic level with 0.08 mg L⁻¹, 0.011 mg L⁻¹, 0.09 mg L⁻¹ and 0.01 mg L⁻¹ for water, mineral, complex and all mediums, respectively. For fish, the toxicity levels show that Ag⁺ has very high toxicity in all mediums (water: 0.163 mg L⁻¹, mineral: 0.09 mg L⁻¹, complex: 0.476 mg L⁻¹, regardless: 0.115 mg L⁻¹). Lastly, for protozoa, median toxicity level in water is calculated as 2 mg L⁻¹ (high toxicity), in mineral media as 2.54 mg L⁻¹ (high toxicity), in complex media as 0.745 mg L⁻¹ (very high toxicity) and considering all L(E)C₅₀ levels regardless of media as 2 mg L⁻¹ (high toxicity). Overall, it may be concluded that the toxicity potential of Ag⁺ in mineral media is the highest one among others. Similarly, Bondarenko et al. reported that Ag⁺ is extremely toxic for all the selected aquatic organisms except protozoa, which fall under very high/high toxicity levels. The same descending order was mentioned for Ag⁺ toxicity on crustaceans, algae, fish and protozoa with median L(E)C₅₀ levels of 0.00085 mg L⁻¹, 0.0076 mg L⁻¹, 0.058 mg L⁻¹ and 1.5 mg L⁻¹, respectively [163].

4.4.3. Effect factor calculation

As mentioned in section 4.3.1, USEtox requires toxicity data for at least three trophic levels along with a minimum of three toxicity values associated with each trophic level. Due to the insufficient number of studies in the majority of size-coating-test medium pairs, effect factors could not be calculated for all of the combinations. Matrices are developed for each option and are included in Appendix C (Figures C8–C12). These matrices are intended to inform research on the EFs for nAg that has specific physicochemical properties. It should be noted that high EF contributes to a higher characterization factor, which eventually defines the freshwater ecotoxicity potential. For instance, considering SPL-RCS scenario, 10.1–20 nm and uncoated nAg in mineral media has an EF of 50,754 PAF m³ kg⁻¹. The EF decreases up to 18,089 PAF m³

kg^{-1} when SPL-CCS scenario is applied. TPL-RCS and TPL-CCS are performed higher EFs for the same size-coating-test medium pair as 48,846 $\text{PAF m}^3 \text{kg}^{-1}$ and 78,107 $\text{PAF m}^3 \text{kg}^{-1}$, respectively. Additionally, cross comparison of EFs are also available using the information from matrices. For example, considering data points collected for all test media, 1–10 nm sized and citrate coated nAg has higher effect factor than same sized and uncoated nAg ($\text{EF}_{\text{SPL-CCS}}$: 21,977 $\text{PAF m}^3 \text{kg}^{-1}$ and $\text{EF}_{\text{SPL-CCS}}$: 7,887 $\text{PAF m}^3 \text{kg}^{-1}$ respectively), which means that citrate coated nAg that have this size range are potentially more impactful when released to the environment than uncoated nAg.

Since size range dependent data were not sufficient for EF calculations for most of the combinations, additional calculations were included such as coating and test medium dependent EFs regardless of size. Figure 24 shows EFs that are calculated using available data per coating and testing environment. An additional EF calculation is performed based on nAg size but independent from coating and test medium, which is included as Figure 24F.

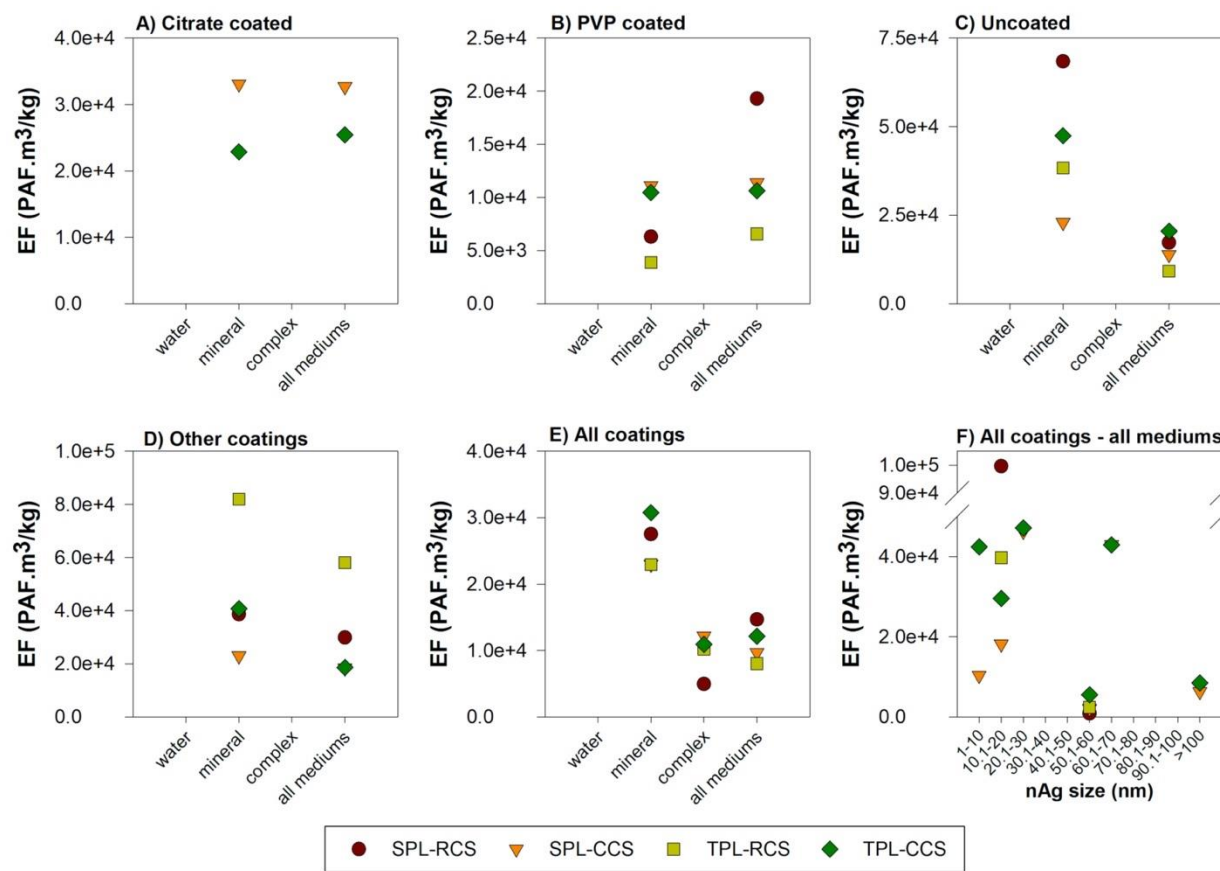


Figure 24. Effect factors for freshwater ecotoxicity impact category under different scenarios A) citrate coated, B) PVP coated, C) uncoated, D) coated with other agents, E) all coatings, F) all coatings and all test mediums but disaggregated based on size.

Previous studies on CF for nAg resulted a wide range of EFs, which are independent from physicochemical characteristics of the examined nAg. The EF developed by Miseljić and Olsen was 8,576 PAF m³ kg⁻¹ [25]. Pu included species level and trophic level calculations and included L(E)C₅₀ values in both cases. For trophic level, Pu calculated the EF as 14,502 PAF m³ kg⁻¹ and for species level as 16,030 PAF m³ kg⁻¹ [189]. Another study by Garvey et al. worked on two different scenarios and one of them was an equivalent of what the current study defines as SPL-CCS, which resulted an EF of 13,497 PAF m³ kg⁻¹. The other scenario was developing the EF using the most sensitive end points for the considered organisms, which resulted in a

significantly higher EF of 281,144 PAF m³ kg⁻¹ [69]. EFs reported in the last column of Figure 24E (all mediums) are the ones that are comparable with previous literature as they are independent from size and coating. Although the currently developed EFs are on the same order of magnitude with the previous literature, they slightly differ considering different scenarios (EF_{SPL-RCS}: 14,675 PAF m³ kg⁻¹; EF_{SPL-CCS}: 9,679 PAF m³ kg⁻¹; EF_{TPL-RCS}: 8,035 PAF m³ kg⁻¹; EF_{TPL-CCS}: 12,130 PAF m³ kg⁻¹). In most of the cases for species level calculation, EFs that are generated based on cumulative scenario are found to be lower than regular scenario. Conversely in the majority of trophic level calculations, effect factors that are generated based on regular scenario (i.e. EC₅₀ only) are found to be lower than cumulative scenario (i.e. EC₅₀, LC₅₀ and IC₅₀). As per species level and trophic level EF comparison, for most of the coating dependent cases TPL performed lower EF then SPL, which was also suggested by Salieri et al. in their nano-TiO₂ study [176]. The effect factor of 10.1–20 nm sized nAg based on species level regular case scenario is found to be significantly higher than the other scenarios due to the inclusion of a very low chronic toxicity value (2.00×10^{-8} kg m⁻³) based on a single species [225, 226]. When excluded, the corresponding species level EF decreases from 99,608 to 53,909 PAF m³ kg⁻¹ (46% decrease) and trophic level EF decreases from 39,755 to 34,339 PAF m³ kg⁻¹ (14% decrease). This also suggests that using trophic level EF calculation should be preferable as excluding/including data points that belong to different species would be treated equally with other data points regardless of the number of data points excluded/included. In other words, species level data availability has a significant impact on EF. For instance, if very few studies are available that belong to a single species in the same trophic level, these data points may skew the results.

Finally, as size and level of toxicity are proved to be inversely proportional for nAg, size dependent EFs regardless of the coating and test environment are developed and presented in Figure 24F. It is expected that smaller sized nAg should have higher EFs, which contribute to higher CF for freshwater ecotoxicity potential. In order to assess the relationship between size and EF, trendlines for each scenario (SPL-RCS, SPL-CCS, TPL-RCS, TPL-CCS) are drawn. Although individual comparisons do not show a clear pattern (e.g. 10.1–20 nm nAg has lower EF than 20.1–30 nm nAg), slopes of the trendlines are negative which means EFs decrease when size range increases (Figure C13). This supports the knowledge of small sized nAg being more toxic to the environment.

4.4.4. Discussion and implications

As argued by Salieri et al., there is a knowledge gap on the potential risks of released ENMs, which causes several uncertainties in LCA results [22]. ENMs can be released from manufacturing (including purification), use and end-of-life stages of nano-enabled consumer products, which affects the overall environmental and human health implications of that particular product [13]. A comprehensive assessment is needed to evaluate the environmental impacts of such products as there are both advantages and detriments of nanoenabling process, e.g. nAg enabled textiles offer less frequent laundering compared to conventional textiles but there is an additional step for nAg manufacturing and a risk for nAg release [60]. As previously discussed, to date, most of the LCA studies excluded the potential impacts resulting from ENMs release, which can be one of the main environmental burdens for an advanced product. Calculating CFs and combining them with potential release patterns will help evaluating the environmental and human health performances of ENMs and/or nano-enabled products in a

holistic way. For instance, Eckelman et al. developed CFs for CNTs that they produced, and found that the life cycle impacts of CNTs production are significantly higher than the impacts resulting from their release [127]. Particularly for nAg, given that they undergo various transformations depending on the release media, calculating CFs and combining them with release patterns will help modeling nano-specific emissions. These then can be combined with conventional LCA results (i.e. non-nanoscale) to conduct a comprehensive impact assessment.

Results of the current study support the previous findings on nAg toxicity, especially the inverse proportion between size and the level of toxicity as well as the potential impacts that coatings may have on the toxicity. As presented earlier, EF decreases when the size of nAg increases, and coating and testing environment have large impact on the results. However, it is found that the literature on toxicity data for nAg in relatively larger sizes (>30 nm) are not broadly studied, which challenges the coating and size dependent EF interpretation, i.e. the majority of cells in matrices cannot be filled as there are not enough data points for specific coating-size-medium pairs (Figure C8–C12). Another finding is the relatively low number of toxicity experiments that are conducted in water and complex mediums compared to mineral. This consideration effects drawing a conclusion about the toxicological impact of nAg in water. More toxicological research is needed to fill these gaps, which then will be used to calculate physicochemical property based EFs for all size ranges, coating options and mediums. It should be noted that, the same methodology that is applied in the current study can be used to collect and handle the physicochemical property based toxicity data points and calculate the specific EFs for different nanomaterials.

EFs that are calculated in the current study can be directly used in any nAg freshwater CF development research. EFs for a certain size-coating-medium combination (when available) can

be paired with XF and FF of interest, and CFs can be calculated. Following this, the calculated CF can be coupled with the mass of nAg released in order to assess the freshwater ecotoxicity potential resulting from the direct (i.e. nano specific) impacts. In other words, physicochemical property based EFs obtained from this present study can be used in modeling impacts resulting from direct release which can be coupled with impacts resulting from raw materials acquisition, production, use and end-of-life [126]. With this, a comprehensive impact assessment (i.e. resulting from both direct and indirect impacts) to evaluate the environmental performances of nAg and/or nAg enabled consumer products can be achieved. Further, these results can be used to estimate the industry-based impacts and to project the overall environmental performances of the sectors where nAg are used (e.g. medical).

4.5. Conclusion

In the current study EFs are calculated using the previously published toxicity data for nAg. Toxicity values of nAg on the selected aquatic organisms are evaluated considering different properties such as size and coating, and test media. The number of toxicity literature was not uniformly distributed for each option (i.e. size-coating-test medium combination). Considering all the data collected from the literature, regardless of size, coating and test media, nAg showed the highest toxicity to crustaceans with median L(E)C₅₀ value of 0.018 mg L⁻¹ (very high toxicity). Algae, fish and protozoa follow crustaceans with median L(E)C₅₀ values of 0.195 mg L⁻¹ (very high toxicity), 1.8 mg L⁻¹ (high toxicity) and 16 mg L⁻¹ (moderate toxicity) respectively. In different test mediums this sequence changed slightly. For instance, in water, the rank from the highest to the lowest toxicity was crustaceans > fish > algae > protozoa; while in complex medium it was crustaceans > algae > protozoa > fish. Collected LC₅₀, EC₅₀ and IC₅₀

values are used to develop physicochemical property (e.g. size, coating) based EFs for nAg. It is found that coating and size affect the overall toxicity of nAg. However, it should be noted that the EF does not recommend the level of freshwater ecotoxicity of a particular nAg, as CF needs to be calculated by incorporating FF and XF factors in addition to EF. In other words, duration that nAg resides in a specific environmental compartment (i.e. FF) as well as dissolved and bioavailable fraction of nAg (i.e. XF) are important considerations when calculating the potential nano-specific impact. EFs developed in the current study can serve as reference values for nano-specific CF calculation. Researchers can pick the EF for their particular sized/coated nAg and incorporate that with the specific fate and exposure patterns that belong to their own environmental model. As mentioned before, there were insufficient number of studies in the majority of size-coating-test medium pairs, therefore, more toxicity research is needed in order to fill these gaps. Future work should develop CFs by incorporating fate and exposure mechanisms for a more thorough evaluation.

4.6. Acknowledgements

Support for this research was provided by the University of Wisconsin – Madison Office of the Vice Chancellor for Research and Graduate Education with funding from the Wisconsin Alumni Research Foundation (WARF). We would like to thank the anonymous reviewers for their time and insightful comments. This work has not been formally reviewed by the WARF, and the findings presented by the authors are their own.

5. Developing physicochemical property-based ecotoxicity characterization factors for silver nanoparticles under mesocosm conditions for use in life cycle assessment

The following chapter has been submitted for consideration for publication with the citation:

Temizel-Sekeryan, S.; Hicks, A.L., Developing physicochemical property-based ecotoxicity characterization factors for silver nanoparticles under mesocosm conditions for use in life cycle assessment.

The article appears as submitted, although style and formatting modifications have been made.

Authorship contribution statement

Sila Temizel-Sekeryan: Designed Research, Performed Research, Analyzed Data, Wrote the Paper.

Andrea L. Hicks: Designed Research, Wrote the Paper.

5.1. Abstract

Global production and consumption of silver nanoparticles (nAg) are forecasted to increase due to their applications in modern technologies. This situation raises concerns related to their environmental and human health consequences, as nAg potentially will be released to the environment during and/or at the end of the product life cycles. Environmental impacts due to nAg production (i.e. non-nanoscale emissions) are widely examined throughout the literature using cradle-to-gate life cycle assessments. However, calculating nano-specific emissions resulting from nAg release is occasionally overlooked, or modeled as ionic silver, due to the lack of characterization factors (CF) to define the follows of impact. The current study seeks to calculate CFs for nAg by combining the principles of colloidal science with the USEtox model to be integrated to cradle-to-grave life cycle assessments. In order to control the variables while modeling fate and behavior of nAg, data from mesocosm conditions are used. Effect and fate factors for CF are calculated considering certain physicochemical properties of nAg in the mesocosm and the composition of aquatic media. Additionally, two different scenarios are computed where the hetero-aggregation is modeled as either removal or transformation process, which significantly changes the final results. Considering different scenarios, a CF range is proposed as $2.19 \times 10^3 - 2.34 \times 10^5$ PAF.m³.day/kg for polyvinylpyrrolidone coated nAg. Moreover, as a result of sensitivity analysis, it is found that the characteristics of the suspended particulate matter largely affect the fate of nAg under both scenarios. Results suggest that using ionic silver to model nAg release will potentially overestimate the environmental impacts.

5.2. Introduction

Silver nanoparticles (nAg) are one of the most used engineered nanomaterials (ENMs) in various consumer products mainly due to their antimicrobial and antibacterial characteristics [1, 7, 60]. They are mostly utilized in the medical industry, followed by textiles, cosmetics, home appliances among other industries [60]. Global production mass and the market value of nAg are expected to increase considerably by 2025 [126, 227]. This suggests that the utilization of nAg in consumer products with several modern technological applications may be advanced accordingly. Although enabling with nAg offers benefits to the consumer products, it will also add burdens to the environment such as impacts resulting from the manufacturing of nAg or the potential release of nAg to air, soil or water [60].

Life cycle assessment (LCA) is a commonly used methodology to investigate the environmental impacts of a product or process [15, 16]. Several papers have been published that reviewed the LCAs implemented for ENMs as well as for nAg [22, 60, 126]. One of the gaps identified by these papers was the lack of characterization factors (CF) to model the release of nAg. Previous LCA studies modeled direct impacts resulting from the nAg release as ionic silver (Ag^+), which potentially resulted in underestimations or overestimations of the impact [38, 58, 60, 65]. In order to develop CFs for ENMs, nano-specific effect factor (EF), fate factor (FF) and exposure factor (XF) are needed to be calculated for the material of interest in a specific environmental media. Section 5.3 of the current study provides a comprehensive background information for developing CFs.

Numerous papers have been broadly reviewed the behavior and potential impacts of ENMs in aquatic environments as well as indicated challenges regarding fate modeling [129, 228–239]. Suhendra et al. grouped the existing environmental exposure models for ENMs under

three classes as material flow analysis models, multimedia compartmental models (e.g. MendNano, SimpleBox4Nano) and spatial river/watershed models (e.g. Nano DUFLOW) [237]. All these models incorporate different fate processes such as dissolution, aggregation and sulfidation. Further, Mortimer and Holden listed and explained the potential fate processes for ENMs in natural environments including agglomeration, dissolution, chemical transformation, nanoparticle formation, sorption of biomolecules, interactions with other contaminants, transformations at the biological receptors and uptake by biota, trophic transfer, degradation and aging [240].

Research suggests that, fate and behavior of ENMs highly depend on the physicochemical properties of ENMs (e.g. size, coating) as well as the environmental conditions (e.g. the level of salinity, organic contamination) [155, 162, 205, 241]. For instance, Li et al. evaluated the potential risks of nAg in different natural aquatic systems and concluded that nAg in freshwater systems is much harmful than nAg in brackish or seawater, due to the inverse proportion between salinity levels and the potential risk of nAg [242]. Besides the characteristics of aquatic environment, information on the initial material properties (e.g. concentration, primary particle size, specific surface area and surface charge) is needed in order to investigate potential behaviors of nAg in environments of interest [243]. Therefore, developing CFs by using predetermined (i.e. generalized) parameters would not be representative. In order to overcome this challenge, in the current study, CFs are developed for nAg using mesocosm conditions. Mesocosms are simulations of aquatic ecosystems under controlled conditions, which help predicting nanomaterial interactions with the environment [129, 244, 245]. Geitner et al. and Stegemeier et al. has published a number of studies on the fate and behavior of nAg under simulated wetland environments, which are utilized to inform this work [246–248].

The goal of this study is to calculate freshwater ecotoxicity CFs for specific sized and coated nAg in a specific environment (i.e. mesocosm) to inform future environmental impact assessment research. Section 5.3 provides contextual information for developing CFs including the considerations for its components, EF, FF and XF, respectively. The current understanding of fate descriptors is also discussed in section 5.3, and the previous literature that calculated CFs for nAg are also summarized. Section 5.4 presents the materials and methods used in the current study, including separate sections for each CF component (i.e. EF, XF, FF) and subsections for relevant processes for calculating FFs. Section 5.5 demonstrates the results and discusses the relevance of the findings for usage in LCAs. Finally, section 5.6 provides the key results of this work and presents the plans for future work.

5.3. Background information for characterization factors

In LCA, the potential impact, or impact scores, of a product/process can be calculated using eqn (5.1),

$$I^i = \sum_{xm} CF_{xm}^i * M_{xm} \quad (5.1)$$

where (x) is the substance of interest, (i) is the impact category of concern, (m) is the media, I^i is the potential impact of (x) for (i), CF_{xm}^i is the characterization factor for (x) emitted to (m) for (i), and M_{xm} is the mass of (x) emitted to (m) [18, 160]. The USEtox model is a recommended for quantifying freshwater ecotoxicity and human toxicity potentials of chemicals in order to be used in LCAs [23, 161]. USEtox calculates CF using eqn (5.2),

$$CF = EF * FF * XF \quad (5.2)$$

where EF is effect factor (PAF.m³/kg), FF is fate factor (day) and XF is exposure factor (%). In the subsequent subsections, the ongoing debate of utilizing the USEtox model for ENMs is

discussed in detail and the three components of CFs are defined. Moreover, Table D1 in the Appendix D presents a summary of previously published studies that developed freshwater ecotoxicity CFs for different ENMs, along with details on considerations and assumptions made. It should be noted that calculation methods for each factor (EF, FF and XF) are discussed separately in section 5.4.

5.3.1. Effect Factor (EF)

Effect factor (EF) represents the toxicological impact of ENMs on the ecosystem, with a unit of $\text{PAF}\cdot\text{m}^3/\text{kg}$ (PAF: potentially affected fraction). In other words, EF is the slope of the concentration – response plot when 50% of the population is affected [26]. For freshwater ecotoxicity category, EF is calculated using toxicological data for aquatic organisms, typically chronic effective concentrations [20]. Numerous papers have been published to investigate the impact of physicochemical properties (such as size and coating) of ENMs on their toxicity [163, 167, 168]. It was concluded that the specific properties have significant impacts on the effective (EC_{50}), lethal (LC_{50}) or inhibitory (IC_{50}) concentrations of the ENMs. For instance, considering nAg, Ivask et al. found that the toxicity of nAg is inversely proportional with the particle size, and Asghari et al. argued that the toxicity of uncoated nAg is slightly higher than the coated ones [167, 214]. Therefore, incorporating the physicochemical properties of ENMs in EF calculations is critical, which has not been applied in the previously developed CFs (Table D1).

5.3.2. Fate Factor (FF)

The FF represents the duration that an ENM resides in a specific environmental compartment such as air, water or soil, and is presented in days [20, 23, 24]. There are various

factors that need to be taken into consideration while calculating the FF. Miseljic and Olsen provided a comprehensive literature review and listed the physicochemical properties of ENMs that drive their fate and behavior. They also suggested various potential environmental pathways that affect the toxicological impact characterization of ENMs. Figure 25A is a summary derived from multiple sources that identified the factors considered while calculating FF [23, 25, 129, 155, 174]. It should be noted that the conditions of the environmental compartment (e.g. presence of organic matter, pH, ionic strength) are also relevant factors that affect the fate as they interact with the surface properties of ENMs [174, 229]. Therefore, physicochemical property based FFs should be calculated specifically for the release media of interest, i.e. case by case evaluation is needed.

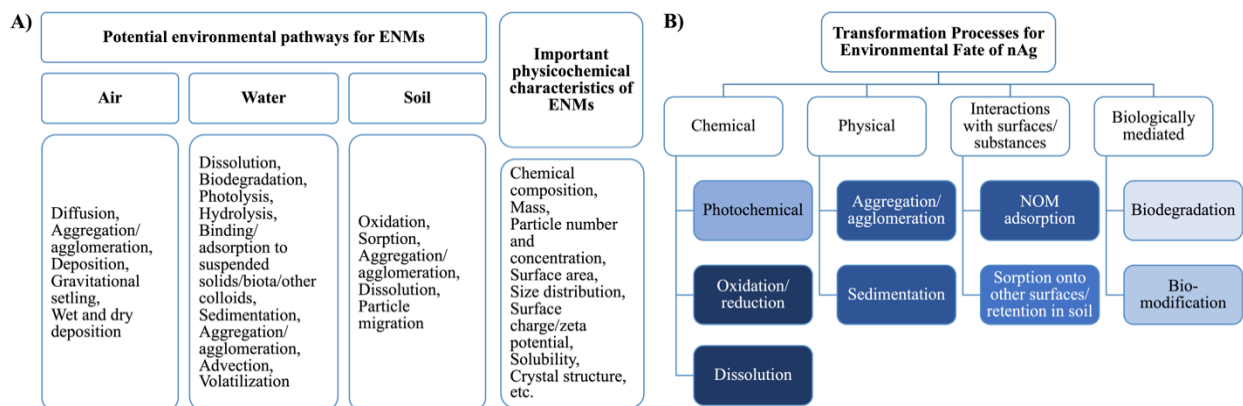


Figure 25. A) Potential environmental pathways for nanomaterials and physicochemical characteristics of ENMs that affect fate factors [23, 25, 129, 155, 174] B) Relative importance of potential transformation processes in modeling environmental fate of nAg (darker shades indicate higher importance) [129, 249].

As the current paper aims to develop freshwater ecotoxicity CF for nAg, studies that define fate and behavior of nAg are reviewed and factors affecting the fate of nAg are listed

[129, 174, 235, 249–253]. Figure 25B shows the processes that are relevant to nAg and illustrates the relative importance of these processes using a color scheme [129]. Throughout the literature, it was found that nAg go through several transformation processes depending on their physicochemical characteristics as well as the properties of the release media with dissolution, oxidation/reduction and aggregation/agglomeration being the most dominant ones among others. Hartmann et al. argued that as nAg are unstable in the presence of light, photochemical transformation process may be neglected. Also, as being an inorganic ENM, the biodegradation of nAg is not expected to be as relevant as the previously mentioned processes [249]. Peng et al. and Peijnenburg et al. provided comprehensive assessments on each of the potential environmental transformation process and the impacts of different conditions on those processes [234, 235]. For instance, after explicitly defining the dynamics of aggregation of metallic ENMs, effects of size, shape, surface coating, pH, ionic strength and presence of organic matter on aggregation are elaborated in detail [234–236].

5.3.2.1. Current understanding of fate descriptors

Currently, there is an evolving debate on the approach used to model fate and behavior of ENMs in the aquatic environments. One approach uses equilibrium partitioning coefficients (K_P) (i.e. mass flow-based model) and the other uses colloidal science (i.e. particle-number based kinetic model). As being the recommended model for use in LCAs, USEtox uses substance specific data, including K_P (e.g. K_P between dissolved organic carbon and water, K_P between suspended solids and water etc.) among others, to model the fate of chemicals in aquatic environments [20, 161]. Conversely, research advised that, ENMs are thermodynamically unstable and their behaviors are controlled by colloidal science rather than equilibrium

assumptions [254–256]. In other words, the surface chemistries of ENMs control the previously mentioned potential transformation processes (e.g. aggregation, sedimentation etc.), therefore instead of K_{ps} , first order kinetics are believed to be more representative for modeling fate of ENMs [22, 244, 254, 255, 257].

Numerous studies have been published where researchers used/suggested using the USEtox framework (i.e. equilibrium partitioning coefficients) [127, 128, 258, 259] or colloidal science [26, 176, 182, 260–262] in order to model the fate of the respective ENMs. While studies tend to prefer one method over another, research suggested that fate models should incorporate both methods to fully cover the behaviors of ENMs [263, 264].

5.3.3. Exposure Factor (XF)

Exposure factor (XF), a dimensionless component of CF, is defined as the bioavailable fraction of a chemical in water [23, 24]. For freshwater ecotoxicity, impacts on biota may occur through invertebrate uptake, plant uptake and bioaccumulation, and microbial interactions [25]. As mentioned previously, the USEtox model is developed primarily for inorganic and organic substances. Therefore, it is believed that the current definition of XF does not fully cover the properties of ENMs [12, 22, 189]. Research suggested that in order to calculate the XF for ENMs, the distinction of soluble and insoluble ENMs should be made to identify respective transformation processes [265]. According to Jacobs et al., ENMs in any form (i.e. dissolved, free, pristine, hetero-aggregated) that are smaller than 450 nm in size should be considered as bioavailable [266]. In their review paper, Salieri et al. recommended that toxicity studies should consider reporting the bioavailable fraction of ENMs in order to overcome this uncertainty in developing CFs [22]. The majority of the published CF papers as summarized in Table D1

assumed a precautionary XF as 1 (i.e. 100% bioavailable). Another approach was conducting Monte Carlo simulations using published partitioning coefficients; however, given that ENMs form thermodynamically unstable suspensions, this approach has not been applied widely [127, 267].

5.3.4. Review of characterization factor literature for nAg

In order to explore the previous studies that calculated CFs for nAg, a literature survey is conducted by using an academic search engine, Web of Science Core Collection, by searching combinations of key terms including characterization factors, nanomaterial, nanosilver and nanosilver-enabled. From this search, three studies were identified where CFs are derived for nAg [25, 69, 189]. Table 5 presents a summary of these studies along with the calculated/assumed FF, XF and EF, and derived CFs.

Table 5. Summary of the literature on developing nAg specific freshwater ecotoxicity CFs.

Considered fate and behavior processes in FF calculation	FF (days)	XF (%)	EF (PAF.m ³ /kg)	CF (PAF.m ³ .day/kg or CTUe/kg)	Ref.
Assumed as one due to many unknowns	1	N/A	8,576	8.57×10 ³	[25]
Sedimentation Advection Dissolution	1.36	100	SPL) 16,030 TPL) 14,502	1.98×10 ⁴	[189]
Calculated using substance specific partitioning coefficients	S1) 30 S2) 130	S1) 60 S2) 80	S1) 13,497 S2) 281,144	S1) 2.43×10 ⁵ S2) 2.92×10 ⁷	[69]

N/A: neglected; S1: Scenario 1; S2: Scenario 2; SPL: Species level; TPL: Trophic level

As being the first CF study for nAg, Miseljic and Olsen used simplifying assumptions to estimate the freshwater ecotoxicity potential of nAg. They suggested that nAg will have a short substance residence time in freshwater (i.e. rapid transformation, aggregation and sedimentation time), which resulted in an FF of 1 [25]. They also assumed that the exposure is equal to the environmental concentration of nAg, and therefore neglected the XF. For EF, Miseljic and Olsen compiled in total of 21 EC₅₀ values for three trophic levels (algae, crustacean and fish) and calculated the EF as 8,576 PAF.m³/kg [25]. Another study by Pu developed a fate model which involves calculating the FF from rate constants of certain transformation processes, such as advection, dissolution, sedimentation [189]. For EF, Pu compiled toxicity data for three trophic levels (algae, crustacean and fish) and calculated the EF as 14,502 PAF.m³/kg. They argued that given that the XF calculation based on USEtox involves partitioning coefficients and they are not representative for ENMs, an *ultra-conservative* XF needs to be assumed which is equal to considering 100% bioavailability [189]. Lastly, Garvey et al. used an adapted version of USEtox model, where they computed *realistic*- and *worst*-case scenarios. They calculated the FF using substance specific partitioning coefficients as USEtox recommended. In order to calculate the EF, Garvey et al. used in total of 73 different toxicity data (including EC₅₀, IC₅₀ and LC₅₀) for four phyla (Arthropoda, Chordata, Chlorophyta and Heterokontophyla) and calculated EF with a range of 13,497 – 281,144 PAF.m³/kg. For XF, they used statistical simulations since empirically determined exposure factors were not available in the literature, and suggested that nAg is 60-80% bioavailable [69].

As previously mentioned, the XF and FF depend on the physicochemical properties of nAg and the conditions of the release media [155, 162]. Additionally, different size and coating of nAg have a significant impact on EF [227]. These factors are needed to be considered while

developing nAg specific CFs. Overall, as discussed in the current section, previous studies that derive nAg-CFs used various approaches and did not take into account the external (i.e. media dependent) and internal (i.e. ENM dependent) factors, which are critically important.

5.4. Materials and Methods

Research recommended that using experimental data obtained from aquatic mesocosms (i.e. specific site) is more representative and approachable in modeling potential fate and behavior of ENMs, rather than including all possible transformation routes discussed previously [244, 245]. Considering this recommendation, in the current study, a CF for freshwater ecotoxicity is developed particularly for the mesocosm conditions examined by Geitner et al. and Stegemeier et al.[246–248]. Following subsections provide detailed information on each of the component of characterization factor.

5.4.1. Effect Factor (EF) Calculation

According to the USEtox, EF is calculated using eqn (5.3) and eqn (5.4), where HC_{50} (hazardous concentration) is calculated by the geometric mean of EC_{50} data, and EC_{50} is the concentration of a substance at which 50% of the population responds (i.e. endpoints may include mortality, immobilization, reproduction, etc.) [20]. The USEtox recommends including at least three chronic or sub-chronic species level toxicity data (n in eq. 5.4) for a minimum of three trophic levels (e.g. crustaceans, fish and algae) in EF calculations [20].

$$EF = \frac{PAF}{HC_{50}} = \frac{0.5}{HC_{50}} \quad (5.3)$$

$$HC_{50} = \sqrt[n]{\prod_{i=1}^n EC_{50,i}} \Rightarrow \log HC_{50} = \frac{1}{n} \sum_{i=1}^n \log EC_{50,i} \quad (5.4)$$

Previous studies performed several adaptations to the USEtox model to calculate the EF. For instance, in order to account for different endpoints, some studies included not only EC_{50} but also LC_{50} and/or IC_{50} values in HC_{50} calculation [26, 69, 127, 176]. Another example may be given from the studies where the EF is calculated using trophic-level (TPL) HC_{50} rather than species-level (SPL) as the USEtox recommends [176, 189]. A literature review by Temizel-Sekeryan and Hicks exhaustively explored the existing nAg toxicity literature and calculated EFs considering different scenarios using a total of 366 data points. As the potential ecotoxicity of released nAg depends on the physicochemical properties of the material and the release media (e.g. whether mineral or complex), we calculated size and coating dependent EFs for different environmental mediums, permitting toxicity data availability [227]. Moreover, using previous suggestions from the literature, we included scenarios for SPL and TPL-EFs to inform the CF development. In the current study, EFs calculated by Temizel-Sekeryan and Hicks are used for the nAg of concern [227]. Due to the limited data availability for PVP coated nAg, size dependent EF could not be extracted from the respective paper. Therefore, EFs that are developed for PVP coated nAg regardless of size are used. In order to provide a CF range, an optimistic (i.e. low toxicity) and a skeptical (i.e. high toxicity) EFs are selected, which are 6,581 $PAF.m^3/kg$ and 19,303 $PAF.m^3/kg$ respectively [227].

5.4.2. Fate Factor (FF) Calculation

Conceptually, FF calculation incorporates the material removal and transport processes as by definition it indicates the persistence of a substance in the environment [20]. Figure 26 lists the processes relevant to the ENMs in aquatic environments. Previous studies that investigated fate of ENMs are constructed based on different opinions (i.e. they focus on/discard different parameters). For instance, a model developed by Meesters et al. assumed the hetero- and/or homo- aggregated ENMs as altered species of the same material, and therefore included aggregation as a transformation process rather than removal [189, 257, 262]. Whereas, various studies that developed CFs for different types of ENMs included aggregation as a removal process and incorporated it in FF calculation [26, 176, 182, 261, 264]. As such, the mechanisms of nAg fate are still not specified explicitly in the literature [174, 189].

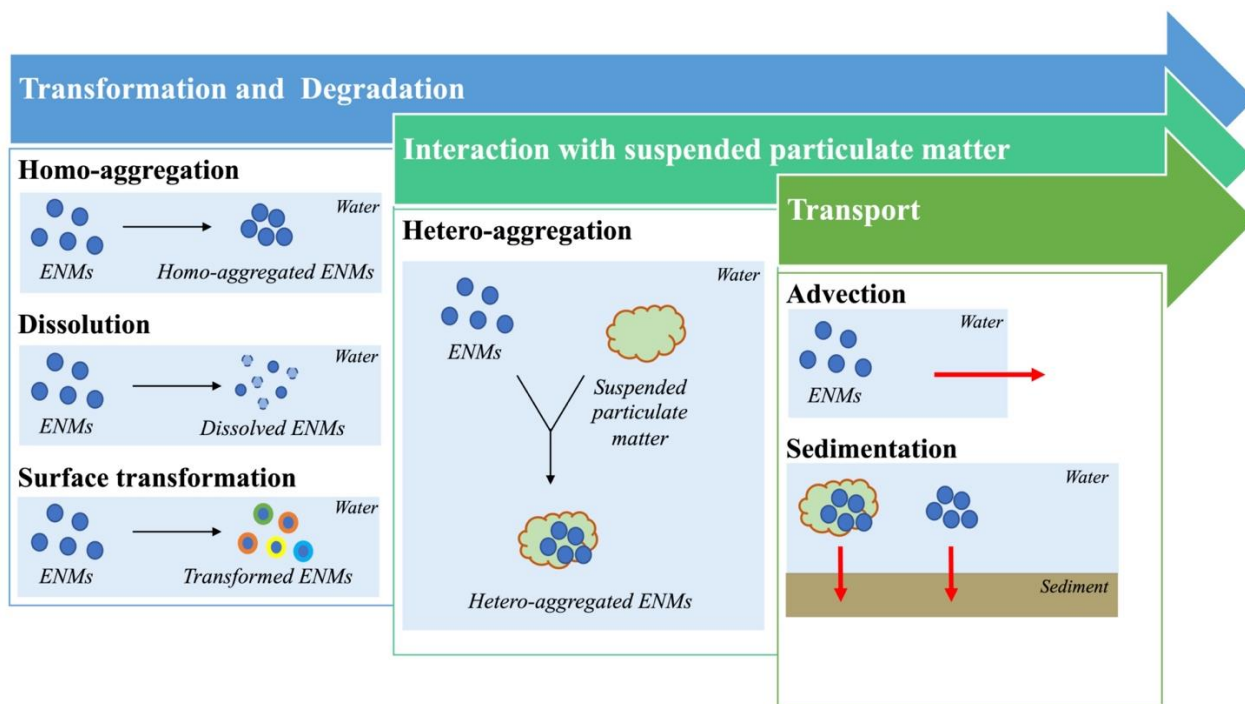


Figure 26. Processes relevant to ENMs in aquatic environments (adapted from [261, 263, 268]).

Acknowledging previous methodologies, two different scenarios for FF calculation is computed in the current study. In scenario 1, FF is calculated using eqn (5.5), which requires calculating rate constants for dissolution (k_{diss}), hetero-aggregation ($k_{het-agg}$), sedimentation (k_{sed}) and advection (k_{adv}) processes [26, 261, 264]. $k_{w,w}$ denotes the removal rate constant for freshwater.

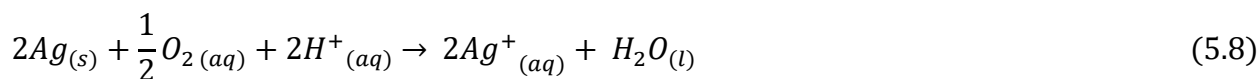
$$FF = \frac{1}{k_{w,w}} = \frac{1}{(k_{diss} + k_{het-agg} + k_{sed} + k_{adv})} \quad (5.5)$$

In scenario 2, aggregation is assumed as a transformation process and the $k_{het-agg}$ is removed from eqn (5.5). Instead, $k_{het-agg}$ is included in the k_{sed} and further calculations are conducted. Following subsections include detailed explanations and calculation frameworks for the components of eqn (5.5). Research suggested that homo-aggregation is negligible compared to hetero-aggregation [162, 176, 257, 260], and no measurable homo-aggregation was detected in nAg mesocosms [246, 247, 269, 270]. For this reason, homo-aggregation is neglected in the current study.

5.4.2.1. Dissolution

In the majority of previously developed CFs (Table D1), dissolution processes were not incorporated because either the ENMs of interest were not soluble (e.g. nano-TiO₂, CNT, GO) or FF calculation method was based on partitioning coefficients [26, 69, 128, 176, 182]. However, as presented in Figure 25B, dissolution is an important transformation mechanism for nAg and has to be incorporated into fate modeling. Furthermore, Pu conducted a sensitivity analysis and suggested that dissolution rate of ENPs in freshwater should be prioritized [189]. So far, the common approach has been assuming a simplified k_{diss} of $0-10^{-5} \text{ s}^{-1}$ provided by Quik et al. for all metallic ENMs that are soluble [236, 262].

Dissolution of nAg is defined as oxidative dissolution where metallic Ag, that is on the surface of nAg, reacts with dissolved oxygen in aqueous media and forms silver(I)oxide (eqn 5.6). Then the silver(I)oxide further dissolves and releases Ag^+ in the presence of protons, thus, pH is an important parameter for this step (eqn 5.7). Eqn (5.8) represents the overall dissolution mechanism of nAg [271].



Dissolution of nAg in aqueous media is affected by several factors including pH, ionic strength, dissolved oxygen, temperature, capping agents, size and shape of nAg, among others [251, 272–278]. For instance, the size of nAg and the level of dissolution are shown to be inversely proportional, meaning that smaller sized nAg will have larger k_{diss} [252, 279–282]. Throughout the literature, the most applied method for calculating the k_{diss} is implementing modified pseudo-first-order kinetic model using experimental data as presented in eqn (5.9),

$$C_t = C_d(1 - e^{-k_{diss}t}) \text{ or } k_{diss} = -\frac{\ln\left(\frac{C_0 - C_{ions}}{C_0}\right)}{t} \quad (5.9)$$

where C_t is the nAg concentration at time t (mg/L), C_d is the concentration when nAg are completely dissolved (mg/L), C_0 is the initial concentration of nAg (mg/L), C_{ions} is the concentration of released ions from nAg at time t (mg/L), k_{diss} is the dissolution rate constant (s^{-1}) and t is the time (s) [189, 257, 283]. Additionally, several studies combined the Arrhenius equation and eqn (5.9) to calculate temperature dependent rate constants or developed individualized kinetic laws for specific conditions (e.g. pH, presence of organic matter, coating) [271, 283, 284]. Similar to the previous literature, in the current study, pseudo-first-order kinetic

model (eqn 5.9) is used to calculate k_{diss} using experimental data from mesocosm conditions as detailed by Geitner et al. and Stegemeier et al. [246–248]. Respective parameters can be found in Table D2.

5.4.2.2. Hetero-aggregation

Hetero-aggregation has been identified as one of the most important processes that greatly impacts the fate of ENMs in aquatic mediums as after the attachment, suspended particulate matter (SPM) dominates the transport behavior of ENMs [246, 270, 285, 286]. In their recent review paper, Praetorius et al. provided a theoretical background for hetero-aggregation process and suggested several experimental approaches for calculating the hetero-aggregation attachment efficiency [270]. Hetero-aggregation process has not been considered as a removal process in any of the previous studies that develop CFs for nAg as detailed in Table 5. Thus, to the best of the authors' knowledge, this is the first study that incorporates the hetero-aggregation as a removal process in FF calculation for nAg (i.e. as scenario 1).

In the current study, hetero-aggregation rate is calculated using eqn (5.10) [26, 176]. One of the factors that affect the hetero-aggregation rate is the hetero-aggregation (or attachment) efficiency, α . It can range from 0 to 1 depending on the surface chemistries of ENMs, the properties of the SPM as well as the characteristics of water [176, 247, 261, 287]. Therefore, it is ideal to obtain the experimental attachment efficiency specific for each study. For reference, Geitner et al. provided a heat-map for α values using different ionic strength and humic acid concentrations, which resulted in a full range of α values (0 to 1) for nAg [247]. Previous nano specific CF literature that applied multimedia fate model for calculation used different theoretical values for attachment efficiencies, e.g. Salieri et al. included both 0.001 and 1 for nano-TiO₂;

Praetorius et al. used a range of 0.001-1 for nano-TiO₂; Deng et al. assumed α as 10⁻⁶ for CNTs; and Deng et al. included α as 0.0015 for graphene oxide nanoparticles [26, 176, 182, 261].

$$k_{het-agg} = k_{coll} * \alpha_{het-agg} * C_{SPM} \quad (5.10)$$

where $\alpha_{het-agg}$ is aggregation efficiency, C_{SPM} is suspended particulate matter concentration (1/m³) and k_{coll} is the collision rate (m³/s). In the current study, a conservative α is selected as 0.012 (the lowest α reported for nAg in the literature) [247] and a sensitivity analysis is conducted in order to identify how sensitive the results to α are. C_{SPM} and k_{coll} require further calculations, which are detailed in the Appendix D (eqn D1-D5). Parameters used to calculate the $k_{het-agg}$ can be found in Tables D2 and D3.

5.4.2.3. Sedimentation

Due to the gravitational settling, free ENMs and ENMs that are attached to SPM and/or organic matter are tend to settle in aquatic environments [230]. The rate of sedimentation is governed by Stoke's Law for gravitational settling of particles, for which, densities and sizes of both nAg and SPM are important parameters [257, 261, 288]. Quik et al. suggested that, a range of 0-10⁻⁴ s⁻¹ is acceptable for the sedimentation rate constant if there are limited nano specific data in the literature [236]. As two scenarios are computed in the current study, two different sedimentation rate constants (k_{sed}^{nAg} and k_{sed}') are calculated. For scenario 1, where hetero-aggregation is considered as a removal process, sedimentation rate constant (k_{sed}^{nAg}) is calculated using eqn (5.11),

$$k_{sed}^{nAg} = \frac{v_{set}^{nAg}}{h_w} \quad (5.11)$$

where v_{set}^{nAg} is the settling velocity (m/s) of nAg and h_w is the depth of the water compartment (m). For scenario 2, where hetero-aggregation is considered as a transformation process rather than removal, sedimentation rate constant (k_{sed}') is calculated using eqn (5.12),

$$k_{sed}' = k_{sed}^{nAg} + k_{agg-sed} + k_{att-sed} \quad (5.12)$$

where k_{sed}^{nAg} is the sedimentation rate constant as calculated in eqn (5.11) (s^{-1}), $k_{agg-sed}$ is the minimum value of either pseudo-sedimentation rate constant for aggregated nAg or the aggregation rate constant (s^{-1}) and $k_{att-sed}$ is the minimum value of either pseudo-sedimentation rate constant for attached nAg or the attachment rate constant (s^{-1}) [189]. As mentioned previously, homo-aggregation is neglected in the current study, therefore $k_{agg-sed}$ is not calculated. Further calculations are detailed in the Appendix D (eqn D6-D10). Parameters used to calculate the k_{sed}^{nAg} and k_{sed}' can be found in Tables D2 and D3.

5.4.2.4. Advection

Advection process can be defined as the transport of ENMs from freshwater to other water compartments (i.e. out of the system), mainly due to precipitation [262, 287]. Quik et al. suggested that, if there are limited nano specific data, using $10^{-6} s^{-1}$, or any value from a range of $0-10^{-5} s^{-1}$, as the advection rate constant is acceptable [236]. If details are available, advection rate constant, k_{adv} , can be calculated using eqn (5.13),

$$k_{adv} = \frac{k_{precipitation} * A_{freshwater} + \varphi * k_{precipitation} * A_{soil}}{V_w} \quad (5.13)$$

where $k_{precipitation}$ is the precipitation rate (mm/yr), $A_{freshwater}$ is the area of freshwater (m^2), A_{soil} (m^2) is the area of soil, φ is the water run-off fraction (%) and V_w is the volume of freshwater (m^3) [26]. Parameters used to calculate the k_{adv} can be found in Tables D2 and D3.

5.4.3. Exposure Factor (XF) Calculation

The USEtox multimedia fate and exposure model suggests calculating the XF using eqn (5.14), which results in a dimensionless element to be incorporated into CFs [20].

$$XF = \frac{1}{1 + (K_{PSS} * SS + K_{DOC} \cdot DOC + BAF * BIO_{mass}) * 10^{-6}} \quad (5.14)$$

where K_{PSS} is the partitioning coefficient between water and suspended solids (L/kg), SS is the concentration of suspended solids in water (mg/L), K_{DOC} is the partitioning coefficient between dissolved carbon and water (L/kg), DOC is the concentration of dissolved organic carbon in water (mg/L), BAF is the bioaccumulation factor in biota (L/kg), and BIO_{mass} is the concentration of biota in water (mg/L) [189]. However, as previously stated, partitioning coefficients are not representative for ENMs. Therefore, the common approach in the literature has been assuming a precautionary XF of 1 for ENMs, which corresponds to 100% bioavailability [25, 176, 189, 262]. In the current study, in accordance with the published body of the literature an XF of 1 is assumed.

5.4.4. Sensitivity Analysis

Due to the variability of data collected from the literature to calculate a CF for nAg, several assumptions are made which may significantly affect the rate constants and therefore the fate factor. A sensitivity analysis is performed for each variable, such as the parameters for SPM (e.g. d_{SPM} , $C_{mass,SPM}$, ρ_{SPM}) and for nAg (e.g. d_{nAg} , ρ_{nAg} , C_0 , C_{ions} , $\alpha_{het-agg}$), to identify the ones to which the rate constants and FF are sensitive to. The value of each parameter is modified by 20% while others are kept constant. Then, the rate constants are re-calculated to determine how the change in the parameters affected the results. A sensitivity threshold is assumed as 2%, and the parameters with a sensitivity factor of $\leq 2\%$ are considered as not sensitive to the system

[289]. Additionally, sensitivities of rate constants (e.g. k_{diss} , $k_{het-agg}$, k_{sed} , k_{adv}) on the FF are analyzed using the same calculation framework.

5.5. Results and Discussions

5.5.1. Fate Factor

As mentioned in section 5.4.2, two scenarios are computed in the current study for FF calculation. Before presenting and discussing the results, it should be noted that smaller removal rate constants indicate that the ENMs are stable and therefore have long residence times in the aquatic environment. In scenario 1, hetero-aggregation is assumed as a removal process, and the corresponding FF is calculated as 8 hours (3 day^{-1}). Pu recommended that the minimum value of FF for nAg can be 3.86×10^{-3} days, which makes the current finding a reasonable duration for the fate [189]. The k_{diss} is found as $3.15 \times 10^{-7} \text{ s}^{-1}$, $k_{het-agg}$ as $3.44 \times 10^{-5} \text{ s}^{-1}$, k_{sed} as $1.09 \times 10^{-8} \text{ s}^{-1}$ and k_{adv} as $2.05 \times 10^{-8} \text{ s}^{-1}$ considering the conditions for scenario 1, which resulted in a $k_{w,w}$ of $3.48 \times 10^{-5} \text{ s}^{-1}$ (Table D4). It is observed that the $k_{het-agg}$ dominates the $k_{w,w}$ for scenario 1, as it is more than two orders of magnitude greater than the other rate constants.

In scenario 2, hetero-aggregation is assumed as a transformation process rather than removal, and the corresponding FF is calculated as 12 days (0.08 day^{-1}). While k_{diss} and k_{adv} remain the same in scenario 2, k_{sed}' is increased to $6.19 \times 10^{-7} \text{ s}^{-1}$ which resulted in a decrease in $k_{w,w}$ with a final result of $9.54 \times 10^{-7} \text{ s}^{-1}$ (Table D4). In this case, it is found that the k_{sed}' dominates the $k_{w,w}$ for scenario 2. These findings are compatible with Espinasse et al., where they hypothesized hetero-aggregation and deposition as primary driving factors for ENMs removal from the aquatic media when SPM is present [269]. For reference, they used glass beads as background particles and found a removal rate of 0.59 day^{-1} ($\approx 6.83 \times 10^{-6} \text{ s}^{-1}$) for PVP coated

nAg [269]. Another study by Colman et al. calculated a removal rate constant of 0.21 ± 0.066 day⁻¹ ($\approx 2.43 \times 10^{-6}$ s⁻¹) for nAg, considering several processes including aggregation, sedimentation, sorption/uptake by plants and sorption/uptake by biofilms [290]. Different from the aforementioned mesocosm studies, Pu calculated a FF for nAg and reported a $k_{w,w}$ of 2.42×10^{-5} s⁻¹ [189].

As mentioned previously, in both scenarios k_{diss} is found as 3.15×10^{-7} s⁻¹ which is in the range of $0-10^{-5}$ s⁻¹ as Quik et al. suggested [236]. Further, the SimpleBox4Nano tool provides a k_{diss} for nAg in freshwater as 1.37×10^{-7} s⁻¹ by default, which is compatible with the rate constant calculated in the current study [291]. It somewhat differs from the literature. For instance, using the same calculation method (section 5.4.2.1), Kittler et al. evaluated the impact of coating on the dissolution and found k_{diss} of PVP coated nAg as 1.17×10^{-2} h⁻¹ ($\approx 3.25 \times 10^{-6}$ s⁻¹) [292].

Regardless of coating, Kent and Vikesland calculated mass-based k_{diss} for 56nm-nAg as ranging from 1.14×10^{-2} d⁻¹ ($\approx 1.32 \times 10^{-7}$ s⁻¹) to 9.87×10^{-2} d⁻¹ ($\approx 1.14 \times 10^{-6}$ s⁻¹) depending on the presence of different levels of sodium chloride (NaCl), which greatly affects nAg dissolution [280].

Further, Liu examined the dissolution kinetics of 65nm-nAg and found that k_{diss} ranges from 2.3×10^{-2} d⁻¹ ($\approx 2.66 \times 10^{-7}$ s⁻¹) to 1.43×10^{-1} d⁻¹ ($\approx 1.66 \times 10^{-6}$ s⁻¹) depending on the temperature of the media [283]. In another study, Pu estimated the dissolution rate constant of nAg by averaging data from the literature, considering only k_{diss} from the studies that have environmental conditions similar to freshwaters (i.e. pH, ionic strength and concentration of organic matter were taken into account in selection) and assumed a k_{diss} of 3.42×10^{-6} s⁻¹ [189]. Finally, in their review paper, Garner and Keller provided residence times using data from the literature and reported that coated nAg has dissolution time frame of weeks which aligns with the results obtained in the current study (≈ 5.2 weeks) [230].

The attachment (or aggregation) efficiency ($\alpha_{het-agg}$) is one of the key parameters while calculating the hetero-aggregation rate. Geitner et al. suggested that attachment efficiency is proportional with ionic strength and inversely proportional with the concentration of organic substances in the media [247]. Quik et al. found similar results and argued that high organic content may have a stabilizing effect which decreases the attachment efficiency and therefore the hetero-aggregation rates [293]. Using a conservative α , $k_{het-agg}$ is found as $3.44 \times 10^{-5} \text{ s}^{-1}$ in the current study, which was the dominating rate constant for scenario 1. Similar to the dissolution time frames, Garner and Keller provided residence times for aggregation. They suggested that coated nAg has aggregation time frame of days which is slightly different from the results obtained herein (≈ 0.34 day) [230]. Since the $k_{het-agg}$ was one of the components of k_{sed}' in scenario 2, it is discussed in the next paragraph.

Based on the scenarios analyzed, two different sedimentation rate constants are calculated. In scenario 1, where only nAg were assumed to settle, k_{sed} is found as $1.09 \times 10^{-8} \text{ s}^{-1}$. This constant is governed solely by the settling velocity of nAg (as calculated by eqn D4), which is found as $1.31 \times 10^{-8} \text{ s}^{-1}$. Quik et al. suggested a range for settling velocities of PVP coated nAg in natural waters as $8.22 \times 10^{-4} \text{ m/d} - 9.98 \times 10^{-3} \text{ m/d}$ ($\approx 9.51 \times 10^{-9} \text{ m/s} - 1.16 \times 10^{-7} \text{ m/s}$) [293], which are compatible with the current findings. Differently, in scenario 2, where the settling of aggregated nAg is also counted in the sedimentation process (as calculated by eqn D6), k_{sed}' is found as $6.19 \times 10^{-7} \text{ s}^{-1}$. It is observed that the settling velocity of SPM is a dominant factor for k_{sed}' . Similar finding is provided by Quik et al., where they stated that hetero-aggregation with SPM plays an important role in the sedimentation process for ENMs [293]. Finally, Garner and Keller suggested that coated nAg has sedimentation time frame of weeks, which is compatible with the findings of scenario 2 (≈ 2.7 weeks), but significantly different from the results obtained

from scenario 1 (≈ 151 weeks) [230]. This may be because of the varying perspectives for inclusion of hetero-aggregation process in the fate modeling. Lastly, the advection rate constant, k_{adv} , is found as $2.05 \times 10^{-8} \text{ s}^{-1}$ for both scenarios. Although it falls in the suggested range of $0-10^{-5} \text{ s}^{-1}$ [236], it slightly differs from the results provided in the literature, e.g. Pu found k_{adv} as $8.1 \times 10^{-9} \text{ s}^{-1}$ [189].

5.5.2. Characterization Factor

Based on the assumed XF and EFs and calculated FFs, different characterization factors are provided in the current study. As previously mentioned, optimistic and skeptical scenarios are computed using the lowest and highest EFs for PVP coated nAg from Temizel-Sekeryan and Hicks [227]. Given that physicochemical properties of nAg (e.g. size and coating) were not considered in the previous research that develop CFs, in order to compare CF values provided by the literature with CFs developed in the current study, additional calculations are performed using EFs that are regardless of coating. Figure 27 shows the CFs collected from the literature (Group A) as well as the ones developed in the current study (Group B and C). The CF for Ag^+ is also included in the figure for comparison. Exact values for EF, XF, FF and CF are provided in Appendix D (Table D5).

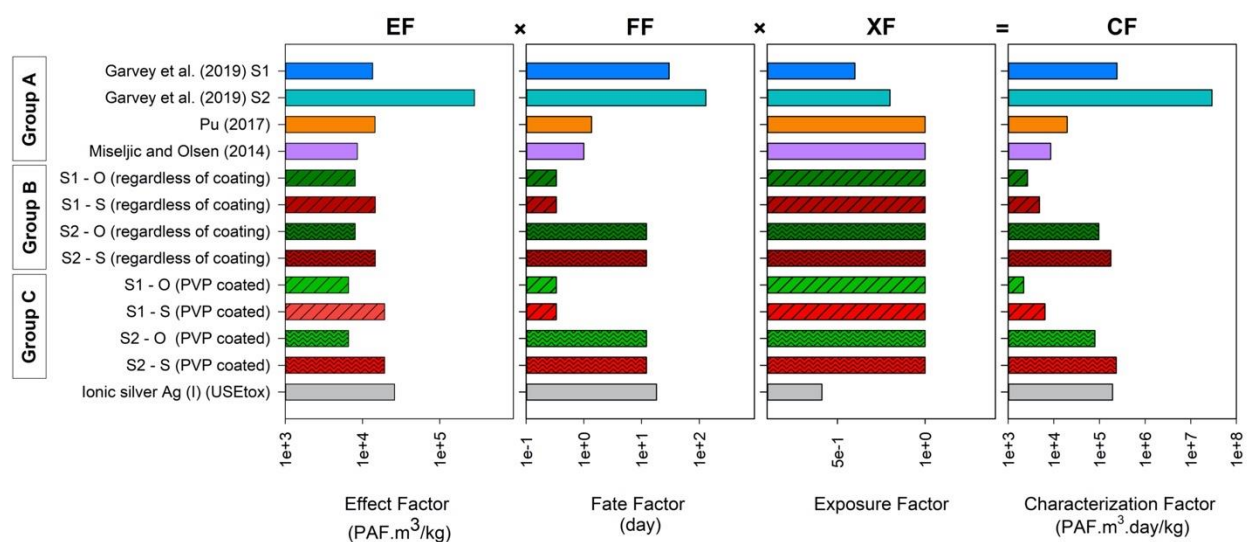


Figure 27. Comparison of characterization factors calculated in the current study with the literature values where Group A shows literature values, Group B shows CF values obtained in the current study using EFs regardless of size and coating (compatible with the literature), and Group C shows CF values obtained in the current study using EFs for PVP coated nAg regardless of size (S1: scenario 1, S2: scenario 2, O: optimistic, S: skeptical).

The CF for PVP coated nAg in the selected mesocosm conditions ranges from 2.19×10^3 to 6.42×10^3 PAF.m³.day/kg assuming hetero-aggregation as a removal process (scenario 1). If hetero-aggregation is considered as a transformation process and included in sedimentation (scenario 2), CF increases to $7.98 \times 10^4 - 2.34 \times 10^5$ PAF.m³.day/kg. This increase is due to the changes in the FF, as the residence time of nAg increases when hetero-aggregation is assumed as a transformation process rather than removal.

The study by Pu is compatible with one of the scenarios modeled in this work, i.e. with scenario 2, as they used multimedia fate model rather than partitioning coefficients and assumed hetero-aggregation as a transformation process [189]. Pu calculated a CF for nAg as 1.97×10^4

PAF.m³.day/kg using an EF regardless of physicochemical properties of nAg. In the current study, using EFs that are developed for nAg regardless of coating resulted in an optimistic CF of 9.74×10^4 PAF.m³.day/kg and a skeptical CF of 1.78×10^5 PAF.m³.day/kg. The difference between the current results and results from Pu may be due to the varying considerations while modeling the FF including values assumed for attachment efficiency, and density and/or size of SPM and/or nAg. Another reason may be differences in calculation methodologies, e.g. Pu used an assumption for k_{diss} rather than actually calculating it or used different formula to calculate the k_{adv} [189]. Also, it should be noted that the FF in the current work is calculated based on the assumptions for PVP coated nAg in the selected mesocosm, which may differ for nAg that are uncoated or coated with other agents.

In order to evaluate the importance of using physicochemical property based EFs, cross comparison between Group B and Group C is analyzed. Using current considerations for FF calculation, incorporating EFs that are developed for nAg regardless of coating resulted in 18% to 32% difference in the developed CFs. Considering optimistic EFs for both scenarios, using coating specific values resulted in lower CFs (Table D5). Interestingly, considering skeptical EFs for both scenarios, using coating specific values resulted in higher CFs (Table D5). These relationships conceivably change in a significant manner if the nAg are uncoated or citrate coated [227].

As mentioned in the introduction section, previous LCA studies modeled released nAg as Ag⁺ [38, 58, 60, 65]. As Gilbertson et al. discussed, this consideration may potentially overestimate toxicity impacts resulting from nAg release [12]. Therefore, cross comparison of CFs developed in the current study with CF of Ag⁺ is also presented in Figure 27. Accordingly, only the CF that is developed using skeptical EF for PVP-nAg in scenario 2 slightly (by 20%)

exceeded the CF for Ag^+ . In other words, the majority of conducted scenarios resulted in lower CFs than CF of Ag^+ . Even in some scenarios, the CFs differed by two orders of magnitude. It can be concluded that, in general, modeling nAg release as Ag^+ likely results in an overestimation of freshwater ecotoxicity impact.

5.5.3. Sensitivity Analysis

For all of the rate constants (e.g. k_{diss} , $k_{het-agg}$, k_{sed} , k_{adv}) and the FF, sensitivity analysis is conducted and sensitivity factors (SFs) are calculated. Figure 28 shows the SFs for each parameter on the rate constants and the FF for scenario 1 (Figure 28A) and scenario 2 (Figure 28B). Red circle in the center shows the cut off value of 2%, therefore, the SFs that fall outside of this red circle are considered as sensitive inputs for the system. SFs for both scenarios are presented in Appendix D as Table D6 and Table D8.

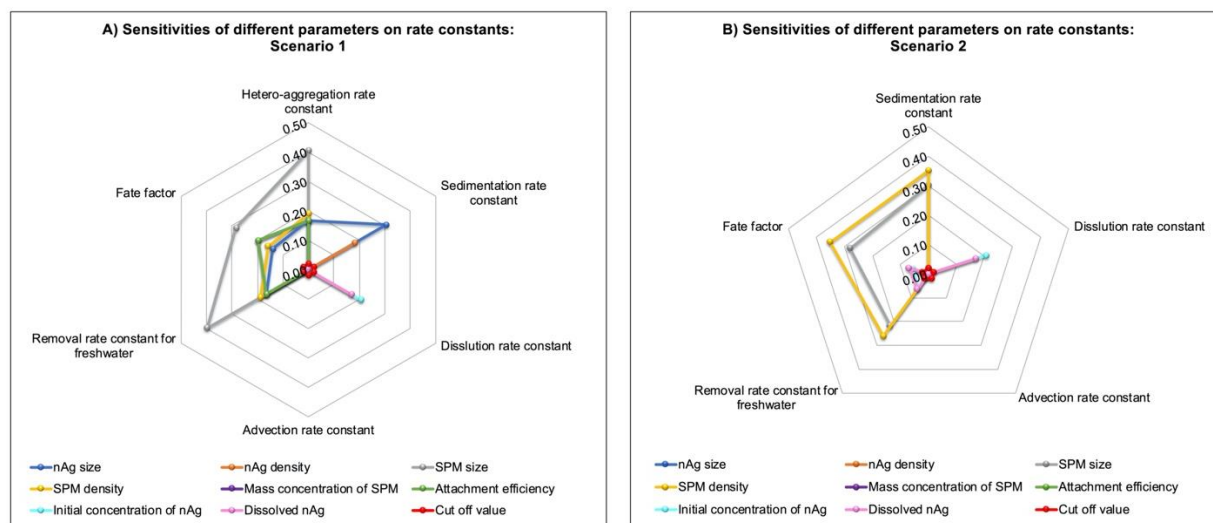


Figure 28. Sensitivity factors (SFs) of the selected inputs on the rate constants for A) Scenario 1 and B) Scenario 2.

As can be seen from Figure 28A, for $k_{het-agg}$, the size and density of SPM, size of nAg, mass concentration of SPM and the attachment efficiency are sensitive parameters, from the most sensitive to the least, respectively. This means that any small change in these parameters will significantly change the $k_{het-agg}$. While the increase in d_{nAg} , d_{SPM} and ρ_{SPM} resulted in a decrease in $k_{het-agg}$ (i.e. inversely proportional); the increase in $C_{mass,SPM}$ and $\alpha_{het-agg}$ resulted in an increase (i.e. proportional). The density and the initial and dissolved concentrations of nAg did not show any sensitivity on the $k_{het-agg}$. In terms of k_{sed} , only the size and density of nAg are identified as sensitive parameters with SFs of 0.31 and 0.18 respectively. For k_{diss} , only the initial (SF \approx 0.21) and dissolved concentrations (SF \approx 0.17) of nAg showed sensitivities, as these parameters are used to calculate the dissolution rate constant. Further, none of the considered parameters showed sensitivities for k_{adv} . Finally, both for $k_{w,w}$ and FF, all of the parameters except ρ_{nAg} , C_0 , C_{ions} are identified as sensitive parameters with varying SFs (Table D6). At the first glance, it can be observed that the d_{SPM} is the most sensitive parameter for the FF, following $C_{mass,SPM}$, $\alpha_{het-agg}$, ρ_{SPM} and d_{nAg} respectively. Also, for scenario 1, the dominating removal rate constant was identified as $k_{het-agg}$, which was the only sensitive rate constant for FF as tabulated in Table D7.

As illustrated in Figure 28B, the aforementioned sensitivity trends changed for scenario 2. Given that the hetero-aggregation is assumed as a transformation process and is included the sedimentation, SFs for only k_{diss} , k_{sed}' , k_{adv} , $k_{w,w}$ and FF are evaluated. While the results for k_{diss} and k_{adv} remained the same, sensitive parameters and SFs for k_{sed}' changed significantly. For k_{sed}' , the size and density of SPM are identified as the sensitive parameters with SFs of 0.30 and 0.35, respectively. Further, both for $k_{w,w}$ and FF ρ_{SPM} , d_{SPM} , C_{ions} and C_0 showed different levels of sensitivities, which are tabulated in Table D8. Finally, as the dominating rate constants

for scenario 2 were k_{diss} and k_{sed}' , they are identified as sensitive constants for FF (Table D9). These findings are compatible with Pu, where they identified the size of SPM as the most important parameter to be considered for freshwater FF calculation [189].

5.5.4. Limitations

Several limitations exist for the calculations conducted in this work. One of the major limitations is assuming an $\alpha_{het-agg}$ for nAg rather than using an α that is calculated specifically for the aquatic media of interest. It should be noted that, while calculating $\alpha_{het-agg}$, the surfaces that nAg are coming in contact with is also another important factor that needs to be considered. As discussed in the previous section, attachment efficiency is one of the sensitive factors for scenario 1, which significantly affects the FF and therefore CF. Another limitation was assuming an averaged value as a density of SPM, which was also identified as one of the sensitive inputs. Additionally, assuming that all the nAg are bioavailable (i.e. XF=100%) is a limitation and may result in an overestimation of CF, as XF has a direct and significant impact on the calculated CF (eqn 5.2). Research stated that functionalization, oxidation and sulfidation are some of the relevant processes that affect the exposure of ENMs, however they are excluded in the current multimedia fate models for being too complex to analyze [22]. In this regard, Mitrano et al. listed possible scenarios for silver release from nano-enabled consumer products with potential transformation routes (e.g. sulfidation, precipitation etc.) [80]. They noted that, nAg may be further speciated, which needs to be taken into account for exposure assessments [80]. Accordingly, incorporating all potential exposure pathways to calculate XF would result in more thorough assessment. Lastly, even though it was reported as acceptable by several papers, neglecting the homo-aggregation process may be listed as one of the limitations for the current

study. One method for improving this work and eliminating the aforementioned limitations would be to create a mesocosm and calculate all the variables (listed in Tables D2 and D3) specifically for that environment.

5.5.5. Implications for LCA

As discussed by Salieri et al. and summarized in Temizel-Sekeryan and Hicks, direct impacts resulting from the release of ENMs are not widely studied in the literature [22, 227]. The main reason of this is identified as the lack of CFs to model nano-specific emissions to air, soil or water [13, 60]. There are four stages in the lifecycle of a product as raw materials acquisition, manufacturing, use and end-of-life [15, 16]. The majority of the LCA literature conducted assessments using cradle-to-gate (i.e. raw materials acquisition and manufacturing) system boundaries, while cradle-to-grave (i.e. all four phases) studies were limited in number [22]. In order to make a comprehensive environmental assessment, not only the indirect impacts (obtained preferably from cradle-to-grave LCAs) but also direct impacts resulting from the released ENMs should be calculated. In the published body of the nAg-LCA literature, release was modeled using CF for Ag^+ [30–32, 39, 64, 65]. However, based on the findings of the present study, this potentially causes an overestimation of results as nAg has different effect, exposure and fate patterns than the Ag^+ .

The current study calculated CF for a specific sized and coated nAg as the physicochemical properties of nAg govern the effect and fate patterns. Combining the CFs with conventional LCA results helps drawing a thorough environmental assessment. For example, Eckelman et al. mentioned that the ecotoxicity impacts resulting from the production (including raw materials) of carbon nanotubes are significantly higher than the direct impacts resulting from

their release (indirect/non-nano ecotoxicity > direct/nano-specific ecotoxicity) [127]. For the case of nAg, Temizel-Sekeryan and Hicks evaluated environmental impacts of different nAg synthesis methods. We conducted Monte Carlo analysis and reported the cradle-to-gate ecotoxicity impact potential as ranging from 7.52×10^3 to 1.31×10^5 CTUe/kg nAg (i.e. PAF.m³.day/kg) considering different physical and chemical methods [126]. When comparing this range with the results obtained from the current study (Table D5), it can be concluded that, in the majority of instances, cradle-to-gate ecotoxicity impacts are found to be higher than the impacts resulting from the nAg release. Only CFs that are calculated using skeptical EFs for both PVP coated and nAg that are regardless of coating under scenario 2 showed slightly higher ecotoxicity impacts. If the exact nAg synthesis method is known, more precise comparison may be drawn. For instance, if the nAg is synthesized by chemical reduction with sodium borohydride, the cradle-to-gate ecotoxicity potential ranges from 1.00×10^4 to 1.09×10^5 CTUe/kg nAg and is higher than the nano-specific impacts [126]. Alternatively, if the nAg is produced by flame spray pyrolysis, the cradle-to-gate ecotoxicity potential decreases by an order of magnitude and is between 7.52×10^3 – 8.50×10^4 CTUe/kg nAg [126].

5.6. Conclusions

In this study, CFs are calculated for specific sized and coated nAg, considering various scenarios and using mesocosm conditions. Given that different fate models have been implemented for ENMs by the published body of the literature, they are addressed in the current work and comparisons are drawn accordingly. Two scenarios are developed for FF calculation in which the hetero-aggregation method is considered either a removal or a transformation process. In order to analyze the dominating variables for the fate of nAg, a sensitivity analysis is

conducted for both scenarios. For scenario 1, the ranking of the sensitivities can be ordered as $d_{SPM} > C_{mass,SPM} > \alpha_{het-agg} > \rho_{SPM} > d_{nAg}$. In scenario 2 the ranking changed to $\rho_{SPM} > d_{SPM} > C_{ions} > C_0$. This suggests that for both scenarios, besides nano-specific parameters, the characteristics of suspended particulate matter also affect the fate of ENMs in aquatic media. Another consideration accounted in this work is using skeptical and optimistic EFs developed for PVP coated nAg to provide a range for the developed CFs. This work elucidates the influence of using physicochemical property based EFs and calculating FFs for a specific environmental media on the developed CFs. Authors suggest using specific EF and FF for CF calculation in order to decrease the potential uncertainties. Authors also recommend that using Ag^+ to model the nAg release in LCAs is likely to result in overestimating the freshwater ecotoxicity impacts. Further research should incorporate indirect (non-nano) cradle-to-grave impacts with direct (nano-specific) release impacts to draw a comprehensive environmental impact assessment of nAg and nAg enabled consumer products.

5.7. Acknowledgements

Support for this research was provided by the Wisconsin Alumni Research Foundation (WARF). This work has not been formally reviewed by the WARF, and the findings presented by the authors are their own.

6. Cradle-to-grave environmental impact assessment of silver enabled t-shirts:

Do direct impacts exceed the indirect emissions?

The following chapter has been submitted for consideration for publication with the citation:

Temizel-Sekeryan, S.; Hicks, A.L., Cradle-to-grave environmental impact assessment of silver enabled t-shirts: Do direct impacts exceed the indirect emissions?

The article appears as submitted, although style and formatting modifications have been made.

Authorship contribution statement

Sila Temizel-Sekeryan: Designed Research, Performed Research, Analyzed Data, Wrote the Paper.

Andrea L. Hicks: Designed Research, Wrote the Paper.

6.1. Abstract

Consumption of silver nanoparticles (nAg) is increasing due to their use in various industries. A comprehensive analysis is needed to elucidate the potential environmental and human health benefits and costs of the silver-enabled consumer products. For this purpose, four commercially available silver enabled textiles with different initial silver loadings (1.07-4,030 $\mu\text{g Ag/g textile}$) are included in the current research and cradle-to-grave life cycle assessments (LCA) are conducted to identify hotspots associated with production and use of these products throughout their lifetimes (100 cycles). Both indirect (non-nano) and direct (nano-specific) impacts are calculated using nano-specific ecotoxicity (EC) characterization factors for nAg, instead of the commonly utilized Ag^+ surrogate. In the majority of environmental impact categories, either textile manufacturing (regardless of Ag/nAg enabling) or laundering were identified as hotspots. It is found that unless the initial silver loading per textile is significantly high, EC and human health (HH) impacts of released silver species would be lower than EC and HH impacts resulting from raw materials acquisition and manufacturing of the antibacterial textiles.

6.2. Introduction

Silver nanoparticles (nAg) are one of the most commercialized engineered nanomaterials (ENMs) due to their use in various consumer products including, but not limited to, textiles, food storage containers, packaging, electronics, etc. [1, 60] The incorporation of these materials into consumer products has brought about the question as to what are the additional environmental costs of these products compared to their conventional counterparts. For this purpose, numerous environmental impact assessments have been conducted using life cycle assessment (LCA) [22]. LCA is a methodology to systematically analyze environmental impacts of any product/process throughout its life cycle (i.e. raw materials acquisition, production, use and disposal) [15, 16]. Considering LCAs conducted for nanomaterials industry, the results generally represent non-nanoscale (or indirect) emissions, which are quantifications of impacts resulting from manufacturing (including raw materials) the ENM or nano-enabled product itself [227]. However, in order to holistically evaluate the environmental benefits and costs associated with nano-enabled products, incorporating the nano-specific (or direct) emissions into LCA is critical, which has not been widely applied in the current state of the literature [12, 22, 60, 126].

Impacts from direct emissions occur mainly during use phase, in which ENMs might be released to soil, air and water as a function of their size and shape, and potentially contribute to human health (HH) and ecotoxicity (EC) impacts. These impacts can be calculated using nano-specific characterization factors (CFs), which requires developing physicochemical property based effect factors (EF), fate factors (FF) and exposure factors (XF) for the ENM of interest [20, 227]. For reference, in their recent work, Temizel-Sekeryan and Hicks (Chapter 5) reviewed the current state of CF literature for nAg and developed a physicochemical property based ecotoxicity CF using mesocosm conditions. Due to the relatively low number of studies in the

toxicity literature for human toxicity of nAg, CFs for HH category have not been developed yet. So far, there are three studies that calculated HH CFs for different ENMs including single- and multi-walled carbon nanotubes [128] and titanium dioxide nanoparticles [294, 295].

Considering the use phase, silver release from Ag/nAg enabled textiles may occur during wearing/weathering and laundering. Significant differences exist among the silver-enabled textiles studied in the literature, such as the initial silver content and its source (nano or conventional), particle size, silver attachment method, type of fabric that silver was enabled in (e.g. polyester, cotton, polyamide), and quantity and the form of silver released. Figure 29A shows the range of the initial silver content in silver-enabled textiles based on silver speciation. The maximum silver content is identified as 53,909 mg Ag/kg textile [296] and the minimum as 0.9 mg Ag/kg textile [297], which is aligned with the previously identified silver concentrations in textiles. In order to make the boxplots more readable, textiles that contain more than 500 mg Ag/kg are excluded from the figure. For reference, Figure E1 shows boxplots that are drawn using all data points. Figure 29B illustrates the percentage of silver released from textiles disaggregated by the initial silver source and based on the number of washing cycles as well as exposure to artificial sweat under different pH conditions. Data used to draw Figure 29A and 29B are extracted from the studies that are presented in Tables E1-E2.

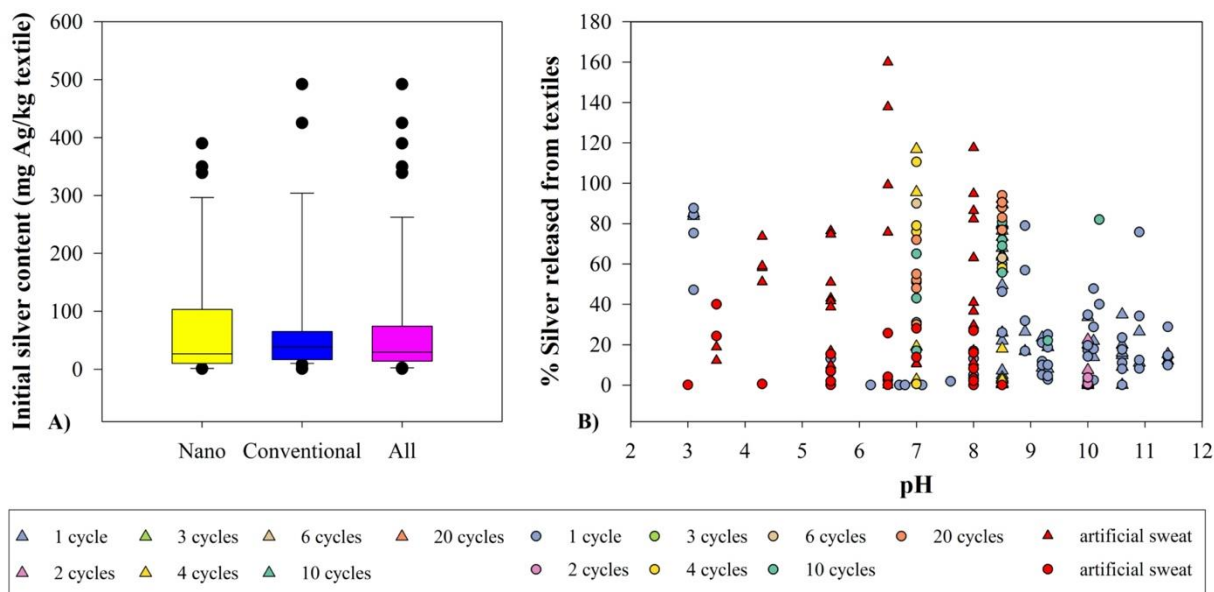


Figure 29. A) The range of the initial silver content in silver-enabled textiles (n indicates the number of data points used to draw the boxplots, initial silver > 500 mg Ag/kg textile are excluded); B) percentage of silver released from textiles due to laundering and exposure to artificial sweat (triangle markers show that initial silver source in textiles were conventional, circle markers indicate that initial silver source in textiles were nano, color scheme illustrates different number of washing cycles) [80, 82, 83, 296–311] (the points that indicate >100% of initial Ag release is due to the Ag/nAg not uniformly distributed in experimental samples).

Research suggested that, although the attachment method may affect the release process, the amount of silver released from antibacterial textiles is proportional to the initial silver loading [30, 32, 303]. Therefore, an ‘ideal product’ (for the lowest environmental cost) should include the lowest possible silver loading for enough efficacy to inhibit bacteria during its useful lifetime. For reference, Spielman-Sun et al. indicated that textiles that include even just <math><10\ \mu\text{g/g}</math> Ag perform high efficacy [311]. While Ureyen and Aslan reported even a slightly lower content of 5 $\mu\text{g/g}$ Ag for a strong antibacterial efficiency [304]. Lastly, Reed et al. conducted efficacy

testing on silver enabled textiles after four laundering cycles, and concluded that 2 $\mu\text{g/g}$ Ag was enough to inhibit >99.9% *E.coli* growth on textiles [303]. Textile characteristics from Reed et al. are considered in the current study [303].

The goal of this study to elucidate the necessity of EC-CFs for Ag/nAg enabled textiles by conducting a cradle-to-grave LCA on four different silver enabled textiles with different initial loadings. Given that this work investigates the contributions resulting from the use and end-of-life phases (i.e. direct impacts), assumptions made for these two phases are presented in the materials and methods section in detail. Later sections demonstrate the results and discuss the implications of manufacturing and using antibacterial textiles along with limitations and suggestions for future research. Results are intended to inform future research agendas in deciding whether there is a need for calculating nano-specific impacts to model direct emissions.

6.3. Materials and Methods

6.3.1. Goal and scope definition

The goal of the current study is to evaluate the cradle-to-grave environmental impacts of four different silver enabled polyester (PES) textiles by combining direct (nano-specific) and indirect (non-nano) emissions resulting from each life cycle stage. Indirect environmental impacts are modeled using LCA with SimaPro 8.5.2 software, and Ecoinvent and USLCI (U.S. Life Cycle Inventory) databases [150, 312, 313]. The tool for the reduction and assessment of chemical and other environmental impacts (TRACI 2.1) is used as an impact assessment method [18]. The TRACI impact categories along with their abbreviations and units are ozone depletion (OD in kg CFC11-eq.), global warming (GW in kg CO₂-eq.), smog (PS in kg O₃-eq.), acidification (AC in kg SO₂-eq.), eutrophication (EU in kg N-eq.), carcinogenics (HHC in

CTUh), non-carcinogenics (HHNC in CTUh), respiratory effects (RE in kg PM_{2.5}-eq.), ecotoxicity (EC in CTUe), and fossil fuel depletion (FF in MJ surplus energy). The functional unit to quantify the performance of the system is selected as 145 gram (g) PES textile, indicates men's t-shirt with a large size [32].

6.3.2. Considerations for developing life cycle inventory informed by the literature

The published body of textile related LCA literature as well as material flow analysis studies are used to develop a cradle-to-grave life cycle inventory for material and energy inputs and emissions associated with producing and using silver enabled textiles. Details on each life cycle stage are explained in the following subsections and the boundaries of the analyzed system is presented in Figure 30. Inventory data and further assumptions are included in Table E3.

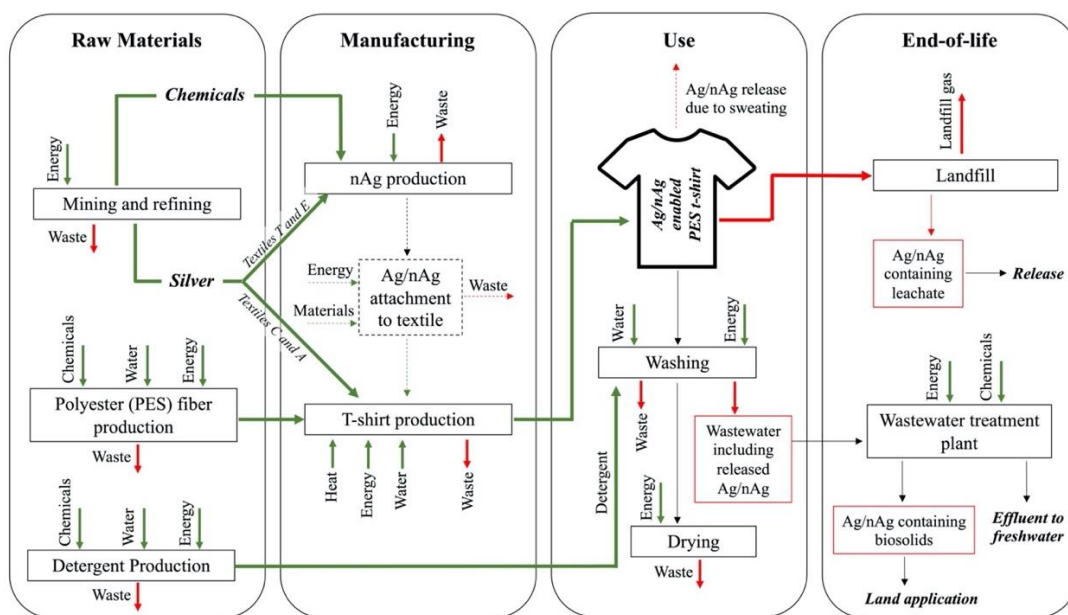


Figure 30. System boundaries considered in the current study along with flows for each life cycle phase. Processes/flows with dashed outlines are not included in the LCA. Green arrows indicate inputs and red arrows represent outputs.

6.3.2.1. Raw materials acquisition and manufacturing

Four different silver enabled PES textiles are analyzed in the current study (referred to as products T, E, A and C for the rest of the work) with different silver loadings. The details for the silver forms (nano, metallic, salt) and concentrations of each textile are described in the literature [32, 303]. Product T (tethered) has a silver concentration of 22.8 micrograms of nAg per gram of textile ($\mu\text{g/g}$) and the nAg is linked to textile with a proprietary linking agent. Product E (electrostatic) has a silver concentration of $1.07 \mu\text{g nAg/g}$ textile and the nAg is attached to textile via surface charge difference. Product A (attached) contains AgCl as a silver source with a concentration of $16.4 \mu\text{g Ag/g}$ textile. Lastly, in product C (coated), metallic silver is incorporated into fibers with a concentration of $4,030 \mu\text{g Ag/g}$. For products T and E, nAg synthesis is modeled using data from Temizel-Sekeryan and Hicks, where the authors mentioned that textile industry mostly uses chemical reduction (CR), flame spray pyrolysis (FSP), arc plasma (AP) and spark methods to synthesize nAg to be embedded in their products [126]. It is known that the AgCl, that is used in product A, is obtained from recycled sources [32]. Due to the lack of information on the exact recycling processes, virgin AgCl is used as a silver source in product A. Finally, for product C, mining and refining of metallic silver is included in the evaluation.

A non-dyed textile (100% PES) is modeled using inventory data from Walser et al., where the authors provided details on material (e.g. polyethylene terephthalate) and energy (e.g. heat, electricity) consumed for producing a single t-shirt [58]. Similar to previous literature, the lifetime of a t-shirt is assumed to be 100 laundering cycles [30, 32, 58]. It should be noted that, due to the lack of information, the Ag/nAg attachment processes themselves are not included in the LCA.

6.3.2.2. Use

The use phase includes wearing and laundering (i.e. washing and drying) processes. Numerous research studies have evaluated potential Ag/nAg release from textiles as a result of sweating as tabulated in Table E2 [308–311]. Given that human sweat has various pH and composition from one individual to another, and that has a significant impact on the quantity of silver lost, Ag/nAg releases due to sweating are excluded in the current work [314]. As laundering process was previously identified to be one of the most impactful step in LCA of textiles [30], several different laundering processes are modeled in the current study using data from Hicks and Theis [32]. Two different washer and dryer options are considered as conventional efficiency (CE) and high efficiency (HE) machines, among which HE consumes less energy, water and detergent when applicable. Scenarios are developed pairing CE washer and dryer (CE/CE), CE washer and line drying (CE/LN), HE washer and dryer (HE/HE) and HE washer and line drying (HE/LN) to project different environmental costs associated with laundering step. Details on the water and energy consumption of these options can be found in Table E3. Detergent input is modeled using the composition of standard laundry detergent in accordance with Reed et al., where they used the formulation from the American Association of Textile Colorists and Chemists [303].

Reed et al. found that the quantity of Ag/nAg released through laundering is not linear with the number of washings. Accordingly, Hicks and Theis modeled the silver losses as a zero-order function (released silver = $k \cdot t$) using experimental data from Reed et al., where the amount of Ag/nAg lost during the first four ($t=4$) washing cycles were provided [32, 303]. As a result, the rate constants (k) are calculated as 3.25 (product T), 0.15 (product E), 0.73 (product A) and 25.25 (product C). Considering these rate constants, only product C will retain 37% of its silver

after 100 laundry cycles, and the rest of the products will lose all of their silver during laundering into the wastewater.

6.3.2.3. End-of-life

Textile materials, at the end of their useful lives, can be recycled, composted, incinerated and landfilled [315]. Although more than 95% of used textiles can be recycled, currently the majority of them are sent to landfills [62, 316]. According to the US EPA, 11.2 million tons of textiles were landfilled, 3.2 million tons were combusted for energy recovery and 2.5 million tons were recycled and repurposed in 2017 in the USA, which correspond to 66%, 19% and 15% of the total amount of textiles disposed of, respectively [317]. As the majority of textiles are disposed of in landfills, in the current study, landfilling is assumed as the disposal scenario and disposed textiles (PES portion) are modeled as inert materials.

If textiles retain a fraction of their initial silver content at the final laundering (in this case product C), an additional release may occur due to their potential contact with landfill leachate. Up to date, only four studies related to silver enabled textiles have included this consideration into their environmental assessments [302, 303, 311, 318], using Toxicity Characteristic Leaching Protocol (TCLP) developed by the US EPA [319]. Limpiteeprakan and Babel applied TCLP into various type of unwashed fabrics to cross compare the amount of silver released as a function of textile type. They found that, up to 81% of silver can be released to leachate from PES fabrics, following by 39% release from cotton and 25% release from 35/65 cotton/PES fabrics in either ionic or particulate forms [318]. Mitrano et al. further investigated whether the laundering step has any impact on landfill leaching. They found that 35-45% of Ag was released from unwashed textiles, whereas only 0.5% of Ag was released from laundered textiles [302].

General conclusion from these studies was that, released silver should not pose a risk because of being unstable in the landfill leachate [302, 311]. In the current study, TCLP findings documented by Reed et al. are used where they mentioned that all the remaining Ag would be released to the environment [32, 303].

Silver released due to laundering is assumed to be treated in a standard wastewater treatment plant (WWTP). For this purpose, municipal WWTP with moderately large treatment capacity is selected in SimaPro software. Literature suggests that 82-95% of silver that enters to WWTP is removed and the rest of it retains in biosolids [320–326]. Biosolids can be used for agricultural (e.g. replacement for chemical fertilizers) and non-agricultural (e.g. reclamation sites, lawn and home gardens) land application purposes as well as can be disposed [327, 328]. In 2019, in the USA, 51% of the generated biosolids were land applied, 22% were landfilled, 16% were incinerated, 10% were stored and 1% were disposed [328]. Given that the majority of biosolids are land applied, questions arise regarding the potential environmental and human health impacts that this action might cause, especially when the biosolids include silver species due to the use of silver enabled consumer products [30].

The silver that remained in the biosolids is mostly (~80-100%) in sulfidated form (Ag_2S), which has a low solubility and bioavailability, and is stable under various pH and ionic strength conditions [322, 323, 329]. According to Zhang et al., nAg do not pose a risk for wastewater ecosystems, because ionic silver (Ag^+) cannot be released from nAg due to anaerobic conditions. Instead, silver complexes and precipitates are formed, which are low in solubility and toxicity compared to nAg and Ag^+ [324]. For reference, toxicity of different silver species that may be present in biosolids is ranked from the least to the most as Ag_2S , AgCl , nAg and AgNO_3 (or Ag^+) respectively [323]. Another study presented similar findings, where authors argued that the

majority of the released silver is paired with chlorine and sulfur when treated in WWTPs, regardless of its initial form (nano or conventional), presence of bleach/detergent and weathering during use phase [314]. Pradas del Real et al. studied the fate of nAg containing biosolids which were applied to agricultural lands. Besides oxidation resistant Ag_2S , they identified Ag-thiol complexes that may be bioavailable for terrestrial organisms and may require more attention [329]. Wang et al. concluded that the risk of land applied biosolids that contain different silver complexes to terrestrial organisms and to human health can be assumed negligible, but the impact of released species should be studied extensively [323]. In the current study, the silver in biosolids are assumed to be Ag_2S and calculations are conducted accordingly.

As mentioned before, the majority of silver that enters to WWTP is removed [325]. Previous LCA studies that modeled cradle-to-grave environmental impacts of silver enabled textiles assumed that the remaining silver is discharged as Ag^+ to freshwaters as WWTP effluent [30, 32, 56, 58]. However, research suggested that 7-8% of the silver that is not removed by WWTPs (i.e. ~5-12% of the released silver is present in the effluent) is in dissolved form and depending on the effluent characteristics, different forms of silver can exist and be discharged to receiving water bodies [330]. Another study, where the behavior of nAg in pilot WWTP was investigated, concluded that about 86% of silver was transformed into Ag_2S and 14% remained in the nano and metallic forms [300, 331]. Azimzada et al. showed that the bioavailability of silver species in WWTP effluent is drastically low due to the presence of inorganic and organic substances in the media. They further characterized the Ag and found that 83-98% of the silver was either complexed or in nano form and the remaining was in free form [332]. A recent study also found that the bioavailability of silver species (to aquatic organisms), that are transformed from nAg, was reduced significantly after treatment and the major form found in the effluent was

Ag₂S [333]. Considering all the aforementioned studies, average characteristics are assumed as effluent consisting of 83% Ag₂S, 7% Ag⁺, 7% nAg and 3% Ag(0). Sensitivity analysis is carried out to identify whether the assumed characteristics of the effluent are sensitive to the overall LCA results.

6.3.3. Ecotoxicity characterization factors for nAg

Direct ecotoxicity impacts resulting from the nAg release are incorporated into LCA results using nano-specific CFs developed in the previous study (Temizel-Sekeryan and Hicks Chapter 5). Using mesocosm conditions and principles of colloidal science, optimistic (i.e. low estimate) CF for nAg is calculated as 2.67×10^3 CTUe/kg, and skeptical (i.e. high estimate) CF is calculated as 1.78×10^5 CTUe/kg nAg. In the current study, direct impact calculations are conducted using high estimate CF to draw a worst-case scenario. In order to calculate impacts due to the release of silver and silver compounds, SimaPro software uses a generic CF from the USEtox as 1.94×10^5 CTUe/kg which is originally for ionic silver [20]. At a first glance, it can be observed that modeling nAg release as Ag⁺ would potentially cause overestimating the results. It should be noted that, due to the lack of nano-specific human health CFs, only direct ecotoxicity impacts are studied in the current research.

6.3.4. Sensitivity and uncertainty analyses

A sensitivity analysis is performed in order to identify the flows/processes to which the LCA results are sensitive. The value of each flow is modified by 20% while others are kept constant. Then, the impact assessment results are recalculated to see how this 20% change in the flows affected the overall LCA results. Sensitivity factors (SF) for each flow are calculated and

the ones with SF of $\leq 2\%$ (assumed cut-off value) are identified as not sensitive to the system [289]. Furthermore, in order to estimate the highest and lowest possible results for each impact category, uncertainty analysis for each scenario is conducted using Monte Carlo simulations in SimaPro (95% confidence interval, 1000 runs) [289].

6.4. Results

6.4.1. Life cycle impact assessment

Environmental impacts of different silver enabled textiles as well as laundering scenarios are evaluated, and the characterization results based on TRACI 2.1 are presented in Tables E4-E19. Figure 31 shows disaggregated cumulative impacts of one article of silver enabled textile under different laundering scenarios throughout its life cycle. Given that several categories performed similar trends, four of them are selected to represent different trends as: GW, HHNC, EC and EU. Figures for the rest of the impact categories are included in Appendix E (Figure E2). For product T and product E, nAg syntheses are modeled using different routes relevant to textile industry as explained in Temizel-Sekeryan and Hicks [126]. However, considering cradle-to-grave impacts, the relative contributions of the nAg synthesis processes are found negligible (up to 1.44% for product T and 0.09% for product E). Therefore, averaged characterization results are used to draw the components of Figure 31. Disaggregated cradle-to-grave LCA results per different nAg synthesis routes can be found in Tables E4-E11 for reference.

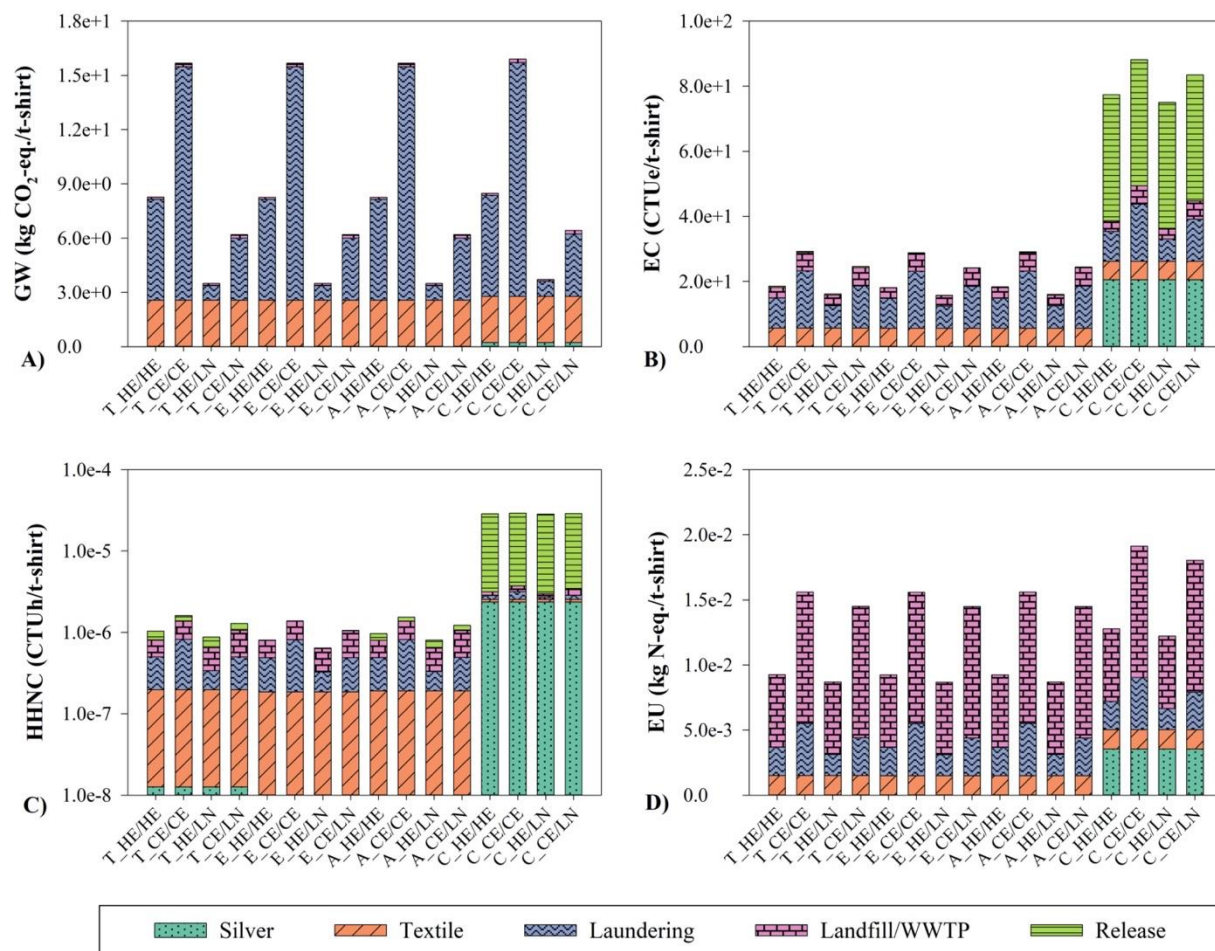


Figure 31. Environmental impacts of various silver enabled textiles under different laundering scenarios A) GW, B) EC, C) HHNC and D) EU (x axis reads product code_type of washer/type of dryer, e.g. T_HE/LN means product T with high efficiency washer and line drying).

The analysis showed that, in the majority of impact categories, the contribution of laundering step dominates the overall LCA results including OD, GW, AC, PS, HHC, RE and FF, which is consistent with previous studies [30, 32, 56, 58]. However, some exceptions exist, and are highlighted. One exception was that, instead of laundering step in HE/LN scenarios, textile manufacturing is identified as the main contributor for GW, PS, AC and RE categories considering all product types. This is mainly due to the potential savings that could be gained

through eliminating the energy consumption of drying. Another one was from FF category, where impacts resulting from textile production step exceeded both HE/LN and CE/LN laundering scenarios for all products. In the case of EU, waste management step showed the highest contribution (44-70%) in all cases mainly due to the wastewater treatment process. Impacts from laundering step followed waste management in all scenarios (19-26%) except for product C, where mining and refining of silver showed the second highest contribution to EU (19-28%). The trends in HHNC and EC categories vary significantly. In terms of HHNC, considering the majority of scenarios (except CE/CE) and products T, E and A, most impact contributions came from waste management step (30-53%), while for CE/CE, laundering is identified as the hotspot. Given that product C has the highest initial silver content, the amount of released silver is significant, and this contributes to more than 87% of HHNC impacts. Similarly, due to the high initial silver loading, release is identified as the hotspot for all scenarios associated with product C with more than 44% contribution. For the rest of the product types and laundering scenarios, laundering was identified as the most impactful process (42-61%). Finally, in order to provide the upper and lower bounds of impacts for each category, uncertainties extracted from Monte Carlo analyses are illustrated in Tables E20-E23.

6.4.2. Sensitivity analysis

For all of the ten environmental impact categories, sensitivity analysis is conducted, and SFs are calculated for each product type (T, E, A and C) and laundering scenario (HE/HE, HE/LN, CE/CE and CE/LN) pairs. Figure 32 shows SFs for each product under HE/LN laundering scenario. HE/LN is selected for the figure as it represents the least impactful laundering option; therefore, a potential change in any of the life cycle steps may affect the

overall result significantly than they would do in other scenarios. In other words, a conservative scenario is selected for inclusion as results are expected to be more sensitive to change in HE/LN. The red line indicates the assumed cut-off value of 2%, and the SFs that are above this line are considered sensitive parameters to the system. SFs for the remaining scenarios are provided in Figures E3-E5.

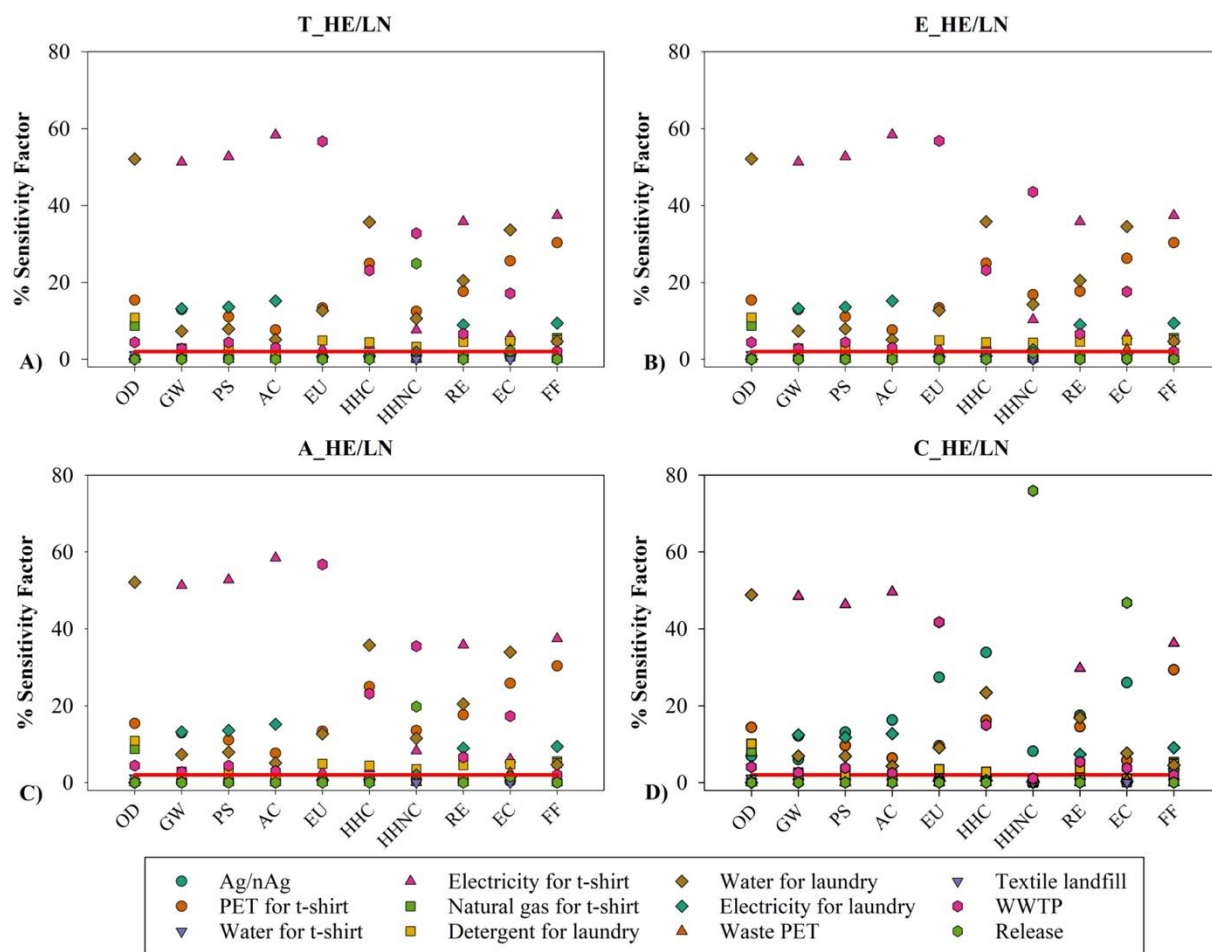


Figure 32. Sensitivity factors of each input/output parameter to environmental impact categories under HE/LN scenario for A) product T, B) product E, C) product A and D) product C.

Considering products T, E and A and HE/LN scenario, the trends for SFs associated with the majority of the impact categories (8 out of 10) are found to be the same except for HHNC and EC. In GW, PS, AC, RE and FF categories, electricity consumed during laundering performed as the most sensitive parameter for all scenarios except for HE/LN, where electricity consumed for textile manufacturing showed the highest sensitivity. In OD, HHC and EC categories, water consumed for laundry was identified as the most sensitive parameter in all scenarios. Lastly for EU and HHNC categories, wastewater treatment performed as the most sensitive parameter. Although the sensitivity rankings and degrees for each process differ within each laundering scenario; the trends for SFs associated with the majority of the impact categories (except EC and HHNC) are found to be the same for products T, E and A. The reason for different trends in EC and HHNC is mainly associated with the amount of silver present in the effluent and biosolids after wastewater treatment step. Silver release from product T (initial loading of 22 $\mu\text{g Ag/g}$ as nAg) and product A (initial loading of 16.4 $\mu\text{g Ag/g}$ as AgCl) showed moderate sensitivities to HHNC in all scenarios with SFs ranging from 0.14 (T_CE/CE) to 0.25 (T_HE/LN) for product T, and 0.11 (A_CE/CE) to 0.20 (A_HE/LN) for product A. In terms of EC, only HE/LN scenario associated with product T showed sensitivity due to silver release. Product E (initial loading of 1.07 $\mu\text{g Ag/g}$ as nAg) did not show any sensitivity in either of the categories due to having very low amount of silver loading and its negligible impact due to release.

Product C (initial loading of 4,030 $\mu\text{g Ag/g}$ as Ag^0) showed varying trends in all environmental impact categories mainly due to its significantly high initial silver loading. Initial silver input (refining and mining) was found sensitive for all of the impact categories in all scenarios considered, with SFs ranging from 1.01% (FF of C_CE/CE) to 33.86% (HHC of

C_HE/LN). In GW, PS, AC, RE and FF categories, electricity consumed during laundering performed as the most sensitive parameter for all scenarios except C_HE/LN, where electricity consumed for textile manufacturing showed the highest sensitivity. In EU, wastewater treatment was identified as the most sensitive parameter in all scenarios. Not surprisingly, for HHNC and EC, silver release performed the highest sensitivities with SFs up to 0.76 and 0.47 respectively. While in C_CE/LN and C_CE/CE, water used for laundering was the most sensitive parameter for HHC; in C_HE/LN and C_HE/HE silver mining and refining performed the most sensitivity. Lastly for OD, water used for laundering was identified as the most sensitive parameter in all scenarios. SFs associated with each product and scenario are tabulated in Tables E24-E27.

6.5. Discussion

6.5.1. Environmental significance

As stated previously, the contributions of this present work into the LCA literature on silver enabled textiles are related to comparing direct and indirect emissions resulting from the product's life cycle. Considering indirect emissions (i.e. emissions excluding Ag/nAg release), current findings corroborated with the published body of the literature, where use phase (laundering) and production of textile (regardless of Ag/nAg enabling step) were identified as impact hotspots for the majority of environmental impact categories [30, 32, 60]. The WWTP has not been analyzed in the previous literature, which slightly changed the trends for EU and HHNC only. Disposal phase (landfill and WWTP combined) contributed to EU the most in all scenarios (up to 70%), and to HHNC in all scenarios (up to 53%) except the ones that used CE washer/dryers as well as product C overall. In general, product C performed differently than

others due to its significantly high silver content affecting the overall indirect LCA results in EU, HHC, HHNC, RE and EC.

Direct emissions modeled in the present work elucidated the evolving debate on the necessity of nano-specific CFs for nAg, in other words, on the applicability of modeling nAg released from textiles as Ag^+ . Both impact assessment and sensitivity analysis showed that silver release contributed to EC and HHNC categories in varying degrees. Even though a skeptical (i.e. high estimate) CF is used to present a worst possible model and SimaPro applying CF for Ag^+ for all silver compounds (e.g. Ag_2S), in the majority of instances, direct impacts resulting from silver release are found to be much lower than indirect cradle-to-grave impacts of silver enabled textiles. For instance, while the indirect EC of T_CE/CE scenario was calculated as 2.89×10^1 CTUe/kg, direct EC was found two orders of magnitude lower as 3.49×10^{-1} CTUe/kg. Similarly, indirect HHNC of T_CE/CE was 1.38×10^{-6} CTUh/kg, whereas direct impacts were 2.30×10^{-7} CTUh/kg. As expected, the EC and HHNC impacts associated with silver release were found to be proportional with the initial silver content. For instance, considering HE/HE scenario, release phase for product C contributed to 89% of HHNC and 50% of EC, product T 22% of HHNC and 2% of EC, product A 17% of HHNC and 1% of EC, and lastly product E 1% of HHNC and 0.1% of EC. Research suggested that the amount of Ag/nAg release during use increases with increased initial silver loading, which supports the findings discussed herein [297, 303].

Given that product C has significantly higher initial silver content than other t-shirts, the trends of direct and indirect impacts associated with its life cycle were different for all categories. In terms of HHNC, direct impacts of product C were found to be one order of magnitude higher for all scenarios. For instance, while indirect impacts of C_CE/CE was calculated as 3.72×10^{-6} CTUh/kg, direct impacts caused 2.55×10^{-5} CTUe/kg emissions.

Considering EC, direct impacts slightly exceeded the indirect impacts only in C_HE/LN scenario by 6%, due to lower electricity requirement associated with using high efficiency washer and no drying.

It can be concluded that, unless there is a very large quantity of initial silver loading per textile, direct impacts would be much lower than indirect impacts. Recent research supports this finding, where authors proved that under anoxic and/or oxic conditions, due to limited levels of ion release, toxicity of nAg is expected to be very low in natural media [334]. Therefore, incorporating an optimized level of silver in order to achieve desired antibacterial efficacy would help decreasing the overall life cycle impacts, because lower amount of Ag/nAg mining/production would be required, and consequently lower amount of Ag/nAg would be released. Also, given that release phase showed sensitivity in the HHNC category in the majority of instances, more focus should be placed on developing nano-specific CFs for this category.

Some limitations exist with the current work such as the lack of human health related (HHC and HHNC) CFs for the released nAg. The reason behind this is that, there are relatively low number of toxicity literature for nAg on human health than ecotoxicity to develop CFs. Another limitation is neglecting the Ag/nAg attachment processes as well as the Ag/nAg release that potentially could occur during production and/or manufacturing of nano-enabled textiles. Giese et al. predicted that 0-1% of Ag/nAg might release during these phases, which is likely to be disposed of together with other wastes generated during fabrication [84]. Given that the form of Ag/nAg and final disposal routes are unknown, release during production and/or manufacturing is neglected in the current work. This might be of concern for product C only, as it has the highest initial silver content comparing to others.

Such comprehensive environmental assessments may help researchers to shed light on grey areas like the necessity of nAg specific CFs for usage in LCAs of nano-enabled textiles. This study uses LCA in order to elaborate the need for nano-specific CFs for antibacterial textiles and direct the future research agenda based on the results. Current findings suggest that, calculating nano-specific impacts and incorporating them into the overall LCA results do not make a significant difference for EC impact category. Therefore, although modeling nAg release as Ag^+ likely results in an overestimation of EC impacts, it may still be applicable as the overall EC results are not sensitive to release. However, this is presumably not the case for HH impacts for which the release showed significant sensitivity for HHNC category. Future work should expand on developing nAg specific CFs for HHC and HHNC categories to be incorporated into LCA results.

6.6. Acknowledgements

Support for this research was provided by the Wisconsin Alumni Research Foundation (WARF). This work has not been formally reviewed by the WARF, and the findings presented by the authors are their own.

7. Conclusions and Future Work

7.1. Summary and Contributions

The first LCA paper (Chapter 2) presented cradle-to-gate impact assessments of six different AgNPs industrially preferred synthesis routes along with thirteen different inventories and a mass based functional unit. Also, it provided models for the annual global environmental impacts of producing AgNPs segmented by industries where the majority of AgNPs are used such as textiles; coatings, paints and pigments; consumer electronics and optics; cosmetics; medical and packaging. Finally, it projected the industrial scale AgNPs syntheses and future life cycle impacts by utilizing simplified scale-up factors. It suggested that the global environmental impact of AgNPs may vary significantly as a function of the synthesis method, scale, and desired product application.

The second LCA paper (Chapter 3) provided cradle-to-gate impact assessments of eight single-walled and seven multi-walled CNTs synthesis processes with a mass based functional unit. Moreover, it presented models for the annual global environmental impacts of producing CNTs segregated by industries where the majority of CNTs are used such as electronics and optics; energy and environment; coatings, paints and pigments; composites; automotive; aerospace and sensors. Finally, it applied hypothetical scaling up scenarios in order to estimate industrial scale impacts of manufacturing CNTs. Similar to the findings from Chapter 2, it suggested that the global environmental impact of CNTs varies significantly as a function of the synthesis process, production scale, and application.

The third paper (Chapter 4) investigated how physicochemical properties affect the effect factors, and therefore the nano-specific characterization factors for nAg. As the potential ecotoxicity of released nAg depends on the physicochemical properties of the material and the

release media, this chapter provided multiple effect factors for different scenarios. It used 366 toxicity data points that belong to various freshwater organisms including crustaceans, algae, fish and protozoa. Results suggested that larger nAg have lower effect factors, and therefore lower nano-specific (or direct) impacts, and coating is an important consideration in toxicity assessment. More broadly, this chapter contributed to the literature by providing effect factors for particular sized/coated nAg. These factors can be incorporated with the specific fate and exposure patterns to project direct life cycle impacts resulting from the released nAg.

The fourth paper (Chapter 5) calculated nano-specific freshwater ecotoxicity characterization factors for nAg by combining the principles of colloidal science with the USEtox model to be integrated to cradle-to-grave LCAs. It compared two different scenarios for fate patterns, in which the hetero-aggregation is modeled as either a removal or transformation process. This chapter further discussed the applicability of using ionic silver to model released nAg and suggested that using ionic silver potentially causes an overestimation as nAg has different effect, exposure and fate patterns than the ionic silver.

The fifth paper (Chapter 6) combined all the aforementioned chapters in order to conduct a cradle-to-grave impact assessment for nAg enabled textiles. It elucidated the necessity of freshwater ecotoxicity and human health characterization factors for nAg enabled textiles. It suggested that unless the initial silver loading per textile is significantly high, ecotoxicity and human health impacts of released silver species (or direct impacts) would be lower than ecotoxicity and human health impacts resulting from raw materials acquisition and manufacturing (or indirect impacts) of the antibacterial textiles. Furthermore, sensitivity analysis showed that human health impacts are more sensitive than ecotoxicity impacts to the release phase, which indicated that human health categories may require future attention.

Overall, this work presented a comprehensive framework for investigating the direct and indirect environmental impacts of nAg and nAg enabled consumer products. It also took the first step for a similar research path for CNTs, by providing cradle-to-gate environmental impact assessments for multiple CNTs production processes. This research could serve as a roadmap for future LCAs, especially for the ones that aim to incorporate direct and indirect environmental impacts to present a holistic evaluation.

7.2. Future Work

Further work on developing nano-specific characterization factors would contribute to this body of research. Human health (carcinogenics and non-carcinogenics) characterization factors should be further explored for nAg and nAg enabled consumer products. Additionally, this work used parameters from mesocosm studies in order to decrease the number of variables while modeling the fate of nAg. Future work may contribute to this area by modeling fate factors using probabilistic tools (such as Monte Carlo) and principles of colloidal science to advance the state of knowledge.

There are 25 different ENMs with varying level of maturities that are commercially available. Although market-based metrics (e.g. production volumes, market demand, growth rate) exist in the literature, environmental and human health implications of the majority of these ENMs are lacking. Future cradle-to-grave LCA research should be encouraged to evaluate the benefits and costs of the ENMs that are not studied.

References

1. Janković NZ, Plata DL (2019) Engineered nanomaterials in the context of global element cycles. *Environmental Science: Nano*, 6(9):2697–2711. <https://doi.org/10.1039/C9EN00322C>
2. ISO (2015) ISO/TS 80004-2: Nanotechnologies — Vocabulary — Part 2: Nano-objects. <https://www.iso.org/standard/54440.html>
3. Klopffer W, Curran MA, Frankl P, Heijungs R, Kohler A, Olsen SI (2007) Nanotechnology and Life Cycle Assessment. A systems approach to Nanotechnology and the environment: Synthesis of Results Obtained at a Workshop Washington, DC 2–3 October 2006.
4. Pourzahedi L (2016) Environmental Impact Assessment of Nanoparticles and Nano-enabled Products Using LCA Frameworks.
5. Keller AA, McFerran S, Lazareva A, Suh S (2013) Global life cycle releases of engineered nanomaterials. *Journal of Nanoparticle Research*, 15(6)<https://doi.org/10.1007/s11051-013-1692-4>
6. Inkwood Research (2019) Global Nanomaterials Market Forecast 2020-2028. <https://www.inkwoodresearch.com/reports/nanomaterials-market/>
7. Inshakova E, Inshakov O (2017) World market for nanomaterials: structure and trends. *MATEC Web of Conferences*, 129:02013. <https://doi.org/10.1051/mateconf/201712902013>
8. Sahu YS (2016) Nanomaterials Market by Type - Global Opportunity Analysis and Industry Forecast, 2014-2022. :178. <https://www.alliedmarketresearch.com/nano-materials-market>
9. Zion Market Research (2018) Nanomaterials Market To Report Impressive Growth, Revenue To Surge To US\$16.8 Billion by 2022. <https://www.zionmarketresearch.com/news/nanomaterials-market>
10. Research and Markets (2019) Global Nanomaterials Market Report 2019-2025. <https://www.prnewswire.com/news-releases/global-nanomaterials-market-report-2019-2025-market-overview-focus-on-select-players-trends--drivers-global-perspective-300943094.html>
11. Grand View Research (2020) Global Nanomaterials Market Size Report, 2020-2027. <https://www.grandviewresearch.com/industry-analysis/nanotechnology-and-nanomaterials-market>
12. Gilbertson LM, Wender BA, Zimmerman JB, Eckelman MJ (2015) Coordinating modeling and experimental research of engineered nanomaterials to improve life cycle assessment studies. *Environmental Science: Nano*, 2(6):669–682. <https://doi.org/10.1039/C5EN00097A>
13. Garvey T (2016) Identifying the Potential Environmental Impacts of Engineered Nanomaterials.

14. Wender B (2015) Developing Anticipatory Life Cycle Assessment Tools to Support Responsible Innovation.
15. ISO (2006) ISO 14040:2006 - Environmental management -- Life cycle assessment -- Principles and framework. <https://www.iso.org/standard/37456.html>
16. ISO (2006) ISO 14044:2006 - Environmental management -- Life cycle assessment -- Requirements and guidelines. <https://www.iso.org/standard/38498.html>
17. Simonen K (2014) Life Cycle Assessment.
18. Bare J (2012) Tool for the Reduction and Assessment of Chemical and Other Environmental Impacts (TRACI) version 2.1. <https://nepis.epa.gov/Adobe/PDF/P100HN53.pdf>
19. Guinée JB, Gorrée M, Heijungs R, Huppes G, Kleijn R, Koning A, Oers L, Wegener Sleeswijk A, Suh S, Udo de Haes HA, Brujin H, Duin R, Huijbregts MAJ (2002) Handbook on life cycle assessment. Operational guide to the ISO standards. I: LCA in perspective. IIA: Guide. IIB: Operational annex. III: Scientific background.
20. Fantke P, Bijster M, Guignard C, Hauschild MZ, Huijbregts M, Jolliet O, Kounina A, Magaud V, Margni M, McKone TE, Posthuma L, Rosenbaum RK, Van De Meent D, Van Zelm R (2017) USEtox® 2.0 Documentation (Version 1.00). <https://doi.org/10.11581/DTU:00000011>
21. Lippiatt BC (2002) BEES 3.0 Building for Environmental and Economic Sustainability Technical Manual and User Guide. :207. https://www.usgbc.org/drupal/legacy/usgbc/docs/LEED_tsac/VSI_BEES.pdf
22. Salieri B, Turner DA, Nowack B, Hirschler R (2018) Life cycle assessment of manufactured nanomaterials: Where are we? *NanoImpact*, 10:108–120. <https://doi.org/10.1016/j.impact.2017.12.003>
23. Rosenbaum RK, Bachmann TM, Gold LS, Huijbregts MAJ, Jolliet O, Juraske R, Koehler A, Larsen HF, MacLeod M, Margni M, McKone TE, Payet J, Schuhmacher M, Meent D van de, Hauschild MZ (2008) USEtox—the UNEP-SETAC toxicity model: recommended characterisation factors for human toxicity and freshwater ecotoxicity in life cycle impact assessment. *The International Journal of Life Cycle Assessment*, 13(7):532–546. <https://doi.org/10.1007/s11367-008-0038-4>
24. Hauschild MZ, Huijbregts M, Jolliet O, Macleod M, Margni M, Meent D van de, Rosenbaum RK, McKone TE (2008) Building a Model Based on Scientific Consensus for Life Cycle Impact Assessment of Chemicals: The Search for Harmony and Parsimony. *Environmental Science & Technology*, 42(19):7032–7037. <https://doi.org/10.1021/es703145t>
25. Miseljic M, Olsen SI (2014) Life-cycle assessment of engineered nanomaterials: a literature review of assessment status. *Journal of Nanoparticle Research*, 16(6):2427. <https://doi.org/10.1007/s11051-014-2427-x>

26. Deng Y, Li J, Li T, Zhang J, Yang F, Yuan C (2017) Life cycle assessment of high capacity molybdenum disulfide lithium-ion battery for electric vehicles. *Energy*, 123:77–88. <https://doi.org/10.1016/j.energy.2017.01.096>
27. Ahari H, Karim G, Anvar AA, Pooyamanesh M, Sajadis A, Mostaghim A, Heydari S (2018) Synthesis of the Silver Nanoparticle by Chemical Reduction Method and Preparation of Nanocomposite based on AgNPS. <https://doi.org/10.11159/iccpe18.125>
28. Bafana A, Kumar SV, Temizel-Sekeryan S, Dahoumane SA, Haselbach L, Jeffryes CS (2018) Evaluating microwave-synthesized silver nanoparticles from silver nitrate with life cycle assessment techniques. *Science of The Total Environment*, 636:936–943. <https://doi.org/10.1016/j.scitotenv.2018.04.345>
29. OECD (2010) List of Manufactured Nanomaterials and List of Endpoints for Phase One of the Sponsorship Programme for the Testing of Manufactured Nanomaterials: Revision.
30. Hicks AL, Gilbertson LM, Yamani JS, Theis TL, Zimmerman JB (2015) Life Cycle Payback Estimates of Nanosilver Enabled Textiles under Different Silver Loading, Release, And Laundering Scenarios Informed by Literature Review. *Environmental Science & Technology*, 49(13):7529–7542. <https://doi.org/10.1021/acs.est.5b01176>
31. Hicks AL, Reed RB, Theis TL, Hanigan D, Huling H, Zaikova T, Hutchison JE, Miller J (2016) Environmental impacts of reusable nanoscale silver-coated hospital gowns compared to single-use, disposable gowns. *Environmental Science: Nano*, 3(5):1124–1132. <https://doi.org/10.1039/C6EN00168H>
32. Hicks AL, Theis TL (2017) A comparative life cycle assessment of commercially available household silver-enabled polyester textiles. *The International Journal of Life Cycle Assessment*, 22(2):256–265. <https://doi.org/10.1007/s11367-016-1145-2>
33. Kelly KL, Coronado E, Zhao LL, Schatz GC (2003) The Optical Properties of Metal Nanoparticles: The Influence of Size, Shape, and Dielectric Environment. *The Journal of Physical Chemistry B*, 107(3):668–677. <https://doi.org/10.1021/jp026731y>
34. Liu P, Zhao M (2009) Silver nanoparticle supported on halloysite nanotubes catalyzed reduction of 4-nitrophenol (4-NP). *Applied Surface Science*, 255(7):3989–3993. <https://doi.org/10.1016/j.apsusc.2008.10.094>
35. Manno D, Filippo E, Di Giulio M, Serra A (2008) Synthesis and characterization of starch-stabilized Ag nanostructures for sensors applications. *Journal of Non-Crystalline Solids*, 354(52–54):5515–5520. <https://doi.org/10.1016/j.jnoncrysol.2008.04.059>
36. Meyer DE, Curran MA, Gonzalez MA (2011) An examination of silver nanoparticles in socks using screening-level life cycle assessment. *Journal of Nanoparticle Research*, 13(1):147–156. <https://doi.org/10.1007/s11051-010-0013-4>
37. Pourzahedi L, Vance M, Eckelman MJ (2017) Life Cycle Assessment and Release Studies for 15 Nanosilver-Enabled Consumer Products: Investigating Hotspots and Patterns of

- Contribution. *Environmental Science & Technology*, 51(12):7148–7158.
<https://doi.org/10.1021/acs.est.6b05923>
38. Pourzahedi L, Eckelman MJ (2015) Environmental Life Cycle Assessment of Nanosilver-Enabled Bandages. *Environmental Science & Technology*, 49(1):361–368.
<https://doi.org/10.1021/es504655y>
39. Westerband EI, Hicks AL (2018) Life cycle impact of nanosilver polymer-food storage containers as a case study informed by literature review. *Environmental Science: Nano*, 5(4):933–945. <https://doi.org/10.1039/C7EN01043E>
40. StatNano (2019) Nanotechnology Products Database (NPD). <http://product.statnano.com/>
41. Pulit-Prociak J, Banach M (2016) Silver nanoparticles – a material of the future...? *Open Chemistry*, 14(1):76–91. <https://doi.org/10.1515/chem-2016-0005>
42. Calderón-Jiménez B, Johnson ME, Montoro Bustos AR, Murphy KE, Winchester MR, Vega Baudrit JR (2017) Silver Nanoparticles: Technological Advances, Societal Impacts, and Metrological Challenges. *Frontiers in Chemistry*, 5 <https://doi.org/10.3389/fchem.2017.00006>
43. Desmau M, Gélabert A, Levard C, Ona-Nguema G, Vidal V, Stubbs JE, Eng PJ, Benedetti MF (2018) Dynamics of silver nanoparticles at the solution/biofilm/mineral interface. *Environmental Science: Nano*, 5(10):2394–2405. <https://doi.org/10.1039/C8EN00331A>
44. Gottschalk F, Sonderer T, Scholz RW, Nowack B (2009) Modeled Environmental Concentrations of Engineered Nanomaterials (TiO₂, ZnO, Ag, CNT, Fullerenes) for Different Regions. *Environmental Science & Technology*, 43(24):9216–9222.
<https://doi.org/10.1021/es9015553>
45. Keller AA, Lazareva A (2014) Predicted Releases of Engineered Nanomaterials: From Global to Regional to Local. *Environmental Science & Technology Letters*, 1(1):65–70.
<https://doi.org/10.1021/ez400106t>
46. Nowack B, Krug HF, Height M (2011) 120 Years of Nanosilver History: Implications for Policy Makers. *Environmental Science & Technology*, 45(4):1177–1183.
<https://doi.org/10.1021/es103316q>
47. Perez J, Bax L, Escolano C (2005) Roadmap Report on Nanoparticles.
<http://nanoparticles.org/pdf/PerezBaxEscolano.pdf>
48. Schmid K, Riediker M (2008) Use of Nanoparticles in Swiss Industry: A Targeted Survey. *Environmental Science & Technology*, 42(7):2253–2260. <https://doi.org/10.1021/es071818o>
49. Grand View Research (2015) Silver Nanoparticles Market By Application And Segment Forecasts To 2022. <https://www.grandviewresearch.com/industry-analysis/silver-nanoparticles-market>

50. Verma V (2018) Silver Nanoparticles Market Size By Application, Industry Analysis Report, Regional Outlook, Growth Potential, Price Trends, Competitive Market Share & Forecast, 2018 – 2024. <https://www.gminsights.com/industry-analysis/silver-nanoparticles-market>
51. Charitidis CA, Georgiou P, Koklioti MA, Trompeta A-F, Markakis V (2014) Manufacturing nanomaterials: from research to industry. *Manufacturing Review*, 1:11. <https://doi.org/10.1051/mfreview/2014009>
52. Meyer DE, Curran MA, Gonzalez MA (2009) An examination of existing data for the industrial manufacture and use of nanocomponents and their role in the life cycle impact of nanoproducts. *Environmental Science & Technology*, 43(5):1256–1263.
53. Pourzahedi L, Eckelman MJ (2015) Comparative life cycle assessment of silver nanoparticle synthesis routes. *Environmental Science: Nano*, 2(4):361–369. <https://doi.org/10.1039/C5EN00075K>
54. Zhang X-F, Liu Z-G, Shen W, Gurunathan S (2016) Silver Nanoparticles: Synthesis, Characterization, Properties, Applications, and Therapeutic Approaches. *International Journal of Molecular Sciences*, 17(9):1534. <https://doi.org/10.3390/ijms17091534>
55. Alaqad K, Saleh TA (2016) Gold and Silver Nanoparticles: Synthesis Methods, Characterization Routes and Applications towards Drugs. *Journal of Environmental & Analytical Toxicology*, 6(4)<https://doi.org/10.4172/2161-0525.1000384>
56. Manda BMK, Worrell E, Patel MK (2015) Prospective life cycle assessment of an antibacterial T-shirt and supporting business decisions to create value. *Resources, Conservation and Recycling*, 103:47–57. <https://doi.org/10.1016/j.resconrec.2015.07.010>
57. Iravani S, Korbekandi H, Mirmohammadi SV, Zolfaghari B (2014) Synthesis of silver nanoparticles: chemical, physical and biological methods. *Research in Pharmaceutical Sciences*, 9(6):385–406.
58. Walser T, Demou E, Lang DJ, Hellweg S (2011) Prospective Environmental Life Cycle Assessment of Nanosilver T-Shirts. *Environmental Science & Technology*, 45(10):4570–4578. <https://doi.org/10.1021/es2001248>
59. Slotte M, Zevenhoven R (2017) Energy requirements and life cycle assessment of production and product integration of silver, copper and zinc nanoparticles. *Journal of Cleaner Production*, 148:948–957. <https://doi.org/10.1016/j.jclepro.2017.01.083>
60. Hicks AL, Temizel-Sekeryan S (2019) Understanding the potential environmental benefits of nanosilver enabled consumer products. *NanoImpact*, 16:100183. <https://doi.org/10.1016/j.impact.2019.100183>
61. Wigger H, Hackmann S, Zimmermann T, Köser J, Thöming J, Gleich A von (2015) Influences of use activities and waste management on environmental releases of engineered nanomaterials. *Science of The Total Environment*, 535:160–171. <https://doi.org/10.1016/j.scitotenv.2015.02.042>

62. Yasin S, Sun D (2019) Propelling textile waste to ascend the ladder of sustainability: EOL study on probing environmental parity in technical textiles. *Journal of Cleaner Production*, 233:1451–1464. <https://doi.org/10.1016/j.jclepro.2019.06.009>
63. Hicks AL (2017) Using multi criteria decision analysis to evaluate nanotechnology: nAg enabled textiles as a case study. *Environmental Science: Nano*, 4(8):1647–1655. <https://doi.org/10.1039/C7EN00429J>
64. Bi Y, Westerband EI, Alum A, Brown FC, Abbaszadegan M, Hristovski KD, Hicks AL, Westerhoff PK (2018) Antimicrobial Efficacy and Life Cycle Impact of Silver-Containing Food Containers. *ACS Sustainable Chemistry & Engineering*, 6(10):13086–13095. <https://doi.org/10.1021/acssuschemeng.8b02639>
65. Westerband EI, Hicks AL (2018) Nanosilver-Enabled Food Storage Container Tradeoffs: Environmental Impacts Versus Food Savings Benefit, Informed by Literature. *Integrated Environmental Assessment and Management*, 14(6):769–776. <https://doi.org/10.1002/ieam.4093>
66. Zhang H, Hortal M, Dobon A, Jorda-Beneyto M, Bermudez JM (2017) Selection of Nanomaterial-Based Active Agents for Packaging Application: Using Life Cycle Assessment (LCA) as a Tool. *Packaging Technology and Science*, 30(9):575–586. <https://doi.org/10.1002/pts.2238>
67. Hischier R, Nowack B, Gottschalk F, Hincapie I, Steinfeldt M, Som C (2015) Life cycle assessment of façade coating systems containing manufactured nanomaterials. *Journal of Nanoparticle Research*, 17(2):68. <https://doi.org/10.1007/s11051-015-2881-0>
68. Ren D, Colosi LM, Smith JA (2013) Evaluating the Sustainability of Ceramic Filters for Point-of-Use Drinking Water Treatment. *Environmental Science & Technology*, 47(19):11206–11213. <https://doi.org/10.1021/es4026084>
69. Garvey T, Moore EA, Babbitt CW, Gaustad G (2019) Comparing ecotoxicity risks for nanomaterial production and release under uncertainty. *Clean Technologies and Environmental Policy*, 21(2):229–242. <https://doi.org/10.1007/s10098-018-1648-6>
70. Piccinno F, Hischier R, Seeger S, Som C (2016) From laboratory to industrial scale: a scale-up framework for chemical processes in life cycle assessment studies. *Journal of Cleaner Production*, 135:1085–1097. <https://doi.org/10.1016/j.jclepro.2016.06.164>
71. Pini M, Cedillo González E, Neri P, Siligardi C, Ferrari A (2017) Assessment of Environmental Performance of TiO₂ Nanoparticles Coated Self-Cleaning Float Glass. *Coatings*, 7(1):8. <https://doi.org/10.3390/coatings7010008>
72. Wu F, Zhou Z, Hicks AL (2019) Life Cycle Impact of Titanium Dioxide Nanoparticle Synthesis through Physical, Chemical, and Biological Routes. *Environmental Science & Technology*, 53(8):4078–4087. <https://doi.org/10.1021/acs.est.8b06800>
73. Gao T, Jelle BP, Sandberg LIC, Gustavsen A (2013) Monodisperse Hollow Silica Nanospheres for Nano Insulation Materials: Synthesis, Characterization, and Life Cycle

Assessment. *ACS Applied Materials & Interfaces*, 5(3):761–767.
<https://doi.org/10.1021/am302303b>

74. Arvidsson R, Molander S (2017) Prospective Life Cycle Assessment of Epitaxial Graphene Production at Different Manufacturing Scales and Maturity. *Journal of Industrial Ecology*, 21(5):1153–1164. <https://doi.org/10.1111/jiec.12526>
75. Piccinno F, Hischier R, Seeger S, Som C (2018) Predicting the environmental impact of a future nanocellulose production at industrial scale: Application of the life cycle assessment scale-up framework. *Journal of Cleaner Production*, 174:283–295.
<https://doi.org/10.1016/j.jclepro.2017.10.226>
76. Falsini S, Bardi U, Abou-Hassan A, Ristori S (2018) Sustainable strategies for large-scale nanotechnology manufacturing in the biomedical field. *Green Chemistry*, 20(17):3897–3907.
<https://doi.org/10.1039/C8GC01248B>
77. Gavankar S, Suh S, Keller AA (2015) The Role of Scale and Technology Maturity in Life Cycle Assessment of Emerging Technologies: A Case Study on Carbon Nanotubes: Carbon Nanotubes Case Study of Scaling and Technology Maturity in LCAs. *Journal of Industrial Ecology*, 19(1):51–60. <https://doi.org/10.1111/jiec.12175>
78. Wigger H (2017) Environmental Release of and Exposure to Iron Oxide and Silver Nanoparticles: Prospective Estimations Based on Product Application Scenarios.
<https://link.springer.com/content/pdf/10.1007/978-3-658-16791-2.pdf>
79. Adam V, Caballero-Guzman A, Nowack B (2018) Considering the forms of released engineered nanomaterials in probabilistic material flow analysis. *Environmental Pollution*, 243:17–27. <https://doi.org/10.1016/j.envpol.2018.07.108>
80. Mitrano DM, Rimmele E, Wichser A, Erni R, Height M, Nowack B (2014) Presence of Nanoparticles in Wash Water from Conventional Silver and Nano-silver Textiles. *ACS Nano*, 8(7):7208–7219. <https://doi.org/10.1021/nn502228w>
81. Donia DT, Carbone M (2019) Fate of the nanoparticles in environmental cycles. *International Journal of Environmental Science and Technology*, 16(1):583–600.
<https://doi.org/10.1007/s13762-018-1960-z>
82. Lombi E, Donner E, Scheckel KG, Sekine R, Lorenz C, Goetz NV, Nowack B (2014) Silver speciation and release in commercial antimicrobial textiles as influenced by washing. *Chemosphere*, 111:352–358. <https://doi.org/10.1016/j.chemosphere.2014.03.116>
83. Mitrano DM, Lombi E, Dasilva YAR, Nowack B (2016) Unraveling the Complexity in the Aging of Nanoenhanced Textiles: A Comprehensive Sequential Study on the Effects of Sunlight and Washing on Silver Nanoparticles. *Environmental Science & Technology*, 50(11):5790–5799.
<https://doi.org/10.1021/acs.est.6b01478>

84. Giese B, Klaessig F, Park B, Kaegi R, Steinfeldt M, Wigger H, Gleich A von, Gottschalk F (2018) Risks, Release and Concentrations of Engineered Nanomaterial in the Environment. *Scientific Reports*, 8(1565)<https://doi.org/10.1038/s41598-018-19275-4>
85. Mueller NC, Nowack B (2008) Exposure Modeling of Engineered Nanoparticles in the Environment. *Environmental Science & Technology*, 42(12):4447–4453. <https://doi.org/10.1021/es7029637>
86. Nowack B, Bornhöft N, Ding Y, Riediker M, Jiménez AS, Sun T, Tongeren M van, Wohlleben W (2015) The Flows of Engineered Nanomaterials from Production, Use, and Disposal to the Environment. *Indoor and Outdoor Nanoparticles*, 48:209–231. https://doi.org/10.1007/698_2015_402
87. Wijnhoven SWP, Peijnenburg WJGM, Herberts CA, Hagens WI, Oomen AG, Heugens EHW, Roszek B, Bisschops J, Gosens I, Meent D van de, Dekkers S, Jong WH de, Zijverden M van, Sips AJAM, Geertsma RE (2009) Nano-silver – a review of available data and knowledge gaps in human and environmental risk assessment. *Nanotoxicology*, 3(2):109–138. <https://doi.org/doi.org/10.1080/17435390902725914>
88. Revelle CS, Whitlatch EE, Wright JR (2004) Civil and Environmental Systems Engineering.
89. Shibasaki M, Fischer M, Barthel L (2007) Effects on Life Cycle Assessment — Scale Up of Processes. *Advances in Life Cycle Engineering for Sustainable Manufacturing Businesses*, :377–381.
90. Shibasaki M, Warburg N, Eyerer P (2006) Upscaling effect and Life Cycle Assessment. *Proceedings of LCE2006*, :61–64. <https://www.mech.kuleuven.be/lce2006/161.pdf>
91. EPA (2018) Inventory of U.S. Greenhouse Gas Emissions and Sinks. <https://www.epa.gov/ghgemissions/inventory-us-greenhouse-gas-emissions-and-sinks>
92. Jolliet O, Rosenbaum RK, Laurent A (2014) Life Cycle Risks and Impacts of Nanotechnologies. *Nanotechnology and Human Health*, :213–277.
93. US EPA (2010) State of the Science Literature Review: Everything Nanosilver and More.
94. Abdalla S, Al-Marzouki F, Al-Ghamdi AA, Abdel-Daiem A (2015) Different Technical Applications of Carbon Nanotubes. *Nanoscale Research Letters*, 10(1):358. <https://doi.org/10.1186/s11671-015-1056-3>
95. Endo M, Strano MS, Ajayan PM (2007) Potential Applications of Carbon Nanotubes. *Topics in Applied Physics*, 111:13–62.
96. Schnorr JM, Swager TM (2011) Emerging Applications of Carbon Nanotubes. *Chemistry of Materials*, 23(3):646–657. <https://doi.org/10.1021/cm102406h>

97. Zhang Q, Huang J-Q, Qian W-Z, Zhang Y-Y, Wei F (2013) The Road for Nanomaterials Industry: A Review of Carbon Nanotube Production, Post-Treatment, and Bulk Applications for Composites and Energy Storage. *Small*, 9(8):1237–1265. <https://doi.org/10.1002/sml.201203252>
98. Bauer C, Buchgeister J, Hischer R, Poganietz WR, Schebek L, Warsen J (2008) Towards a framework for life cycle thinking in the assessment of nanotechnology. *Journal of Cleaner Production*, 16(8–9):910–926. <https://doi.org/10.1016/j.jclepro.2007.04.022>
99. Upadhyayula VKK, Meyer DE, Curran MA, Gonzalez MA (2012) Life cycle assessment as a tool to enhance the environmental performance of carbon nanotube products: a review. *Journal of Cleaner Production*, 26:37–47. <https://doi.org/10.1016/j.jclepro.2011.12.018>
100. Healy ML, Dahlben LJ, Isaacs JA (2008) Environmental Assessment of Single-Walled Carbon Nanotube Processes. *Journal of Industrial Ecology*, 12(3):376–393. <https://doi.org/10.1111/j.1530-9290.2008.00058.x>
101. Hendren CO, Mesnard X, Dröge J, Wiesner MR (2011) Estimating Production Data for Five Engineered Nanomaterials As a Basis for Exposure Assessment. *Environmental Science & Technology*, 45(7):2562–2569. <https://doi.org/10.1021/es103300g>
102. Kuzma J (2005) The Nanotechnology-Biology Interface: Exploring Models for Oversight.
103. Ray PC, Yu H, Fu PP (2009) Toxicity and Environmental Risks of Nanomaterials: Challenges and Future Needs. *Journal of Environmental Science and Health, Part C*, 27(1):1–35. <https://doi.org/10.1080/10590500802708267>
104. Nanotechmag (2014) The Global Market For Carbon Nanotubes. 2:20–22.
105. Nanowerk (2011) Global carbon nanotubes market - industry beckons. <https://www.nanowerk.com/spotlight/spotid=23118.php>
106. Statista (2015) Market size of carbon nanotubes worldwide from 2012 to 2022, by application (in tons). <https://www.statista.com/statistics/714708/carbon-nanotube-global-market-size-by-application/>
107. Sahu YS (2016) Carbon Nanotubes Market by Type (Single-Walled Carbon Nanotubes, Multi-Walled Carbon Nanotubes), Application (Structural Polymer, Conductive Polymer, Conductive Adhesives, Metal Matrix Composites, Li-ion Battery Electrodes) and End-User (Electricals & Electronics, Aerospace & Defense, Energy, Sporting Goods, Automotive) - Global Opportunity Analysis and Industry Forecast, 2014 - 2022. :128. <https://www.alliedmarketresearch.com/carbon-nanotube-market>
108. Markets and Markets (2018) Carbon Nanotubes (CNT) Market by Type (Single, Multi Walled), Method (Chemical Vapor Deposition, Catalytic Chemical Vapor Deposition, High Pressure Carbon Monoxide), Application (Electronics, Chemical, Batteries, Energy, Medical) - Global Forecast to 2023. <https://www.marketsandmarkets.com/Market-Reports/carbon-nanotubes-139.html>

109. Research and Markets (2018) The Global Carbon Nanotubes (CNT) Market (2018-2023) is Projected to Grow at a CAGR of 16.7% - Technological Advancements and Decreasing Production Cost is Driving Growth. <https://www.prnewswire.com/news-releases/the-global-carbon-nanotubes-cnt-market-2018-2023-is-projected-to-grow-at-a-cagr-of-16-7---technological-advancements-and-decreasing-production-cost-is-driving-growth-300752102.html>
110. Reports and Data (2019) Carbon Nanotubes Market To Reach USD 15.02 Billion By 2026. <https://www.globenewswire.com/news-release/2019/07/17/1884106/0/en/Carbon-Nanotubes-Market-To-Reach-USD-15-02-Billion-By-2026-Reports-And-Data.html>
111. US Patent and Trademark Office (2019) Patent Full-Text Databases. <http://patft.uspto.gov/netahtml/PTO/index.html>
112. Borm PJ, Robbins D, Haubold S, Kuhlbusch T, Fissan H, Donaldson K, Schins R, Stone V, Kreyling W, Lademann J, Krutmann J, Warheit D, Oberdorster E (2006) The potential risks of nanomaterials: a review carried out for ECETOC. *Particle and Fibre Toxicology*, 3(1):11. <https://doi.org/10.1186/1743-8977-3-11>
113. Pulidindi K, Pandey H (2018) Carbon Nanotubes Market Size By Product (Single-Walled Carbon Nanotubes, Multi-Walled Carbon Nanotubes), By Application (Polymers, Energy, Electrical & Electronics), Industry Analysis Report, Regional Outlook, Growth Potential, Price Trends, Competitive Market Share & Forecast, 2018 – 2024. <https://www.gminsights.com/industry-analysis/carbon-nanotubes-market>
114. Ghaffarzadeh K (2018) Graphene, 2D Materials and Carbon Nanotubes: Markets, Technologies and Opportunities 2018-2020. <https://www.idtechex.com/en/research-report/graphene-2d-materials-and-carbon-nanotubes-markets-technologies-and-opportunities-2019-2029/669>
115. Eatemadi A, Daraee H, Karimkhanloo H, Kouhi M, Zarghami N, Akbarzadeh A, Abasi M, Hanifehpour Y, Joo S (2014) Carbon nanotubes: properties, synthesis, purification, and medical applications. *Nanoscale Research Letters*, 9(1):393. <https://doi.org/10.1186/1556-276X-9-393>
116. Sengupta J (2018) Carbon Nanotube Fabrication at Industrial Scale. *Handbook of Nanomaterials for Industrial Applications*, :172–194. <https://doi.org/10.1016/B978-0-12-813351-4.00010-9>
117. Rahman G, Najaf Z, Mehmood A, Bilal S, Shah A, Mian S, Ali G (2019) An Overview of the Recent Progress in the Synthesis and Applications of Carbon Nanotubes. *Journal of Carbon Research*, 5(3):31. <https://doi.org/10.3390/c5010003>
118. Isaacs JA, Tanwani A, Healy ML, Dahlben LJ (2010) Economic assessment of single-walled carbon nanotube processes. *Journal of Nanoparticle Research*, 12(2):551–562. <https://doi.org/10.1007/s11051-009-9673-3>
119. Roes AL, Tabak LB, Shen L, Nieuwlaar E, Patel MK (2010) Influence of using nanoobjects as filler on functionality-based energy use of nanocomposites. *Journal of Nanoparticle Research*, 12(6):2011–2028. <https://doi.org/10.1007/s11051-009-9819-3>

120. Zhang Q, Huang J-Q, Zhao M-Q, Qian W-Z, Wei F (2011) Carbon Nanotube Mass Production: Principles and Processes. *ChemSusChem*, 4(7):864–889. <https://doi.org/10.1002/cssc.201100177>
121. Das R, Shahnava Z, Ali MdE, Islam MM, Abd Hamid SB (2016) Can We Optimize Arc Discharge and Laser Ablation for Well-Controlled Carbon Nanotube Synthesis? *Nanoscale Research Letters*, 11(1):510. <https://doi.org/10.1186/s11671-016-1730-0>
122. Kawajiri K, Goto T, Sakurai S, Hata K, Tahara K (2020) Development of life cycle assessment of an emerging technology at research and development stage: A case study on single-wall carbon nanotube produced by super growth method. *Journal of Cleaner Production*, 255:120015. <https://doi.org/10.1016/j.jclepro.2020.120015>
123. Pallas G, Vijver MG, Peijnenburg WJGM, Guinée J (2020) Life cycle assessment of emerging technologies at the lab scale: The case of nanowire-based solar cells. *Journal of Industrial Ecology*, 24(1):193–204. <https://doi.org/10.1111/jiec.12855>
124. Maranghi S, Parisi ML, Basosi R, Sinicropi A (2020) LCA as a Support Tool for the Evaluation of Industrial Scale-Up. *Life Cycle Assessment in the Chemical Product Chain*, :125–143. https://doi.org/10.1007/978-3-030-34424-5_6
125. Teah HY, Sato T, Namiki K, Asaka M, Feng K, Noda S (2020) Life Cycle Greenhouse Gas Emissions of Long and Pure Carbon Nanotubes Synthesized via On-Substrate and Fluidized-Bed Chemical Vapor Deposition. *ACS Sustainable Chemistry & Engineering*, 8(4):1730–1740. <https://doi.org/10.1021/acssuschemeng.9b04542>
126. Temizel-Sekeryan S, Hicks AL (2020) Global environmental impacts of silver nanoparticle production methods supported by life cycle assessment. *Resources, Conservation and Recycling*, 156:104676. <https://doi.org/10.1016/j.resconrec.2019.104676>
127. Eckelman MJ, Mauter MS, Isaacs JA, Elimelech M (2012) New Perspectives on Nanomaterial Aquatic Ecotoxicity: Production Impacts Exceed Direct Exposure Impacts for Carbon Nanotubes. *Environmental Science & Technology*, 46(5):2902–2910. <https://doi.org/10.1021/es203409a>
128. Rodriguez-Garcia G, Zimmermann B, Weil M (2014) Nanotoxicity and Life Cycle Assessment: First attempt towards the determination of characterization factors for carbon nanotubes. *IOP Conference Series: Materials Science and Engineering*, 64:012029. <https://doi.org/10.1088/1757-899X/64/1/012029>
129. Baun A, Sayre P, Steinhäuser KG, Rose J (2017) Regulatory relevant and reliable methods and data for determining the environmental fate of manufactured nanomaterials. *NanoImpact*, 8:1–10. <https://doi.org/10.1016/j.impact.2017.06.004>
130. Moore EA, Babbitt CW, Tomaszewski B, Tyler AC (2020) Spatial perspectives enhance modeling of nanomaterial risks. *Journal of Industrial Ecology*, 24(4):855–870. <https://doi.org/10.1111/jiec.12976>

131. Parsons S, Murphy RJ, Lee J, Sims G (2015) Uncertainty communication in the environmental life cycle assessment of carbon nanotubes. *International Journal of Nanotechnology*, 12(8/9):620. <https://doi.org/10.1504/IJNT.2015.068883>
132. Upadhyayula VKK, Meyer DE, Curran MA, Gonzalez MA (2014) Evaluating the Environmental Impacts of a Nano-Enhanced Field Emission Display Using Life Cycle Assessment: A Screening-Level Study. *Environmental Science & Technology*, 48(2):1194–1205. <https://doi.org/10.1021/es4034638>
133. Hischer R, Walser T (2012) Life cycle assessment of engineered nanomaterials: State of the art and strategies to overcome existing gaps. *Science of The Total Environment*, 425:271–282. <https://doi.org/10.1016/j.scitotenv.2012.03.001>
134. Singh A, Lou HH, Pike RW, Agboola A, Li X, Hopper JR, Yaws CL (2008) Environmental Impact Assessment for Potential Continuous Processes for the Production of Carbon Nanotubes. *American Journal of Environmental Sciences*, 4(5):522–534. <https://doi.org/10.3844/ajessp.2008.522.534>
135. Celik I, Mason BE, Phillips AB, Heben MJ, Apul D (2017) Environmental Impacts from Photovoltaic Solar Cells Made with Single Walled Carbon Nanotubes. *Environmental Science & Technology*, 51(8):4722–4732. <https://doi.org/10.1021/acs.est.6b06272>
136. Ganter MJ, Seager TP, Schauerman CM, Landi BJ, Raffaele RP (2009) A life-cycle energy analysis of single wall carbon nanotubes produced through laser vaporization. *2009 IEEE International Symposium on Sustainable Systems and Technology*, :1–4. <https://doi.org/10.1109/ISSST.2009.5156719>
137. Liu B-C, Tang S-H, Liang Q, Gao L-Z, Zhang B-L, Qu M-Z, Yu Z-L (2001) Production of Carbon Nanotubes over Pre-reduced LaCoO₃ by Using Fluidized-bed Catalytic Reactor. *Chinese Journal of Chemistry*, 19:983–986. <https://doi.org/10.1002/cjoc.20010191013>
138. Mauron P, Emmenegger C, Sudan P, Wenger P, Rentsch S, Züttel A (2003) Fluidised-bed CVD synthesis of carbon nanotubes on Fe₂O₃yMgO. *Diamond and Related Materials*, :6.
139. Griffiths OG, O’Byrne JP, Torrente-Murciano L, Jones MD, Mattia D, McManus MC (2013) Identifying the largest environmental life cycle impacts during carbon nanotube synthesis via chemical vapour deposition. *Journal of Cleaner Production*, 42:180–189. <https://doi.org/10.1016/j.jclepro.2012.10.040>
140. Trompeta A-F, Koklioti MA, Perivoliotis DK, Lynch I, Charitidis CA (2016) Towards a holistic environmental impact assessment of carbon nanotube growth through chemical vapour deposition. *Journal of Cleaner Production*, 129:384–394. <https://doi.org/10.1016/j.jclepro.2016.04.044>
141. Fan Y-Y, Kaufmann A, Mukasyan A, Varma A (2006) Single- and multi-wall carbon nanotubes produced using the floating catalyst method: Synthesis, purification and hydrogen uptake. *Carbon*, 44(11):2160–2170. <https://doi.org/10.1016/j.carbon.2006.03.009>

142. Ishigami M, Cumings J, Zettl A, Chen S (2000) A simple method for the continuous production of carbon nanotubes. *Chemical Physics Letters*, 319(5–6):457–459. [https://doi.org/10.1016/S0009-2614\(00\)00151-2](https://doi.org/10.1016/S0009-2614(00)00151-2)
143. Cucurachi S, Giesen C van der, Guinée J (2018) Ex-ante LCA of Emerging Technologies. *Procedia CIRP*, 69:463–468. <https://doi.org/10.1016/j.procir.2017.11.005>
144. Tsoy N, Steubing B, Giesen C van der, Guinée J (2020) Upscaling methods used in ex ante life cycle assessment of emerging technologies: a review. *The International Journal of Life Cycle Assessment*, 25(9):1680–1692. <https://doi.org/10.1007/s11367-020-01796-8>
145. Piccinno F, Gottschalk F, Seeger S, Nowack B (2012) Industrial production quantities and uses of ten engineered nanomaterials in Europe and the world. *Journal of Nanoparticle Research*, 14(9)<https://doi.org/10.1007/s11051-012-1109-9>
146. Project on Emerging Nanotechnologies (2013) Consumer Products Inventory. <http://www.nanotechproject.org/cpi>
147. DTU Environment, Danish Ecological Council, Danish Consumer Council (2019) The Nanodatabase (Denmark). <http://nanodb.dk/en/>
148. Sun TY, Gottschalk F, Hungerbühler K, Nowack B (2014) Comprehensive probabilistic modelling of environmental emissions of engineered nanomaterials. *Environmental Pollution*, 185:69–76. <https://doi.org/10.1016/j.envpol.2013.10.004>
149. Promentilla MAB, Janairo JIB, Yu DEC, Pausta CMJ, Beltran AB, Huelgas-Orbecido AP, Tapia JFD, Aviso KB, Tan RR (2018) A stochastic fuzzy multi-criteria decision-making model for optimal selection of clean technologies. *Journal of Cleaner Production*, 183:1289–1299. <https://doi.org/10.1016/j.jclepro.2018.02.183>
150. NREL (2020) U.S. Life Cycle Inventory Database. *U.S. Life Cycle Inventory (USLCI) Database*, <https://www.nrel.gov/lci/>
151. International Energy Agency (2020) World Energy Balances: Total energy supply (TES) by source, World 1990-2018. *Data and Statistics*, [https://www.iea.org/data-and-statistics?country=WORLD&fuel=Energy%20supply&indicator=Total%20energy%20supply%20\(TES\)%20by%20source](https://www.iea.org/data-and-statistics?country=WORLD&fuel=Energy%20supply&indicator=Total%20energy%20supply%20(TES)%20by%20source)
152. Heijungs R (2014) Ten easy lessons for good communication of LCA. *The International Journal of Life Cycle Assessment*, 19(3):473–476. <https://doi.org/10.1007/s11367-013-0662-5>
153. Arvidsson R, Tillman A-M, Sandén BA, Janssen M, Nordelöf A, Kushnir D, Molander S (2018) Environmental Assessment of Emerging Technologies: Recommendations for Prospective LCA. *Journal of Industrial Ecology*, 22(6):1286–1294. <https://doi.org/10.1111/jiec.12690>

154. Gilbertson LM, Busnaina AA, Isaacs JA, Zimmerman JB, Eckelman MJ (2014) Life Cycle Impacts and Benefits of a Carbon Nanotube-Enabled Chemical Gas Sensor. *Environmental Science & Technology*, 48(19):11360–11368. <https://doi.org/10.1021/es5006576>
155. Lamon L, Asturiol D, Vilchez A, Ruperez-Illescas R, Cabellos J, Richarz A, Worth A (2019) Computational models for the assessment of manufactured nanomaterials: Development of model reporting standards and mapping of the model landscape. *Computational Toxicology*, 9:143–151. <https://doi.org/10.1016/j.comtox.2018.12.002>
156. International Energy Agency (2020) Global CO2 emissions by sector, 2018. <https://www.iea.org/data-and-statistics/charts/global-co2-emissions-by-sector-2018>
157. Schauer MW, White MA (2015) Tailoring Industrial Scale CNT Production to Specialty Markets. *MRS Proceedings*, 1752:103–109. <https://doi.org/10.1557/opl.2015.90>
158. Market Study Report (2018) Nanomaterials Market Set to Register USD \$98 Billion by 2025. <https://www.reuters.com/brandfeatures/venture-capital/article?id=65231>
159. Hicks AL (2018) Chapter 5 - Environmental assessment of medical nanotechnologies; Subchapter 5.1. What we have learnt from the life-cycle impacts of nanosilver products. *Nanotechnologies in Preventive and Regenerative Medicine: An Emerging Big Picture-Micro and Nano Technologies*, :381–397.
160. Hauschild MZ, Huijbregts MAJ (2015) Introducing Life Cycle Impact Assessment. *Life Cycle Impact Assessment*, :1–16. https://doi.org/10.1007/978-94-017-9744-3_1
161. Hauschild M, Goedkoop M, Guinee J, Heijungs R, Huijbregts M, Joliet O, Margni M, De Schryver A (2011) Recommendations for Life Cycle Impact Assessment in the European context - based on existing environmental impact assessment models and factors (International Reference Life Cycle Data System - ILCD handbook). <https://publications.jrc.ec.europa.eu/repository/handle/111111111/26229>
162. Westerhoff P, Nowack B (2013) Searching for Global Descriptors of Engineered Nanomaterial Fate and Transport in the Environment. *Accounts of Chemical Research*, 46(3):844–853. <https://doi.org/10.1021/ar300030n>
163. Bondarenko O, Juganson K, Ivask A, Kasemets K, Mortimer M, Kahru A (2013) Toxicity of Ag, CuO and ZnO nanoparticles to selected environmentally relevant test organisms and mammalian cells in vitro: a critical review. *Archives of Toxicology*, 87(7):1181–1200. <https://doi.org/10.1007/s00204-013-1079-4>
164. Coll C, Notter D, Gottschalk F, Sun T, Som C, Nowack B (2016) Probabilistic environmental risk assessment of five nanomaterials (nano-TiO₂, nano-Ag, nano-ZnO, CNT, and fullerenes). *Nanotoxicology*, 10(4):436–444. <https://doi.org/10.3109/17435390.2015.1073812>
165. Fabrega J, Luoma SN, Tyler CR, Galloway TS, Lead JR (2011) Silver nanoparticles: Behaviour and effects in the aquatic environment. *Environment International*, 37(2):517–531. <https://doi.org/10.1016/j.envint.2010.10.012>

166. Hund-Rinke K, Schlich K, Kühnel D, Hellack B, Kaminski H, Nickel C (2018) Grouping concept for metal and metal oxide nanomaterials with regard to their ecotoxicological effects on algae, daphnids and fish embryos. *NanoImpact*, 9:52–60. <https://doi.org/10.1016/j.impact.2017.10.003>
167. Ivask A, Kurvet I, Kasemets K, Blinova I, Aruoja V, Suppi S, Vija H, Käkinen A, Titma T, Heinlaan M, Visnapuu M, Koller D, Kisand V, Kahru A (2014) Size-Dependent Toxicity of Silver Nanoparticles to Bacteria, Yeast, Algae, Crustaceans and Mammalian Cells In Vitro. *PLoS ONE*, 9(7):e102108. <https://doi.org/10.1371/journal.pone.0102108>
168. Juganson K, Ivask A, Blinova I, Mortimer M, Kahru A (2015) NanoE-Tox: New and in-depth database concerning ecotoxicity of nanomaterials. *Beilstein Journal of Nanotechnology*, 6:1788–1804. <https://doi.org/10.3762/bjnano.6.183>
169. Kahru A, Dubourguier H-C (2010) From ecotoxicology to nanoecotoxicology. *Toxicology*, 269(2–3):105–119. <https://doi.org/10.1016/j.tox.2009.08.016>
170. Kalantzi I, Mylona K, Toncelli C, Bucheli TD, Knauer K, Pergantis SA, Pitta P, Tsiola A, Tsapakis M (2019) Ecotoxicity of silver nanoparticles on plankton organisms: a review. *Journal of Nanoparticle Research*, 21(3):65. <https://doi.org/10.1007/s11051-019-4504-7>
171. Liang SXT, Wong LS, Dhanapal ACTA, Djearmane S (2020) Toxicity of Metals and Metallic Nanoparticles on Nutritional Properties of Microalgae. *Water, Air, & Soil Pollution*, 231(2):52. <https://doi.org/10.1007/s11270-020-4413-5>
172. Minetto D, Volpi Ghirardini A, Libralato G (2016) Saltwater ecotoxicology of Ag, Au, CuO, TiO₂, ZnO and C60 engineered nanoparticles: An overview. *Environment International*, 92–93:189–201. <https://doi.org/10.1016/j.envint.2016.03.041>
173. Tang Y, Xin H, Yang F, Long X (2018) A historical review and bibliometric analysis of nanoparticles toxicity on algae. *Journal of Nanoparticle Research*, 20(4):92. <https://doi.org/10.1007/s11051-018-4196-4>
174. Tortella GR, Rubilar O, Durán N, Diez MC, Martínez M, Parada J, Seabra AB (2020) Silver nanoparticles: Toxicity in model organisms as an overview of its hazard for human health and the environment. *Journal of Hazardous Materials*, 390:121974. <https://doi.org/10.1016/j.jhazmat.2019.121974>
175. Larsen HF, Hauschild M (2007) GM-troph: A Low Data Demand Ecotoxicity Effect Indicator for Use in LCIA (13+3 pp). *The International Journal of Life Cycle Assessment*, 12(2):79–91. <https://doi.org/10.1065/lca2006.12.288>
176. Salieri B, Righi S, Pasteris A, Olsen SI (2015) Freshwater ecotoxicity characterisation factor for metal oxide nanoparticles: A case study on titanium dioxide nanoparticle. *Science of The Total Environment*, 505:494–502. <https://doi.org/10.1016/j.scitotenv.2014.09.107>

177. Hou P, Zhao B, Jolliet O, Zhu J, Wang P, Xu M (2020) Rapid Prediction of Chemical Ecotoxicity Through Genetic Algorithm Optimized Neural Network Models. *ACS Sustainable Chemistry & Engineering*, 8(32):12168–12176. <https://doi.org/10.1021/acssuschemeng.0c03660>
178. Wang Z, Chen J, Li X, Shao J, Peijnenburg WJGM (2012) Aquatic toxicity of nanosilver colloids to different trophic organisms: Contributions of particles and free silver ion. *Environmental Toxicology and Chemistry*, 31(10):2408–2413. <https://doi.org/10.1002/etc.1964>
179. González AG, Fernández-Rojo L, Leflaive J, Pokrovsky OS, Rols J-L (2016) Response of three biofilm-forming benthic microorganisms to Ag nanoparticles and Ag⁺: the diatom *Nitzschia palea*, the green alga *Uronema confervicolum* and the cyanobacteria *Leptolyngbya* sp. *Environmental Science and Pollution Research*, 23(21):22136–22150. <https://doi.org/10.1007/s11356-016-7259-z>
180. Pokhrel LR, Dubey B, Scheuerman PR (2013) Impacts of Select Organic Ligands on the Colloidal Stability, Dissolution Dynamics, and Toxicity of Silver Nanoparticles. *Environmental Science & Technology*, 47(22):12877–12885. <https://doi.org/10.1021/es403462j>
181. Voelker D, Schlich K, Hohndorf L, Koch W, Kuehnen U, Polleichtner C, Kussatz C, Hund-Rinke K (2015) Approach on environmental risk assessment of nanosilver released from textiles. *Environmental Research*, 140:661–672. <https://doi.org/10.1016/j.envres.2015.05.011>
182. Deng Y, Li J, Qiu M, Yang F, Zhang J, Yuan C (2017) Deriving characterization factors on freshwater ecotoxicity of graphene oxide nanomaterial for life cycle impact assessment. *The International Journal of Life Cycle Assessment*, 22(2):222–236. <https://doi.org/10.1007/s11367-016-1151-4>
183. Dong Y, Gandhi N, Hauschild MZ (2014) Development of Comparative Toxicity Potentials of 14 cationic metals in freshwater. *Chemosphere*, 112:26–33. <https://doi.org/10.1016/j.chemosphere.2014.03.046>
184. Harmon AR, Kennedy AJ, Laird JG, Bednar AJ, Steevens JA (2017) Comparison of acute to chronic ratios between silver and gold nanoparticles, using *Ceriodaphnia dubia*. *Nanotoxicology*, 11(9–10):1127–1139. <https://doi.org/10.1080/17435390.2017.1399219>
185. Handy RD, Brink N van den, Chappell M, Mühling M, Behra R, Dušinská M, Simpson P, Ahtiainen J, Jha AN, Seiter J, Bednar A, Kennedy A, Fernandes TF, Riediker M (2012) Practical considerations for conducting ecotoxicity test methods with manufactured nanomaterials: what have we learnt so far? *Ecotoxicology*, 21(4):933–972. <https://doi.org/10.1007/s10646-012-0862-y>
186. Hobbs DA, Warne MSJ, Markich SJ (2005) Evaluation of criteria used to assess the quality of aquatic toxicity data. *Integrated Environmental Assessment and Management*, 1(3):174–180. <https://doi.org/10.1897/2004-003r.1>
187. Lubinski L, Urbaszek P, Gajewicz A, Cronin MTD, Enoch SJ, Madden JC, Leszczynska D, Leszczynski J, Puzyn T (2013) Evaluation criteria for the quality of published experimental data

- on nanomaterials and their usefulness for QSAR modelling. *SAR and QSAR in Environmental Research*, 24(12):995–1008. <https://doi.org/10.1080/1062936X.2013.840679>
188. Przybylak KR, Madden JC, Cronin MTD, Hewitt M (2012) Assessing toxicological data quality: basic principles, existing schemes and current limitations. *SAR and QSAR in Environmental Research*, 23(5–6):435–459. <https://doi.org/10.1080/1062936X.2012.664825>
189. Pu Y (2017) Toxicity assessment of engineered nanoparticles. <https://tel.archives-ouvertes.fr/tel-02002324>
190. Buist HE, Hischier R, Westerhout J, Brouwer DH (2017) Derivation of health effect factors for nanoparticles to be used in LCIA. *NanoImpact*, 7:41–53. <https://doi.org/10.1016/j.impact.2017.05.002>
191. Salieri B, Kaiser J-P, Rösslein M, Nowack B, Hischier R, Wick P (2020) Relative potency factor approach enables the use of *in vitro* information for estimation of human effect factors for nanoparticle toxicity in life-cycle impact assessment. *Nanotoxicology*, 14(2):275–286. <https://doi.org/10.1080/17435390.2019.1710872>
192. Hoheisel SM, Diamond S, Mount D (2012) Comparison of nanosilver and ionic silver toxicity in *Daphnia magna* and *Pimephales promelas*. *Environmental Toxicology and Chemistry*, 31(11):2557–2563. <https://doi.org/10.1002/etc.1978>
193. Kwak JI, Cui R, Nam S-H, Kim SW, Chae Y, An Y-J (2016) Multispecies toxicity test for silver nanoparticles to derive hazardous concentration based on species sensitivity distribution for the protection of aquatic ecosystems. *Nanotoxicology*, 10(5):521–530. <https://doi.org/10.3109/17435390.2015.1090028>
194. Hou J, Zhou Y, Wang C, Li S, Wang X (2017) Toxic Effects and Molecular Mechanism of Different Types of Silver Nanoparticles to the Aquatic Crustacean *Daphnia magna*. *Environmental Science & Technology*, 51(21):12868–12878. <https://doi.org/10.1021/acs.est.7b03918>
195. Ribeiro F, Gallego-Urrea JA, Jurkschat K, Crossley A, Hassellöv M, Taylor C, Soares AMVM, Loureiro S (2014) Silver nanoparticles and silver nitrate induce high toxicity to *Pseudokirchneriella subcapitata*, *Daphnia magna* and *Danio rerio*. *Science of The Total Environment*, 466–467:232–241. <https://doi.org/10.1016/j.scitotenv.2013.06.101>
196. Valerio-García RC, Carbajal-Hernández AL, Martínez-Ruíz EB, Jarquín-Díaz VH, Haro-Pérez C, Martínez-Jerónimo F (2017) Exposure to silver nanoparticles produces oxidative stress and affects macromolecular and metabolic biomarkers in the goodeid fish *Chapalichthys pardalis*. *Science of The Total Environment*, 583:308–318. <https://doi.org/10.1016/j.scitotenv.2017.01.070>
197. Burkart C, Tümping W von, Berendonk T, Jungmann D (2015) Nanoparticles in wastewater treatment plants: a novel acute toxicity test for ciliates and its implementation in risk assessment. *Environmental Science and Pollution Research*, 22(10):7485–7494. <https://doi.org/10.1007/s11356-014-4057-3>

198. Lacave JM, Fanjul Á, Bilbao E, Gutierrez N, Barrio I, Arostegui I, Cajaraville MP, Orbea A (2017) Acute toxicity, bioaccumulation and effects of dietary transfer of silver from brine shrimp exposed to PVP/PEI-coated silver nanoparticles to zebrafish. *Comparative Biochemistry and Physiology Part C: Toxicology & Pharmacology*, 199:69–80. <https://doi.org/10.1016/j.cbpc.2017.03.008>
199. McLaughlin J, Bonzongo J-CJ (2012) Effects of natural water chemistry on nanosilver behavior and toxicity to *Ceriodaphnia dubia* and *Pseudokirchneriella subcapitata*: nAg-natural water suspensions: Behavior and toxicity. *Environmental Toxicology and Chemistry*, 31(1):168–175. <https://doi.org/10.1002/etc.720>
200. Resano M, Lapeña AC, Belarra MA (2013) Potential of solid sampling high-resolution continuum source graphite furnace atomic absorption spectrometry to monitor the Ag body burden in individual *Daphnia magna* specimens exposed to Ag nanoparticles. *Analytical Methods*, 5(5):1130. <https://doi.org/10.1039/c2ay26456k>
201. Sharma VK, Siskova KM, Zboril R, Gardea-Torresdey JL (2014) Organic-coated silver nanoparticles in biological and environmental conditions: Fate, stability and toxicity. *Advances in Colloid and Interface Science*, 204:15–34. <https://doi.org/10.1016/j.cis.2013.12.002>
202. Akter M, Sikder MdT, Rahman MdM, Ullah AKMA, Hossain KFB, Banik S, Hosokawa T, Saito T, Kurasaki M (2018) A systematic review on silver nanoparticles-induced cytotoxicity: Physicochemical properties and perspectives. *Journal of Advanced Research*, 9:1–16. <https://doi.org/10.1016/j.jare.2017.10.008>
203. Falinski MM, Plata DL, Chopra SS, Theis TL, Gilbertson LM, Zimmerman JB (2018) A framework for sustainable nanomaterial selection and design based on performance, hazard, and economic considerations. *Nature Nanotechnology*, 13(8):708–714. <https://doi.org/10.1038/s41565-018-0120-4>
204. Martínez-Castañón GA, Niño-Martínez N, Martínez-Gutierrez F, Martínez-Mendoza JR, Ruiz F (2008) Synthesis and antibacterial activity of silver nanoparticles with different sizes. *Journal of Nanoparticle Research*, 10(8):1343–1348. <https://doi.org/10.1007/s11051-008-9428-6>
205. Lekamge S, Miranda AF, Ball AS, Shukla R, Nugegoda D (2019) The toxicity of coated silver nanoparticles to *Daphnia carinata* and trophic transfer from alga *Raphidocelis subcapitata*. *PLOS ONE*, 14(4):e0214398. <https://doi.org/10.1371/journal.pone.0214398>
206. Salas P, Odzak N, Echegoyen Y, Kägi R, Sancho MC, Navarro E (2019) The role of size and protein shells in the toxicity to algal photosynthesis induced by ionic silver delivered from silver nanoparticles. *Science of The Total Environment*, 692:233–239. <https://doi.org/10.1016/j.scitotenv.2019.07.237>
207. Schiavo S, Duroudier N, Bilbao E, Mikolaczyk M, Schäfer J, Cajaraville MP, Manzo S (2017) Effects of PVP/PEI coated and uncoated silver NPs and PVP/PEI coating agent on three species of marine microalgae. *Science of The Total Environment*, 577:45–53. <https://doi.org/10.1016/j.scitotenv.2016.10.051>

208. Angel BM, Batley GE, Jarolimek CV, Rogers NJ (2013) The impact of size on the fate and toxicity of nanoparticulate silver in aquatic systems. *Chemosphere*, 93(2):359–365. <https://doi.org/10.1016/j.chemosphere.2013.04.096>
209. Kleiven M, Macken A, Oughton DH (2019) Growth inhibition in *Raphidocelis subcapita* – Evidence of nanospecific toxicity of silver nanoparticles. *Chemosphere*, 221:785–792. <https://doi.org/10.1016/j.chemosphere.2019.01.055>
210. Silva TU (2011) An Evaluation of Coating Material Dependent Toxicity of Silver Nanoparticles. <https://dc.etsu.edu/etd/1229>
211. University of Michigan (2020) Animal Diversity Web. *Animal Diversity Web (ADW)*, <https://animaldiversity.org/>
212. Flanders Marine Institute (2020) World Register of Marine Species. *World Register of Marine Species (WoRMS)*, <http://www.marinespecies.org/index.php>
213. US EPA (2011) Design for the Environment Program Alternatives Assessment Criteria for Hazard Evaluation (Version 2.0). https://www.epa.gov/sites/production/files/2014-01/documents/aa_criteria_v2.pdf
214. Asghari S, Johari SA, Lee JH, Kim YS, Jeon YB, Choi HJ, Moon MC, Yu IJ (2012) Toxicity of various silver nanoparticles compared to silver ions in *Daphnia magna*. *Journal of Nanobiotechnology*, 10(1):14. <https://doi.org/10.1186/1477-3155-10-14>
215. Gao J, Youn S, Hovsepian A, Llaneza VL, Wang Y, Bitton G, Bonzongo J-CJ (2009) Dispersion and Toxicity of Selected Manufactured Nanomaterials in Natural River Water Samples: Effects of Water Chemical Composition. *Environmental Science & Technology*, 43(9):3322–3328. <https://doi.org/10.1021/es803315v>
216. Guiry MD, Guiry GM (2020) AlgaeBase. *AlgaeBase: World-wide electronic publication*, <https://www.algaebase.org/>
217. Wang Z, Quik JTK, Song L, Van Den Brandhof E-J, Wouterse M, Peijnenburg WJGM (2015) Humic substances alleviate the aquatic toxicity of polyvinylpyrrolidone-coated silver nanoparticles to organisms of different trophic levels: Humic substances alleviate the aquatic toxicity of PVP-AgNPs. *Environmental Toxicology and Chemistry*, 34(6):1239–1245. <https://doi.org/10.1002/etc.2936>
218. Froese R, Pauly D (2019) FishBase. www.fishbase.org
219. Massarsky A, Trudeau VL, Moon TW (2014) Predicting the environmental impact of nanosilver. *Environmental Toxicology and Pharmacology*, 38(3):861–873. <https://doi.org/10.1016/j.etap.2014.10.006>
220. Pavagadhi S, Sathishkumar M, Balasubramanian R (2014) Uptake of Ag and TiO₂ nanoparticles by zebrafish embryos in the presence of other contaminants in the aquatic environment. *Water Research*, 55:280–291. <https://doi.org/10.1016/j.watres.2014.02.036>

221. Blaser SA, Scheringer M, MacLeod M, Hungerbühler K (2008) Estimation of cumulative aquatic exposure and risk due to silver: Contribution of nano-functionalized plastics and textiles. *Science of The Total Environment*, 390(2–3):396–409. <https://doi.org/10.1016/j.scitotenv.2007.10.010>
222. Maurya R, Pandey AK (2020) Importance of protozoa Tetrahymena in toxicological studies: A review. *Science of The Total Environment*, :140058. <https://doi.org/10.1016/j.scitotenv.2020.140058>
223. Cho J-G, Kim K-T, Ryu T-K, Lee J, Kim J-E, Kim J, Lee B-C, Jo E-H, Yoon J, Eom I, Choi K, Kim P (2013) Stepwise Embryonic Toxicity of Silver Nanoparticles on *Oryzias latipes*. *BioMed Research International*, 2013:1–7. <https://doi.org/10.1155/2013/494671>
224. Shaw BJ, Handy RD (2011) Physiological effects of nanoparticles on fish: A comparison of nanometals versus metal ions. *Environment International*, 37(6):1083–1097. <https://doi.org/10.1016/j.envint.2011.03.009>
225. Wang P, Ng QX, Zhang H, Zhang B, Ong CN, He Y (2018) Metabolite changes behind faster growth and less reproduction of *Daphnia similis* exposed to low-dose silver nanoparticles. *Ecotoxicology and Environmental Safety*, 163:266–273. <https://doi.org/10.1016/j.ecoenv.2018.07.080>
226. Zhang B, Zhang H, Du C, Ng QX, Hu C, He Y, Ong CN (2017) Metabolic responses of the growing *Daphnia similis* to chronic AgNPs exposure as revealed by GC-Q-TOF/MS and LC-Q-TOF/MS. *Water Research*, 114:135–143. <https://doi.org/10.1016/j.watres.2017.02.046>
227. Temizel-Sekeryan S, Hicks AL (2020) Emerging investigator series: Calculating size- and coating- dependent effect factors for silver nanoparticles to inform characterization factor development for usage in life cycle assessment. *Environmental Science: Nano*, :10.1039/D0EN00675K. <https://doi.org/10.1039/D0EN00675K>
228. Adam V, Loyaux-Lawniczak S, Quaranta G (2015) Characterization of engineered TiO₂ nanomaterials in a life cycle and risk assessments perspective. *Environmental Science and Pollution Research*, 22(15):11175–11192. <https://doi.org/10.1007/s11356-015-4661-x>
229. Batley GE, Kirby JK, McLaughlin MJ (2013) Fate and Risks of Nanomaterials in Aquatic and Terrestrial Environments. *Accounts of Chemical Research*, 46(3):854–862. <https://doi.org/10.1021/ar2003368>
230. Garner KL, Keller AA (2014) Emerging patterns for engineered nanomaterials in the environment: a review of fate and toxicity studies. *Journal of Nanoparticle Research*, 16(8)<https://doi.org/10.1007/s11051-014-2503-2>
231. Ju-Nam Y, Lead J (2016) Properties, Sources, Pathways, and Fate of Nanoparticles in the Environment. *Engineered Nanoparticles and the Environment: Biophysicochemical Processes and Toxicity*, :95–117. <https://doi.org/10.1002/9781119275855>

232. Lowry GV, Gregory KB, Apte SC, Lead JR (2012) Transformations of Nanomaterials in the Environment. *Environmental Science & Technology*, 46(13):6893–6899. <https://doi.org/10.1021/es300839e>
233. Nowack B (2017) Evaluation of environmental exposure models for engineered nanomaterials in a regulatory context. *NanoImpact*, 8:38–47. <https://doi.org/10.1016/j.impact.2017.06.005>
234. Peijnenburg WJGM, Baalousha M, Chen J, Chaudry Q, Von der kammer F, Kuhlbusch TAJ, Lead J, Nickel C, Quik JTK, Renker M, Wang Z, Koelmans AA (2015) A Review of the Properties and Processes Determining the Fate of Engineered Nanomaterials in the Aquatic Environment. *Critical Reviews in Environmental Science and Technology*, 45(19):2084–2134. <https://doi.org/10.1080/10643389.2015.1010430>
235. Peng C, Zhang W, Gao H, Li Y, Tong X, Li K, Zhu X, Wang Y, Chen Y (2017) Behavior and Potential Impacts of Metal-Based Engineered Nanoparticles in Aquatic Environments. *Nanomaterials*, 7(1):21. <https://doi.org/10.3390/nano7010021>
236. Quik JTK, Vonk JA, Hansen SF, Baun A, Van De Meent D (2011) How to assess exposure of aquatic organisms to manufactured nanoparticles? *Environment International*, 37(6):1068–1077. <https://doi.org/10.1016/j.envint.2011.01.015>
237. Suhendra E, Chang C-H, Hou W-C, Hsieh Y-C (2020) A Review on the Environmental Fate Models for Predicting the Distribution of Engineered Nanomaterials in Surface Waters. *International Journal of Molecular Sciences*, 21(12):4554. <https://doi.org/10.3390/ijms21124554>
238. Tao M, Keller AA (2020) ChemFate: A fate and transport modeling framework for evaluating radically different chemicals under comparable conditions. *Chemosphere*, 255:126897. <https://doi.org/10.1016/j.chemosphere.2020.126897>
239. Williams RJ, Harrison S, Keller V, Kuenen J, Lofts S, Praetorius A, Svendsen C, Vermeulen LC, Wijnen J van (2019) Models for assessing engineered nanomaterial fate and behaviour in the aquatic environment. *Current Opinion in Environmental Sustainability*, 36:105–115. <https://doi.org/10.1016/j.cosust.2018.11.002>
240. Mortimer M, Holden PA (2019) Chapter 3 - Fate of engineered nanomaterials in natural environments and impacts on ecosystems. *Exposure to Engineered Nanomaterials in the Environment*, :61–103. <https://doi.org/10.1016/B978-0-12-814835-8.00003-0>
241. Ellis L-JA, Baalousha M, Valsami-Jones E, Lead JR (2018) Seasonal variability of natural water chemistry affects the fate and behaviour of silver nanoparticles. *Chemosphere*, 191:616–625. <https://doi.org/10.1016/j.chemosphere.2017.10.006>
242. Li P, Su M, Wang X, Zou X, Sun X, Shi J, Zhang H (2020) Environmental fate and behavior of silver nanoparticles in natural estuarine systems. *Journal of Environmental Sciences*, 88:248–259. <https://doi.org/10.1016/j.jes.2019.09.013>

243. O'Brien NJ, Cummins EJ (2016) Environmental Exposure Modeling Methods for Engineered Nanomaterials. *Engineered Nanoparticles and the Environment: Biophysicochemical Processes and Toxicity*, :118–138. <https://doi.org/10.1002/9781119275855>
244. Baalousha M, Cornelis G, Kuhlbusch TAJ, Lynch I, Nickel C, Peijnenburg W, Brink NW van den (2016) Modeling nanomaterial fate and uptake in the environment: current knowledge and future trends. *Environmental Science: Nano*, 3(2):323–345. <https://doi.org/10.1039/C5EN00207A>
245. Holden PA, Gardea-Torresdey JL, Klaessig F, Turco RF, Mortimer M, Hund-Rinke K, Cohen Hubal EA, Avery D, Barceló D, Behra R, Cohen Y, Deydier-Stephan L, Ferguson PL, Fernandes TF, Herr Harthorn B, Henderson WM, Hoke RA, Hristozov D, Johnston JM, Kane AB, Kapustka L, Keller AA, Lenihan HS, Lovell W, Murphy CJ, Nisbet RM, Petersen EJ, Salinas ER, Scheringer M, Sharma M, Speed DE, Sultan Y, Westerhoff P, White JC, Wiesner MR, Wong EM, Xing B, Steele Horan M, Godwin HA, Nel AE (2016) Considerations of Environmentally Relevant Test Conditions for Improved Evaluation of Ecological Hazards of Engineered Nanomaterials. *Environmental Science & Technology*, 50(12):6124–6145. <https://doi.org/10.1021/acs.est.6b00608>
246. Geitner NK, Bossa N, Wiesner MR (2019) Formulation and Validation of a Functional Assay-Driven Model of Nanoparticle Aquatic Transport. *Environmental Science & Technology*, 53(6):3104–3109. <https://doi.org/10.1021/acs.est.8b06283>
247. Geitner NK, O'Brien NJ, Turner AA, Cummins EJ, Wiesner MR (2017) Measuring Nanoparticle Attachment Efficiency in Complex Systems. *Environmental Science & Technology*, 51(22):13288–13294. <https://doi.org/10.1021/acs.est.7b04612>
248. Stegemeier JP, Colman BP, Schwab F, Wiesner MR, Lowry GV (2017) Uptake and Distribution of Silver in the Aquatic Plant *Landoltia punctata* (Duckweed) Exposed to Silver and Silver Sulfide Nanoparticles. *Environmental Science & Technology*, 51(9):4936–4943. <https://doi.org/10.1021/acs.est.6b06491>
249. Hartmann NB, Skjolding LM, Hansen SF, Kjølholt J, Gottschalck F, Baun A (2014) Environmental fate and behaviour of nanomaterials - new knowledge on important transformation processes. :12. http://www.nanopartikel.info/files/downloads/Report_Environmental_fate-and-behaviour-of-nanomaterials-2014.pdf
250. Dale AL, Lowry GV, Casman EA (2013) Modeling Nanosilver Transformations in Freshwater Sediments. *Environmental Science & Technology*, 47(22):12920–12928. <https://doi.org/10.1021/es402341t>
251. Furtado LM, Norman BC, Xenopoulos MA, Frost PC, Metcalfe CD, Hintelmann H (2015) Environmental Fate of Silver Nanoparticles in Boreal Lake Ecosystems. *Environmental Science & Technology*, 49(14):8441–8450. <https://doi.org/10.1021/acs.est.5b01116>

252. Levard C, Hotze EM, Lowry GV, Brown GE (2012) Environmental Transformations of Silver Nanoparticles: Impact on Stability and Toxicity. *Environmental Science & Technology*, 46(13):6900–6914. <https://doi.org/10.1021/es2037405>
253. Maiga DT, Nyoni H, Mamba BB, Msagati TAM (2020) The role and influence of hydrogeochemistry in the behaviour and fate of silver nanoparticles in freshwater systems. *SN Applied Sciences*, 2(3):326. <https://doi.org/10.1007/s42452-020-2130-8>
254. Cornelis G (2015) Fate descriptors for engineered nanoparticles: the good, the bad, and the ugly. *Environmental Science: Nano*, 2(1):19–26. <https://doi.org/10.1039/C4EN00122B>
255. Praetorius A, Tufenkji N, Goss K-U, Scheringer M, Kammer F von der, Elimelech M (2014) The road to nowhere: equilibrium partition coefficients for nanoparticles. *Environ. Sci.: Nano*, 1(4):317–323. <https://doi.org/10.1039/C4EN00043A>
256. Wiesner MR, Lowry GV, Jones KL, Hochella, Jr. MF, Di Giulio RT, Casman E, Bernhardt ES (2009) Decreasing Uncertainties in Assessing Environmental Exposure, Risk, and Ecological Implications of Nanomaterials^{† ‡}. *Environmental Science & Technology*, 43(17):6458–6462. <https://doi.org/10.1021/es803621k>
257. Meesters JAJ, Koelmans AA, Quik JTK, Hendriks AJ, Meent D van de (2014) Multimedia Modeling of Engineered Nanoparticles with SimpleBox4nano: Model Definition and Evaluation. *Environmental Science & Technology*, 48(10):5726–5736. <https://doi.org/10.1021/es500548h>
258. Dale AL, Lowry GV, Casman EA (2015) Much ado about α : reframing the debate over appropriate fate descriptors in nanoparticle environmental risk modeling. *Environmental Science: Nano*, 2(1):27–32. <https://doi.org/10.1039/C4EN00170B>
259. Liu HH, Cohen Y (2014) Multimedia Environmental Distribution of Engineered Nanomaterials. *Environmental Science & Technology*, 48(6):3281–3292. <https://doi.org/10.1021/es405132z>
260. Garner KL, Suh S, Keller AA (2017) Assessing the Risk of Engineered Nanomaterials in the Environment: Development and Application of the nanoFate Model. *Environmental Science & Technology*, 51(10):5541–5551. <https://doi.org/10.1021/acs.est.6b05279>
261. Praetorius A, Scheringer M, Hungerbühler K (2012) Development of Environmental Fate Models for Engineered Nanoparticles—A Case Study of TiO₂ Nanoparticles in the Rhine River. *Environmental Science & Technology*, 46(12):6705–6713. <https://doi.org/10.1021/es204530n>
262. Pu Y, Tang F, Adam P-M, Laratte B, Ionescu RE (2016) Fate and Characterization Factors of Nanoparticles in Seventeen Subcontinental Freshwaters: A Case Study on Copper Nanoparticles. *Environmental Science & Technology*, 50(17):9370–9379. <https://doi.org/10.1021/acs.est.5b06300>
263. Dale AL, Casman EA, Lowry GV, Lead JR, Viparelli E, Baalousha M (2015) Modeling Nanomaterial Environmental Fate in Aquatic Systems. *Environmental Science & Technology*, 49(5):2587–2593. <https://doi.org/10.1021/es505076w>

264. Salieri B, Hischier R, Quik JTK, Jolliet O (2019) Fate modelling of nanoparticle releases in LCA: An integrative approach towards “USEtox4Nano.” *Journal of Cleaner Production*, 206:701–712. <https://doi.org/10.1016/j.jclepro.2018.09.187>
265. Skjolding LM, Sørensen SN, Hartmann NB, Hjorth R, Hansen SF, Baun A (2016) Aquatic Ecotoxicity Testing of Nanoparticles—The Quest To Disclose Nanoparticle Effects. *Angewandte Chemie International Edition*, 55(49):15224–15239. <https://doi.org/10.1002/anie.201604964>
266. Jacobs R, Meesters JAJ, Braak CJF ter, Meent D van de, Voet H van der (2016) Combining exposure and effect modeling into an integrated probabilistic environmental risk assessment for nanoparticles. *Environmental Toxicology and Chemistry*, 35(12):2958–2967. <https://doi.org/10.1002/etc.3476>
267. Wender BA, Foley RW, Prado-Lopez V, Ravikumar D, Eisenberg DA, Hottle TA, Sadowski J, Flanagan WP, Fisher A, Laurin L, Bates ME, Linkov I, Seager TP, Fraser MP, Guston DH (2014) Illustrating Anticipatory Life Cycle Assessment for Emerging Photovoltaic Technologies. *Environmental Science & Technology*, 48(18):10531–10538. <https://doi.org/10.1021/es5016923>
268. Quik JTK, Klein JJM de, Koelmans AA (2015) Spatially explicit fate modelling of nanomaterials in natural waters. *Water Research*, 80:200–208. <https://doi.org/10.1016/j.watres.2015.05.025>
269. Espinasse BP, Geitner NK, Schierz A, Therezien M, Richardson CJ, Lowry GV, Ferguson L, Wiesner MR (2018) Comparative Persistence of Engineered Nanoparticles in a Complex Aquatic Ecosystem. *Environmental Science & Technology*, 52(7):4072–4078. <https://doi.org/10.1021/acs.est.7b06142>
270. Praetorius A, Badetti E, Brunelli A, Clavier A, Gallego-Urrea JA, Gondikas A, Hassellöv M, Hofmann T, Mackevica A, Marcomini A, Peijnenburg W, Quik JTK, Seijo M, Stoll S, Tepe N, Walch H, Kammer F von der (2020) Strategies for determining heteroaggregation attachment efficiencies of engineered nanoparticles in aquatic environments. *Environmental Science: Nano*, 7(2):351–367. <https://doi.org/10.1039/C9EN01016E>
271. Liu J, Hurt RH (2010) Ion Release Kinetics and Particle Persistence in Aqueous Nano-Silver Colloids. *Environmental Science & Technology*, 44(6):2169–2175. <https://doi.org/10.1021/es9035557>
272. Delay M, Dolt T, Woellhaf A, Sembritzki R, Frimmel FH (2011) Interactions and stability of silver nanoparticles in the aqueous phase: Influence of natural organic matter (NOM) and ionic strength. *Journal of Chromatography A*, 1218(27):4206–4212. <https://doi.org/10.1016/j.chroma.2011.02.074>
273. Johnston KA, Stabryla LM, Gilbertson LM, Millstone JE (2019) Emerging investigator series: connecting concepts of coinage metal stability across length scales. *Environmental Science: Nano*, 6(9):2674–2696. <https://doi.org/10.1039/C9EN00407F>

274. Liu C, Leng W, Vikesland PJ (2018) Controlled Evaluation of the Impacts of Surface Coatings on Silver Nanoparticle Dissolution Rates. *Environmental Science & Technology*, 52(5):2726–2734. <https://doi.org/10.1021/acs.est.7b05622>
275. Liu W, Zhou Q, Liu J, Fu J, Liu S, Jiang G (2011) Environmental and biological influences on the stability of silver nanoparticles. *Chinese Science Bulletin*, 56(19):2009–2015. <https://doi.org/10.1007/s11434-010-4332-8>
276. Sotiriou GA, Meyer A, Knijnenburg JTN, Panke S, Pratsinis SE (2012) Quantifying the Origin of Released Ag⁺ Ions from Nanosilver. *Langmuir*, 28(45):15929–15936. <https://doi.org/10.1021/la303370d>
277. Stabryla LM, Johnston KA, Millstone JE, Gilbertson LM (2018) Emerging investigator series: it's not all about the ion: support for particle-specific contributions to silver nanoparticle antimicrobial activity. *Environmental Science: Nano*, 5(9):2047–2068. <https://doi.org/10.1039/C8EN00429C>
278. Stebounova LV, Guio E, Grassian VH (2011) Silver nanoparticles in simulated biological media: a study of aggregation, sedimentation, and dissolution. *Journal of Nanoparticle Research*, 13(1):233–244. <https://doi.org/10.1007/s11051-010-0022-3>
279. Ho C-M, Yau SK-W, Lok C-N, So M-H, Che C-M (2010) Oxidative Dissolution of Silver Nanoparticles by Biologically Relevant Oxidants: A Kinetic and Mechanistic Study. *Chemistry - An Asian Journal*, 5(2):285–293. <https://doi.org/10.1002/asia.200900387>
280. Kent RD, Vikesland PJ (2012) Controlled Evaluation of Silver Nanoparticle Dissolution Using Atomic Force Microscopy. *Environmental Science & Technology*, 46(13):6977–6984. <https://doi.org/10.1021/es203475a>
281. Ma R, Levard C, Marinakos SM, Cheng Y, Liu J, Michel FM, Brown GE, Lowry GV (2012) Size-Controlled Dissolution of Organic-Coated Silver Nanoparticles. *Environmental Science & Technology*, 46(2):752–759. <https://doi.org/10.1021/es201686j>
282. Peretyazhko TS, Zhang Q, Colvin VL (2014) Size-Controlled Dissolution of Silver Nanoparticles at Neutral and Acidic pH Conditions: Kinetics and Size Changes. *Environmental Science & Technology*, 48(20):11954–11961. <https://doi.org/10.1021/es5023202>
283. Liu C (2020) Controlled Evaluation of Silver Nanoparticle Dissolution: Surface Coating, Size and Temperature Effects. https://techworks.lib.vt.edu/bitstream/handle/10919/97509/Liu_C_D_2020.pdf?sequence=1&isAllowed=y
284. Zhang W, Yao Y, Sullivan N, Chen Y (2011) Modeling the Primary Size Effects of Citrate-Coated Silver Nanoparticles on Their Ion Release Kinetics. *Environmental Science & Technology*, 45(10):4422–4428. <https://doi.org/10.1021/es104205a>

285. Dong F, Zhou Y (2020) Distinct mechanisms in the heteroaggregation of silver nanoparticles with mineral and microbial colloids. *Water Research*, 170:115332. <https://doi.org/10.1016/j.watres.2019.115332>
286. Therezien M, Thill A, Wiesner MR (2014) Importance of heterogeneous aggregation for NP fate in natural and engineered systems. *Science of The Total Environment*, 485–486:309–318. <https://doi.org/10.1016/j.scitotenv.2014.03.020>
287. Quik JTK (2013) Fate of nanoparticles in the aquatic environment: removal of engineered nanomaterials from the water phase under environmental conditions.
288. Salieri B (2013) The challenges and the limitations in Life Cycle Impact Assessment for metal oxide nanoparticles, a case study on nano- TiO₂. http://amsdottorato.unibo.it/5227/1/Beatrice_Salieri_Tesi.pdf
289. Temizel-Sekeryan S, Wu F, Hicks AL (2020) Life Cycle Assessment of Struvite Precipitation from Anaerobically Digested Dairy Manure: A Wisconsin Perspective. *Integrated Environmental Assessment and Management*, :ieam.4318. <https://doi.org/10.1002/ieam.4318>
290. Colman BP, Espinasse B, Richardson CJ, Matson CW, Lowry GV, Hunt DE, Wiesner MR, Bernhardt ES (2014) Emerging Contaminant or an Old Toxin in Disguise? Silver Nanoparticle Impacts on Ecosystems. *Environmental Science & Technology*, 48(9):5229–5236. <https://doi.org/10.1021/es405454v>
291. Dutch National Institute for Public Health and the Environment (2019) SimpleBox4nano | RIVM. <https://www.rivm.nl/en/soil-and-water/simplebox4nano>
292. Kittler S, Greulich C, Diendorf J, Köller M, Epple M (2010) Toxicity of Silver Nanoparticles Increases during Storage Because of Slow Dissolution under Release of Silver Ions. *Chemistry of Materials*, 22(16):4548–4554. <https://doi.org/10.1021/cm100023p>
293. Quik JTK, Velzeboer I, Wouterse M, Koelmans AA, Meent D van de (2014) Heteroaggregation and sedimentation rates for nanomaterials in natural waters. *Water Research*, 48:269–279. <https://doi.org/10.1016/j.watres.2013.09.036>
294. Ettrup K, Kounina A, Hansen SF, Meesters JAJ, Veia EB, Laurent A (2017) Development of Comparative Toxicity Potentials of TiO₂ Nanoparticles for Use in Life Cycle Assessment. *Environmental Science & Technology*, 51(7):4027–4037. <https://doi.org/10.1021/acs.est.6b05049>
295. Pini M, Salieri B, Ferrari AM, Nowack B, Hirsch R (2016) Human health characterization factors of nano-TiO₂ for indoor and outdoor environments. *The International Journal of Life Cycle Assessment*, 21(10):1452–1462. <https://doi.org/10.1007/s11367-016-1115-8>
296. Ding D, Chen L, Dong S, Cai H, Chen J, Jiang C, Cai T (2016) Natural ageing process accelerates the release of Ag from functional textile in various exposure scenarios. *Scientific Reports*, 6(1):37314. <https://doi.org/10.1038/srep37314>

297. Benn TM, Westerhoff P (2008) Nanoparticle Silver Released into Water from Commercially Available Sock Fabrics. *Environmental Science & Technology*, 42(11):4133–4139. <https://doi.org/10.1021/es7032718>
298. Geranio L, Heuberger M, Nowack B (2009) The Behavior of Silver Nanotextiles during Washing. *Environmental Science & Technology*, 43(21):8113–8118. <https://doi.org/10.1021/es9018332>
299. Benn T, Cavanagh B, Hristovski K, Posner JD, Westerhoff P (2010) The Release of Nanosilver from Consumer Products Used in the Home. *Journal of Environmental Quality*, 39(6):1875–1882. <https://doi.org/10.2134/jeq2009.0363>
300. Lorenz C, Windler L, Goetz N von, Lehmann RP, Schuppler M, Hungerbühler K, Heuberger M, Nowack B (2012) Characterization of silver release from commercially available functional (nano)textiles. *Chemosphere*, 89(7):817–824. <https://doi.org/10.1016/j.chemosphere.2012.04.063>
301. Limpiteprakan P, Babel S, Lohwacharin J, Takizawa S (2016) Release of silver nanoparticles from fabrics during the course of sequential washing. *Environmental Science and Pollution Research*, 23(22):22810–22818. <https://doi.org/10.1007/s11356-016-7486-3>
302. Mitrano DM, Limpiteprakan P, Babel S, Nowack B (2016) Durability of nano-enhanced textiles through the life cycle: releases from landfilling after washing. *Environmental Science: Nano*, 3(2):375–387. <https://doi.org/10.1039/C6EN00023A>
303. Reed RB, Zaikova T, Barber A, Simonich M, Lankone R, Marco M, Hristovski K, Herckes P, Passantino L, Fairbrother DH, Tanguay R, Ranville JF, Hutchison JE, Westerhoff PK (2016) Potential Environmental Impacts and Antimicrobial Efficacy of Silver- and Nanosilver-Containing Textiles. *Environmental Science & Technology*, 50(7):4018–4026. <https://doi.org/10.1021/acs.est.5b06043>
304. Üreyen ME, Aslan C (2016) Determination of silver release from antibacterial finished cotton and polyester fabrics into water. *The Journal of The Textile Institute*, :1–8. <https://doi.org/10.1080/00405000.2016.1222855>
305. Gagnon V, Button M, Boparai HK, Nearing M, O’Carroll DM, Weber KP (2019) Influence of realistic wearing on the morphology and release of silver nanomaterials from textiles. *Environmental Science: Nano*, 6(2):411–424. <https://doi.org/10.1039/C8EN00803E>
306. Kulthong K, Srisung S, Boonpavanitchakul K, Kangwansupamonkon W, Maniratanachote R (2010) Determination of silver nanoparticle release from antibacterial fabrics into artificial sweat. *Particle and Fibre Toxicology*, 7(1):8. <https://doi.org/10.1186/1743-8977-7-8>
307. Yan Y, Yang H, Li J, Lu X, Wang C (2012) Release behavior of nano-silver textiles in simulated perspiration fluids. *Textile Research Journal*, 82(14):1422–1429. <https://doi.org/10.1177/0040517512439922>

308. Goetz N von, Lorenz C, Windler L, Nowack B, Heuberger M, Hungerbühler K (2013) Migration of Ag- and TiO₂-(Nano)particles from Textiles into Artificial Sweat under Physical Stress: Experiments and Exposure Modeling. *Environmental Science & Technology*, 47(17):9979–9987. <https://doi.org/10.1021/es304329w>
309. Wagener S, Dommershausen N, Jungnickel H, Laux P, Mitrano D, Nowack B, Schneider G, Luch A (2016) Textile Functionalization and Its Effects on the Release of Silver Nanoparticles into Artificial Sweat. *Environmental Science & Technology*, 50(11):5927–5934. <https://doi.org/10.1021/acs.est.5b06137>
310. Kim JB, Kim JY, Yoon TH (2017) Determination of silver nanoparticle species released from textiles into artificial sweat and laundry wash for a risk assessment. *Human and Ecological Risk Assessment: An International Journal*, 23(4):741–750. <https://doi.org/10.1080/10807039.2016.1277417>
311. Spielman-Sun E, Zaikova T, Dankovich T, Yun J, Ryan M, Hutchison JE, Lowry GV (2018) Effect of silver concentration and chemical transformations on release and antibacterial efficacy in silver-containing textiles. *NanoImpact*, 11:51–57. <https://doi.org/10.1016/j.impact.2018.02.002>
312. PRé Sustainability (2020) SimaPro LCA software. *Sustainability software for fact-based decisions*, <https://pre-sustainability.com/solutions/tools/simapro/>
313. ecoinvent (2020) Ecoinvent 3. *ecoinvent - the world's mostconsistent & transparentlife cycle inventory database*, <https://www.ecoinvent.org/>
314. Mohan S, Princz J, Ormeci B, DeRosa MC (2019) Morphological Transformation of Silver Nanoparticles from Commercial Products: Modeling from Product Incorporation, Weathering through Use Scenarios, and Leaching into Wastewater. *Nanomaterials*, 9(9):1258. <https://doi.org/10.3390/nano9091258>
315. Ellen MacArthur Foundation (2017) A New Textiles Economy: Redesigning Fashion's Future. https://www.ellenmacarthurfoundation.org/assets/downloads/publications/A-New-Textiles-Economy_Full-Report.pdf
316. Ütebay B, Çelik P, Çay A (2020) Textile Wastes: Status and Perspectives. *Waste in Textile and Leather Sectors*, <https://doi.org/10.5772/intechopen.92234>
317. US EPA (2020) Textiles: Material-Specific Data. *Facts and Figures about Materials, Waste and Recycling*, <https://www.epa.gov/facts-and-figures-about-materials-waste-and-recycling/textiles-material-specific-data#TextilesTableandGraph>
318. Limpiteprakan P, Babel S (2016) Leaching potential of silver from nanosilver-treated textile products. *Environmental Monitoring and Assessment*, 188(3):156. <https://doi.org/10.1007/s10661-016-5158-x>
319. US EPA (1992) SW-846 Test Method 1311: Toxicity Characteristic Leaching Procedure. *Hazardous Waste Test Methods / SW-846*, <https://www.epa.gov/hw-sw846/sw-846-test-method->

1311-toxicity-characteristic-leaching-procedure#:~:text=Related%20Topics%3A-,SW%2D846%20Test%20Method%20201311%3A%20Toxicity%20Characteristic%20Leaching%20Procedure,%2C%20solid%2C%20and%20multiphasic%20wastes.

320. Hendren CO, Badireddy AR, Casman E, Wiesner MR (2013) Modeling nanomaterial fate in wastewater treatment: Monte Carlo simulation of silver nanoparticles (nano-Ag). *Science of The Total Environment*, 449:418–425. <https://doi.org/10.1016/j.scitotenv.2013.01.078>

321. Huang Y, Keller AA, Cervantes-Avilés P, Nelson J (2020) Fast Multielement Quantification of Nanoparticles in Wastewater and Sludge Using Single-Particle ICP-MS. *ACS ES&T Water*, <https://doi.org/10.1021/acsestwater.0c00083>

322. Ma R, Levard C, Judy JD, Unrine JM, Durenkamp M, Martin B, Jefferson B, Lowry GV (2014) Fate of Zinc Oxide and Silver Nanoparticles in a Pilot Wastewater Treatment Plant and in Processed Biosolids. *Environmental Science & Technology*, 48(1):104–112. <https://doi.org/10.1021/es403646x>

323. Wang P, Lombi E, W. Menzies N, Zhao F-J, M. Kopittke P (2018) Engineered silver nanoparticles in terrestrial environments: a meta-analysis shows that the overall environmental risk is small. *Environmental Science: Nano*, 5(11):2531–2544. <https://doi.org/10.1039/C8EN00486B>

324. Zhang C, Hu Z, Li P, Gajaraj S (2016) Governing factors affecting the impacts of silver nanoparticles on wastewater treatment. *Science of The Total Environment*, 572:852–873. <https://doi.org/10.1016/j.scitotenv.2016.07.145>

325. Nabi MM, Wang J, Meyer M, Croteau M-N, Ismail N, Baalousha M (2021) Concentrations and size distribution of TiO₂ and Ag engineered particles in five wastewater treatment plants in the United States. *Science of The Total Environment*, 753:142017. <https://doi.org/10.1016/j.scitotenv.2020.142017>

326. Som C, Wick P, Krug H, Nowack B (2011) Environmental and health effects of nanomaterials in nanotextiles and façade coatings. *Environment International*, 37(6):1131–1142. <https://doi.org/10.1016/j.envint.2011.02.013>

327. DEQ (2014) What are biosolids, how are they used, and are they safe? https://www.michigan.gov/documents/deq/deq-ess-faq-water-wb-septagebiosolids-whatarethey_206712_7.pdf

328. US EPA (2020) Basic Information about Biosolids. <https://www.epa.gov/biosolids/basic-information-about-biosolids>

329. Pradas del Real AE, Castillo-Michel H, Kaegi R, Sinnet B, Magnin V, Findling N, Villanova J, Carrière M, Santaella C, Fernández-Martínez A, Levard C, Sarret G (2016) Fate of Ag-NPs in Sewage Sludge after Application on Agricultural Soils. *Environmental Science & Technology*, 50(4):1759–1768. <https://doi.org/10.1021/acs.est.5b04550>

330. Georgantzopoulou A, Almeida Carvalho P, Vogelsang C, Tilahun M, Ndungu K, Booth AM, Thomas KV, Macken A (2018) Ecotoxicological Effects of Transformed Silver and Titanium Dioxide Nanoparticles in the Effluent from a Lab-Scale Wastewater Treatment System. *Environmental Science & Technology*, 52(16):9431–9441. <https://doi.org/10.1021/acs.est.8b01663>
331. Kaegi R, Voegelin A, Sinnet B, Zuleeg S, Hagendorfer H, Burkhardt M, Siegrist H (2011) Behavior of Metallic Silver Nanoparticles in a Pilot Wastewater Treatment Plant. *Environmental Science & Technology*, 45(9):3902–3908. <https://doi.org/10.1021/es1041892>
332. Azimzada A, Tufenkji N, Wilkinson KJ (2017) Transformations of silver nanoparticles in wastewater effluents: links to Ag bioavailability. *Environmental Science: Nano*, 4(6):1339–1349. <https://doi.org/10.1039/C7EN00093F>
333. Zeumer R, Hermsen L, Kaegi R, Kühn S, Knopf B, Schlechtriem C (2020) Bioavailability of silver from wastewater and planktonic food borne silver nanoparticles in the rainbow trout *Oncorhynchus mykiss*. *Science of The Total Environment*, 706:135695. <https://doi.org/10.1016/j.scitotenv.2019.135695>
334. Mulenos MR, Liu J, Lujan H, Guo B, Lichtfouse E, Sharma VK, Sayes CM (2020) Copper, silver, and titania nanoparticles do not release ions under anoxic conditions and release only minute ion levels under oxic conditions in water: Evidence for the low toxicity of nanoparticles. *Environmental Chemistry Letters*, 18(4):1319–1328. <https://doi.org/10.1007/s10311-020-00985-z>

Appendix A

Electronic supplemental information from Chapter 2 and associated references.

Synthesis Methods and LCA Inventories

Wet Chemistry

Microwave (MW)

In the microwave (MW) technique applied by Bafana et al., glucose was used as a reducing agent for silver nitrate, and food-grade starch was used as a stabilizing agent [1]. A laboratory-grade microwave was used for this synthesis (which consumes 1250 MJ electricity to produce 1 kg of AgNPs) which allows modification of heating rates and monitoring the reaction easily, and also completes AgNPs production within 5 minutes. In the current study, inventory used for microwave method (MW) for 1 kg AgNP is adjusted from Bafana et al. [1] and is given in Table A1.

Table A1. Inventory used for microwave method (MW) for 1 kg AgNP.

Microwave (MW) for 1 kg AgNP			
Input	Unit	Amount	Database
Electricity	MJ	1250	ELCD
Potato starch	1.31	kg	Ecoinvent 3
Silver Nitrate (AgNO ₃)	1.57	kg	Table A15
Water, deionized	773	kg	Ecoinvent 3
Glucose	2.50	kg	USLCI
Output	Unit	Amount	Database
AgNP	kg	1	-

Chemical Reduction (CR)

The chemical reduction (CR) technique uses different reducing agents (such as plant extracts, biological or chemical agents, or irradiation methods) to reduce silver ions and to produce AgNPs. Also capping agents are added to block overgrowth and to control structural characteristics of AgNPs (i.e. size) [2, 3]. This method has mild reaction conditions, consumes low energy and has high yield [3]. The current paper examines five different CR approaches including reduction of silver nitrate with trisodium citrate [4], with sodium borohydride [4, 5], with ethylene glycol [4] and with soluble starch [4]. In the current study, inventories used for chemical reduction methods for 1 kg AgNP are adjusted from Pourzahedi and Eckelman [4] and are given in Table A2-A5.

Table A2. Inventory used for chemical reduction with trisodium citrate for 1 kg AgNP.

Chemical Reduction with Trisodium Citrate (CR-TSC) for 1 kg AgNP			
Input	Unit	Amount	Database
Silver Nitrate (AgNO ₃)	1.57	kg	Table A15
Water, deionized	9277	kg	Ecoinvent 3
Heat	2912	MJ	Ecoinvent 3
Trisodium citrate [4]	0.8	kg	-
Output	Unit	Amount	Database
AgNP	kg	1	-
Hydrogen -emissions to air-	kg	0.006	-
Oxygen -emissions to air-	kg	0.12	-
Citric acid -emissions to water-	kg	0.59	-
Sodium nitrate -emissions to water-	kg	0.79	-

Table A3. Inventory used for chemical reduction with sodium borohydride for 1 kg AgNP.

Chemical Reduction with Sodium Borohydride (CR-SB) for 1 kg AgNP			
Input	Unit	Amount	Database
Silver Nitrate (AgNO ₃)	1.57	kg	Table A15
Cooling water	24	kg	Ecoinvent 3
Water, deionized	13915	kg	Ecoinvent 3
Sodium borohydride [4]	0.35	kg	-
Output	Unit	Amount	Database
AgNP	kg	1	-
Hydrogen -emissions to air-	kg	0.009	-
Diborane -emissions to air-	kg	0.13	-
Sodium nitrate -emissions to water-	kg	0.79	-

Table A4. Inventory used for chemical reduction with ethylene glycol for 1 kg AgNP.

Chemical Reduction with Ethylene Glycol (CR-EG) for 1 kg AgNP			
Input	Unit	Amount	Database
Silver Nitrate (AgNO ₃)	1.57	kg	Table A15
Water, deionized	261	kg	Ecoinvent 3
Ethylene glycol	29.1	kg	Ecoinvent 3
PVP [4]	47.2	kg	-
Output	Unit	Amount	Database
AgNP	kg	1	-

Table A5. Inventory used for chemical reduction with starch for 1 kg AgNP.

Chemical Reduction with Starch (CR-starch) for 1 kg AgNP			
Input	Unit	Amount	Database
Silver Nitrate (AgNO ₃)	1.57	kg	Table A15
Water, deionized	10000	kg	Ecoinvent 3
Heat	1915	MJ	Ecoinvent 3
Potato starch	90	kg	Ecoinvent 3
Output	Unit	Amount	Database
AgNP	kg	1	-

Dry Chemistry

Flame Spray Pyrolysis (FSP)

The flame spray pyrolysis (FSP) method is used to produce commercial quantities of nanoparticles [6], and because of being rapid and scalable, it is found highly promising and versatile [7]. This is a one step process in which a solvent, including dissolved metal precursors, is sprayed with an oxidizing gas into a flame, then it is combusted, and precursors are converted into nanoparticles. Depending on the desired characteristics of ENMs, operating conditions and precursor types may change [8]. For AgNPs production with FSP, silver acetate, silver benzoate, and silver nitrate may be used as metal precursors; 2-ethylhexanoate-toluene, pyridine, xylene-tetraisopropoxide and ethanol may be used as solvents [7]. The current study examines FSP method with melt-spun incorporation [9]. The inventory used for this method is adjusted from Walser et al. [9] and is given in Table A6-A8.

Table A6. Inventory used for flame spray pyrolysis with melt-spun incorporation method (FSP-MS) for 1 kg AgNP.

Flame Spray Pyrolysis with Melt-Spun Incorporation (FSP-MS) for 1 kg AgNP			
Input	Unit	Amount	Database
Oxygen	kg	33.4	Ecoinvent 3
Methane	m ³	1.004	Ecoinvent 3
Water, deionized	kg	62.8	Ecoinvent 3
Silver-octanoate (Ag-C ₈ H ₁₅ O ₂)	kg	2.35	Table A8
2-ethylhexanoic acid (C ₈ H ₁₆ O ₂)	kg	6.29	Table A7
Xylene	kg	6.29	Ecoinvent 3
Electricity	kWh	25.1	ELCD
Output	Unit	Amount	Database
AgNP	kg	1	-
Nitrogen oxide -emissions to air-	kg	0.387	-
Water -emissions to air-	kg	16.8	-

Table A7. Inventory used for 1 kg of 2-ethylhexanoic acid ($C_8H_{16}O_2$) [9].

Production Inventory for 1 kg of 2-ethylhexanoic acid ($C_8H_{16}O_2$)			
Input	Unit	Amount	Database
Steam, in chemical industry	kg	0.000716	Ecoinvent 3
Hydroformylation of propylene *	kg	1.02	Ecoinvent 3
Transport, freight, lorry	t-km	10.8	Ecoinvent 3
Output	Unit	Amount	Database
2-ethylhexanoic acid ($C_8H_{16}O_2$)	kg	1	-
Carbon dioxide, fossil -emissions to air-	kg	0.0499	-

*n-butyraldehyde is a high-production volume chemical produced from hydroformylation of propylene [10].

Table A8. Inventory used for 1 kg of Silver-octanoate ($AgC_8H_{15}O_2$) [9].

Production Inventory 1 kg of Silver-octanoate ($AgC_8H_{15}O_2$)			
Input	Unit	Amount	Database
Fatty acid [#]	kg	2.7085	Ecoinvent 3
Sodium hydroxide	kg	0.3785	Ecoinvent 3
Silver Nitrate ($AgNO_3$)	kg	2.575	Table A15
Water, deionized	kg	0.901	Ecoinvent 3
Output	Unit	Amount	Database
Silver-octanoate ($AgC_8H_{15}O_2$)	kg	1	-

[#]Octanoic acid is an eight-carbon saturated fatty acid and is naturally found in coconut oil.

Arc Plasma (AP) and Spark System

Arc plasma (AP) and spark methods use energy delivered through the electrical discharge to produce pure metallic nanoparticles. The difference between these two setups is the energy delivery techniques. While a continuous arc discharge delivers the energy to AP, sparks supply the energy with varying frequencies to the spark system [11]. The current paper analyses five different AP methods (one from Pourzahedi and Eckelman [4] and four from Slotte and Zevenhoven [11]) and a spark system (from Slotte and Zevenhoven [11]) method. Inventories

used for these methods are adjusted from aforementioned studies and can be found in Table A9-A13.

Table A9. Inventory used for arc discharge method (AP) for 1 kg AgNP.

Arc Discharge (AP) for 1 kg AgNP			
Input	Unit	Amount	Database
Silver	kg	1	Ecoinvent 3
Argon	kg	7.4	Ecoinvent 3
Electricity	kWh	41.67	ELCD
Output	Unit	Amount	Database
AgNP	kg	1	-

Table A10. Inventory used for arc discharge method (AP-UDE1) for 1 kg AgNP.

Arc discharge by University of Duisburg- Essen, Germany (UDE1) for 1 kg AgNP			
Input	Unit	Amount	Database
Electricity	kWh	570	ELCD
Silver	kg	3.2	Ecoinvent 3
Transport, freight, sea	kgkm	48000	Ecoinvent 3
Nitrogen	kg	32.2	Ecoinvent 3
Transport, freight, lorry	kgkm	644	Ecoinvent 3
Output	Unit	Amount	Database
AgNP	kg	1	-
Nitrogen, total -emissions to air-	kg	32.2	-
Silver	kg	2.2	Ecoinvent 3

Table A11. Inventory used for arc discharge method (AP-UDE2) for 1 kg AgNP.

Arc discharge by University of Duisburg- Essen, Germany (UDE2) for 1 kg AgNP			
Input	Unit	Amount	Database
Electricity	kWh	743.75	ELCD
Silver	kg	4.25	Ecoinvent 3
Transport, freight, sea	kgkm	63750	Ecoinvent 3
Nitrogen	kg	20.13	Ecoinvent 3
Transport, freight, lorry	kgkm	402.5	Ecoinvent 3
Output	Unit	Amount	Database
AgNP	kg	1	-
Nitrogen, total -emissions to air-	kg	20.13	-
Silver	kg	3.25	Ecoinvent 3

Table A12. Inventory used for arc discharge method (AP-UDE3) for 1 kg AgNP.

Arc discharge by University of Duisburg- Essen, Germany (UDE3) for 1 kg AgNP			
Input	Unit	Amount	Database
Electricity	kWh	960	ELCD
Silver	kg	7.2	Ecoinvent 3
Transport, freight, sea	kgkm	108000	Ecoinvent 3
Nitrogen	kg	16.1	Ecoinvent 3
Transport, freight, lorry	kgkm	322	Ecoinvent 3
Output	Unit	Amount	Database
AgNP	kg	1	-
Nitrogen, total -emissions to air-	kg	16.1	-
Silver	kg	6.2	Ecoinvent 3

Table A13. Inventory used for arc discharge method (AP-MNL) for 1 kg AgNP.

Arc discharge by Metal Nanopowders Ltd., United Kingdom (MNL) for 1 kg AgNP			
Input	Unit	Amount	Database
Electricity	kWh	615	ELCD
Silver	kg	5.35	Ecoinvent 3
Transport, freight, sea	kgkm	80250	Ecoinvent 3
Nitrogen	kg	2.69	Ecoinvent 3
Transport, freight, lorry	kgkm	53.8	Ecoinvent 3
Output	Unit	Amount	Database
AgNP	kg	1	-
Nitrogen, total -emissions to air-	kg	2.69	-
Silver	kg	4.35	Ecoinvent 3

Table A14. Inventory used for spark system method (Spark-TUD) for 1 kg AgNP.

Spark system Delft University of Technology, the Netherlands (TUD) for 1 kg AgNP			
Input	Unit	Amount	Database
Electricity	kWh	500	ELCD
Silver	kg	1.25	Ecoinvent 3
Transport, freight, sea	kgkm	18750	Ecoinvent 3
Argon	kg	75	Ecoinvent 3
Transport, freight, lorry	kgkm	1500	Ecoinvent 3
Output	Unit	Amount	Database
AgNP	kg	1	-
Argon -emissions to air-	kg	75	-
Silver	kg	0.25	Ecoinvent 3

Table A15. Inventory used for 1 kg of Silver Nitrate (AgNO₃) [4].

Production Inventory 1 kg of Silver Nitrate (AgNO₃)			
Input	Unit	Amount	Database
Nitric acid	kg	0.49	Ecoinvent 3
Silver	kg	0.64	Ecoinvent 3
Output	Unit	Amount	Database
Silver Nitrate (AgNO ₃)	kg	1	-
Water -emissions to air-	kg	0.07	-
Nitrogen oxides -emissions to air-	kg	0.06	-

Reactive Magnetron Sputtering (RMS)

In reactive magnetron sputtering (RMS) method, argon (Ar) is used for bombardment of the sputtering target (which is Ag). A mixture of Ar and reactive gases (nitrogen) is used to place films of oxide or nitride forms of the target material onto the substrate surface [4]. In the current study, inventory used for RMS method for 1 kg AgNP is adjusted from Pourzahedi and Eckelman [4] and is given in Table A16.

Table A16. Inventory used for reactive magnetron sputtering (RMS-Ar-N) for 1 kg AgNP.

Reactive Magnetron Sputtering (RMS-Ar-N) for 1 kg AgNP			
Input	Unit	Amount	Database
Silver	kg	1	Ecoinvent 3
Argon	g	123.6	Ecoinvent 3
Nitrogen	g	10.4	Ecoinvent 3
Electricity	kWh	27.8	ELCD
Output	Unit	Amount	Database
AgNP	kg	1	-

Table A17. Potential environmental impact categories of TRACI 2.1, CML (baseline), IMPACT 2002+ and ReCiPe Midpoint impact assessment methodologies with their abbreviations and units.

Methodology	Potential Environmental Impact Categories
TRACI 2.1 [12]	ozone depletion (ODP in kg CFC11-eq.), global warming (GWP in kg CO ₂ -eq.), smog (SP in kg O ₃ -eq.), acidification (AP in kg SO ₂ -eq.), eutrophication (EP in kg N-eq.), carcinogenics (HHCP in CTUh), non-carcinogenics (HHNCP in CTUh), respiratory effects (RP in kg PM _{2.5} -eq.), ecotoxicity (ETP in CTUe), and fossil fuel depletion (FFP in MJ surplus energy).
CML (baseline) [13]	abiotic depletion (ADP in kg Sb-eq.), abiotic depletion-fossil fuels (ADP(FF) in MJ), global warming (GWP100a in kg CO ₂ -eq.), ozone layer depletion (ODP in kg CFC11-eq.), human toxicity (HTP in kg 1,4-DB-eq.), fresh water aquatic ecotoxicity (FWAEP in kg 1,4-DB-eq.), marine aquatic ecotoxicity (MAEP in kg 1,4-DB-eq.), terrestrial ecotoxicity (TEP in kg 1,4-DB-eq.), photochemical oxidation (POxP in kg C ₂ H ₄ -eq.), acidification (AP in kg SO ₂ -eq.), and eutrophication (EP in kg PO ₄ -eq.).
IMPACT 2002+ [14]	carcinogens (CP in kg C ₂ H ₃ Cl-eq.), non-carcinogens (NCP in kg C ₂ H ₃ Cl-eq.), respiratory inorganics (RaIP in kg PM _{2.5} -eq.), ionizing radiation (IR in Bq C-14-eq.), ozone layer depletion (ODP in kg CFC11-eq.), respiratory organics (RaOP in kg C ₂ H ₄ -eq.), aquatic ecotoxicity (AEP in kg TEG water), terrestrial ecotoxicity (TEP in kg TEG soil), terrestrial acidification (tAP in kg SO ₂ -eq.), land occupation (LO in m ² org.arable), aquatic acidification (aAP in kg SO ₂ -eq.), aquatic eutrophication (EP in kg PO ₄ P-lim), global warming (GWP in kg CO ₂ -eq.), non-renewable energy (NRE in MJ primary), and mineral extraction (ME in MJ surplus).
ReCiPe Midpoint [15]	climate change (GWP in kg CO ₂ -eq.), ozone depletion (ODP in kg CFC11-eq.), terrestrial acidification (tAP in kg SO ₂ -eq.), freshwater eutrophication (FWEP in kg P-eq.), marine eutrophication (MEP in kg N-eq.), human toxicity (HTP in kg 1,4-DB-eq.), photochemical oxidant formation (POxP in kg NMVOC), particulate matter formation (RP in kg PM ₁₀ -eq.), terrestrial ecotoxicity (TEP in kg 1,4-DB-eq.), freshwater ecotoxicity (FWAEP in kg 1,4-DB-eq.), marine ecotoxicity (MAEP in kg 1,4-DB-eq.), ionizing radiation (IR in kBq U235 eq.), agricultural land occupation (ALO in m ² a), urban land occupation (ULO in m ² a), natural land transformation (NLT in m ²), water depletion (WDP in m ³), metal depletion (MD in kg Fe eq.), and fossil depletion (FFP in kg oil eq.).

Uncertainty Analysis

Table A18. Uncertainties around each production method simulated by Monte Carlo Analysis in SimaPro 8.5.2 (per FUn: 1 kg AgNP)

C1*	C2	MW	CR-TSC	CR-SB	CR-EG	CR-starch	FSP-MS	AP	AP-UDE1	AP-UDE2	AP-UDE3	AP-MNL	Spark-TUD	RMS-Ar-N
ODP	LB	6.69E-05	3.81E-05	2.50E-05	3.42E-05	3.18E-05	1.86E-05	1.30E-05	1.01E-04	1.28E-04	1.62E-04	1.08E-04	9.83E-05	1.21E-05
	M	7.53E-05	6.08E-05	3.38E-05	5.28E-05	5.14E-05	2.79E-05	2.17E-05	1.11E-04	1.38E-04	1.71E-04	1.17E-04	1.12E-04	2.08E-05
	UB	9.90E-05	1.23E-04	6.09E-05	9.44E-05	1.04E-04	5.12E-05	4.79E-05	1.31E-04	1.60E-04	1.94E-04	1.39E-04	1.45E-04	4.50E-05
GWP	LB	4.91E+02	6.33E+02	4.03E+02	5.42E+02	5.30E+02	3.46E+02	3.33E+02	6.27E+02	7.25E+02	8.56E+02	6.49E+02	7.08E+02	3.08E+02
	M	5.92E+02	7.62E+02	5.07E+02	6.82E+02	6.49E+02	4.18E+02	4.29E+02	7.30E+02	8.30E+02	9.56E+02	7.46E+02	8.53E+02	4.06E+02
	UB	7.42E+02	9.37E+02	6.61E+02	8.81E+02	8.01E+02	5.33E+02	5.79E+02	8.92E+02	9.71E+02	1.10E+03	8.99E+02	1.12E+03	5.60E+02
SP	LB	3.68E+01	4.20E+01	3.38E+01	4.44E+01	4.08E+01	2.61E+01	3.00E+01	3.79E+01	4.20E+01	4.56E+01	3.93E+01	4.45E+01	2.90E+01
	M	5.80E+01	6.39E+01	5.54E+01	6.64E+01	6.25E+01	4.21E+01	5.13E+01	5.87E+01	6.17E+01	6.58E+01	5.85E+01	6.62E+01	5.05E+01
	UB	1.07E+02	1.12E+02	1.02E+02	1.12E+02	1.09E+02	7.72E+01	9.39E+01	1.04E+02	1.08E+02	1.13E+02	1.06E+02	1.14E+02	9.16E+01
AP	LB	7.91E+00	7.82E+00	6.77E+00	7.96E+00	7.89E+00	5.21E+00	6.69E+00	8.68E+00	9.42E+00	1.03E+01	8.92E+00	9.06E+00	6.47E+00
	M	1.04E+01	1.05E+01	9.37E+00	1.04E+01	1.04E+01	7.09E+00	9.10E+00	1.12E+01	1.20E+01	1.28E+01	1.13E+01	1.19E+01	9.05E+00
	UB	1.42E+01	1.48E+01	1.31E+01	1.42E+01	1.43E+01	9.80E+00	1.27E+01	1.49E+01	1.58E+01	1.63E+01	1.52E+01	1.56E+01	1.26E+01
EP	LB	2.35E+00	2.63E+00	2.28E+00	3.01E+00	3.30E+00	1.89E+00	2.19E+00	2.34E+00	2.30E+00	2.36E+00	2.31E+00	2.94E+00	2.33E+00
	M	5.04E+00	5.40E+00	5.01E+00	5.83E+00	5.96E+00	3.99E+00	5.21E+00	4.95E+00	4.94E+00	4.97E+00	4.97E+00	5.71E+00	5.00E+00
	UB	1.79E+01	1.92E+01	1.65E+01	1.80E+01	1.76E+01	1.31E+01	1.87E+01	1.71E+01	1.62E+01	1.62E+01	1.64E+01	1.74E+01	1.55E+01
HHCP	LB	3.20E-05	3.42E-05	3.18E-05	3.69E-05	3.62E-05	2.53E-05	3.04E-05	3.26E-05	3.11E-05	2.96E-05	3.06E-05	3.57E-05	2.89E-05
	M	8.04E-05	8.73E-05	7.92E-05	9.16E-05	8.95E-05	6.13E-05	7.91E-05	8.30E-05	7.96E-05	8.13E-05	8.25E-05	8.97E-05	7.71E-05
	UB	4.49E-04	4.07E-04	3.81E-04	3.84E-04	3.73E-04	3.19E-04	3.54E-04	3.69E-04	4.04E-04	3.73E-04	4.15E-04	4.03E-04	4.51E-04
HHNCP	LB	1.42E-03	1.47E-03	1.43E-03	1.42E-03	1.73E-03	1.06E-03	1.37E-03	1.41E-03	1.42E-03	1.47E-03	1.45E-03	1.53E-03	1.33E-03
	M	3.22E-03	3.45E-03	3.34E-03	3.35E-03	3.73E-03	2.55E-03	3.21E-03	3.34E-03	3.21E-03	3.32E-03	3.30E-03	3.47E-03	3.19E-03
	UB	1.02E-02	1.12E-02	1.17E-02	1.20E-02	1.21E-02	8.04E-03	1.00E-02	1.06E-02	1.02E-02	1.14E-02	1.10E-02	1.16E-02	1.10E-02
RP	LB	7.64E-01	7.87E-01	6.57E-01	9.57E-01	8.31E-01	5.55E-01	6.88E-01	8.34E-01	8.76E-01	9.53E-01	8.37E-01	1.03E+00	6.50E-01
	M	9.49E-01	1.01E+00	8.70E-01	1.24E+00	1.03E+00	7.05E-01	8.81E-01	1.04E+00	1.09E+00	1.15E+00	1.03E+00	1.32E+00	8.48E-01
	UB	1.25E+00	1.35E+00	1.18E+00	1.64E+00	1.33E+00	8.96E-01	1.17E+00	1.35E+00	1.40E+00	1.44E+00	1.31E+00	1.80E+00	1.12E+00
ETP	LB	9.75E+03	1.01E+04	1.00E+04	1.10E+04	1.36E+04	7.52E+03	9.57E+03	1.02E+04	1.03E+04	9.52E+03	1.02E+04	1.14E+04	1.02E+04
	M	2.72E+04	2.83E+04	2.68E+04	2.85E+04	3.11E+04	2.06E+04	2.64E+04	2.68E+04	2.59E+04	2.64E+04	2.68E+04	2.81E+04	2.74E+04
	UB	1.06E+05	1.08E+05	1.09E+05	1.31E+05	1.17E+05	8.50E+04	1.17E+05	1.06E+05	1.04E+05	1.09E+05	1.08E+05	1.14E+05	1.07E+05
FFP	LB	3.17E+02	5.70E+02	2.67E+02	6.49E+02	4.56E+02	2.96E+02	2.00E+02	4.13E+02	4.76E+02	5.67E+02	4.24E+02	4.56E+02	1.85E+02
	M	3.96E+02	7.16E+02	3.53E+02	8.15E+02	5.87E+02	3.70E+02	2.86E+02	4.97E+02	5.63E+02	6.48E+02	5.04E+02	5.81E+02	2.70E+02
	UB	5.53E+02	9.65E+02	5.23E+02	1.07E+03	7.79E+02	5.04E+02	4.38E+02	6.47E+02	7.22E+02	8.04E+02	6.72E+02	8.04E+02	4.16E+02
CED	LB	6.92E+03	6.91E+03	4.27E+03	7.67E+03	6.69E+03	4.18E+03	3.45E+03	9.72E+03	1.17E+04	1.43E+04	1.01E+04	1.06E+04	3.03E+03
	M	8.05E+03	8.69E+03	5.41E+03	1.01E+04	8.74E+03	5.25E+03	4.56E+03	1.09E+04	1.29E+04	1.54E+04	1.13E+04	1.27E+04	4.14E+03
	UB	9.88E+03	1.13E+04	7.43E+03	1.34E+04	1.18E+04	6.80E+03	6.36E+03	1.27E+04	1.47E+04	1.72E+04	1.29E+04	1.66E+04	5.91E+03

C1: Potential environmental impact categories considered in the current study.

C2: Lower bound (LB), median (M) and upper bound (UB) of emissions based on 95% confidence intervals for the uncertainties.

* ODP in kg CFC11-eq., GWP in kg CO₂-eq., SP in kg O₃-eq., AP in kg SO₂-eq., EP in kg N-eq., HHCP in CTUh, HHNCP in CTUh, RP in kg PM_{2.5}-eq., ETP in CTUe, FFP in MJ surplus energy, CED in MJ.

Table A19. When SF =2, the GWP (tons CO₂-eq.) associated with each synthesis are:

	Scaling Up Factor	Median (tons CO ₂ -eq./year)	Lower Bound (tons CO ₂ -eq./year)	Upper Bound (tons CO ₂ -eq./year)
MW	2	2.96E+02	2.46E+02	3.71E+02
CR-TSC	2	3.81E+02	3.17E+02	4.69E+02
CR-SB	2	2.54E+02	2.02E+02	3.31E+02
CR-EG	2	3.41E+02	2.71E+02	4.41E+02
CR-starch	2	3.25E+02	2.65E+02	4.01E+02
FSP-MS	2	2.09E+02	1.73E+02	2.67E+02
AP	2	2.15E+02	1.67E+02	2.90E+02
AP-UDE1	2	3.65E+02	3.14E+02	4.46E+02
AP-UDE2	2	4.15E+02	3.63E+02	4.86E+02
AP-UDE3	2	4.78E+02	4.28E+02	5.50E+02
AP-MNL	2	3.73E+02	3.25E+02	4.50E+02
Spark-TUD	2	4.27E+02	3.54E+02	5.60E+02
RMS-AR-N	2	2.03E+02	1.54E+02	2.80E+02

Table A20. The projected GWP (tons CO₂-eq.) in 2018 using the skeptical production volume and the industrial weighting for physical and wet chemistry method.

#	Weighting [16]		GWP, Skeptical w/ Weighting		
			Median (tons CO ₂ -eq./year)	Lower Bound (tons CO ₂ -eq./year)	Upper Bound (tons CO ₂ -eq./year)
1	MW	0.42	5.10E+04	4.23E+04	6.39E+04
2	CR-TSC	0.42	6.56E+04	5.45E+04	8.07E+04
3	CR-SB	0.42	4.37E+04	3.47E+04	5.69E+04
4	CR-EG	0.42	5.87E+04	4.67E+04	7.59E+04
5	CR-starch	0.42	5.59E+04	4.56E+04	6.90E+04
6	FSP-MS	0.43	3.68E+04	3.05E+04	4.70E+04
7	AP	0.43	3.78E+04	2.94E+04	5.10E+04
8	AP-UDE1	0.43	6.43E+04	5.53E+04	7.86E+04
9	AP-UDE2	0.43	7.32E+04	6.39E+04	8.56E+04
10	AP-UDE3	0.43	8.43E+04	7.55E+04	9.70E+04
11	AP-MNL	0.43	6.58E+04	5.72E+04	7.92E+04
12	Spark-TUD	0.43	7.52E+04	6.24E+04	9.87E+04
13	RMS-AR-N	0.43	3.58E+04	2.72E+04	4.94E+04

Table A21. Overall projected GWP (tons CO₂-eq.) in 2018 with different combinations considered.

Combination of methods	Median (tons CO ₂ -eq./year)	Lower Bound (tons CO ₂ -eq./year)	Upper Bound (tons CO ₂ -eq./year)	Combination of methods	Median (tons CO ₂ -eq./year)	Lower Bound (tons CO ₂ -eq./year)	Upper Bound (tons CO ₂ -eq./year)
1+6	8.78E+04	7.28E+04	1.11E+05	4+6	9.56E+04	7.72E+04	1.23E+05
1+7	8.88E+04	7.16E+04	1.15E+05	4+7	9.65E+04	7.60E+04	1.27E+05
1+8	1.15E+05	9.75E+04	1.43E+05	4+8	1.23E+05	1.02E+05	1.54E+05
1+9	1.24E+05	1.06E+05	1.49E+05	4+9	1.32E+05	1.11E+05	1.61E+05
1+10	1.35E+05	1.18E+05	1.61E+05	4+10	1.43E+05	1.22E+05	1.73E+05
1+11	1.17E+05	9.95E+04	1.43E+05	4+11	1.24E+05	1.04E+05	1.55E+05
1+12	1.26E+05	1.05E+05	1.63E+05	4+12	1.34E+05	1.09E+05	1.75E+05
1+13	8.68E+04	6.94E+04	1.13E+05	4+13	9.45E+04	7.38E+04	1.25E+05
2+6	1.02E+05	8.50E+04	1.28E+05	5+6	9.27E+04	7.61E+04	1.16E+05
2+7	1.03E+05	8.39E+04	1.32E+05	5+7	9.37E+04	7.50E+04	1.20E+05
2+8	1.30E+05	1.10E+05	1.59E+05	5+8	1.20E+05	1.01E+05	1.48E+05
2+9	1.39E+05	1.18E+05	1.66E+05	5+9	1.29E+05	1.10E+05	1.55E+05
2+10	1.50E+05	1.30E+05	1.78E+05	5+10	1.40E+05	1.21E+05	1.66E+05
2+11	1.31E+05	1.12E+05	1.60E+05	5+11	1.22E+05	1.03E+05	1.48E+05
2+12	1.41E+05	1.17E+05	1.79E+05	5+12	1.31E+05	1.08E+05	1.68E+05
2+13	1.01E+05	8.17E+04	1.30E+05	5+13	9.17E+04	7.28E+04	1.18E+05
3+6	8.05E+04	6.52E+04	1.04E+05	MEAN	1.17E+05		
3+7	8.15E+04	6.41E+04	1.08E+05	STDDEV	2.81E+04		
3+8	1.08E+05	9.00E+04	1.36E+05				
3+9	1.17E+05	9.86E+04	1.43E+05				
3+10	1.28E+05	1.10E+05	1.54E+05				
3+11	1.09E+05	9.19E+04	1.36E+05				
3+12	1.19E+05	9.71E+04	1.56E+05				
3+13	7.94E+04	6.18E+04	1.06E+05				

Table A22. Comprehensive table for AgNPs synthesis methods considered in this study, and their applications in different industries.

Method	Yield	Size Range	Surface Area	Known Applications	Reference
MW	99%	1-10 nm	190 m ² /g	Medical or biological	[1]
CR-TSC	N/A	100 nm	N/A	Catalysis, optics, microelectronics	[17] cited in [4]
				Medical, food storage, textile, baby goods, towel	[18]
CR-SB	N/A	10-14 nm	N/A	N/A	[19] cited in [4]
				Food containers	[20]
				Textile	[21] cited in [5]
CR-EG	45%	8.1-10.4 nm	N/A	Optical sensors	[22] cited in [4]
CR-starch	N/A	6-8 nm	N/A	Industrial	[23] cited in [4]
FSP-MS	95%	1-2 nm	N/A	Textile	[9] cited in [5] and [4]
AP	0.5-1.3 g/min	5-65 nm	23.81 m ² /g	Catalyst, microelectronic elements, photoelectronic devices, lubricants, conductive materials, activation, and sintering materials	[24] cited in [4]
AP-UDE1	N/A	1-100 nm	N/A	Textile	[11]
AP-UDE2	N/A	1-100 nm	N/A	Textile	[11]
AP-UDE3	N/A	1-100 nm	N/A	Textile	[11]
AP-MNL	N/A	20-100 nm	N/A	Textile	[11]
Spark-TUD	N/A	1-10 nm	N/A	Textile	[11]
RMS-AR-N	N/A	50-60 nm	N/A	Mechanical, optical, electronic and magnetic applications	[25] cited in [4]
				Bandages	[4]

Table A23. Characterization results of multiple synthesis routes for 1 kg AgNPs using TRACI 2.1 IA Methodology

Routes	ODP (kg CFC11-eq)	GWP (kg CO₂-eq)	SP (kg O₃-eq)	AP (kg SO₂-eq)	EP (kg N-q)	HHCP (CTUh)	HHNCP (CTUh)	RP (kg PM_{2.5}-eq)	ETP (CTUe)	FFP (MJ surplus energy)
MW	7.74E-05	5.98E+02	6.05E+01	1.05E+01	6.13E+00	1.10E-04	4.06E-03	9.64E-01	3.55E+04	4.07E+02
CR-TSC	6.53E-05	7.65E+02	6.71E+01	1.06E+01	6.54E+00	1.15E-04	4.08E-03	1.02E+00	3.59E+04	7.34E+02
CR-SB	3.64E-05	5.13E+02	5.81E+01	9.51E+00	6.18E+00	1.11E-04	4.05E-03	8.82E-01	3.55E+04	3.61E+02
CR-EG	5.60E-05	6.89E+02	6.84E+01	1.06E+01	7.05E+00	1.23E-04	4.11E-03	1.25E+00	3.75E+04	8.28E+02
CR-starch	5.63E-05	6.54E+02	6.59E+01	1.06E+01	7.25E+00	1.21E-04	4.41E-03	1.05E+00	3.91E+04	5.96E+02
FSP-MS	1.00E-04	1.65E+03	2.13E+02	3.54E+01	2.38E+01	4.27E-04	1.56E-02	3.36E+00	1.37E+05	1.19E+03
AP	2.36E-05	4.37E+02	5.45E+01	9.32E+00	6.14E+00	1.10E-04	4.03E-03	8.93E-01	3.54E+04	2.92E+02
AP-UDE1	1.13E-04	7.38E+02	6.26E+01	1.14E+01	6.15E+00	1.10E-04	4.04E-03	1.06E+00	3.53E+04	5.03E+02
AP-UDE2	1.39E-04	8.35E+02	6.55E+01	1.21E+01	6.14E+00	1.10E-04	4.04E-03	1.10E+00	3.53E+04	5.71E+02
AP-UDE3	1.73E-04	9.62E+02	6.94E+01	1.30E+01	6.15E+00	1.10E-04	4.05E-03	1.16E+00	3.53E+04	6.59E+02
AP-MNL	1.19E-04	7.52E+02	6.28E+01	1.15E+01	6.10E+00	1.10E-04	4.04E-03	1.04E+00	3.53E+04	5.14E+02
Spark-TUD	1.14E-04	8.67E+02	6.95E+01	1.19E+01	6.92E+00	1.18E-04	4.07E-03	1.35E+00	3.64E+04	5.91E+02
RMS-Ar-N	2.25E-05	4.09E+02	5.29E+01	9.15E+00	6.06E+00	1.09E-04	4.03E-03	8.57E-01	3.52E+04	2.74E+02

Table A24. Characterization results of multiple synthesis routes for 1 kg AgNPs using Cumulative Energy Demand (CED).

Routes	Cumulative Energy Demand (MJ/kg AgNP)		
	Renewable (biomass, wind, solar, geothermal, water)	Non-renewable (fossil, nuclear and biomass)	TOTAL
MW	6.00E+02	7.53E+03	8.13E+03
CR-TSC	4.08E+02	8.39E+03	8.79E+03
CR-SB	3.65E+02	5.13E+03	5.50E+03
CR-EG	6.93E+02	9.46E+03	1.02E+04
CR-starch	1.88E+03	6.95E+03	8.83E+03
FSP-MS	1.54E+03	1.61E+04	1.76E+04
AP	3.26E+02	4.32E+03	4.65E+03
AP-UDE1	8.07E+02	1.01E+04	1.10E+04
AP-UDE2	9.49E+02	1.20E+04	1.30E+04
AP-UDE3	1.13E+03	1.44E+04	1.55E+04
AP-MNL	8.28E+02	1.05E+04	1.13E+04
Spark-TUD	1.03E+03	1.19E+04	1.29E+04
RMS-AR-N	3.00E+02	3.93E+03	4.23E+03

Table A25. Characterization results of multiple synthesis routes for 1 kg AgNPs using CML (baseline) IA Methodology.

Routes	ADP (kg Sb-eq.)	ADP(FF) (MJ)	GWP 100a (kg CO ₂ -eq)	ODP (kg CFC11-eq)	HTP (kg 1,4-DB-eq)	FWAEP (kg 1,4-DB-eq)	MAEP (kg 1,4-DB-eq)	TEP (kg 1,4-DB-eq)	POxP (kg C ₂ H ₄ -eq)	AP (kg SO ₂ -eq)	EP (kg PO ₄ -eq)
MW	1.28E+00	5.54E+03	5.98E+02	6.79E-05	1.18E+03	6.83E+02	2.01E+06	2.21E+00	4.47E-01	1.15E+01	2.94E+00
CR-TSC	1.28E+00	7.80E+03	7.65E+02	5.15E-05	1.22E+03	7.10E+02	2.07E+06	2.33E+00	4.51E-01	1.15E+01	3.13E+00
CR-SB	1.28E+00	4.48E+03	5.13E+02	3.02E-05	1.18E+03	6.83E+02	1.95E+06	2.13E+00	3.97E-01	1.04E+01	2.95E+00
CR-EG	1.28E+00	8.63E+03	6.89E+02	4.49E-05	1.29E+03	7.72E+02	2.25E+06	2.57E+00	4.74E-01	1.15E+01	3.35E+00
CR-starch	1.28E+00	6.53E+03	6.54E+02	4.48E-05	1.25E+03	7.36E+02	2.10E+06	3.18E+00	4.32E-01	1.14E+01	3.49E+00
FSP-MS	4.95E+00	1.47E+04	1.65E+03	7.90E-05	4.54E+03	2.66E+03	7.51E+06	1.15E+01	1.48E+00	3.87E+01	1.13E+01
AP	1.28E+00	4.02E+03	4.37E+02	1.84E-05	1.18E+03	6.85E+02	1.98E+06	2.10E+00	4.01E-01	1.02E+01	2.90E+00
AP-UDE1	1.28E+00	7.01E+03	7.38E+02	1.00E-04	1.19E+03	6.83E+02	2.07E+06	2.31E+00	4.95E-01	1.24E+01	1.65E+01
AP-UDE2	1.28E+00	8.01E+03	8.35E+02	1.25E-04	1.19E+03	6.82E+02	2.10E+06	2.38E+00	5.30E-01	1.32E+01	1.14E+01
AP-UDE3	1.28E+00	9.31E+03	9.62E+02	1.56E-04	1.20E+03	6.82E+02	2.15E+06	2.46E+00	5.76E-01	1.42E+01	9.77E+00
AP-MNL	1.28E+00	7.15E+03	7.52E+02	1.06E-04	1.19E+03	6.79E+02	2.06E+06	2.31E+00	5.02E-01	1.26E+01	4.08E+00
Spark-TUD	1.28E+00	8.51E+03	8.67E+02	1.00E-04	1.24E+03	7.44E+02	2.28E+06	2.65E+00	5.15E-01	1.30E+01	3.32E+00
RMS-AR-N	1.28E+00	3.69E+03	4.09E+02	1.75E-05	1.17E+03	6.79E+02	1.95E+06	2.06E+00	3.89E-01	1.00E+01	2.86E+00

Table A26. Characterization results of multiple synthesis routes for 1 kg AgNPs using IMPACT 2002+ IA Methodology.

Routes	CP (kg C ₂ H ₃ Cl-eq)	NCP (kg C ₂ H ₃ Cl-eq)	RAiP (kg PM _{2.5} -eq)	IR (Bq C-14-eq)	ODP (kg CFC11-eq)	RaoP (kg C ₂ H ₄ -eq)	AEP (kg TEG water)	TEP (kg TEG soil)	tAP (kg SO ₂ -eq.)	LO (m ² org. arable)	AP (kg SO ₂ -eq)	EP (kg PO ₄ P-lim)	GWP (kg CO ₂ -eq)	NRE (MJ primary)	ME (MJ surplus)
MW	9.47E+01	8.55E+02	1.38E+00	7.69E+03	7.10E-05	2.09E-01	3.57E+05	9.80E+04	2.58E+01	9.09E+00	1.05E+01	8.72E-01	5.73E+02	7.53E+03	1.03E+03
CR-TSC	1.01E+02	8.57E+02	1.45E+00	3.87E+03	5.20E-05	2.50E-01	3.73E+05	1.03E+05	2.67E+01	9.09E+00	1.06E+01	9.11E-01	7.34E+02	8.39E+03	1.04E+03
CR-SB	9.49E+01	8.55E+02	1.26E+00	3.22E+03	3.09E-05	2.05E-01	3.57E+05	9.79E+04	2.41E+01	7.33E+00	9.52E+00	8.94E-01	4.92E+02	5.13E+03	1.04E+03
CR-EG	1.06E+02	8.58E+02	1.67E+00	5.60E+03	4.49E-05	3.30E-01	3.73E+05	1.02E+05	2.68E+01	1.17E+01	1.06E+01	9.28E-01	6.54E+02	9.46E+03	1.05E+03
CR-starch	1.00E+02	8.78E+02	1.47E+00	3.46E+03	4.48E-05	2.49E-01	3.97E+05	1.48E+05	2.88E+01	1.29E+02	1.06E+01	9.28E-01	6.20E+02	6.95E+03	1.05E+03
FSP-MS	3.67E+02	3.30E+03	4.73E+00	8.96E+03	7.92E-05	7.98E-01	1.38E+06	3.78E+05	8.82E+01	6.32E+01	3.54E+01	3.37E+00	1.58E+03	1.60E+04	3.99E+03
AP	9.44E+01	8.51E+02	1.25E+00	2.20E+03	1.84E-05	2.14E-01	3.58E+05	9.74E+04	2.28E+01	7.38E+00	9.33E+00	8.69E-01	4.18E+02	4.32E+03	1.03E+03
AP-UDE1	9.45E+01	8.51E+02	1.50E+00	1.16E+04	1.05E-4	2.17E-01	3.56E+05	9.77E+04	2.73E+01	7.39E+00	1.14E+01	8.71E-01	7.08E+02	1.01E+04	1.03E+03
AP-UDE2	9.44E+01	8.52E+02	1.57E+00	1.44E+04	1.31E-04	2.23E-01	3.55E+05	9.77E+04	2.88E+01	7.33E+00	1.21E+01	8.71E-01	8.02E+02	1.20E+04	1.03E+03
AP-UDE3	9.44E+01	8.52E+02	1.68E+00	1.80E+04	1.64E-04	2.31E-01	3.55E+05	9.78E+04	3.08E+01	7.31E+00	1.30E+01	8.72E-01	9.24E+02	1.44E+04	1.03E+03
AP-MNL	9.43E+01	8.51E+02	1.49E+00	1.22E+04	1.11E-04	2.18E-01	3.55E+05	9.76E+04	2.75E+01	7.25E+00	1.15E+01	8.69E-1	7.22E+02	1.05E+04	1.03E+03
Spark-TUD	9.74E+01	8.53E+02	1.82E+00	1.41E+04	1.05E-04	2.31E-01	3.62E+05	9.92E+04	2.91E+01	9.66E+00	1.19E+01	9.07E-01	8.31E+02	1.19E+04	1.03E+03
RMS-AR-N	9.41E+01	8.51E+02	1.20E+00	1.84E+03	1.75E-05	2.06E-01	3.56E+05	9.73E+04	2.23E+01	7.23E+00	9.15E+00	8.66E-01	3.91E+02	3.93E+03	1.03E+03

Table A27. Characterization results of multiple synthesis routes for 1 kg AgNPs using ReCiPe Midpoint IA Methodology.

Routes	GWP (kg CO ₂ -eq)	ODP (kg CFC11-eq)	tAP (kg SO ₂ -eq)	FWEP (kg P-eq)	MEP (kg N-eq)	HTP (kg 1,4-DB-eq)	POxP (kg NMVOC)	HHAP (kg PM ₁₀ -eq)	TEP (kg 1,4-DB-eq)	FWAEP (kg 1,4-DB-eq)	MAEP (kg 1,4-DB-eq)	IR (kBq U235 eq)	ALO (m ² a)	ULO (m ² a)	NLT (m ²)	WDP (m ³)	MD (kg Fe eq)	FFP (kg oil eq)
MW	5.98E+02	6.82E-05	1.02E+01	8.15E-01	2.63E-01	3.48E+03	3.60E+00	2.86E+00	4.92E-02	2.83E+01	2.61E+01	7.87E+01	2.90E+01	5.49E+00	5.03E-02	1.81E+01	4.53E+02	1.24E+02
CR-TSC	7.65E+02	5.18E-05	1.02E+01	8.60E-01	2.85E-01	3.52E+03	3.87E+00	2.96E+00	8.57E-02	2.93E+01	2.72E+01	3.87E+01	3.01E+01	6.59E+00	1.05E-01	2.70E+01	4.54E+02	1.74E+02
CR-SB	5.13E+02	3.04E-05	9.24E+00	8.16E-01	2.63E-01	3.48E+03	3.38E+00	2.62E+00	4.74E-02	2.85E+01	2.62E+01	3.24E+01	2.74E+01	5.53E+00	5.14E-02	3.12E+01	4.53E+02	1.00E+02
CR-EG	6.89E+02	4.55E-05	1.02E+01	9.36E-01	2.90E-01	3.58E+03	4.00E+00	3.22E+00	6.96E-02	3.21E+01	2.97E+01	5.50E+01	5.20E+01	7.40E+00	9.79E-02	7.38E+01	4.65E+02	1.92E+02
CR-starch	6.54E+02	4.61E-05	1.04E+01	8.79E-01	8.64E-01	3.54E+03	3.75E+00	2.99E+00	2.20E-01	3.08E+01	2.87E+01	3.41E+01	1.47E+02	7.10E+00	9.61E-02	2.90E+01	4.64E+02	1.46E+02
FSP-MS	1.65E+03	8.01E-05	3.45E+01	3.17E+00	9.89E-01	1.34E+04	1.23E+01	9.79E+00	6.30E-01	1.10E+02	1.01E+02	8.83E+01	1.28E+02	2.21E+01	5.44E-01	7.98E+01	1.75E+03	3.29E+02
AP	4.37E+02	1.87E-05	9.08E+00	8.20E-01	2.38E-01	3.47E+03	3.17E+00	2.58E+00	4.30E-02	2.83E+01	2.62E+01	2.16E+01	2.78E+01	5.55E+00	5.16E-02	2.31E+01	4.51E+02	9.02E+01
AP-UDE1	7.38E+02	1.00E-04	1.10E+01	8.18E-01	2.61E-01	3.47E+03	3.83E+00	3.11E+00	5.05E-02	2.84E+01	2.62E+01	1.19E+02	2.77E+01	5.55E+00	5.16E-02	2.22E+01	4.51E+02	1.57E+02
AP-UDE2	8.35E+02	1.25E-04	1.17E+01	8.15E-01	2.68E-01	3.48E+03	4.06E+00	3.27E+00	5.25E-02	2.83E+01	2.61E+01	1.49E+02	2.75E+01	5.51E+00	5.10E-02	2.07E+01	4.51E+02	1.80E+02
AP-UDE3	9.62E+02	1.56E-04	1.25E+01	8.15E-01	2.78E-01	3.48E+03	4.36E+00	3.49E+00	5.52E-02	2.83E+01	2.61E+01	1.86E+02	2.74E+01	5.50E+00	5.10E-02	2.05E+01	4.51E+02	2.09E+02
AP-MNL	7.52E+02	1.06E-04	1.11E+01	8.11E-01	2.60E-01	3.47E+03	3.87E+00	3.11E+00	5.03E-02	2.82E+01	2.60E+01	1.25E+02	2.71E+01	5.46E+00	5.03E-02	1.80E+01	4.50E+02	1.60E+02
Spark-TUD	8.67E+02	1.01E-04	1.15E+01	9.20E-01	2.97E-01	3.54E+03	4.15E+00	3.54E+00	6.03E-02	3.07E+01	2.83E+01	1.43E+02	3.82E+01	6.55E+00	7.01E-02	8.44E+01	4.53E+02	1.91E+02
RMS-AR-N	4.09E+02	1.78E-05	8.92E+00	8.10E-01	2.33E-01	3.46E+03	3.09E+00	2.50E+00	4.23E-02	2.81E+01	2.59E+01	1.81E+01	2.71E+01	5.45E+00	4.98E-02	1.68E+01	4.50E+02	8.26E+01

Table A28. Overall comparison of AgNPs synthesis methods using TRACI 2.1 Impact Assessment Methodology and Cumulative Energy Demand (CED) per functional unit.

Potential Environmental Impact Categories	AgNP Synthesis Method		
	Minimum	Median	Maximum
ODP (kg CFC11-eq.)	RMS-Ar-N	MW	AP-UDE
GWP (kg CO₂-eq.)	RMS-Ar-N	AP-UDE1	FSP-MS
SAP (kg O₃-eq.)	RMS-Ar-N	AP-UDE2	FSP-MS
AP (kg SO₂-eq.)	RMS-Ar-N	CR-TSC	FSP-MS
EP (kg N-eq.)	RMS-Ar-N	AP-UDE	FSP-MS
HHCP (CTUh)	RMS-Ar-N	AP	FSP-MS
HHNCP (CTUh)	RMS-Ar-N	AP-UDE3	FSP-MS
RP (kg PM_{2.5}-eq.)	RMS-Ar-N	CR-starch	FSP-MS
ETP (CTUe)	RMS-Ar-N	CR-SB	FSP-MS
FFP (MJ surplus energy)	RMS-Ar-N	AP-UDE2	FSP-MS
CED (MJ)	RMS-Ar-N	CR-EG	FSP-MS

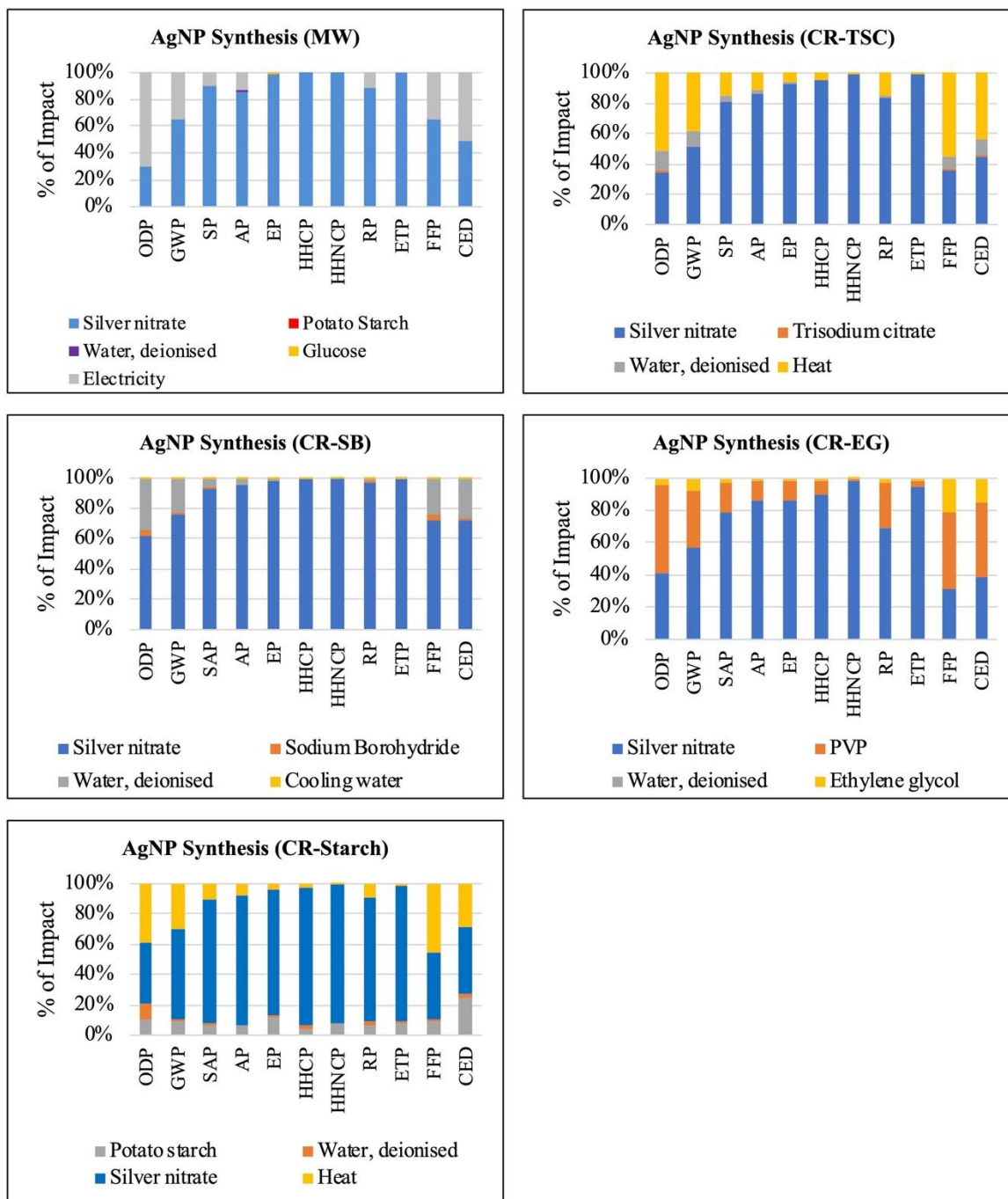


Figure A1. Midpoint LCA results for 1kg of AgNPs production with wet chemistry methods.

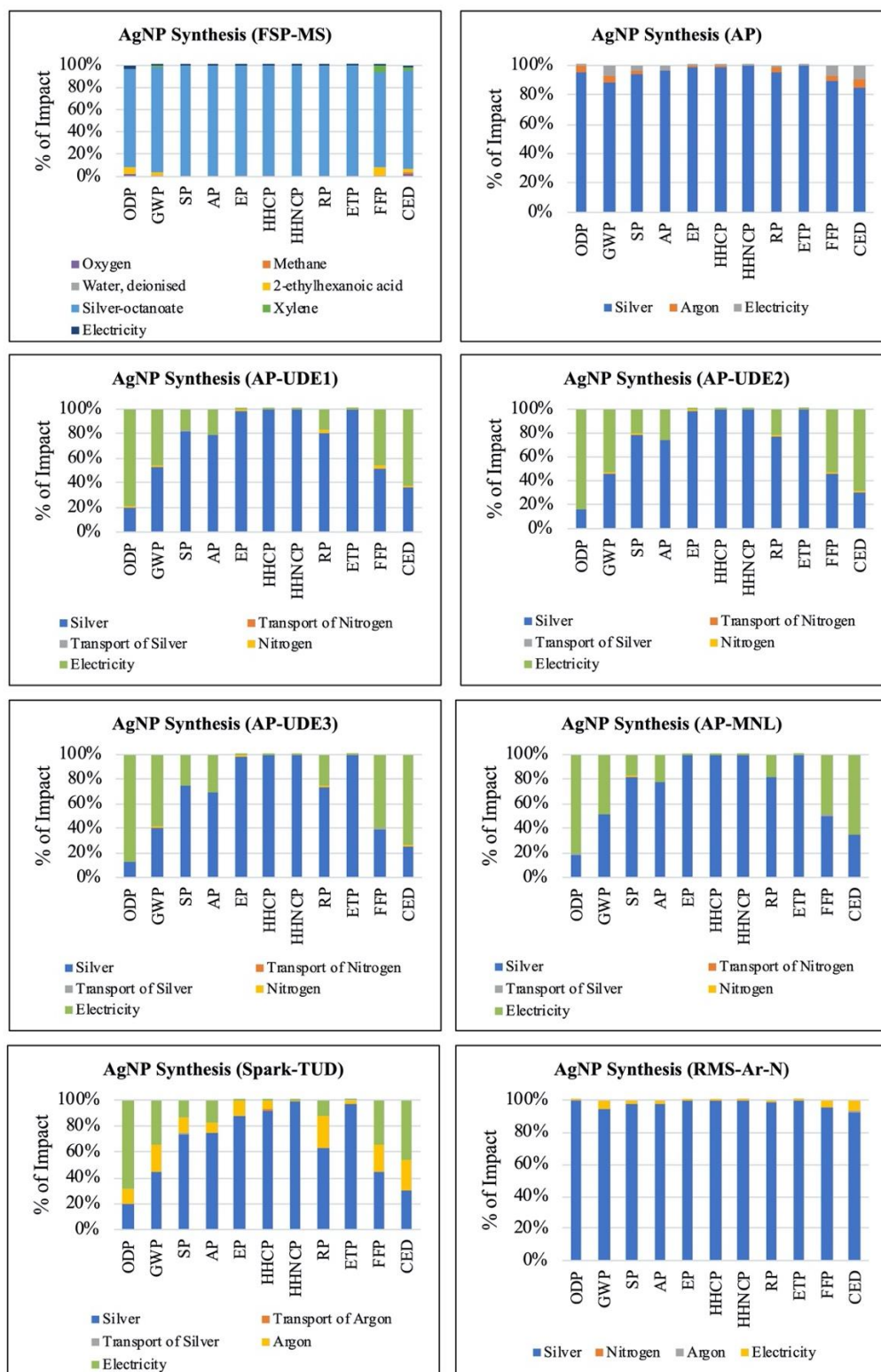


Figure A2. Midpoint LCA results for 1kg of AgNPs production with physical chemistry methods.

Table A29. The projected GWP (tons CO₂-eq.) from 2018 to 2025 using different combination of synthesis procedures and scaling up factors (SF) of 2, 4 and 6.

	Laboratory Scale		SF=2		SF=4		SF=6		
	Year	Mean	StdDev	Mean	StdDev	Mean	StdDev	Mean	StdDev
Skeptical Production	2018	1.20E+05	2.88E+04	6.00E+04	1.44E+04	3.00E+04	7.19E+03	2.00E+04	4.80E+03
	2019	1.31E+05	3.15E+04	6.57E+04	1.58E+04	3.29E+04	7.88E+03	2.19E+04	5.25E+03
	2020	1.46E+05	3.49E+04	7.29E+04	1.75E+04	3.64E+04	8.73E+03	2.43E+04	5.82E+03
	2021	1.60E+05	3.84E+04	8.00E+04	1.92E+04	4.00E+04	9.59E+03	2.67E+04	6.39E+03
	2022	1.77E+05	4.25E+04	8.86E+04	2.12E+04	4.43E+04	1.06E+04	2.95E+04	7.08E+03
	2023	2.00E+05	4.80E+04	1.00E+05	2.40E+04	5.00E+04	1.20E+04	3.34E+04	7.99E+03
	2024	2.17E+05	5.21E+04	1.09E+05	2.60E+04	5.43E+04	1.30E+04	3.62E+04	8.68E+03
	2025	2.34E+05	5.62E+04	1.17E+05	2.81E+04	5.86E+04	1.40E+04	3.91E+04	9.36E+03
Optimistic Production	Laboratory Scale		SF=2		SF=4		SF=6		
	Year	Mean	StdDev	Mean	StdDev	Mean	StdDev	Mean	StdDev
	2018	3.03E+05	7.26E+04	1.52E+05	3.63E+04	7.58E+04	1.82E+04	5.05E+04	1.21E+04
	2019	3.20E+05	7.67E+04	1.60E+05	3.84E+04	8.00E+04	1.92E+04	5.34E+04	1.28E+04
	2020	3.43E+05	8.22E+04	1.72E+05	4.11E+04	8.58E+04	2.06E+04	5.72E+04	1.37E+04
	2021	3.63E+05	8.70E+04	1.82E+05	4.35E+04	9.08E+04	2.18E+04	6.05E+04	1.45E+04
	2022	3.83E+05	9.18E+04	1.92E+05	4.59E+04	9.58E+04	2.30E+04	6.38E+04	1.53E+04
	2023	4.06E+05	9.73E+04	2.03E+05	4.86E+04	1.01E+05	2.43E+04	6.77E+04	1.62E+04
	2024	4.31E+05	1.03E+05	2.15E+05	5.16E+04	1.08E+05	2.58E+04	7.18E+04	1.72E+04
2025	4.56E+05	1.09E+05	2.28E+05	5.47E+04	1.14E+05	2.73E+04	7.60E+04	1.82E+04	

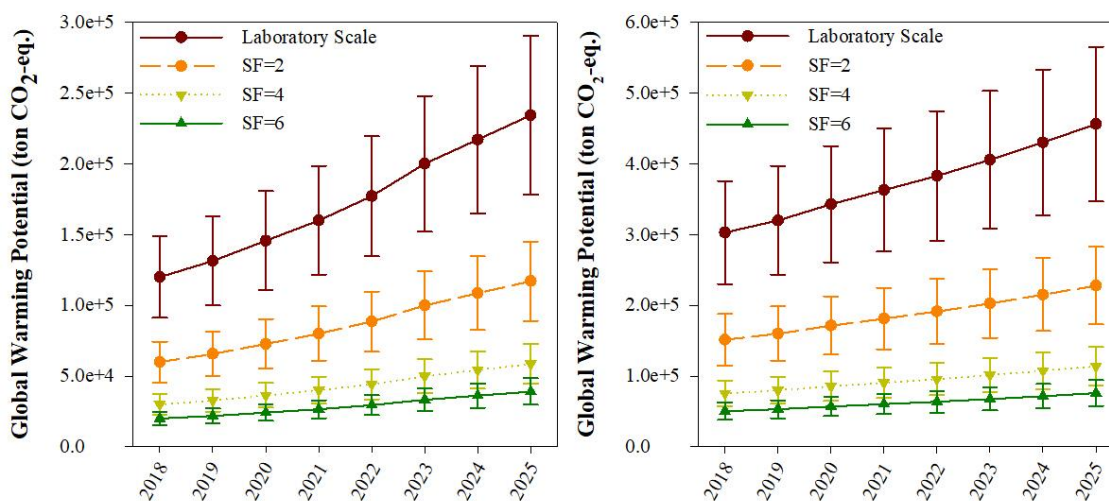


Figure A3. Global annual environmental impacts using different scale-up factors (2, 4 and 6) as well as laboratory scale results for GWP (tons CO₂-eq.) [skeptical left, optimistic right].

Table A30. The projected ODP (tons CFC11-eq.) from 2018 to 2025 using different combination of synthesis procedures and scaling up factors (SF) of 2, 4 and 6.

	Laboratory Scale		SF=2		SF=4		SF=6		
	Year	Mean	StdDev	Mean	StdDev	Mean	StdDev	Mean	StdDev
Skeptical Production	2018	1.41E-02	6.17E-03	7.07E-03	3.09E-03	3.54E-03	1.54E-03	2.36E-03	1.03E-03
	2019	1.55E-02	6.76E-03	7.75E-03	3.38E-03	3.87E-03	1.69E-03	2.58E-03	1.13E-03
	2020	1.72E-02	7.49E-03	8.59E-03	3.75E-03	4.30E-03	1.87E-03	2.86E-03	1.25E-03
	2021	1.89E-02	8.23E-03	9.43E-03	4.11E-03	4.72E-03	2.06E-03	3.14E-03	1.37E-03
	2022	2.09E-02	9.11E-03	1.04E-02	4.56E-03	5.22E-03	2.28E-03	3.48E-03	1.52E-03
	2023	2.36E-02	1.03E-02	1.18E-02	5.14E-03	5.90E-03	2.57E-03	3.93E-03	1.71E-03
	2024	2.56E-02	1.12E-02	1.28E-02	5.58E-03	6.40E-03	2.79E-03	4.27E-03	1.86E-03
	2025	2.76E-02	1.20E-02	1.38E-02	6.02E-03	6.91E-03	3.01E-03	4.60E-03	2.01E-03
	Optimistic Production	2018	3.57E-02	1.56E-02	1.79E-02	7.79E-03	8.93E-03	3.89E-03	5.95E-03
2019		3.77E-02	1.65E-02	1.89E-02	8.23E-03	9.43E-03	4.11E-03	6.29E-03	2.74E-03
2020		4.04E-02	1.76E-02	2.02E-02	8.82E-03	1.01E-02	4.41E-03	6.74E-03	2.94E-03
2021		4.28E-02	1.87E-02	2.14E-02	9.33E-03	1.07E-02	4.67E-03	7.13E-03	3.11E-03
2022		4.51E-02	1.97E-02	2.26E-02	9.84E-03	1.13E-02	4.92E-03	7.52E-03	3.28E-03
2023		4.78E-02	2.09E-02	2.39E-02	1.04E-02	1.20E-02	5.22E-03	7.97E-03	3.48E-03
2024		5.07E-02	2.21E-02	2.54E-02	1.11E-02	1.27E-02	5.53E-03	8.46E-03	3.69E-03
2025		5.38E-02	2.35E-02	2.69E-02	1.17E-02	1.34E-02	5.86E-03	8.96E-03	3.91E-03

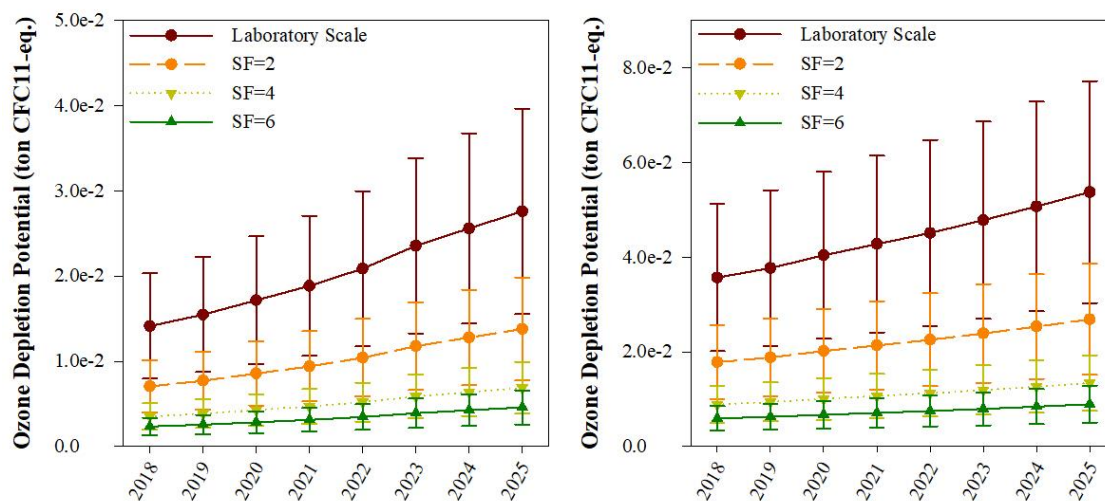


Figure A4. Global annual environmental impacts using different scale-up factors (2, 4 and 6) as well as laboratory scale results for ODP (tons CFC11-eq.) [skeptical left, optimistic right].

Table A31. The projected SP (tons O₃-eq.) from 2018 to 2025 using different combination of synthesis procedures and scaling up factors (SF) of 2, 4 and 6.

	Laboratory Scale		SF=2		SF=4		SF=6		
	Year	Mean	StdDev	Mean	StdDev	Mean	StdDev	Mean	StdDev
Skeptical Production	2018	1.20E+04	5.05E+03	6.00E+03	2.53E+03	3.00E+03	1.26E+03	2.00E+03	8.42E+02
	2019	1.32E+04	5.54E+03	6.58E+03	2.77E+03	3.29E+03	1.38E+03	2.19E+03	9.23E+02
	2020	1.46E+04	6.14E+03	7.29E+03	3.07E+03	3.65E+03	1.53E+03	2.43E+03	1.02E+03
	2021	1.60E+04	6.74E+03	8.01E+03	3.37E+03	4.00E+03	1.68E+03	2.67E+03	1.12E+03
	2022	1.77E+04	7.46E+03	8.86E+03	3.73E+03	4.43E+03	1.87E+03	2.95E+03	1.24E+03
	2023	2.00E+04	8.42E+03	1.00E+04	4.21E+03	5.00E+03	2.11E+03	3.34E+03	1.40E+03
	2024	2.17E+04	9.15E+03	1.09E+04	4.57E+03	5.43E+03	2.29E+03	3.62E+03	1.52E+03
	2025	2.34E+04	9.87E+03	1.17E+04	4.93E+03	5.86E+03	2.47E+03	3.91E+03	1.64E+03
	Optimistic Production	2018	3.03E+04	1.28E+04	1.52E+04	6.38E+03	7.58E+03	3.19E+03	5.05E+03
2019		3.20E+04	1.35E+04	1.60E+04	6.74E+03	8.01E+03	3.37E+03	5.34E+03	2.25E+03
2020		3.43E+04	1.44E+04	1.72E+04	7.22E+03	8.58E+03	3.61E+03	5.72E+03	2.41E+03
2021		3.63E+04	1.53E+04	1.82E+04	7.64E+03	9.08E+03	3.82E+03	6.05E+03	2.55E+03
2022		3.83E+04	1.61E+04	1.92E+04	8.06E+03	9.58E+03	4.03E+03	6.39E+03	2.69E+03
2023		4.06E+04	1.71E+04	2.03E+04	8.54E+03	1.01E+04	4.27E+03	6.77E+03	2.85E+03
2024		4.31E+04	1.81E+04	2.15E+04	9.06E+03	1.08E+04	4.53E+03	7.18E+03	3.02E+03
2025		4.56E+04	1.92E+04	2.28E+04	9.60E+03	1.14E+04	4.80E+03	7.61E+03	3.20E+03

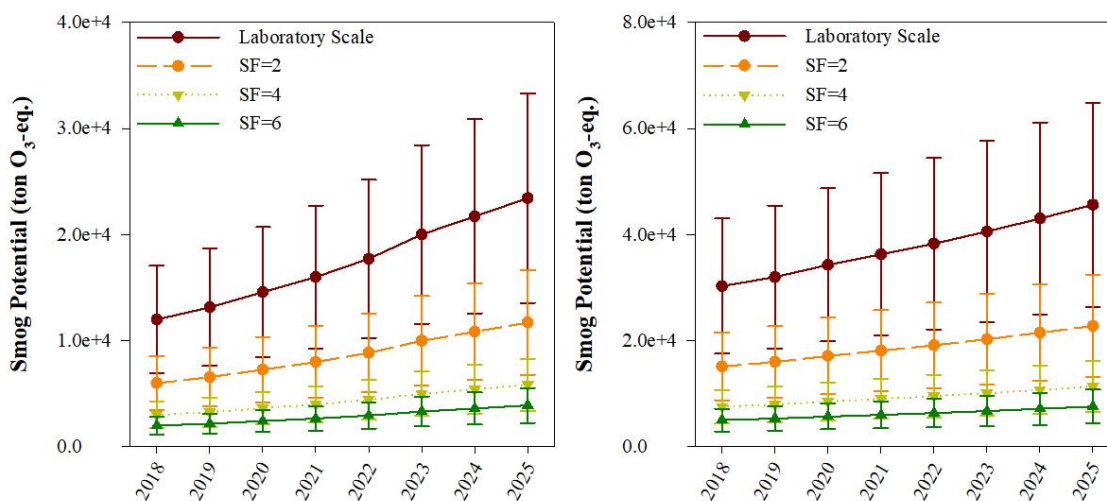


Figure A5. Global annual environmental impacts using different scale-up factors (2, 4 and 6) as well as laboratory scale results for SP (tons O₃-eq.) [skeptical left, optimistic right].

Table A32. The projected AP (tons SO₂-eq.) from 2018 to 2025 using different combination of synthesis procedures and scaling up factors (SF) of 2, 4 and 6.

	Laboratory Scale		SF=2		SF=4		SF=6		
	Year	Mean	StdDev	Mean	StdDev	Mean	StdDev	Mean	StdDev
Skeptical Production	2018	1.93E+03	4.91E+02	9.64E+02	2.45E+02	4.82E+02	1.23E+02	3.21E+02	8.18E+01
	2019	2.11E+03	5.37E+02	1.06E+03	2.69E+02	5.28E+02	1.34E+02	3.52E+02	8.96E+01
	2020	2.34E+03	5.96E+02	1.17E+03	2.98E+02	5.85E+02	1.49E+02	3.90E+02	9.93E+01
	2021	2.57E+03	6.54E+02	1.28E+03	3.27E+02	6.42E+02	1.64E+02	4.28E+02	1.09E+02
	2022	2.84E+03	7.24E+02	1.42E+03	3.62E+02	7.11E+02	1.81E+02	4.74E+02	1.21E+02
	2023	3.21E+03	8.18E+02	1.61E+03	4.09E+02	8.03E+02	2.04E+02	5.35E+02	1.36E+02
	2024	3.49E+03	8.88E+02	1.74E+03	4.44E+02	8.72E+02	2.22E+02	5.81E+02	1.48E+02
	2025	3.76E+03	9.58E+02	1.88E+03	4.79E+02	9.41E+02	2.39E+02	6.27E+02	1.60E+02
	Optimistic Production	Laboratory Scale		SF=2		SF=4		SF=6	
Year		Mean	StdDev	Mean	StdDev	Mean	StdDev	Mean	StdDev
2018		4.86E+03	1.24E+03	2.43E+03	6.19E+02	1.22E+03	3.10E+02	8.11E+02	2.06E+02
2019		5.14E+03	1.31E+03	2.57E+03	6.54E+02	1.28E+03	3.27E+02	8.56E+02	2.18E+02
2020		5.51E+03	1.40E+03	2.75E+03	7.01E+02	1.38E+03	3.50E+02	9.18E+02	2.34E+02
2021		5.83E+03	1.48E+03	2.91E+03	7.42E+02	1.46E+03	3.71E+02	9.71E+02	2.47E+02
2022		6.15E+03	1.57E+03	3.07E+03	7.83E+02	1.54E+03	3.91E+02	1.02E+03	2.61E+02
2023		6.52E+03	1.66E+03	3.26E+03	8.29E+02	1.63E+03	4.15E+02	1.09E+03	2.76E+02
2024		6.91E+03	1.76E+03	3.45E+03	8.80E+02	1.73E+03	4.40E+02	1.15E+03	2.93E+02
2025	7.32E+03	1.86E+03	3.66E+03	9.32E+02	1.83E+03	4.66E+02	1.22E+03	3.11E+02	

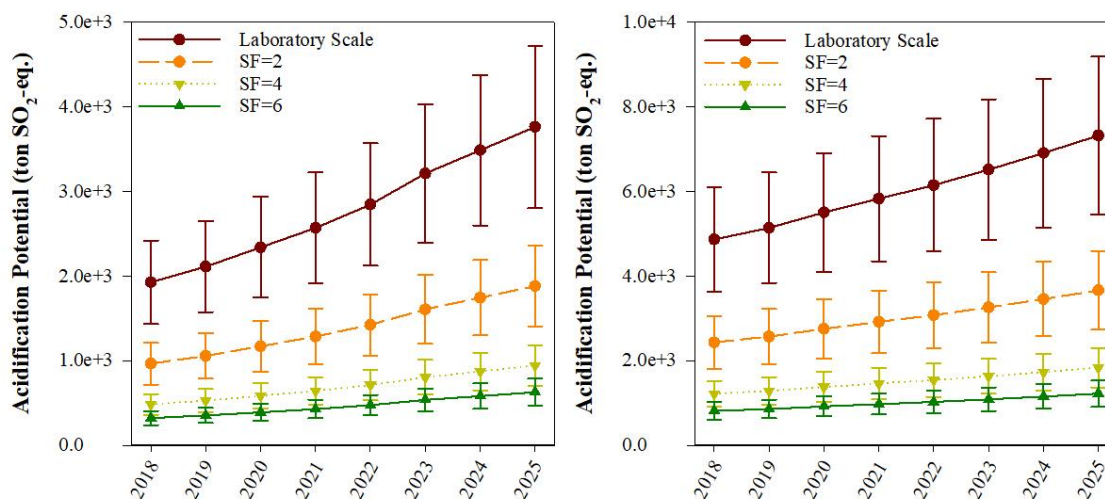


Figure A6. Global annual environmental impacts using different scale-up factors (2, 4 and 6) as well as laboratory scale results for AP (tons SO₂-eq.) [skeptical left, optimistic right].

Table A33. The projected EP (tons N-eq.) from 2018 to 2025 using different combination of synthesis procedures and scaling up factors (SF) of 2, 4 and 6.

		Laboratory Scale		SF=2		SF=4		SF=6	
	Year	Mean	StdDev	Mean	StdDev	Mean	StdDev	Mean	StdDev
Skeptical Production	2018	1.93E+03	4.91E+02	9.64E+02	2.45E+02	4.82E+02	1.23E+02	3.21E+02	8.18E+01
	2019	2.11E+03	5.37E+02	1.06E+03	2.69E+02	5.28E+02	1.34E+02	3.52E+02	8.96E+01
	2020	2.34E+03	5.96E+02	1.17E+03	2.98E+02	5.85E+02	1.49E+02	3.90E+02	9.93E+01
	2021	2.57E+03	6.54E+02	1.28E+03	3.27E+02	6.42E+02	1.64E+02	4.28E+02	1.09E+02
	2022	2.84E+03	7.24E+02	1.42E+03	3.62E+02	7.11E+02	1.81E+02	4.74E+02	1.21E+02
	2023	3.21E+03	8.18E+02	1.61E+03	4.09E+02	8.03E+02	2.04E+02	5.35E+02	1.36E+02
	2024	3.49E+03	8.88E+02	1.74E+03	4.44E+02	8.72E+02	2.22E+02	5.81E+02	1.48E+02
	2025	3.76E+03	9.58E+02	1.88E+03	4.79E+02	9.41E+02	2.39E+02	6.27E+02	1.60E+02
	Optimistic Production	2018	4.86E+03	1.24E+03	2.43E+03	6.19E+02	1.22E+03	3.10E+02	8.11E+02
2019		5.14E+03	1.31E+03	2.57E+03	6.54E+02	1.28E+03	3.27E+02	8.56E+02	2.18E+02
2020		5.51E+03	1.40E+03	2.75E+03	7.01E+02	1.38E+03	3.50E+02	9.18E+02	2.34E+02
2021		5.83E+03	1.48E+03	2.92E+03	7.40E+02	1.46E+03	3.70E+02	9.72E+02	2.47E+02
2022		6.15E+03	1.57E+03	3.07E+03	7.83E+02	1.54E+03	3.91E+02	1.02E+03	2.61E+02
2023		6.52E+03	1.66E+03	3.26E+03	8.29E+02	1.63E+03	4.15E+02	1.09E+03	2.76E+02
2024		6.91E+03	1.76E+03	3.45E+03	8.80E+02	1.73E+03	4.40E+02	1.15E+03	2.93E+02
2025		7.32E+03	1.86E+03	3.66E+03	9.32E+02	1.83E+03	4.66E+02	1.22E+03	3.11E+02

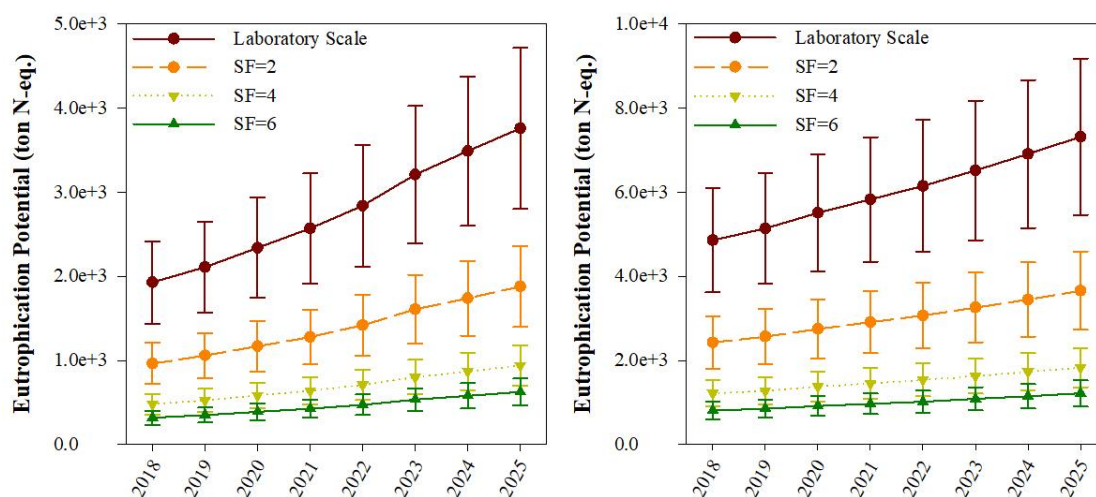


Figure A7. Global annual environmental impacts using different scale-up factors (2, 4 and 6) as well as laboratory scale results for EP (tons N-eq.) [skeptical left, optimistic right].

Table A34. The projected HHCP (CTUh) from 2018 to 2025 using different combination of synthesis procedures and scaling up factors (SF) of 2, 4 and 6.

	Laboratory Scale		SF=2		SF=4		SF=6		
	Year	Mean	StdDev	Mean	StdDev	Mean	StdDev	Mean	StdDev
Skeptical Production	2018	3.02E+01	2.86E+01	1.51E+01	1.43E+01	7.54E+00	7.16E+00	5.03E+00	4.77E+00
	2019	3.30E+01	3.14E+01	1.65E+01	1.57E+01	8.26E+00	7.84E+00	5.51E+00	5.23E+00
	2020	3.66E+01	3.48E+01	1.83E+01	1.74E+01	9.16E+00	8.70E+00	6.11E+00	5.80E+00
	2021	4.02E+01	3.82E+01	2.01E+01	1.91E+01	1.01E+01	9.55E+00	6.70E+00	6.37E+00
	2022	4.45E+01	4.23E+01	2.23E+01	2.11E+01	1.11E+01	1.06E+01	7.42E+00	7.05E+00
	2023	5.03E+01	4.77E+01	2.51E+01	2.39E+01	1.26E+01	1.19E+01	8.38E+00	7.96E+00
	2024	5.46E+01	5.18E+01	2.73E+01	2.59E+01	1.36E+01	1.30E+01	9.10E+00	8.64E+00
	2025	5.89E+01	5.59E+01	2.95E+01	2.80E+01	1.47E+01	1.40E+01	9.82E+00	9.32E+00
	Optimistic Production	2018	7.61E+01	7.23E+01	3.81E+01	3.62E+01	1.90E+01	1.81E+01	1.27E+01
2019		8.05E+01	7.64E+01	4.02E+01	3.82E+01	2.01E+01	1.91E+01	1.34E+01	1.27E+01
2020		8.62E+01	8.19E+01	4.31E+01	4.09E+01	2.15E+01	2.05E+01	1.44E+01	1.36E+01
2021		9.12E+01	8.66E+01	4.56E+01	4.33E+01	2.28E+01	2.17E+01	1.52E+01	1.44E+01
2022		9.63E+01	9.14E+01	4.81E+01	4.57E+01	2.41E+01	2.29E+01	1.60E+01	1.52E+01
2023		1.02E+02	9.69E+01	5.10E+01	4.84E+01	2.55E+01	2.42E+01	1.70E+01	1.61E+01
2024		1.08E+02	1.03E+02	5.41E+01	5.14E+01	2.70E+01	2.57E+01	1.80E+01	1.71E+01
2025		1.15E+02	1.09E+02	5.73E+01	5.44E+01	2.87E+01	2.72E+01	1.91E+01	1.81E+01

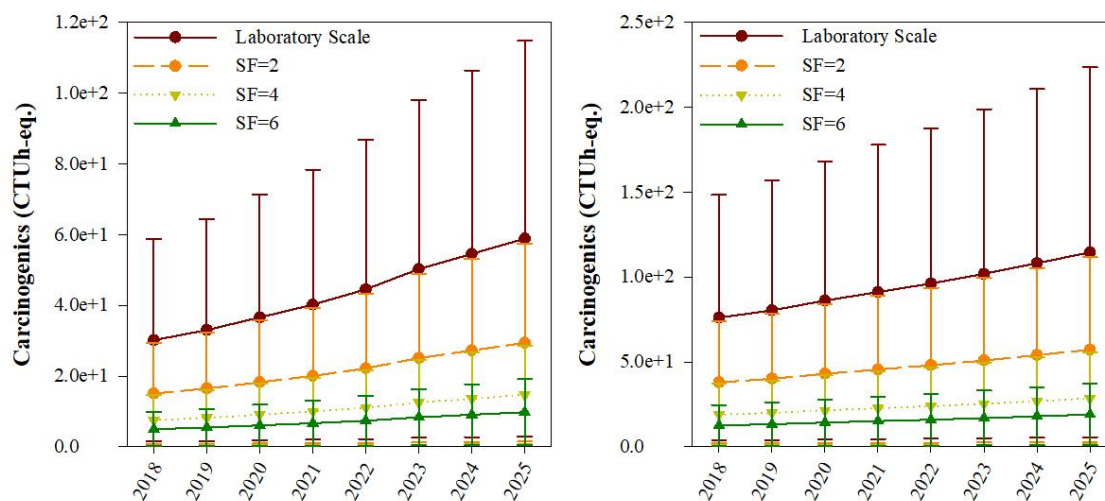


Figure A8. Global annual environmental impacts using different scale-up factors (2, 4 and 6) as well as laboratory scale results for HHCP (CTUh) [skeptical left, optimistic right]

Table A35. The projected HHNCP (CTUh) from 2018 to 2025 using different combination of synthesis procedures and scaling up factors (SF) of 2, 4 and 6.

	Laboratory Scale		SF=2		SF=4		SF=6		
	Year	Mean	StdDev	Mean	StdDev	Mean	StdDev	Mean	StdDev
Skeptical Production	2018	9.34E+02	7.41E+02	4.67E+02	3.71E+02	2.34E+02	1.85E+02	1.56E+02	1.24E+02
	2019	1.02E+03	8.12E+02	5.11E+02	4.06E+02	2.56E+02	2.03E+02	1.70E+02	1.35E+02
	2020	1.13E+03	9.00E+02	5.67E+02	4.50E+02	2.84E+02	2.25E+02	1.89E+02	1.50E+02
	2021	1.25E+03	9.88E+02	6.23E+02	4.94E+02	3.11E+02	2.47E+02	2.08E+02	1.65E+02
	2022	1.38E+03	1.09E+03	6.89E+02	5.47E+02	3.45E+02	2.74E+02	2.30E+02	1.82E+02
	2023	1.56E+03	1.24E+03	7.78E+02	6.18E+02	3.89E+02	3.09E+02	2.59E+02	2.06E+02
	2024	1.69E+03	1.34E+03	8.45E+02	6.71E+02	4.23E+02	3.35E+02	2.82E+02	2.24E+02
	2025	1.82E+03	1.45E+03	9.12E+02	7.24E+02	4.56E+02	3.62E+02	3.04E+02	2.41E+02
	Optimistic Production	2018	2.36E+03	1.87E+03	1.18E+03	9.35E+02	5.89E+02	4.68E+02	3.93E+02
2019		2.49E+03	1.98E+03	1.25E+03	9.88E+02	6.23E+02	4.94E+02	4.15E+02	3.29E+02
2020		2.67E+03	2.12E+03	1.33E+03	1.06E+03	6.67E+02	5.29E+02	4.45E+02	3.53E+02
2021		2.82E+03	2.24E+03	1.41E+03	1.12E+03	7.06E+02	5.60E+02	4.71E+02	3.74E+02
2022		2.98E+03	2.36E+03	1.49E+03	1.18E+03	7.45E+02	5.91E+02	4.97E+02	3.94E+02
2023		3.16E+03	2.51E+03	1.58E+03	1.25E+03	7.89E+02	6.26E+02	5.26E+02	4.18E+02
2024		3.35E+03	2.66E+03	1.67E+03	1.33E+03	8.37E+02	6.64E+02	5.58E+02	4.43E+02
2025		3.55E+03	2.82E+03	1.77E+03	1.41E+03	8.87E+02	7.04E+02	5.92E+02	4.69E+02

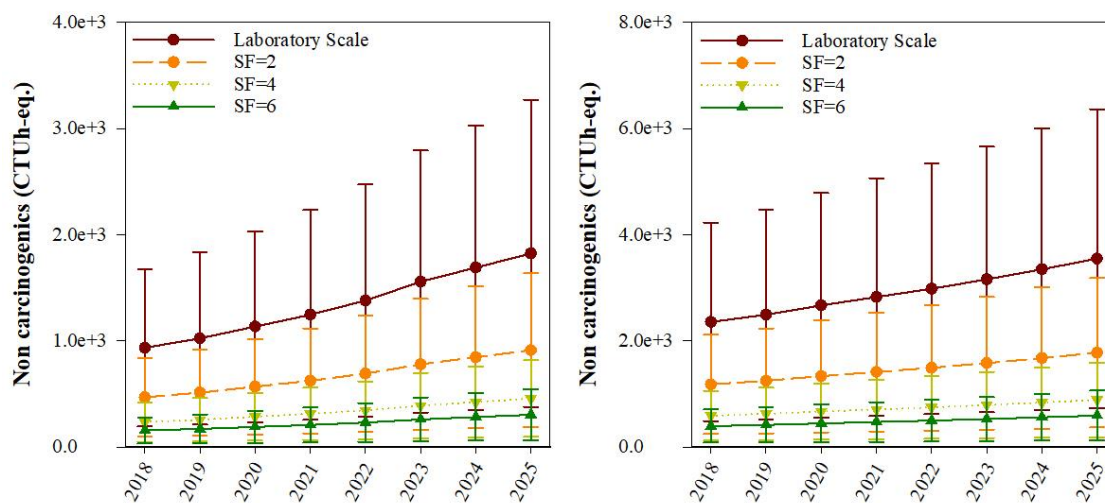


Figure A9. Global annual environmental impacts using different scale-up factors (2, 4 and 6) as well as laboratory scale results for HHNCP (CTUh) [skeptical left, optimistic right].

Table A36. The projected RP (tons PM_{2.5}-eq.) from 2018 to 2025 using different combination of synthesis procedures and scaling up factors (SF) of 2, 4 and 6.

	Laboratory Scale		SF=2		SF=4		SF=6		
	Year	Mean	StdDev	Mean	StdDev	Mean	StdDev	Mean	StdDev
Skeptical Production	2018	1.87E+02	4.43E+01	9.36E+01	2.22E+01	4.68E+01	1.11E+01	3.12E+01	7.39E+00
	2019	2.05E+02	4.86E+01	1.02E+02	2.43E+01	5.12E+01	1.21E+01	3.42E+01	8.10E+00
	2020	2.27E+02	5.39E+01	1.14E+02	2.69E+01	5.68E+01	1.35E+01	3.79E+01	8.98E+00
	2021	2.50E+02	5.91E+01	1.25E+02	2.96E+01	6.24E+01	1.48E+01	4.16E+01	9.86E+00
	2022	2.76E+02	6.55E+01	1.38E+02	3.27E+01	6.91E+01	1.64E+01	4.60E+01	1.09E+01
	2023	3.12E+02	7.39E+01	1.56E+02	3.70E+01	7.80E+01	1.85E+01	5.20E+01	1.23E+01
	2024	3.39E+02	8.03E+01	1.69E+02	4.01E+01	8.47E+01	2.01E+01	5.64E+01	1.34E+01
	2025	3.65E+02	8.66E+01	1.83E+02	4.33E+01	9.13E+01	2.16E+01	6.09E+01	1.44E+01
	Optimistic Production	2018	4.72E+02	1.12E+02	2.36E+02	5.60E+01	1.18E+02	2.80E+01	7.87E+01
2019		4.99E+02	1.18E+02	2.50E+02	5.91E+01	1.25E+02	2.96E+01	8.32E+01	1.97E+01
2020		5.35E+02	1.27E+02	2.67E+02	6.34E+01	1.34E+02	3.17E+01	8.91E+01	2.11E+01
2021		5.66E+02	1.34E+02	2.83E+02	6.71E+01	1.41E+02	3.35E+01	9.43E+01	2.24E+01
2022		5.97E+02	1.41E+02	2.99E+02	7.07E+01	1.49E+02	3.54E+01	9.95E+01	2.36E+01
2023		6.33E+02	1.50E+02	3.16E+02	7.50E+01	1.58E+02	3.75E+01	1.05E+02	2.50E+01
2024		6.71E+02	1.59E+02	3.35E+02	7.95E+01	1.68E+02	3.98E+01	1.12E+02	2.65E+01
2025		7.11E+02	1.69E+02	3.56E+02	8.43E+01	1.78E+02	4.21E+01	1.19E+02	2.81E+01

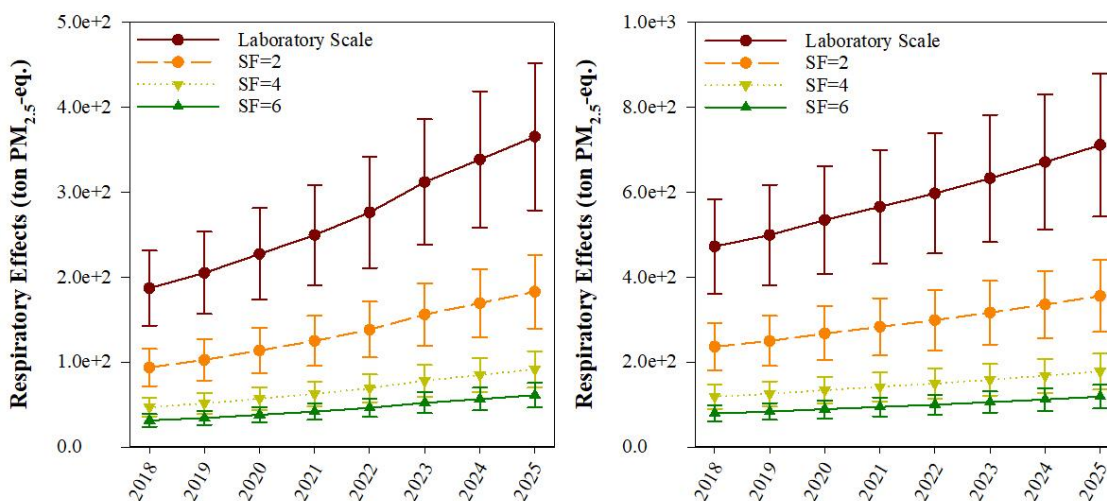


Figure A10. Global annual environmental impacts using different scale-up factors (2, 4 and 6) as well as laboratory scale results for RP (tons PM_{2.5}-eq.) [skeptical left, optimistic right].

Table A37. The projected ETP (CTUe) from 2018 to 2025 using different combination of synthesis procedures and scaling up factors (SF) of 2, 4 and 6.

	Laboratory Scale		SF=2		SF=4		SF=6		
	Year	Mean	StdDev	Mean	StdDev	Mean	StdDev	Mean	StdDev
Skeptical Production	2018	8.79E+09	7.85E+09	4.40E+09	3.92E+09	2.20E+09	1.96E+09	1.47E+09	1.31E+09
	2019	9.63E+09	8.60E+09	4.81E+09	4.30E+09	2.41E+09	2.15E+09	1.60E+09	1.43E+09
	2020	1.07E+10	9.53E+09	5.34E+09	4.77E+09	2.67E+09	2.38E+09	1.78E+09	1.59E+09
	2021	1.17E+10	1.05E+10	5.86E+09	5.23E+09	2.93E+09	2.62E+09	1.95E+09	1.74E+09
	2022	1.30E+10	1.16E+10	6.49E+09	5.79E+09	3.24E+09	2.90E+09	2.16E+09	1.93E+09
	2023	1.47E+10	1.31E+10	7.33E+09	6.54E+09	3.66E+09	3.27E+09	2.44E+09	2.18E+09
	2024	1.59E+10	1.42E+10	7.95E+09	7.10E+09	3.98E+09	3.55E+09	2.65E+09	2.37E+09
	2025	1.72E+10	1.53E+10	8.58E+09	7.66E+09	4.29E+09	3.83E+09	2.86E+09	2.55E+09
	Optimistic Production	2018	2.22E+10	1.98E+10	1.11E+10	9.91E+09	5.55E+09	4.95E+09	3.70E+09
2019		2.34E+10	2.09E+10	1.17E+10	1.05E+10	5.86E+09	5.23E+09	3.91E+09	3.49E+09
2020		2.51E+10	2.24E+10	1.26E+10	1.12E+10	6.28E+09	5.61E+09	4.19E+09	3.74E+09
2021		2.66E+10	2.37E+10	1.33E+10	1.19E+10	6.65E+09	5.93E+09	4.43E+09	3.96E+09
2022		2.80E+10	2.50E+10	1.40E+10	1.25E+10	7.01E+09	6.26E+09	4.67E+09	4.17E+09
2023		2.97E+10	2.65E+10	1.49E+10	1.33E+10	7.43E+09	6.64E+09	4.95E+09	4.42E+09
2024		3.15E+10	2.81E+10	1.58E+10	1.41E+10	7.88E+09	7.04E+09	5.25E+09	4.69E+09
2025		3.34E+10	2.98E+10	1.67E+10	1.49E+10	8.35E+09	7.46E+09	5.57E+09	4.97E+09

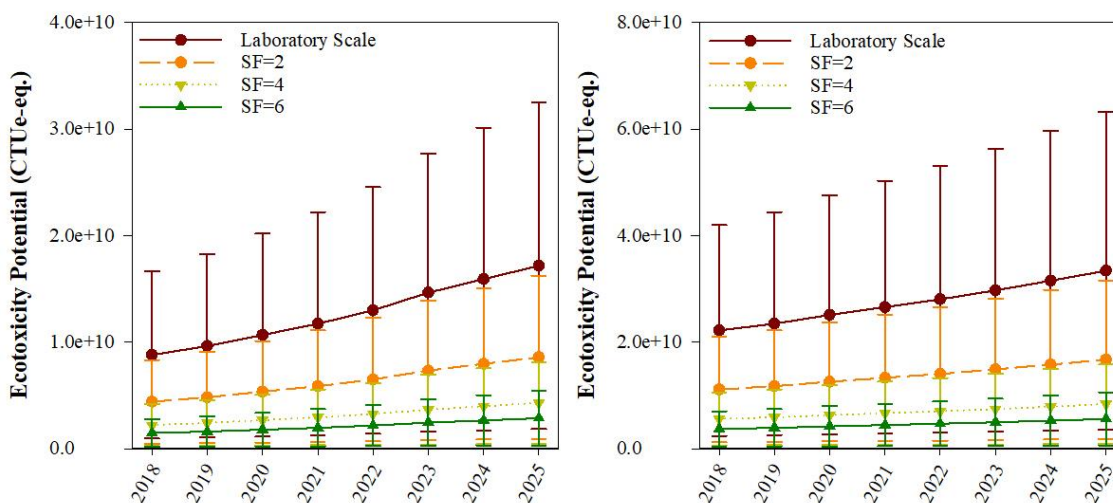


Figure A11. Global annual environmental impacts using different scale-up factors (2, 4 and 6) as well as laboratory scale results for ETP (CTUe) [skeptical left, optimistic right].

Table A38. The projected FFP (MJ surplus energy) from 2018 to 2025 using different combination of synthesis procedures and scaling up factors (SF) of 2, 4 and 6.

		Laboratory Scale		SF=2		SF=4		SF=6	
	Year	Mean	StdDev	Mean	StdDev	Mean	StdDev	Mean	StdDev
Skeptical Production	2018	9.72E+07	2.94E+07	4.86E+07	1.47E+07	2.43E+07	7.35E+06	1.62E+07	4.90E+06
	2019	1.06E+08	3.22E+07	5.32E+07	1.61E+07	2.66E+07	8.05E+06	1.77E+07	5.36E+06
	2020	1.18E+08	3.57E+07	5.90E+07	1.78E+07	2.95E+07	8.92E+06	1.97E+07	5.95E+06
	2021	1.30E+08	3.92E+07	6.48E+07	1.96E+07	3.24E+07	9.80E+06	2.16E+07	6.53E+06
	2022	1.43E+08	4.34E+07	7.17E+07	2.17E+07	3.59E+07	1.08E+07	2.39E+07	7.23E+06
	2023	1.62E+08	4.90E+07	8.10E+07	2.45E+07	4.05E+07	1.22E+07	2.70E+07	8.16E+06
	2024	1.76E+08	5.32E+07	8.79E+07	2.66E+07	4.40E+07	1.33E+07	2.93E+07	8.86E+06
	2025	1.90E+08	5.74E+07	9.49E+07	2.87E+07	4.74E+07	1.43E+07	3.16E+07	9.56E+06
Optimistic Production		Laboratory Scale		SF=2		SF=4		SF=6	
	Year	Mean	StdDev	Mean	StdDev	Mean	StdDev	Mean	StdDev
	2018	2.45E+08	7.42E+07	1.23E+08	3.71E+07	6.13E+07	1.85E+07	4.09E+07	1.24E+07
	2019	2.59E+08	7.84E+07	1.30E+08	3.92E+07	6.48E+07	1.96E+07	4.32E+07	1.31E+07
	2020	2.78E+08	8.40E+07	1.39E+08	4.20E+07	6.94E+07	2.10E+07	4.63E+07	1.40E+07
	2021	2.94E+08	8.89E+07	1.47E+08	4.44E+07	7.35E+07	2.22E+07	4.90E+07	1.48E+07
	2022	3.10E+08	9.38E+07	1.55E+08	4.69E+07	7.75E+07	2.34E+07	5.17E+07	1.56E+07
	2023	3.29E+08	9.94E+07	1.64E+08	4.97E+07	8.22E+07	2.48E+07	5.48E+07	1.66E+07
	2024	3.49E+08	1.05E+08	1.74E+08	5.27E+07	8.71E+07	2.63E+07	5.81E+07	1.76E+07
2025	3.69E+08	1.12E+08	1.85E+08	5.58E+07	9.23E+07	2.79E+07	6.16E+07	1.86E+07	

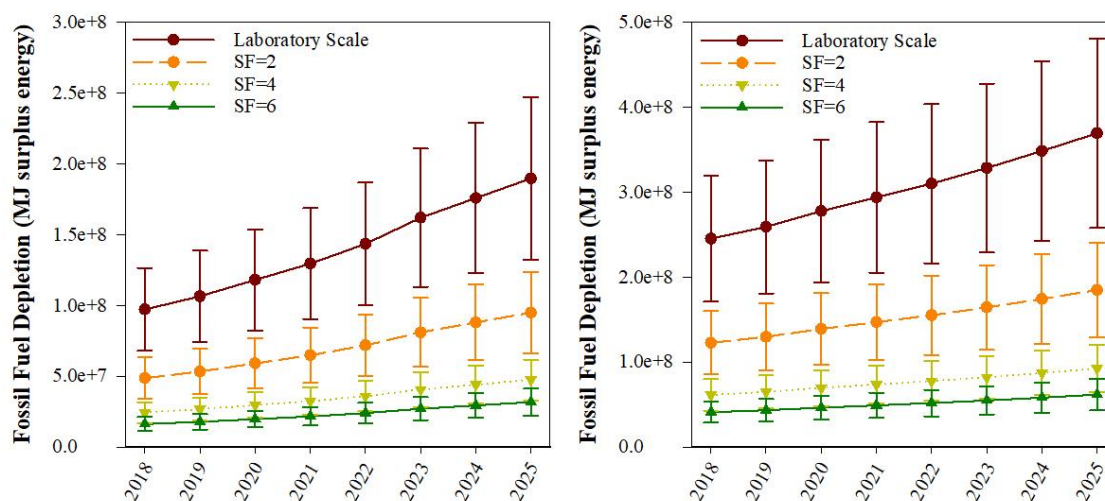


Figure A12. Global annual environmental impacts using different scale-up factors (2, 4 and 6) as well as laboratory scale results for FFP (MJ surplus energy) [skeptical left, optimistic right].

Table A39. The projected CED (MJ eq.) from 2018 to 2025 using different combination of synthesis procedures and scaling up factors (SF) of 2, 4 and 6.

	Laboratory Scale		SF=2		SF=4		SF=6		
	Year	Mean	StdDev	Mean	StdDev	Mean	StdDev	Mean	StdDev
Skeptical Production	2018	1.64E+09	4.88E+08	8.21E+08	2.44E+08	4.10E+08	1.22E+08	2.74E+08	8.13E+07
	2019	1.80E+09	5.34E+08	8.99E+08	2.67E+08	4.49E+08	1.34E+08	3.00E+08	8.90E+07
	2020	1.99E+09	5.92E+08	9.97E+08	2.96E+08	4.98E+08	1.48E+08	3.32E+08	9.87E+07
	2021	2.19E+09	6.50E+08	1.09E+09	3.25E+08	5.47E+08	1.63E+08	3.65E+08	1.08E+08
	2022	2.42E+09	7.20E+08	1.21E+09	3.60E+08	6.06E+08	1.80E+08	4.04E+08	1.20E+08
	2023	2.74E+09	8.13E+08	1.37E+09	4.06E+08	6.84E+08	2.03E+08	4.56E+08	1.35E+08
	2024	2.97E+09	8.83E+08	1.49E+09	4.41E+08	7.43E+08	2.21E+08	4.95E+08	1.47E+08
	2025	3.20E+09	9.52E+08	1.60E+09	4.76E+08	8.01E+08	2.38E+08	5.34E+08	1.59E+08
	Optimistic Production	2018	4.14E+09	1.23E+09	2.07E+09	6.16E+08	1.04E+09	3.08E+08	6.90E+08
2019		4.38E+09	1.30E+09	2.19E+09	6.50E+08	1.09E+09	3.25E+08	7.30E+08	2.17E+08
2020		4.69E+09	1.39E+09	2.35E+09	6.97E+08	1.17E+09	3.48E+08	7.82E+08	2.32E+08
2021		4.96E+09	1.47E+09	2.48E+09	7.37E+08	1.24E+09	3.69E+08	8.27E+08	2.46E+08
2022		5.24E+09	1.56E+09	2.62E+09	7.78E+08	1.31E+09	3.89E+08	8.73E+08	2.59E+08
2023		5.55E+09	1.65E+09	2.77E+09	8.25E+08	1.39E+09	4.12E+08	9.25E+08	2.75E+08
2024		5.89E+09	1.75E+09	2.94E+09	8.75E+08	1.47E+09	4.37E+08	9.81E+08	2.92E+08
2025		6.24E+09	1.85E+09	3.12E+09	9.27E+08	1.56E+09	4.63E+08	1.04E+09	3.09E+08

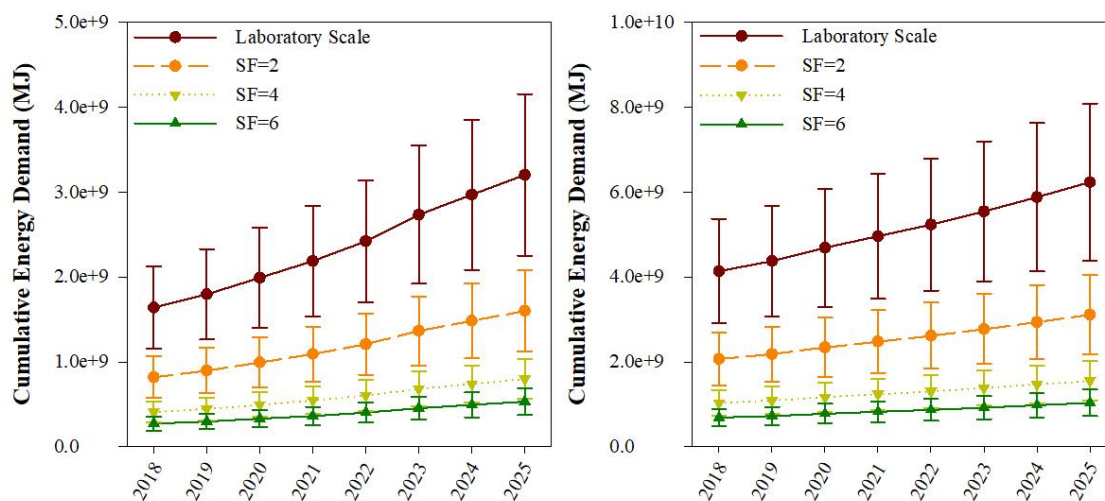


Figure A13. Global annual environmental impacts using different scale-up factors (2, 4 and 6) as well as laboratory scale results for CED (MJ eq.) [skeptical left, optimistic right].

Industry Based Environmental Impact Predictions

Industry-based potential environmental impacts are calculated using below equations and Sankey diagrams are developed for each impact category considered to better illustrate the follows of impact before scaling up. n is the number of methods applied for that industry and i is the respective AgNPs synthesis method(s).

$$\sum_i^n \frac{\text{industrial proportions} * \frac{\text{skeptical AgNPs production}}{\text{year}}}{n} * GWP_i \left(\text{in } \frac{\text{kg } CO_2 - \text{eq.}}{\text{kg AgNPs}} \right)$$

$$\sum_i^n \frac{\text{industrial proportions} * \frac{\text{optimistic AgNPs production}}{\text{year}}}{n} * GWP_i \left(\text{in } \frac{\text{kg } CO_2 - \text{eq.}}{\text{kg AgNPs}} \right)$$

Example calculation of GWP for medical industry with skeptical production on 2018:

$$\sum \left[\frac{0.31 * 210 \text{ t AgNPs}}{3} * \left(5.98E + 02 \frac{\text{kg } CO_2 - \text{eq.}}{\text{kg AgNPs}} \right) + \frac{0.31 * 210 \text{ t AgNPs}}{3} \right]$$

$$* \left(7.65 + 02 \frac{\text{kg } CO_2 - \text{eq.}}{\text{kg AgNPs}} \right) + \frac{0.31 * 210 \text{ t AgNPs}}{3} * \left(4.09E + 02 \frac{\text{kg } CO_2 - \text{eq.}}{\text{kg AgNPs}} \right) \Big]$$

$$= 38,694 \text{ t } CO_2 - \text{eq./year}$$

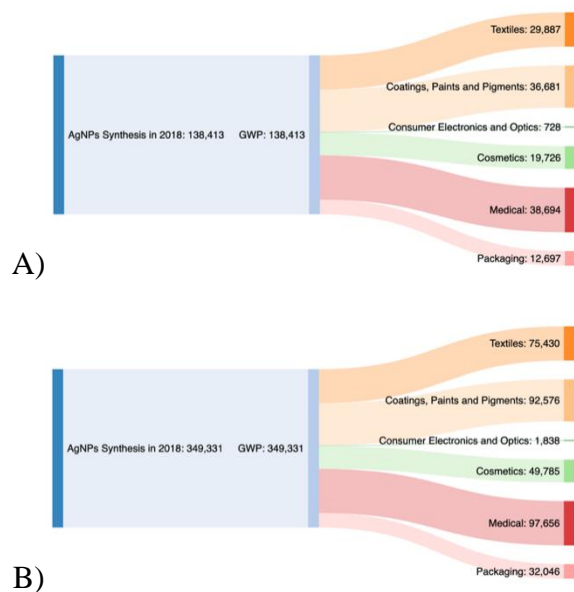


Figure A14. Sankey diagrams for sectoral GWP (tons CO₂-eq.) impacts (before scaling up) in 2018 for A) Skeptical and B) Optimistic estimations.

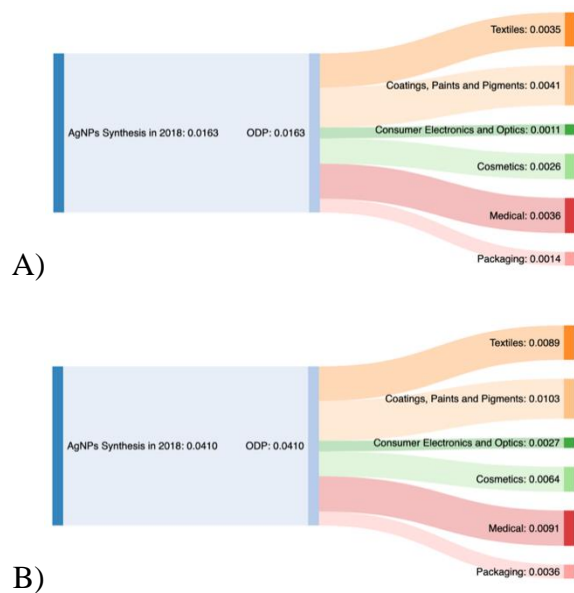


Figure A15. Sankey diagrams for sectoral ODP (tons CFC11-eq.) impacts (before scaling up) in 2018 for A) Skeptical and B) Optimistic estimations.

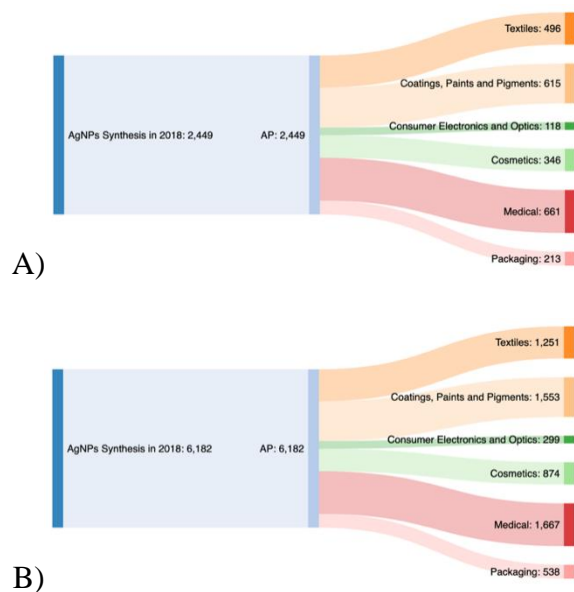


Figure A16. Sankey diagrams for sectoral AP (tons SO₂-eq.) impacts (before scaling up) in 2018 for A) Skeptical and B) Optimistic estimations.

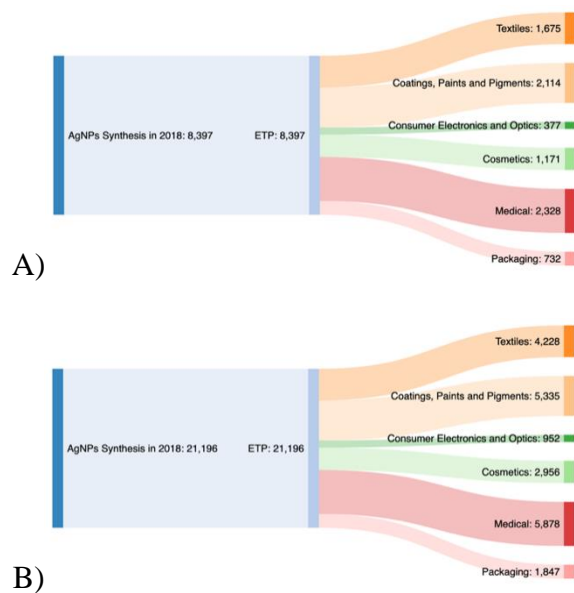


Figure A17. Sankey diagrams for sectoral ETP (x10⁶ CTUe) impacts (before scaling up) in 2018 for A) Skeptical and B) Optimistic estimations.

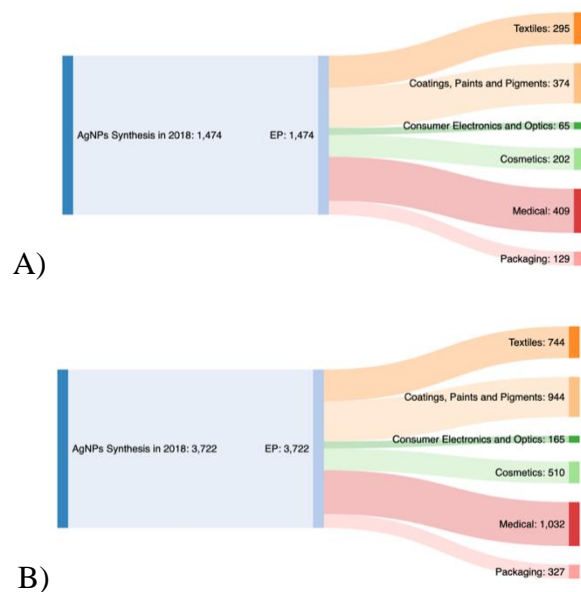


Figure A18. Sankey diagrams for sectoral EP (tons N-eq.) impacts (before scaling up) in 2018 for A) Skeptical and B) Optimistic estimations.

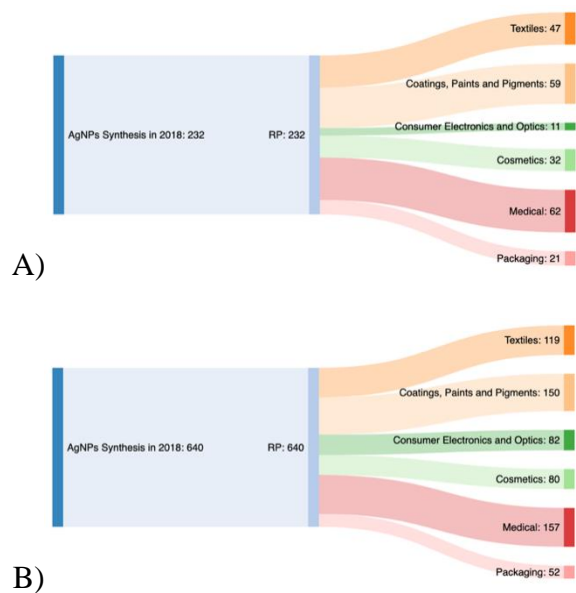


Figure A19. Sankey diagrams for sectoral RP (tons PM_{2.5}-eq.) impacts (before scaling up) in 2018 for A) Skeptical and B) Optimistic estimations.

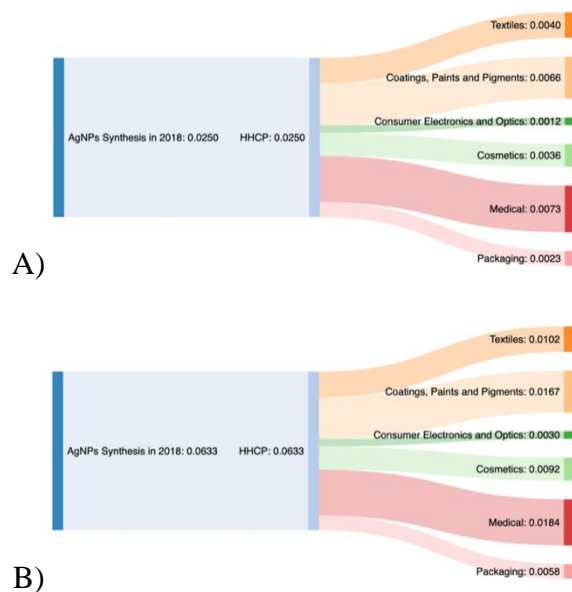


Figure A20. Sankey diagrams for sectoral HHCP ($\times 10^3$ CTUh) impacts (before scaling up) in 2018 for A) Skeptical and B) Optimistic estimations.

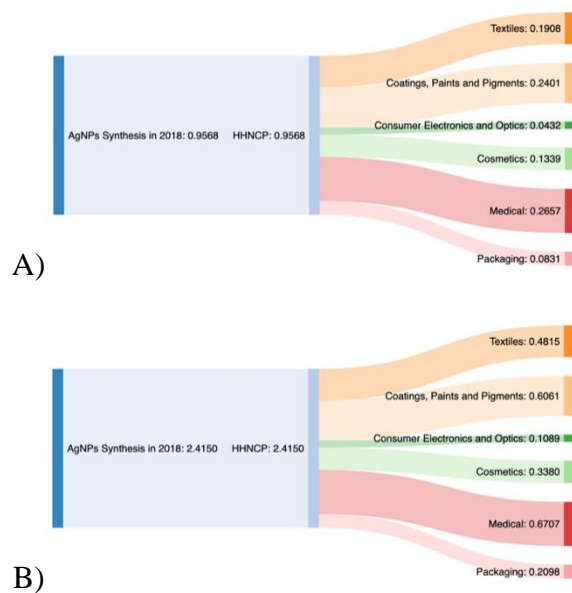


Figure A21. Sankey diagrams for sectoral HHNCP ($\times 10^3$ CTUh) impacts (before scaling up) in 2018 for A) Skeptical and B) Optimistic estimations.

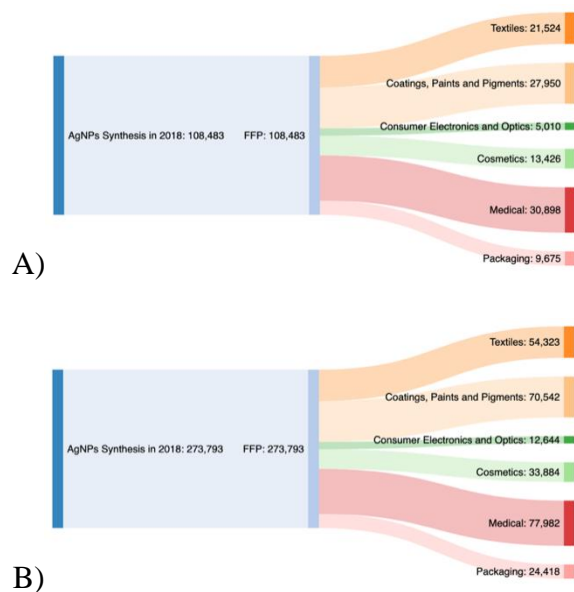


Figure A22. Sankey diagrams for sectoral FFP ($\times 10^3$ MJ surplus energy) impacts (before scaling up) in 2018 for A) Skeptical and B) Optimistic estimations.

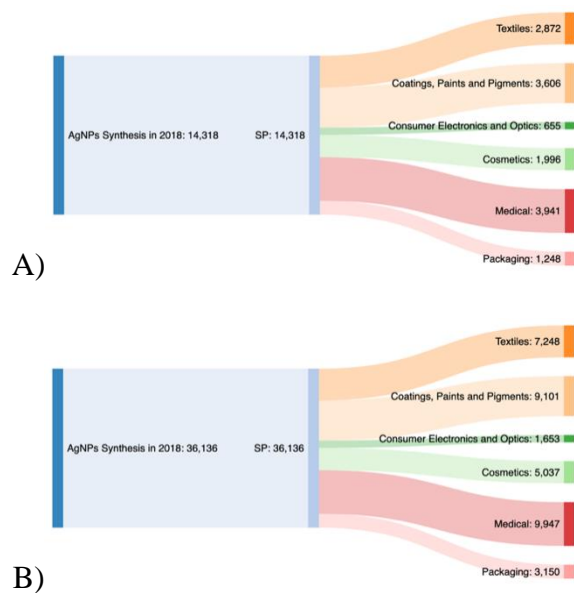


Figure A23. Sankey diagrams for industry-based SP (tons O₃-eq.) impacts (before scaling up) in 2018 for A) Skeptical and B) Optimistic estimations.

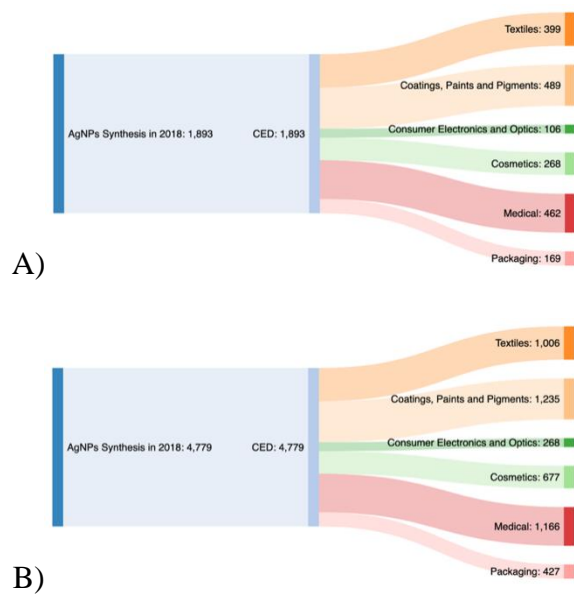


Figure A24. Sankey diagrams for sectoral CED (x10⁶ MJ) impacts (before scaling up) in 2018 for A) Skeptical and B) Optimistic estimations.

References-Appendix A

1. Bafana A, Kumar SV, Temizel-Sekeryan S, Dahoumane SA, Haselbach L, Jeffryes CS (2018) Evaluating microwave-synthesized silver nanoparticles from silver nitrate with life cycle assessment techniques. *Science of The Total Environment*, 636:936–943. <https://doi.org/10.1016/j.scitotenv.2018.04.345>
2. Phan CM, Nguyen HM (2017) Role of Capping Agent in Wet Synthesis of Nanoparticles. *The Journal of Physical Chemistry A*, 121(17):3213–3219. <https://doi.org/10.1021/acs.jpca.7b02186>
3. Ahari H, Karim G, Anvar AA, Pooyamanesh M, Sajadis A, Mostaghim A, Heydari S (2018) Synthesis of the Silver Nanoparticle by Chemical Reduction Method and Preparation of Nanocomposite based on AgNPS. <https://doi.org/10.11159/iccpe18.125>
4. Pourzahedi L, Eckelman MJ (2015) Comparative life cycle assessment of silver nanoparticle synthesis routes. *Environmental Science: Nano*, 2(4):361–369. <https://doi.org/10.1039/C5EN00075K>
5. Hicks AL, Gilbertson LM, Yamani JS, Theis TL, Zimmerman JB (2015) Life Cycle Payback Estimates of Nanosilver Enabled Textiles under Different Silver Loading, Release, And Laundering Scenarios Informed by Literature Review. *Environmental Science & Technology*, 49(13):7529–7542. <https://doi.org/10.1021/acs.est.5b01176>
6. Kammler HK, Mädler L, Pratsinis SE (2001) Flame Synthesis of Nanoparticles. *Chemical Engineering & Technology*, 24(6):583–596. [https://doi.org/10.1002/1521-4125\(200106\)24:6<583::AID-CEAT583>3.0.CO;2-H](https://doi.org/10.1002/1521-4125(200106)24:6<583::AID-CEAT583>3.0.CO;2-H)
7. Teoh WY, Amal R, Mädler L (2010) Flame spray pyrolysis: An enabling technology for nanoparticles design and fabrication. *Nanoscale*, 2(8):1324. <https://doi.org/10.1039/c0nr00017e>
8. Thiébaud B (2011) Flame Spray Pyrolysis: A Unique Facility for the Production of Nanopowders. *Platinum Metals Review*, 55(2):149–151. <https://doi.org/10.1595/147106711X567680>
9. Walser T, Demou E, Lang DJ, Hellweg S (2011) Prospective Environmental Life Cycle Assessment of Nanosilver T-Shirts. *Environmental Science & Technology*, 45(10):4570–4578. <https://doi.org/10.1021/es2001248>
10. Ku JT, Simanjuntak W, Lan EI (2017) Renewable synthesis of n-butyraldehyde from glucose by engineered *Escherichia coli*. *Biotechnology for Biofuels*, 10(1)<https://doi.org/10.1186/s13068-017-0978-7>
11. Slotte M, Zevenhoven R (2017) Energy requirements and life cycle assessment of production and product integration of silver, copper and zinc nanoparticles. *Journal of Cleaner Production*, 148:948–957. <https://doi.org/10.1016/j.jclepro.2017.01.083>
12. Bare J (2012) Tool for the Reduction and Assessment of Chemical and Other Environmental Impacts (TRACI) version 2.1. <https://nepis.epa.gov/Adobe/PDF/P100HN53.pdf>

13. Guinée JB, Gorrée M, Heijungs R, Huppes G, Kleijn R, Koning A, Oers L, Wegener Sleswijk A, Suh S, Udo de Haes HA, Brujin H, Duin R, Huijbregts MAJ (2002) Handbook on life cycle assessment. Operational guide to the ISO standards. I: LCA in perspective. IIa: Guide. IIb: Operational annex. III: Scientific background.
14. Jolliet O, Margni M, Charles R, Humbert S, Payet J, Rebitzer G, Rosenbaum R (2003) IMPACT 2002+: A new life cycle impact assessment methodology. *The International Journal of Life Cycle Assessment*, 8(6):324–330. <https://doi.org/10.1007/BF02978505>
15. Goedkoop M, Heijungs R, Huijbregts M, Schryver AD, Strujis J, Zelm R van (2013) ReCiPe 2008: Characterisation. https://www.pre-sustainability.com/download/ReCiPe_main_report_MAY_2013.pdf
16. Charitidis CA, Georgiou P, Koklioti MA, Trompeta A-F, Markakis V (2014) Manufacturing nanomaterials: from research to industry. *Manufacturing Review*, 1:11. <https://doi.org/10.1051/mfreview/2014009>
17. Sileikaite A, Prosycevas I, Puiso J, Juraitis A, Guobiene A (2006) Analysis of Silver Nanoparticles Produced by Chemical Reduction of Silver Salt Solution. *Materials Science*, 12(4):5.
18. Pourzahedi L, Vance M, Eckelman MJ (2017) Life Cycle Assessment and Release Studies for 15 Nanosilver-Enabled Consumer Products: Investigating Hotspots and Patterns of Contribution. *Environmental Science & Technology*, 51(12):7148–7158. <https://doi.org/10.1021/acs.est.6b05923>
19. Mulfinger L, Solomon SD, Bahadory M, Jeyarajasingam AV, Rutkowsky SA, Boritz C (2007) Synthesis and Study of Silver Nanoparticles. *Journal of Chemical Education*, 84(2):322. <https://doi.org/10.1021/ed084p322>
20. Westerband EI, Hicks AL (2018) Life cycle impact of nanosilver polymer-food storage containers as a case study informed by literature review. *Environmental Science: Nano*, 5(4):933–945. <https://doi.org/10.1039/C7EN01043E>
21. Solomon SD, Bahadory M, Jeyarajasingam AV, Rutkowsky SA, Boritz C (2007) Synthesis and Study of Silver Nanoparticles. *Journal of Chemical Education*, 84(2):322. <https://doi.org/10.1021/ed084p322>
22. Slistan-Grijalva A, Herrera-Urbina R, Rivas-Silva JF, Ávalos-Borja M, Castellón-Barraza FF, Posada-Amarillas A (2005) Assessment of growth of silver nanoparticles synthesized from an ethylene glycol–silver nitrate–polyvinylpyrrolidone solution. *Physica E: Low-dimensional Systems and Nanostructures*, 25(4):438–448. <https://doi.org/10.1016/j.physe.2004.07.010>
23. El-Rafie MH, El-Naggar ME, Ramadan MA, Fouda MMG, Al-Deyab SS, Hebeish A (2011) Environmental synthesis of silver nanoparticles using hydroxypropyl starch and their characterization. *Carbohydrate Polymers*, 86(2):630–635. <https://doi.org/10.1016/j.carbpol.2011.04.088>

24. Zhou M, Wei Z, Qiao H, Zhu L, Yang H, Xia T (2009) Particle Size and Pore Structure Characterization of Silver Nanoparticles Prepared by Confined Arc Plasma. *Journal of Nanomaterials*, 2009:1–5. <https://doi.org/10.1155/2009/968058>
25. Pierson JF, Wiederkehr D, Billard A (2005) Reactive magnetron sputtering of copper, silver, and gold. *Thin Solid Films*, 478(1–2):196–205. <https://doi.org/10.1016/j.tsf.2004.10.043>

Appendix B

Electronic supplemental information from Chapter 3 and associated references.

the search query used for total CNTs patents:

ABST/(carbon AND nanotube) AND ISD/1/1/1980->31/12/2019

the search query used for SWCNTs patents:

ABST/(carbon AND nanotube AND single AND (wall OR walled)) AND ISD/1/1/1996->31/12/2019

the search query used for MWCNTs patents:

ABST/(carbon AND nanotube AND multi AND (wall OR walled)) AND ISD/1/1/1996->31/12/2019

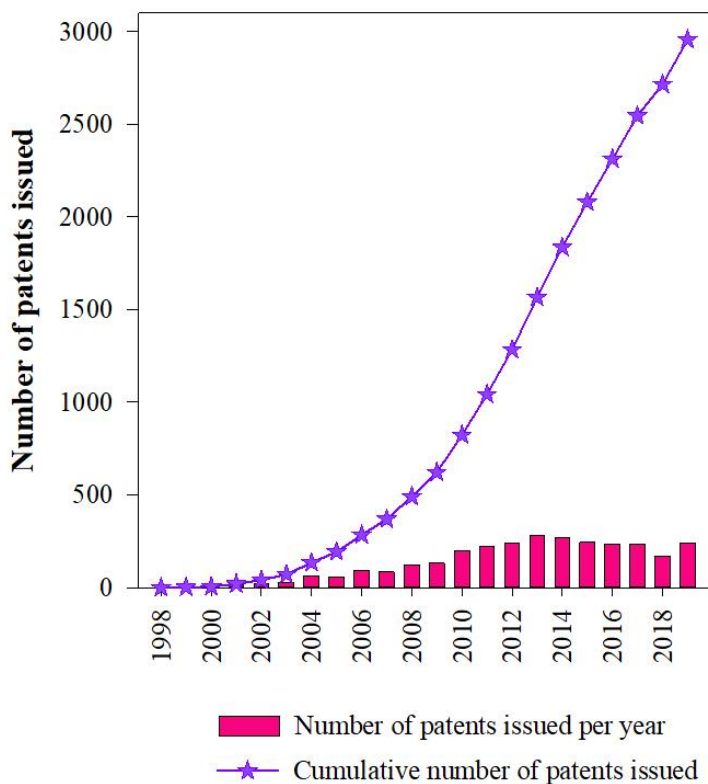


Figure B1. Number of CNTs patents issued by United States Patent and Trademark Office [1].

Table B1. Detailed literature compilation* on previously applied life cycle assessments for SWCNTs/MWCNTs (listed by the year of publication).

Title	Synthesis process(es) applied	SWCNT/ MWCNT	Software (S)/ Method (M)/ Database (D)/ Functional Unit (FUn)	Life cycle inventory (LCI) source	System boundaries	How results are presented?	Study reference
Towards a framework for life cycle thinking in the assessment of nanotechnology	CVD (lab scale)	SWCNT	S: Umberto D: Ecoinvent v1.2 M: CED and CML 2001 FUn: one 15"-FED screen	[2, 3]	Cradle-to-grave	Although individual LCA results for CNTs were not shared, results for one 15"-FED screen were provided graphically (without actual numbers).	[4]
Environmental Assessment of Single-Walled Carbon Nanotube Processes	AD, CVD, HiPCO (lab scale)	SWCNT	S: SimaPro D: N/A M: EPS 2000, EcoIndicator 99 FUn: 1 g SWCNT	[5, 6]	Cradle-to-gate	Internally normalized life cycle results were provided graphically (without actual numbers).	[3, 7]
Environmental Assessment of SWNT Production				Own derived inventory data			[6]
Energy Requirements of Carbon Nanoparticle Production	CVD, HiPCO, LV, AD (lab scale)	SWCNT	S: N/A D: N/A M: CED FUn: 1 kg CNTs	[6]	Cradle-to-gate	Cumulative energy requirements of different methods were provided.	[8]
	CVD, LV, AD, Solar Furnace Synthesis (lab scale)	MWCNT					

Title	Synthesis process(es) applied	SWCNT/ MWCNT	Software (S)/ Method (M)/ Database (D)/ Functional Unit (FUn)	Life cycle inventory (LCI) source	System boundaries	How results are presented?	Study reference
Environmental Impact Assessment for Potential Continuous Processes for the Production of Carbon Nanotubes	HiPCO, CoMoCat (lab and large scales)	SWCNT	S: SimaPro 7.0 D: N/A M: TRACI FUn: 1 kg of SWCNT	[9]	Cradle-to-gate	Results for 1 kg SWCNT were provided.	[10]
Environmental Assessment of Manufacturing with Carbon Nanotubes	HiPCO (lab scale)	SWCNT	S: SimaPro D: N/A M: EcoIndicator 1999 (H) FUn: one device (e.g. CNT switch or unit area of CNT-polymer mesh)	[7]	Cradle-to-gate	Although individual LCA results for CNTs were not shared (showed graphically), results for one CNT switch and one CNT-polymer mesh were provided.	[11]
A Life-Cycle Energy Analysis of Single Wall Carbon Nanotubes Produced Through Laser Vaporization	LV (lab scale)	SWCNT	S: Economic Input-Output (EIO) LCA and SimaPro D: N/A M: CED FUn: 1 kg SWCNT	Own derived inventory data	Cradle-to-gate	Only life-cycle energy consumption (electrical and material embodied energy) was calculated in MJ.	[12]
Influence of using nanoobjects as filler on functionality-based energy use of nanocomposites	CVD (large scale)	SWCNT/ MWCNT	S: SimaPro D: Ecoinvent M: non-renewable energy use (NREU) FUn: 1 kg CNT	Bayer Material Science AG (proprietary)	Cradle-to-grave	Results were presented for GW (kg CO ₂ -eq/kg) and NREU (MJ/kg) for both SWCNT and MWCNT.	[13]
Environmental relief effects of nanotechnologies by the example of CNT composite materials and films	CVD (lab scale)	MWCNT	S: Umberto D: N/A M: CED and CML FUn: 1 kg MWCNT	Own derived inventory data	Cradle-to-grave	Results for 1 kg MWCNT were provided.	[14]

Title	Synthesis process(es) applied	SWCNT/ MWCNT	Software (S)/ Method (M)/ Database (D)/ Functional Unit (FUn)	Life cycle inventory (LCI) source	System boundaries	How results are presented?	Study reference
Towards Prospective Life Cycle Assessment: Single Wall Carbon Nanotubes for Lithium-ion Batteries	LV (lab scale)	SWCNT	S: <i>N/A</i> D: <i>N/A</i> M: <i>N/A</i> FUn: kWh energy storage capacity in the battery	[12]	Cradle-to-gate	Results on SWCNT anode manufacturing were provided graphically (without actual numbers).	[15]
New Perspectives on Nanomaterial Aquatic Ecotoxicity: Production Impacts Exceed Direct Exposure Impacts for Carbon Nanotubes	AD, CVD, HiPCO	SWCNT	S: SimaPro 7.3 D: <i>N/A</i> M: USEtox model FUn: 1 kg SWCNT	[7]	Cradle-to-gate and release	Only aquatic ecotoxicity impacts were quantified as Comparative Toxic Units for Ecosystems (CTUe).	[16]
Environmental and economic assessment of ITO-free electrodes for organic solar cells	AD (lab scale)	SWCNT	S: <i>N/A</i> D: ProcessOne M: ProcessOne FUn: <i>N/A</i>	[8, 17, 18]	Cradle-to-gate	Embedded energy results were provided for SWCNTs graphically (without actual numbers) as an alternative of transparent conductor to replace the indium–tin oxide conductors.	[19]
Ecological assessment of nano-enabled supercapacitors for automotive applications	LV (lab scale)	SWCNT	S: <i>N/A</i> D: <i>N/A</i> M: CED FUn: 1 kg SWCNT	Own derived inventory data	Cradle-to-gate	CED results for producing one kg SWCNT were published.	[20]

Title	Synthesis process(es) applied	SWCNT/ MWCNT	Software (S)/ Method (M)/ Database (D)/ Functional Unit (FUn)	Life cycle inventory (LCI) source	System boundaries	How results are presented?	Study reference
Environmental Life Cycle Assessment of a Carbon Nanotube-Enabled Semiconductor Device	HiPCO (lab scale)	SWCNT	S: SimaPro 7.3 D: Ecoinvent v2.2 M: TRACI 2 FUn: all devices manufactured on a single wafer	[7]	Cradle-to-gate	Although individual LCA results for CNTs were not shared, results for fabrication step of semiconductor device and for material and energy input were provided graphically (without actual numbers).	[21]
Identifying the largest environmental life cycle impacts during carbon nanotube synthesis via chemical vapor deposition	CVD (lab scale)	MWCNT	S: SimaPro D: Ecoinvent v2.2 M: ReCiPe FUn: 300 mg of MWCNT	Own derived inventory data	Cradle-to-gate	Results for producing one batch MWCNT were published.	[22]
Life Cycle Impacts and Benefits of a Carbon Nanotube-Enabled Chemical Gas Sensor	CVD (lab scale)	SWCNT	S: SimaPro 7.3.3 D: US-EI v2.2 and Ecoinvent v2.2 M: TRACI 2 and ReCiPe FUn: 1 Chip, 16 Sensors/Chip, 36 Chips/Wafer	[7]	Cradle-to-gate	Results for each individual life cycle stage were shared in DALYs. Also, internally normalized midpoint results for each stage were provided graphically (without actual numbers).	[23]

Title	Synthesis process(es) applied	SWCNT/ MWCNT	Software (S)/ Method (M)/ Database (D)/ Functional Unit (FUn)	Life cycle inventory (LCI) source	System boundaries	How results are presented?	Study reference
Evaluating the Environmental Impacts of a Nano-Enhanced Field Emission Display Using Life Cycle Assessment: A Screening-Level Study	CVD (lab scale)	N/A	S: SimaPro 7.3 D: USLCI and Ecoinvent v2.0 M: TRACI 2.1 FUn: 10,000 viewing Hours (lifespan of a CNT-FED)	[8, 24–26]	Cradle-to-grave	Results for screening-level LCA were provided along with contribution analysis.	[27]
The Role of Scale and Technology Maturity in Life Cycle Assessment of Emerging Technologies: A Case Study on Carbon Nanotubes	CoMoCat (small scale)	SWCNT	S: not mentioned D: Comprehensive Environmental Data Archive (CEDA) M: TRACI (unspecified version) FUn: 1 kg SWCNT	Proprietary (on-site data by the manufacturer)	Cradle-to-gate	Results both small and industrial scale (estimation) manufacturing processes of SWCNTs were provided.	[28]
Green catalysis by nanoparticulate catalysts developed for flow processing? Case study of glucose hydrogenation	CVD (lab scale)	N/A	S: Umberto® NXT LCA D: Ecoinvent v3.0 M: ReCiPe 2008 FUn: 1 kg sorbitol	Own derived inventory data	Cradle-to-gate	Internally normalized life cycle results were provided graphically (without actual numbers) for nitrogen doped CNTs.	[29]

Title	Synthesis process(es) applied	SWCNT/ MWCNT	Software (S)/ Method (M)/ Database (D)/ Functional Unit (FUn)	Life cycle inventory (LCI) source	System boundaries	How results are presented?	Study reference
Life cycle assessment study of a field emission display television device	CVD (lab scale)	SWCNT	S: not mentioned D: Ecoinvent v2.2 M: ReCiPe and USEtox FUn: (1) 36-in FED television device over its complete life cycle, and (2) one square-inch of display during 1 h of active use	[7, 30]	Cradle-to-grave	Although individual LCA results for CNTs were not shared, results for the field emission display television device were provided.	[31]
Life cycle assessment of PEM FC applications: electric mobility and μ -CHP	CVD (lab scale)	MWCNT	S: SimaPro (unspecified version) M: ReCiPe 2008 D: Ecoinvent v2.2 FUn: 10 kW HT PEM fuel cell unit	Own derived inventory data for functionalized MWCNT	Cradle-to-gate	Results for manufacturing 1 kg MWCNT were provided.	[32]
Towards a holistic environmental impact assessment of carbon nanotube growth through chemical vapour deposition	CVD (lab scale)	MWCNT	S: SimaPro 8 M: ReCiPe (H) D: Ecoinvent v3.1 FUn: 1 kg MWCNT	Own derived inventory data	Cradle-to-gate	Results for manufacturing 1 kg MWCNT were provided.	[33]

Title	Synthesis process(es) applied	SWCNT/ MWCNT	Software (S)/ Method (M)/ Database (D)/ Functional Unit (FUn)	Life cycle inventory (LCI) source	System boundaries	How results are presented?	Study reference
Net energy benefits of carbon nanotube applications	CVD (industrial scale)	SWCNT and MWCNT	S: N/A M: CED v1.08 D: Ecoinvent v2.2 FUn: (1) 1,000 kg mass of cement, (2) 16 Gb capacity of memory, and (3) 16 kWh capacity of battery	[8]	Cradle-to-grave	Net energy benefits were reported for different CNT uses, e.g. SWCNT switch flash memory, SWCNT Li-ion battery anodes, MWCNT-reinforced cement, and MWCNT Li-ion battery cathodes	[34]
Environmental Impacts from Photovoltaic Solar Cells Made with Single Walled Carbon Nanotubes	CoMoCat (lab scale)	SWCNT	S: GaBi 6.0 M: TRACI 2.1 D: Ecoinvent v2.1 FUn: 1 m ² SWCNT	[9, 28, 35]	Cradle-to-grave (excluding transportation and disposal)	Normalized impact assessment results for solar PV were provided.	[36]
Life cycle assessment of high capacity molybdenum disulfide lithium-ion battery for electric vehicles	LV (lab scale)	SWCNT	S: GaBi 6.0 M: ReCiPe D: Ecoinvent v2.2 FUn: 1 km driving of a mid-sized EV for 10 years (200,000 km)	[37]	Cradle-to-grave	Although individual LCA results for CNTs were not shared, results for life cycle of the NMC-MoS ₂ battery pack were provided.	[38]
Life cycle inventories of the commonly used materials for lithium-ion batteries in China	N/A	N/A	S: GaBi 6.0 and GREET M: N/A D: CLCD v0.8, Ecoinvent v3.0 FUn: 1 kg CNT	Nantong Dongheng New Energy Co., Ltd.	Cradle-to-gate	Criteria air pollutants (CO, NMVOC, SO ₂ and NO _x emissions), GW and CED impacts were provided graphically (without actual numbers).	[39]

Title	Synthesis process(es) applied	SWCNT/ MWCNT	Software (S)/ Method (M)/ Database (D)/ Functional Unit (FUn)	Life cycle inventory (LCI) source	System boundaries	How results are presented?	Study reference
Development of life cycle assessment of an emerging technology at research and development stage: A case study on single-wall carbon nanotube produced by super growth method	CVD (lab and pilot scales)	SWCNT	S: N/A M: N/A D: IDEA v2.1.3 FUn: 1 kg SWCNT	[40, 41]	Cradle-to-gate	GHG (i.e. GW) impacts for lab scale, pilot scale and commercial scale (estimated via scaling up method) SWCNTs production were provided.	[42]
Life Cycle Greenhouse Gas Emissions of Long and Pure Carbon Nanotubes Synthesized via On-Substrate and Fluidized-Bed Chemical Vapor Deposition	CVD (lab scale)	Single-wall to few-wall CNTs	S: openLCA v1.7 M: IPCC D: Ecoinvent v3.4 FUn: 1 g single-wall to few-wall CNTs	[43–45]	Cradle-to-gate	GHG (i.e. GW) impacts for on-substrate and fluidized-bed CVD processes were provided.	[46]
Assessing the environmental impact and payback of carbon nanotube supported CO ₂ capture technologies using LCA methodology	CVD (pilot scale)	MWCNT	S: SimaPro 8.5 M: TRACI 2.1 D: Ecoinvent v3 and USLCI FUn: (1) 1 kg of material synthesis cost, and (2) materials required to adsorb 1 kg CO ₂	[47]	Cradle-to-gate	Results for manufacturing 1 kg MWCNT were provided.	[48]

* Search query from Web of Science Core Collection: (("life cycle assessment" OR "LCA" OR "life cycle analysis" OR "life cycle impact assessment" OR "life cycle impacts" OR "life cycle impact" OR "environmental impact assessment") AND ("carbon nanotube" OR "carbon nanotubes" OR "CNT" OR "CNTs" OR "carbonnanotube" OR "carbonnanotubes" OR "single walled" OR "single-walled" OR "multi walled" OR "multi-walled" OR "SWCNT" OR "SWNT" OR "MWCNT" OR "MWNT" OR "SWCNTs" OR "SWNTs" OR "MWCNTs" OR "MWNTs")) and the following papers [49–52]

Life Cycle Inventories Considered for SWCNT Production Processes

Eight production processes are considered in this work for SWCNTs. Either cradle-to-gate inventories or detailed experimental processes are collected from the literature for different synthesis routes. From the detailed experimental research found in the literature, cradle-to-gate inventories are developed for different synthesis routes. In this section, life cycle inventories used for SWCNT synthesis processes are presented for 1 kg of SWCNTs.

Chemical Vapor Deposition

Table B2. Inventory used for S-CVD1 for 1 kg SWCNT [7].

Synthesis Input	Unit	Amount	Database
Ammonia	kg	0.0024	Industry data 2.0
Magnesium	kg	3.27	Ecoinvent 3
Cobalt	kg	0.02	Ecoinvent 3
Citric acid	kg	0.13	Ecoinvent 3
Methane	m ³	63.8 ^a	Ecoinvent 3
Hydrogen	kg	42.07	Ecoinvent 3
Argon	kg	833.67	Ecoinvent 3
Electricity	GJ	828.86	USLCI
Synthesis Output	Unit	Amount	Database
Methane -emissions to air-	kg	40.62	-
Hydrogen -emissions to air-	kg	42.07	-
Argon -emissions to air-	kg	833.67	-
Purification Input	Unit	Amount	Database
Deionized water ^b	kg	6024.86	Ecoinvent 3
Nitric acid	kg	696.31	Ecoinvent 3
Electricity	GJ	53.17	USLCI
Purification Output	Unit	Amount	Database
SWCNT	kg	1	-
Water -emissions to water- ^c	kg	6721.41	-

^a Density of methane = 0.656 kg/m³ → 41.85 kg methane/1 kg SWCNT = 63.8 m³/kg SWCNT.

^b Deionized water and Triton X100 input as deionized water [7].

^c Deionized water and filtration output as deionized water [7].

Table B3. Inventory used for **S-CVD2** for 1 kg SWCNT [4, 50].

Input	Unit	Amount	Database
Acetylene	kg	10	Ecoinvent 3
Hydrogen	kg	16 ^a	Ecoinvent 3
Argon	kg	317 ^a	Ecoinvent 3
Electricity	GJ	2750	USLCI
Output			
SWCNT	kg	1	-
Hydrogen -emissions to air-	kg	11.2	-

^a As a carrier material, multiple inputs (H₂ and Ar) were represented by a total amount of 333 kg Hischer and Walser [50]. A ratio of H₂ and Ar is calculated by using data from Healy et al. [7] and applied for this inventory.

High-Pressure Carbon Monoxide Reaction

Table B4. Inventory used for **S-HiPCO1** for 1 kg SWCNT [7].

Synthesis Input	Unit	Amount	Database
Chemical, organic ^a	kg	0.09	Ecoinvent 3
Carbon monoxide	kg	14.86	Ecoinvent 3
Argon	kg	0.04	Ecoinvent 3
Electricity	GJ	95.36	USLCI
Synthesis Output			
Carbon monoxide -emissions to air-	kg	13.71	-
Argon -emissions to air-	kg	0.04	-
Purification Input			
Deionized water ^b	kg	5590.05	Ecoinvent 3
Nitric acid	kg	646.06	Ecoinvent 3
Electricity	GJ	49.36	USLCI
Purification Output			
SWCNT	kg	1	-
Water -emissions to water- ^c	kg	6236.26	-

^a Catalyst Fe(CO)₅ input is assumed as chemicals organic [7].

^b Deionized water and Triton X100 input as deionized water [7].

^c Deionized water and filtration output as deionized water [7].

Table B5. Inventory used for **S-HiPCO₂*** for 1 kg SWCNT [10, 50].

Input	Unit	Amount	Database
Chemical, organic ^a	kg	1.05	Ecoinvent 3
Carbon monoxide	kg	4.43	Ecoinvent 3
Electricity	MJ	6.39	USLCI
Heat/vapor	MJ	59.4	Ecoinvent 3
Output			
SWCNT	kg	1	-
Carbon dioxide -emissions to air-	kg	4.48	-
Iron (III) oxide -waste to treatment-	kg	0.43	-
Water -emissions to water-	kg	108	-

^a Catalyst Fe(CO)₅ input is assumed as chemicals organic [7].

Cobalt-Molybdenum Catalytic Process

Table B6. Inventory used for **S-CoMoCat1** for 1 kg SWCNT [36].

Input	Unit	Amount	Database
Carbon monoxide	kg	25.1	Ecoinvent 3
Chemical, organic ^a	kg	0.274	Ecoinvent 3
Oxygen	kg	0.065	Ecoinvent 3
Sodium hydroxide	kg	3.53	Ecoinvent 3
Deionized water	kg	2.08	Ecoinvent 3
Electricity	GJ	532	USLCI
Output			
SWCNT	kg	1	-
Carbon dioxide -emissions to air-	kg	19.7	-
Carbon monoxide -emissions to air-	kg	2.52	-
Hydrogen -emissions to air-	kg	0.181	-
Water -emissions to water-	kg	1.84	-
Hazardous waste	kg	2.04	-

^a Catalyst Co-Mo input is assumed as chemicals organic [7].

Table B7. Inventory used for **S-CoMoCat2*** for 1 kg SWCNT [10, 50].

Input	Unit	Amount	Database
Chemical, organic ^a	kg	1 ^b	Ecoinvent 3
Carbon monoxide	kg	5.83	Ecoinvent 3
Electricity	MJ	2.34	USLCI
Heat/vapor	MJ	74.8	Ecoinvent 3
Output			
SWCNT	kg	1	-
Sodium hydroxide -emissions to soil-	kg	0.383	-
Carbon dioxide -emissions to air-	kg	4.58	-
Carbon monoxide -emissions to air-	kg	0.587	-
Hydrogen -emissions to air-	kg	0.042	-
Water -emissions to water-	kg	121.6	-

^a Catalyst Co-Mo input is assumed as chemicals organic [7].

^b In Hischer and Walser [50], no information was available for the mass of Co-Mo Catalyst used. Therefore, the amount of Co-Mo Catalyst was assumed as 1 kg.

Arc Process

Table B8. Inventory used for **S-AP** for 1 kg SWCNT [7].

Synthesis Input	Unit	Amount	Database
Iron pellet	kg	13.5	Ecoinvent 3
Rare earth concentrate	kg	3.4	Ecoinvent 3
Sulfur	kg	1.82	Ecoinvent 3
Carbon black	kg	1.7	Ecoinvent 3
Helium	kg	173.61	Ecoinvent 3
Carbon black ^a	kg	169.33	Ecoinvent 3
Electricity	GJ	251.03	USLCI
Synthesis Output			
Carbon -emissions to air-	kg	50.53	-
Carbon -emissions to soil-	kg	136.57	-
Helium -emissions to air-	kg	173.61	-
Purification Input			
Deionized water ^b	kg	9524.03	Ecoinvent 3
Nitric acid	kg	1342.88	Ecoinvent 3
Electricity	GJ	102.56	USLCI
Purification Output			
SWCNT	kg	1	-
Water -emissions to water- ^c	kg	12963.57	-

^a Anode and Cathode mass input as carbon [7].

^b Deionized water and Triton X100 input as deionized water [7].

^c Deionized water and filtration output as deionized water [7].

Laser Vaporization

Table B9. Inventory used for **S-LV** for 1 kg SWCNT [12].

Synthesis Input	Unit	Amount	Database
Graphite	kg	3.133	Ecoinvent 3
Cobalt	kg	0.1	Ecoinvent 3
Nickel	kg	0.1	Ecoinvent 3
Argon	kg	0.7125	Ecoinvent 3
Electricity	GJ	330.48	USLCI
Synthesis Output			
Argon -emissions to air-	kg	0.7125	-
Purification Input			
Nitric acid	kg	1.258	Ecoinvent 3
Hydrochloric acid	kg	0.472	Ecoinvent 3
Deionized water	kg	5	Ecoinvent 3
Acetone	kg	0.658	Ecoinvent 3
Electricity	GJ	79.2	USLCI
Purification Output			
SWCNT	kg	1	-
Water -emissions to water- ^a	kg	7.388	-

^a According to Ganter et al. [12], most material inputs become waste at the laboratory scale. Acid reflux (nitric acid, hydrochloric acid and deionized water) and filtration (acetone and deionized water) outputs are based on the assumption made in this work (the sum of inputs is considered equal to the sum of outputs).

Life Cycle Inventories Considered for MWCNT Production Processes

An arc process and six different chemical vapor deposition processes are considered in this work. Either cradle-to-gate inventories or detailed experimental processes are collected from the literature for different synthesis routes. From the detailed experimental research found in the literature, cradle-to-gate inventories are developed for different synthesis routes. In this section, life cycle inventories used for MWCNT synthesis processes are presented.

Chemical Vapor Deposition

Table B10. Inventory used for **M-CVD1** for 1 kg MWCNT [53].

Input	Unit	Amount	Database
Cobalt	kg	0.0012	Ecoinvent 3
Citric acid	kg	0.0013	Ecoinvent 3
Nitrogen	kg	0.1024 ^a	Ecoinvent 3
Hydrogen	kg	0.0061 ^b	Ecoinvent 3
Acetylene	kg	1.0471 ^c	Ecoinvent 3
Lanthanum oxide	kg	0.00211	Ecoinvent 3
Electricity	MJ	954	USLCI
Output			
MWCNT	kg	1	-

^a Density of nitrogen = 1.251 g/L → 81.8 L nitrogen/1 kg MWCNT = 0.1024 kg/kg MWCNT.

^b Density of hydrogen = 0.0893 g/L → 68.2 L hydrogen/1 kg MWCNT = 0.0061 kg/kg MWCNT.

^c Density of acetylene = 1.097 g/L → 954.5 L acetylene/1 kg MWCNT = 1.0471 kg/kg MWCNT.

Table B11. Inventory used for **M-CVD2** for 1 kg MWCNT [54].

Input	Unit	Amount	Database
Magnesium oxide	kg	1.0968	Ecoinvent 3
Iron pellet	kg	0.4032	Ecoinvent 3
Argon	kg	1.388 ^a	Ecoinvent 3
Acetylene	kg	0.049 ^b	Ecoinvent 3
Hydrochloric acid	kg	119 ^c	Ecoinvent 3
Ethanol	kg	157.84 ^d	Ecoinvent 3
Electricity	MJ	626	USLCI
Output			
MWCNT	kg	1	-

^a Density of argon = 1.784 mg/cm³ → 778 cm³ argon/1 g MWCNT = 1.388 kg argon/kg MWCNT.

^b Density of acetylene = 1.171 mg/cm³ → 42 cm³ acetylene/1 g MWCNT = 0.049 kg/kg MWCNT.

^c Density of hydrochloric acid = 1.19 g/mL → 100 mL hydrochloric acid/1 g MWCNT = 119 kg/kg MWCNT.

^d Density of ethanol = 0.7892 g/mL → 200 mL ethanol/1 g MWCNT = 157.84 kg/kg MWCNT.

Table B12. Inventory used for 1 kg Ferrocene production [22].

Input	Unit	Amount	Database
Iron (III) chloride	kg	0.507	Ecoinvent 3
Iron scrap	kg	0.253	Ecoinvent 3
Deionized water	kg	6.647	Ecoinvent 3
Sodium metoxide	kg	0.715	Ecoinvent 3
Benzene	kg	0.776	Ecoinvent 3
Methanol	kg	2.776	Ecoinvent 3
Sulfuric acid	kg	18.882	Ecoinvent 3
Nitrogen	kg	0.002	Ecoinvent 3
Electricity	kWh	2.829	USLCI
Natural gas	kWh	0.124	USLCI
Output			
Wastewater-untreated, organic contaminated	kg	1	-
Ferrocene	kg	1	-

Table B13. Inventory used for **M-CVD3** for 1 kg MWCNT [22].

Input	Unit	Amount	Database
Ferrocene	kg	0.667	Table 12
Toluene	kg	28.9	Ecoinvent 3
Hydrogen	kg	0.823	Ecoinvent 3
Argon	kg	245.07	Ecoinvent 3
Hydrochloric acid	kg	78.93	Ecoinvent 3
Electricity	GJ	15.86	USLCI
Output			
MWCNT	kg	1	-

Table B14. Inventory used for **M-CVD4** for 1 kg MWCNT [33].

Input	Unit	Amount	Database
Camphor (palm oil)	kg	22.22	Ecoinvent 3
Ferrocene	kg	1.11	Table B12
Silicon wafer	m ²	0.67	Ecoinvent 3
Nitrogen	kg	39.04	Ecoinvent 3
Electricity	MJ	2480	USLCI
Output			
MWCNT	kg	1	-
Nitrogen -emissions to air-	kg	39.04	-
Camphor (palm oil) -emissions to treatment-	kg	11.11	-
VOCs -emissions to air-	kg	8.89	-
PAHs -emissions to air-	kg	0.11	-
Soot -emissions to air-	kg	2.22	-

Table B15. Inventory used for **M-CVD5** for 1 kg MWCNT [33].

Input	Unit	Amount	Database
Acetylene	kg	2.45	Ecoinvent 3
Nitrogen	kg	21.81	Ecoinvent 3
Electricity	MJ	1114	USLCI
Iron chloride, 40% in water	kg	0.16	Ecoinvent 3
Zeolite	kg	0.03	Ecoinvent 3
DI water	kg	0.29	Ecoinvent 3
Output			
MWCNT	kg	1	-
Nitrogen -emissions to air-	kg	21.81	-
Acetylene	kg	0.73	-
VOCs -emissions to air-	kg	0.53	-
PAHs -emissions to air-	kg	0.01	-
Soot -emissions to air-	kg	0.13	-

Table B16. Inventory used for **M-CVD6*** for 1 kg MWCNT [47].

Input	Unit	Amount	Database
Benzene	kg	13.146 ^a	Ecoinvent 3
Ferrocene	kg	0.15	Table B12
Hydrogen	kg	0.00054 ^b	Ecoinvent 3
Argon	kg	2.676 ^c	Ecoinvent 3
Water, decarbonized	kg	5	Ecoinvent 3
Hydrochloric acid	kg	30.417 ^d	Ecoinvent 3
Electricity	MJ	482	USLCI
Output			
MWCNT	kg	1	-

^a Density of benzene = 0.8765 g/mL → 300 mL benzene/20 g MWCNT = 13.146 kg benzene/kg MWCNT.

^b Density of hydrogen = 0.0893 g/L → 120 mL hydrogen/20 g MWCNT = 0.00054 kg hydrogen/kg MWCNT.

^c Density of argon = 1.784 mg/cm³ → 30 L argon/20 g MWCNT = 2.676 kg argon/kg MWCNT.

^d 5 M HCl = 182.5 g/20 g MWCNT → with 30% purity = 608.34 g/20 g MWCNT → 30.417 kg/kg MWCNT.

Arc Process

Table B17. Inventory used for **M-AP** for 1 kg MWCNT [55].

Input	Unit	Amount	Database
Nitrogen	kg	0.183 ^a	Ecoinvent 3
Carbon black	kg	0.0425	Ecoinvent 3
Electricity	MJ	65.92	USLCI
Output			
MWCNT	kg	1	-

^a Density of nitrogen = 1.251 g/L → 146.46 L nitrogen/1 kg MWCNT = 0.183 kg/kg MWCNT.

Table B18. Environmental impact categories of TRACI, CML, IMPACT 2002+ and ReCiPe impact assessment methods with their abbreviations and units.

Method	Environmental Impact Categories
TRACI [56]	ozone depletion (OD in kg CFC11-eq.), global warming (GW in kg CO ₂ -eq.), smog (PS in kg O ₃ -eq.), acidification (AC in kg SO ₂ -eq.), eutrophication (EU in kg N-eq.), carcinogenics (HHC in CTUh), non carcinogenics (HHNC in CTUh), respiratory effects (RE in kg PM _{2.5} -eq.), ecotoxicity (EC in CTUe), and fossil fuel depletion (FF in MJ surplus energy).
CML [57]	abiotic depletion (AD in kg Sb-eq.), abiotic depletion-fossil fuels (AD(FF) in MJ), global warming (GW100a in kg CO ₂ -eq.), ozone layer depletion (OD in kg CFC11-eq.), human toxicity (HT in kg 1,4-DB-eq.), fresh water aquatic ecotoxicity (FWAEC in kg 1,4-DB-eq.), marine aquatic ecotoxicity (MAEC in kg 1,4-DB-eq.), terrestrial ecotoxicity (TEC in kg 1,4-DB-eq.), photochemical oxidation (POx in kg C ₂ H ₄ -eq.), acidification (AC in kg SO ₂ -eq.), and eutrophication (EU in kg PO ₄ -eq.).
IMPACT 2002+ [58]	carcinogens (HHC in kg C ₂ H ₃ Cl-eq.), non-carcinogens (HHNC in kg C ₂ H ₃ Cl-eq.), respiratory inorganics (REI in kg PM _{2.5} -eq.), ionizing radiation (IR in Bq C-14-eq.), ozone layer depletion (OD in kg CFC11-eq.), respiratory organics (REO in kg C ₂ H ₄ -eq.), aquatic ecotoxicity (AEC in kg TEG water), terrestrial ecotoxicity (TEC in kg TEG soil), terrestrial acidification (TAC in kg SO ₂ -eq.), land occupation (LO in m ² org.arable), aquatic acidification (AAC in kg SO ₂ -eq.), aquatic eutrophication (AEU in kg PO ₄ P-lim), global warming (GW in kg CO ₂ -eq.), non-renewable energy (NRE in MJ primary), and mineral extraction (ME in MJ surplus).
ReCiPe [59]	climate change (GW in kg CO ₂ -eq.), ozone depletion (OD in kg CFC11-eq.), terrestrial acidification (tAC in kg SO ₂ -eq.), freshwater eutrophication (FWEU in kg P-eq.), marine eutrophication (MEU in kg N-eq.), human toxicity (HT in kg 1,4-DB-eq.), photochemical oxidant formation (POx in kg NMVOC), particulate matter formation (RE in kg PM ₁₀ -eq.), terrestrial ecotoxicity (TEC in kg 1,4-DB-eq.), freshwater ecotoxicity (FWAEC in kg 1,4-DB-eq.), marine ecotoxicity (MAEC in kg 1,4-DB-eq.), ionizing radiation (IR in kBq U235 eq.), agricultural land occupation (ALO in m ² a), urban land occupation (ULO in m ² a), natural land transformation (NLT in m ²), water depletion (WDP in m ³), metal depletion (MD in kg Fe eq.), and fossil depletion (FF in kg oil eq.).

Table B19. Uncertainties around each production process simulated by Monte Carlo Analysis (per 1 kg SWCNTs).

C1*	C2	S-CVD1	S-CVD2	S-HiPCO1	S-HiPCO2*	S-CoMoCat1	S-CoMoCat2*	S-AP	S-LV
AC	LB	1.66E+03	5.13E+03	2.76E+02	6.87E-02	9.93E+02	7.32E-02	6.84E+02	7.65E+02
	M	1.67E+03	5.14E+03	2.79E+02	8.34E-02	9.93E+02	9.39E-02	6.94E+02	7.65E+02
	UB	1.68E+03	5.14E+03	2.83E+02	1.09E-01	9.93E+02	1.26E-01	7.15E+02	7.65E+02
HHC	LB	3.81E-04	1.11E-03	6.39E-05	2.09E-07	2.14E-04	2.44E-07	1.85E-04	1.65E-04
	M	4.23E-04	1.12E-03	7.36E-05	4.02E-07	2.15E-04	4.89E-07	2.37E-04	1.65E-04
	UB	9.30E-04	1.31E-03	1.30E-04	2.29E-06	2.24E-04	3.33E-06	4.91E-04	1.66E-04
EC	LB	8.24E+04	2.34E+05	1.39E+04	4.96E+01	4.51E+04	6.27E+01	3.86E+04	3.46E+04
	M	9.28E+04	2.37E+05	1.67E+04	8.48E+01	4.53E+04	1.07E+02	4.73E+04	3.46E+04
	UB	1.24E+05	2.48E+05	3.17E+04	1.79E+02	4.58E+04	2.28E+02	8.42E+04	3.49E+04
EU	LB	2.74E+01	7.34E+01	4.68E+00	2.33E-02	1.41E+01	2.91E-02	1.30E+01	1.08E+01
	M	3.34E+01	7.57E+01	5.26E+00	4.58E-02	1.42E+01	5.79E-02	1.57E+01	1.08E+01
	UB	6.00E+01	8.66E+01	7.52E+00	1.24E-01	1.47E+01	1.50E-01	2.43E+01	1.09E+01
FF	LB	1.22E+05	3.75E+05	2.05E+04	3.23E+01	7.26E+04	3.81E+01	5.71E+04	5.58E+04
	M	1.23E+05	3.75E+05	2.11E+04	4.40E+01	7.26E+04	5.25E+01	6.43E+04	5.58E+04
	UB	1.26E+05	3.76E+05	2.24E+04	6.37E+01	7.27E+04	8.02E+01	7.90E+04	5.58E+04
GW	LB	1.95E+05	5.95E+05	3.27E+04	1.79E+01	1.15E+05	1.96E+01	8.10E+04	8.86E+04
	M	1.96E+05	5.96E+05	3.35E+04	2.03E+01	1.15E+05	2.29E+01	8.28E+04	8.86E+04
	UB	1.99E+05	5.97E+05	3.48E+04	2.33E+01	1.15E+05	2.69E+01	8.58E+04	8.86E+04
HHNC	LB	6.34E-03	1.91E-02	1.04E-03	1.41E-06	3.69E-03	1.66E-06	2.68E-03	2.84E-03
	M	6.61E-03	1.92E-02	1.11E-03	2.53E-06	3.69E-03	3.19E-06	2.92E-03	2.84E-03
	UB	7.90E-03	1.95E-02	1.55E-03	6.58E-06	3.72E-03	8.51E-06	4.17E-03	2.85E-03
OD	LB	1.80E-04	3.81E-05	6.22E-05	1.98E-06	1.25E-05	2.54E-06	5.06E-04	2.25E-06
	M	3.34E-04	7.19E-05	1.47E-04	3.74E-06	2.16E-05	4.80E-06	1.00E-03	2.64E-06
	UB	7.00E-04	1.67E-04	4.23E-04	8.31E-06	4.69E-05	1.13E-05	2.19E-03	3.45E-06
RE	LB	8.23E+01	2.49E+02	1.35E+01	7.78E-03	4.81E+01	9.20E-03	3.47E+01	3.71E+01
	M	8.44E+01	2.50E+02	1.38E+01	9.62E-03	4.82E+01	1.16E-02	3.59E+01	3.71E+01
	UB	9.05E+01	2.53E+02	1.44E+01	1.22E-02	4.82E+01	1.48E-02	3.80E+01	3.71E+01
PS	LB	1.30E+04	4.00E+04	2.16E+03	5.77E-01	7.74E+03	6.52E-01	5.33E+03	5.96E+03
	M	1.30E+04	4.00E+04	2.20E+03	7.15E-01	7.74E+03	8.35E-01	5.40E+03	5.96E+03
	UB	1.32E+04	4.01E+04	2.26E+03	9.58E-01	7.74E+03	1.17E+00	5.55E+03	5.96E+03
CED	LB	2.70E+06	8.34E+06	4.45E+05	3.24E+02	1.61E+06	3.80E+02	1.14E+06	1.24E+06
	M	2.72E+06	8.35E+06	4.50E+05	4.36E+02	1.61E+06	5.25E+02	1.19E+06	1.24E+06
	UB	2.77E+06	8.36E+06	4.60E+05	6.34E+02	1.61E+06	7.79E+02	1.31E+06	1.24E+06

C1: Environmental impact categories considered in the current study.

C2: Lower bound (LB), median (M) and upper bound (UB) of emissions based on 95% confidence intervals for the uncertainties.

* OD in kg CFC11-eq., GW in kg CO₂-eq., PS in kg O₃-eq., AC in kg SO₂-eq., EU in kg N-eq., HHC in CTUh, HHNC in CTUh, RE in kg PM_{2.5}-eq., EC in CTUe, FF in MJ surplus energy, CED in MJ.

Table B20. Uncertainties around each production process simulated by Monte Carlo Analysis (per 1 kg MWCNTs).

C1*	C2	M-CVD1	M-CVD2	M-CVD3	M-CVD4	M-CVD5	M-CVD6*	M-AP
AC	LB	1.79E+00	2.11E+00	3.11E+01	5.21E+00	2.15E+00	1.08E+00	1.24E-01
	M	1.81E+00	2.39E+00	3.27E+01	5.32E+00	2.19E+00	1.13E+00	1.24E-01
	UB	1.84E+00	2.82E+00	3.70E+01	5.48E+00	2.27E+00	1.21E+00	1.24E-01
HHC	LB	4.36E-07	6.44E-06	1.36E-05	3.20E-06	7.68E-07	1.31E-06	2.77E-08
	M	5.32E-07	1.26E-05	2.52E-05	4.56E-06	1.11E-06	2.43E-06	2.94E-08
	UB	2.08E-06	4.89E-05	1.60E-04	1.80E-05	5.46E-06	7.22E-06	4.58E-08
EC	LB	9.68E+01	1.39E+03	3.26E+03	5.89E+02	1.70E+02	2.99E+02	5.88E+00
	M	1.17E+02	2.78E+03	5.97E+03	8.08E+02	2.31E+02	5.73E+02	6.19E+00
	UB	1.79E+02	7.22E+03	1.36E+04	1.49E+03	4.55E+02	1.69E+03	7.15E+00
EU	LB	3.25E-02	7.52E-01	1.21E+00	4.01E-01	6.33E-02	6.25E-02	1.95E-03
	M	4.67E-02	1.30E+00	2.75E+00	5.90E-01	1.14E-01	1.21E-01	2.14E-03
	UB	8.94E-02	2.80E+00	9.72E+00	1.11E+00	2.70E-01	3.30E-01	2.75E-03
FF	LB	1.32E+02	8.59E+02	2.62E+03	4.27E+02	1.62E+02	2.05E+02	9.35E+00
	M	1.34E+02	1.16E+03	2.85E+03	4.46E+02	1.67E+02	2.12E+02	9.55E+00
	UB	1.38E+02	1.57E+03	3.43E+03	4.70E+02	1.76E+02	2.23E+02	9.88E+00
GW	LB	2.09E+02	3.75E+02	3.72E+03	6.70E+02	2.56E+02	1.41E+02	1.44E+01
	M	2.12E+02	4.41E+02	4.06E+03	7.02E+02	2.64E+02	1.49E+02	1.44E+01
	UB	2.18E+02	5.40E+02	4.92E+03	7.41E+02	2.78E+02	1.63E+02	1.45E+01
HHNC	LB	6.97E-06	5.66E-05	1.52E-04	1.41E-05	9.41E-06	7.90E-06	4.64E-07
	M	7.55E-06	1.05E-04	2.24E-04	2.53E-05	1.13E-05	1.43E-05	4.73E-07
	UB	9.70E-06	3.28E-04	5.51E-04	6.18E-05	2.05E-05	5.61E-05	5.10E-07
OD	LB	1.88E-07	5.22E-05	7.29E-05	6.93E-06	9.42E-07	1.49E-05	2.65E-08
	M	3.79E-07	9.20E-05	1.23E-04	9.58E-06	1.52E-06	2.81E-05	5.86E-08
	UB	8.40E-07	1.73E-04	2.29E-04	1.58E-05	2.77E-06	6.00E-05	1.51E-07
RE	LB	9.22E-02	1.77E-01	1.88E+00	3.80E-01	1.31E-01	6.99E-02	6.12E-03
	M	9.84E-02	2.22E-01	2.51E+00	4.30E-01	1.48E-01	8.35E-02	6.19E-03
	UB	1.10E-01	3.07E-01	4.16E+00	4.92E-01	1.79E-01	1.11E-01	6.34E-03
PS	LB	1.40E+01	2.48E+01	2.48E+02	7.30E+01	1.89E+01	9.68E+00	9.63E-01
	M	1.42E+01	2.86E+01	2.64E+02	7.39E+01	1.93E+01	1.04E+01	9.65E-01
	UB	1.44E+01	3.39E+01	3.07E+02	7.52E+01	2.00E+01	1.14E+01	9.70E-01
CED	LB	2.93E+03	9.22E+03	5.46E+04	9.55E+03	3.59E+03	2.73E+03	2.03E+02
	M	2.98E+03	1.19E+04	5.99E+04	1.01E+04	3.72E+03	2.92E+03	2.05E+02
	UB	3.06E+03	1.61E+04	7.47E+04	1.10E+04	3.94E+03	3.28E+03	2.07E+02

C1: Environmental impact categories considered in the current study.

C2: Lower bound (LB), median (M) and upper bound (UB) of emissions based on 95% confidence intervals for the uncertainties.

* OD in kg CFC11-eq., GW in kg CO₂-eq., PS in kg O₃-eq., AC in kg SO₂-eq., EU in kg N-eq., HHC in CTUh, HHNC in CTUh, RE in kg PM_{2.5}-eq., EC in CTUe, FF in MJ surplus energy, CED in MJ.

Table B21. Uncertainties around each production process (large scale-S1) simulated by Monte Carlo Analysis (per 1 kg SWCNTs).

C1*	C2	S-CVD1	S-CVD2	S-HiPCO1	S-CoMoCat1	S-AP	S-LV
AC	LB	2.20E+02	6.68E+02	3.83E+01	1.29E+02	9.31E+01	9.94E+01
	M	2.23E+02	6.68E+02	3.96E+01	1.29E+02	9.59E+01	9.95E+01
	UB	2.29E+02	6.71E+02	4.16E+01	1.29E+02	1.00E+02	9.96E+01
HHC	LB	5.67E-05	1.45E-04	1.00E-05	2.81E-05	2.63E-05	2.14E-05
	M	7.55E-05	1.50E-04	1.46E-05	2.84E-05	3.74E-05	2.15E-05
	UB	2.95E-04	2.17E-04	4.35E-05	3.18E-05	1.03E-04	2.21E-05
EC	LB	1.30E+04	3.07E+04	2.35E+03	5.92E+03	5.71E+03	4.51E+03
	M	1.70E+04	3.17E+04	3.76E+03	5.99E+03	8.97E+03	4.54E+03
	UB	2.88E+04	3.56E+04	1.05E+04	6.19E+03	2.34E+04	4.67E+03
EU	LB	4.72E+00	9.71E+00	8.95E-01	1.86E+00	2.19E+00	1.41E+00
	M	7.11E+00	1.05E+01	1.14E+00	1.91E+00	2.74E+00	1.42E+00
	UB	1.59E+01	1.35E+01	2.07E+00	2.05E+00	5.09E+00	1.44E+00
FF	LB	1.64E+04	4.88E+04	2.91E+03	9.45E+03	7.40E+03	7.26E+03
	M	1.69E+04	4.89E+04	3.23E+03	9.48E+03	8.21E+03	7.26E+03
	UB	1.79E+04	4.92E+04	3.86E+03	9.52E+03	9.64E+03	7.26E+03
GW	LB	2.61E+04	7.74E+04	4.79E+03	1.50E+04	1.15E+04	1.15E+04
	M	2.68E+04	7.76E+04	5.20E+03	1.50E+04	1.23E+04	1.15E+04
	UB	2.81E+04	7.80E+04	5.88E+03	1.50E+04	1.37E+04	1.15E+04
HHNC	LB	8.73E-04	2.49E-03	1.51E-04	4.81E-04	3.68E-04	3.69E-04
	M	9.88E-04	2.52E-03	1.83E-04	4.83E-04	4.46E-04	3.70E-04
	UB	1.42E-03	2.67E-03	4.18E-04	4.93E-04	8.92E-04	3.76E-04
OD	LB	7.56E-05	8.54E-06	2.97E-05	4.68E-06	7.97E-05	5.09E-07
	M	1.43E-04	2.04E-05	7.19E-05	7.98E-06	1.74E-04	6.98E-07
	UB	3.22E-04	5.46E-05	2.02E-04	1.62E-05	4.71E-04	1.10E-06
RE	LB	1.14E+01	3.25E+01	1.91E+00	6.27E+00	4.69E+00	4.82E+00
	M	1.22E+01	3.28E+01	2.03E+00	6.27E+00	4.97E+00	4.82E+00
	UB	1.45E+01	3.37E+01	2.36E+00	6.28E+00	5.63E+00	4.83E+00
PS	LB	1.72E+03	5.20E+03	3.02E+02	1.01E+03	7.30E+02	7.75E+02
	M	1.76E+03	5.21E+03	3.20E+02	1.01E+03	7.67E+02	7.75E+02
	UB	1.82E+03	5.23E+03	3.53E+02	1.01E+03	8.37E+02	7.75E+02
CED	LB	3.59E+05	1.08E+06	6.00E+04	2.10E+05	1.49E+05	1.61E+05
	M	3.67E+05	1.09E+06	6.25E+04	2.10E+05	1.55E+05	1.61E+05
	UB	3.87E+05	1.10E+06	6.77E+04	2.11E+05	1.66E+05	1.61E+05

C1: Environmental impact categories considered in the current study.

C2: Lower bound (LB), median (M) and upper bound (UB) of emissions based on 95% confidence intervals for the uncertainties.

* OD in kg CFC11-eq., GW in kg CO₂-eq., PS in kg O₃-eq., AC in kg SO₂-eq., EU in kg N-eq., HHC in CTUh, HHNC in CTUh, RE in kg PM_{2.5}-eq., EC in CTUe, FF in MJ surplus energy, CED in MJ.

Table B22. Uncertainties around each production process (large scale-S1) simulated by Monte Carlo Analysis (per 1 kg MWCNTs).

C1*	C2	M-CVD1	M-CVD2	M-CVD3	M-CVD4	M-CVD5	M-AP
AC	LB	2.32E-01	6.24E-01	4.38E+00	8.23E-01	2.84E-01	1.61E-02
	M	2.33E-01	7.65E-01	5.01E+00	8.76E-01	2.91E-01	1.61E-02
	UB	2.34E-01	9.78E-01	6.74E+00	9.69E-01	3.02E-01	1.62E-02
HHC	LB	5.33E-08	3.06E-06	3.43E-06	1.55E-06	2.01E-07	3.70E-09
	M	5.77E-08	6.48E-06	8.20E-06	2.10E-06	2.53E-07	4.10E-09
	UB	1.13E-07	2.61E-05	6.19E-05	7.78E-06	8.67E-07	1.03E-08
EC	LB	1.14E+01	6.92E+02	1.02E+03	1.67E+02	2.63E+01	8.05E-01
	M	1.23E+01	1.37E+03	2.04E+03	2.71E+02	3.75E+01	8.85E-01
	UB	1.51E+01	3.57E+03	5.18E+03	5.51E+02	6.44E+01	1.13E+00
EU	LB	3.66E-03	3.82E-01	3.41E-01	8.55E-02	1.01E-02	2.73E-04
	M	4.26E-03	6.42E-01	9.29E-01	1.61E-01	1.91E-02	3.36E-04
	UB	6.43E-03	1.44E+00	3.73E+00	4.24E-01	4.91E-02	5.90E-04
FF	LB	1.70E+01	4.04E+02	3.70E+02	8.50E+01	2.16E+01	1.20E+00
	M	1.71E+01	5.51E+02	4.56E+02	9.42E+01	2.25E+01	1.21E+00
	UB	1.73E+01	7.82E+02	6.91E+02	1.08E+02	2.39E+01	1.22E+00
GW	LB	2.70E+01	1.39E+02	5.43E+02	1.04E+02	3.41E+01	1.88E+00
	M	2.71E+01	1.71E+02	6.64E+02	1.12E+02	3.55E+01	1.89E+00
	UB	2.73E+01	2.18E+02	1.00E+03	1.27E+02	3.77E+01	1.90E+00
HHNC	LB	8.81E-07	2.70E-05	3.31E-05	5.38E-06	1.34E-06	6.13E-08
	M	9.06E-07	5.09E-05	6.07E-05	8.50E-06	1.66E-06	6.37E-08
	UB	1.04E-06	1.52E-04	1.73E-04	2.42E-05	2.89E-06	7.40E-08
OD	LB	1.33E-08	2.71E-05	2.79E-05	3.20E-06	2.00E-07	2.37E-09
	M	2.21E-08	4.67E-05	5.22E-05	4.42E-06	2.99E-07	3.94E-09
	UB	4.39E-08	8.72E-05	9.22E-05	7.21E-06	5.24E-07	8.12E-09
RE	LB	1.15E-02	6.88E-02	3.54E-01	8.33E-02	1.89E-02	8.15E-04
	M	1.18E-02	8.98E-02	5.80E-01	1.03E-01	2.16E-02	8.38E-04
	UB	1.22E-02	1.29E-01	1.30E+00	1.34E-01	2.64E-02	8.75E-04
PS	LB	1.81E+00	8.96E+00	3.65E+01	3.84E+01	4.15E+00	1.26E-01
	M	1.82E+00	1.10E+01	4.25E+01	3.88E+01	4.22E+00	1.26E-01
	UB	1.83E+00	1.35E+01	5.91E+01	3.95E+01	4.33E+00	1.27E-01
CED	LB	3.78E+02	3.79E+03	8.22E+03	1.61E+03	4.78E+02	2.64E+01
	M	3.80E+02	5.18E+03	1.03E+04	1.79E+03	4.99E+02	2.65E+01
	UB	3.84E+02	7.26E+03	1.63E+04	2.07E+03	5.39E+02	2.68E+01

C1: Environmental impact categories considered in the current study.

C2: Lower bound (LB), median (M) and upper bound (UB) of emissions based on 95% confidence intervals for the uncertainties.

* OD in kg CFC11-eq., GW in kg CO₂-eq., PS in kg O₃-eq., AC in kg SO₂-eq., EU in kg N-eq., HHC in CTUh, HHNC in CTUh, RE in kg PM_{2.5}-eq., EC in CTUe, FF in MJ surplus energy, CED in MJ.

Table B23. Uncertainties around each production process (large scale-S2) simulated by Monte Carlo Analysis (per 1 kg SWCNTs).

C1*	C2	S-CVD1	S-CVD2	S-HiPCO1	S-CoMoCat1	S-AP	S-LV
AC	LB	1.92E+02	5.66E+02	3.69E+01	1.11E+02	1.00E+02	8.42E+01
	M	1.95E+02	5.68E+02	4.00E+01	1.11E+02	1.09E+02	8.42E+01
	UB	2.00E+02	5.70E+02	4.40E+01	1.12E+02	1.22E+02	8.44E+01
HHC	LB	6.16E-05	1.27E-04	1.67E-05	3.01E-05	5.58E-05	1.82E-05
	M	8.73E-05	1.38E-04	3.03E-05	3.83E-05	1.05E-04	1.84E-05
	UB	2.85E-04	2.60E-04	1.08E-04	1.42E-04	3.59E-04	1.95E-05
EC	LB	1.54E+04	2.75E+04	4.37E+03	6.91E+03	1.13E+04	3.84E+03
	M	2.05E+04	2.95E+04	8.06E+03	8.69E+03	2.34E+04	3.90E+03
	UB	3.99E+04	3.51E+04	2.25E+04	1.42E+04	7.60E+04	4.15E+03
EU	LB	5.70E+00	8.86E+00	1.86E+00	2.37E+00	6.11E+00	1.21E+00
	M	7.79E+00	1.03E+01	2.91E+00	3.50E+00	9.12E+00	1.22E+00
	UB	1.37E+01	1.52E+01	6.32E+00	8.13E+00	1.58E+01	1.26E+00
FF	LB	1.49E+04	4.16E+04	3.43E+03	8.84E+03	2.19E+04	6.15E+03
	M	1.56E+04	4.18E+04	4.41E+03	9.43E+03	3.00E+04	6.15E+03
	UB	1.69E+04	4.21E+04	5.92E+03	1.06E+04	4.30E+04	6.15E+03
GW	LB	3.34E+04	6.58E+04	5.03E+03	1.31E+04	1.48E+04	9.75E+03
	M	3.43E+04	6.61E+04	5.82E+03	1.32E+04	1.72E+04	9.76E+03
	UB	3.57E+04	6.66E+04	7.12E+03	1.34E+04	2.10E+04	9.76E+03
HHNC	LB	1.02E-03	2.14E-03	1.85E-04	4.53E-04	4.99E-04	3.13E-04
	M	1.31E-03	2.20E-03	2.83E-04	5.00E-04	7.91E-04	3.15E-04
	UB	2.47E-03	2.41E-03	9.66E-04	7.08E-04	2.65E-03	3.27E-04
OD	LB	1.34E-04	2.78E-05	1.11E-04	8.84E-05	1.12E-03	8.08E-07
	M	2.32E-04	4.66E-05	2.47E-04	1.65E-04	2.48E-03	1.18E-06
	UB	5.52E-04	8.83E-05	6.34E-04	4.26E-04	6.79E-03	2.27E-06
RE	LB	1.05E+01	2.81E+01	2.03E+00	5.49E+00	6.57E+00	4.09E+00
	M	1.11E+01	2.87E+01	2.30E+00	5.57E+00	8.05E+00	4.09E+00
	UB	1.20E+01	2.98E+01	2.93E+00	5.69E+00	1.21E+01	4.10E+00
PS	LB	1.53E+03	4.42E+03	3.05E+02	8.65E+02	8.01E+02	6.56E+02
	M	1.57E+03	4.43E+03	3.41E+02	8.71E+02	8.93E+02	6.56E+02
	UB	1.64E+03	4.46E+03	4.09E+02	8.82E+02	1.09E+03	6.56E+02
CED	LB	3.28E+05	9.23E+05	6.06E+04	1.87E+05	2.38E+05	1.37E+05
	M	3.40E+05	9.27E+05	6.78E+04	1.93E+05	2.95E+05	1.37E+05
	UB	3.59E+05	9.35E+05	8.28E+04	2.03E+05	3.96E+05	1.37E+05

C1: Environmental impact categories considered in the current study.

C2: Lower bound (LB), median (M) and upper bound (UB) of emissions based on 95% confidence intervals for the uncertainties.

* OD in kg CFC11-eq., GW in kg CO₂-eq., PS in kg O₃-eq., AC in kg SO₂-eq., EU in kg N-eq., HHC in CTUh, HHNC in CTUh, RE in kg PM_{2.5}-eq., EC in CTUe, FF in MJ surplus energy, CED in MJ.

Table B24. Uncertainties around each production process (large scale-S2) simulated by Monte Carlo Analysis (per 1 kg MWCNTs).

C1*	C2	M-CVD1	M-CVD2	M-CVD3	M-CVD4	M-CVD5	M-AP
AC	LB	3.37E-01	1.07E+00	4.80E+00	1.99E+00	5.81E-01	1.62E-02
	M	4.79E-01	1.35E+00	5.02E+00	2.37E+00	9.08E-01	1.77E-02
	UB	7.73E-01	1.78E+00	5.46E+00	2.84E+00	1.59E+00	2.06E-02
HHC	LB	5.13E-07	6.60E-06	7.42E-06	4.58E-06	1.28E-06	7.82E-09
	M	1.41E-06	1.29E-05	1.41E-05	7.19E-06	3.50E-06	1.56E-08
	UB	1.20E-05	6.55E-05	3.94E-05	1.96E-05	3.37E-05	5.25E-08
EC	LB	1.68E+02	1.38E+03	1.31E+03	1.02E+03	3.96E+02	1.39E+00
	M	3.68E+02	2.72E+03	2.24E+03	1.46E+03	8.58E+02	2.77E+00
	UB	9.32E+02	6.92E+03	5.02E+03	2.51E+03	2.13E+03	1.10E+01
EU	LB	7.52E-02	7.54E-01	3.15E-01	1.67E+00	1.82E-01	9.15E-04
	M	2.17E-01	1.26E+00	5.89E-01	2.45E+00	4.96E-01	1.45E-03
	UB	7.19E-01	3.03E+00	1.43E+00	3.57E+00	1.61E+00	2.69E-03
FF	LB	3.34E+01	7.97E+02	2.90E+03	1.58E+02	6.25E+01	4.10E+00
	M	5.23E+01	1.08E+03	2.93E+03	1.86E+02	1.06E+02	6.19E+00
	UB	8.88E+01	1.49E+03	2.99E+03	2.24E+02	1.95E+02	9.56E+00
GW	LB	5.05E+01	2.55E+02	8.79E+02	7.16E+02	9.62E+01	2.25E+00
	M	7.90E+01	3.19E+02	9.17E+02	9.46E+02	1.61E+02	2.61E+00
	UB	1.35E+02	4.08E+02	1.01E+03	1.25E+03	3.00E+02	3.20E+00
HHNC	LB	4.54E-06	5.28E-05	3.11E-05	-1.14E-04	9.76E-06	7.54E-08
	M	1.02E-05	1.01E-04	5.31E-05	-5.65E-05	2.23E-05	1.09E-07
	UB	3.31E-05	2.82E-04	1.77E-04	9.39E-05	7.23E-05	3.95E-07
OD	LB	1.66E-06	5.32E-05	4.92E-05	9.12E-06	4.13E-06	2.21E-07
	M	3.58E-06	9.29E-05	8.46E-05	1.33E-05	8.53E-06	5.22E-07
	UB	7.72E-06	1.71E-04	1.53E-04	2.25E-05	1.91E-05	1.44E-06
RE	LB	6.57E-02	1.28E-01	3.56E-01	4.60E-01	1.54E-01	1.05E-03
	M	1.27E-01	1.72E-01	4.30E-01	6.50E-01	2.87E-01	1.39E-03
	UB	2.50E-01	2.56E-01	6.02E-01	1.04E+00	6.01E-01	2.42E-03
PS	LB	3.05E+00	1.67E+01	4.67E+01	5.00E+01	7.46E+00	1.24E-01
	M	4.50E+00	2.06E+01	4.93E+01	5.43E+01	1.08E+01	1.37E-01
	UB	7.34E+00	2.57E+01	5.39E+01	6.04E+01	1.78E+01	1.68E-01
CED	LB	7.38E+02	7.43E+03	2.52E+04	9.44E+03	1.37E+03	4.54E+01
	M	1.17E+03	1.02E+04	2.60E+04	1.23E+04	2.31E+03	5.89E+01
	UB	2.00E+03	1.41E+04	2.78E+04	1.65E+04	4.34E+03	8.45E+01

C1: Environmental impact categories considered in the current study.

C2: Lower bound (LB), median (M) and upper bound (UB) of emissions based on 95% confidence intervals for the uncertainties.

* OD in kg CFC11-eq., GW in kg CO₂-eq., PS in kg O₃-eq., AC in kg SO₂-eq., EU in kg N-eq., HHC in CTUh, HHNC in CTUh, RE in kg PM_{2.5}-eq., EC in CTUe, FF in MJ surplus energy, CED in MJ.

Table B25. Uncertainties around each production process (large scale-S3) simulated by Monte Carlo Analysis (per 1 kg SWCNTs).

C1*	C2	S-CVD1	S-CVD2	S-HiPCO1	S-CoMoCat1	S-AP	S-LV
AC	LB	2.55E+02	7.90E+02	4.25E+01	1.53E+02	1.05E+02	1.18E+02
	M	2.56E+02	7.90E+02	4.29E+01	1.53E+02	1.07E+02	1.18E+02
	UB	2.59E+02	7.91E+02	4.35E+01	1.53E+02	1.10E+02	1.18E+02
HHC	LB	5.86E-05	1.71E-04	9.83E-06	3.30E-05	2.84E-05	2.53E-05
	M	6.50E-05	1.73E-04	1.13E-05	3.31E-05	3.64E-05	2.53E-05
	UB	1.43E-04	2.01E-04	2.00E-05	3.45E-05	7.55E-05	2.55E-05
EC	LB	1.27E+04	3.59E+04	2.14E+03	6.94E+03	5.93E+03	5.32E+03
	M	1.43E+04	3.64E+04	2.56E+03	6.97E+03	7.28E+03	5.33E+03
	UB	1.91E+04	3.82E+04	4.88E+03	7.05E+03	1.30E+04	5.37E+03
EU	LB	4.22E+00	1.13E+01	7.19E-01	2.18E+00	2.00E+00	1.67E+00
	M	5.13E+00	1.16E+01	8.09E-01	2.19E+00	2.41E+00	1.67E+00
	UB	9.23E+00	1.33E+01	1.16E+00	2.26E+00	3.73E+00	1.68E+00
FF	LB	1.88E+04	5.77E+04	3.15E+03	1.12E+04	8.78E+03	8.59E+03
	M	1.90E+04	5.77E+04	3.25E+03	1.12E+04	9.89E+03	8.59E+03
	UB	1.94E+04	5.79E+04	3.45E+03	1.12E+04	1.21E+04	8.59E+03
GW	LB	3.00E+04	9.16E+04	5.03E+03	1.77E+04	1.25E+04	1.36E+04
	M	3.02E+04	9.16E+04	5.16E+03	1.77E+04	1.27E+04	1.36E+04
	UB	3.07E+04	9.18E+04	5.36E+03	1.77E+04	1.32E+04	1.36E+04
HHNC	LB	9.76E-04	2.94E-03	1.60E-04	5.67E-04	4.12E-04	4.36E-04
	M	1.02E-03	2.95E-03	1.71E-04	5.68E-04	4.49E-04	4.37E-04
	UB	1.21E-03	3.01E-03	2.39E-04	5.72E-04	6.41E-04	4.38E-04
OD	LB	2.76E-05	5.86E-06	9.57E-06	1.93E-06	7.79E-05	3.46E-07
	M	5.13E-05	1.11E-05	2.25E-05	3.32E-06	1.54E-04	4.05E-07
	UB	1.08E-04	2.57E-05	6.51E-05	7.22E-06	3.37E-04	5.30E-07
RE	LB	1.27E+01	3.84E+01	2.08E+00	7.41E+00	5.33E+00	5.70E+00
	M	1.30E+01	3.85E+01	2.12E+00	7.41E+00	5.53E+00	5.70E+00
	UB	1.39E+01	3.89E+01	2.22E+00	7.41E+00	5.85E+00	5.71E+00
PS	LB	1.99E+03	6.15E+03	3.33E+02	1.19E+03	8.19E+02	9.16E+02
	M	2.00E+03	6.16E+03	3.38E+02	1.19E+03	8.31E+02	9.16E+02
	UB	2.03E+03	6.17E+03	3.47E+02	1.19E+03	8.54E+02	9.16E+02
CED	LB	4.16E+05	1.28E+06	6.84E+04	2.48E+05	1.76E+05	1.91E+05
	M	4.19E+05	1.28E+06	6.92E+04	2.48E+05	1.83E+05	1.91E+05
	UB	4.27E+05	1.29E+06	7.07E+04	2.48E+05	2.02E+05	1.91E+05

C1: Environmental impact categories considered in the current study.

C2: Lower bound (LB), median (M) and upper bound (UB) of emissions based on 95% confidence intervals for the uncertainties.

* OD in kg CFC11-eq., GW in kg CO₂-eq., PS in kg O₃-eq., AC in kg SO₂-eq., EU in kg N-eq., HHC in CTUh, HHNC in CTUh, RE in kg PM_{2.5}-eq., EC in CTUe, FF in MJ surplus energy, CED in MJ.

Table B26. Uncertainties around each production process (large scale-S3) simulated by Monte Carlo Analysis (per 1 kg MWCNTs).

C1*	C2	M-CVD1	M-CVD2	M-CVD3	M-CVD4	M-CVD5	M-AP
AC	LB	2.76E-01	3.24E-01	4.78E+00	8.02E-01	3.31E-01	1.90E-02
	M	2.78E-01	3.68E-01	5.03E+00	8.19E-01	3.38E-01	1.90E-02
	UB	2.83E-01	4.34E-01	5.69E+00	8.43E-01	3.49E-01	1.91E-02
HHC	LB	6.71E-08	9.91E-07	2.10E-06	4.92E-07	1.18E-07	4.27E-09
	M	8.18E-08	1.94E-06	3.88E-06	7.02E-07	1.70E-07	4.52E-09
	UB	3.20E-07	7.52E-06	2.46E-05	2.77E-06	8.40E-07	7.04E-09
EC	LB	1.49E+01	2.15E+02	5.01E+02	9.06E+01	2.62E+01	9.05E-01
	M	1.80E+01	4.28E+02	9.18E+02	1.24E+02	3.56E+01	9.52E-01
	UB	2.75E+01	1.11E+03	2.10E+03	2.29E+02	7.00E+01	1.10E+00
EU	LB	4.99E-03	1.16E-01	1.86E-01	6.17E-02	9.74E-03	3.00E-04
	M	7.18E-03	2.00E-01	4.23E-01	9.07E-02	1.75E-02	3.29E-04
	UB	1.37E-02	4.30E-01	1.50E+00	1.71E-01	4.16E-02	4.24E-04
FF	LB	2.03E+01	1.32E+02	4.03E+02	6.57E+01	2.49E+01	1.44E+00
	M	2.06E+01	1.78E+02	4.39E+02	6.87E+01	2.57E+01	1.47E+00
	UB	2.12E+01	2.42E+02	5.28E+02	7.23E+01	2.71E+01	1.52E+00
GW	LB	3.22E+01	5.77E+01	5.73E+02	1.03E+02	3.94E+01	2.21E+00
	M	3.26E+01	6.79E+01	6.25E+02	1.08E+02	4.06E+01	2.22E+00
	UB	3.35E+01	8.30E+01	7.57E+02	1.14E+02	4.27E+01	2.23E+00
HHNC	LB	1.07E-06	8.70E-06	2.34E-05	2.16E-06	1.45E-06	7.14E-08
	M	1.16E-06	1.61E-05	3.45E-05	3.89E-06	1.74E-06	7.28E-08
	UB	1.49E-06	5.05E-05	8.47E-05	9.51E-06	3.15E-06	7.84E-08
OD	LB	2.90E-08	8.03E-06	1.12E-05	1.07E-06	1.45E-07	4.07E-09
	M	5.84E-08	1.42E-05	1.89E-05	1.47E-06	2.34E-07	9.02E-09
	UB	1.29E-07	2.66E-05	3.52E-05	2.44E-06	4.26E-07	2.32E-08
RE	LB	1.42E-02	2.72E-02	2.89E-01	5.84E-02	2.01E-02	9.41E-04
	M	1.51E-02	3.42E-02	3.87E-01	6.61E-02	2.28E-02	9.53E-04
	UB	1.69E-02	4.73E-02	6.40E-01	7.57E-02	2.76E-02	9.76E-04
PS	LB	2.16E+00	3.81E+00	3.81E+01	1.12E+01	2.90E+00	1.48E-01
	M	2.18E+00	4.40E+00	4.07E+01	1.14E+01	2.97E+00	1.49E-01
	UB	2.22E+00	5.22E+00	4.73E+01	1.16E+01	3.08E+00	1.49E-01
CED	LB	4.51E+02	1.42E+03	8.40E+03	1.47E+03	5.52E+02	3.12E+01
	M	4.58E+02	1.82E+03	9.21E+03	1.56E+03	5.72E+02	3.15E+01
	UB	4.71E+02	2.48E+03	1.15E+04	1.70E+03	6.07E+02	3.19E+01

C1: Environmental impact categories considered in the current study.

C2: Lower bound (LB), median (M) and upper bound (UB) of emissions based on 95% confidence intervals for the uncertainties.

* OD in kg CFC11-eq., GW in kg CO₂-eq., PS in kg O₃-eq., AC in kg SO₂-eq., EU in kg N-eq., HHC in CTUh, HHNC in CTUh, RE in kg PM_{2.5}-eq., EC in CTUe, FF in MJ surplus energy, CED in MJ.

Table B27. Characterization results of multiple synthesis processes for 1 kg CNTs (S- and M-) using CML (baseline) Method.

Routes	AD (kg Sb- eq.)	AD(FF) (MJ)	GW 100a (kg CO ₂ - eq)	OD (kg CFC11- eq)	HT (kg 1,4-DB- eq)	FWAEC (kg 1,4-DB- eq)	MAEC (kg 1,4-DB- eq)	TEC (kg 1,4-DB- eq)	Pox (kg C ₂ H ₄ - eq)	AC (kg SO ₂ -eq)	EU (kg PO ₄ - eq)
S-CVD1	6.73E-03	2.71E+06	1.97E+05	2.91E-04	4.68E+04	7.49E+03	2.29E+08	1.04E+02	1.58E+02	1.78E+03	7.16E+01
S-CVD2	5.99E-04	8.34E+06	5.96E+05	6.01E-05	1.42E+05	2.05E+04	7.03E+08	3.05E+02	4.89E+02	5.49E+03	1.99E+02
S-HiPCO1	3.68E-03	4.49E+05	3.36E+04	1.30E-04	7.89E+03	1.22E+03	3.74E+07	1.72E+01	2.63E+01	2.97E+02	1.34E+01
S-HiPCO2*	3.11E-05	3.81E+02	2.03E+01	3.23E-06	6.18E+00	4.31E+00	1.50E+04	2.72E-02	5.41E-03	8.93E-02	2.43E-02
S-CoMoCat1	1.69E-04	1.61E+06	1.15E+05	1.82E-05	2.74E+04	3.94E+03	1.36E+08	5.89E+01	9.47E+01	1.06E+03	3.83E+01
S-CoMoCat2*	3.93E-05	4.56E+02	2.30E+01	4.17E-06	7.17E+00	5.46E+00	1.76E+04	3.40E-02	2.15E-02	1.01E-01	3.06E-02
S-AP	9.90E-03	1.20E+06	8.29E+04	8.50E-04	1.99E+04	3.36E+03	9.27E+07	4.39E+01	6.43E+01	7.42E+02	3.35E+01
S-LV	1.97E-05	1.24E+06	8.86E+04	1.67E-06	2.11E+04	3.02E+03	1.05E+08	4.52E+01	7.29E+01	8.18E+02	2.94E+01
M-CVD1	7.61E-06	2.96E+03	2.12E+02	3.20E-07	5.12E+01	9.14E+00	2.52E+05	1.18E-01	1.72E-01	1.94E+00	8.09E-02
M-CVD2	1.64E-03	1.04E+04	4.45E+02	9.47E-05	1.67E+02	1.18E+02	4.76E+05	1.81E+00	3.69E-01	2.52E+00	7.06E-01
M-CVD3	1.36E-03	5.74E+04	4.13E+03	1.20E-04	1.07E+03	3.77E+02	4.98E+06	3.31E+00	2.97E+00	3.53E+01	2.58E+00
M-CVD4	1.73E-04	8.78E+03	7.04E+02	8.23E-06	1.67E+02	9.51E+01	7.55E+05	2.12E+01	5.11E-01	5.67E+00	1.69E+01
M-CVD5	2.42E-05	3.64E+03	2.65E+02	1.28E-06	6.51E+01	1.64E+01	3.16E+05	1.70E-01	2.05E-01	2.35E+00	9.29E+00
M-CVD6*	3.54E-04	2.59E+03	1.50E+02	2.93E-05	5.27E+01	2.17E+01	1.69E+05	1.70E-01	9.76E-02	1.20E+00	9.62E-02
M-AP	2.22E-07	2.04E+02	1.44E+01	5.02E-08	3.43E+00	5.20E-01	1.70E+04	7.49E-03	1.18E-02	1.32E-01	4.94E-03

Table B28. Characterization results of multiple synthesis processes for 1 kg CNTs (S- and M-) using ReCiPe (H) Method.

Routes	GW (kg CO ₂ - eq)	OD (kg CFCl11-eq)	tAC (kg SO ₂ - eq)	FWEU (kg P-eq)	MEU (kg N-eq)	HT (kg 1,4- DB-eq)	Pox (kg NMVOC)	RE (kg PM ₁₀ -eq)	TEC (kg 1,4- DB-eq)	FWAEC (kg 1,4-DB- eq)	MAEC (kg 1,4- DB-eq)	IR (kBq U235 eq)	ALO (m ² a)	ULO (m ² a)	NLT (m ²)	WDP (m ²)	MD (kg Fe eq)	FF (kg oil eq)
S-CVD1	1.97E+05	2.93E-04	1.56E+03	1.51E+00	2.05E+01	1.79E+04	7.70E+02	3.78E+02	2.20E+00	1.71E+02	1.68E+02	5.05E+02	4.03E+02	2.04E+01	5.10E-01	7.60E+02	8.36E+01	6.10E+04
S-CVD2	5.96E+05	6.03E-05	4.79E+03	4.99E-01	6.09E+01	5.23E+04	2.37E+03	1.15E+03	5.42E+00	4.20E+02	4.14E+02	1.71E+02	5.07E+01	4.96E+00	9.18E-02	3.03E+02	1.30E+01	1.87E+05
S-HPCO1	3.36E+04	1.31E-04	2.62E+02	1.21E-01	3.63E+00	2.99E+03	1.29E+02	6.29E+01	4.53E-01	2.97E+01	3.04E+01	7.21E+01	1.99E+01	3.13E+00	2.55E-01	1.24E+01	4.63E+01	1.01E+04
S-HPCO2'	2.03E+01	3.24E-06	7.91E-02	6.11E-03	2.85E-03	4.96E+00	4.57E-02	2.61E-02	1.73E-03	1.80E-01	1.69E-01	3.46E+00	8.64E-01	8.38E-02	6.00E-03	6.51E-02	4.80E-01	8.56E+00
S-CoMoCat1	1.15E+05	1.83E-05	9.27E+02	2.98E-02	1.18E+01	1.01E+04	4.58E+02	2.22E+02	1.04E+00	7.99E+01	7.88E+01	1.86E+01	4.73E+00	3.51E-01	2.72E-02	7.30E-01	2.49E+00	3.63E+04
S-CoMoCat2'	2.30E+01	4.18E-06	8.91E-02	7.84E-03	3.48E-03	6.21E+00	7.83E-02	3.01E-02	2.17E-03	2.29E-01	2.15E-01	4.51E+00	1.12E+00	1.06E-01	7.76E-03	8.04E-02	6.07E-01	1.02E+01
S-AP	8.29E+04	8.52E-04	6.52E+02	6.96E-01	8.95E+00	7.76E+03	3.20E+02	1.58E+02	1.31E+00	9.68E+01	8.75E+01	3.23E+02	9.22E+01	1.51E+01	1.67E+00	3.05E+01	1.86E+02	2.68E+04
S-LV	8.86E+04	1.67E-06	7.14E+02	4.41E-03	9.05E+00	7.75E+03	3.52E+02	1.71E+02	8.01E-01	6.10E+01	6.03E+01	8.78E-01	3.54E-01	1.48E-01	1.69E-03	7.23E-01	4.05E-01	2.79E+04
M-CVD1	2.12E+02	3.23E-07	1.69E+00	3.38E-03	2.24E-02	2.04E+01	8.37E-01	4.18E-01	2.22E-03	2.27E-01	2.18E-01	9.51E-01	2.99E-01	4.02E-02	6.99E-04	2.03E+00	1.34E-01	6.65E+01
M-CVD2	4.45E+02	9.52E-05	2.24E+00	1.86E-01	7.22E-02	2.05E+02	1.77E+00	7.09E-01	1.26E-01	5.23E+00	5.70E+00	5.35E+01	2.66E+01	1.87E+00	2.46E-02	7.71E+00	2.13E+01	2.33E+02
M-CVD3	4.13E+03	1.20E-04	3.09E+01	3.95E-01	5.07E-01	6.17E+02	1.54E+01	8.64E+00	1.42E-01	1.33E+01	1.29E+01	1.32E+02	4.37E+01	4.44E+00	1.39E-01	2.26E+02	2.09E+01	1.29E+03
M-CVD4	7.04E+02	8.29E-06	5.01E+00	4.69E-02	2.72E-01	8.53E+01	2.50E+00	1.40E+00	2.71E+00	2.03E+00	1.53E+00	1.26E+01	3.91E+01	6.78E-01	4.79E-01	1.21E+01	2.79E+00	1.97E+02
M-CVD5	2.65E+02	1.28E-06	2.05E+00	1.31E-02	2.97E-02	3.02E+01	1.02E+00	5.42E-01	5.21E-03	4.90E-01	4.60E-01	3.68E+00	1.14E+00	1.48E-01	2.59E-03	7.84E+00	4.54E-01	8.17E+01
M-CVD6'	1.50E+02	2.94E-05	1.05E+00	1.52E-02	1.87E-02	4.08E+01	5.61E-01	2.93E-01	2.98E-02	1.05E+00	1.18E+00	3.90E+00	2.91E+00	3.48E-01	2.80E-02	5.07E+00	4.39E+00	5.80E+01
M-AP	1.44E+01	5.02E-08	1.16E-01	4.91E-05	1.48E-03	1.28E+00	5.71E-02	2.79E-02	1.36E-04	1.13E-02	1.10E-02	2.88E-02	4.56E-03	8.13E-04	1.03E-04	2.63E-02	3.93E-03	4.59E+00

Table B29. Characterization results of multiple synthesis processes for 1 kg CNTs (S- and M-) using IMPACT 2002+ Method.

Routes	HHC (kg C ₂ H ₃ Cl- eq)	HHNC (kg C ₂ H ₃ Cl- eq)	REI (kg PM _{2.5} - eq)	IR (Bq C-14- eq)	OD (kg CFC11- eq)	REO (kg C ₂ H ₄ - eq)	AEC (kg TEG water)	TEC (kg TEG soil)	TAC (kg SO ₂ - eq.)	LO (m ² org. arable)	AAC (kg SO ₂ -eq)	AEU (kg PO ₄ P-lim)	GW (kg CO ₂ -eq)	NRE (MJ primary)	ME (MJ surplus)
S-CVD1	1.58E+02	1.99E+03	1.66E+02	5.14E+04	2.92E-04	1.09E+02	1.26E+07	9.16E+04	3.99E+03	7.16E+01	1.67E+03	1.04E+00	1.88E+05	2.72E+06	8.25E+01
S-CVD2	2.72E+02	6.12E+03	5.00E+02	1.75E+04	6.01E-05	3.35E+02	3.89E+07	1.46E+05	1.22E+04	1.10E+01	5.14E+03	1.35E+00	5.74E+05	8.35E+06	9.47E+00
S-HiPCO1	2.06E+01	3.28E+02	2.76E+01	7.25E+03	1.31E-04	1.78E+01	2.08E+06	1.98E+04	6.89E+02	4.87E+00	2.79E+02	2.04E-01	3.17E+04	4.50E+05	5.40E+01
S-HiPCO2*	3.23E-01	1.35E-01	1.38E-02	3.51E+02	3.23E-06	6.60E-03	1.21E+03	2.87E+02	2.27E-01	1.91E-01	8.47E-02	3.53E-03	1.96E+01	4.29E+02	4.59E-01
S-CoMoCat1	5.01E+01	1.18E+03	9.65E+01	1.89E+03	1.82E-05	6.48E+01	7.53E+06	2.78E+04	2.35E+03	9.68E-01	9.94E+02	2.42E-01	1.11E+05	1.61E+06	2.41E+00
S-CoMoCat2*	3.68E-01	1.55E-01	1.68E-02	4.57E+02	4.17E-06	7.14E-03	1.44E+03	3.63E+02	2.58E-01	2.46E-01	9.56E-02	4.50E-03	2.31E+01	5.18E+02	5.79E-01
S-AP	5.08E+02	8.64E+02	6.99E+01	3.26E+04	8.50E-04	4.51E+01	5.32E+06	6.96E+04	1.70E+03	2.33E+01	6.96E+02	7.15E-01	7.84E+04	1.20E+06	1.69E+02
S-LV	3.84E+01	9.11E+02	7.43E+01	8.94E+01	1.67E-06	4.99E+01	5.80E+06	2.11E+04	1.81E+03	1.61E-01	7.65E+02	1.78E-01	8.54E+04	1.24E+06	2.98E-01
M-CVD1	2.08E-01	2.17E+00	1.87E-01	9.72E+01	3.20E-07	1.18E-01	1.37E+04	1.09E+02	4.31E+00	7.29E-02	1.81E+00	1.70E-03	2.05E+02	2.97E+03	1.22E-01
M-CVD2	1.59E+01	4.50E+00	3.52E-01	5.46E+03	9.47E-05	4.29E-01	2.49E+04	3.94E+03	6.74E+00	4.94E+00	2.41E+00	2.37E-01	4.18E+02	1.15E+04	2.35E+01
M-CVD3	1.47E+01	4.13E+01	4.26E+00	1.35E+04	1.20E-04	2.04E+00	2.52E+05	8.10E+03	8.05E+01	9.43E+00	3.31E+01	1.62E-01	3.97E+03	5.96E+04	2.05E+01
M-CVD4	3.92E+02	6.07E+00	6.83E-01	1.28E+03	8.23E-06	3.17E+00	3.85E+04	-1.07E+03	1.34E+01	3.52E+01	5.34E+00	2.72E-02	6.78E+02	8.97E+03	2.71E+00
M-CVD5	3.59E+01	2.68E+00	2.56E-01	3.76E+02	1.28E-06	3.11E-01	1.70E+04	2.71E+02	5.28E+00	2.68E-01	2.20E+00	5.37E-03	2.55E+02	3.69E+03	4.35E-01
M-CVD6*	1.33E+00	1.65E+00	1.40E-01	4.01E+02	2.93E-05	8.17E-02	8.95E+03	7.59E+02	2.82E+00	6.07E-01	1.13E+00	1.06E-02	1.42E+02	2.68E+03	5.19E+00
M-AP	8.35E-03	1.48E-01	1.22E-02	2.91E+00	5.02E-08	8.08E-03	9.44E+02	5.97E+00	2.94E-01	1.23E-03	1.24E-01	6.56E-05	1.39E+01	2.05E+02	3.73E-03

Table B30. SWCNTs applications in different industries and respective synthesis processes for product-based impact estimations.

Process	Size Range	Known Applications	Reference
CVD	<i>N/A</i>	Electronics (field emission display screen), Chemical gas sensor	[4] [23]
	0.6-1.2 nm	Energy storage, medical	[60]
	0.8-2 nm	Composite materials, energy storage and environment, microelectronics, biotechnology	[61]
	<i>N/A</i>	Polymer filler, Flash memory, Li-ion battery	[13] [34]
	<i>N/A</i>	Field emission display television device	[31]
HiPCO	<i>N/A</i>	Electronics (Cellular phone flash memory semiconductor device)	[21]
	<i>N/A</i>	Electronics and optics	[10]
CoMoCat	0.7-1.1 nm	Electronics and displays	[28]
	<i>N/A</i>	Electronics and optics	[10]
	7.5 nm	Photovoltaic Solar Cells	[36]
AP	1.2-1.4 nm	Energy storage, medical	[60]
	<i>N/A</i>	Electrodes for organic solar cells	[19]
	1.3-1.8 nm	Electronics (electromagnetic interference)	[62]
	0.7-7 nm	Tennis racquet, field emission display	[63]
LV	5-20 nm	Energy storage, medical	[60]
	<i>N/A</i>	Li-ion batteries, Supercapacitors for automotive applications	[64] [20]

N/A: information is not available.

Table B31. MWCNTs applications in different industries and respective synthesis processes for product-based impact estimations.

Process	Size Range	Known Applications	Reference
CVD	20-70 nm	Electrode and sensor	[65]
	5-20 nm	Composite materials, energy storage and environment, biotechnology	[61]
	N/A	Flat panel displays, thermal interface materials	[25]
	N/A	Composite materials	[14]
	N/A	Polymer filler	[13]
	15–35 nm (>10 μm length)	Fuel cell	[32]
	N/A	Cement, li-ion battery	[34]
	10-20 nm (10-30 μm length)	Electronics (electromagnetic radiation shielding)	[66]
	150 nm (10–20 μm length)	Electronics (electromagnetic interference shielding)	[67]
	10 nm	Electronics (electromagnetic interference)	[68]
AP	1-3 nm	Energy storage, medical	[60]
	0.7-7 nm	Tennis racquet, field emission display	[63]

N/A: information is not available.

Table B32. Characterization results of multiple synthesis processes for 1 kg CNTs (S- and M-) using TRACI 2.1 Method.

Routes	OD (kg CFC11-eq)	GW (kg CO₂-eq)	PS (kg O₃-eq)	AP (kg SO₂-eq)	EP (kg N-q)	CP (CTUh)	NCP (CTUh)	RP (kg PM_{2.5}-eq)	EC (CTUe)	FFP (MJ surplus energy)
S-CVD1	3.63E-04	1.97E+05	1.30E+04	1.67E+03	3.56E+01	4.92E-04	6.75E-03	8.50E+01	9.57E+04	1.24E+05
S-CVD2	7.74E-05	5.96E+05	4.00E+04	5.14E+03	7.64E+01	1.14E-03	1.92E-02	2.50E+02	2.37E+05	3.75E+05
S-HiPCO1	1.70E-04	3.36E+04	2.20E+03	2.79E+02	5.41E+00	7.98E-05	1.16E-03	1.38E+01	1.81E+04	2.12E+04
S-HiPCO2*	4.15E-06	2.03E+01	7.28E-01	8.47E-02	5.19E-02	6.32E-07	3.02E-06	9.73E-03	9.37E+01	4.46E+01
S-CoMoCat1	2.35E-05	1.15E+05	7.74E+03	9.93E+02	1.43E+01	2.16E-04	3.69E-03	4.82E+01	4.53E+04	7.26E+04
S-CoMoCat2*	5.35E-06	2.30E+01	8.58E-01	9.55E-02	6.62E-02	7.94E-07	3.79E-06	1.17E-02	1.18E+02	5.43E+01
S-AP	1.10E-03	8.29E+04	5.41E+03	6.96E+02	1.65E+01	2.63E-04	3.06E-03	3.61E+01	5.09E+04	6.56E+04
S-LV	2.69E-06	8.86E+04	5.96E+03	7.65E+02	1.08E+01	1.65E-04	2.84E-03	3.71E+01	3.47E+04	5.58E+04
M-CVD1	4.09E-07	2.12E+02	1.42E+01	1.81E+00	5.12E-02	6.72E-07	7.78E-06	9.90E-02	1.22E+02	1.34E+02
M-CVD2	9.73E-05	4.45E+02	2.88E+01	2.41E+00	1.44E+00	1.79E-05	1.23E-04	2.28E-01	3.15E+03	1.18E+03
M-CVD3	1.29E-04	4.13E+03	2.68E+02	3.31E+01	3.45E+00	4.18E-05	2.59E-04	2.66E+00	6.81E+03	2.90E+03
M-CVD4	1.00E-05	7.04E+02	7.40E+01	5.33E+00	6.33E-01	6.36E-06	2.79E-05	4.33E-01	8.72E+02	4.48E+02
M-CVD5	1.61E-06	2.65E+02	1.93E+01	2.20E+00	1.30E-01	1.66E-06	1.21E-05	1.50E-01	2.50E+02	1.67E+02
M-CVD6*	2.98E-05	1.50E+02	1.04E+01	1.13E+00	1.34E-01	2.98E-06	1.84E-05	8.48E-02	6.56E+02	2.12E+02
M-AP	6.67E-08	1.44E+01	9.66E-01	1.24E-01	2.20E-03	3.15E-08	4.78E-07	6.21E-03	6.30E+00	9.57E+00

Table B33. Characterization results of multiple synthesis routes for 1 kg CNTs (S- and M-) using Cumulative Energy Demand (CED).

Routes	Cumulative Energy Demand (MJ/kg CNTs)		
	Renewable (biomass, wind, solar, geothermal, water)	Non-renewable (fossil, nuclear and biomass)	TOTAL
S-CVD1	5.68E+03	2.72E+06	2.73E+06
S-CVD2	1.39E+03	8.35E+06	8.35E+06
S-HiPCO1	2.94E+02	4.50E+05	4.50E+05
S-HiPCO2*	1.72E+01	4.29E+02	4.46E+02
S-CoMoCat1	9.42E+01	1.61E+06	1.61E+06
S-CoMoCat2*	2.23E+01	5.18E+02	5.40E+02
S-AP	1.74E+03	1.20E+06	1.20E+06
S-LV	8.86E+00	1.24E+06	1.24E+06
M-CVD1	8.87E+00	2.97E+03	2.98E+03
M-CVD2	4.27E+02	1.15E+04	1.19E+04
M-CVD3	1.68E+03	5.95E+04	6.12E+04
M-CVD4	9.12E+02	9.26E+03	1.02E+04
M-CVD5	3.39E+01	3.69E+03	3.73E+03
M-CVD6*	2.66E+02	2.68E+03	2.94E+03
M-AP	1.23E-01	2.05E+02	2.05E+02

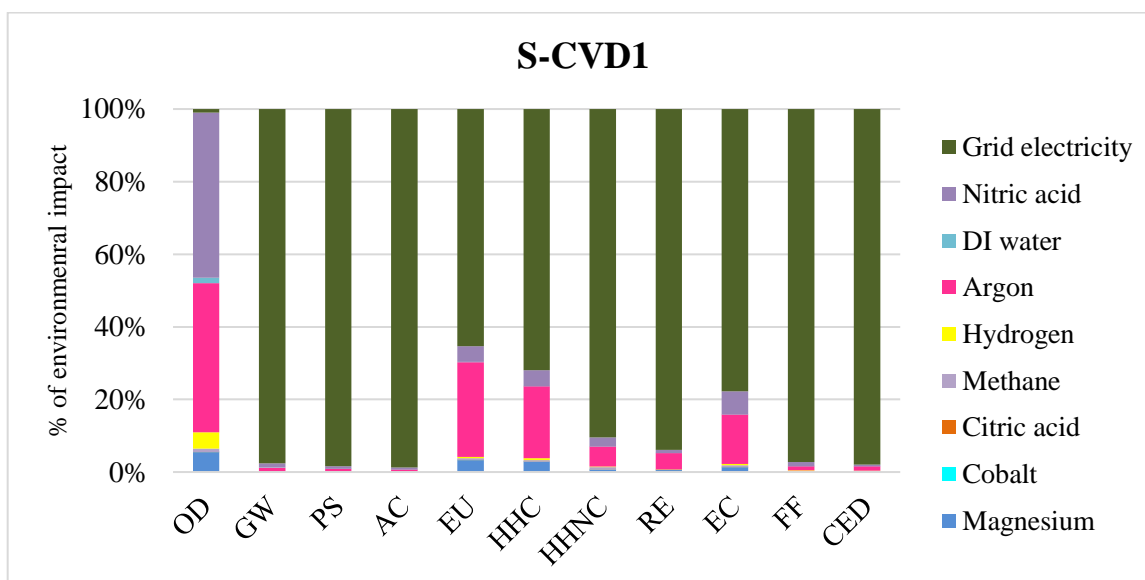


Figure B2. Midpoint LCA results for the 1 kg of SWCNTs production with S-CVD1.

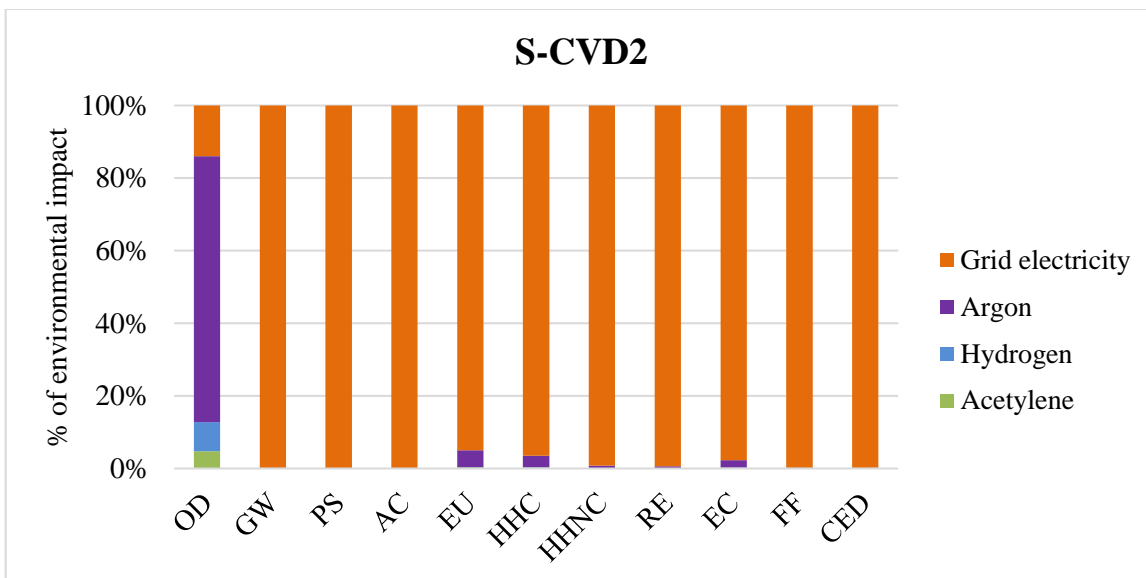


Figure B3. Midpoint LCA results for the 1 kg of SWCNTs production with S-CVD2.

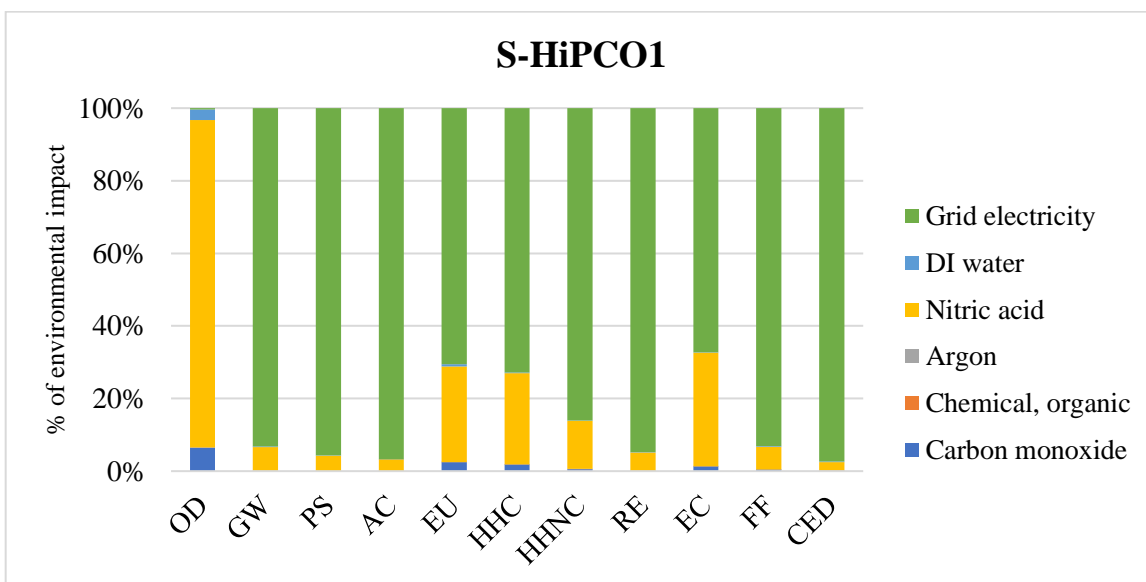


Figure B4. Midpoint LCA results for the 1 kg of SWCNTs production with S-HiPCO1.

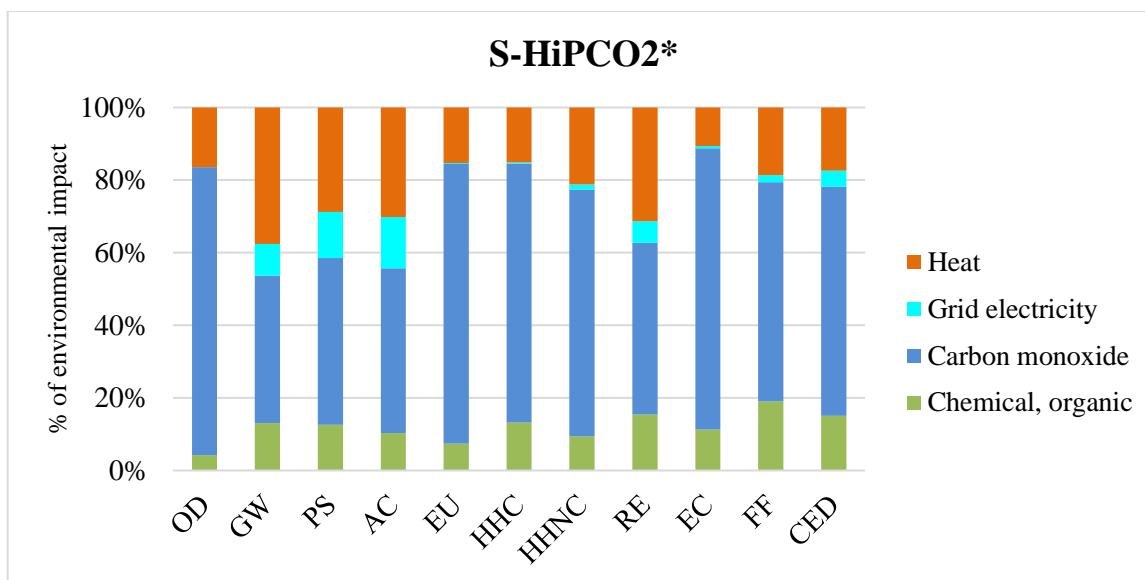


Figure B5. Midpoint LCA results for the 1 kg of SWCNTs production with S-HiPCO2*.

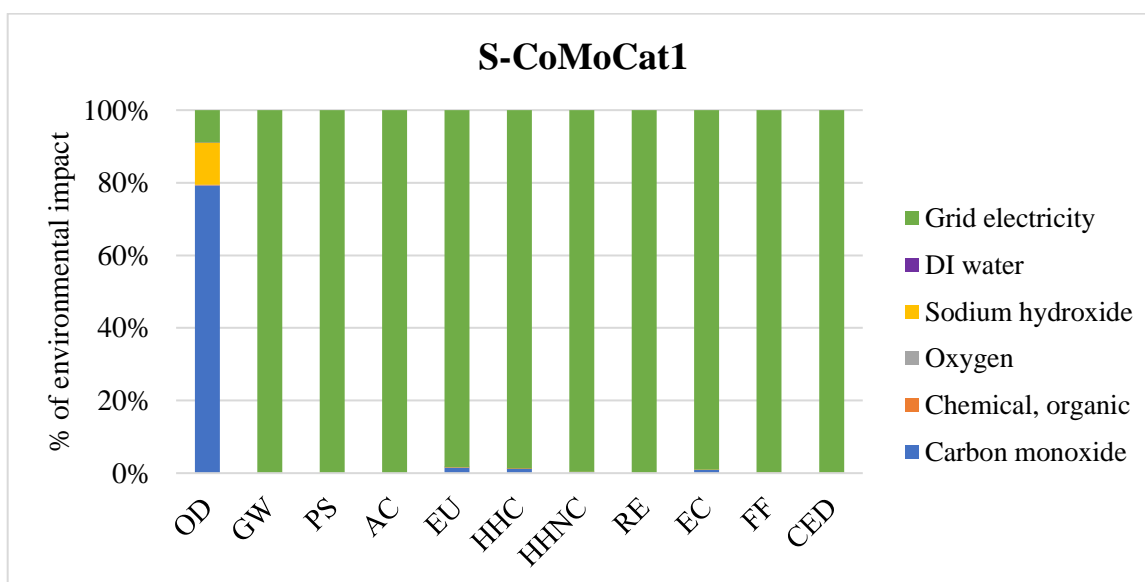


Figure B6. Midpoint LCA results for the 1 kg of SWCNTs production with S-CoMoCat1.

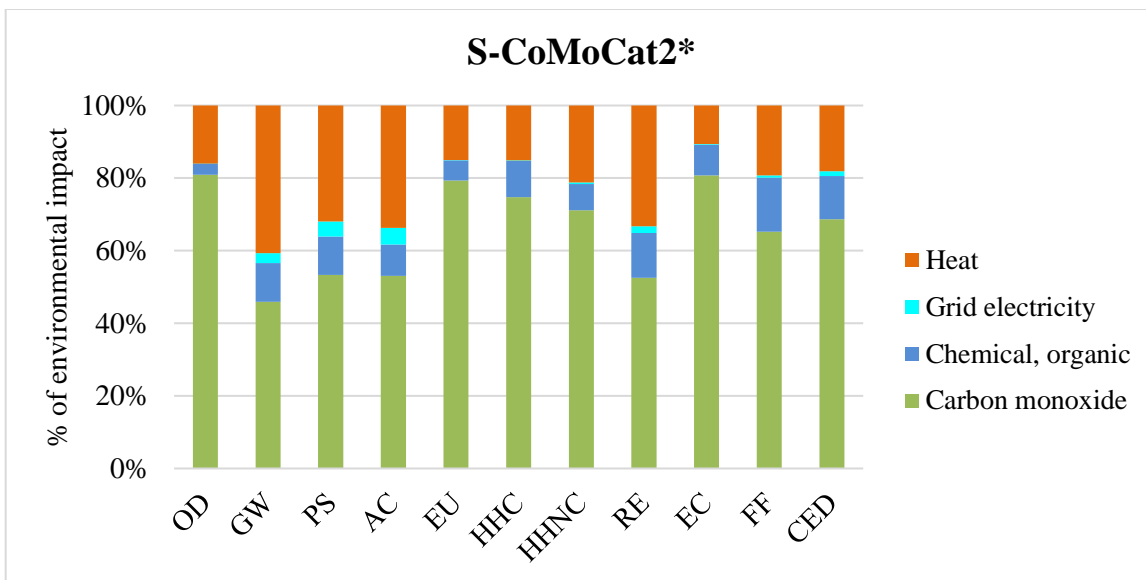


Figure B7. Midpoint LCA results for the 1 kg of SWCNTs production with S-CoMoCat2*.

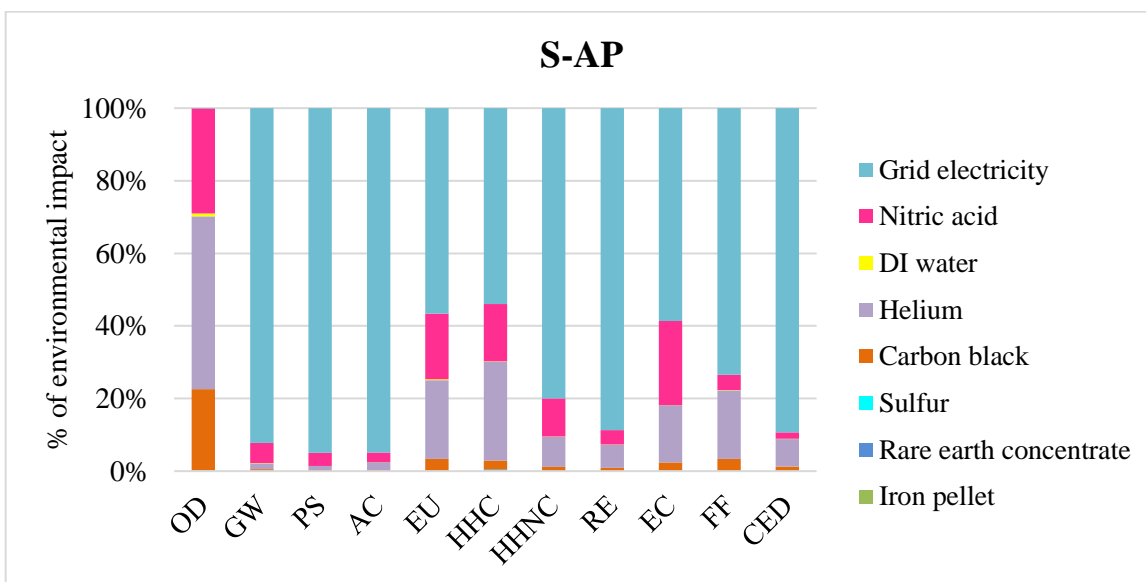


Figure B8. Midpoint LCA results for the 1 kg of SWCNTs production with S-AP.

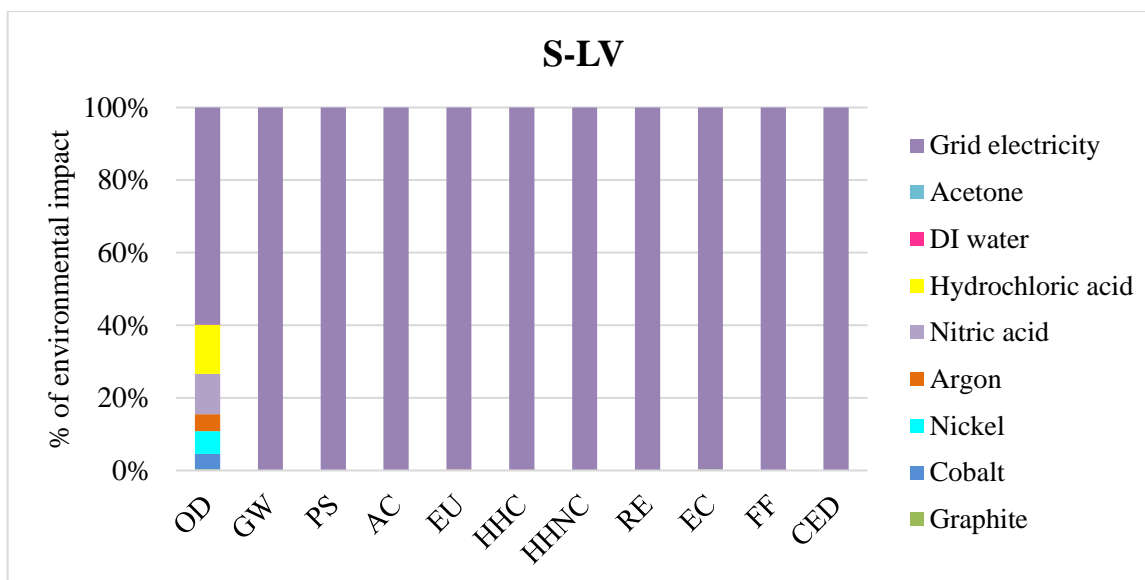


Figure B9. Midpoint LCA results for the 1 kg of SWCNTs production with S-LV.

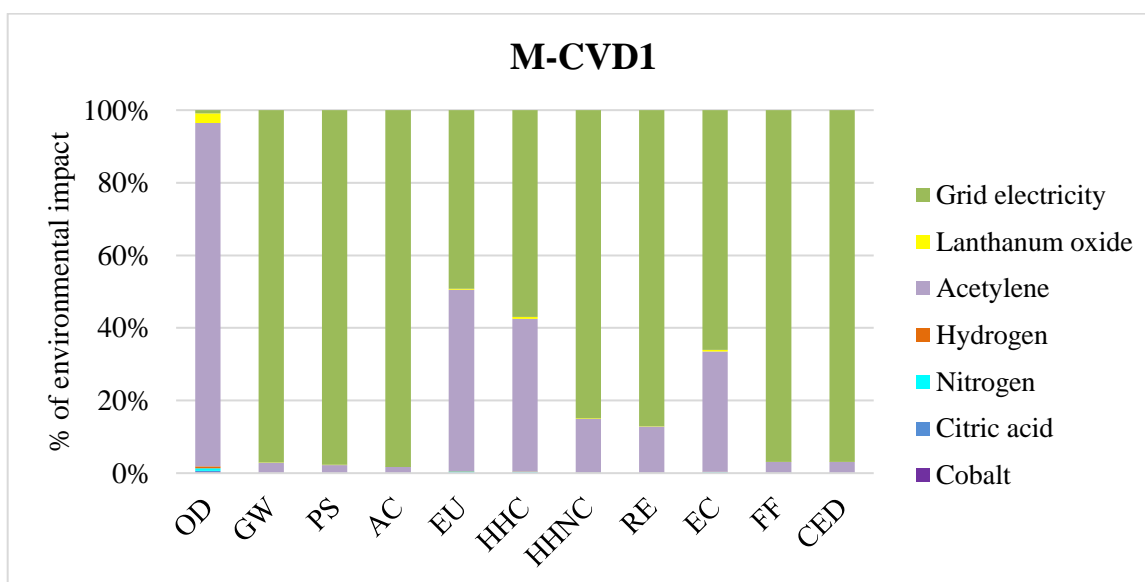


Figure B10. Midpoint LCA results for the 1 kg of MWCNTs production with M-CVD1.

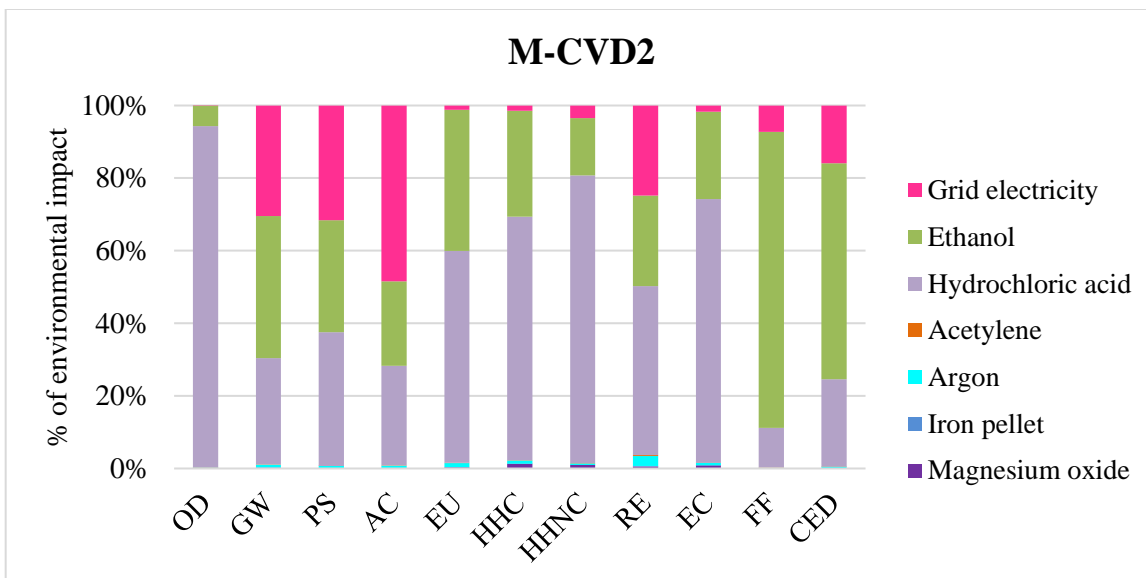


Figure B11. Midpoint LCA results for the 1 kg of MWCNTs production with M-CVD2.

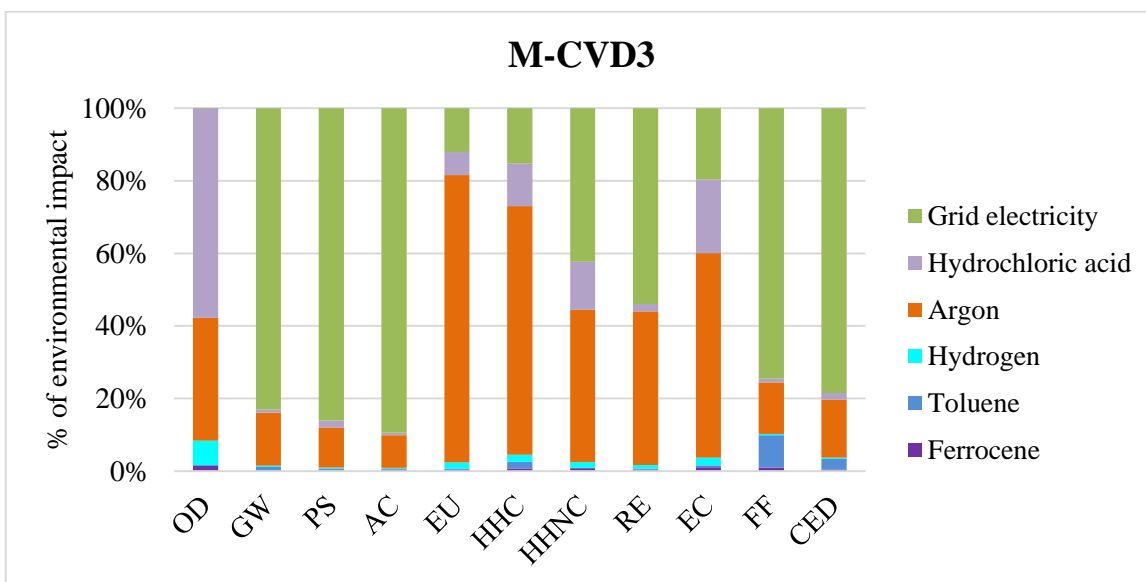


Figure B12. Midpoint LCA results for the 1 kg of MWCNTs production with M-CVD3.

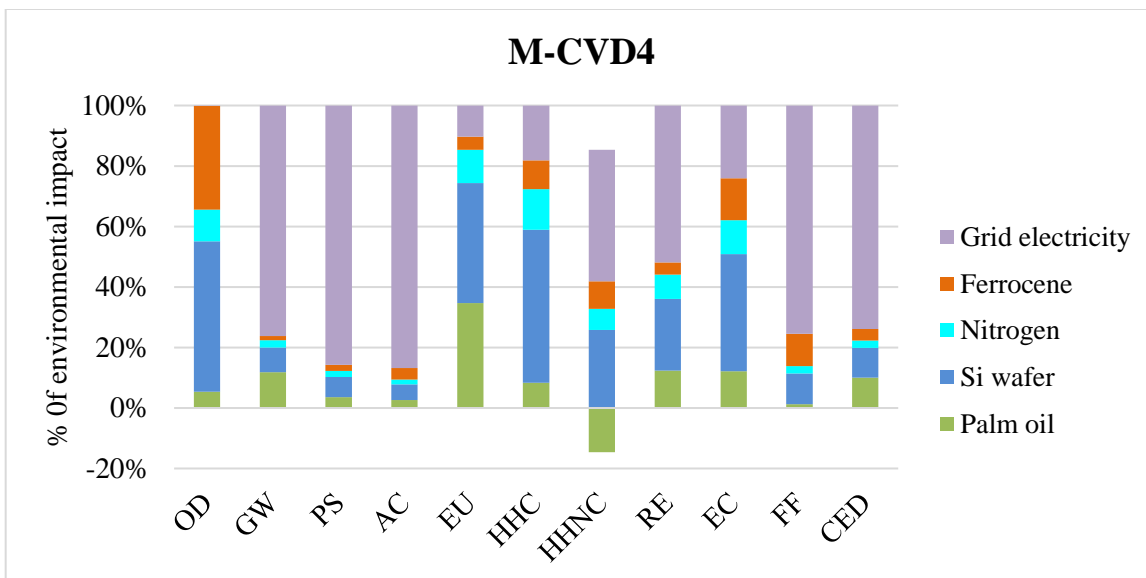


Figure B13. Midpoint LCA results for the 1 kg of MWCNTs production with M-CVD4.

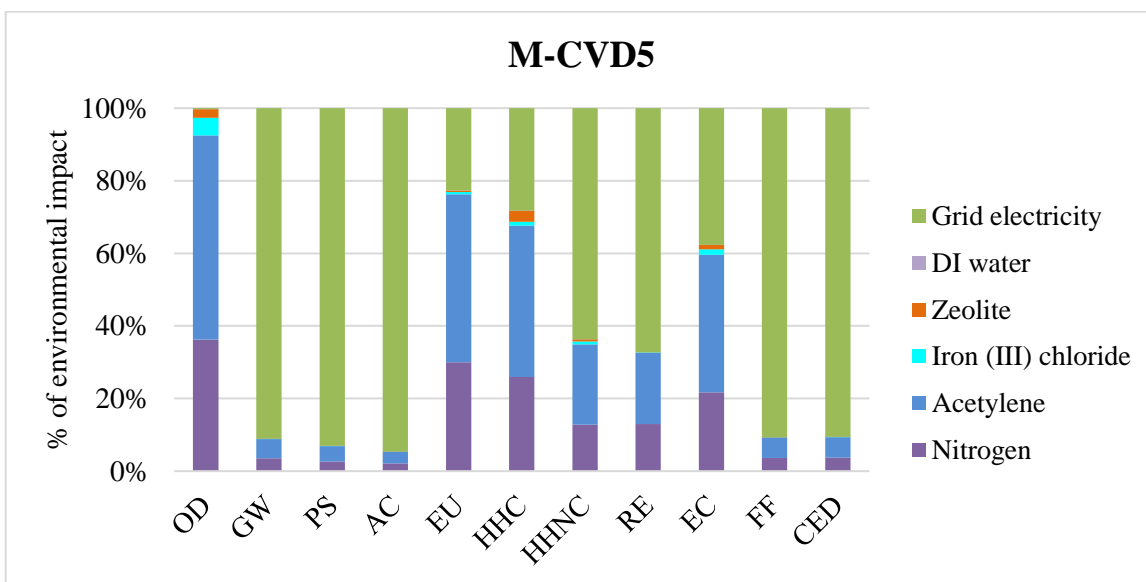


Figure B14. Midpoint LCA results for the 1 kg of MWCNTs production with M-CVD5.

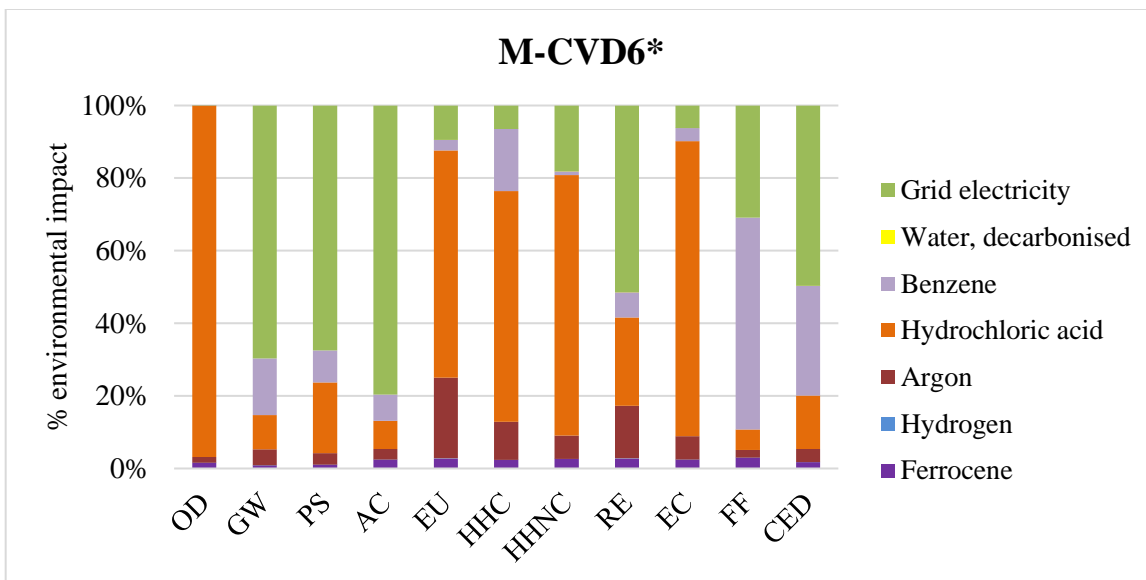


Figure B15. Midpoint LCA results for the 1 kg of MWCNTs production with M-CVD6*.

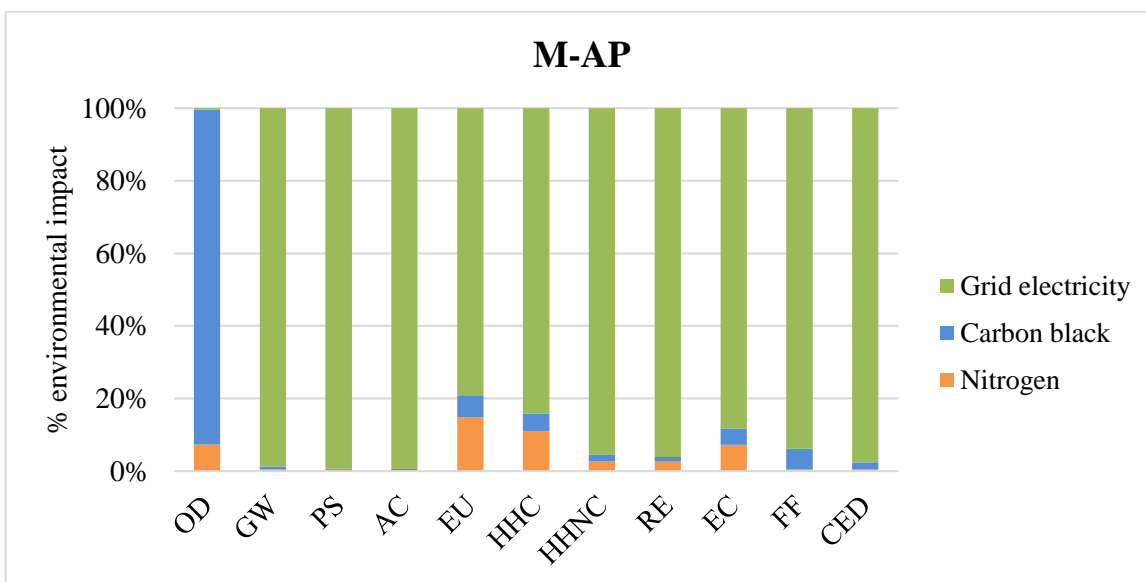


Figure B16. Midpoint LCA results for the 1 kg of MWCNTs production with M-AP.

Table B34. Environmental impact rankings (lowest, medium and highest) grouped by wall number (SWCNTs and MWCNTs).

Category	SWCNTs Synthesis Processes			MWCNTs Synthesis Processes		
	Low	Medium	High	Low	Medium	High
AC	S-HiPCO2*	S-AP	S-CVD2	M-AP	M-CVD5	M-CVD3
ET	S-HiPCO2*	S-LV	S-CVD2	M-AP	M-CVD6*	M-CVD3
EU	S-HiPCO2*	S-LV	S-CVD2	M-AP	M-CVD6*	M-CVD3
GW	S- HiPCO2*	S-AP	S-CVD2	M-AP	M-CVD5	M-CVD3
RE	S-HiPCO2*	S-AP	S-CVD2	M-AP	M-CVD5	M-CVD3
PS	S-HiPCO2*	S-AP	S-CVD2	M-AP	M-CVD5	M-CVD3
HHC	S-HiPCO2*	S-LV	S-CVD2	M-AP	M-CVD6*	M-CVD3
HHNC	S-HiPCO2*	S-LV	S-CVD2	M-AP	M-CVD6*	M-CVD3
OD	S-LV	S-CoMoCat1	S-AP	M-AP	M-CVD4	M-CVD3
FF	S-HiPCO2*	S-LV	S-CVD2	M-AP	M-CVD6*	M-CVD3
CED	S-HiPCO2*	S-LV	S-CVD2	M-AP	M-CVD5	M-CVD3

Table B35. Different electricity scenarios and their corresponding environmental impacts for SWCNTs production.

	IC	S-CVD1	S-CVD2	S-HiPCO1	S-HiPCO2*	S-CoMoCat1	S-CoMoCat2*	S-AP	S-LV
Grid Electricity (base case)	OD	3.63E-04	7.74E-05	1.70E-04	4.15E-06	2.35E-05	5.35E-06	1.10E-03	2.69E-06
	GW	1.97E+05	5.96E+05	3.36E+04	2.03E+01	1.15E+05	2.30E+01	8.29E+04	8.86E+04
	PS	1.30E+04	4.00E+04	2.20E+03	7.28E-01	7.74E+03	8.58E-01	5.41E+03	5.96E+03
	AC	1.67E+03	5.14E+03	2.79E+02	8.47E-02	9.93E+02	9.55E-02	6.96E+02	7.65E+02
	EU	3.56E+01	7.64E+01	5.41E+00	5.19E-02	1.43E+01	6.62E-02	1.65E+01	1.08E+01
	HHC	4.92E-04	1.14E-03	7.98E-05	6.32E-07	2.16E-04	7.94E-07	2.63E-04	1.65E-04
	HHNC	6.75E-03	1.92E-02	1.16E-03	3.02E-06	3.69E-03	3.79E-06	3.06E-03	2.84E-03
	RE	8.50E+01	2.50E+02	1.38E+01	9.73E-03	4.82E+01	1.17E-02	3.61E+01	3.71E+01
	EC	9.57E+04	2.37E+05	1.81E+04	9.37E+01	4.53E+04	1.18E+02	5.09E+04	3.47E+04
	FF	1.24E+05	3.75E+05	2.12E+04	4.46E+01	7.26E+04	5.43E+01	6.56E+04	5.58E+04
CED	2.73E+06	8.35E+06	4.50E+05	4.46E+02	1.61E+06	5.40E+02	1.20E+06	1.24E+06	
Solar	OD	6.07E-03	1.79E-02	1.11E-03	3.89E-06	3.47E-03	5.00E-06	3.39E-03	2.65E-03
	GW	3.56E+04	9.40E+04	7.17E+03	1.52E+01	1.81E+04	1.76E+01	1.84E+04	1.39E+04
	PS	1.90E+03	5.30E+03	3.72E+02	5.52E-01	1.02E+03	7.07E-01	9.47E+02	7.84E+02
	AC	2.07E+02	5.83E+02	3.96E+01	6.11E-02	1.12E+02	7.52E-02	1.10E+02	8.63E+01
	EU	2.09E+02	6.18E+02	3.39E+01	5.85E-02	1.19E+02	7.34E-02	8.61E+01	9.16E+01
	HHC	3.75E-03	1.13E-02	6.15E-04	8.04E-07	2.18E-03	9.89E-07	1.57E-03	1.68E-03
	HHNC	2.92E-02	8.93E-02	4.85E-03	4.46E-06	1.73E-02	5.47E-06	1.21E-02	1.33E-02
	RE	5.72E+01	1.64E+02	9.25E+00	9.98E-03	3.14E+01	1.22E-02	2.49E+01	2.42E+01
EC	2.11E+06	6.51E+06	3.48E+05	2.39E+02	1.26E+06	2.88E+02	8.57E+05	9.69E+05	

	IC	S-CVD1	S-CVD2	S-HiPCO1	S-HiPCO2*	S-CoMoCat1	S-CoMoCat2*	S-AP	S-LV
	FF	2.99E+04	8.34E+04	5.81E+03	3.74E+01	1.61E+04	4.58E+01	2.80E+04	1.23E+04
	CED	1.47E+06	4.43E+06	2.44E+05	4.55E+02	8.55E+05	5.59E+02	6.96E+05	6.57E+05
Wind	OD	1.66E-03	4.12E-03	3.83E-04	3.56E-06	8.06E-04	4.61E-06	1.62E-03	6.05E-04
	GW	1.37E+04	2.56E+04	3.57E+03	1.36E+01	4.84E+03	1.57E+01	9.62E+03	3.69E+03
	PS	8.11E+02	1.90E+03	1.93E+02	4.70E-01	3.61E+02	6.12E-01	5.09E+02	2.77E+02
	AC	9.07E+01	2.21E+02	2.06E+01	5.24E-02	4.21E+01	6.51E-02	6.37E+01	3.24E+01
	EU	1.12E+02	3.13E+02	1.79E+01	5.12E-02	6.01E+01	6.49E-02	4.69E+01	4.61E+01
	HHC	3.55E-03	1.07E-02	5.82E-04	7.89E-07	2.06E-03	9.72E-07	1.49E-03	1.59E-03
	HHNC	2.33E-02	7.07E-02	3.88E-03	4.02E-06	1.37E-02	4.95E-06	9.69E-03	1.05E-02
	RE	2.02E+01	4.83E+01	3.19E+00	7.22E-03	9.08E+00	9.00E-03	1.01E+01	6.98E+00
	EC	5.39E+06	1.68E+07	8.87E+05	4.84E+02	3.24E+06	5.75E+02	2.17E+06	2.49E+06
	FF	1.18E+04	2.69E+04	2.84E+03	3.60E+01	5.22E+03	4.42E+01	2.08E+04	3.91E+03
	CED	1.11E+06	3.31E+06	1.85E+05	4.28E+02	6.39E+05	5.27E+02	5.52E+05	4.91E+05
Hydro	OD	3.82E-04	1.36E-04	1.73E-04	3.47E-06	3.48E-05	4.50E-06	1.11E-03	1.14E-05
	GW	1.17E+04	1.95E+04	3.25E+03	1.34E+01	3.67E+03	1.56E+01	8.84E+03	2.79E+03
	PS	2.51E+02	1.50E+02	1.01E+02	4.29E-01	2.31E+01	5.63E-01	2.85E+02	1.68E+01
	AC	2.32E+01	1.03E+01	9.51E+00	4.74E-02	1.42E+00	5.91E-02	3.66E+01	1.09E+00
	EU	1.26E+01	4.69E+00	1.64E+00	4.38E-02	4.15E-01	5.62E-02	7.26E+00	1.66E-01
	HHC	1.52E-04	8.62E-05	2.41E-05	5.36E-07	1.16E-05	6.74E-07	1.27E-04	7.19E-06
	HHNC	6.83E-04	2.83E-04	1.70E-04	2.34E-06	3.78E-05	2.97E-06	6.31E-04	2.35E-05
	RE	5.30E+00	1.97E+00	7.46E-01	6.11E-03	1.09E-01	7.70E-03	4.13E+00	7.45E-02
	EC	2.18E+04	6.98E+03	6.01E+03	8.32E+01	7.52E+02	1.06E+02	2.12E+04	3.57E+02
	FF	3.78E+03	1.83E+03	1.52E+03	3.54E+01	3.69E+02	4.35E+01	1.76E+04	1.76E+02
CED	1.19E+06	3.56E+06	1.99E+05	4.34E+02	6.88E+05	5.34E+02	5.85E+05	5.29E+05	
Natural gas	OD	1.61E-02	4.92E-02	2.75E-03	4.64E-06	9.53E-03	5.88E-06	7.42E-03	7.32E-03
	GW	1.56E+05	4.69E+05	2.69E+04	2.42E+01	9.06E+04	2.82E+01	6.66E+04	6.97E+04
	PS	3.31E+03	9.70E+03	6.04E+02	6.57E-01	1.87E+03	8.31E-01	1.51E+03	1.44E+03
	AC	4.76E+02	1.42E+03	8.38E+01	8.12E-02	2.75E+02	9.88E-02	2.18E+02	2.12E+02
	EU	4.58E+01	1.08E+02	7.09E+00	4.63E-02	2.04E+01	5.91E-02	2.06E+01	1.56E+01
	HHC	1.03E-03	2.83E-03	1.68E-04	6.01E-07	5.42E-04	7.51E-07	4.80E-04	4.16E-04
	HHNC	5.41E-03	1.50E-02	9.45E-04	2.69E-06	2.89E-03	3.38E-06	2.53E-03	2.22E-03
	RE	3.82E+01	1.05E+02	6.14E+00	8.56E-03	2.00E+01	1.06E-02	1.73E+01	1.54E+01
	EC	1.38E+05	3.69E+05	2.51E+04	9.19E+01	7.08E+04	1.16E+02	6.78E+04	5.43E+04
	FF	3.93E+05	1.21E+06	6.53E+04	6.44E+01	2.35E+05	7.75E+01	1.73E+05	1.81E+05
CED	2.69E+06	8.24E+06	4.45E+05	5.46E+02	1.59E+06	6.66E+02	1.19E+06	1.23E+06	
Nuclear	OD	3.61E-04	7.17E-05	1.70E-04	3.47E-06	2.24E-05	4.50E-06	1.10E-03	1.85E-06
	GW	8.59E+03	9.66E+03	2.74E+03	1.32E+01	1.76E+03	1.53E+01	7.57E+03	1.32E+03
	PS	6.43E+02	1.37E+03	1.66E+02	4.58E-01	2.60E+02	5.97E-01	4.42E+02	1.99E+02
	AC	8.95E+01	2.17E+02	2.04E+01	5.23E-02	4.14E+01	6.49E-02	6.32E+01	3.19E+01
	EU	1.33E+01	6.73E+00	1.75E+00	4.38E-02	8.10E-01	5.63E-02	7.52E+00	4.70E-01
	HHC	1.46E-04	6.48E-05	2.29E-05	5.35E-07	7.50E-06	6.74E-07	1.24E-04	4.00E-06
	HHNC	1.02E-03	1.33E-03	2.25E-04	2.36E-06	2.40E-04	3.00E-06	7.65E-04	1.79E-04

	IC	S-CVD1	S-CVD2	S-HiPCO1	S-HiPCO2*	S-CoMoCat1	S-CoMoCat2*	S-AP	S-LV
	RE	8.70E+00	1.26E+01	1.30E+00	6.36E-03	2.16E+00	8.00E-03	5.50E+00	1.66E+00
	EC	3.34E+04	4.32E+04	7.92E+03	8.41E+01	7.77E+03	1.07E+02	2.59E+04	5.76E+03
	FF	5.89E+03	8.42E+03	1.87E+03	3.56E+01	1.64E+03	4.37E+01	1.84E+04	1.16E+03
	CED	9.53E+04	1.40E+05	1.85E+04	3.52E+02	2.60E+04	4.38E+02	1.45E+05	1.88E+04
Coal	OD	3.66E-03	1.04E-02	7.11E-04	3.71E-06	2.01E-03	4.79E-06	2.42E-03	1.53E-03
	GW	2.62E+05	8.01E+05	4.44E+04	3.21E+01	1.55E+05	3.75E+01	1.09E+05	1.19E+05
	PS	2.12E+04	6.54E+04	3.53E+03	1.99E+00	1.26E+04	2.39E+00	8.67E+03	9.74E+03
	AC	2.22E+03	6.85E+03	3.69E+02	2.11E-01	1.32E+03	2.51E-01	9.16E+02	1.02E+03
	EU	1.28E+03	3.96E+03	2.10E+02	1.38E-01	7.65E+02	1.67E-01	5.16E+02	5.89E+02
	HHC	1.47E-02	4.54E-02	2.41E-03	1.62E-06	8.77E-03	1.94E-06	5.95E-03	6.75E-03
	HHNC	5.05E-02	1.56E-01	8.35E-03	6.05E-06	3.01E-02	7.33E-06	2.06E-02	2.32E-02
	RE	2.03E+02	6.18E+02	3.32E+01	2.08E-02	1.19E+02	2.50E-02	8.34E+01	9.19E+01
	EC	1.28E+06	3.92E+06	2.12E+05	1.77E+02	7.57E+05	2.15E+02	5.24E+05	5.83E+05
	FF	4.30E+04	1.24E+05	7.96E+03	3.83E+01	2.40E+04	4.69E+01	3.33E+04	1.84E+04
	CED	2.91E+06	8.93E+06	4.81E+05	5.62E+02	1.73E+06	6.85E+02	1.27E+06	1.33E+06
Oil	OD	5.63E-02	1.74E-01	9.34E-03	7.64E-06	3.37E-02	9.39E-06	2.35E-02	2.60E-02
	GW	2.40E+05	7.30E+05	4.07E+04	3.04E+01	1.41E+05	3.55E+01	1.00E+05	1.09E+05
	PS	1.94E+04	5.97E+04	3.24E+03	1.85E+00	1.15E+04	2.23E+00	7.94E+03	8.89E+03
	AC	1.89E+03	5.84E+03	3.16E+02	1.87E-01	1.13E+03	2.23E-01	7.86E+02	8.70E+02
	EU	1.75E+02	5.12E+02	2.84E+01	5.59E-02	9.86E+01	7.05E-02	7.25E+01	7.58E+01
	HHC	1.58E-03	4.54E-03	2.58E-04	6.42E-07	8.73E-04	7.99E-07	6.99E-04	6.70E-04
	HHNC	8.20E-03	2.37E-02	1.40E-03	2.90E-06	4.57E-03	3.63E-06	3.64E-03	3.52E-03
	RE	1.34E+02	4.04E+02	2.19E+01	1.57E-02	7.78E+01	1.90E-02	5.58E+01	5.99E+01
	EC	2.88E+05	8.36E+05	4.97E+04	1.03E+02	1.61E+05	1.29E+02	1.28E+05	1.24E+05
	FF	4.96E+05	1.54E+06	8.22E+04	7.21E+01	2.97E+05	8.65E+01	2.15E+05	2.29E+05
	CED	3.55E+06	1.09E+07	5.86E+05	6.10E+02	2.11E+06	7.41E+02	1.53E+06	1.62E+06

Table B36. Different electricity scenarios and their corresponding environmental impacts for MWCNTs production.

	IC	M-CVD1	M-CVD2	M-CVD3	M-CVD4	M-CVD5	M-CVD6*	M-AP
Grid Electricity (base case)	OD	4.09E-07	9.73E-05	1.29E-04	1.00E-05	1.61E-06	2.98E-05	6.67E-08
	GW	2.12E+02	4.45E+02	4.13E+03	7.04E+02	2.65E+02	1.50E+02	1.44E+01
	PS	1.42E+01	2.88E+01	2.68E+02	7.40E+01	1.93E+01	1.04E+01	9.66E-01
	AC	1.81E+00	2.41E+00	3.31E+01	5.33E+00	2.20E+00	1.13E+00	1.24E-01
	EU	5.12E-02	1.44E+00	3.45E+00	6.33E-01	1.30E-01	1.34E-01	2.20E-03
	HHC	6.72E-07	1.79E-05	4.18E-05	6.36E-06	1.66E-06	2.98E-06	3.15E-08
	HHNC	7.78E-06	1.23E-04	2.59E-04	2.79E-05	1.21E-05	1.84E-05	4.78E-07
	RE	9.90E-02	2.28E-01	2.66E+00	4.33E-01	1.50E-01	8.48E-02	6.21E-03

	IC	M-CVD1	M-CVD2	M-CVD3	M-CVD4	M-CVD5	M-CVD6*	M-AP
	EC	1.22E+02	3.15E+03	6.81E+03	8.72E+02	2.50E+02	6.56E+02	6.30E+00
	FF	1.34E+02	1.18E+03	2.90E+03	4.48E+02	1.67E+02	2.12E+02	9.57E+00
	CED	2.98E+03	1.19E+04	6.12E+04	1.02E+04	3.73E+03	2.94E+03	2.05E+02
Solar	OD	6.58E-06	1.01E-04	2.32E-04	2.61E-05	8.82E-06	3.29E-05	4.93E-07
	GW	3.84E+01	3.31E+02	1.24E+03	2.51E+02	6.14E+01	6.18E+01	2.42E+00
	PS	2.15E+00	2.09E+01	6.78E+01	4.27E+01	5.26E+00	4.30E+00	1.33E-01
	AC	2.32E-01	1.38E+00	6.85E+00	1.23E+00	3.54E-01	3.32E-01	1.47E-02
	EU	2.39E-01	1.56E+00	6.58E+00	1.12E+00	3.49E-01	2.29E-01	1.52E-02
	HHC	4.20E-06	2.02E-05	1.00E-04	1.55E-05	5.78E-06	4.76E-06	2.75E-07
	HHNC	3.21E-05	1.39E-04	6.63E-04	9.11E-05	4.05E-05	3.07E-05	2.16E-06
	RE	6.90E-02	2.08E-01	2.16E+00	3.54E-01	1.15E-01	6.96E-02	4.13E-03
	EC	2.30E+03	4.58E+03	4.30E+04	6.53E+03	2.79E+03	1.76E+03	1.57E+02
	FF	3.29E+01	1.11E+03	1.22E+03	1.84E+02	4.92E+01	1.61E+02	2.57E+00
CED	1.62E+03	1.11E+04	3.86E+04	6.63E+03	2.14E+03	2.25E+03	1.11E+02	
Wind	OD	1.81E-06	9.82E-05	1.53E-04	1.37E-05	3.24E-06	3.05E-05	1.64E-07
	GW	1.47E+01	3.15E+02	8.45E+02	1.90E+02	3.37E+01	4.98E+01	7.76E-01
	PS	9.67E-01	2.02E+01	4.81E+01	3.96E+01	3.88E+00	3.70E+00	5.18E-02
	AC	1.06E-01	1.29E+00	4.76E+00	9.00E-01	2.07E-01	2.68E-01	6.01E-03
	EU	1.33E-01	1.49E+00	4.82E+00	8.47E-01	2.26E-01	1.76E-01	7.88E-03
	HHC	3.98E-06	2.01E-05	9.69E-05	1.50E-05	5.53E-06	4.65E-06	2.60E-07
	HHNC	2.57E-05	1.35E-04	5.57E-04	7.44E-05	3.30E-05	2.74E-05	1.71E-06
	RE	2.89E-02	1.82E-01	1.49E+00	2.50E-01	6.82E-02	4.94E-02	1.36E-03
	EC	5.85E+03	6.91E+03	1.02E+05	1.58E+04	6.94E+03	3.55E+03	4.02E+02
	FF	1.33E+01	1.10E+03	8.89E+02	1.33E+02	2.63E+01	1.51E+02	1.22E+00
CED	1.23E+03	1.08E+04	3.22E+04	5.63E+03	1.69E+03	2.06E+03	8.39E+01	
Hydro	OD	4.29E-07	9.73E-05	1.30E-04	1.01E-05	1.63E-06	2.98E-05	6.81E-08
	GW	1.26E+01	3.14E+02	8.10E+02	1.84E+02	3.12E+01	4.87E+01	6.30E-01
	PS	3.61E-01	1.98E+01	3.81E+01	3.80E+01	3.17E+00	3.40E+00	9.96E-03
	AC	3.32E-02	1.25E+00	3.55E+00	7.11E-01	1.22E-01	2.31E-01	9.66E-04
	EU	2.63E-02	1.42E+00	3.04E+00	5.69E-01	1.01E-01	1.22E-01	4.80E-04
	HHC	3.05E-07	1.76E-05	3.57E-05	5.41E-06	1.24E-06	2.80E-06	6.09E-09
	HHNC	1.22E-06	1.19E-04	1.50E-04	1.08E-05	4.46E-06	1.51E-05	2.48E-08
	RE	1.29E-02	1.72E-01	1.23E+00	2.09E-01	4.94E-02	4.12E-02	2.52E-04
	EC	4.19E+01	3.10E+03	5.48E+03	6.64E+02	1.57E+02	6.16E+02	7.79E-01
	FF	4.60E+00	1.09E+03	7.45E+02	1.11E+02	1.62E+01	1.47E+02	6.19E-01
CED	1.32E+03	1.09E+04	3.36E+04	5.86E+03	1.79E+03	2.10E+03	9.01E+01	
Natu	OD	1.74E-05	1.09E-04	4.13E-04	5.43E-05	2.15E-05	3.84E-05	1.24E-06
	GW	1.68E+02	4.16E+02	3.40E+03	5.89E+02	2.13E+02	1.27E+02	1.14E+01

	IC	M-CVD1	M-CVD2	M-CVD3	M-CVD4	M-CVD5	M-CVD6*	M-AP
	PS	3.67E+00	2.19E+01	9.31E+01	4.67E+01	7.04E+00	5.07E+00	2.39E-01
	AC	5.23E-01	1.57E+00	1.17E+01	1.98E+00	6.94E-01	4.79E-01	3.48E-02
	EU	6.22E-02	1.45E+00	3.64E+00	6.62E-01	1.43E-01	1.40E-01	2.96E-03
	HHC	1.26E-06	1.83E-05	5.15E-05	7.88E-06	2.35E-06	3.28E-06	7.18E-08
	HHNC	6.33E-06	1.23E-04	2.35E-04	2.41E-05	1.04E-05	1.77E-05	3.78E-07
	RE	4.85E-02	1.95E-01	1.82E+00	3.01E-01	9.10E-02	5.92E-02	2.71E-03
	EC	1.68E+02	3.18E+03	7.57E+03	9.90E+02	3.03E+02	6.79E+02	9.46E+00
	FF	4.25E+02	1.37E+03	7.73E+03	1.20E+03	5.07E+02	3.59E+02	2.97E+01
	CED	2.95E+03	1.19E+04	6.06E+04	1.01E+04	3.68E+03	2.92E+03	2.02E+02
Nuclear	OD	4.07E-07	9.73E-05	1.29E-04	1.00E-05	1.60E-06	2.97E-05	6.66E-08
	GW	9.19E+00	3.11E+02	7.53E+02	1.75E+02	2.73E+01	4.70E+01	3.94E-01
	PS	7.85E-01	2.00E+01	4.51E+01	3.91E+01	3.67E+00	3.61E+00	3.93E-02
	AC	1.05E-01	1.29E+00	4.74E+00	8.97E-01	2.06E-01	2.68E-01	5.92E-03
	EU	2.70E-02	1.42E+00	3.05E+00	5.70E-01	1.01E-01	1.22E-01	5.29E-04
	HHC	2.97E-07	1.76E-05	3.56E-05	5.39E-06	1.23E-06	2.79E-06	5.58E-09
	HHNC	1.58E-06	1.19E-04	1.56E-04	1.18E-05	4.88E-06	1.53E-05	4.98E-08
	RE	1.66E-02	1.74E-01	1.29E+00	2.18E-01	5.37E-02	4.31E-02	5.07E-04
	EC	5.45E+01	3.11E+03	5.69E+03	6.97E+02	1.71E+02	6.22E+02	1.65E+00
	FF	6.88E+00	1.09E+03	7.83E+02	1.17E+02	1.88E+01	1.48E+02	7.77E-01
	CED	1.36E+02	1.01E+04	1.39E+04	2.77E+03	4.04E+02	1.50E+03	8.00E+00
Coal	OD	3.97E-06	9.97E-05	1.89E-04	1.93E-05	5.77E-06	3.16E-05	3.13E-07
	GW	2.84E+02	4.91E+02	5.32E+03	8.89E+02	3.48E+02	1.86E+02	1.94E+01
	PS	2.30E+01	3.46E+01	4.14E+02	9.69E+01	2.96E+01	1.48E+01	1.57E+00
	AC	2.40E+00	2.80E+00	4.30E+01	6.88E+00	2.89E+00	1.43E+00	1.65E-01
	EU	1.40E+00	2.32E+00	2.58E+01	4.13E+00	1.70E+00	8.15E-01	9.53E-02
	HHC	1.60E-05	2.79E-05	2.97E-04	4.62E-05	1.96E-05	1.07E-05	1.09E-06
	HHNC	5.51E-05	1.55E-04	1.05E-03	1.51E-04	6.74E-05	4.23E-05	3.75E-06
	RE	2.27E-01	3.12E-01	4.78E+00	7.64E-01	2.99E-01	1.49E-01	1.50E-02
	EC	1.40E+03	3.99E+03	2.80E+04	4.19E+03	1.74E+03	1.30E+03	9.45E+01
	FF	4.71E+01	1.12E+03	1.45E+03	2.21E+02	6.58E+01	1.68E+02	3.55E+00
	CED	3.18E+03	1.21E+04	6.46E+04	1.07E+04	3.96E+03	3.04E+03	2.19E+02
Oil	OD	6.09E-05	1.37E-04	1.13E-03	1.67E-04	7.22E-05	6.03E-05	4.24E-06
	GW	2.59E+02	4.75E+02	4.91E+03	8.25E+02	3.19E+02	1.73E+02	1.77E+01
	PS	2.10E+01	3.33E+01	3.82E+02	9.18E+01	2.73E+01	1.38E+01	1.44E+00
	AC	2.06E+00	2.57E+00	3.72E+01	5.97E+00	2.48E+00	1.25E+00	1.41E-01
	EU	2.02E-01	1.54E+00	5.97E+00	1.03E+00	3.06E-01	2.10E-01	1.26E-02
	HHC	1.85E-06	1.87E-05	6.14E-05	9.42E-06	3.04E-06	3.58E-06	1.13E-07
	HHNC	9.35E-06	1.25E-04	2.85E-04	3.20E-05	1.40E-05	1.92E-05	5.87E-07

	IC	M-CVD1	M-CVD2	M-CVD3	M-CVD4	M-CVD5	M-CVD6*	M-AP
	RE	1.52E-01	2.63E-01	3.54E+00	5.71E-01	2.12E-01	1.12E-01	9.88E-03
	EC	3.30E+02	3.29E+03	1.03E+04	1.41E+03	4.93E+02	7.61E+02	2.07E+01
	FF	5.37E+02	1.44E+03	9.59E+03	1.49E+03	6.38E+02	4.16E+02	3.74E+01
	CED	3.88E+03	1.25E+04	7.61E+04	1.25E+04	4.77E+03	3.39E+03	2.66E+02

Table B37. Projected global warming (GW) with and without scaling up approach for pessimistic production estimations of SWCNTs, MWCNTs and total CNTs (σ represents standard deviation).

Global Warming (tons CO ₂ -eq./year)						
Year	Lab Scale (SWCNT)		Lab Scale (MWCNT)		Lab Scale (CNTs total)	
	Mean	σ	Mean	σ	Mean	σ
2018	1.81E+07	9.09E+04	4.48E+05	4.62E+04	1.85E+07	1.02E+05
2019	1.91E+07	9.58E+04	4.73E+05	4.87E+04	1.96E+07	1.07E+05
2020	1.98E+07	9.93E+04	4.90E+05	5.05E+04	2.03E+07	1.11E+05
2021	2.09E+07	1.05E+05	5.17E+05	5.33E+04	2.14E+07	1.18E+05
2022	2.19E+07	1.10E+05	5.42E+05	5.58E+04	2.24E+07	1.23E+05
2023	2.25E+07	1.13E+05	5.59E+05	5.76E+04	2.31E+07	1.27E+05
2024	2.37E+07	1.19E+05	5.86E+05	6.04E+04	2.43E+07	1.33E+05
2025	2.55E+07	1.28E+05	6.31E+05	6.50E+04	2.61E+07	1.44E+05
Year	S1 (SWCNT)		S1 (MWCNT)		S1 (CNTs total)	
	Mean	σ	Mean	σ	Mean	σ
2018	2.42E+06	4.01E+04	9.23E+04	1.82E+04	2.51E+06	4.40E+04
2019	2.55E+06	4.23E+04	9.73E+04	1.92E+04	2.65E+06	4.65E+04
2020	2.65E+06	4.38E+04	1.01E+05	1.99E+04	2.75E+06	4.81E+04
2021	2.80E+06	4.63E+04	1.06E+05	2.10E+04	2.91E+06	5.08E+04
2022	2.93E+06	4.85E+04	1.11E+05	2.20E+04	3.04E+06	5.33E+04
2023	3.02E+06	5.00E+04	1.15E+05	2.27E+04	3.14E+06	5.49E+04
2024	3.17E+06	5.25E+04	1.21E+05	2.38E+04	3.29E+06	5.76E+04
2025	3.41E+06	5.65E+04	1.30E+05	2.57E+04	3.54E+06	6.21E+04
Year	S2 (SWCNT)		S2 (MWCNT)		S2 (CNTs total)	
	Mean	σ	Mean	σ	Mean	σ
2018	2.39E+06	7.85E+04	1.98E+05	3.44E+04	2.59E+06	8.57E+04
2019	2.52E+06	8.27E+04	2.08E+05	3.62E+04	2.73E+06	9.03E+04
2020	2.62E+06	8.57E+04	2.16E+05	3.76E+04	2.84E+06	9.36E+04
2021	2.76E+06	9.05E+04	2.28E+05	3.97E+04	2.99E+06	9.88E+04
2022	2.89E+06	9.48E+04	2.39E+05	4.15E+04	3.13E+06	1.03E+05
2023	2.98E+06	9.78E+04	2.46E+05	4.29E+04	3.23E+06	1.07E+05
2024	3.13E+06	1.03E+05	2.58E+05	4.50E+04	3.39E+06	1.12E+05
2025	3.37E+06	1.10E+05	2.78E+05	4.84E+04	3.65E+06	1.20E+05
Year	S3 (SWCNT)		S3 (MWCNT)		S3 (CNTs total)	
	Mean	σ	Mean	σ	Mean	σ
2018	2.78E+06	1.41E+04	7.85E+04	7.67E+03	2.86E+06	1.61E+04
2019	2.93E+06	1.48E+04	8.27E+04	8.08E+03	3.01E+06	1.69E+04
2020	3.04E+06	1.54E+04	8.57E+04	8.37E+03	3.13E+06	1.75E+04
2021	3.21E+06	1.62E+04	9.06E+04	8.85E+03	3.30E+06	1.85E+04
2022	3.36E+06	1.70E+04	9.48E+04	9.26E+03	3.45E+06	1.94E+04
2023	3.47E+06	1.75E+04	9.78E+04	9.55E+03	3.57E+06	1.99E+04
2024	3.64E+06	1.84E+04	1.03E+05	1.00E+04	3.74E+06	2.09E+04
2025	3.92E+06	1.98E+04	1.10E+05	1.08E+04	4.03E+06	2.26E+04

Table B38. Projected global warming (GW) with and without scaling up approach for optimistic production estimations of SWCNTs, MWCNTs and total CNTs (σ represents standard deviation).

Global Warming (tons CO ₂ -eq./year)						
Year	Lab Scale (SWCNT)		Lab Scale (MWCNT)		Lab Scale (CNTs total)	
	Mean	σ	Mean	σ	Mean	σ
2018	9.19E+07	4.62E+05	2.28E+06	2.35E+05	9.42E+07	5.18E+05
2019	9.74E+07	4.90E+05	2.41E+06	2.49E+05	9.98E+07	5.50E+05
2020	1.04E+08	5.25E+05	2.59E+06	2.67E+05	1.07E+08	5.89E+05
2021	1.11E+08	5.60E+05	2.76E+06	2.84E+05	1.14E+08	6.28E+05
2022	1.20E+08	6.01E+05	2.97E+06	3.06E+05	1.23E+08	6.74E+05
2023	1.59E+08	7.97E+05	3.93E+06	4.05E+05	1.63E+08	8.94E+05
2024	1.70E+08	8.53E+05	4.21E+06	4.34E+05	1.74E+08	9.57E+05
2025	1.95E+08	9.79E+05	4.83E+06	4.98E+05	2.00E+08	1.10E+06
Year	S1 (SWCNT)		S1 (MWCNT)		S1 (CNTs total)	
	Mean	σ	Mean	σ	Mean	σ
2018	1.23E+07	2.04E+05	4.69E+05	9.25E+04	1.28E+07	2.24E+05
2019	1.30E+07	2.16E+05	4.97E+05	9.81E+04	1.35E+07	2.37E+05
2020	1.40E+07	2.31E+05	5.32E+05	1.05E+05	1.45E+07	2.54E+05
2021	1.49E+07	2.47E+05	5.68E+05	1.12E+05	1.55E+07	2.71E+05
2022	1.60E+07	2.65E+05	6.10E+05	1.21E+05	1.66E+07	2.91E+05
2023	2.12E+07	3.52E+05	8.09E+05	1.60E+05	2.20E+07	3.87E+05
2024	2.27E+07	3.76E+05	8.66E+05	1.71E+05	2.36E+07	4.13E+05
2025	2.61E+07	4.32E+05	9.94E+05	1.96E+05	2.71E+07	4.74E+05
Year	S2 (SWCNT)		S2 (MWCNT)		S2 (CNTs total)	
	Mean	σ	Mean	σ	Mean	σ
2018	1.22E+07	3.98E+05	1.00E+06	1.75E+05	1.32E+07	4.35E+05
2019	1.29E+07	4.22E+05	1.06E+06	1.85E+05	1.40E+07	4.61E+05
2020	1.38E+07	4.53E+05	1.14E+06	1.98E+05	1.49E+07	4.94E+05
2021	1.47E+07	4.83E+05	1.22E+06	2.12E+05	1.59E+07	5.27E+05
2022	1.58E+07	5.19E+05	1.31E+06	2.27E+05	1.71E+07	5.66E+05
2023	2.10E+07	6.88E+05	1.73E+06	3.02E+05	2.27E+07	7.51E+05
2024	2.25E+07	7.36E+05	1.85E+06	3.23E+05	2.44E+07	8.04E+05
2025	2.58E+07	8.45E+05	2.13E+06	3.70E+05	2.79E+07	9.22E+05
Year	S3 (SWCNT)		S3 (MWCNT)		S3 (CNTs total)	
	Mean	σ	Mean	σ	Mean	σ
2018	1.41E+07	7.14E+04	3.98E+05	3.89E+04	1.45E+07	8.13E+04
2019	1.50E+07	7.57E+04	4.23E+05	4.13E+04	1.54E+07	8.62E+04
2020	1.61E+07	8.11E+04	4.53E+05	4.42E+04	1.66E+07	9.24E+04
2021	1.71E+07	8.65E+04	4.83E+05	4.72E+04	1.76E+07	9.85E+04
2022	1.84E+07	9.30E+04	5.19E+05	5.07E+04	1.89E+07	1.06E+05
2023	2.44E+07	1.23E+05	6.88E+05	6.72E+04	2.51E+07	1.40E+05
2024	2.61E+07	1.32E+05	7.37E+05	7.19E+04	2.68E+07	1.50E+05
2025	3.00E+07	1.51E+05	8.45E+05	8.26E+04	3.08E+07	1.72E+05

Table B39. Projected acidification (AC) with and without scaling up approach for pessimistic production estimations of SWCNTs, MWCNTs and total CNTs (σ represents standard deviation).

Acidification (tons SO ₂ -eq./year)						
Year	Lab Scale (SWCNT)		Lab Scale (MWCNT)		Lab Scale (CNTs total)	
	Mean	σ	Mean	σ	Mean	σ
2018	1.55E+05	4.77E+02	3.47E+03	2.25E+02	1.58E+05	5.27E+02
2019	1.63E+05	5.03E+02	3.65E+03	2.37E+02	1.67E+05	5.56E+02
2020	1.69E+05	5.21E+02	3.79E+03	2.46E+02	1.73E+05	5.76E+02
2021	1.79E+05	5.51E+02	4.00E+03	2.60E+02	1.83E+05	6.09E+02
2022	1.87E+05	5.76E+02	4.19E+03	2.72E+02	1.91E+05	6.37E+02
2023	1.93E+05	5.95E+02	4.32E+03	2.81E+02	1.97E+05	6.58E+02
2024	2.03E+05	6.24E+02	4.53E+03	2.94E+02	2.08E+05	6.90E+02
2025	2.18E+05	6.72E+02	4.88E+03	3.17E+02	2.23E+05	7.43E+02
Year	S1 (SWCNT)		S1 (MWCNT)		S1 (CNTs total)	
	Mean	σ	Mean	σ	Mean	σ
2018	2.04E+04	1.50E+02	6.49E+02	9.41E+01	2.10E+04	1.77E+02
2019	2.15E+04	1.58E+02	6.84E+02	9.92E+01	2.22E+04	1.87E+02
2020	2.23E+04	1.64E+02	7.09E+02	1.03E+02	2.30E+04	1.94E+02
2021	2.36E+04	1.73E+02	7.49E+02	1.09E+02	2.43E+04	2.04E+02
2022	2.47E+04	1.81E+02	7.84E+02	1.14E+02	2.55E+04	2.14E+02
2023	2.55E+04	1.87E+02	8.09E+02	1.17E+02	2.63E+04	2.21E+02
2024	2.67E+04	1.96E+02	8.49E+02	1.23E+02	2.75E+04	2.31E+02
2025	2.88E+04	2.11E+02	9.13E+02	1.33E+02	2.97E+04	2.49E+02
Year	S2 (SWCNT)		S2 (MWCNT)		S2 (CNTs total)	
	Mean	σ	Mean	σ	Mean	σ
2018	1.80E+04	2.81E+02	8.62E+02	1.17E+02	1.89E+04	3.04E+02
2019	1.90E+04	2.96E+02	9.09E+02	1.23E+02	1.99E+04	3.21E+02
2020	1.97E+04	3.07E+02	9.42E+02	1.28E+02	2.06E+04	3.33E+02
2021	2.08E+04	3.24E+02	9.95E+02	1.35E+02	2.18E+04	3.51E+02
2022	2.18E+04	3.39E+02	1.04E+03	1.41E+02	2.28E+04	3.67E+02
2023	2.25E+04	3.50E+02	1.07E+03	1.46E+02	2.36E+04	3.79E+02
2024	2.36E+04	3.67E+02	1.13E+03	1.53E+02	2.47E+04	3.98E+02
2025	2.54E+04	3.95E+02	1.21E+03	1.65E+02	2.66E+04	4.28E+02
Year	S3 (SWCNT)		S3 (MWCNT)		S3 (CNTs total)	
	Mean	σ	Mean	σ	Mean	σ
2018	2.39E+04	7.39E+01	6.05E+02	3.81E+01	2.45E+04	8.31E+01
2019	2.51E+04	7.79E+01	6.37E+02	4.02E+01	2.57E+04	8.77E+01
2020	2.61E+04	8.08E+01	6.61E+02	4.17E+01	2.68E+04	9.09E+01
2021	2.75E+04	8.53E+01	6.98E+02	4.40E+01	2.82E+04	9.60E+01
2022	2.88E+04	8.93E+01	7.30E+02	4.61E+01	2.95E+04	1.00E+02
2023	2.97E+04	9.21E+01	7.54E+02	4.75E+01	3.05E+04	1.04E+02
2024	3.12E+04	9.67E+01	7.91E+02	4.99E+01	3.20E+04	1.09E+02
2025	3.36E+04	1.04E+02	8.51E+02	5.37E+01	3.45E+04	1.17E+02

Table B40. Projected acidification (AC) with and without scaling up approach for optimistic production estimations of SWCNTs, MWCNTs and total CNTs (σ represents standard deviation).

Acidification (tons SO ₂ -eq./year)						
Year	Lab Scale (SWCNT)		Lab Scale (MWCNT)		Lab Scale (CNTs total)	
	Mean	σ	Mean	σ	Mean	σ
2018	7.87E+05	2.42E+03	1.76E+04	1.14E+03	8.05E+05	2.68E+03
2019	8.35E+05	2.57E+03	1.87E+04	1.21E+03	8.54E+05	2.84E+03
2020	8.94E+05	2.75E+03	2.00E+04	1.30E+03	9.14E+05	3.04E+03
2021	9.54E+05	2.94E+03	2.13E+04	1.39E+03	9.75E+05	3.25E+03
2022	1.03E+06	3.16E+03	2.29E+04	1.49E+03	1.05E+06	3.49E+03
2023	1.36E+06	4.18E+03	3.04E+04	1.97E+03	1.39E+06	4.62E+03
2024	1.45E+06	4.48E+03	3.25E+04	2.11E+03	1.48E+06	4.95E+03
2025	1.67E+06	5.14E+03	3.73E+04	2.42E+03	1.71E+06	5.68E+03
Year	S1 (SWCNT)		S1 (MWCNT)		S1 (CNTs total)	
	Mean	σ	Mean	σ	Mean	σ
2018	1.04E+05	7.61E+02	3.29E+03	4.78E+02	1.07E+05	8.99E+02
2019	1.10E+05	8.07E+02	3.49E+03	5.07E+02	1.13E+05	9.53E+02
2020	1.18E+05	8.64E+02	3.74E+03	5.43E+02	1.22E+05	1.02E+03
2021	1.26E+05	9.22E+02	3.99E+03	5.79E+02	1.30E+05	1.09E+03
2022	1.35E+05	9.91E+02	4.29E+03	6.23E+02	1.39E+05	1.17E+03
2023	1.79E+05	1.31E+03	5.69E+03	8.25E+02	1.85E+05	1.55E+03
2024	1.92E+05	1.41E+03	6.09E+03	8.83E+02	1.98E+05	1.66E+03
2025	2.20E+05	1.61E+03	6.99E+03	1.01E+03	2.27E+05	1.90E+03
Year	S2 (SWCNT)		S2 (MWCNT)		S2 (CNTs total)	
	Mean	σ	Mean	σ	Mean	σ
2018	9.16E+04	1.43E+03	4.38E+03	5.93E+02	9.60E+04	1.55E+03
2019	9.72E+04	1.51E+03	4.64E+03	6.29E+02	1.02E+05	1.64E+03
2020	1.04E+05	1.62E+03	4.98E+03	6.74E+02	1.09E+05	1.75E+03
2021	1.11E+05	1.73E+03	5.31E+03	7.19E+02	1.16E+05	1.87E+03
2022	1.19E+05	1.86E+03	5.71E+03	7.73E+02	1.25E+05	2.01E+03
2023	1.58E+05	2.46E+03	7.56E+03	1.03E+03	1.66E+05	2.67E+03
2024	1.69E+05	2.63E+03	8.09E+03	1.10E+03	1.77E+05	2.85E+03
2025	1.94E+05	3.02E+03	9.29E+03	1.26E+03	2.03E+05	3.27E+03
Year	S3 (SWCNT)		S3 (MWCNT)		S3 (CNTs total)	
	Mean	σ	Mean	σ	Mean	σ
2018	1.21E+05	3.75E+02	3.07E+03	1.94E+02	1.24E+05	4.22E+02
2019	1.28E+05	3.98E+02	3.26E+03	2.05E+02	1.31E+05	4.48E+02
2020	1.38E+05	4.27E+02	3.49E+03	2.20E+02	1.41E+05	4.80E+02
2021	1.47E+05	4.55E+02	3.72E+03	2.35E+02	1.51E+05	5.12E+02
2022	1.58E+05	4.89E+02	4.00E+03	2.52E+02	1.62E+05	5.50E+02
2023	2.09E+05	6.48E+02	5.30E+03	3.34E+02	2.14E+05	7.29E+02
2024	2.24E+05	6.94E+02	5.68E+03	3.58E+02	2.30E+05	7.81E+02
2025	2.57E+05	7.96E+02	6.51E+03	4.11E+02	2.64E+05	8.96E+02

Table B41. Projected eutrophication (EU) with and without scaling up approach for pessimistic production estimations of SWCNTs, MWCNTs and total CNTs (σ represents standard deviation).

Eutrophication (tons N-eq./year)						
Year	Lab Scale (SWCNT)		Lab Scale (MWCNT)		Lab Scale (CNTs total)	
	Mean	σ	Mean	σ	Mean	σ
2018	2.72E+03	4.26E+02	5.39E+02	3.78E+02	3.26E+03	5.70E+02
2019	2.87E+03	4.49E+02	5.68E+02	3.99E+02	3.44E+03	6.01E+02
2020	2.98E+03	4.66E+02	5.89E+02	4.13E+02	3.57E+03	6.23E+02
2021	3.14E+03	4.92E+02	6.22E+02	4.36E+02	3.76E+03	6.57E+02
2022	3.29E+03	5.15E+02	6.51E+02	4.57E+02	3.94E+03	6.89E+02
2023	3.39E+03	5.31E+02	6.72E+02	4.71E+02	4.06E+03	7.10E+02
2024	3.56E+03	5.57E+02	7.05E+02	4.95E+02	4.27E+03	7.45E+02
2025	3.83E+03	6.00E+02	7.59E+02	5.32E+02	4.59E+03	8.02E+02
Year	S1 (SWCNT)		S1 (MWCNT)		S1 (CNTs total)	
	Mean	σ	Mean	σ	Mean	σ
2018	4.66E+02	1.36E+02	2.16E+02	1.64E+02	6.82E+02	2.13E+02
2019	4.91E+02	1.43E+02	2.28E+02	1.73E+02	7.19E+02	2.24E+02
2020	5.09E+02	1.49E+02	2.36E+02	1.79E+02	7.45E+02	2.33E+02
2021	5.38E+02	1.57E+02	2.50E+02	1.89E+02	7.88E+02	2.46E+02
2022	5.63E+02	1.64E+02	2.61E+02	1.98E+02	8.24E+02	2.57E+02
2023	5.81E+02	1.70E+02	2.70E+02	2.04E+02	8.51E+02	2.66E+02
2024	6.09E+02	1.78E+02	2.83E+02	2.14E+02	8.92E+02	2.78E+02
2025	6.56E+02	1.92E+02	3.05E+02	2.31E+02	9.61E+02	3.00E+02
Year	S2 (SWCNT)		S2 (MWCNT)		S2 (CNTs total)	
	Mean	σ	Mean	σ	Mean	σ
2018	6.60E+02	2.38E+02	4.68E+02	2.39E+02	1.13E+03	3.37E+02
2019	6.96E+02	2.51E+02	4.93E+02	2.52E+02	1.19E+03	3.56E+02
2020	7.21E+02	2.61E+02	5.11E+02	2.61E+02	1.23E+03	3.69E+02
2021	7.62E+02	2.75E+02	5.39E+02	2.76E+02	1.30E+03	3.90E+02
2022	7.97E+02	2.88E+02	5.65E+02	2.89E+02	1.36E+03	4.08E+02
2023	8.23E+02	2.97E+02	5.83E+02	2.98E+02	1.41E+03	4.21E+02
2024	8.63E+02	3.12E+02	6.11E+02	3.12E+02	1.47E+03	4.41E+02
2025	9.29E+02	3.36E+02	6.58E+02	3.36E+02	1.59E+03	4.75E+02
Year	S3 (SWCNT)		S3 (MWCNT)		S3 (CNTs total)	
	Mean	σ	Mean	σ	Mean	σ
2018	4.21E+02	6.69E+01	9.37E+01	6.54E+01	5.15E+02	9.36E+01
2019	4.44E+02	7.05E+01	9.87E+01	6.89E+01	5.43E+02	9.86E+01
2020	4.60E+02	7.31E+01	1.02E+02	7.14E+01	5.62E+02	1.02E+02
2021	4.86E+02	7.72E+01	1.08E+02	7.55E+01	5.94E+02	1.08E+02
2022	5.08E+02	8.08E+01	1.13E+02	7.90E+01	6.21E+02	1.13E+02
2023	5.25E+02	8.33E+01	1.17E+02	8.15E+01	6.42E+02	1.17E+02
2024	5.51E+02	8.75E+01	1.22E+02	8.55E+01	6.73E+02	1.22E+02
2025	5.93E+02	9.42E+01	1.32E+02	9.21E+01	7.25E+02	1.32E+02

Table B42. Projected eutrophication (EU) with and without scaling up approach for optimistic production estimations of SWCNTs, MWCNTs and total CNTs (σ represents standard deviation).

Eutrophication (tons N-eq./year)						
Year	Lab Scale (SWCNT)		Lab Scale (MWCNT)		Lab Scale (CNTs total)	
	Mean	σ	Mean	σ	Mean	σ
2018	1.38E+04	2.16E+03	2.74E+03	1.92E+03	1.65E+04	2.89E+03
2019	1.47E+04	2.30E+03	2.90E+03	2.04E+03	1.76E+04	3.07E+03
2020	1.57E+04	2.46E+03	3.11E+03	2.18E+03	1.88E+04	3.29E+03
2021	1.68E+04	2.62E+03	3.32E+03	2.33E+03	2.01E+04	3.51E+03
2022	1.80E+04	2.82E+03	3.56E+03	2.50E+03	2.16E+04	3.77E+03
2023	2.39E+04	3.74E+03	4.73E+03	3.32E+03	2.86E+04	5.00E+03
2024	2.56E+04	4.00E+03	5.06E+03	3.55E+03	3.07E+04	5.35E+03
2025	2.93E+04	4.59E+03	5.80E+03	4.07E+03	3.51E+04	6.13E+03
Year	S1 (SWCNT)		S1 (MWCNT)		S1 (CNTs total)	
	Mean	σ	Mean	σ	Mean	σ
2018	2.37E+03	6.91E+02	1.10E+03	8.32E+02	3.47E+03	1.08E+03
2019	2.51E+03	7.33E+02	1.17E+03	8.82E+02	3.68E+03	1.15E+03
2020	2.69E+03	7.85E+02	1.25E+03	9.45E+02	3.94E+03	1.23E+03
2021	2.87E+03	8.37E+02	1.33E+03	1.01E+03	4.20E+03	1.31E+03
2022	3.08E+03	9.00E+02	1.43E+03	1.08E+03	4.51E+03	1.41E+03
2023	4.09E+03	1.19E+03	1.90E+03	1.44E+03	5.99E+03	1.87E+03
2024	4.37E+03	1.28E+03	2.03E+03	1.54E+03	6.40E+03	2.00E+03
2025	5.02E+03	1.47E+03	2.33E+03	1.76E+03	7.35E+03	2.29E+03
Year	S2 (SWCNT)		S2 (MWCNT)		S2 (CNTs total)	
	Mean	σ	Mean	σ	Mean	σ
2018	3.35E+03	1.21E+03	2.37E+03	1.21E+03	5.72E+03	1.71E+03
2019	3.55E+03	1.28E+03	2.52E+03	1.29E+03	6.07E+03	1.82E+03
2020	3.81E+03	1.38E+03	2.70E+03	1.38E+03	6.51E+03	1.95E+03
2021	4.06E+03	1.47E+03	2.88E+03	1.47E+03	6.94E+03	2.08E+03
2022	4.37E+03	1.58E+03	3.09E+03	1.58E+03	7.46E+03	2.23E+03
2023	5.79E+03	2.09E+03	4.10E+03	2.10E+03	9.89E+03	2.96E+03
2024	6.19E+03	2.24E+03	4.39E+03	2.24E+03	1.06E+04	3.17E+03
2025	7.11E+03	2.57E+03	5.04E+03	2.57E+03	1.22E+04	3.63E+03
Year	S3 (SWCNT)		S3 (MWCNT)		S3 (CNTs total)	
	Mean	σ	Mean	σ	Mean	σ
2018	2.14E+03	3.40E+02	4.75E+02	3.32E+02	2.62E+03	4.75E+02
2019	2.27E+03	3.60E+02	5.04E+02	3.52E+02	2.77E+03	5.03E+02
2020	2.43E+03	3.86E+02	5.40E+02	3.77E+02	2.97E+03	5.40E+02
2021	2.59E+03	4.12E+02	5.76E+02	4.02E+02	3.17E+03	5.76E+02
2022	2.79E+03	4.42E+02	6.20E+02	4.33E+02	3.41E+03	6.19E+02
2023	3.69E+03	5.87E+02	8.21E+02	5.73E+02	4.51E+03	8.20E+02
2024	3.95E+03	6.28E+02	8.79E+02	6.14E+02	4.83E+03	8.78E+02
2025	4.53E+03	7.20E+02	1.01E+03	7.04E+02	5.54E+03	1.01E+03

Table B43. Projected ecotoxicity (EC) with and without scaling up approach for pessimistic production estimations of SWCNTs, MWCNTs and total CNTs (σ represents standard deviation).

Ecotoxicity (CTUe/year)						
Year	Lab Scale (SWCNT)		Lab Scale (MWCNT)		Lab Scale (CNTs total)	
	Mean	σ	Mean	σ	Mean	σ
2018	8.08E+06	8.45E+05	1.01E+06	5.96E+05	9.09E+06	1.03E+06
2019	8.51E+06	8.91E+05	1.07E+06	6.28E+05	9.58E+06	1.09E+06
2020	8.82E+06	9.23E+05	1.11E+06	6.51E+05	9.93E+06	1.13E+06
2021	9.32E+06	9.75E+05	1.17E+06	6.88E+05	1.05E+07	1.19E+06
2022	9.75E+06	1.02E+06	1.23E+06	7.20E+05	1.10E+07	1.25E+06
2023	1.01E+07	1.05E+06	1.26E+06	7.43E+05	1.14E+07	1.29E+06
2024	1.06E+07	1.11E+06	1.33E+06	7.80E+05	1.19E+07	1.36E+06
2025	1.14E+07	1.19E+06	1.43E+06	8.39E+05	1.28E+07	1.46E+06
Year	S1 (SWCNT)		S1 (MWCNT)		S1 (CNTs total)	
	Mean	σ	Mean	σ	Mean	σ
2018	1.32E+06	3.31E+05	4.36E+05	2.81E+05	1.76E+06	4.34E+05
2019	1.39E+06	3.49E+05	4.59E+05	2.96E+05	1.85E+06	4.58E+05
2020	1.44E+06	3.62E+05	4.76E+05	3.07E+05	1.92E+06	4.75E+05
2021	1.52E+06	3.82E+05	5.03E+05	3.24E+05	2.02E+06	5.01E+05
2022	1.60E+06	4.00E+05	5.26E+05	3.39E+05	2.13E+06	5.24E+05
2023	1.65E+06	4.12E+05	5.43E+05	3.50E+05	2.19E+06	5.41E+05
2024	1.73E+06	4.33E+05	5.70E+05	3.68E+05	2.30E+06	5.68E+05
2025	1.86E+06	4.66E+05	6.13E+05	3.96E+05	2.47E+06	6.12E+05
Year	S2 (SWCNT)		S2 (MWCNT)		S2 (CNTs total)	
	Mean	σ	Mean	σ	Mean	σ
2018	1.93E+06	8.61E+05	7.93E+05	4.63E+05	2.72E+06	9.78E+05
2019	2.03E+06	9.07E+05	8.35E+05	4.88E+05	2.87E+06	1.03E+06
2020	2.11E+06	9.41E+05	8.66E+05	5.05E+05	2.98E+06	1.07E+06
2021	2.23E+06	9.94E+05	9.14E+05	5.34E+05	3.14E+06	1.13E+06
2022	2.33E+06	1.04E+06	9.57E+05	5.59E+05	3.29E+06	1.18E+06
2023	2.40E+06	1.07E+06	9.88E+05	5.77E+05	3.39E+06	1.22E+06
2024	2.52E+06	1.13E+06	1.04E+06	6.05E+05	3.56E+06	1.28E+06
2025	2.71E+06	1.21E+06	1.12E+06	6.51E+05	3.83E+06	1.37E+06
Year	S3 (SWCNT)		S3 (MWCNT)		S3 (CNTs total)	
	Mean	σ	Mean	σ	Mean	σ
2018	1.25E+06	1.32E+05	2.10E+05	1.30E+05	1.46E+06	1.85E+05
2019	1.31E+06	1.39E+05	2.21E+05	1.37E+05	1.53E+06	1.95E+05
2020	1.36E+06	1.44E+05	2.29E+05	1.42E+05	1.59E+06	2.02E+05
2021	1.44E+06	1.52E+05	2.42E+05	1.49E+05	1.68E+06	2.13E+05
2022	1.50E+06	1.59E+05	2.53E+05	1.56E+05	1.75E+06	2.23E+05
2023	1.55E+06	1.64E+05	2.62E+05	1.61E+05	1.81E+06	2.30E+05
2024	1.63E+06	1.72E+05	2.74E+05	1.69E+05	1.90E+06	2.41E+05
2025	1.75E+06	1.85E+05	2.95E+05	1.82E+05	2.05E+06	2.60E+05

Table B44. Projected ecotoxicity (EC) with and without scaling up approach for optimistic production estimations of SWCNTs, MWCNTs and total CNTs (σ represents standard deviation).

Ecotoxicity (CTUe/year)						
Year	Lab Scale (SWCNT)		Lab Scale (MWCNT)		Lab Scale (CNTs total)	
	Mean	σ	Mean	σ	Mean	σ
2018	4.10E+07	4.29E+06	5.15E+06	3.03E+06	4.62E+07	5.25E+06
2019	4.35E+07	4.55E+06	5.46E+06	3.21E+06	4.90E+07	5.57E+06
2020	4.66E+07	4.88E+06	5.85E+06	3.44E+06	5.25E+07	5.97E+06
2021	4.97E+07	5.20E+06	6.25E+06	3.67E+06	5.60E+07	6.36E+06
2022	5.34E+07	5.59E+06	6.71E+06	3.94E+06	6.01E+07	6.84E+06
2023	7.08E+07	7.41E+06	8.90E+06	5.23E+06	7.97E+07	9.07E+06
2024	7.58E+07	7.93E+06	9.52E+06	5.59E+06	8.53E+07	9.70E+06
2025	8.70E+07	9.10E+06	1.09E+07	6.42E+06	9.79E+07	1.11E+07
Year	S1 (SWCNT)		S1 (MWCNT)		S1 (CNTs total)	
	Mean	σ	Mean	σ	Mean	σ
2018	6.71E+06	1.68E+06	2.21E+06	1.43E+06	8.92E+06	2.21E+06
2019	7.11E+06	1.78E+06	2.35E+06	1.51E+06	9.46E+06	2.33E+06
2020	7.62E+06	1.91E+06	2.51E+06	1.62E+06	1.01E+07	2.50E+06
2021	8.13E+06	2.04E+06	2.68E+06	1.73E+06	1.08E+07	2.67E+06
2022	8.74E+06	2.19E+06	2.88E+06	1.86E+06	1.16E+07	2.87E+06
2023	1.16E+07	2.90E+06	3.82E+06	2.47E+06	1.54E+07	3.81E+06
2024	1.24E+07	3.11E+06	4.09E+06	2.64E+06	1.65E+07	4.08E+06
2025	1.42E+07	3.56E+06	4.69E+06	3.03E+06	1.89E+07	4.67E+06
Year	S2 (SWCNT)		S2 (MWCNT)		S2 (CNTs total)	
	Mean	σ	Mean	σ	Mean	σ
2018	9.79E+06	4.37E+06	4.02E+06	2.35E+06	1.38E+07	4.96E+06
2019	1.04E+07	4.64E+06	4.27E+06	2.49E+06	1.47E+07	5.27E+06
2020	1.11E+07	4.97E+06	4.57E+06	2.67E+06	1.57E+07	5.64E+06
2021	1.19E+07	5.30E+06	4.88E+06	2.85E+06	1.68E+07	6.02E+06
2022	1.28E+07	5.70E+06	5.24E+06	3.06E+06	1.80E+07	6.47E+06
2023	1.69E+07	7.55E+06	6.95E+06	4.06E+06	2.39E+07	8.57E+06
2024	1.81E+07	8.08E+06	7.44E+06	4.34E+06	2.55E+07	9.17E+06
2025	2.08E+07	9.27E+06	8.53E+06	4.98E+06	2.93E+07	1.05E+07
Year	S3 (SWCNT)		S3 (MWCNT)		S3 (CNTs total)	
	Mean	σ	Mean	σ	Mean	σ
2018	6.32E+06	6.69E+05	1.07E+06	6.58E+05	7.39E+06	9.38E+05
2019	6.71E+06	7.09E+05	1.13E+06	6.98E+05	7.84E+06	9.95E+05
2020	7.19E+06	7.60E+05	1.21E+06	7.47E+05	8.40E+06	1.07E+06
2021	7.67E+06	8.11E+05	1.29E+06	7.97E+05	8.96E+06	1.14E+06
2022	8.24E+06	8.72E+05	1.39E+06	8.57E+05	9.63E+06	1.22E+06
2023	1.09E+07	1.16E+06	1.84E+06	1.14E+06	1.27E+07	1.63E+06
2024	1.17E+07	1.24E+06	1.97E+06	1.22E+06	1.37E+07	1.74E+06
2025	1.34E+07	1.42E+06	2.26E+06	1.40E+06	1.57E+07	1.99E+06

Table B45. Projected carcinogenics (HHC) with and without scaling up approach for pessimistic production estimations of SWCNTs, MWCNTs and total CNTs (σ represents standard deviation).

Carcinogenics (CTUh/year)						
Year	Lab Scale (SWCNT)		Lab Scale (MWCNT)		Lab Scale (CNTs total)	
	Mean	σ	Mean	σ	Mean	σ
2018	4.12E-02	8.30E-03	7.77E-03	7.21E-03	4.90E-02	1.10E-02
2019	4.35E-02	8.75E-03	8.18E-03	7.60E-03	5.17E-02	1.16E-02
2020	4.50E-02	9.07E-03	8.48E-03	7.88E-03	5.35E-02	1.20E-02
2021	4.76E-02	9.58E-03	8.96E-03	8.32E-03	5.66E-02	1.27E-02
2022	4.98E-02	1.00E-02	9.38E-03	8.71E-03	5.92E-02	1.33E-02
2023	5.14E-02	1.03E-02	9.68E-03	8.99E-03	6.11E-02	1.37E-02
2024	5.39E-02	1.09E-02	1.02E-02	9.43E-03	6.41E-02	1.44E-02
2025	5.80E-02	1.17E-02	1.09E-02	1.02E-02	6.89E-02	1.55E-02
Year	S1 (SWCNT)		S1 (MWCNT)		S1 (CNTs total)	
	Mean	σ	Mean	σ	Mean	σ
2018	7.22E-03	3.15E-03	3.30E-03	3.14E-03	1.05E-02	4.45E-03
2019	7.61E-03	3.32E-03	3.47E-03	3.31E-03	1.11E-02	4.69E-03
2020	7.89E-03	3.44E-03	3.60E-03	3.43E-03	1.15E-02	4.86E-03
2021	8.34E-03	3.64E-03	3.80E-03	3.63E-03	1.21E-02	5.14E-03
2022	8.72E-03	3.81E-03	3.98E-03	3.80E-03	1.27E-02	5.38E-03
2023	9.00E-03	3.93E-03	4.11E-03	3.92E-03	1.31E-02	5.55E-03
2024	9.45E-03	4.12E-03	4.31E-03	4.11E-03	1.38E-02	5.82E-03
2025	1.02E-02	4.44E-03	4.64E-03	4.43E-03	1.48E-02	6.27E-03
Year	S2 (SWCNT)		S2 (MWCNT)		S2 (CNTs total)	
	Mean	σ	Mean	σ	Mean	σ
2018	1.03E-02	6.28E-03	5.96E-03	5.15E-03	1.63E-02	8.12E-03
2019	1.09E-02	6.62E-03	6.28E-03	5.42E-03	1.72E-02	8.56E-03
2020	1.13E-02	6.86E-03	6.51E-03	5.62E-03	1.78E-02	8.87E-03
2021	1.19E-02	7.25E-03	6.88E-03	5.94E-03	1.88E-02	9.37E-03
2022	1.25E-02	7.59E-03	7.20E-03	6.21E-03	1.97E-02	9.81E-03
2023	1.29E-02	7.83E-03	7.43E-03	6.41E-03	2.03E-02	1.01E-02
2024	1.35E-02	8.21E-03	7.80E-03	6.73E-03	2.13E-02	1.06E-02
2025	1.45E-02	8.84E-03	8.39E-03	7.24E-03	2.29E-02	1.14E-02
Year	S3 (SWCNT)		S3 (MWCNT)		S3 (CNTs total)	
	Mean	σ	Mean	σ	Mean	σ
2018	6.38E-03	1.31E-03	1.42E-03	1.27E-03	7.80E-03	1.82E-03
2019	6.72E-03	1.38E-03	1.50E-03	1.34E-03	8.22E-03	1.92E-03
2020	6.96E-03	1.43E-03	1.56E-03	1.39E-03	8.52E-03	1.99E-03
2021	7.36E-03	1.51E-03	1.64E-03	1.47E-03	9.00E-03	2.11E-03
2022	7.70E-03	1.58E-03	1.72E-03	1.53E-03	9.42E-03	2.20E-03
2023	7.94E-03	1.63E-03	1.78E-03	1.58E-03	9.72E-03	2.27E-03
2024	8.34E-03	1.71E-03	1.86E-03	1.66E-03	1.02E-02	2.38E-03
2025	8.97E-03	1.84E-03	2.01E-03	1.79E-03	1.10E-02	2.57E-03

Table B46. Projected carcinogenics (HHC) with and without scaling up approach for optimistic production estimations of SWCNTs, MWCNTs and total CNTs (σ represents standard deviation).

Carcinogenics (CTUh/year)						
Year	Lab Scale (SWCNT)		Lab Scale (MWCNT)		Lab Scale (CNTs total)	
	Mean	σ	Mean	σ	Mean	σ
2018	2.09E-01	4.21E-02	3.94E-02	3.66E-02	2.48E-01	5.58E-02
2019	2.22E-01	4.47E-02	4.18E-02	3.88E-02	2.64E-01	5.92E-02
2020	2.38E-01	4.79E-02	4.48E-02	4.16E-02	2.83E-01	6.34E-02
2021	2.54E-01	5.11E-02	4.78E-02	4.44E-02	3.02E-01	6.77E-02
2022	2.73E-01	5.49E-02	5.14E-02	4.77E-02	3.24E-01	7.27E-02
2023	3.62E-01	7.28E-02	6.81E-02	6.33E-02	4.30E-01	9.65E-02
2024	3.87E-01	7.79E-02	7.29E-02	6.77E-02	4.60E-01	1.03E-01
2025	4.44E-01	8.94E-02	8.36E-02	7.77E-02	5.28E-01	1.18E-01
Year	S1 (SWCNT)		S1 (MWCNT)		S1 (CNTs total)	
	Mean	σ	Mean	σ	Mean	σ
2018	3.67E-02	1.60E-02	1.67E-02	1.60E-02	5.34E-02	2.26E-02
2019	3.89E-02	1.70E-02	1.77E-02	1.69E-02	5.66E-02	2.40E-02
2020	4.17E-02	1.82E-02	1.90E-02	1.81E-02	6.07E-02	2.57E-02
2021	4.45E-02	1.94E-02	2.03E-02	1.93E-02	6.48E-02	2.74E-02
2022	4.78E-02	2.08E-02	2.18E-02	2.08E-02	6.96E-02	2.94E-02
2023	6.34E-02	2.76E-02	2.89E-02	2.76E-02	9.23E-02	3.90E-02
2024	6.78E-02	2.96E-02	3.09E-02	2.95E-02	9.87E-02	4.18E-02
2025	7.78E-02	3.39E-02	3.55E-02	3.39E-02	1.13E-01	4.79E-02
Year	S2 (SWCNT)		S2 (MWCNT)		S2 (CNTs total)	
	Mean	σ	Mean	σ	Mean	σ
2018	5.25E-02	3.19E-02	3.03E-02	2.61E-02	8.28E-02	4.12E-02
2019	5.56E-02	3.38E-02	3.21E-02	2.77E-02	8.77E-02	4.37E-02
2020	5.96E-02	3.62E-02	3.44E-02	2.97E-02	9.40E-02	4.68E-02
2021	6.36E-02	3.87E-02	3.67E-02	3.17E-02	1.00E-01	5.00E-02
2022	6.83E-02	4.16E-02	3.94E-02	3.40E-02	1.08E-01	5.37E-02
2023	9.06E-02	5.51E-02	5.23E-02	4.51E-02	1.43E-01	7.12E-02
2024	9.70E-02	5.90E-02	5.60E-02	4.83E-02	1.53E-01	7.62E-02
2025	1.11E-01	6.76E-02	6.42E-02	5.54E-02	1.75E-01	8.74E-02
Year	S3 (SWCNT)		S3 (MWCNT)		S3 (CNTs total)	
	Mean	σ	Mean	σ	Mean	σ
2018	3.24E-02	6.65E-03	7.23E-03	6.45E-03	3.96E-02	9.26E-03
2019	3.43E-02	7.05E-03	7.67E-03	6.84E-03	4.20E-02	9.82E-03
2020	3.68E-02	7.55E-03	8.22E-03	7.33E-03	4.50E-02	1.05E-02
2021	3.92E-02	8.06E-03	8.77E-03	7.82E-03	4.80E-02	1.12E-02
2022	4.22E-02	8.66E-03	9.42E-03	8.40E-03	5.16E-02	1.21E-02
2023	5.59E-02	1.15E-02	1.25E-02	1.11E-02	6.84E-02	1.60E-02
2024	5.98E-02	1.23E-02	1.34E-02	1.19E-02	7.32E-02	1.71E-02
2025	6.87E-02	1.41E-02	1.53E-02	1.37E-02	8.40E-02	1.97E-02

Table B47. Projected non carcinogenics (HHNC) with and without scaling up approach for pessimistic production estimations of SWCNTs, MWCNTs and total CNTs (σ represents standard deviation).

Non Carcinogenics (CTUh/year)						
Year	Lab Scale (SWCNT)		Lab Scale (MWCNT)		Lab Scale (CNTs total)	
	Mean	σ	Mean	σ	Mean	σ
2018	6.05E-01	2.89E-02	4.12E-02	2.52E-02	6.46E-01	3.83E-02
2019	6.38E-01	3.05E-02	4.34E-02	2.66E-02	6.81E-01	4.05E-02
2020	6.61E-01	3.16E-02	4.50E-02	2.76E-02	7.06E-01	4.20E-02
2021	6.98E-01	3.33E-02	4.75E-02	2.91E-02	7.46E-01	4.42E-02
2022	7.31E-01	3.49E-02	4.97E-02	3.05E-02	7.81E-01	4.63E-02
2023	7.54E-01	3.60E-02	5.13E-02	3.14E-02	8.05E-01	4.78E-02
2024	7.92E-01	3.78E-02	5.38E-02	3.30E-02	8.46E-01	5.02E-02
2025	8.52E-01	4.07E-02	5.80E-02	3.55E-02	9.10E-01	5.40E-02
Year	S1 (SWCNT)		S1 (MWCNT)		S1 (CNTs total)	
	Mean	σ	Mean	σ	Mean	σ
2018	8.67E-02	1.10E-02	1.54E-02	1.08E-02	1.02E-01	1.54E-02
2019	9.13E-02	1.16E-02	1.62E-02	1.13E-02	1.08E-01	1.62E-02
2020	9.47E-02	1.20E-02	1.68E-02	1.18E-02	1.12E-01	1.68E-02
2021	1.00E-01	1.27E-02	1.78E-02	1.24E-02	1.18E-01	1.77E-02
2022	1.05E-01	1.33E-02	1.86E-02	1.30E-02	1.24E-01	1.86E-02
2023	1.08E-01	1.37E-02	1.92E-02	1.34E-02	1.27E-01	1.92E-02
2024	1.13E-01	1.44E-02	2.01E-02	1.41E-02	1.33E-01	2.02E-02
2025	1.22E-01	1.55E-02	2.17E-02	1.52E-02	1.44E-01	2.17E-02
Year	S2 (SWCNT)		S2 (MWCNT)		S2 (CNTs total)	
	Mean	σ	Mean	σ	Mean	σ
2018	1.06E-01	3.51E-02	2.11E-02	2.31E-02	1.27E-01	4.20E-02
2019	1.12E-01	3.70E-02	2.22E-02	2.44E-02	1.34E-01	4.43E-02
2020	1.16E-01	3.84E-02	2.30E-02	2.53E-02	1.39E-01	4.60E-02
2021	1.22E-01	4.05E-02	2.43E-02	2.67E-02	1.46E-01	4.85E-02
2022	1.28E-01	4.24E-02	2.55E-02	2.79E-02	1.54E-01	5.08E-02
2023	1.32E-01	4.38E-02	2.63E-02	2.88E-02	1.58E-01	5.24E-02
2024	1.39E-01	4.59E-02	2.76E-02	3.02E-02	1.67E-01	5.49E-02
2025	1.49E-01	4.95E-02	2.97E-02	3.26E-02	1.79E-01	5.93E-02
Year	S3 (SWCNT)		S3 (MWCNT)		S3 (CNTs total)	
	Mean	σ	Mean	σ	Mean	σ
2018	9.32E-02	4.52E-03	7.97E-03	5.22E-03	1.01E-01	6.90E-03
2019	9.83E-02	4.76E-03	8.40E-03	5.50E-03	1.07E-01	7.27E-03
2020	1.02E-01	4.93E-03	8.71E-03	5.71E-03	1.11E-01	7.54E-03
2021	1.08E-01	5.21E-03	9.20E-03	6.03E-03	1.17E-01	7.97E-03
2022	1.13E-01	5.45E-03	9.63E-03	6.31E-03	1.23E-01	8.34E-03
2023	1.16E-01	5.63E-03	9.94E-03	6.51E-03	1.26E-01	8.61E-03
2024	1.22E-01	5.91E-03	1.04E-02	6.83E-03	1.32E-01	9.03E-03
2025	1.31E-01	6.36E-03	1.12E-02	7.35E-03	1.42E-01	9.72E-03

Table B48. Projected non carcinogenics (HHNC) with and without scaling up approach for optimistic production estimations of SWCNTs, MWCNTs and total CNTs (σ represents standard deviation).

Non Carcinogenics (CTUh/year)						
Year	Lab Scale (SWCNT)		Lab Scale (MWCNT)		Lab Scale (CNTs total)	
	Mean	σ	Mean	σ	Mean	σ
2018	3.07E+00	1.47E-01	2.09E-01	1.28E-01	3.28E+00	1.95E-01
2019	3.26E+00	1.56E-01	2.22E-01	1.36E-01	3.48E+00	2.07E-01
2020	3.49E+00	1.67E-01	2.38E-01	1.46E-01	3.73E+00	2.22E-01
2021	3.72E+00	1.78E-01	2.53E-01	1.55E-01	3.97E+00	2.36E-01
2022	4.00E+00	1.91E-01	2.72E-01	1.67E-01	4.27E+00	2.54E-01
2023	5.31E+00	2.53E-01	3.61E-01	2.21E-01	5.67E+00	3.36E-01
2024	5.68E+00	2.71E-01	3.86E-01	2.37E-01	6.07E+00	3.60E-01
2025	6.52E+00	3.11E-01	4.43E-01	2.72E-01	6.96E+00	4.13E-01
Year	S1 (SWCNT)		S1 (MWCNT)		S1 (CNTs total)	
	Mean	σ	Mean	σ	Mean	σ
2018	4.40E-01	5.59E-02	7.82E-02	5.47E-02	5.18E-01	7.82E-02
2019	4.67E-01	5.93E-02	8.29E-02	5.80E-02	5.50E-01	8.29E-02
2020	5.00E-01	6.36E-02	8.89E-02	6.21E-02	5.89E-01	8.89E-02
2021	5.33E-01	6.78E-02	9.48E-02	6.63E-02	6.28E-01	9.48E-02
2022	5.73E-01	7.29E-02	1.02E-01	7.12E-02	6.75E-01	1.02E-01
2023	7.60E-01	9.66E-02	1.35E-01	9.44E-02	8.95E-01	1.35E-01
2024	8.13E-01	1.03E-01	1.45E-01	1.01E-01	9.58E-01	1.44E-01
2025	9.33E-01	1.19E-01	1.66E-01	1.16E-01	1.10E+00	1.66E-01
Year	S2 (SWCNT)		S2 (MWCNT)		S2 (CNTs total)	
	Mean	σ	Mean	σ	Mean	σ
2018	5.38E-01	1.78E-01	1.07E-01	1.17E-01	6.45E-01	2.13E-01
2019	5.70E-01	1.89E-01	1.14E-01	1.25E-01	6.84E-01	2.27E-01
2020	6.11E-01	2.03E-01	1.22E-01	1.33E-01	7.33E-01	2.43E-01
2021	6.52E-01	2.16E-01	1.30E-01	1.42E-01	7.82E-01	2.58E-01
2022	7.01E-01	2.32E-01	1.39E-01	1.53E-01	8.40E-01	2.78E-01
2023	9.29E-01	3.08E-01	1.85E-01	2.03E-01	1.11E+00	3.69E-01
2024	9.94E-01	3.30E-01	1.98E-01	2.17E-01	1.19E+00	3.95E-01
2025	1.14E+00	3.78E-01	2.27E-01	2.49E-01	1.37E+00	4.53E-01
Year	S3 (SWCNT)		S3 (MWCNT)		S3 (CNTs total)	
	Mean	σ	Mean	σ	Mean	σ
2018	4.73E-01	2.29E-02	4.05E-02	2.65E-02	5.14E-01	3.50E-02
2019	5.02E-01	2.43E-02	4.29E-02	2.81E-02	5.45E-01	3.71E-02
2020	5.38E-01	2.61E-02	4.60E-02	3.01E-02	5.84E-01	3.98E-02
2021	5.74E-01	2.78E-02	4.91E-02	3.21E-02	6.23E-01	4.25E-02
2022	6.17E-01	2.99E-02	5.27E-02	3.46E-02	6.70E-01	4.57E-02
2023	8.18E-01	3.96E-02	6.99E-02	4.58E-02	8.88E-01	6.05E-02
2024	8.75E-01	4.24E-02	7.48E-02	4.90E-02	9.50E-01	6.48E-02
2025	1.00E+00	4.86E-02	8.59E-02	5.62E-02	1.09E+00	7.43E-02

Table B49. Projected respiratory effects (RE) with and without scaling up approach for pessimistic production estimations of SWCNTs, MWCNTs and total CNTs (σ represents standard deviation).

Respiratory effects (tons PM _{2.5} /year)						
Year	Lab Scale (SWCNT)		Lab Scale (MWCNT)		Lab Scale (CNTs total)	
	Mean	σ	Mean	σ	Mean	σ
2018	7.67E+03	1.08E+02	2.87E+02	8.21E+01	7.96E+03	1.36E+02
2019	8.08E+03	1.14E+02	3.03E+02	8.65E+01	8.38E+03	1.43E+02
2020	8.38E+03	1.18E+02	3.14E+02	8.97E+01	8.69E+03	1.48E+02
2021	8.85E+03	1.24E+02	3.31E+02	9.48E+01	9.18E+03	1.56E+02
2022	9.26E+03	1.30E+02	3.47E+02	9.92E+01	9.61E+03	1.64E+02
2023	9.56E+03	1.34E+02	3.58E+02	1.02E+02	9.92E+03	1.68E+02
2024	1.00E+04	1.41E+02	3.76E+02	1.07E+02	1.04E+04	1.77E+02
2025	1.08E+04	1.52E+02	4.04E+02	1.16E+02	1.12E+04	1.91E+02
Year	S1 (SWCNT)		S1 (MWCNT)		S1 (CNTs total)	
	Mean	σ	Mean	σ	Mean	σ
2018	1.04E+03	3.92E+01	7.95E+01	3.49E+01	1.12E+03	5.25E+01
2019	1.10E+03	4.13E+01	8.38E+01	3.68E+01	1.18E+03	5.53E+01
2020	1.14E+03	4.29E+01	8.69E+01	3.81E+01	1.23E+03	5.74E+01
2021	1.20E+03	4.53E+01	9.18E+01	4.03E+01	1.29E+03	6.06E+01
2022	1.26E+03	4.74E+01	9.60E+01	4.21E+01	1.36E+03	6.34E+01
2023	1.30E+03	4.89E+01	9.91E+01	4.35E+01	1.40E+03	6.54E+01
2024	1.36E+03	5.13E+01	1.04E+02	4.56E+01	1.46E+03	6.86E+01
2025	1.47E+03	5.52E+01	1.12E+02	4.91E+01	1.58E+03	7.39E+01
Year	S2 (SWCNT)		S2 (MWCNT)		S2 (CNTs total)	
	Mean	σ	Mean	σ	Mean	σ
2018	9.92E+02	6.68E+01	1.45E+02	5.05E+01	1.14E+03	8.37E+01
2019	1.05E+03	7.04E+01	1.53E+02	5.32E+01	1.20E+03	8.82E+01
2020	1.08E+03	7.30E+01	1.58E+02	5.52E+01	1.24E+03	9.15E+01
2021	1.14E+03	7.71E+01	1.67E+02	5.83E+01	1.31E+03	9.67E+01
2022	1.20E+03	8.07E+01	1.75E+02	6.10E+01	1.38E+03	1.01E+02
2023	1.24E+03	8.32E+01	1.80E+02	6.29E+01	1.42E+03	1.04E+02
2024	1.30E+03	8.73E+01	1.89E+02	6.60E+01	1.49E+03	1.09E+02
2025	1.40E+03	9.40E+01	2.04E+02	7.11E+01	1.60E+03	1.18E+02
Year	S3 (SWCNT)		S3 (MWCNT)		S3 (CNTs total)	
	Mean	σ	Mean	σ	Mean	σ
2018	1.18E+03	1.66E+01	4.97E+01	1.37E+01	1.23E+03	2.15E+01
2019	1.24E+03	1.75E+01	5.24E+01	1.44E+01	1.29E+03	2.27E+01
2020	1.29E+03	1.82E+01	5.43E+01	1.50E+01	1.34E+03	2.36E+01
2021	1.36E+03	1.92E+01	5.74E+01	1.58E+01	1.42E+03	2.49E+01
2022	1.43E+03	2.01E+01	6.00E+01	1.65E+01	1.49E+03	2.60E+01
2023	1.47E+03	2.07E+01	6.20E+01	1.71E+01	1.53E+03	2.68E+01
2024	1.54E+03	2.18E+01	6.50E+01	1.79E+01	1.61E+03	2.82E+01
2025	1.66E+03	2.34E+01	7.00E+01	1.93E+01	1.73E+03	3.03E+01

Table B50. Projected respiratory effects (RE) with and without scaling up approach for optimistic production estimations of SWCNTs, MWCNTs and total CNTs (σ represents standard deviation).

Respiratory effects (tons PM2.5/year)						
Year	Lab Scale (SWCNT)		Lab Scale (MWCNT)		Lab Scale (CNTs total)	
	Mean	σ	Mean	σ	Mean	σ
2018	3.89E+04	5.48E+02	1.46E+03	4.17E+02	4.04E+04	6.89E+02
2019	4.13E+04	5.81E+02	1.55E+03	4.42E+02	4.29E+04	7.30E+02
2020	4.42E+04	6.22E+02	1.66E+03	4.74E+02	4.59E+04	7.82E+02
2021	4.72E+04	6.64E+02	1.77E+03	5.05E+02	4.90E+04	8.34E+02
2022	5.07E+04	7.13E+02	1.90E+03	5.43E+02	5.26E+04	8.96E+02
2023	6.72E+04	9.46E+02	2.52E+03	7.20E+02	6.97E+04	1.19E+03
2024	7.20E+04	1.01E+03	2.70E+03	7.71E+02	7.47E+04	1.27E+03
2025	8.26E+04	1.16E+03	3.09E+03	8.84E+02	8.57E+04	1.46E+03
Year	S1 (SWCNT)		S1 (MWCNT)		S1 (CNTs total)	
	Mean	σ	Mean	σ	Mean	σ
2018	5.29E+03	1.99E+02	4.04E+02	1.77E+02	5.69E+03	2.66E+02
2019	5.61E+03	2.11E+02	4.28E+02	1.88E+02	6.04E+03	2.83E+02
2020	6.01E+03	2.26E+02	4.59E+02	2.01E+02	6.47E+03	3.02E+02
2021	6.41E+03	2.41E+02	4.89E+02	2.15E+02	6.90E+03	3.23E+02
2022	6.89E+03	2.60E+02	5.26E+02	2.31E+02	7.42E+03	3.48E+02
2023	9.13E+03	3.44E+02	6.97E+02	3.06E+02	9.83E+03	4.60E+02
2024	9.77E+03	3.68E+02	7.46E+02	3.27E+02	1.05E+04	4.92E+02
2025	1.12E+04	4.23E+02	8.56E+02	3.76E+02	1.21E+04	5.66E+02
Year	S2 (SWCNT)		S2 (MWCNT)		S2 (CNTs total)	
	Mean	σ	Mean	σ	Mean	σ
2018	5.04E+03	3.39E+02	7.35E+02	2.56E+02	5.78E+03	4.25E+02
2019	5.34E+03	3.60E+02	7.80E+02	2.72E+02	6.12E+03	4.51E+02
2020	5.72E+03	3.85E+02	8.36E+02	2.91E+02	6.56E+03	4.83E+02
2021	6.10E+03	4.11E+02	8.91E+02	3.11E+02	6.99E+03	5.15E+02
2022	6.56E+03	4.42E+02	9.58E+02	3.34E+02	7.52E+03	5.54E+02
2023	8.70E+03	5.86E+02	1.27E+03	4.43E+02	9.97E+03	7.35E+02
2024	9.31E+03	6.27E+02	1.36E+03	4.74E+02	1.07E+04	7.86E+02
2025	1.07E+04	7.19E+02	1.56E+03	5.44E+02	1.23E+04	9.02E+02
Year	S3 (SWCNT)		S3 (MWCNT)		S3 (CNTs total)	
	Mean	σ	Mean	σ	Mean	σ
2018	5.99E+03	8.45E+01	2.52E+02	6.96E+01	6.24E+03	1.09E+02
2019	6.35E+03	8.96E+01	2.68E+02	7.38E+01	6.62E+03	1.16E+02
2020	6.81E+03	9.60E+01	2.87E+02	7.90E+01	7.10E+03	1.24E+02
2021	7.26E+03	1.02E+02	3.06E+02	8.43E+01	7.57E+03	1.32E+02
2022	7.81E+03	1.10E+02	3.29E+02	9.06E+01	8.14E+03	1.43E+02
2023	1.03E+04	1.46E+02	4.36E+02	1.20E+02	1.07E+04	1.89E+02
2024	1.11E+04	1.56E+02	4.67E+02	1.29E+02	1.16E+04	2.02E+02
2025	1.27E+04	1.79E+02	5.35E+02	1.48E+02	1.32E+04	2.32E+02

Table B51. Projected fossil fuel depletion (FF) with and without scaling up approach for pessimistic production estimations of SWCNTs, MWCNTs and total CNTs (σ represents standard deviation).

Fossil fuel depletion (MJ surplus energy/year)						
Year	Lab Scale (SWCNT)		Lab Scale (MWCNT)		Lab Scale (CNTs total)	
	Mean	σ	Mean	σ	Mean	σ
2018	1.16E+07	1.96E+05	3.82E+05	4.95E+04	1.20E+07	2.02E+05
2019	1.23E+07	2.06E+05	4.02E+05	5.22E+04	1.27E+07	2.13E+05
2020	1.27E+07	2.14E+05	4.17E+05	5.41E+04	1.31E+07	2.21E+05
2021	1.34E+07	2.26E+05	4.40E+05	5.71E+04	1.38E+07	2.33E+05
2022	1.41E+07	2.37E+05	4.61E+05	5.98E+04	1.46E+07	2.44E+05
2023	1.45E+07	2.44E+05	4.76E+05	6.17E+04	1.50E+07	2.52E+05
2024	1.52E+07	2.56E+05	4.99E+05	6.48E+04	1.57E+07	2.64E+05
2025	1.64E+07	2.76E+05	5.37E+05	6.97E+04	1.69E+07	2.85E+05
Year	S1 (SWCNT)		S1 (MWCNT)		S1 (CNTs total)	
	Mean	σ	Mean	σ	Mean	σ
2018	1.54E+06	3.55E+04	1.07E+05	2.29E+04	1.65E+06	4.22E+04
2019	1.62E+06	3.74E+04	1.12E+05	2.42E+04	1.73E+06	4.45E+04
2020	1.68E+06	3.88E+04	1.16E+05	2.50E+04	1.80E+06	4.62E+04
2021	1.77E+06	4.10E+04	1.23E+05	2.64E+04	1.89E+06	4.88E+04
2022	1.86E+06	4.29E+04	1.29E+05	2.77E+04	1.99E+06	5.11E+04
2023	1.92E+06	4.43E+04	1.33E+05	2.86E+04	2.05E+06	5.27E+04
2024	2.01E+06	4.65E+04	1.39E+05	3.00E+04	2.15E+06	5.53E+04
2025	2.16E+06	5.00E+04	1.50E+05	3.23E+04	2.31E+06	5.95E+04
Year	S2 (SWCNT)		S2 (MWCNT)		S2 (CNTs total)	
	Mean	σ	Mean	σ	Mean	σ
2018	1.78E+06	1.87E+05	3.46E+05	3.25E+04	2.13E+06	1.90E+05
2019	1.88E+06	1.97E+05	3.64E+05	3.43E+04	2.24E+06	2.00E+05
2020	1.95E+06	2.04E+05	3.78E+05	3.56E+04	2.33E+06	2.07E+05
2021	2.06E+06	2.16E+05	3.99E+05	3.76E+04	2.46E+06	2.19E+05
2022	2.15E+06	2.26E+05	4.18E+05	3.93E+04	2.57E+06	2.29E+05
2023	2.22E+06	2.33E+05	4.31E+05	4.06E+04	2.65E+06	2.37E+05
2024	2.33E+06	2.45E+05	4.52E+05	4.26E+04	2.78E+06	2.49E+05
2025	2.51E+06	2.63E+05	4.87E+05	4.58E+04	3.00E+06	2.67E+05
Year	S3 (SWCNT)		S3 (MWCNT)		S3 (CNTs total)	
	Mean	σ	Mean	σ	Mean	σ
2018	1.79E+06	3.06E+04	7.21E+04	8.08E+03	1.86E+06	3.16E+04
2019	1.89E+06	3.22E+04	7.60E+04	8.52E+03	1.97E+06	3.33E+04
2020	1.96E+06	3.34E+04	7.88E+04	8.83E+03	2.04E+06	3.45E+04
2021	2.07E+06	3.53E+04	8.32E+04	9.33E+03	2.15E+06	3.65E+04
2022	2.16E+06	3.69E+04	8.71E+04	9.76E+03	2.25E+06	3.82E+04
2023	2.23E+06	3.81E+04	8.99E+04	1.01E+04	2.32E+06	3.94E+04
2024	2.34E+06	4.00E+04	9.43E+04	1.06E+04	2.43E+06	4.14E+04
2025	2.52E+06	4.30E+04	1.02E+05	1.14E+04	2.62E+06	4.45E+04

Table B52. Projected fossil fuel depletion (FF) with and without scaling up approach for optimistic production estimations of SWCNTs, MWCNTs and total CNTs (σ represents standard deviation).

Fossil fuel depletion (MJ surplus energy/year)						
Year	Lab Scale (SWCNT)		Lab Scale (MWCNT)		Lab Scale (CNTs total)	
	Mean	σ	Mean	σ	Mean	σ
2018	5.91E+07	9.95E+05	1.94E+06	2.51E+05	6.10E+07	1.03E+06
2019	6.26E+07	1.05E+06	2.06E+06	2.67E+05	6.47E+07	1.08E+06
2020	6.71E+07	1.13E+06	2.20E+06	2.86E+05	6.93E+07	1.17E+06
2021	7.16E+07	1.21E+06	2.35E+06	3.05E+05	7.40E+07	1.25E+06
2022	7.70E+07	1.30E+06	2.53E+06	3.28E+05	7.95E+07	1.34E+06
2023	1.02E+08	1.72E+06	3.35E+06	4.34E+05	1.05E+08	1.77E+06
2024	1.09E+08	1.84E+06	3.58E+06	4.65E+05	1.13E+08	1.90E+06
2025	1.25E+08	2.11E+06	4.11E+06	5.33E+05	1.29E+08	2.18E+06
Year	S1 (SWCNT)		S1 (MWCNT)		S1 (CNTs total)	
	Mean	σ	Mean	σ	Mean	σ
2018	7.80E+06	1.80E+05	5.41E+05	1.16E+05	8.34E+06	2.14E+05
2019	8.28E+06	1.91E+05	5.74E+05	1.23E+05	8.85E+06	2.27E+05
2020	8.87E+06	2.05E+05	6.15E+05	1.32E+05	9.49E+06	2.44E+05
2021	9.46E+06	2.19E+05	6.56E+05	1.41E+05	1.01E+07	2.60E+05
2022	1.02E+07	2.35E+05	7.05E+05	1.52E+05	1.09E+07	2.80E+05
2023	1.35E+07	3.12E+05	9.35E+05	2.01E+05	1.44E+07	3.71E+05
2024	1.44E+07	3.33E+05	1.00E+06	2.15E+05	1.54E+07	3.96E+05
2025	1.66E+07	3.83E+05	1.15E+06	2.47E+05	1.78E+07	4.56E+05
Year	S2 (SWCNT)		S2 (MWCNT)		S2 (CNTs total)	
	Mean	σ	Mean	σ	Mean	σ
2018	9.05E+06	9.50E+05	1.76E+06	1.65E+05	1.08E+07	9.64E+05
2019	9.60E+06	1.01E+06	1.86E+06	1.75E+05	1.15E+07	1.03E+06
2020	1.03E+07	1.08E+06	1.99E+06	1.88E+05	1.23E+07	1.10E+06
2021	1.10E+07	1.15E+06	2.13E+06	2.00E+05	1.31E+07	1.17E+06
2022	1.18E+07	1.24E+06	2.29E+06	2.15E+05	1.41E+07	1.26E+06
2023	1.56E+07	1.64E+06	3.03E+06	2.85E+05	1.86E+07	1.66E+06
2024	1.67E+07	1.76E+06	3.25E+06	3.05E+05	2.00E+07	1.79E+06
2025	1.92E+07	2.01E+06	3.72E+06	3.51E+05	2.29E+07	2.04E+06
Year	S3 (SWCNT)		S3 (MWCNT)		S3 (CNTs total)	
	Mean	σ	Mean	σ	Mean	σ
2018	9.09E+06	1.55E+05	3.66E+05	4.10E+04	9.46E+06	1.60E+05
2019	9.65E+06	1.65E+05	3.88E+05	4.35E+04	1.00E+07	1.71E+05
2020	1.03E+07	1.76E+05	4.16E+05	4.66E+04	1.07E+07	1.82E+05
2021	1.10E+07	1.88E+05	4.44E+05	4.97E+04	1.14E+07	1.94E+05
2022	1.19E+07	2.02E+05	4.77E+05	5.35E+04	1.24E+07	2.09E+05
2023	1.57E+07	2.68E+05	6.33E+05	7.09E+04	1.63E+07	2.77E+05
2024	1.68E+07	2.87E+05	6.77E+05	7.59E+04	1.75E+07	2.97E+05
2025	1.93E+07	3.29E+05	7.77E+05	8.71E+04	2.01E+07	3.40E+05

Table B53. Projected cumulative energy demand (CED) with and without scaling up approach for pessimistic production estimations of SWCNTs, MWCNTs and total CNTs (σ represents standard deviation).

Cumulative energy demand (MJ/year)						
Year	Lab Scale (SWCNT)		Lab Scale (MWCNT)		Lab Scale (CNTs total)	
	Mean	σ	Mean	σ	Mean	σ
2018	2.54E+08	1.96E+06	7.10E+06	9.19E+05	2.61E+08	2.16E+06
2019	2.67E+08	2.06E+06	7.48E+06	9.69E+05	2.74E+08	2.28E+06
2020	2.77E+08	2.14E+06	7.76E+06	1.00E+06	2.85E+08	2.36E+06
2021	2.93E+08	2.26E+06	8.19E+06	1.06E+06	3.01E+08	2.50E+06
2022	3.06E+08	2.36E+06	8.58E+06	1.11E+06	3.15E+08	2.61E+06
2023	3.16E+08	2.44E+06	8.85E+06	1.15E+06	3.25E+08	2.70E+06
2024	3.32E+08	2.56E+06	9.29E+06	1.20E+06	3.41E+08	2.83E+06
2025	3.57E+08	2.75E+06	1.00E+07	1.29E+06	3.67E+08	3.04E+06
Year	S1 (SWCNT)		S1 (MWCNT)		S1 (CNTs total)	
	Mean	σ	Mean	σ	Mean	σ
2018	3.34E+07	4.43E+05	1.69E+06	3.91E+05	3.51E+07	5.91E+05
2019	3.52E+07	4.67E+05	1.78E+06	4.12E+05	3.70E+07	6.23E+05
2020	3.64E+07	4.84E+05	1.84E+06	4.27E+05	3.82E+07	6.45E+05
2021	3.85E+07	5.11E+05	1.95E+06	4.51E+05	4.05E+07	6.82E+05
2022	4.03E+07	5.35E+05	2.04E+06	4.72E+05	4.23E+07	7.13E+05
2023	4.16E+07	5.52E+05	2.10E+06	4.87E+05	4.37E+07	7.36E+05
2024	4.36E+07	5.79E+05	2.21E+06	5.11E+05	4.58E+07	7.72E+05
2025	4.70E+07	6.24E+05	2.38E+06	5.50E+05	4.94E+07	8.32E+05
Year	S2 (SWCNT)		S2 (MWCNT)		S2 (CNTs total)	
	Mean	σ	Mean	σ	Mean	σ
2018	3.22E+07	1.62E+06	4.21E+06	6.48E+05	3.64E+07	1.74E+06
2019	3.40E+07	1.71E+06	4.44E+06	6.82E+05	3.84E+07	1.84E+06
2020	3.52E+07	1.77E+06	4.60E+06	7.07E+05	3.98E+07	1.91E+06
2021	3.72E+07	1.87E+06	4.86E+06	7.47E+05	4.21E+07	2.01E+06
2022	3.89E+07	1.95E+06	5.08E+06	7.82E+05	4.40E+07	2.10E+06
2023	4.02E+07	2.02E+06	5.25E+06	8.07E+05	4.55E+07	2.18E+06
2024	4.21E+07	2.12E+06	5.50E+06	8.47E+05	4.76E+07	2.28E+06
2025	4.54E+07	2.28E+06	5.93E+06	9.12E+05	5.13E+07	2.46E+06
Year	S3 (SWCNT)		S3 (MWCNT)		S3 (CNTs total)	
	Mean	σ	Mean	σ	Mean	σ
2018	3.90E+07	3.05E+05	1.28E+06	1.56E+05	4.03E+07	3.43E+05
2019	4.11E+07	3.21E+05	1.35E+06	1.64E+05	4.25E+07	3.60E+05
2020	4.26E+07	3.33E+05	1.40E+06	1.70E+05	4.40E+07	3.74E+05
2021	4.50E+07	3.52E+05	1.48E+06	1.80E+05	4.65E+07	3.95E+05
2022	4.71E+07	3.68E+05	1.55E+06	1.88E+05	4.87E+07	4.13E+05
2023	4.86E+07	3.80E+05	1.59E+06	1.94E+05	5.02E+07	4.27E+05
2024	5.10E+07	3.99E+05	1.67E+06	2.04E+05	5.27E+07	4.48E+05
2025	5.49E+07	4.29E+05	1.80E+06	2.19E+05	5.67E+07	4.82E+05

Table B54. Projected cumulative energy demand (CED) with and without scaling up approach for optimistic production estimations of SWCNTs, MWCNTs and total CNTs (σ represents standard deviation).

Cumulative energy demand (MJ/year)						
Year	Lab Scale (SWCNT)		Lab Scale (MWCNT)		Lab Scale (CNTs total)	
	Mean	σ	Mean	σ	Mean	σ
2018	1.29E+09	9.93E+06	3.61E+07	4.67E+06	1.33E+09	1.10E+07
2019	1.37E+09	1.05E+07	3.82E+07	4.95E+06	1.41E+09	1.16E+07
2020	1.46E+09	1.13E+07	4.10E+07	5.30E+06	1.50E+09	1.25E+07
2021	1.56E+09	1.20E+07	4.37E+07	5.66E+06	1.60E+09	1.33E+07
2022	1.68E+09	1.29E+07	4.70E+07	6.08E+06	1.73E+09	1.43E+07
2023	2.22E+09	1.71E+07	6.23E+07	8.06E+06	2.28E+09	1.89E+07
2024	2.38E+09	1.84E+07	6.66E+07	8.63E+06	2.45E+09	2.03E+07
2025	2.73E+09	2.11E+07	7.65E+07	9.90E+06	2.81E+09	2.33E+07
Year	S1 (SWCNT)		S1 (MWCNT)		S1 (CNTs total)	
	Mean	σ	Mean	σ	Mean	σ
2018	1.69E+08	2.25E+06	8.57E+06	1.99E+06	1.78E+08	3.00E+06
2019	1.80E+08	2.39E+06	9.09E+06	2.11E+06	1.89E+08	3.19E+06
2020	1.92E+08	2.56E+06	9.74E+06	2.26E+06	2.02E+08	3.41E+06
2021	2.05E+08	2.73E+06	1.04E+07	2.41E+06	2.15E+08	3.64E+06
2022	2.21E+08	2.93E+06	1.12E+07	2.59E+06	2.32E+08	3.91E+06
2023	2.93E+08	3.88E+06	1.48E+07	3.43E+06	3.08E+08	5.18E+06
2024	3.13E+08	4.16E+06	1.58E+07	3.67E+06	3.29E+08	5.55E+06
2025	3.59E+08	4.77E+06	1.82E+07	4.21E+06	3.77E+08	6.36E+06
Year	S2 (SWCNT)		S2 (MWCNT)		S2 (CNTs total)	
	Mean	σ	Mean	σ	Mean	σ
2018	1.64E+08	8.21E+06	2.14E+07	3.29E+06	1.85E+08	8.84E+06
2019	1.74E+08	8.71E+06	2.27E+07	3.49E+06	1.97E+08	9.38E+06
2020	1.86E+08	9.33E+06	2.43E+07	3.74E+06	2.10E+08	1.01E+07
2021	1.98E+08	9.96E+06	2.59E+07	3.98E+06	2.24E+08	1.07E+07
2022	2.13E+08	1.07E+07	2.78E+07	4.28E+06	2.41E+08	1.15E+07
2023	2.83E+08	1.42E+07	3.69E+07	5.68E+06	3.20E+08	1.53E+07
2024	3.02E+08	1.52E+07	3.95E+07	6.08E+06	3.42E+08	1.64E+07
2025	3.47E+08	1.74E+07	4.53E+07	6.97E+06	3.92E+08	1.87E+07
Year	S3 (SWCNT)		S3 (MWCNT)		S3 (CNTs total)	
	Mean	σ	Mean	σ	Mean	σ
2018	1.98E+08	1.55E+06	6.50E+06	7.91E+05	2.05E+08	1.74E+06
2019	2.10E+08	1.64E+06	6.89E+06	8.39E+05	2.17E+08	1.84E+06
2020	2.25E+08	1.76E+06	7.38E+06	8.98E+05	2.32E+08	1.98E+06
2021	2.40E+08	1.88E+06	7.87E+06	9.58E+05	2.48E+08	2.11E+06
2022	2.58E+08	2.02E+06	8.46E+06	1.03E+06	2.66E+08	2.27E+06
2023	3.42E+08	2.67E+06	1.12E+07	1.37E+06	3.53E+08	3.00E+06
2024	3.66E+08	2.86E+06	1.20E+07	1.46E+06	3.78E+08	3.21E+06
2025	4.20E+08	3.28E+06	1.38E+07	1.68E+06	4.34E+08	3.69E+06

Table B55. Projected ozone depletion (OD) with and without scaling up approach for pessimistic production estimations of SWCNTs, MWCNTs and total CNTs (σ represents standard deviation).

Ozone depletion (tons CFC11-eq./year)						
Year	Lab Scale (SWCNT)		Lab Scale (MWCNT)		Lab Scale (CNTs total)	
	Mean	σ	Mean	σ	Mean	σ
2018	3.22E-02	1.88E-02	2.19E-02	1.03E-02	5.41E-02	2.14E-02
2019	3.39E-02	1.98E-02	2.31E-02	1.09E-02	5.70E-02	2.26E-02
2020	3.51E-02	2.05E-02	2.39E-02	1.13E-02	5.90E-02	2.34E-02
2021	3.71E-02	2.17E-02	2.52E-02	1.19E-02	6.23E-02	2.47E-02
2022	3.89E-02	2.27E-02	2.64E-02	1.24E-02	6.53E-02	2.59E-02
2023	4.01E-02	2.34E-02	2.73E-02	1.28E-02	6.74E-02	2.67E-02
2024	4.21E-02	2.45E-02	2.86E-02	1.35E-02	7.07E-02	2.80E-02
2025	4.53E-02	2.64E-02	3.08E-02	1.45E-02	7.61E-02	3.01E-02
Year	S1 (SWCNT)		S1 (MWCNT)		S1 (CNTs total)	
	Mean	σ	Mean	σ	Mean	σ
2018	9.30E-03	6.10E-03	1.12E-02	5.37E-03	2.05E-02	8.13E-03
2019	9.80E-03	6.42E-03	1.18E-02	5.66E-03	2.16E-02	8.56E-03
2020	1.02E-02	6.66E-03	1.22E-02	5.87E-03	2.24E-02	8.88E-03
2021	1.07E-02	7.03E-03	1.29E-02	6.20E-03	2.36E-02	9.37E-03
2022	1.12E-02	7.36E-03	1.35E-02	6.49E-03	2.47E-02	9.81E-03
2023	1.16E-02	7.60E-03	1.40E-02	6.69E-03	2.56E-02	1.01E-02
2024	1.22E-02	7.97E-03	1.46E-02	7.03E-03	2.68E-02	1.06E-02
2025	1.31E-02	8.58E-03	1.58E-02	7.56E-03	2.89E-02	1.14E-02
Year	S2 (SWCNT)		S2 (MWCNT)		S2 (CNTs total)	
	Mean	σ	Mean	σ	Mean	σ
2018	7.14E-02	4.86E-02	1.98E-02	9.32E-03	9.12E-02	4.95E-02
2019	7.53E-02	5.12E-02	2.08E-02	9.83E-03	9.61E-02	5.21E-02
2020	7.80E-02	5.31E-02	2.16E-02	1.02E-02	9.96E-02	5.41E-02
2021	8.24E-02	5.61E-02	2.28E-02	1.08E-02	1.05E-01	5.71E-02
2022	8.62E-02	5.87E-02	2.39E-02	1.13E-02	1.10E-01	5.98E-02
2023	8.90E-02	6.06E-02	2.46E-02	1.16E-02	1.14E-01	6.17E-02
2024	9.34E-02	6.36E-02	2.58E-02	1.22E-02	1.19E-01	6.48E-02
2025	1.01E-01	6.84E-02	2.78E-02	1.31E-02	1.29E-01	6.96E-02
Year	S3 (SWCNT)		S3 (MWCNT)		S3 (CNTs total)	
	Mean	σ	Mean	σ	Mean	σ
2018	5.10E-03	2.98E-03	5.52E-03	2.78E-03	1.06E-02	4.08E-03
2019	5.37E-03	3.14E-03	5.82E-03	2.93E-03	1.12E-02	4.29E-03
2020	5.57E-03	3.25E-03	6.03E-03	3.03E-03	1.16E-02	4.44E-03
2021	5.88E-03	3.43E-03	6.37E-03	3.20E-03	1.23E-02	4.69E-03
2022	6.16E-03	3.59E-03	6.67E-03	3.35E-03	1.28E-02	4.91E-03
2023	6.36E-03	3.71E-03	6.88E-03	3.46E-03	1.32E-02	5.07E-03
2024	6.67E-03	3.89E-03	7.22E-03	3.63E-03	1.39E-02	5.32E-03
2025	7.18E-03	4.19E-03	7.78E-03	3.91E-03	1.50E-02	5.73E-03

Table B56. Projected ozone depletion (OD) with and without scaling up approach for optimistic production estimations of SWCNTs, MWCNTs and total CNTs (σ represents standard deviation).

Ozone depletion (tons CFC11-eq./year)						
Year	Lab Scale (SWCNT)		Lab Scale (MWCNT)		Lab Scale (CNTs total)	
	Mean	σ	Mean	σ	Mean	σ
2018	1.63E-01	9.53E-02	1.11E-01	5.23E-02	2.74E-01	1.09E-01
2019	1.73E-01	1.01E-01	1.18E-01	5.55E-02	2.91E-01	1.15E-01
2020	1.86E-01	1.08E-01	1.26E-01	5.94E-02	3.12E-01	1.23E-01
2021	1.98E-01	1.16E-01	1.35E-01	6.34E-02	3.33E-01	1.32E-01
2022	2.13E-01	1.24E-01	1.45E-01	6.82E-02	3.58E-01	1.42E-01
2023	2.82E-01	1.65E-01	1.92E-01	9.03E-02	4.74E-01	1.88E-01
2024	3.02E-01	1.76E-01	2.05E-01	9.67E-02	5.07E-01	2.01E-01
2025	3.47E-01	2.02E-01	2.36E-01	1.11E-01	5.83E-01	2.30E-01
Year	S1 (SWCNT)		S1 (MWCNT)		S1 (CNTs total)	
	Mean	σ	Mean	σ	Mean	σ
2018	4.72E-02	3.09E-02	5.69E-02	2.73E-02	1.04E-01	4.12E-02
2019	5.01E-02	3.28E-02	6.03E-02	2.89E-02	1.10E-01	4.37E-02
2020	5.37E-02	3.52E-02	6.46E-02	3.10E-02	1.18E-01	4.69E-02
2021	5.72E-02	3.75E-02	6.89E-02	3.31E-02	1.26E-01	5.00E-02
2022	6.15E-02	4.03E-02	7.41E-02	3.55E-02	1.36E-01	5.37E-02
2023	8.16E-02	5.35E-02	9.82E-02	4.71E-02	1.80E-01	7.13E-02
2024	8.73E-02	5.72E-02	1.05E-01	5.04E-02	1.92E-01	7.62E-02
2025	1.00E-01	6.56E-02	1.21E-01	5.79E-02	2.21E-01	8.75E-02
Year	S2 (SWCNT)		S2 (MWCNT)		S2 (CNTs total)	
	Mean	σ	Mean	σ	Mean	σ
2018	3.63E-01	2.47E-01	1.00E-01	4.73E-02	4.63E-01	2.51E-01
2019	3.85E-01	2.62E-01	1.06E-01	5.02E-02	4.91E-01	2.67E-01
2020	4.12E-01	2.81E-01	1.14E-01	5.38E-02	5.26E-01	2.86E-01
2021	4.39E-01	2.99E-01	1.22E-01	5.74E-02	5.61E-01	3.04E-01
2022	4.72E-01	3.22E-01	1.31E-01	6.17E-02	6.03E-01	3.28E-01
2023	6.26E-01	4.26E-01	1.73E-01	8.18E-02	7.99E-01	4.34E-01
2024	6.70E-01	4.56E-01	1.85E-01	8.75E-02	8.55E-01	4.64E-01
2025	7.69E-01	5.24E-01	2.13E-01	1.00E-01	9.82E-01	5.33E-01
Year	S3 (SWCNT)		S3 (MWCNT)		S3 (CNTs total)	
	Mean	σ	Mean	σ	Mean	σ
2018	2.59E-02	1.51E-02	2.80E-02	1.41E-02	5.39E-02	2.07E-02
2019	2.75E-02	1.60E-02	2.97E-02	1.50E-02	5.72E-02	2.19E-02
2020	2.94E-02	1.72E-02	3.19E-02	1.60E-02	6.13E-02	2.35E-02
2021	3.14E-02	1.83E-02	3.40E-02	1.71E-02	6.54E-02	2.50E-02
2022	3.37E-02	1.97E-02	3.65E-02	1.84E-02	7.02E-02	2.70E-02
2023	4.47E-02	2.61E-02	4.84E-02	2.43E-02	9.31E-02	3.57E-02
2024	4.79E-02	2.79E-02	5.18E-02	2.61E-02	9.97E-02	3.82E-02
2025	5.49E-02	3.20E-02	5.95E-02	2.99E-02	1.14E-01	4.38E-02

Table B57. Projected smog (PS) with and without scaling up approach for pessimistic production estimations of SWCNTs, MWCNTs and total CNTs (σ represents standard deviation).

Smog (tons O ₃ -eq./year)						
Year	Lab Scale (SWCNT)		Lab Scale (MWCNT)		Lab Scale (CNTs total)	
	Mean	σ	Mean	σ	Mean	σ
2018	1.21E+06	4.41E+03	3.13E+04	2.31E+03	1.24E+06	4.98E+03
2019	1.27E+06	4.65E+03	3.30E+04	2.43E+03	1.30E+06	5.25E+03
2020	1.32E+06	4.82E+03	3.42E+04	2.52E+03	1.35E+06	5.44E+03
2021	1.40E+06	5.09E+03	3.61E+04	2.67E+03	1.44E+06	5.75E+03
2022	1.46E+06	5.33E+03	3.78E+04	2.79E+03	1.50E+06	6.02E+03
2023	1.51E+06	5.50E+03	3.90E+04	2.88E+03	1.55E+06	6.21E+03
2024	1.58E+06	5.77E+03	4.09E+04	3.02E+03	1.62E+06	6.51E+03
2025	1.70E+06	6.21E+03	4.41E+04	3.25E+03	1.74E+06	7.01E+03
Year	S1 (SWCNT)		S1 (MWCNT)		S1 (CNTs total)	
	Mean	σ	Mean	σ	Mean	σ
2018	1.60E+05	1.92E+03	8.38E+03	9.38E+02	1.68E+05	2.14E+03
2019	1.69E+05	2.02E+03	8.83E+03	9.88E+02	1.78E+05	2.25E+03
2020	1.75E+05	2.10E+03	9.15E+03	1.02E+03	1.84E+05	2.33E+03
2021	1.85E+05	2.21E+03	9.66E+03	1.08E+03	1.95E+05	2.46E+03
2022	1.94E+05	2.32E+03	1.01E+04	1.13E+03	2.04E+05	2.58E+03
2023	2.00E+05	2.39E+03	1.04E+04	1.17E+03	2.10E+05	2.66E+03
2024	2.10E+05	2.51E+03	1.10E+04	1.23E+03	2.21E+05	2.80E+03
2025	2.26E+05	2.70E+03	1.18E+04	1.32E+03	2.38E+05	3.01E+03
Year	S2 (SWCNT)		S2 (MWCNT)		S2 (CNTs total)	
	Mean	σ	Mean	σ	Mean	σ
2018	1.43E+05	3.80E+03	1.14E+04	1.31E+03	1.54E+05	4.02E+03
2019	1.51E+05	4.00E+03	1.20E+04	1.38E+03	1.63E+05	4.23E+03
2020	1.57E+05	4.15E+03	1.25E+04	1.43E+03	1.70E+05	4.39E+03
2021	1.66E+05	4.38E+03	1.32E+04	1.51E+03	1.79E+05	4.63E+03
2022	1.73E+05	4.59E+03	1.38E+04	1.58E+03	1.87E+05	4.85E+03
2023	1.79E+05	4.73E+03	1.42E+04	1.63E+03	1.93E+05	5.00E+03
2024	1.88E+05	4.97E+03	1.49E+04	1.71E+03	2.03E+05	5.26E+03
2025	2.02E+05	5.35E+03	1.60E+04	1.85E+03	2.18E+05	5.66E+03
Year	S3 (SWCNT)		S3 (MWCNT)		S3 (CNTs total)	
	Mean	σ	Mean	σ	Mean	σ
2018	1.86E+05	6.84E+02	5.48E+03	3.99E+02	1.91E+05	7.92E+02
2019	1.96E+05	7.21E+02	5.77E+03	4.21E+02	2.02E+05	8.35E+02
2020	2.03E+05	7.47E+02	5.98E+03	4.36E+02	2.09E+05	8.65E+02
2021	2.15E+05	7.89E+02	6.32E+03	4.61E+02	2.21E+05	9.14E+02
2022	2.25E+05	8.26E+02	6.61E+03	4.82E+02	2.32E+05	9.56E+02
2023	2.32E+05	8.52E+02	6.82E+03	4.98E+02	2.39E+05	9.87E+02
2024	2.43E+05	8.94E+02	7.16E+03	5.22E+02	2.50E+05	1.04E+03
2025	2.62E+05	9.63E+02	7.71E+03	5.62E+02	2.70E+05	1.11E+03

Table B58. Projected smog (PS) with and without scaling up approach for optimistic production estimations of SWCNTs, MWCNTs and total CNTs (σ represents standard deviation).

Smog (tons O ₃ -eq./year)						
Year	Lab Scale (SWCNT)		Lab Scale (MWCNT)		Lab Scale (CNTs total)	
	Mean	σ	Mean	σ	Mean	σ
2018	6.14E+06	2.24E+04	1.59E+05	1.17E+04	6.30E+06	2.53E+04
2019	6.51E+06	2.38E+04	1.69E+05	1.24E+04	6.68E+06	2.68E+04
2020	6.98E+06	2.54E+04	1.81E+05	1.33E+04	7.16E+06	2.87E+04
2021	7.44E+06	2.71E+04	1.93E+05	1.42E+04	7.63E+06	3.06E+04
2022	8.00E+06	2.92E+04	2.07E+05	1.53E+04	8.21E+06	3.30E+04
2023	1.06E+07	3.87E+04	2.75E+05	2.03E+04	1.09E+07	4.37E+04
2024	1.13E+07	4.14E+04	2.94E+05	2.17E+04	1.16E+07	4.67E+04
2025	1.30E+07	4.75E+04	3.37E+05	2.49E+04	1.33E+07	5.36E+04
Year	S1 (SWCNT)		S1 (MWCNT)		S1 (CNTs total)	
	Mean	σ	Mean	σ	Mean	σ
2018	8.14E+05	9.74E+03	4.25E+04	4.76E+03	8.57E+05	1.08E+04
2019	8.63E+05	1.03E+04	4.51E+04	5.05E+03	9.08E+05	1.15E+04
2020	9.25E+05	1.11E+04	4.83E+04	5.41E+03	9.73E+05	1.23E+04
2021	9.87E+05	1.18E+04	5.15E+04	5.77E+03	1.04E+06	1.31E+04
2022	1.06E+06	1.27E+04	5.54E+04	6.20E+03	1.12E+06	1.41E+04
2023	1.41E+06	1.68E+04	7.34E+04	8.22E+03	1.48E+06	1.87E+04
2024	1.50E+06	1.80E+04	7.86E+04	8.80E+03	1.58E+06	2.00E+04
2025	1.73E+06	2.07E+04	9.02E+04	1.01E+04	1.82E+06	2.30E+04
Year	S2 (SWCNT)		S2 (MWCNT)		S2 (CNTs total)	
	Mean	σ	Mean	σ	Mean	σ
2018	7.28E+05	1.93E+04	5.79E+04	6.66E+03	7.86E+05	2.04E+04
2019	7.72E+05	2.05E+04	6.14E+04	7.06E+03	8.33E+05	2.17E+04
2020	8.28E+05	2.19E+04	6.58E+04	7.57E+03	8.94E+05	2.32E+04
2021	8.83E+05	2.34E+04	7.02E+04	8.07E+03	9.53E+05	2.48E+04
2022	9.49E+05	2.51E+04	7.54E+04	8.67E+03	1.02E+06	2.66E+04
2023	1.26E+06	3.33E+04	1.00E+05	1.15E+04	1.36E+06	3.52E+04
2024	1.35E+06	3.57E+04	1.07E+05	1.23E+04	1.46E+06	3.78E+04
2025	1.54E+06	4.09E+04	1.23E+05	1.41E+04	1.66E+06	4.33E+04
Year	S3 (SWCNT)		S3 (MWCNT)		S3 (CNTs total)	
	Mean	σ	Mean	σ	Mean	σ
2018	9.45E+05	3.47E+03	2.78E+04	2.03E+03	9.73E+05	4.02E+03
2019	1.00E+06	3.68E+03	2.95E+04	2.15E+03	1.03E+06	4.26E+03
2020	1.07E+06	3.94E+03	3.16E+04	2.30E+03	1.10E+06	4.56E+03
2021	1.15E+06	4.21E+03	3.37E+04	2.46E+03	1.18E+06	4.88E+03
2022	1.23E+06	4.52E+03	3.62E+04	2.64E+03	1.27E+06	5.23E+03
2023	1.63E+06	6.00E+03	4.80E+04	3.50E+03	1.68E+06	6.95E+03
2024	1.75E+06	6.42E+03	5.14E+04	3.75E+03	1.80E+06	7.43E+03
2025	2.00E+06	7.36E+03	5.90E+04	4.30E+03	2.06E+06	8.52E+03

Table B59. Cross comparison of impacts using different scenarios for pessimistic CNTs production in 2019 (red: the highest, orange/yellow: medium-high, light green: medium-low, dark green: the lowest).

	Laboratory	S1	S2	S3
AC (ton SO ₂ -eq.)	1.67E+05	2.22E+04	1.99E+04	2.57E+04
HHC (CTUh-eq.)	5.17E-02	1.11E-02	1.72E-02	8.22E-03
EC (CTUe-eq.)	9.58E+06	1.85E+06	2.87E+06	1.53E+06
EU (ton N-eq.)	3.44E+03	7.19E+02	1.19E+03	5.43E+02
FF (MJ surplus)	1.27E+07	1.73E+06	2.24E+06	1.97E+06
GW (ton CO ₂ -eq.)	1.96E+07	2.65E+06	2.73E+06	3.01E+06
HHNC (CTUh-eq.)	6.81E-01	1.08E-01	1.34E-01	1.07E-01
OD (ton CFC11-eq.)	5.70E-02	2.16E-02	9.61E-02	1.12E-02
RE (ton PM _{2.5} -eq.)	8.38E+03	1.18E+03	1.20E+03	1.29E+03
PS (ton O ₃ -eq.)	1.30E+06	1.78E+05	1.63E+05	2.02E+05
CED (MJ)	2.74E+08	3.70E+07	3.84E+07	4.25E+07

Industry Based Environmental Impact Predictions- Example Calculation

Mass of SWCNTs produced is assumed as = 0.2*total CNTs, mass of MWCNTs produced is assumed as = 0.8*total CNTs. Example calculation of GW for energy and environment industry with pessimistic SWCNTs production on 2019 (lab scale):

$$\begin{aligned}
 & \sum \left[\frac{0.23 * 137 \text{ t SWCNTs}}{4} * \left(8.29E + 04 \frac{\text{kg CO}_2 - \text{eq.}}{\text{kg SWCNTs}} \right) + \frac{0.23 * 137 \text{ t SWCNTs}}{4} \right. \\
 & \quad * \left(8.86E + 04 \frac{\text{kg CO}_2 - \text{eq.}}{\text{kg SWCNTs}} \right) + \frac{0.23 * 137 \text{ t SWCNTs}}{4} * \left(1.97E + 05 \frac{\text{kg CO}_2 - \text{eq.}}{\text{kg SWCNTs}} \right) \\
 & \quad \left. + \frac{0.23 * 137 \text{ t SWCNTs}}{4} * \left(5.96E + 05 \frac{\text{kg CO}_2 - \text{eq.}}{\text{kg SWCNTs}} \right) \right] \\
 & = 7.59E + 06 \text{ t CO}_2 - \text{eq./year}
 \end{aligned}$$

Table B60. Industry based GW (tons CO₂-eq./year) estimations separated by SW- and MW-CNTs and laboratory scale synthesis in 2019.

Industry	tons CO ₂ -eq./year		
	SWCNTs	MWCNTs	TOTAL
Electronics and Optics	4.81E+06	1.11E+05	4.92E+06
Composites	1.36E+07	1.35E+05	1.37E+07
Energy and Environment	7.59E+06	1.07E+05	7.70E+06
Automotive	4.02E+06	5.40E+04	4.07E+06
Aerospace	8.77E+05	2.32E+04	9.00E+05
Coatings, Paints and Pigments	1.75E+06	4.64E+04	1.80E+06
Sensors	1.63E+06	1.62E+04	1.65E+06
TOTAL (Laboratory scale w/ pessimistic estimations)	3.43E+07	4.93E+05	3.48E+07
Industry	tons CO ₂ -eq./year		
	SWCNTs	MWCNTs	TOTAL
Electronics and Optics	2.46E+07	5.69E+05	2.52E+07
Composites	6.93E+07	6.89E+05	7.00E+07
Energy and Environment	3.88E+07	5.45E+05	3.93E+07
Automotive	2.06E+07	2.76E+05	2.09E+07
Aerospace	4.48E+06	1.18E+05	4.60E+06
Coatings, Paints and Pigments	8.96E+06	2.37E+05	9.20E+06
Sensors	8.32E+06	8.27E+04	8.40E+06
TOTAL (Laboratory scale w/ optimistic estimations)	1.75E+08	2.52E+06	1.78E+08

Table B61. Industry based AP (tons SO₂-eq./year) estimations separated by SW- and MW-CNTs and laboratory scale synthesis in 2019.

Industry	tons SO ₂ -eq./year		
	SWCNTs	MWCNTs	TOTAL
Electronics and Optics	4.12E+04	8.66E+02	4.21E+04
Composites	1.16E+05	1.05E+03	1.17E+05
Energy and Environment	6.51E+04	8.30E+02	6.59E+04
Automotive	3.46E+04	4.20E+02	3.50E+04
Aerospace	7.51E+03	1.81E+02	7.69E+03
Coatings, Paints and Pigments	1.50E+04	3.61E+02	1.54E+04
Sensors	1.40E+04	1.26E+02	1.41E+04
TOTAL (Laboratory scale w/ pessimistic estimations)	2.94E+05	3.83E+03	2.98E+05
Industry	tons SO ₂ -eq./year		
	SWCNTs	MWCNTs	TOTAL
Electronics and Optics	2.10E+05	4.43E+03	2.14E+05
Composites	5.95E+05	5.37E+03	6.00E+05
Energy and Environment	3.33E+05	4.24E+03	3.37E+05
Automotive	1.77E+05	2.15E+03	1.79E+05
Aerospace	3.84E+04	9.22E+02	3.93E+04
Coatings, Paints and Pigments	7.67E+04	1.84E+03	7.85E+04
Sensors	7.14E+04	6.44E+02	7.20E+04
TOTAL (Laboratory scale w/ optimistic estimations)	1.50E+06	1.96E+04	1.52E+06

Table B62. Industry based EC (CTUe/year) estimations separated by SW- and MW- CNTs and laboratory scale synthesis in 2019.

Industry	CTUe/year		
	SWCNTs	MWCNTs	TOTAL
Electronics and Optics	2.10E+06	2.23E+05	2.32E+06
Composites	5.70E+06	2.71E+05	5.97E+06
Energy and Environment	3.30E+06	2.14E+05	3.51E+06
Automotive	1.68E+06	1.08E+05	1.79E+06
Aerospace	3.83E+05	4.65E+04	4.30E+05
Coatings, Paints and Pigments	7.67E+05	9.29E+04	8.60E+05
Sensors	6.84E+05	3.25E+04	7.17E+05
TOTAL (Laboratory scale w/ pessimistic estimations)	1.46E+07	9.88E+05	1.56E+07
Industry	CTUe/year		
	SWCNTs	MWCNTs	TOTAL
Electronics and Optics	1.07E+07	1.14E+06	1.18E+07
Composites	2.91E+07	1.38E+06	3.05E+07
Energy and Environment	1.68E+07	1.09E+06	1.79E+07
Automotive	8.58E+06	5.54E+05	9.13E+06
Aerospace	1.96E+06	2.37E+05	2.20E+06
Coatings, Paints and Pigments	3.92E+06	4.75E+05	4.40E+06
Sensors	3.50E+06	1.66E+05	3.67E+06
TOTAL (Laboratory scale w/ optimistic estimations)	7.47E+07	5.05E+06	7.98E+07

Table B63. Industry based HHC (CTUh/year) estimations separated by SW- and MW- CNTs and laboratory scale synthesis in 2019.

Industry	CTUh/year		
	SWCNTs	MWCNTs	TOTAL
Electronics and Optics	1.03E-02	1.34E-03	1.16E-02
Composites	2.80E-02	1.63E-03	2.96E-02
Energy and Environment	1.63E-02	1.29E-03	1.76E-02
Automotive	8.23E-03	6.52E-04	8.88E-03
Aerospace	1.88E-03	2.80E-04	2.16E-03
Coatings, Paints and Pigments	3.76E-03	5.59E-04	4.32E-03
Sensors	3.36E-03	1.96E-04	3.56E-03
TOTAL (Laboratory scale w/ pessimistic estimations)	7.18E-02	5.94E-03	7.77E-02
Industry	CTUh/year		
	SWCNTs	MWCNTs	TOTAL
Electronics and Optics	5.27E-02	6.86E-03	5.96E-02
Composites	1.43E-01	8.33E-03	1.51E-01
Energy and Environment	8.31E-02	6.57E-03	8.97E-02
Automotive	4.20E-02	3.33E-03	4.53E-02
Aerospace	9.61E-03	1.43E-03	1.10E-02
Coatings, Paints and Pigments	1.92E-02	2.86E-03	2.21E-02
Sensors	1.72E-02	9.99E-04	1.82E-02
TOTAL (Laboratory scale w/ optimistic estimations)	3.67E-01	3.04E-02	3.97E-01

Table B64. Industry based HHNC (CTUh/year) estimations separated by SW- and MW- CNTs and laboratory scale synthesis in 2019.

Industry	CTUh/year		
	SWCNTs	MWCNTs	TOTAL
Electronics and Optics	1.59E-01	8.44E-03	1.67E-01
Composites	4.44E-01	1.03E-02	4.54E-01
Energy and Environment	2.51E-01	8.09E-03	2.59E-01
Automotive	1.31E-01	4.10E-03	1.35E-01
Aerospace	2.90E-02	1.76E-03	3.08E-02
Coatings, Paints and Pigments	5.80E-02	3.52E-03	6.15E-02
Sensors	5.33E-02	1.23E-03	5.45E-02
TOTAL (Laboratory scale w/ pessimistic estimations)	1.13E+00	3.74E-02	1.17E+00
Industry	CTUh/year		
	SWCNTs	MWCNTs	TOTAL
Electronics and Optics	8.13E-01	4.31E-02	8.56E-01
Composites	2.27E+00	5.24E-02	2.32E+00
Energy and Environment	1.28E+00	4.13E-02	1.32E+00
Automotive	6.71E-01	2.10E-02	6.92E-01
Aerospace	1.48E-01	8.99E-03	1.57E-01
Coatings, Paints and Pigments	2.96E-01	1.80E-02	3.14E-01
Sensors	2.72E-01	6.29E-03	2.78E-01
TOTAL (Laboratory scale w/ optimistic estimations)	5.75E+00	1.91E-01	5.94E+00

Table B65. Industry based EU (tons N-eq./year) estimations separated by SW- and MW- CNTs and laboratory scale synthesis in 2019.

Industry	tons N-eq./year		
	SWCNTs	MWCNTs	TOTAL
Electronics and Optics	6.97E+02	1.10E+02	8.07E+02
Composites	1.92E+03	1.33E+02	2.05E+03
Energy and Environment	1.10E+03	1.05E+02	1.21E+03
Automotive	5.61E+02	5.33E+01	6.14E+02
Aerospace	1.27E+02	2.29E+01	1.50E+02
Coatings, Paints and Pigments	2.54E+02	4.57E+01	3.00E+02
Sensors	2.30E+02	1.60E+01	2.46E+02
TOTAL (Laboratory scale w/ pessimistic estimations)	4.89E+03	4.86E+02	5.38E+03
Industry	tons N-eq./year		
	SWCNTs	MWCNTs	TOTAL
Electronics and Optics	3.56E+03	5.61E+02	4.12E+03
Composites	9.80E+03	6.81E+02	1.05E+04
Energy and Environment	5.61E+03	5.37E+02	6.15E+03
Automotive	2.87E+03	2.72E+02	3.14E+03
Aerospace	6.49E+02	1.17E+02	7.66E+02
Coatings, Paints and Pigments	1.30E+03	2.34E+02	1.53E+03
Sensors	1.18E+03	8.17E+01	1.26E+03
TOTAL (Laboratory scale w/ optimistic estimations)	2.50E+04	2.48E+03	2.75E+04

Table B66. Industry based RE (tons PM_{2.5}-eq./year) estimations separated by SW- and MW-CNTs and laboratory scale synthesis in 2019.

Industry	tons PM _{2.5} -eq./year		
	SWCNTs	MWCNTs	TOTAL
Electronics and Optics	2.04E+03	6.87E+01	2.11E+03
Composites	5.74E+03	8.34E+01	5.82E+03
Energy and Environment	3.22E+03	6.59E+01	3.29E+03
Automotive	1.70E+03	3.34E+01	1.73E+03
Aerospace	3.71E+02	1.43E+01	3.85E+02
Coatings, Paints and Pigments	7.42E+02	2.86E+01	7.71E+02
Sensors	6.89E+02	1.00E+01	6.99E+02
TOTAL (Laboratory scale w/ pessimistic estimations)	1.45E+04	3.04E+02	1.48E+04
Industry	tons PM _{2.5} -eq./year		
	SWCNTs	MWCNTs	TOTAL
Electronics and Optics	1.04E+04	3.51E+02	1.08E+04
Composites	2.93E+04	4.26E+02	2.97E+04
Energy and Environment	1.64E+04	3.37E+02	1.67E+04
Automotive	8.69E+03	1.70E+02	8.86E+03
Aerospace	1.90E+03	7.32E+01	1.97E+03
Coatings, Paints and Pigments	3.79E+03	1.46E+02	3.94E+03
Sensors	3.52E+03	5.11E+01	3.57E+03
TOTAL (Laboratory scale w/ optimistic estimations)	7.41E+04	1.56E+03	7.57E+04

Table B67. Industry based FF (MJ surplus energy/year) estimations separated by SW- and MW-CNTs and laboratory scale synthesis in 2019.

Industry	MJ surplus energy/year		
	SWCNTs	MWCNTs	TOTAL
Electronics and Optics	3.09E+06	9.48E+04	3.18E+06
Composites	8.54E+06	1.15E+05	8.66E+06
Energy and Environment	4.89E+06	9.09E+04	4.98E+06
Automotive	2.53E+06	4.60E+04	2.58E+06
Aerospace	5.64E+05	1.98E+04	5.84E+05
Coatings, Paints and Pigments	1.13E+06	3.95E+04	1.17E+06
Sensors	1.03E+06	1.38E+04	1.04E+06
TOTAL (Laboratory scale w/ pessimistic estimations)	2.18E+07	4.20E+05	2.22E+07
Industry	MJ surplus energy/year		
	SWCNTs	MWCNTs	TOTAL
Electronics and Optics	1.58E+07	4.84E+05	1.63E+07
Composites	4.37E+07	5.88E+05	4.43E+07
Energy and Environment	2.50E+07	4.64E+05	2.55E+07
Automotive	1.29E+07	2.35E+05	1.31E+07
Aerospace	2.88E+06	1.01E+05	2.98E+06
Coatings, Paints and Pigments	5.76E+06	2.02E+05	5.96E+06
Sensors	5.24E+06	7.05E+04	5.31E+06
TOTAL (Laboratory scale w/ optimistic estimations)	1.11E+08	2.14E+06	1.13E+08

Table B68. Industry based CED (MJ/year) estimations separated by SW- and MW- CNTs and laboratory scale synthesis in 2019.

Industry	MJ/year		
	SWCNTs	MWCNTs	TOTAL
Electronics and Optics	6.74E+07	1.75E+06	6.92E+07
Composites	1.90E+08	2.12E+06	1.92E+08
Energy and Environment	1.07E+08	1.68E+06	1.09E+08
Automotive	5.63E+07	8.49E+05	5.71E+07
Aerospace	1.23E+07	3.65E+05	1.27E+07
Coatings, Paints and Pigments	2.46E+07	7.29E+05	2.53E+07
Sensors	2.28E+07	2.55E+05	2.31E+07
TOTAL (Laboratory scale w/ pessimistic estimations)	4.79E+08	7.75E+06	4.87E+08
Industry	MJ/year		
	SWCNTs	MWCNTs	TOTAL
Electronics and Optics	3.44E+08	8.94E+06	3.53E+08
Composites	9.70E+08	1.08E+07	9.81E+08
Energy and Environment	5.44E+08	8.57E+06	5.53E+08
Automotive	2.87E+08	4.34E+06	2.91E+08
Aerospace	6.27E+07	1.86E+06	6.46E+07
Coatings, Paints and Pigments	1.25E+08	3.73E+06	1.29E+08
Sensors	1.16E+08	1.30E+06	1.17E+08
TOTAL (Laboratory scale w/ optimistic estimations)	2.45E+09	3.96E+07	2.49E+09

Table B69. Industry based PS (tons O₃-eq./year) estimations separated by SW- and MW- CNTs and laboratory scale synthesis in 2019.

Industry	tons O ₃ -eq./year		
	SWCNTs	MWCNTs	TOTAL
Electronics and Optics	3.21E+05	7.81E+03	3.29E+05
Composites	9.09E+05	9.47E+03	9.18E+05
Energy and Environment	5.08E+05	7.49E+03	5.15E+05
Automotive	2.70E+05	3.79E+03	2.74E+05
Aerospace	5.86E+04	1.63E+03	6.02E+04
Coatings, Paints and Pigments	1.17E+05	3.25E+03	1.20E+05
Sensors	1.09E+05	1.14E+03	1.10E+05
TOTAL (Laboratory scale w/ pessimistic estimations)	2.29E+06	3.46E+04	2.32E+06
Industry	tons O ₃ -eq./year		
	SWCNTs	MWCNTs	TOTAL
Electronics and Optics	1.64E+06	3.99E+04	1.68E+06
Composites	4.64E+06	4.84E+04	4.69E+06
Energy and Environment	2.59E+06	3.82E+04	2.63E+06
Automotive	1.38E+06	1.94E+04	1.40E+06
Aerospace	2.99E+05	8.31E+03	3.07E+05
Coatings, Paints and Pigments	5.99E+05	1.66E+04	6.16E+05
Sensors	5.57E+05	5.81E+03	5.63E+05
TOTAL (Laboratory scale w/ optimistic estimations)	1.17E+07	1.77E+05	1.19E+07

Table B70. Industry based OD (tons CFC11-eq./year) estimations separated by SW- and MW-CNTs and laboratory scale synthesis in 2019.

Industry	tons CFC11-eq./year		
	SWCNTs	MWCNTs	TOTAL
Electronics and Optics	8.20E-03	5.05E-03	1.33E-02
Composites	7.54E-03	6.13E-03	1.37E-02
Energy and Environment	1.22E-02	4.84E-03	1.70E-02
Automotive	2.02E-03	2.45E-03	4.47E-03
Aerospace	1.50E-03	1.05E-03	2.55E-03
Coatings, Paints and Pigments	2.99E-03	2.10E-03	5.09E-03
Sensors	9.05E-04	7.36E-04	1.64E-03
TOTAL (Laboratory scale w/ pessimistic estimations)	3.53E-02	2.24E-02	5.77E-02
Industry	tons CFC11-eq./year		
	SWCNTs	MWCNTs	TOTAL
Electronics and Optics	4.19E-02	2.58E-02	6.77E-02
Composites	3.85E-02	3.13E-02	6.98E-02
Energy and Environment	6.22E-02	2.47E-02	8.69E-02
Automotive	1.03E-02	1.25E-02	2.28E-02
Aerospace	7.64E-03	5.37E-03	1.30E-02
Coatings, Paints and Pigments	1.53E-02	1.07E-02	2.60E-02
Sensors	4.62E-03	3.76E-03	8.38E-03
TOTAL (Laboratory scale w/ optimistic estimations)	1.81E-01	1.14E-01	2.95E-01

References-Appendix B

1. US Patent and Trademark Office (2019) Patent Full-Text Databases. <http://patft.uspto.gov/netahtml/PTO/index.html>
2. Hwang C-L, Ting J, Chiang J-S, Chuang C (2005) Process of direct growth of carbon nanotubes on a substrate at low temperature. <https://patentimages.storage.googleapis.com/27/74/9f/665fc732cd0ee7/US6855376.pdf>
3. Healy ML, Tanwani A, Isaacs JA (2006) NSTI Nanotech 2006: 2006 NSTI Nanotechnology Conference and Trade Show, Boston, May 7-11, 2006. 2
4. Bauer C, Buchgeister J, Hischer R, Poganietz WR, Schebek L, Warsen J (2008) Towards a framework for life cycle thinking in the assessment of nanotechnology. *Journal of Cleaner Production*, 16(8–9):910–926. <https://doi.org/10.1016/j.jclepro.2007.04.022>
5. Healy ML (2006) Environmental and economic comparison of single-wall carbon nanotube production alternatives.
6. Isaacs JA, Tanwani A, Healy ML (2006) Environmental Assessment of SWNT Production. *Proceedings of the 2006 IEEE International Symposium on Electronics and the Environment, 2006.*, :38–41. <https://doi.org/10.1109/ISEE.2006.1650028>
7. Healy ML, Dahlben LJ, Isaacs JA (2008) Environmental Assessment of Single-Walled Carbon Nanotube Processes. *Journal of Industrial Ecology*, 12(3):376–393. <https://doi.org/10.1111/j.1530-9290.2008.00058.x>
8. Kushnir D, Sandén BA (2008) Energy Requirements of Carbon Nanoparticle Production. *Journal of Industrial Ecology*, 12(3):360–375. <https://doi.org/10.1111/j.1530-9290.2008.00057.x>
9. Agboola AE (2005) Development and model formulation of scalable carbon nanotube processes: HiPCO and CoMoCAT process models. https://digitalcommons.lsu.edu/gradschool_theses/1635
10. Singh A, Lou HH, Pike RW, Agboola A, Li X, Hopper JR, Yaws CL (2008) Environmental Impact Assessment for Potential Continuous Processes for the Production of Carbon Nanotubes. *American Journal of Environmental Sciences*, 4(5):522–534. <https://doi.org/10.3844/ajessp.2008.522.534>

11. Dahlben LJ, Isaacs JA (2009) Environmental assessment of manufacturing with carbon nanotubes. *2009 IEEE International Symposium on Sustainable Systems and Technology*, :1–5. <https://doi.org/10.1109/ISSST.2009.5156767>
12. Ganter MJ, Seager TP, Schauerman CM, Landi BJ, Raffaele RP (2009) A life-cycle energy analysis of single wall carbon nanotubes produced through laser vaporization. *2009 IEEE International Symposium on Sustainable Systems and Technology*, :1–4. <https://doi.org/10.1109/ISSST.2009.5156719>
13. Roes AL, Tabak LB, Shen L, Nieuwlaar E, Patel MK (2010) Influence of using nanoobjects as filler on functionality-based energy use of nanocomposites. *Journal of Nanoparticle Research*, 12(6):2011–2028. <https://doi.org/10.1007/s11051-009-9819-3>
14. Steinfeldt M (2010) Nanosustain: Development of sustainable solutions for nanotechnology-based products based on hazard characterization and LCA. <https://www.tecdesign.uni-bremen.de/forschungsprojekte-nanosustain.php>
15. Wender BA, Seager TP (2011) Towards prospective life cycle assessment: Single wall carbon nanotubes for lithium-ion batteries. *Proceedings of the 2011 IEEE International Symposium on Sustainable Systems and Technology*, :1–4. <https://doi.org/10.1109/ISSST.2011.5936889>
16. Eckelman MJ, Mauter MS, Isaacs JA, Elimelech M (2012) New Perspectives on Nanomaterial Aquatic Ecotoxicity: Production Impacts Exceed Direct Exposure Impacts for Carbon Nanotubes. *Environmental Science & Technology*, 46(5):2902–2910. <https://doi.org/10.1021/es203409a>
17. Zhang D, Ryu K, Liu X, Polikarpov E, Ly J, Tompson ME, Zhou C (2006) Transparent, Conductive, and Flexible Carbon Nanotube Films and Their Application in Organic Light-Emitting Diodes. *Nano Letters*, 6(9):1880–1886. <https://doi.org/10.1021/nl0608543>
18. Kim S, Yim J, Wang X, Bradley DDC, Lee S, deMello JC (2010) Spin- and Spray-Deposited Single-Walled Carbon-Nanotube Electrodes for Organic Solar Cells. *Advanced Functional Materials*, 20(14):2310–2316. <https://doi.org/10.1002/adfm.200902369>
19. Emmott CJM, Urbina A, Nelson J (2012) Environmental and economic assessment of ITO-free electrodes for organic solar cells. *Solar Energy Materials and Solar Cells*, 97:14–21. <https://doi.org/10.1016/j.solmat.2011.09.024>

20. Weil M, Dura H, Shimon B, Baumann M, Zimmermann B, Ziemann S, Lei C, Markoulidis F, Lekakou T, Decker M (2012) Ecological assessment of nano-enabled supercapacitors for automotive applications. *IOP Conference Series: Materials Science and Engineering*, 40:012013. <https://doi.org/10.1088/1757-899X/40/1/012013>
21. Dahlben LJ, Eckelman MJ, Hakimian A, Somu S, Isaacs JA (2013) Environmental Life Cycle Assessment of a Carbon Nanotube-Enabled Semiconductor Device. *Environmental Science & Technology*, 47(15):8471–8478. <https://doi.org/10.1021/es305325y>
22. Griffiths OG, O’Byrne JP, Torrente-Murciano L, Jones MD, Mattia D, McManus MC (2013) Identifying the largest environmental life cycle impacts during carbon nanotube synthesis via chemical vapour deposition. *Journal of Cleaner Production*, 42:180–189. <https://doi.org/10.1016/j.jclepro.2012.10.040>
23. Gilbertson LM, Busnaina AA, Isaacs JA, Zimmerman JB, Eckelman MJ (2014) Life Cycle Impacts and Benefits of a Carbon Nanotube-Enabled Chemical Gas Sensor. *Environmental Science & Technology*, 48(19):11360–11368. <https://doi.org/10.1021/es5006576>
24. Liu J, Harris AT (2009) Synthesis of multiwalled carbon nanotubes on Al₂O₃ supported Ni catalysts in a fluidized-bed. *AIChE Journal*, :102–113. <https://doi.org/10.1002/aic.11974>
25. Plata DL, Hart AJ, Reddy CM, Gschwend PM (2009) Early Evaluation of Potential Environmental Impacts of Carbon Nanotube Synthesis by Chemical Vapor Deposition. *Environmental Science & Technology*, 43(21):8367–8373. <https://doi.org/10.1021/es901626p>
26. Zhang Q, Huang J-Q, Zhao M-Q, Qian W-Z, Wei F (2011) Carbon Nanotube Mass Production: Principles and Processes. *ChemSusChem*, 4(7):864–889. <https://doi.org/10.1002/cssc.201100177>
27. Upadhyayula VKK, Meyer DE, Curran MA, Gonzalez MA (2014) Evaluating the Environmental Impacts of a Nano-Enhanced Field Emission Display Using Life Cycle Assessment: A Screening-Level Study. *Environmental Science & Technology*, 48(2):1194–1205. <https://doi.org/10.1021/es4034638>
28. Gavankar S, Suh S, Keller AA (2015) The Role of Scale and Technology Maturity in Life Cycle Assessment of Emerging Technologies: A Case Study on Carbon Nanotubes: Carbon Nanotubes Case Study of Scaling and Technology

Maturity in LCAs. *Journal of Industrial Ecology*, 19(1):51–60.
<https://doi.org/10.1111/jiec.12175>

29. Gericke D, Ott D, Matveeva VG, Sulman E, Aho A, Murzin DYu, Roggan S, Danilova L, Hessel V, Loeb P, Kralisch D (2015) Green catalysis by nanoparticulate catalysts developed for flow processing? Case study of glucose hydrogenation. *RSC Advances*, 5(21):15898–15908.
<https://doi.org/10.1039/C4RA14559C>

30. Isaacs JA, Tanwani A, Healy ML, Dahlben LJ (2010) Economic assessment of single-walled carbon nanotube processes. *Journal of Nanoparticle Research*, 12(2):551–562. <https://doi.org/10.1007/s11051-009-9673-3>

31. Hischier R (2015) Life cycle assessment study of a field emission display television device. *The International Journal of Life Cycle Assessment*, 20(1):61–73. <https://doi.org/10.1007/s11367-014-0806-2>

32. Notter DA, Kouravelou K, Karachalios T, Daletou MK, Haberland NT (2015) Life cycle assessment of PEM FC applications: electric mobility and μ -CHP. *Energy & Environmental Science*, 8(7):1969–1985.
<https://doi.org/10.1039/C5EE01082A>

33. Trompeta A-F, Koklioti MA, Perivoliotis DK, Lynch I, Charitidis CA (2016) Towards a holistic environmental impact assessment of carbon nanotube growth through chemical vapour deposition. *Journal of Cleaner Production*, 129:384–394.
<https://doi.org/10.1016/j.jclepro.2016.04.044>

34. Zhai P, Isaacs JA, Eckelman MJ (2016) Net energy benefits of carbon nanotube applications. *Applied Energy*, 173:624–634.
<https://doi.org/10.1016/j.apenergy.2016.04.001>

35. Monzon A, Lolli G, Cosma S, Mohamed SB, Resasco DE (2008) Kinetic Modeling of the SWNT Growth by CO Disproportionation on CoMo Catalysts. *Journal of Nanoscience and Nanotechnology*, 8(11):6141–6152.
<https://doi.org/10.1166/jnn.2008.SW21>

36. Celik I, Mason BE, Phillips AB, Heben MJ, Apul D (2017) Environmental Impacts from Photovoltaic Solar Cells Made with Single Walled Carbon Nanotubes. *Environmental Science & Technology*, 51(8):4722–4732.
<https://doi.org/10.1021/acs.est.6b06272>

37. Weil M, Dura H, Simon B, Baumann M, Zimmermann B, Ziemann S, Lei C, Markoulidis F, Lekakou T, Decker M (2013) Ecological Assessment of Nano Materials for the Production of Electrostatic/Electrochemical Energy Storage Systems. *Structural Nanocomposites*, :259–269. https://doi.org/10.1007/978-3-642-40322-4_12
38. Deng Y, Li J, Li T, Zhang J, Yang F, Yuan C (2017) Life cycle assessment of high capacity molybdenum disulfide lithium-ion battery for electric vehicles. *Energy*, 123:77–88. <https://doi.org/10.1016/j.energy.2017.01.096>
39. Yin R, Hu S, Yang Y (2019) Life cycle inventories of the commonly used materials for lithium-ion batteries in China. *Journal of Cleaner Production*, 227:960–971. <https://doi.org/10.1016/j.jclepro.2019.04.186>
40. Shibuya A, Kawata K, Arakawa K, Hata K, Yumura M (2009) Equipment and method for producing orientated carbon nano-tube aggregates. (2008–107327, 2009–029129)<https://patentscope2.wipo.int/search/en/detail.jsf?docId=WO2009128349&tab=PCTBIBLIO>
41. Hata K (2016) A super-growth method for single-walled carbon nanotube synthesis: Development of a mass production technique for industrial application. *Synthesiology English edition*, 9(3):167–179. https://doi.org/10.5571/syntheng.9.3_167
42. Kawajiri K, Goto T, Sakurai S, Hata K, Tahara K (2020) Development of life cycle assessment of an emerging technology at research and development stage: A case study on single-wall carbon nanotube produced by super growth method. *Journal of Cleaner Production*, 255:120015. <https://doi.org/10.1016/j.jclepro.2020.120015>
43. Kim DY, Sugime H, Hasegawa K, Osawa T, Noda S (2011) Sub-millimeter-long carbon nanotubes repeatedly grown on and separated from ceramic beads in a single fluidized bed reactor. *Carbon*, 49(6):1972–1979. <https://doi.org/10.1016/j.carbon.2011.01.022>
44. Kim DY, Sugime H, Hasegawa K, Osawa T, Noda S (2012) Fluidized-bed synthesis of sub-millimeter-long single walled carbon nanotube arrays. *Carbon*, 50(4):1538–1545. <https://doi.org/10.1016/j.carbon.2011.11.032>
45. Sato T, Sugime H, Noda S (2018) CO₂-assisted growth of millimeter-tall single-wall carbon nanotube arrays and its advantage against H₂O for large-scale

and uniform synthesis. *Carbon*, 136:143–149.
<https://doi.org/10.1016/j.carbon.2018.04.060>

46. Teah HY, Sato T, Namiki K, Asaka M, Feng K, Noda S (2020) Life Cycle Greenhouse Gas Emissions of Long and Pure Carbon Nanotubes Synthesized via On-Substrate and Fluidized-Bed Chemical Vapor Deposition. *ACS Sustainable Chemistry & Engineering*, 8(4):1730–1740.
<https://doi.org/10.1021/acssuschemeng.9b04542>

47. Fan Y-Y, Kaufmann A, Mukasyan A, Varma A (2006) Single- and multi-wall carbon nanotubes produced using the floating catalyst method: Synthesis, purification and hydrogen up-take. *Carbon*, 44(11):2160–2170.
<https://doi.org/10.1016/j.carbon.2006.03.009>

48. Wu F, Zhou Z, Temizel-Sekeryan S, Ghamkhar R, Hicks AL (2020) Assessing the environmental impact and payback of carbon nanotube supported CO₂ capture technologies using LCA methodology. *Journal of Cleaner Production*, :122465.
<https://doi.org/10.1016/j.jclepro.2020.122465>

49. Gavankar S, Suh S, Keller AF (2012) Life cycle assessment at nanoscale: review and recommendations. *The International Journal of Life Cycle Assessment*, 17(3):295–303. <https://doi.org/10.1007/s11367-011-0368-5>

50. Hischier R, Walser T (2012) Life cycle assessment of engineered nanomaterials: State of the art and strategies to overcome existing gaps. *Science of The Total Environment*, 425:271–282.
<https://doi.org/10.1016/j.scitotenv.2012.03.001>

51. Upadhyayula VKK, Meyer DE, Curran MA, Gonzalez MA (2012) Life cycle assessment as a tool to enhance the environmental performance of carbon nanotube products: a review. *Journal of Cleaner Production*, 26:37–47.
<https://doi.org/10.1016/j.jclepro.2011.12.018>

52. Salieri B, Turner DA, Nowack B, Hischier R (2018) Life cycle assessment of manufactured nanomaterials: Where are we? *NanoImpact*, 10:108–120.
<https://doi.org/10.1016/j.impact.2017.12.003>

53. Liu B-C, Tang S-H, Liang Q, Gao L-Z, Zhang B-L, Qu M-Z, Yu Z-L (2001) Production of Carbon Nanotubes over Pre-reduced LaCoO₃ by Using Fluidized-bed Catalytic Reactor. *Chinese Journal of Chemistry*, 19:983–986.
<https://doi.org/10.1002/cjoc.20010191013>

54. Mauron P, Emmenegger C, Sudan P, Wenger P, Rentsch S, Züttel A (2003) Fluidised-bed CVD synthesis of carbon nanotubes on Fe₂O₃yMgO. *Diamond and Related Materials*, :6.
55. Ishigami M, Cumings J, Zettl A, Chen S (2000) A simple method for the continuous production of carbon nanotubes. *Chemical Physics Letters*, 319(5–6):457–459. [https://doi.org/10.1016/S0009-2614\(00\)00151-2](https://doi.org/10.1016/S0009-2614(00)00151-2)
56. Bare J (2012) Tool for the Reduction and Assessment of Chemical and Other Environmental Impacts (TRACI) version 2.1. <https://nepis.epa.gov/Adobe/PDF/P100HN53.pdf>
57. Guinée JB, Gorrée M, Heijungs R, Huppes G, Kleijn R, Koning A, Oers L, Wegener Sleeswijk A, Suh S, Udo de Haes HA, Brujin H, Duin R, Huijbregts MAJ (2002) Handbook on life cycle assessment. Operational guide to the ISO standards. I: LCA in perspective. IIa: Guide. IIb: Operational annex. III: Scientific background.
58. Jolliet O, Margni M, Charles R, Humbert S, Payet J, Rebitzer G, Rosenbaum R (2003) IMPACT 2002+: A new life cycle impact assessment methodology. *The International Journal of Life Cycle Assessment*, 8(6):324–330. <https://doi.org/10.1007/BF02978505>
59. Goedkoop M, Heijungs R, Huijbregts M, Schryver AD, Struijs J, Zelm R van (2013) ReCiPe 2008: Characterisation. https://www.pre-sustainability.com/download/ReCiPe_main_report_MAY_2013.pdf
60. Ganesh EN (2013) Single Walled and Multi Walled Carbon Nanotube Structure, Synthesis and Applications. 2(4):10.
61. De Volder MFL, Tawfick SH, Baughman RH, Hart AJ (2013) Carbon Nanotubes: Present and Future Commercial Applications. *Science*, 339(6119):535–539. <https://doi.org/10.1126/science.1222453>
62. Huang Y, Li N, Ma Y, Du F, Li F, He X, Lin X, Gao H, Chen Y (2007) The influence of single-walled carbon nanotube structure on the electromagnetic interference shielding efficiency of its epoxy composites. *Carbon*, 45(8):1614–1621. <https://doi.org/10.1016/j.carbon.2007.04.016>
63. Wardak A, Gorman ME, Swami N, Deshpande S (2008) Identification of Risks in the Life Cycle of Nanotechnology-Based Products. *Journal of Industrial Ecology*, 12(3):435–448. <https://doi.org/10.1111/j.1530-9290.2008.00029.x>

64. Wender BA, Foley RW, Guston DH, Seager TP, Wiek A (2012) Anticipatory Governance and Anticipatory Life Cycle Assessment of Single Wall Carbon Nanotube Anode Lithium ion Batteries. *Nanotechnology Law & Business*, 9(3):201–216.
65. Baddour CE, Fadlallah F, Nasuhoglu D, Mitra R, Vandsburger L, Meunier J-L (2009) A simple thermal CVD method for carbon nanotube synthesis on stainless steel 304 without the addition of an external catalyst. *Carbon*, 47(1):313–318. <https://doi.org/10.1016/j.carbon.2008.10.038>
66. Wang H, Wang G, Li W, Wang Q, Wei W, Jiang Z, Zhang S (2012) A material with high electromagnetic radiation shielding effectiveness fabricated using multi-walled carbon nanotubes wrapped with poly(ether sulfone) in a poly(ether ether ketone) matrix. *Journal of Materials Chemistry*, 22(39):21232–21237. <https://doi.org/10.1039/C2JM35129C>
67. Zhang C-S, Ni Q-Q, Fu S-Y, Kurashiki K (2007) Electromagnetic interference shielding effect of nanocomposites with carbon nanotube and shape memory polymer. *Composites Science and Technology*, 67(14):2973–2980. <https://doi.org/10.1016/j.compscitech.2007.05.011>
68. Thomassin J-M, Pagnouille C, Bednarz L, Huynen I, Jerome R, Detrembleur C (2008) Foams of polycaprolactone/MWNT nanocomposites for efficient EMI reduction. *Journal of Materials Chemistry*, 18(7):792–796. <https://doi.org/10.1039/B709864B>

Appendix C

Electronic supplemental information from Chapter 4 and associated references.

Search Queries for Toxicity Literature Survey

Crustaceans

TOPIC ("toxicity" OR "LC50" OR "LC 50" OR "EC50" OR "EC 50" OR "acute" OR "chronic")
AND ("crustaceans" OR "crustacean") AND ("silver nanoparticle" OR "silver nanoparticles" OR
"nanosilver" OR "nano silver" OR "AgNP" OR "AgNPs" OR "nAg")

Algae

TOPIC ("toxicity" OR "LC50" OR "LC 50" OR "EC50" OR "EC 50" OR "acute" OR "chronic")
AND ("algae" OR "alga") AND ("silver nanoparticle" OR "silver nanoparticles" OR "nanosilver"
OR "nano silver" OR "AgNP" OR "AgNPs" OR "nAg")

Fish

TOPIC ("toxicity" OR "LC50" OR "LC 50" OR "EC50" OR "EC 50" OR "acute" OR "chronic")
AND ("fish" OR "fishes") AND ("silver nanoparticle" OR "silver nanoparticles" OR
"nanosilver" OR "nano silver" OR "AgNP" OR "AgNPs" OR "nAg")

Protozoa

TOPIC ("toxicity" OR "LC50" OR "LC 50" OR "EC50" OR "EC 50") AND ("ciliate" OR
"ciliates" OR "protozoa" OR "protozoan" OR "protozoans") AND ("silver nanoparticle" OR
"silver nanoparticles" OR "nanosilver" OR "nano silver" OR "AgNP" OR "AgNPs" OR "nAg")

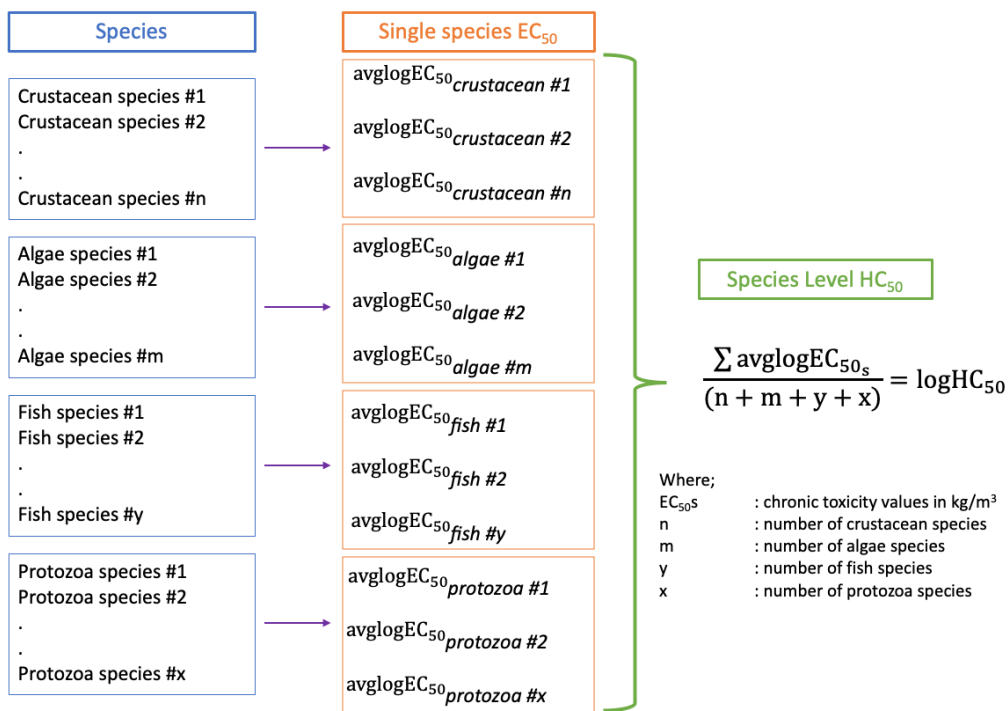


Figure C1. Species level (SPL) HC₅₀ calculation scheme.

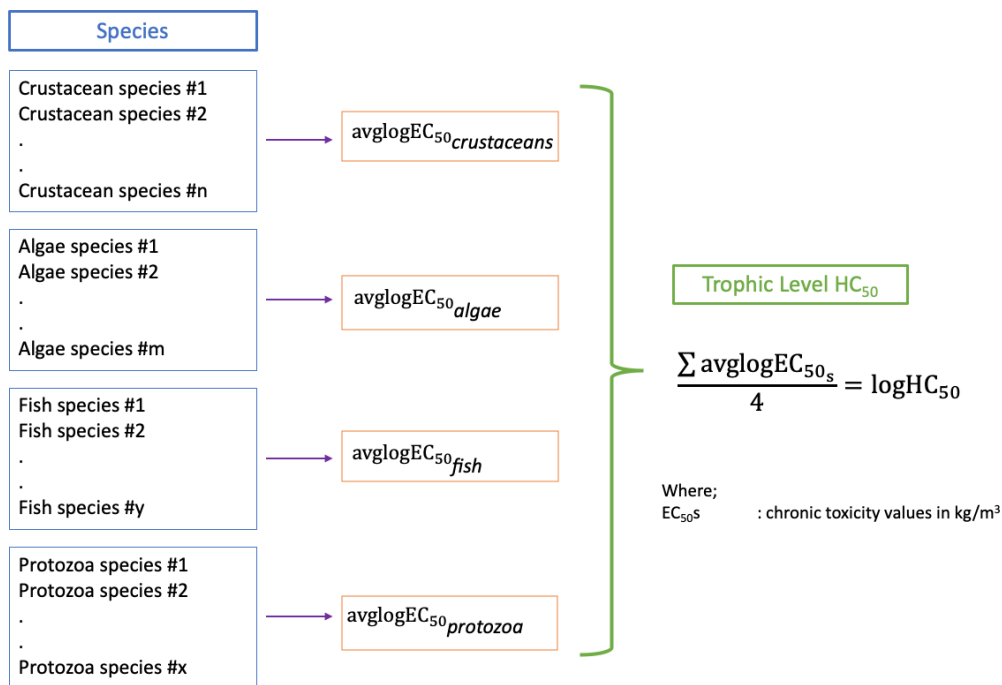


Figure C2. Trophic level (TPL) HC₅₀ calculation scheme.

Table C1. Number of papers disaggregated based on coating, test medium and size for each aquatic organism.

Size (nm)	Organism	Water Medium					Mineral Medium					Complex Medium					Regardless of Medium				
		cit	PVP	un	o	sum	cit	PVP	un	o	sum	cit	PVP	un	o	sum	cit	PVP	un	o	sum
1-10	C	0	0	1	0	1	9	2	6	10	27	2	7	0	0	9	11	9	7	10	37
	A	0	1	0	0	1	5	1	3	6	15	0	1	0	0	1	5	3	3	6	17
	F	0	1	4	0	5	6	0	2	3	11	2	0	0	0	2	8	1	6	3	18
	P	0	0	2	0	2	0	0	0	0	0	0	0	0	1	1	0	0	2	1	3
10.1-20	C	2	2	0	6	10	5	7	8	7	27	1	0	0	6	7	8	9	8	19	44
	A	0	0	0	6	6	9	0	15	2	26	3	0	0	0	3	12	0	15	8	35
	F	0	0	14	1	15	1	5	11	3	20	6	0	6	0	12	7	5	31	4	47
	P	0	0	0	2	2	0	0	0	0	0	0	0	2	0	2	0	0	2	2	4
20.1-30	C	1	0	0	5	6	4	4	4	4	16	1	1	5	0	7	6	5	9	9	29
	A	0	0	0	0	0	6	3	3	10	22	0	0	2	0	2	6	3	5	10	24
	F	0	4	0	0	4	1	3	4	4	12	0	1	0	0	1	1	8	4	4	17
	P	0	0	0	0	0	0	2	0	0	2	0	0	0	0	0	0	2	0	0	2
30.1-40	C	2	1	0	1	4	3	0	7	3	13	1	0	0	0	1	6	1	7	4	18
	A	0	0	0	0	0	1	0	4	2	7	0	0	0	0	0	1	0	4	2	7
	F	0	0	0	0	0	0	0	4	1	5	0	0	0	0	0	0	0	4	1	5
	P	0	2	2	1	5	0	0	0	0	0	0	0	0	0	0	0	2	2	1	5
40.1-50	C	0	0	0	0	0	0	2	3	0	5	0	0	0	0	0	0	2	3	0	5
	A	0	0	0	0	0	0	1	3	2	6	0	0	0	0	0	0	1	3	2	6
	F	0	0	2	0	2	2	1	6	2	11	0	1	3	0	4	2	2	11	2	17
	P	0	0	0	0	0	0	0	0	0	0	0	0	0	0	0	0	0	0	0	0
50.1-60	C	1	0	0	0	1	5	1	1	0	7	0	0	0	0	0	6	1	1	0	8
	A	0	0	0	0	0	1	5	0	0	6	0	0	0	0	0	1	5	0	0	6
	F	0	0	0	0	0	0	7	2	2	11	0	0	0	0	0	0	7	2	2	11
	P	0	0	0	0	0	0	0	0	0	0	0	0	0	0	0	0	0	0	0	0

Size (nm)	Organism	Water Medium					Mineral Medium					Complex Medium					Regardless of Medium				
		cit	PVP	un	o	sum	cit	PVP	un	o	sum	cit	PVP	un	o	sum	cit	PVP	un	o	sum
60.1-70	C	1	0	0	0	1	1	2	0	3	6	0	0	0	0	0	2	2	0	3	7
	A	0	0	0	0	0	1	0	2	4	7	0	0	0	0	0	1	0	2	4	7
	F	0	0	4	0	4	0	0	0	1	1	0	0	0	0	0	0	0	4	1	5
	P	0	0	0	0	0	0	0	0	0	0	0	0	0	0	0	0	0	0	0	0
70.1-80	C	1	0	0	0	1	3	1	4	0	8	0	0	0	1	1	4	1	4	1	10
	A	0	0	0	0	0	1	1	0	0	2	0	0	0	0	0	1	1	0	0	2
	F	1	0	1	0	2	0	1	4	0	5	0	0	0	1	1	1	1	5	1	8
	P	0	0	0	0	0	0	0	1	0	1	0	0	0	0	0	0	0	1	0	1
80.1-90	C	0	0	0	0	0	0	0	0	0	0	0	0	0	0	0	0	0	0	0	0
	A	0	0	0	0	0	0	1	1	0	2	0	0	0	0	0	0	1	1	0	2
	F	0	0	0	0	0	0	2	5	0	7	0	0	0	0	0	0	2	5	0	7
	P	0	0	0	0	0	0	0	0	0	0	0	0	0	0	0	0	0	0	0	0
90.1-100	C	0	0	1	0	1	1	0	1	1	3	1	0	0	0	1	2	0	2	1	5
	A	0	0	0	0	0	0	0	0	0	0	0	0	0	0	0	0	0	0	0	0
	F	1	6	8	0	15	0	1	0	1	2	0	0	0	0	0	1	7	8	1	17
	P	0	0	2	0	2	0	0	0	0	0	0	0	0	0	0	0	0	2	0	2
>100	C	1	1	0	2	4	1	0	6	1	8	0	0	1	0	1	2	1	7	3	13
	A	0	0	0	0	0	0	0	2	1	3	0	1	0	0	1	0	1	2	1	4
	F	0	0	4	0	4	2	3	2	4	11	0	1	0	0	1	2	4	6	4	16
	P	0	0	0	0	0	0	0	0	0	0	0	0	0	0	0	0	0	0	0	0

C: crustaceans, A: algae, F: fish, P: protozoa, cit: citrate coated, PVP: polyvinylpyrrolidone, un: uncoated, o: other coatings, sum: regardless of coating

A) Crustaceans																				
nAg size	Water				Mineral				Complex				All Media (i.e. regardless)				All coatings (i.e. regardless)			
	Citrate	PVP	Uncoated	Other	Citrate	PVP	Uncoated	Other	Citrate	PVP	Uncoated	Other	Citrate	PVP	Uncoated	Other	Water	Mineral	Complex	All Media
1-10	0	0	1	0	9	2	6	10	2	7	0	0	11	9	7	10	1	27	9	37
10.1-20	2	2	0	6	5	7	8	7	1	0	0	6	8	9	8	19	10	27	7	44
20.1-30	1	0	0	5	4	4	4	4	1	1	5	0	6	5	9	9	6	16	7	29
30.1-40	2	1	0	1	3	0	7	3	1	0	0	0	6	1	7	4	4	13	1	18
40.1-50	0	0	0	0	5	1	1	0	0	0	0	0	0	2	3	0	0	7	0	5
50.1-60	1	0	0	0	5	1	1	0	0	0	0	0	6	1	1	0	1	7	0	8
60.1-70	1	0	0	0	1	2	0	3	0	0	0	0	2	2	0	3	1	6	0	7
70.1-80	1	0	0	0	1	1	0	0	0	0	1	0	4	1	4	1	1	2	1	10
80.1-90	0	0	0	0	0	0	0	0	0	0	0	0	0	0	0	0	0	0	0	0
90.1-100	0	0	1	0	1	0	1	1	1	0	0	0	2	0	2	1	1	3	1	5
>100	1	1	0	2	1	0	6	1	0	0	1	0	2	1	7	3	4	8	1	13

B) Algae																				
nAg size	Water				Mineral				Complex				All Media (i.e. regardless)				All coatings (i.e. regardless)			
	Citrate	PVP	Uncoated	Other	Citrate	PVP	Uncoated	Other	Citrate	PVP	Uncoated	Other	Citrate	PVP	Uncoated	Other	Water	Mineral	Complex	All Media
1-10	0	1	0	0	5	1	3	6	0	1	0	0	5	3	3	6	1	15	1	17
10.1-20	0	0	0	6	9	0	15	2	3	0	0	0	12	0	15	8	6	26	3	35
20.1-30	0	0	0	0	6	3	3	10	0	0	2	0	6	3	5	10	0	22	2	24
30.1-40	0	0	0	0	1	0	4	2	0	0	0	0	1	0	4	2	0	7	0	7
40.1-50	0	0	0	0	0	1	3	2	0	0	0	0	0	1	3	2	0	6	0	6
50.1-60	0	0	0	0	1	5	0	0	0	0	0	0	1	5	0	0	0	6	0	6
60.1-70	0	0	0	0	1	0	2	4	0	0	0	0	1	0	2	4	0	7	0	7
70.1-80	0	0	0	0	1	1	0	0	0	0	0	0	1	1	0	0	0	2	0	2
80.1-90	0	0	0	0	0	1	1	0	0	0	0	0	0	1	1	0	0	2	0	2
90.1-100	0	0	0	0	0	0	0	0	0	0	0	0	0	0	0	0	0	0	0	0
>100	0	0	0	0	0	0	2	1	0	1	0	0	0	1	2	1	0	3	1	4

C) Fish																				
nAg size	Water				Mineral				Complex				All Media (i.e. regardless)				All coatings (i.e. regardless)			
	Citrate	PVP	Uncoated	Other	Citrate	PVP	Uncoated	Other	Citrate	PVP	Uncoated	Other	Citrate	PVP	Uncoated	Other	Water	Mineral	Complex	All Media
1-10	0	1	4	0	6	0	2	3	2	0	0	0	8	1	6	3	5	11	2	18
10.1-20	0	0	14	1	1	5	11	3	6	0	6	0	7	5	31	4	15	20	12	47
20.1-30	0	4	0	0	1	3	4	4	0	1	0	0	1	8	4	4	4	12	1	17
30.1-40	0	0	0	0	0	0	4	1	0	0	0	0	0	0	4	1	0	5	0	5
40.1-50	0	0	2	0	2	1	6	2	0	1	3	0	2	2	11	2	2	11	4	17
50.1-60	0	0	0	0	0	7	2	2	0	0	0	0	0	7	2	2	0	11	0	11
60.1-70	0	0	4	0	0	0	0	1	0	0	0	0	0	0	4	1	4	1	0	5
70.1-80	1	0	1	0	0	1	4	0	0	0	1	0	1	1	5	1	2	5	1	8
80.1-90	0	0	0	0	0	2	5	0	0	0	0	0	0	2	5	0	0	7	0	7
90.1-100	1	6	8	0	0	1	0	1	0	0	0	0	1	7	8	1	15	2	0	17
>100	0	0	4	0	2	3	2	4	0	1	0	0	2	4	6	4	4	11	1	16

D) Protozoa																				
nAg size	Water				Mineral				Complex				All Media (i.e. regardless)				All coatings (i.e. regardless)			
	Citrate	PVP	Uncoated	Other	Citrate	PVP	Uncoated	Other	Citrate	PVP	Uncoated	Other	Citrate	PVP	Uncoated	Other	Water	Mineral	Complex	All Media
1-10	0	0	2	0	0	0	0	0	0	0	0	1	0	0	2	1	2	0	1	3
10.1-20	0	0	0	2	0	0	0	0	0	0	2	0	0	0	2	2	2	0	2	4
20.1-30	0	0	0	0	0	2	0	0	0	0	0	0	0	2	0	0	0	2	0	2
30.1-40	0	2	2	1	0	0	0	0	0	0	0	0	0	2	2	1	5	0	0	5
40.1-50	0	0	0	0	0	0	0	0	0	0	0	0	0	0	0	0	0	0	0	0
50.1-60	0	0	0	0	0	0	0	0	0	0	0	0	0	0	0	0	0	0	0	0
60.1-70	0	0	0	0	0	0	0	0	0	0	0	0	0	0	0	0	0	0	0	0
70.1-80	0	0	0	0	0	0	1	0	0	0	0	0	0	0	1	0	0	1	0	1
80.1-90	0	0	0	0	0	0	0	0	0	0	0	0	0	0	0	0	0	0	0	0
90.1-100	0	0	2	0	0	0	0	0	0	0	0	0	0	0	2	0	2	0	0	2
>100	0	0	0	0	0	0	0	0	0	0	0	0	0	0	0	0	0	0	0	0

Figure C3. Number of toxicity data disaggregated by the test medium, nAg size and coating for A) crustaceans, B) algae, C) fish and D) protozoa.

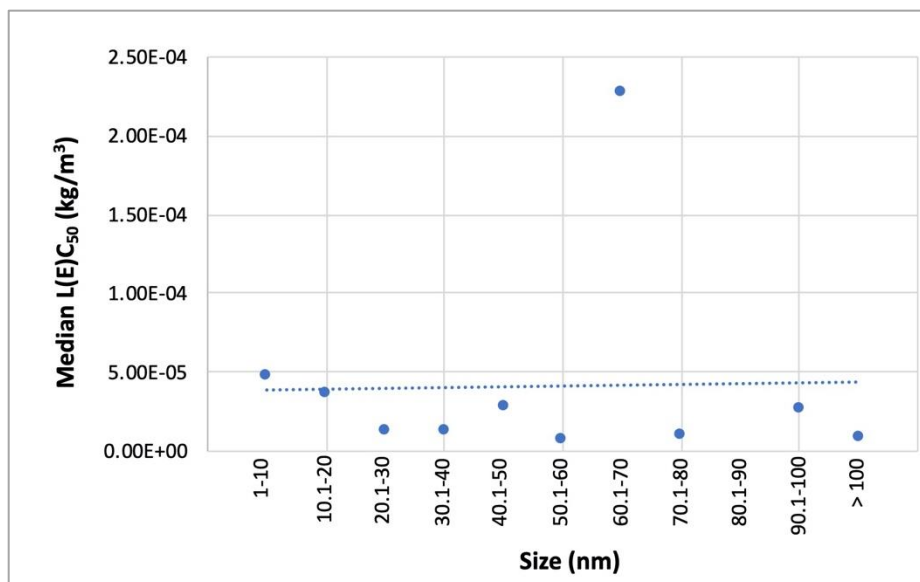


Figure C4. Size versus Median L(E)C₅₀ values for crustaceans.

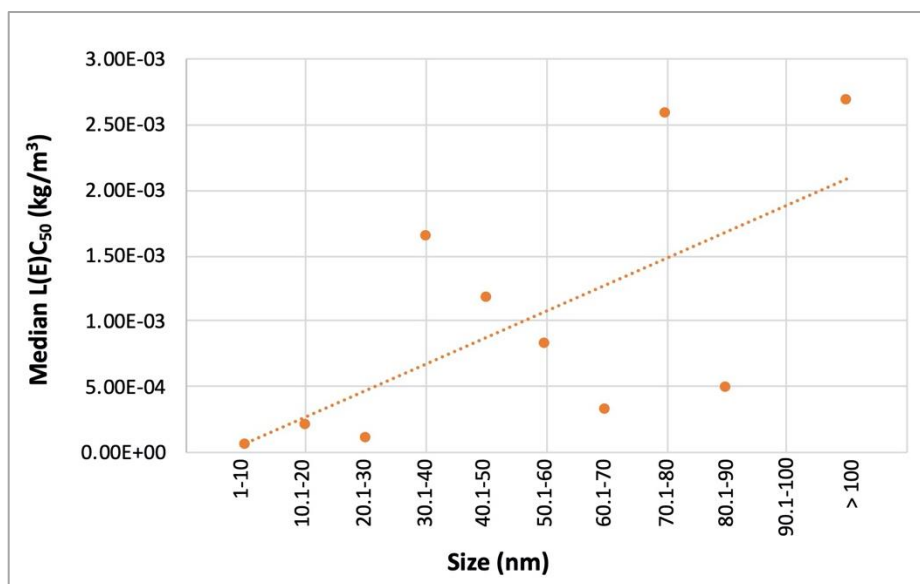


Figure C5. Size versus Median L(E)C₅₀ values for algae.

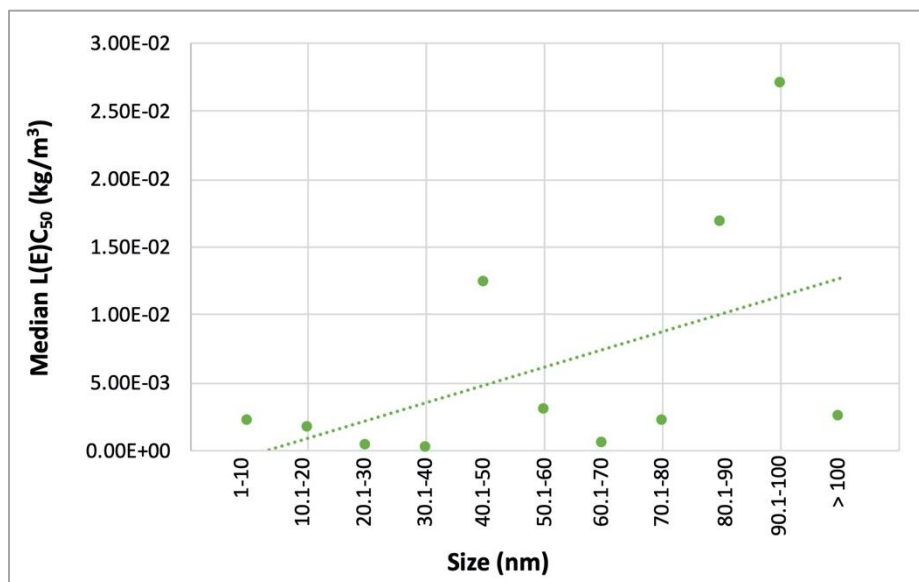


Figure C6. Size versus Median L(E)C₅₀ values for fish.

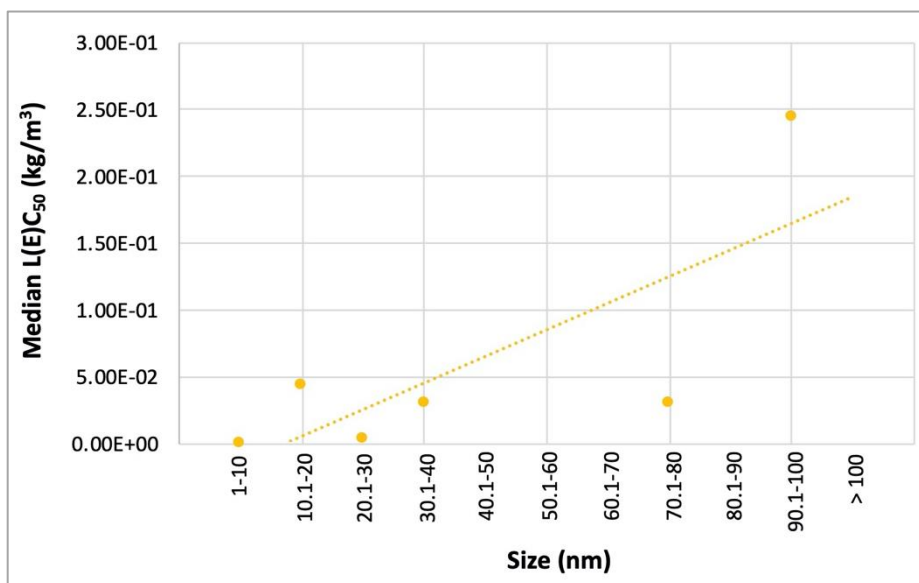


Figure C7. Size versus Median L(E)C₅₀ values for protozoa.

COATING: PVP

	1-10 nm	10.1-20 nm	20.1-30 nm	30.1-40 nm	40.1-50 nm	50.1-60 nm	60.1-70 nm	70.1-80 nm	80.1-90 nm	90.1-100 nm	> 100 nm	All sizes
A) Water	RCS N/A	CCS N/A	RCS N/A	CCS N/A	RCS N/A	CCS N/A	RCS N/A	CCS N/A	RCS N/A	CCS N/A	RCS N/A	CCS N/A
	TPL SPL N/A	TPL SPL N/A	TPL SPL N/A	TPL SPL N/A	TPL SPL N/A	TPL SPL N/A	TPL SPL N/A	TPL SPL N/A	TPL SPL N/A	TPL SPL N/A	TPL SPL N/A	TPL SPL N/A
B) Mineral Medium	RCS N/A	CCS N/A	RCS N/A	CCS N/A	RCS N/A	CCS N/A	RCS N/A	CCS N/A	RCS N/A	CCS N/A	RCS N/A	CCS N/A
	TPL SPL N/A	TPL SPL N/A	TPL SPL N/A	TPL SPL N/A	TPL SPL N/A	TPL SPL N/A	TPL SPL N/A	TPL SPL N/A	TPL SPL N/A	TPL SPL N/A	TPL SPL N/A	TPL SPL 6,321 3,897
C) Complex Medium	RCS N/A	CCS N/A	RCS N/A	CCS N/A	RCS N/A	CCS N/A	RCS N/A	CCS N/A	RCS N/A	CCS N/A	RCS N/A	CCS N/A
	TPL SPL N/A	TPL SPL N/A	TPL SPL N/A	TPL SPL N/A	TPL SPL N/A	TPL SPL N/A	TPL SPL N/A	TPL SPL N/A	TPL SPL N/A	TPL SPL N/A	TPL SPL N/A	TPL SPL N/A
D) All test media	RCS N/A	CCS N/A	RCS N/A	CCS N/A	RCS N/A	CCS N/A	RCS N/A	CCS N/A	RCS N/A	CCS N/A	RCS N/A	CCS N/A
	TPL SPL N/A	TPL SPL N/A	TPL SPL N/A	TPL SPL N/A	TPL SPL N/A	TPL SPL N/A	TPL SPL N/A	TPL SPL N/A	TPL SPL N/A	TPL SPL N/A	TPL SPL N/A	TPL SPL 19,303 6,581

N/A: not enough data for calculation were available, therefore the corresponding EF could not be calculated.

Figure C8. Effect factors (PAF.m³/kg) for PVP coated nAg based on size and test media.

COATING: Citrate

	1-10 nm	10.1-20 nm	20.1-30 nm	30.1-40 nm	40.1-50 nm	50.1-60 nm	60.1-70 nm	70.1-80 nm	80.1-90 nm	90.1-100 nm	> 100 nm	All sizes
A) Water	RCS N/A	CCS N/A	RCS N/A	CCS N/A	RCS N/A	CCS N/A	RCS N/A	CCS N/A	RCS N/A	CCS N/A	RCS N/A	CCS N/A
	TPL SPL N/A	TPL SPL N/A	TPL SPL N/A	TPL SPL N/A	TPL SPL N/A	TPL SPL N/A	TPL SPL N/A	TPL SPL N/A	TPL SPL N/A	TPL SPL N/A	TPL SPL N/A	TPL SPL N/A
B) Mineral Medium	RCS N/A	CCS 37,360	RCS N/A	CCS N/A	RCS N/A	CCS N/A	RCS N/A	CCS N/A	RCS N/A	CCS N/A	RCS N/A	CCS 33,092
	TPL SPL N/A	TPL SPL 35,441	TPL SPL N/A	TPL SPL N/A	TPL SPL N/A	TPL SPL N/A	TPL SPL N/A	TPL SPL N/A	TPL SPL N/A	TPL SPL N/A	TPL SPL N/A	TPL SPL 22,871
C) Complex Medium	RCS N/A	CCS N/A	RCS N/A	CCS N/A	RCS N/A	CCS N/A	RCS N/A	CCS N/A	RCS N/A	CCS N/A	RCS N/A	CCS N/A
	TPL SPL N/A	TPL SPL N/A	TPL SPL N/A	TPL SPL N/A	TPL SPL N/A	TPL SPL N/A	TPL SPL N/A	TPL SPL N/A	TPL SPL N/A	TPL SPL N/A	TPL SPL N/A	TPL SPL N/A
D) All test mediums	RCS N/A	CCS 21,977	RCS N/A	CCS N/A	RCS N/A	CCS N/A	RCS N/A	CCS N/A	RCS N/A	CCS N/A	RCS N/A	CCS 32,686
	TPL SPL N/A	TPL SPL 28,698	TPL SPL N/A	TPL SPL N/A	TPL SPL N/A	TPL SPL N/A	TPL SPL N/A	TPL SPL N/A	TPL SPL N/A	TPL SPL N/A	TPL SPL N/A	TPL SPL 25,447

N/A: not enough data for calculation were available, therefore the corresponding EF could not be calculated.

Figure C9. Effect factors (PAF.m³/kg) for citrate coated nAg based on size and test media.

COATING: Uncoated

	1-10 nm	10.1-20 nm	20.1-30 nm	30.1-40 nm	40.1-50 nm	50.1-60 nm	60.1-70 nm	70.1-80 nm	80.1-90 nm	90.1-100 nm	> 100 nm	All sizes
A) Water	RCS CCS N/A N/A	RCS CCS N/A N/A	RCS CCS N/A N/A	RCS CCS N/A N/A	RCS CCS N/A N/A	RCS CCS N/A N/A	RCS CCS N/A N/A	RCS CCS N/A N/A	RCS CCS N/A N/A	RCS CCS N/A N/A	RCS CCS N/A N/A	RCS CCS N/A N/A
	TPL SPL N/A N/A	TPL SPL N/A N/A	TPL SPL N/A N/A	TPL SPL N/A N/A	TPL SPL N/A N/A	TPL SPL N/A N/A	TPL SPL N/A N/A	TPL SPL N/A N/A	TPL SPL N/A N/A	TPL SPL N/A N/A	TPL SPL N/A N/A	TPL SPL N/A N/A
B) Mineral Medium	RCS CCS N/A N/A	RCS CCS 50,754 18,089	RCS CCS N/A 160,934	RCS CCS N/A N/A	RCS CCS N/A N/A	RCS CCS N/A N/A	RCS CCS N/A N/A	RCS CCS N/A N/A	RCS CCS N/A N/A	RCS CCS N/A N/A	RCS CCS N/A N/A	RCS CCS 68,441 22,950
	TPL SPL N/A N/A	TPL SPL 48,846 78,107	TPL SPL N/A 81,575	TPL SPL N/A N/A	TPL SPL N/A N/A	TPL SPL N/A N/A	TPL SPL N/A N/A	TPL SPL N/A N/A	TPL SPL N/A N/A	TPL SPL N/A N/A	TPL SPL N/A N/A	TPL SPL 38,372 47,452
C) Complex Medium	RCS CCS N/A N/A	RCS CCS N/A N/A	RCS CCS N/A N/A	RCS CCS N/A N/A	RCS CCS N/A N/A	RCS CCS N/A N/A	RCS CCS N/A N/A	RCS CCS N/A N/A	RCS CCS N/A N/A	RCS CCS N/A N/A	RCS CCS N/A N/A	RCS CCS N/A N/A
	TPL SPL N/A N/A	TPL SPL N/A N/A	TPL SPL N/A N/A	TPL SPL N/A N/A	TPL SPL N/A N/A	TPL SPL N/A N/A	TPL SPL N/A N/A	TPL SPL N/A N/A	TPL SPL N/A N/A	TPL SPL N/A N/A	TPL SPL N/A N/A	TPL SPL N/A N/A
D) All test media	RCS CCS N/A 7,887	RCS CCS 50,754 13,476	RCS CCS N/A 87,991	RCS CCS N/A N/A	RCS CCS N/A N/A	RCS CCS N/A N/A	RCS CCS N/A N/A	RCS CCS N/A N/A	RCS CCS N/A N/A	RCS CCS N/A N/A	RCS CCS N/A N/A	RCS CCS 17,290 13,844
	TPL SPL N/A 10,721	TPL SPL 48,846 42,457	TPL SPL N/A 85,346	TPL SPL N/A N/A	TPL SPL N/A N/A	TPL SPL N/A N/A	TPL SPL N/A N/A	TPL SPL N/A N/A	TPL SPL N/A N/A	TPL SPL N/A N/A	TPL SPL N/A N/A	TPL SPL 9,236 20,524

N/A: not enough data for calculation were available, therefore the corresponding EF could not be calculated.

Figure C10. Effect factors (PAF.m³/kg) for uncoated nAg based on size and test media.

COATING: Other

	1-10 nm	10.1-20 nm	20.1-30 nm	30.1-40 nm	40.1-50 nm	50.1-60 nm	60.1-70 nm	70.1-80 nm	80.1-90 nm	90.1-100 nm	> 100 nm	All sizes
A) Water	RCS CCS N/A N/A	RCS CCS N/A N/A	RCS CCS N/A N/A	RCS CCS N/A N/A	RCS CCS N/A N/A	RCS CCS N/A N/A	RCS CCS N/A N/A	RCS CCS N/A N/A	RCS CCS N/A N/A	RCS CCS N/A N/A	RCS CCS N/A N/A	RCS CCS N/A N/A
	TPL SPL N/A N/A	TPL SPL N/A N/A	TPL SPL N/A N/A	TPL SPL N/A N/A	TPL SPL N/A N/A	TPL SPL N/A N/A	TPL SPL N/A N/A	TPL SPL N/A N/A	TPL SPL N/A N/A	TPL SPL N/A N/A	TPL SPL N/A N/A	TPL SPL N/A N/A
B) Mineral Medium	RCS CCS N/A 66,050	RCS CCS N/A N/A	RCS CCS N/A 47,108	RCS CCS N/A N/A	RCS CCS N/A N/A	RCS CCS N/A N/A	RCS CCS N/A N/A	RCS CCS N/A N/A	RCS CCS N/A N/A	RCS CCS N/A N/A	RCS CCS N/A N/A	RCS CCS 38,645 22,961
	TPL SPL N/A 206,055	TPL SPL N/A N/A	TPL SPL N/A 37,139	TPL SPL N/A N/A	TPL SPL N/A N/A	TPL SPL N/A N/A	TPL SPL N/A N/A	TPL SPL N/A N/A	TPL SPL N/A N/A	TPL SPL N/A N/A	TPL SPL N/A N/A	TPL SPL 81,999 40,793
C) Complex Medium	RCS CCS N/A N/A	RCS CCS N/A N/A	RCS CCS N/A N/A	RCS CCS N/A N/A	RCS CCS N/A N/A	RCS CCS N/A N/A	RCS CCS N/A N/A	RCS CCS N/A N/A	RCS CCS N/A N/A	RCS CCS N/A N/A	RCS CCS N/A N/A	RCS CCS N/A N/A
	TPL SPL N/A N/A	TPL SPL N/A N/A	TPL SPL N/A N/A	TPL SPL N/A N/A	TPL SPL N/A N/A	TPL SPL N/A N/A	TPL SPL N/A N/A	TPL SPL N/A N/A	TPL SPL N/A N/A	TPL SPL N/A N/A	TPL SPL N/A N/A	TPL SPL N/A N/A
D) All test mediums	RCS CCS N/A 61,170	RCS CCS N/A N/A	RCS CCS N/A 30,818	RCS CCS N/A N/A	RCS CCS N/A N/A	RCS CCS N/A N/A	RCS CCS N/A N/A	RCS CCS N/A N/A	RCS CCS N/A N/A	RCS CCS N/A N/A	RCS CCS N/A N/A	RCS CCS 29,906 18,390
	TPL SPL N/A 181,313	TPL SPL N/A N/A	TPL SPL N/A 12,079	TPL SPL N/A N/A	TPL SPL N/A N/A	TPL SPL N/A N/A	TPL SPL N/A N/A	TPL SPL N/A N/A	TPL SPL N/A N/A	TPL SPL N/A N/A	TPL SPL N/A N/A	TPL SPL 58,129 18,581

N/A: not enough data for calculation were available, therefore the corresponding EF could not be calculated.

Figure C11. Effect factors (PAF.m³/kg) for nAg coated with other capping agents based on size and test media.

COATING: All coatings (i.e. regardless of coating)

	1-10 nm	10.1-20 nm	20.1-30 nm	30.1-40 nm	40.1-50 nm	50.1-60 nm	60.1-70 nm	70.1-80 nm	80.1-90 nm	90.1-100 nm	> 100 nm	All sizes
A) Water	RCS CCS N/A N/A	RCS CCS N/A N/A	RCS CCS N/A N/A	RCS CCS N/A N/A	RCS CCS N/A N/A	RCS CCS N/A N/A	RCS CCS N/A N/A	RCS CCS N/A N/A	RCS CCS N/A N/A	RCS CCS N/A N/A	RCS CCS N/A N/A	RCS CCS N/A N/A
	TPL SPL N/A N/A	TPL SPL N/A N/A	TPL SPL N/A N/A	TPL SPL N/A N/A	TPL SPL N/A N/A	TPL SPL N/A N/A	TPL SPL N/A N/A	TPL SPL N/A N/A	TPL SPL N/A N/A	TPL SPL N/A N/A	TPL SPL N/A N/A	TPL SPL N/A N/A
B) Mineral Medium	RCS CCS 30,035 20,964	RCS CCS 123,660 27,372	RCS CCS N/A 38,002	RCS CCS N/A 18,393	RCS CCS N/A N/A	RCS CCS 899 2,015	RCS CCS N/A N/A	RCS CCS N/A N/A	RCS CCS N/A N/A	RCS CCS N/A N/A	RCS CCS N/A N/A	RCS CCS 27,523 22,981
	TPL SPL 73,795 70,984	TPL SPL 49,456 53,118	TPL SPL N/A 54,419	TPL SPL N/A 20,432	TPL SPL N/A N/A	TPL SPL 2,374 5,149	TPL SPL N/A N/A	TPL SPL N/A N/A	TPL SPL N/A N/A	TPL SPL N/A N/A	TPL SPL N/A N/A	TPL SPL 22,948 30,745
C) Complex Medium	RCS CCS N/A N/A	RCS CCS N/A 12,515	RCS CCS N/A N/A	RCS CCS N/A N/A	RCS CCS N/A N/A	RCS CCS N/A N/A	RCS CCS N/A N/A	RCS CCS N/A N/A	RCS CCS N/A N/A	RCS CCS N/A N/A	RCS CCS N/A N/A	RCS CCS 4,959 12,189
	TPL SPL N/A N/A	TPL SPL N/A 8,989	TPL SPL N/A N/A	TPL SPL N/A N/A	TPL SPL N/A N/A	TPL SPL N/A N/A	TPL SPL N/A N/A	TPL SPL N/A N/A	TPL SPL N/A N/A	TPL SPL N/A N/A	TPL SPL N/A N/A	TPL SPL 10,233 10,928
D) All test mediums	RCS CCS N/A 10,362	RCS CCS 99,608 18,169	RCS CCS N/A 46,313	RCS CCS N/A N/A	RCS CCS N/A N/A	RCS CCS 899 2,088	RCS CCS N/A 42,943	RCS CCS N/A N/A	RCS CCS N/A N/A	RCS CCS N/A N/A	RCS CCS N/A 6,333	RCS CCS 14,675 9,679
	TPL SPL N/A 42,431	TPL SPL 39,755 29,523	TPL SPL N/A 47,163	TPL SPL N/A N/A	TPL SPL N/A N/A	TPL SPL 2,374 5,527	TPL SPL N/A 42,943	TPL SPL N/A N/A	TPL SPL N/A N/A	TPL SPL N/A N/A	TPL SPL N/A 8,477	TPL SPL 8,035 12,130

N/A: not enough data for calculation were available, therefore the corresponding EF could not be calculated.

Figure C12. Effect factors (PAF.m³/kg) for nAg based on size and test media regardless of coating.

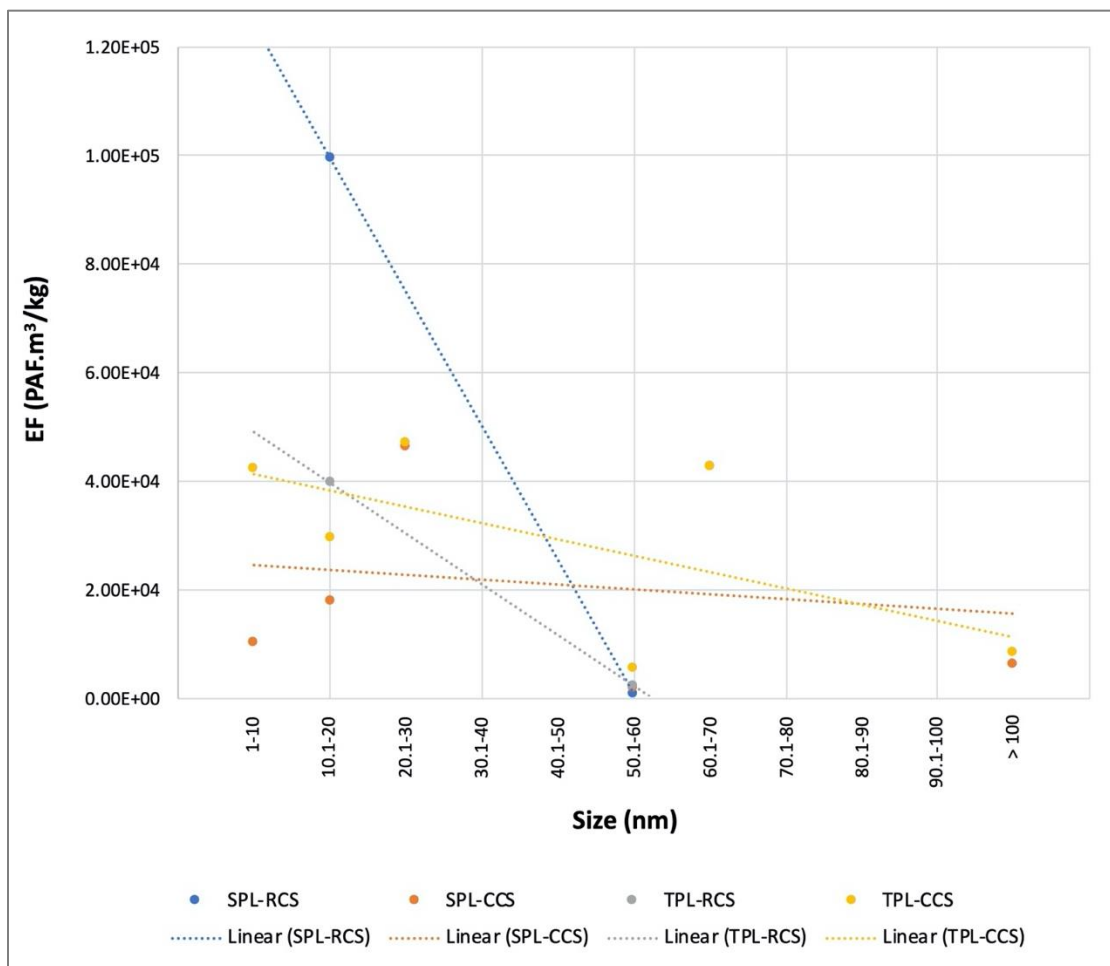


Figure C13. Size dependent effect factors for different scenarios and respective trendlines.

Table C2. The LC₅₀/EC₅₀/IC₅₀ values collected from the literature for silver nanoparticles for freshwater crustaceans (listed in alphabetical order based on references).

Species	Endpoint	Exposure Time (hours, days)	Acute/ Chronic (Based on USEtox)	Reported LC ₅₀ / EC ₅₀ / IC ₅₀	LC ₅₀ / EC ₅₀ / IC ₅₀ (kg Ag/m ³)	Avg Size (nm)	Coating	Method	Test Medium	LC ₅₀ / EC ₅₀ / IC ₅₀ for Ag ⁺ (kg Ag/m ³)	Ref.
<i>Daphnia magna</i>	mortality	48 h	A	LC50	1.10E-06	5.94	citrate	US EPA 600/4-90/027F	mineral (MHRW)	1.10E-06	[1]
<i>Daphnia magna</i>	mortality	48 h	A	LC50	3.15E-05	39.4	coated (proprietary)	US EPA 600/4-90/027F	mineral (MHRW)	1.10E-06	[1]
<i>Daphnia magna</i>	mortality	48 h	A	LC50	1.67E-05	681.4	uncoated	US EPA 600/4-90/027F	mineral (MHRW)	1.10E-06	[1]
<i>Daphnia magna</i>	mortality	48 h	A	LC50	1.00E-06	773.6	coffee	US EPA 600/4-90/027F	mineral (MHRW)	1.10E-06	[1]
<i>Daphnia magna</i>	mortality	48 h	A	LC50	4.40E-06	39.4	coated (proprietary)	US EPA 600/4-90/027F	mineral (MHRW)	7.00E-07	[1]
<i>Daphnia magna</i>	mortality	48 h	A	LC50	1.40E-06	681.4	uncoated	US EPA 600/4-90/027F	mineral (MHRW)	7.00E-07	[1]
<i>Daphnia magna</i>	immobilization	48 h	A	EC50	2.00E-06	6.47	uncoated	OECD 202	mineral (M4)	2.30E-06	[2]
<i>Daphnia magna</i>	immobilization	48 h	A	EC50	4.00E-06	7.32	citrate	OECD 202	mineral (M4)	2.30E-06	[2]
<i>Daphnia magna</i>	immobilization	48 h	A	EC50	1.87E-04	17.97	uncoated	OECD 202	mineral (M4)	2.30E-06	[2]
<i>Ceriodaphnia cornuta</i>	mortality	24 h	A	LC50	3.86E-02	9.4	Camellia sinensis	N/A	mineral (OECD)	1.92E-02	[3]
<i>Daphnia magna</i>	immobilization	48 h	A	EC50	5.40E-05	8.4	PVP	OECD 202	mineral (AFW)	2.20E-06	[4]

Species	Endpoint	Exposure Time (hours, days)	Acute/ Chronic (Based on USEtox)	Reported LC ₅₀ / EC ₅₀ / IC ₅₀	LC ₅₀ / EC ₅₀ / IC ₅₀ (kg Ag/m ³)	Avg Size (nm)	Coating	Method	Test Medium	LC ₅₀ / EC ₅₀ / IC ₅₀ for Ag ⁺ (kg Ag/m ³)	Ref.
<i>Thamnocephalus platyurus</i>	mortality	24 h	A	LC50	6.88E-05	8.4	PVP	OECD 202	mineral (AFW)	5.70E-06	[4]
<i>Daphnia magna</i>	immobilization	48 h	A	EC50	1.37E-04	8.4	PVP	OECD 202	complex (river)	1.40E-05	[4]
<i>Thamnocephalus platyurus</i>	mortality	24 h	A	LC50	1.91E-04	8.4	PVP	OECD 202	complex (river)	1.07E-05	[4]
<i>Daphnia magna</i>	immobilization	48 h	A	EC50	1.89E-04	8.4	PVP	OECD 202	complex (lake)	9.00E-06	[4]
<i>Thamnocephalus platyurus</i>	mortality	24 h	A	LC50	3.90E-04	8.4	PVP	OECD 202	complex (lake)	1.68E-05	[4]
<i>Daphnia magna</i>	reproduction/ mortality	21 d	C	-	5.80E-05	8.4	PVP	OECD 211	complex (river)	N/A	[4]
<i>Daphnia magna</i>	immobilization	48 h	A	EC50	4.94E-05	12.5	protein	OECD 202	mineral (AFW)	2.20E-06	[4]
<i>Thamnocephalus platyurus</i>	mortality	24 h	A	LC50	2.56E-04	12.5	protein	OECD 202	mineral (AFW)	5.70E-06	[4]
<i>Daphnia magna</i>	immobilization	48 h	A	EC50	4.89E-05	12.5	protein	OECD 202	complex (river)	1.40E-05	[4]
<i>Thamnocephalus platyurus</i>	mortality	24 h	A	LC50	1.62E-04	12.5	protein	OECD 202	complex (river)	1.07E-05	[4]
<i>Daphnia magna</i>	immobilization	48 h	A	EC50	6.30E-05	12.5	protein	OECD 202	complex (lake)	9.00E-06	[4]
<i>Thamnocephalus platyurus</i>	mortality	24 h	A	LC50	2.50E-04	12.5	protein	OECD 202	complex (lake)	1.68E-05	[4]
<i>Daphnia magna</i>	reproduction/ mortality	21 d	C	-	3.70E-05	12.5	protein	OECD 211	complex (river)	N/A	[4]
<i>Daphnia magna</i>	reproduction/ mortality	21 d	C	-	7.40E-05	12.5	protein	OECD 211	complex (lake)	N/A	[4]
<i>Moina macrocopa</i>	mortality	48 h	A	LC50	1.10E-04	20.8	PVP	OECD 202	mineral (MHRW)	N/A	[5]
<i>Moina macrocopa</i>	mortality	48 h	A	LC50	1.16E-03	40.04	L Tyrosine	OECD 202	mineral (MHRW)	N/A	[5]

Species	Endpoint	Exposure Time (hours, days)	Acute/ Chronic (Based on USEtox)	Reported LC ₅₀ / EC ₅₀ / IC ₅₀	LC ₅₀ / EC ₅₀ / IC ₅₀ (kg Ag/m ³)	Avg Size (nm)	Coating	Method	Test Medium	LC ₅₀ / EC ₅₀ / IC ₅₀ for Ag ⁺ (kg Ag/m ³)	Ref.
<i>Daphnia magna</i>	growth and survival	48 h	A	LC50	1.70E-05	10	CPA	US EPA 821/R-02/012	mineral (COMBO)	N/A	[6]
<i>Daphnia magna</i>	mortality	48 h	A	LC50	2.75E-06	1–10	CPA	OECD 202	mineral (COMBO)	N/A	[7]
<i>Daphnia magna</i>	growth and mortality	96 h	A	LC50	1.00E-04	35	uncoated	US EPA 821/R-02/012	mineral (MHRW)	N/A	[8]
<i>Daphnia magna</i>	moulting	21 d	C	LC50	1.00E-06	35	uncoated	US EPA 821/R-02/012	mineral (MHRW)	N/A	[8]
<i>Daphnia magna</i>	moulting	21 d	C	LC50	5.00E-06	35	uncoated	US EPA 821/R-02/012	mineral (MHRW)	N/A	[8]
<i>Ceriodaphnia dubia</i>	mortality and/or immobilization	48 h	A	LC50	4.60E-07	20-30	N/A	US EPA 3050B	complex (Suwannee River)	N/A	[9]
<i>Ceriodaphnia dubia</i>	mortality and/or immobilization	48 h	A	LC50	6.18E-06	20-30	N/A	US EPA 3050B	complex (Suwannee River)	N/A	[9]
<i>Ceriodaphnia dubia</i>	mortality and/or immobilization	48 h	A	LC50	7.71E-07	20-30	N/A	US EPA 3050B	complex (Suwannee River)	N/A	[9]
<i>Ceriodaphnia dubia</i>	mortality and/or immobilization	48 h	A	LC50	6.96E-07	20-30	N/A	US EPA 3050B	complex (Suwannee River)	N/A	[9]
<i>Daphnia magna</i>	immobilization	48 h	A	EC50	1.20E-04	20	N/A	OECD 202	mineral (OECD)	1.40E-06	[10]
<i>Daphnia magna</i>	immobilization	48 h	A	EC50	1.20E-06	23	N/A	OECD 202	mineral (OECD)	1.40E-06	[10]
<i>Daphnia magna</i>	immobilization	48 h	A	EC50	2.00E-05	27	N/A	OECD 202	mineral (OECD)	1.40E-06	[10]

Species	Endpoint	Exposure Time (hours, days)	Acute/ Chronic (Based on USEtox)	Reported LC ₅₀ / EC ₅₀ / IC ₅₀	LC ₅₀ / EC ₅₀ / IC ₅₀ (kg Ag/m ³)	Avg Size (nm)	Coating	Method	Test Medium	LC ₅₀ / EC ₅₀ / IC ₅₀ for Ag ⁺ (kg Ag/m ³)	Ref.
<i>Daphnia magna</i>	immobilization	48 h	A	EC50	6.50E-04	200	N/A	OECD 202	mineral (OECD)	1.40E-06	[10]
<i>Ceriodaphnia dubia</i>	mortality and/or immobilization	48 h	A	LC50	6.70E-05	26.6	metal oxide	US EPA 821/R-02/013	mineral (MHFW)	1.60E-04	[11]
<i>Daphnia pulex</i>	mortality and/or immobilization	48 h	A	LC50	4.00E-05	26.6	metal oxide	US EPA 821/R-02/013	mineral (MHFW)	8.00E-06	[12]
<i>Daphnia magna</i>	mortality	7 d	SC	LC50	8.50E-06	20	citrate	US EPA 812/R-02/012	mineral (VSRW)	N/A	[12]
<i>Daphnia magna</i>	mortality	7 d	SC	LC50	9.09E-06	20	citrate	US EPA 812/R-02/012	mineral (SRW)	N/A	[12]
<i>Daphnia magna</i>	mortality	7 d	SC	LC50	7.03E-06	54	citrate	US EPA 812/R-02/012	mineral (VSRW)	N/A	[12]
<i>Daphnia magna</i>	mortality	7 d	SC	LC50	5.98E-06	54	citrate	US EPA 812/R-02/012	mineral (SRW)	N/A	[12]
<i>Daphnia magna</i>	mortality	7 d	SC	LC50	7.00E-06	76	citrate	US EPA 812/R-02/012	mineral (VSRW)	N/A	[12]
<i>Daphnia magna</i>	mortality	7 d	SC	LC50	1.08E-05	76	citrate	US EPA 812/R-02/012	mineral (SRW)	N/A	[12]
<i>Daphnia magna</i>	immobilization	48 h	A	EC50	1.94E-06	21	PVP	OECD 202	complex (lake)	9.30E-07	[13]
<i>Daphnia magna</i>	mortality	48 h	A	LC50	7.00E-06	10	uncoated	US EPA 600/4-90/027F	mineral (Lake Superior)	5.70E-07	[14]

Species	Endpoint	Exposure Time (hours, days)	Acute/ Chronic (Based on USEtox)	Reported LC ₅₀ / EC ₅₀ / IC ₅₀	LC ₅₀ / EC ₅₀ / IC ₅₀ (kg Ag/m ³)	Avg Size (nm)	Coating	Method	Test Medium	LC ₅₀ / EC ₅₀ / IC ₅₀ for Ag ⁺ (kg Ag/m ³)	Ref.
<i>Daphnia magna</i>	mortality	48 h	A	LC50	1.10E-05	20	uncoated	US EPA 600/4-90/027F	mineral (Lake Superior)	5.70E-07	[14]
<i>Daphnia magna</i>	mortality	48 h	A	LC50	1.80E-05	30	uncoated	US EPA 600/4-90/027F	mineral (Lake Superior)	5.70E-07	[14]
<i>Daphnia magna</i>	mortality	48 h	A	LC50	2.74E-05	50	uncoated	US EPA 600/4-90/027F	mineral (Lake Superior)	5.70E-07	[14]
<i>Daphnia magna</i>	lethality	24 h	A	LC50	2.50E-05	40	PVP	US EPA 812/R-02/012	water	N/A	[15]
<i>Daphnia magna</i>	lethality	24 h	A	LC50	8.90E-06	40	citrate	US EPA 812/R-02/012	water	N/A	[15]
<i>Daphnia magna</i>	lethality	24 h	A	LC50	3.84E-05	110	PVP	US EPA 812/R-02/012	water	N/A	[15]
<i>Daphnia magna</i>	lethality	24 h	A	LC50	1.74E-05	110	citrate	US EPA 812/R-02/012	water	N/A	[15]
<i>Daphnia magna</i>	mortality	21 d	C	EC50	3.20E-04	8.6	citrate	OECD 211	mineral (M4)	1.20E-06	[16]
<i>Daphnia magna</i>	immobilization	24 h	A	EC50	1.05E-04	8.6	citrate	OECD 202	mineral (M4)	2.80E-06	[16]
<i>Daphnia magna</i>	immobilization	24 h	A	EC50	2.70E-04	8.6	citrate	OECD 202	complex (lake)	7.50E-06	[16]
<i>Daphnia magna</i>	immobilization	48 h	A	EC50	1.10E-04	8.6	citrate	OECD 202	mineral (M4)	1.80E-06	[16]
<i>Daphnia magna</i>	immobilization	48 h	A	EC50	2.70E-04	8.6	citrate	OECD 202	complex (lake)	8.00E-06	[16]
<i>Daphnia magna</i>	immobilization	48 h	A	EC50	3.70E-05	15	uncoated	OECD 202	mineral (OECD)	N/A	[17]

Species	Endpoint	Exposure Time (hours, days)	Acute/ Chronic (Based on USEtox)	Reported LC ₅₀ / EC ₅₀ / IC ₅₀	LC ₅₀ / EC ₅₀ / IC ₅₀ (kg Ag/m ³)	Avg Size (nm)	Coating	Method	Test Medium	LC ₅₀ / EC ₅₀ / IC ₅₀ for Ag ⁺ (kg Ag/m ³)	Ref.
<i>Daphnia magna</i>	immobilization	48 h	A	EC50	1.60E-06	44	uncoated	OECD 202	mineral (OECD)	N/A	[17]
<i>Daphnia magna</i>	immobilization	48 h	A	EC50	8.50E-06	241	uncoated	OECD 202	mineral (OECD)	N/A	[17]
<i>Daphnia magna</i>	immobilization	48 h	A	EC50	1.00E-05	10	citrate	OECD 202	mineral (AFW)	2.00E-06	[18]
<i>Daphnia magna</i>	immobilization	48 h	A	EC50	3.40E-05	20	citrate	OECD 202	mineral (AFW)	2.00E-06	[18]
<i>Daphnia magna</i>	immobilization	48 h	A	EC50	1.41E-04	40	citrate	OECD 202	mineral (AFW)	2.00E-06	[18]
<i>Daphnia magna</i>	immobilization	48 h	A	EC50	1.68E-04	60	citrate	OECD 202	mineral (AFW)	2.00E-06	[18]
<i>Daphnia magna</i>	immobilization	48 h	A	EC50	2.18E-04	80	citrate	OECD 202	mineral (AFW)	2.00E-06	[18]
<i>Daphnia magna</i>	immobilization	48 h	A	EC50	2.50E-06	20.4	PVP	OECD 202	mineral (AFW)	1.00E-06	[19]
<i>Ceriodaphnia cornuta</i>	mortality	1 h	A	LC50	2.35E-02	8.2	N/A	OECD, US EPA	water (SSF)	1.47E-02	[20]
<i>Daphnia magna</i>	immobilization	24 h	A	EC50	1.00E-05	<100	N/A	US EPA	mineral (MHRW)	3.20E-06	[21]
<i>Daphnia magna</i>	mortality	48 h	A	LC50	5.40E-06	10	N/A	US EPA 812/R-02/012	mineral (MHRW)	1.20E-06	[22]
<i>Daphnia magna</i>	mortality	48 h	A	LC50	5.30E-06	20	N/A	US EPA 812/R-02/012	mineral (MHRW)	1.20E-06	[22]
<i>Daphnia magna</i>	mortality	48 h	A	LC50	1.11E-05	29	citrate	US EPA 812/R-02/012	mineral (MHRW)	1.20E-06	[22]
<i>Daphnia magna</i>	mortality	48 h	A	LC50	1.80E-06	31	N/A	US EPA 812/R-02/012	mineral (MHRW)	1.20E-06	[22]

Species	Endpoint	Exposure Time (hours, days)	Acute/ Chronic (Based on USEtox)	Reported LC ₅₀ / EC ₅₀ / IC ₅₀	LC ₅₀ / EC ₅₀ / IC ₅₀ (kg Ag/m ³)	Avg Size (nm)	Coating	Method	Test Medium	LC ₅₀ / EC ₅₀ / IC ₅₀ for Ag ⁺ (kg Ag/m ³)	Ref.
<i>Daphnia magna</i>	mortality	48 h	A	LC50	1.49E-05	36	N/A	US EPA 812/R-02/012	mineral (MHRW)	1.20E-06	[22]
<i>Daphnia magna</i>	mortality	48 h	A	LC50	9.70E-05	41	PVP	US EPA 812/R-02/012	mineral (MHRW)	1.20E-06	[22]
<i>Daphnia magna</i>	mortality	48 h	A	LC50	5.40E-06	50	N/A	US EPA 812/R-02/012	mineral (MHRW)	1.20E-06	[22]
<i>Daphnia magna</i>	mortality	48 h	A	LC50	1.77E-05	80	N/A	US EPA 812/R-02/012	mineral (MHRW)	1.20E-06	[22]
<i>Ceriodaphnia dubia</i>	mortality	48 h	A	LC50	4.80E-06	20	citrate	US EPA 812/R-02/012	mineral (MHRW)	7.00E-07	[22]
<i>Ceriodaphnia dubia</i>	mortality	48 h	A	LC50	>4.65E-05	20	citrate	US EPA 812/R-02/012	complex	1.90E-06	[22]
<i>Ceriodaphnia dubia</i>	mortality	48 h	A	LC50	2.67E-05	100	citrate	US EPA 812/R-02/012	mineral (MHRW)	7.00E-07	[22]
<i>Ceriodaphnia dubia</i>	mortality	48 h	A	LC50	>4.14E-05	100	citrate	US EPA 812/R-02/012	complex	1.90E-06	[22]
<i>Daphnia magna</i>	immobilization	48 h	A	EC50	1.00E-06	60	uncoated	OECD 202	mineral (M4)	5.00E-07	[23]
<i>Daphnia magna</i>	immobilization	48 h	A	EC50	1.40E-06	300	uncoated	OECD 202	mineral (M4)	5.00E-07	[23]
<i>Daphnia magna</i>	immobilization	24 h	A	EC50	4.10E-05	20	uncoated	OECD 202	mineral (OECD)	2.30E-06	[24]
<i>Daphnia magna</i>	immobilization	48 h	A	EC50	4.50E-05	56.6	PVP	OECD 202	mineral (MHW)	N/A	[25]

Species	Endpoint	Exposure Time (hours, days)	Acute/ Chronic (Based on USEtox)	Reported LC ₅₀ / EC ₅₀ / IC ₅₀	LC ₅₀ / EC ₅₀ / IC ₅₀ (kg Ag/m ³)	Avg Size (nm)	Coating	Method	Test Medium	LC ₅₀ / EC ₅₀ / IC ₅₀ for Ag ⁺ (kg Ag/m ³)	Ref.
<i>Daphnia magna</i>	immobilization	48 h	A	EC50	7.98E-06	13.3	citrate	N/A	mineral (M4)	5.70E-07	[26]
<i>Daphnia magna</i>	immobilization	48 h	A	EC50	7.50E-07	60-100	uncoated	N/A	mineral (M4)	5.70E-07	[26]
<i>Daphnia carinata</i>	immobilization	48 h	A	EC50	4.97E-05	10.56	tyrosine	OECD 202	mineral (MHW) ASTM	1.21E-06	[27]
<i>Daphnia carinata</i>	immobilization	48 h	A	EC50	1.94E-05	9.27	epigallocatechin gallate	OECD 202	mineral (MHW) ASTM	1.21E-06	[27]
<i>Daphnia carinata</i>	immobilization	48 h	A	EC50	2.14E-05	13.68	curcumin	OECD 202	mineral (MHW) ASTM	1.21E-06	[27]
<i>Daphnia magna</i>	mortality	48 h	A	LC50	1.20E-05	30	citrate-Au	OECD	water (SSF)	2.00E-06	[28]
<i>Daphnia magna</i>	mortality	48 h	A	LC50	4.50E-06	36	citrate	OECD	water (SSF)	2.00E-06	[28]
<i>Daphnia magna</i>	mortality	48 h	A	LC50	6.50E-06	52	citrate	OECD	water (SSF)	2.00E-06	[28]
<i>Daphnia magna</i>	mortality	48 h	A	LC50	1.00E-05	66	citrate	OECD	water (SSF)	2.00E-06	[28]
<i>Daphnia magna</i>	mortality	48 h	A	LC50	1.50E-05	72	citrate-Au	OECD	water (SSF)	2.00E-06	[28]
<i>Daphnia magna</i>	immobilization	48 h	A	EC50	4.76E-05	30	citrate	OECD 202	mineral (M7)	7.50E-07	[29]
<i>Daphnia magna</i>	reproduction	21 d	C	-	2.00E-05	30	citrate	OECD 211	mineral (M7)	N/A	[29]
<i>Ceriodaphnia dubia</i>	mortality	48 h	A	LC50	2.21E-04	76.8	carbon	US EPA	complex (Prairie Creek Preserve)	N/A	[30]

Species	Endpoint	Exposure Time (hours, days)	Acute/ Chronic (Based on USEtox)	Reported LC ₅₀ / EC ₅₀ / IC ₅₀	LC ₅₀ / EC ₅₀ / IC ₅₀ (kg Ag/m ³)	Avg Size (nm)	Coating	Method	Test Medium	LC ₅₀ / EC ₅₀ / IC ₅₀ for Ag ⁺ (kg Ag/m ³)	Ref.
<i>Ceriodaphnia dubia</i>	mortality	48 h	A	LC50	4.33E-07	25.4	uncoated	US EPA	complex (Ichetucknee River)	N/A	[30]
<i>Ceriodaphnia dubia</i>	mortality	48 h	A	LC50	4.82E-07	25.4	uncoated	US EPA	mineral (MHRW)	N/A	[30]
<i>Daphnia magna</i>	reproduction	21 d	C	-	1.07E-04	8.4	PVP	N/A	complex (E7)	1.20E-05	[31]
<i>Daphnia magna</i>	immobilization	24 h	A	EC50	2.90E-04	8.4	PVP	N/A	complex (E7)	1.39E-05	[31]
<i>Daphnia magna</i>	mortality	24 h	A	LC50	1.50E-06	<100	N/A	OECD 211	water	N/A	[32]
<i>Daphnia lumholtzi</i>	mortality	24 h	A	LC50	6.93E-05	9.8	N/A	OECD 202	mineral (COMBO)	N/A	[33]
<i>Daphnia lumholtzi</i>	mortality	48 h	A	LC50	5.76E-05	9.8	N/A	OECD 202	mineral (COMBO)	N/A	[33]
<i>Daphnia lumholtzi</i>	survival, growth and reproduction	21 d	C	-	>5.00E-07	9.8	N/A	OECD 202	mineral (COMBO)	N/A	[33]
<i>Daphnia magna</i>	mortality	48 h	A	EC50	7.98E-04	56.5	citrate	US EPA	mineral (MHW)	4.30E-06	[34]
<i>Daphnia magna</i>	mortality	24 h	A	LC50	6.10E-06	35	uncoated	US EPA	mineral (MHRW)	4.00E-07	[35]
<i>Daphnia magna</i>	mortality	24 h	A	LC50	1.80E-06	40	citrate	US EPA	mineral (MHRW)	4.00E-07	[35]
<i>Daphnia magna</i>	mortality	24 h	A	LC50	1.06E-05	35-50	PVP	US EPA	mineral (MHRW)	4.00E-07	[35]
<i>Daphnia magna</i>	immobilization	48 h	A	EC50	4.72E-05	3-11.4	citrate	OECD	mineral	4.50E-06	[36]
<i>Daphnia magna</i>	mortality	24 h	A	LC50	2.65E-01	17	protein	US EPA 821/R-02/012	water (SSF)	N/A	[37]

Species	Endpoint	Exposure Time (hours, days)	Acute/ Chronic (Based on USEtox)	Reported LC ₅₀ / EC ₅₀ / IC ₅₀	LC ₅₀ / EC ₅₀ / IC ₅₀ (kg Ag/m ³)	Avg Size (nm)	Coating	Method	Test Medium	LC ₅₀ / EC ₅₀ / IC ₅₀ for Ag ⁺ (kg Ag/m ³)	Ref.
<i>Daphnia magna</i>	mortality	48 h	A	LC50	1.18E-01	17	protein	US EPA 821/R-02/012	water (SSF)	N/A	[37]
<i>Daphnia magna</i>	mortality	24 h	A	LC50	1.62E-01	18	protein	US EPA 821/R-02/012	water (SSF)	N/A	[37]
<i>Daphnia magna</i>	mortality	48 h	A	LC50	8.06E-02	18	protein	US EPA 821/R-02/012	water (SSF)	N/A	[37]
<i>Daphnia magna</i>	mortality	24 h	A	LC50	1.42E-01	27	protein	US EPA 821/R-02/012	water (SSF)	N/A	[37]
<i>Daphnia magna</i>	mortality	48 h	A	LC50	7.53E-02	27	protein	US EPA 821/R-02/012	water (SSF)	N/A	[37]
<i>Daphnia magna</i>	mortality	24 h	A	LC50	1.33E-01	28	protein	US EPA 821/R-02/012	water (SSF)	N/A	[37]
<i>Daphnia magna</i>	mortality	48 h	A	LC50	6.88E-02	28	protein	US EPA 821/R-02/012	water (SSF)	N/A	[37]
<i>Daphnia magna</i>	mortality	24 h	A	LC50	1.27E-01	120	protein	US EPA 821/R-02/012	water (SSF)	N/A	[37]
<i>Daphnia magna</i>	mortality	48 h	A	LC50	6.20E-02	120	protein	US EPA 821/R-02/012	water (SSF)	N/A	[37]
<i>Daphnia magna</i>	mortality	48 h	A	LC50	5.00E-05	20-40	N/A	N/A	mineral (RHFV)	3.50E-06	[38]
<i>Daphnia magna</i>	feeding inhibition	24 h	A	EC50	1.36E-05	7.5	alkane	N/A	mineral (MHW) ASTM	2.03E-06	[39]

Species	Endpoint	Exposure Time (hours, days)	Acute/ Chronic (Based on USEtox)	Reported LC ₅₀ / EC ₅₀ / IC ₅₀	LC ₅₀ / EC ₅₀ / IC ₅₀ (kg Ag/m ³)	Avg Size (nm)	Coating	Method	Test Medium	LC ₅₀ / EC ₅₀ / IC ₅₀ for Ag ⁺ (kg Ag/m ³)	Ref.
<i>Daphnia magna</i>	lethality	24 h	A	EC50	1.14E-05	7.5	alkane	N/A	mineral (MHW) ASTM	1.36E-06	[39]
<i>Daphnia magna</i>	lethality	48 h	A	EC50	1.10E-05	7.5	alkane	N/A	mineral (MHW) ASTM	1.04E-06	[39]
<i>Daphnia magna</i>	immobilization	24 h	A	EC50	1.02E-05	7.5	alkane	OECD 202	mineral (MHW) ASTM	1.05E-06	[39]
<i>Daphnia magna</i>	reproduction	21 d	C	EC50	1.00E-06	7.5	alkane	OECD 211	mineral (MHW) ASTM	3.80E-07	[39]
<i>Daphnia magna</i>	immobilization	24 h	A	EC50	7.46E-06	7	citrate	OECD 202	mineral (OECD and ISO)	N/A	[40]
<i>Daphnia magna</i>	immobilization	48 h	A	EC50	2.43E-06	79.9	uncoated	OECD 202	mineral (OECD)	2.50E-07	[41]
<i>Daphnia galeata</i>	immobilization	48 h	A	EC50	2.16E-06	79.9	uncoated	OECD 202	mineral (OECD)	1.60E-07	[41]
<i>Bosmina longirostris</i>	immobilization	48 h	A	EC50	2.90E-06	79.9	uncoated	OECD 202	mineral (OECD)	2.20E-07	[41]
<i>Daphnia magna</i>	mortality	24 h	A	LC50	4.21E-04	30	PVP	US EPA	mineral (COMBO)	8.00E-07	[42]
<i>Daphnia magna</i>	mortality	24 h	A	LC50	1.55E-04	30	SiO ₂	US EPA	mineral (COMBO)	8.00E-07	[42]
<i>Daphnia magna</i>	mortality	24 h	A	LC50	2.61E-04	30	PVP	US EPA	mineral (MHW)	6.00E-07	[42]
<i>Daphnia magna</i>	mortality	24 h	A	LC50	3.60E-06	30	SiO ₂	US EPA	mineral (MHW)	6.00E-07	[42]

Species	Endpoint	Exposure Time (hours, days)	Acute/ Chronic (Based on USEtox)	Reported LC ₅₀ / EC ₅₀ / IC ₅₀	LC ₅₀ / EC ₅₀ / IC ₅₀ (kg Ag/m ³)	Avg Size (nm)	Coating	Method	Test Medium	LC ₅₀ / EC ₅₀ / IC ₅₀ for Ag ⁺ (kg Ag/m ³)	Ref.
<i>Daphnia magna</i>	mortality	24 h	A	LC50	2.34E-04	65	PVP	US EPA	mineral (COMBO)	8.00E-07	[42]
<i>Daphnia magna</i>	mortality	24 h	A	LC50	5.22E-04	65	SiO ₂	US EPA	mineral (COMBO)	8.00E-07	[42]
<i>Daphnia magna</i>	mortality	24 h	A	LC50	4.15E-04	65	PVP	US EPA	mineral (MHW)	6.00E-07	[42]
<i>Daphnia magna</i>	mortality	24 h	A	LC50	2.27E-04	65	SiO ₂	US EPA	mineral (MHW)	6.00E-07	[42]
<i>Daphnia magna</i>	immobilization	48 h	A	EC50	4.12E-06	26	citrate	OECD 202	mineral (RHFw)	2.47E-05	[43]
<i>Daphnia magna</i>	immobilization	48 h	A	EC50	1.26E-06	26	citrate	OECD 202	complex	2.40E-05	[43]
<i>Daphnia magna</i>	mortality	21 d	C	-	5.02E-05	35	citrate	OECD 211	mineral (RHFw)	2.47E-05	[43]
<i>Daphnia magna</i>	mortality	21 d	C	-	5.99E-05	35	citrate	OECD 211	complex	2.40E-05	[43]
<i>Daphnia magna</i>	immobilization	48 h	A	EC50	7.35E-07	68	citrate	OECD 202	mineral (RHFw)	2.47E-05	[43]
<i>Daphnia magna</i>	immobilization	48 h	A	EC50	2.14E-06	106	citrate	OECD 202	mineral (RHFw)	2.47E-05	[43]
<i>Daphnia magna</i>	immobilization	48 h	A	EC50	5.74E-06	144	uncoated	OECD 202	mineral (RHFw)	2.47E-05	[43]
<i>Daphnia magna</i>	immobilization	48 h	A	EC50	3.39E-06	144	uncoated	OECD 202	complex	2.40E-05	[43]
<i>Ceriodaphnia cornuta</i>	immobilization	24 h	A	EC50	5.00E-05	18.7-63.4	BLCFE	OECD 202	water (SSF)	2.20E-05	[44]
<i>Daphnia magna</i>	mortality	48 h	A	LC50	4.10E-07	10	BPEI	US EPA/600/8-87/011	mineral (MHW)	N/A	[45]
<i>Daphnia magna</i>	mortality	48 h	A	LC50	2.88E-06	56	citrate	US EPA/600/8-87/011	mineral (MHW)	N/A	[45]

Species	Endpoint	Exposure Time (hours, days)	Acute/ Chronic (Based on USEtox)	Reported LC ₅₀ / EC ₅₀ / IC ₅₀	LC ₅₀ / EC ₅₀ / IC ₅₀ (kg Ag/m ³)	Avg Size (nm)	Coating	Method	Test Medium	LC ₅₀ / EC ₅₀ / IC ₅₀ for Ag ⁺ (kg Ag/m ³)	Ref.
<i>Daphnia magna</i>	mortality	48 h	A	LC50	4.79E-06	72	PVP	US EPA/600/8-87/011	mineral (MHW)	N/A	[45]
<i>Daphnia magna</i>	immobilization	48 h	A	EC50	1.20E-05	5	citrate	OECD 202	mineral (M4)	N/A	[46]
<i>Daphnia magna</i>	immobilization and mortality	24 h	A	EC50	1.38E-05	18.2	citrate	OECD	water	5.40E-06	[47]
<i>Daphnia magna</i>	immobilization and mortality	48 h	A	EC50	1.24E-05	18.2	citrate	OECD	water	2.60E-06	[47]
<i>Ceriodaphnia cornuta</i>	mortality	24 h	A	LC50	7.94E-06	23	SA	US EPA 821/R-02/012	water (SSF)	3.20E-06	[48]
<i>Daphnia magna</i>	immobilization	48 h	A	EC50	4.10E-05	15	coated (proprietary)	OECD 202	mineral (OECD)	N/A	[49]
<i>Daphnia magna</i>	immobilization	4 d	A	EC50	3.10E-05	15	coated (proprietary)	OECD 202	mineral (OECD)	N/A	[49]
<i>Daphnia magna</i>	immobilization	48 h	A	EC50	1.21E-04	15	PVP	OECD 202	mineral (M4)	1.10E-06	[50]
<i>Daphnia magna</i>	mortality	21 d	C	-	9.20E-07	15	PVP	OECD 211	mineral (M4)	N/A	[50]
<i>Daphnia pulex</i>	immobilization	48 h	A	EC50	8.95E-06	15	PVP	OECD 202	mineral (M4)	6.80E-07	[50]
<i>Daphnia pulex</i>	mortality	21 d	C	-	2.25E-06	15	PVP	OECD 211	mineral (M4)	N/A	[50]
<i>Daphnia galeata</i>	immobilization	48 h	A	EC50	1.39E-05	15	PVP	OECD 202	mineral (M4)	2.13E-06	[50]
<i>Daphnia galeata</i>	mortality	21 d	C	-	3.45E-06	15	PVP	OECD 211	mineral (M4)	N/A	[50]
<i>Chydorus sphaericus</i>	immobilization	48 h	A	EC50	3.02E-05	35	uncoated	OECD 202	mineral (OECD)	4.31E-06	[51]
<i>Chydorus sphaericus</i>	immobilization	48 h	A	EC50	8.63E-06	15	coated (proprietary)	OECD 202	mineral (OECD)	4.31E-06	[51]

Species	Endpoint	Exposure Time (hours, days)	Acute/ Chronic (Based on USEtox)	Reported LC ₅₀ / EC ₅₀ / IC ₅₀	LC ₅₀ / EC ₅₀ / IC ₅₀ (kg Ag/m ³)	Avg Size (nm)	Coating	Method	Test Medium	LC ₅₀ / EC ₅₀ / IC ₅₀ for Ag ⁺ (kg Ag/m ³)	Ref.
<i>Chydorus sphaericus</i>	immobilization	48 h	A	EC50	1.29E-05	80	PVP	OECD 202	mineral (OECD)	4.31E-06	[51]
<i>Chydorus sphaericus</i>	immobilization	48 h	A	EC50	7.98E-04	200	PVP	OECD 202	complex	9.71E-06	[52]
<i>Daphnia similis</i>	survival	21 d	C	-	2.00E-08	20	PVP	OECD 211	water	N/A	[53]
<i>Daphnia similis</i>	mortality	48 h	A	LC50	1.59E-06	20	PVP	OECD 211	water	N/A	[53]
<i>Daphnia magna</i>	mortality	48 h	A	LC50	2.20E-04	70	PEG, Si, Ami-Si	N/A	mineral	N/A	[54]
<i>Daphnia similis</i>	baseline metabolite change	48 h	A	LC50	1.59E-06	20	N/A	OECD	mineral (RHFW)	N/A	[55]
<i>Daphnia similis</i>	baseline metabolite change	21 d	C	-	2.00E-08	20	N/A	OECD	mineral (RHFW)	N/A	[55]
<i>Daphnia magna</i>	mortality	48 h	A	LC50	>5.00E-04	20	carbonate	OECD 202	water (SSF)	2.51E-06	[56]
<i>Daphnia magna</i>	reproduction	21 d	C	-	5.00E-05	20	carbonate	OECD 211	water (SSF)	1.60E-06	[56]
<i>Daphnia magna</i>	mortality	48 h	A	LC50	2.87E-05	<100	lactate	OECD 202	mineral	8.80E-07	[57]
<i>Daphnia magna</i>	mortality	48 h	A	LC50	2.00E-06	10-20	PVP	OECD 202	mineral	8.80E-07	[57]
<i>Daphnia magna</i>	mortality	48 h	A	LC50	1.10E-06	10-20	SDBS	OECD 202	mineral	8.80E-07	[57]

Table C3. The LC₅₀/EC₅₀/IC₅₀ values collected from the literature for silver nanoparticles for freshwater algae (listed in alphabetical order based on references).

Species	Endpoint	Exposure Time (hours, days)	Acute/Chronic (Based on USEtox)	Reported LC ₅₀ /EC ₅₀ /IC ₅₀	LC ₅₀ /EC ₅₀ /IC ₅₀ (kg Ag/m ³)	Avg Size (nm)	Coating	Method	Test Medium	LC ₅₀ /EC ₅₀ /IC ₅₀ for Ag ⁺ (kg Ag/m ³)	Ref.
<i>Pseudokirchneriella subcapitata</i>	growth inhibition	72 h	C	IC50	3.67E-05	4.2	PVP	US EPA 600-4-91-002	complex	1.10E-06	[58]
<i>Pseudokirchneriella subcapitata</i>	growth inhibition	72 h	C	IC50	1.95E-05	5.9	PVP	US EPA 600-4-91-002	water (SSF)	1.10E-06	[58]
<i>Pseudokirchneriella subcapitata</i>	growth inhibition	72 h	C	IC50	3.00E-06	13.4	citrate	US EPA 600-4-91-002	mineral (SSF)	1.10E-06	[58]
<i>Pseudokirchneriella subcapitata</i>	growth inhibition	72 h	C	IC50	5.20E-06	14.7	citrate	US EPA 600-4-91-002	complex	1.10E-06	[58]
<i>Microcystis aeruginosa</i>	growth inhibition	10 d	C	EC50	7.50E-06	10-18	citrate	N/A	mineral (synthetic culture medium)	N/A	[59]
<i>Desmodesmus subspicatus</i>	growth inhibition	72 h	C	EC50	2.20E-03	20	N/A	ISO 8692	mineral (ISO)	4.20E-05	[10]
<i>Desmodesmus subspicatus</i>	growth inhibition	72 h	C	EC50	3.40E-05	23	N/A	ISO 8692	mineral (ISO)	4.20E-05	[10]
<i>Desmodesmus subspicatus</i>	growth inhibition	72 h	C	EC50	3.30E-04	27	N/A	ISO 8692	mineral (ISO)	4.20E-05	[10]
<i>Desmodesmus subspicatus</i>	growth inhibition	72 h	C	EC50	3.70E-03	200	N/A	ISO 8692	mineral (ISO)	4.20E-05	[10]
<i>Uronema confervicolum</i>	growth inhibition	48 h	A	EC50	5.00E-04	20	citrate	N/A	mineral (COMBO)	4.20E-06	[60]
<i>Uronema confervicolum</i>	growth inhibition	5 d	C	EC50	1.00E-03	20	citrate	N/A	mineral (COMBO)	3.36E-05	[60]
<i>Uronema confervicolum</i>	growth inhibition	14 d	C	EC50	1.00E-03	20	citrate	N/A	mineral (COMBO)	3.94E-04	[60]

Species	Endpoint	Exposure Time (hours, days)	Acute/Chronic (Based on USEtox)	Reported LC ₅₀ /EC ₅₀ /IC ₅₀	LC ₅₀ /EC ₅₀ /IC ₅₀ (kg Ag/m ³)	Avg Size (nm)	Coating	Method	Test Medium	LC ₅₀ /EC ₅₀ /IC ₅₀ for Ag ⁺ (kg Ag/m ³)	Ref.
<i>Pseudokirchneriella subcapitata</i>	growth inhibition	96 h	C	-	1.90E-04	26.6	metal oxide	US EPA 821/R-02/013	mineral (MHFW)	N/A	[11]
<i>Microcystis aeruginosa</i>	growth inhibition	72 h	C	EC50	6.56E-04	6.24	HA	N/A	mineral (OECD)	N/A	[61]
<i>Pseudokirchneriella subcapitata</i>	growth inhibition	72 h	C	EC50	4.80E-05	15	uncoated	OECD 201	mineral (OECD)	N/A	[17]
<i>Pseudokirchneriella subcapitata</i>	growth inhibition	72 h	C	EC50	2.17E-05	44	uncoated	OECD 201	mineral (OECD)	N/A	[17]
<i>Pseudokirchneriella subcapitata</i>	growth inhibition	72 h	C	EC50	2.37E-03	241	uncoated	OECD 201	mineral (OECD)	N/A	[17]
<i>Pseudokirchneriella subcapitata</i>	growth inhibition	72 h	C	EC50	1.80E-04	10	citrate	OECD 201	mineral (synthetic culture medium)	7.00E-06	[18]
<i>Pseudokirchneriella subcapitata</i>	growth inhibition	72 h	C	EC50	5.20E-04	20	citrate	OECD 201	mineral (synthetic culture medium)	7.00E-06	[18]
<i>Pseudokirchneriella subcapitata</i>	growth inhibition	72 h	C	EC50	8.20E-04	40	citrate	OECD 201	mineral (synthetic culture medium)	7.00E-06	[18]
<i>Pseudokirchneriella subcapitata</i>	growth inhibition	72 h	C	EC50	9.40E-04	60	citrate	OECD 201	mineral (synthetic culture medium)	7.00E-06	[18]
<i>Pseudokirchneriella subcapitata</i>	growth inhibition	72 h	C	EC50	1.14E-03	80	citrate	OECD 201	mineral (synthetic culture medium)	7.00E-06	[18]
<i>Pseudokirchneriella subcapitata</i>	growth inhibition	72 h	C	EC50	8.60E-06	20.4	PVP	OECD 201	mineral	7.10E-06	[19]

Species	Endpoint	Exposure Time (hours, days)	Acute/Chronic (Based on USEtox)	Reported LC ₅₀ /EC ₅₀ /IC ₅₀	LC ₅₀ /EC ₅₀ /IC ₅₀ (kg Ag/m ³)	Avg Size (nm)	Coating	Method	Test Medium	LC ₅₀ /EC ₅₀ /IC ₅₀ for Ag ⁺ (kg Ag/m ³)	Ref.
<i>Pseudokirchneriella subcapitata</i>	growth inhibition	24 h	A	EC50	5.77E-06	11	N/A	OECD 201	mineral (OECD)	4.19E-06	[62]
<i>Pseudokirchneriella subcapitata</i>	growth inhibition	48 h	A	EC50	9.67E-06	11	N/A	OECD 201	mineral (OECD)	3.36E-06	[62]
<i>Pseudokirchneriella subcapitata</i>	growth inhibition	72 h	C	EC50	9.74E-06	11	N/A	OECD 201	mineral (OECD)	7.09E-06	[62]
<i>Pseudokirchneriella subcapitata</i>	growth inhibition	24 h	A	EC50	1.28E-05	16	N/A	OECD 201	mineral (OECD)	4.19E-06	[62]
<i>Pseudokirchneriella subcapitata</i>	growth inhibition	48 h	A	EC50	2.95E-05	16	N/A	OECD 201	mineral (OECD)	3.36E-06	[62]
<i>Pseudokirchneriella subcapitata</i>	growth inhibition	72 h	C	EC50	2.42E-05	16	N/A	OECD 201	mineral (OECD)	7.09E-06	[62]
<i>Pseudokirchneriella subcapitata</i>	growth inhibition	72 h	C	EC50	6.17E-04	20	uncoated	OECD 201	mineral	1.61E-05	[24]
<i>Scenedesmus vacuolatus</i>	growth inhibition	24 h	A	EC50	1.40E-03	20	uncoated	N/A	mineral	8.40E-06	[24]
<i>Pseudokirchneriella subcapitata</i>	growth inhibition	72 h	C	EC50	1.63E-03	34	uncoated	OECD	mineral (OECD)	N/A	[63]
<i>Chlamydomonas reinhardtii</i>	growth inhibition	72 h	C	EC50	1.35E-02	56.6	PVP	OECD 201	mineral (TAP)	N/A	[25]
<i>Chlorococcum infusionum</i>	growth inhibition	72 h	C	EC50	6.80E-04	56.6	PVP	OECD 201	mineral (MHW)	N/A	[25]
<i>Chlamydomonas reinhardtii</i>	growth inhibition	72 h	C	-	2.15E-03	56.6	PVP	OECD 201	mineral (TAP)	N/A	[25]
<i>Chlorococcum infusionum</i>	growth inhibition	72 h	C	-	1.00E-04	56.6	PVP	OECD 201	mineral (MHW)	N/A	[25]
<i>Pseudokirchneriella subcapitata</i>	growth inhibition	48 h	A	EC50	5.40E-06	10	PEG	OECD	mineral (OECD)	3.15E-06	[64]
<i>Pseudokirchneriella subcapitata</i>	growth inhibition	48 h	A	EC50	2.31E-05	10	citrate	OECD	mineral (OECD)	3.15E-06	[64]
<i>Pseudokirchneriella subcapitata</i>	growth inhibition	48 h	A	EC50	2.29E-05	10	BPEI	OECD	mineral (OECD)	3.15E-06	[64]

Species	Endpoint	Exposure Time (hours, days)	Acute/Chronic (Based on USEtox)	Reported LC ₅₀ /EC ₅₀ /IC ₅₀	LC ₅₀ /EC ₅₀ /IC ₅₀ (kg Ag/m ³)	Avg Size (nm)	Coating	Method	Test Medium	LC ₅₀ /EC ₅₀ /IC ₅₀ for Ag ⁺ (kg Ag/m ³)	Ref.
<i>Pseudokirchneriella subcapitata</i>	growth inhibition	48 h	A	EC50	1.19E-05	30	PEG	OECD	mineral (OECD)	3.15E-06	[64]
<i>Pseudokirchneriella subcapitata</i>	growth inhibition	48 h	A	EC50	3.83E-05	30	citrate	OECD	mineral (OECD)	3.15E-06	[64]
<i>Pseudokirchneriella subcapitata</i>	growth inhibition	48 h	A	EC50	6.71E-05	30	BPEI	OECD	mineral (OECD)	3.15E-06	[64]
<i>Pseudokirchneriella subcapitata</i>	growth inhibition	48 h	A	EC50	6.65E-05	70	PEG	OECD	mineral (OECD)	3.15E-06	[64]
<i>Pseudokirchneriella subcapitata</i>	growth inhibition	48 h	A	EC50	1.18E-04	70	citrate	OECD	mineral (OECD)	3.15E-06	[64]
<i>Pseudokirchneriella subcapitata</i>	growth inhibition	48 h	A	EC50	3.07E-04	70	BPEI	OECD	mineral (OECD)	3.15E-06	[64]
<i>Pseudokirchneriella subcapitata</i>	growth inhibition	96 h	C	IC50	1.60E-03	25.4	uncoated	US EPA 821-R-02-013	complex (Prairie Creek Preserve)	N/A	[30]
<i>Pseudokirchneriella subcapitata</i>	growth inhibition	96 h	C	IC50	4.61E-06	25.4	uncoated	US EPA 821-R-02-013	mineral (synthetic culture medium)	N/A	[30]
<i>Pseudokirchneriella subcapitata</i>	growth inhibition	96 h	C	IC50	2.26E-05	25.4	uncoated	US EPA 821-R-02-013	complex (Ichetucknee River)	N/A	[30]
<i>Pseudokirchneriella subcapitata</i>	growth inhibition	72 h	C	EC50	5.36E-06	8.4	PVP	N/A	mineral (AAP)	2.52E-06	[31]
<i>Euglena gracilis</i>	photosynthetic yield	1 h	A	EC50	2.00E-04	20	citrate	OECD	complex	9.17E-06	[65]
<i>Euglena gracilis</i>	photosynthetic yield	2 h	A	EC50	1.60E-04	20	citrate	OECD	complex	9.60E-06	[65]
<i>Chlorococcum infusionum</i>	growth inhibition	72 h	C	EC50	1.00E-04	57	PVP	OECD 201	mineral (MHW)	N/A	[66]
<i>Chlamydomonas reinhardtii</i>	growth inhibition	1 h	A	EC50	3.60E-04	25	carbonate	N/A	mineral	2.00E-05	[67]

Species	Endpoint	Exposure Time (hours, days)	Acute/Chronic (Based on USEtox)	Reported LC ₅₀ /EC ₅₀ /IC ₅₀	LC ₅₀ /EC ₅₀ /IC ₅₀ (kg Ag/m ³)	Avg Size (nm)	Coating	Method	Test Medium	LC ₅₀ /EC ₅₀ /IC ₅₀ for Ag ⁺ (kg Ag/m ³)	Ref.
<i>Chlamydomonas reinhardtii</i>	growth inhibition	2 h	A	EC50	1.10E-04	25	carbonate	N/A	mineral	2.00E-05	[67]
<i>Chlamydomonas reinhardtii</i>	growth inhibition	3 h	A	EC50	9.50E-05	25	carbonate	N/A	mineral	N/A	[67]
<i>Chlamydomonas reinhardtii</i>	growth inhibition	5 h	A	EC50	8.90E-05	25	carbonate	N/A	mineral	N/A	[67]
<i>Chlamydomonas reinhardtii</i>	growth inhibition	4 h	A	EC50	8.60E-05	25	carbonate	N/A	mineral	N/A	[67]
<i>Chlamydomonas reinhardtii</i>	photosynthetic yield	1 h	A	EC50	5.66E-04	17	citrate	N/A	mineral (synthetic culture medium)	1.94E-05	[68]
<i>Chlamydomonas reinhardtii</i>	photosynthetic yield	1 h	A	EC50	3.51E-04	25	CHI	N/A	mineral (synthetic culture medium)	1.94E-05	[68]
<i>Chlamydomonas reinhardtii</i>	photosynthetic yield	1 h	A	EC50	2.18E-04	35	LAC	N/A	mineral (synthetic culture medium)	1.94E-05	[68]
<i>Chlamydomonas reinhardtii</i>	photosynthetic yield	1 h	A	EC50	3.15E-04	40	carbonate	N/A	mineral (synthetic culture medium)	1.94E-05	[68]
<i>Chlamydomonas reinhardtii</i>	photosynthetic yield	1 h	A	EC50	5.09E-04	42	GEL	N/A	mineral (synthetic culture medium)	1.94E-05	[68]
<i>Chlamydomonas reinhardtii</i>	photosynthetic yield	1 h	A	EC50	4.06E-04	45	SDBS	N/A	mineral (synthetic culture medium)	1.94E-05	[68]

Species	Endpoint	Exposure Time (hours, days)	Acute/ Chronic (Based on USEtox)	Reported LC ₅₀ / EC ₅₀ / IC ₅₀	LC ₅₀ / EC ₅₀ / IC ₅₀ (kg Ag/m ³)	Avg Size (nm)	Coating	Method	Test Medium	LC ₅₀ / EC ₅₀ / IC ₅₀ for Ag ⁺ (kg Ag/m ³)	Ref.
<i>Chlamydomonas reinhardtii</i>	photosynthetic yield	1 h	A	EC50	1.28E-04	70	PEG	N/A	mineral (synthetic culture medium)	1.94E-05	[68]
<i>Chlamydomonas reinhardtii</i>	photosynthetic yield	1 h	A	EC50	8.52E-05	84	PVP	N/A	mineral (synthetic culture medium)	1.94E-05	[68]
<i>Chlamydomonas reinhardtii</i>	photosynthetic yield	1 h	A	EC50	3.02E-05	456	DEX	N/A	mineral (synthetic culture medium)	1.94E-05	[68]
<i>Scenedesmus acuminatus</i>	growth inhibition	96 h	C	EC50	3.85E-05	9.8	N/A	OECD 202	mineral (COMBO)	N/A	[33]
<i>Scenedesmus sp. (Chlorophyceae)</i>	growth inhibition	72 h	C	EC50	8.99E-05	6-10	PVA	OECD 202	mineral (COMBO)	N/A	[33]
<i>Pseudokirchneriella subcapitata</i>	growth inhibition	24 h	A	EC50	3.24E-05	7.5	alkane	OECD 201	mineral (MHW) ASTM	3.38E-05	[39]
<i>Chlamydomonas reinhardtii</i>	photosynthetic yield	1 h	A	EC50	7.75E-04	10.67	protein (Vitelinato)	N/A	nanopure water	8.40E-05	[69]
<i>Chlamydomonas reinhardtii</i>	photosynthetic yield	2 h	A	EC50	7.88E-04	10.67	protein (Vitelinato)	N/A	nanopure water	8.03E-05	[69]
<i>Chlamydomonas reinhardtii</i>	photosynthetic yield	1 h	A	EC50	1.17E-02	12.93	protein (Colargol)	N/A	nanopure water	8.40E-05	[69]
<i>Chlamydomonas reinhardtii</i>	photosynthetic yield	2 h	A	EC50	1.00E-02	12.93	protein (Colargol)	N/A	nanopure water	8.03E-05	[69]

Species	Endpoint	Exposure Time (hours, days)	Acute/Chronic (Based on USEtox)	Reported LC ₅₀ /EC ₅₀ /IC ₅₀	LC ₅₀ /EC ₅₀ /IC ₅₀ (kg Ag/m ³)	Avg Size (nm)	Coating	Method	Test Medium	LC ₅₀ /EC ₅₀ /IC ₅₀ for Ag ⁺ (kg Ag/m ³)	Ref.
<i>Chlamydomonas reinhardtii</i>	photosynthetic yield	1 h	A	EC50	2.52E-02	17.96	protein (Proteinato)	N/A	nanopure water	8.40E-05	[69]
<i>Chlamydomonas reinhardtii</i>	photosynthetic yield	2 h	A	EC50	2.06E-02	17.96	protein (Proteinato)	N/A	nanopure water	8.03E-05	[69]
<i>Chlamydomonas reinhardtii</i>	growth inhibition	72 h	C	EC50	1.00E-05	16.7	N/A	OECD	mineral (AFW)	N/A	[70]
<i>Pseudokirchneriella subcapitata</i>	growth inhibition	72 h	C	EC50	7.40E-04	5	citrate	OECD 201	mineral (OECD)	N/A	[46]
<i>Pseudokirchneriella subcapitata</i>	growth inhibition	48 h	A	EC50	1.40E-04	15	uncoated	OECD	mineral (ISO)	4.90E-06	[71]
<i>Pseudokirchneriella subcapitata</i>	¹⁴ C assimilation	2 h	A	EC50	5.00E-05	15	uncoated	OECD	mineral (ISO)	6.00E-06	[71]
<i>Pseudokirchneriella subcapitata</i>	growth inhibition	48 h	A	EC50	3.10E-04	30	citrate	OECD	mineral (ISO)	4.90E-06	[71]
<i>Pseudokirchneriella subcapitata</i>	growth inhibition	48 h	A	EC50	7.50E-05	30	citrate	OECD	mineral (ISO)	4.90E-06	[71]
<i>Pseudokirchneriella subcapitata</i>	¹⁴ C assimilation	2 h	A	EC50	7.10E-04	30	citrate	OECD	mineral (ISO)	6.00E-06	[71]
<i>Pseudokirchneriella subcapitata</i>	¹⁴ C assimilation	2 h	A	EC50	1.50E-04	30	citrate	OECD	mineral (ISO)	6.00E-06	[71]
<i>Chlamydomonas reinhardtii</i>	growth inhibition	72 h	C	EC50	1.82E-03	50	PVP	OECD 201	mineral (MBL Woodshole medium)	4.30E-05	[72]
<i>Chlamydomonas reinhardtii</i>	growth inhibition	72 h	C	EC50	9.93E-04	3-8	alkane	OECD 201	mineral (MBL Woodshole medium)	4.30E-05	[72]

Species	Endpoint	Exposure Time (hours, days)	Acute/Chronic (Based on USEtox)	Reported LC ₅₀ /EC ₅₀ /IC ₅₀	LC ₅₀ /EC ₅₀ /IC ₅₀ (kg Ag/m ³)	Avg Size (nm)	Coating	Method	Test Medium	LC ₅₀ /EC ₅₀ /IC ₅₀ for Ag ⁺ (kg Ag/m ³)	Ref.
<i>Desmodesmus subspicatus</i>	growth inhibition	48 h	A	EC50	6.80E-05	15	coated (proprietary)	OECD 201	mineral (OECD)	N/A	[49]
<i>Pseudokirchneriella subcapitata</i>	immobilization	4.5 h	A	EC50	8.96E-04	15	coated (proprietary)	OECD 202	mineral (RHFV)	3.13E-05	[51]
<i>Pseudokirchneriella subcapitata</i>	immobilization	4.5 h	A	EC50	2.11E-02	35	uncoated	OECD 202	mineral (RHFV)	3.13E-05	[51]
<i>Pseudokirchneriella subcapitata</i>	immobilization	4.5 h	A	EC50	4.01E-03	80	PVP	OECD 202	mineral (RHFV)	3.13E-05	[51]
<i>Pseudokirchneriella subcapitata</i>	photosynthetic yield	4.5 h	A	EC50	2.99E-03	200	PVP	OECD 202	complex	1.62E-05	[52]
<i>Chlamydomonas reinhardtii</i>	mortality	48 h	A	LC50	6.05E-04	70	PEG, Si, Ami-Si	N/A	mineral	N/A	[54]
<i>Microcystis aeruginosa</i>	growth inhibition	96 h	C	EC50	1.08E-07	10	citrate	OECD	mineral (OECD)	N/A	[73]
<i>Microcystis aeruginosa</i>	growth inhibition	10 d	C	EC50	1.35E-04	10	citrate	OECD	mineral (OECD)	N/A	[73]
<i>Chlorella sp.</i>	growth inhibition	48 h	A	EC50	8.90E-04	84	N/A	OECD 201	mineral (OECD)	3.90E-04	[74]
<i>Euglena gracilis</i>	photosynthetic yield	24 h	A	EC50	1.85E-04	19.4	citrate	N/A	mineral	1.00E-05	[75]
<i>Microcystis aeruginosa</i>	growth inhibition	96 h	C	LC50	1.30E-04	23.4	PVP	N/A	mineral (HGZ-145)	N/A	[76]
<i>Chlorella vulgaris</i>	growth inhibition	72 h	C	EC50	7.00E-05	22.03	citrate	OECD 201	mineral (OECD)	N/A	[77]
<i>Chlorella vulgaris</i>	growth inhibition	72 h	C	EC50	5.00E-05	28.98	PEI	OECD 201	mineral (OECD)	N/A	[77]
<i>Chlorella pyrenoidosa</i>	growth inhibition	96 h	C	IC50	3.92E-05	19	citrate	OECD	mineral (OECD)	1.20E-05	[78]
<i>Chlorella pyrenoidosa</i>	growth inhibition	96 h	C	IC50	1.40E-04	22	PVP	OECD	mineral (OECD)	1.20E-05	[78]

Species	Endpoint	Exposure Time (hours, days)	Acute/Chronic (Based on USEtox)	Reported LC ₅₀ /EC ₅₀ /IC ₅₀	LC ₅₀ /EC ₅₀ /IC ₅₀ (kg Ag/m ³)	Avg Size (nm)	Coating	Method	Test Medium	LC ₅₀ /EC ₅₀ /IC ₅₀ for Ag ⁺ (kg Ag/m ³)	Ref.
<i>Scenedesmus quadricauda</i>	growth inhibition	96 h	C	EC50	2.00E-03	5	N/A	N/A	mineral (Knopp medium)	1.00E-03	[79]
<i>Chlorella vulgaris</i>	growth inhibition	96 h	C	EC50	1.00E-03	5	N/A	N/A	mineral (Knopp medium)	1.10E-03	[79]
<i>Scenedesmus quadricauda</i>	growth inhibition	96 h	C	EC50	5.10E-03	20	N/A	N/A	mineral (Knopp medium)	1.00E-03	[79]
<i>Chlorella vulgaris</i>	growth inhibition	96 h	C	EC50	2.00E-03	20	N/A	N/A	mineral (Knopp medium)	1.10E-03	[79]
<i>Scenedesmus quadricauda</i>	growth inhibition	96 h	C	EC50	4.00E-03	37	N/A	N/A	mineral (Knopp medium)	1.00E-03	[79]
<i>Chlorella vulgaris</i>	growth inhibition	96 h	C	EC50	5.00E-03	37	N/A	N/A	mineral (Knopp medium)	1.10E-03	[79]
<i>Scenedesmus quadricauda</i>	growth inhibition	96 h	C	EC50	8.00E-03	43	N/A	N/A	mineral (Knopp medium)	1.00E-03	[79]
<i>Chlorella vulgaris</i>	growth inhibition	96 h	C	EC50	2.30E-03	43	N/A	N/A	mineral (Knopp medium)	1.10E-03	[79]
<i>Scenedesmus quadricauda</i>	growth inhibition	96 h	C	EC50	7.60E-03	70	N/A	N/A	mineral (Knopp medium)	1.00E-03	[79]
<i>Chlorella vulgaris</i>	growth inhibition	96 h	C	EC50	4.50E-03	70	N/A	N/A	mineral (Knopp medium)	1.10E-03	[79]

Table C4. The LC₅₀/EC₅₀/IC₅₀ values collected from the literature for silver nanoparticles for freshwater fish (listed in alphabetical order based on references).

Species	Endpoint	Exposure Time (hours, days)	Acute/ Chronic (Based on USEtox)	Reported LC ₅₀ / EC ₅₀ / IC ₅₀	<i>In vivo/in vitro</i>	LC ₅₀ / EC ₅₀ / IC ₅₀ (kg Ag/m ³)	Avg Size (nm)	Coating	Method	Test Medium	LC ₅₀ / EC ₅₀ / IC ₅₀ for Ag ⁺ (kg Ag/m ³)	Ref.
<i>Oreochromis niloticus</i>	mortality	96 h	A	LC50	<i>in vivo</i>	1.95E-02	<100	PVP	US EPA	water	N/A	[80]
<i>Tilapia zillii</i>	mortality	96 h	A	LC50	<i>in vivo</i>	2.00E-02	<100	PVP	US EPA	water	N/A	[80]
<i>Oreochromis niloticus</i>	mortality	24 h	A	LC50	<i>in vivo</i>	2.65E-02	<100	PVP	US EPA	water	N/A	[80]
<i>Tilapia zillii</i>	mortality	24 h	A	LC50	<i>in vivo</i>	2.69E-02	<100	PVP	US EPA	water	N/A	[80]
<i>Oreochromis niloticus</i>	mortality	48 h	A	LC50	<i>in vivo</i>	2.40E-02	<100	PVP	US EPA	water	N/A	[80]
<i>Tilapia zillii</i>	mortality	48 h	A	LC50	<i>in vivo</i>	2.46E-02	<100	PVP	US EPA	water	N/A	[80]
<i>Danio rerio</i> (zebrafish)	inhibition of hatchability	48 h	A	EC50	<i>in vitro</i>	7.20E-05	21.5	PEG	OECD 236	mineral	3.40E-05	[81]
<i>Danio rerio</i> (zebrafish)	mortality	48 h	A	LC50	<i>in vivo</i>	3.06E-04	21.5	PEG	OECD 236	mineral	2.35E-04	[81]
<i>Acipenser persicus</i> (Persian sturgeon)	mortality	96 h	A	LC50	<i>in vivo</i>	8.90E-04	16.6	N/A	OECD 203	mineral (FW)	N/A	[82]
<i>Acipenser persicus</i> (Persian sturgeon)	mortality	96 h	A	LC50	<i>in vivo</i>	1.83E-03	16.6	N/A	OECD 203	mineral (brackish water)	N/A	[82]
<i>Poecilia reticulata</i> (Guppy fish)	mortality	24 h	A	LC50	<i>in vivo</i>	3.90E-03	9.4	N/A	N/A	mineral	3.90E-04	[3]
<i>Poeciliopsis lucida</i> (topminnow fish)	metabolic activity	24 h	A	EC50	<i>in vitro</i>	8.76E-03	20	uncoated	OECD	complex (culture)	1.37E-03	[83]
<i>Poeciliopsis lucida</i> (topminnow fish)	cell membrane integrity	24 h	A	EC50	<i>in vitro</i>	3.45E-02	20	uncoated	OECD	complex (culture)	8.80E-04	[83]
<i>Poeciliopsis lucida</i> (topminnow fish)	lysosomal functioning	24 h	A	EC50	<i>in vitro</i>	1.49E-02	20	uncoated	OECD	complex (culture)	6.50E-04	[83]
<i>Danio rerio</i> (zebrafish)	mortality	48 h	A	LC50	<i>in vivo</i>	8.40E-05	81	PVP	OECD	mineral (OECD)	2.50E-05	[84]
<i>Danio rerio</i> (zebrafish)	mortality	48 h	A	LC50	<i>in vivo</i>	8.90E-05	81	PVP	OECD	mineral (OECD)	2.80E-05	[84]

Species	Endpoint	Exposure Time (hours, days)	Acute/ Chronic (Based on USEtox)	Reported LC ₅₀ / EC ₅₀ / IC ₅₀	In vivo/in vitro	LC ₅₀ / EC ₅₀ / IC ₅₀ (kg Ag/m ³)	Avg Size (nm)	Coating	Method	Test Medium	LC ₅₀ / EC ₅₀ / IC ₅₀ for Ag ⁺ (kg Ag/m ³)	Ref.
<i>Poecilia reticulata</i> (Guppy fish)	mortality	24 h	A	LC50	in vivo	9.13E-03	76	N/A	N/A	water	N/A	[85]
<i>Danio rerio</i> (zebrafish)	mortality	96 h	A	LC50	in vivo	4.31E-03	30.7	maltose/gelatine	OECD 236	mineral (OECD)	5.84E-05	[86]
<i>Danio rerio</i> (zebrafish)	mortality	96 h	A	LC50	in vivo	1.00E-01	58.4	PVP	OECD 236	mineral (OECD)	5.84E-05	[86]
<i>Oryzias latipes</i> (Japanese medaka)	mortality	96 h	A	LC50	in vivo	3.46E-05	49.6	N/A	US EPA 712/C-96/118	water	3.65E-05	[87]
<i>Oryzias latipes</i> (Japanese medaka)	lethality	96 h	A	LC50	in vivo	8.40E-04	8.3	citrate	OECD 203	mineral (OECD)	N/A	[88]
<i>Oryzias latipes</i> (Japanese medaka)	lethality	96 h	A	LC50	in vivo	8.00E-04	8.3	citrate	OECD 203	mineral (OECD)	N/A	[88]
<i>Danio rerio</i> (zebrafish)	mortality and delayed hatching	24 h	A	LC50	in vitro	2.50E-01	5-20	N/A	N/A	water	N/A	[89]
<i>Oncorhynchus mykiss</i> (Rainbow trout)	liver cell line	24 h	A	IC50	in vitro	7.59E-02	20	uncoated	N/A	complex	1.10E-02	[90]
<i>Oncorhynchus mykiss</i> (Rainbow trout)	hepatoma cell line	24 h	A	IC50	in vitro	1.98E-02	20	uncoated	N/A	complex	1.10E-03	[90]
<i>Oncorhynchus mykiss</i> (Rainbow trout)	fibroblast-like gonadal cell line	24 h	A	IC50	in vitro	4.17E-02	20	uncoated	N/A	complex	2.80E-03	[90]
<i>Danio rerio</i> (zebrafish)	mortality and sublethal toxicity	24 h	A	LC50	in vivo	5.28E-03	42	N/A	OECD 203, 210, 212	mineral (FSEW)	N/A	[91]
<i>Danio rerio</i> (zebrafish)	mortality and sublethal toxicity	48 h	A	LC50	in vivo	6.62E-03	42	N/A	OECD 203, 210, 212	mineral (FSEW)	N/A	[91]
<i>Danio rerio</i> (zebrafish)	mortality and sublethal toxicity	24 h	A	LC50	in vivo	1.51E-02	46	citrate	OECD 203, 210, 212	mineral (FSEW)	N/A	[91]
<i>Danio rerio</i> (zebrafish)	mortality and sublethal toxicity	48 h	A	LC50	in vivo	1.84E-02	46	citrate	OECD 203, 210, 212	mineral (FSEW)	N/A	[91]

Species	Endpoint	Exposure Time (hours, days)	Acute/ Chronic (Based on USEtox)	Reported LC ₅₀ / EC ₅₀ / IC ₅₀	In vivo/in vitro	LC ₅₀ / EC ₅₀ / IC ₅₀ (kg Ag/m ³)	Avg Size (nm)	Coating	Method	Test Medium	LC ₅₀ / EC ₅₀ / IC ₅₀ for Ag ⁺ (kg Ag/m ³)	Ref.
<i>Danio rerio</i> (zebrafish)	mortality and sublethal toxicity	24 h	A	LC50	<i>in vivo</i>	5.74E-02	48	gelatin	OECD 203, 210, 212	mineral (FSEW)	N/A	[91]
<i>Danio rerio</i> (zebrafish)	mortality and sublethal toxicity	48 h	A	LC50	<i>in vivo</i>	4.35E-02	48	gelatin	OECD 203, 210, 212	mineral (FSEW)	N/A	[91]
<i>Danio rerio</i> (zebrafish)	mortality and sublethal toxicity	24 h	A	LC50	<i>in vivo</i>	4.64E-04	52	PVP	OECD 203, 210, 212	mineral (FSEW)	N/A	[91]
<i>Danio rerio</i> (zebrafish)	mortality and sublethal toxicity	48 h	A	LC50	<i>in vivo</i>	4.06E-04	52	PVP	OECD 203, 210, 212	mineral (FSEW)	N/A	[91]
<i>Danio rerio</i> (zebrafish)	mortality and sublethal toxicity	24 h	A	LC50	<i>in vivo</i>	6.16E-03	53	thiol	OECD 203, 210, 212	mineral (FSEW)	N/A	[91]
<i>Danio rerio</i> (zebrafish)	mortality and sublethal toxicity	48 h	A	LC50	<i>in vivo</i>	1.05E-02	53	thiol	OECD 203, 210, 212	mineral (FSEW)	N/A	[91]
<i>Danio rerio</i> (zebrafish)	mortality and sublethal toxicity	24 h	A	LC50	<i>in vivo</i>	3.46E-03	77	N/A	OECD 203, 210, 212	mineral (FSEW)	N/A	[91]
<i>Danio rerio</i> (zebrafish)	mortality and sublethal toxicity	48 h	A	LC50	<i>in vivo</i>	3.09E-03	77	N/A	OECD 203, 210, 212	mineral (FSEW)	N/A	[91]
<i>Danio rerio</i> (zebrafish)	mortality and sublethal toxicity	24 h	A	LC50	<i>in vivo</i>	8.45E-05	108	thiol	OECD 203, 210, 212	mineral (FSEW)	N/A	[91]
<i>Danio rerio</i> (zebrafish)	mortality and sublethal toxicity	48 h	A	LC50	<i>in vivo</i>	3.45E-05	108	thiol	OECD 203, 210, 212	mineral (FSEW)	N/A	[91]
<i>Danio rerio</i> (zebrafish)	mortality and sublethal toxicity	24 h	A	LC50	<i>in vivo</i>	6.92E-03	110	citrate	OECD 203, 210, 212	mineral (FSEW)	N/A	[91]
<i>Danio rerio</i> (zebrafish)	mortality and sublethal toxicity	48 h	A	LC50	<i>in vivo</i>	2.43E-03	110	citrate	OECD 203, 210, 212	mineral (FSEW)	N/A	[91]

Species	Endpoint	Exposure Time (hours, days)	Acute/ Chronic (Based on USEtox)	Reported LC ₅₀ / EC ₅₀ / IC ₅₀	In vivo/in vitro	LC ₅₀ / EC ₅₀ / IC ₅₀ (kg Ag/m ³)	Avg Size (nm)	Coating	Method	Test Medium	LC ₅₀ / EC ₅₀ / IC ₅₀ for Ag ⁺ (kg Ag/m ³)	Ref.
<i>Danio rerio</i> (zebrafish)	mortality and sublethal toxicity	24 h	A	LC50	in vivo	6.10E-05	140	PVP	OECD 203, 210, 212	mineral (FSEW)	N/A	[91]
<i>Danio rerio</i> (zebrafish)	mortality and sublethal toxicity	48 h	A	LC50	in vivo	2.28E-04	140	PVP	OECD 203, 210, 212	mineral (FSEW)	N/A	[91]
<i>Danio rerio</i> (zebrafish)	mortality and sublethal toxicity	24 h	A	LC50	in vivo	5.89E-03	155	gelatin	OECD 203, 210, 212	mineral (FSEW)	N/A	[91]
<i>Danio rerio</i> (zebrafish)	mortality and sublethal toxicity	48 h	A	LC50	in vivo	3.04E-03	155	gelatin	OECD 203, 210, 212	mineral (FSEW)	N/A	[91]
<i>Oryzias melastigma</i>	cell viability	48 h	A	EC50	in vitro	7.25E-06	46.6	PVP	N/A	complex (culture)	4.20E-05	[92]
<i>Oryzias melastigma</i>	cell viability	48 h	A	EC50	in vitro	9.24E-04	74.2	oleic acid	N/A	complex (culture)	4.20E-05	[92]
<i>Oncorhynchus mykiss</i> (Rainbow trout)	inhibition of metabolic activity	48 h	A	EC50	in vitro	2.60E-03	1-10	citrate	N/A	complex (culture)	1.10E-03	[93]
<i>Oncorhynchus mykiss</i> (Rainbow trout)	membrane stability	48 h	A	EC50	in vitro	3.50E-03	1-10	citrate	N/A	complex (culture)	1.39E-02	[93]
<i>Oncorhynchus mykiss</i> (Rainbow trout)	inhibition of metabolic activity	48 h	A	EC50	in vitro	2.50E-03	1-10	citrate	N/A	mineral (culture)	1.10E-03	[93]
<i>Oncorhynchus mykiss</i> (Rainbow trout)	membrane stability	48 h	A	EC50	in vitro	4.90E-03	1-10	citrate	N/A	mineral (culture)	1.39E-02	[93]
<i>Oreochromis mossambicus</i>	mortality	8 d	SC	LC50	in vitro	1.26E-02	60-80	citrate	N/A	water	N/A	[94]
<i>Danio rerio</i> (zebrafish)	mortality and/or immobilization	48 h	A	LC50	in vivo	7.07E-03	26.6	metal oxide	US EPA 821/R-02/013	mineral (MHFW)	2.22E-05	[11]
<i>Danio rerio</i> (zebrafish)	mortality and/or immobilization	48 h	A	LC50	in vivo	7.20E-03	26.6	metal oxide	US EPA 821/R-02/013	mineral (MHFW)	>1.00E-02	[11]
<i>Danio rerio</i> (zebrafish)	immobilization	96 h	A	EC50	in vivo	2.45E-05	21	PVP	OECD 236	complex (lake)	1.55E-05	[13]

Species	Endpoint	Exposure Time (hours, days)	Acute/ Chronic (Based on USEtox)	Reported LC ₅₀ / EC ₅₀ / IC ₅₀	In vivo/in vitro	LC ₅₀ / EC ₅₀ / IC ₅₀ (kg Ag/m ³)	Avg Size (nm)	Coating	Method	Test Medium	LC ₅₀ / EC ₅₀ / IC ₅₀ for Ag ⁺ (kg Ag/m ³)	Ref.
<i>Pimephales promelas</i>	mortality and growth inhibition	96 h	A	LC50	in vivo	8.94E-05	10	uncoated	US EPA 600/4-90/027F, US EPA 821/R-02/013	water	4.70E-06	[14]
<i>Danio rerio</i> (zebrafish)	not specified	72 h	A	EC50	in vivo	5.36E-04	15	uncoated	OECD 236	mineral (OECD)	N/A	[17]
<i>Danio rerio</i> (zebrafish)	not specified	72 h	A	EC50	in vivo	2.03E-04	44	uncoated	OECD 236	mineral (OECD)	N/A	[17]
<i>Danio rerio</i> (zebrafish)	not specified	72 h	A	EC50	in vivo	2.04E-02	241	uncoated	OECD 236	mineral (OECD)	N/A	[17]
<i>Hypophthalmichthys molitrix</i>	mortality	96 h	A	LC50	in vivo	6.64E-02	<100	N/A	N/A	water	N/A	[95]
<i>Carassius auratus</i> (Goldfish)	mortality	96 h	A	LC50	in vivo	8.39E-02	<100	N/A	N/A	water	N/A	[95]
<i>Hypophthalmichthys molitrix</i>	mortality	24 h	A	LC50	in vivo	1.13E-01	<100	N/A	N/A	water	N/A	[95]
<i>Carassius auratus</i> (Goldfish)	mortality	24 h	A	LC50	in vivo	1.44E-01	<100	N/A	N/A	water	N/A	[95]
<i>Hypophthalmichthys molitrix</i>	mortality	48 h	A	LC50	in vivo	1.01E-01	<100	N/A	N/A	water	N/A	[95]
<i>Carassius auratus</i> (Goldfish)	mortality	48 h	A	LC50	in vivo	1.44E-01	<100	N/A	N/A	water	N/A	[95]
<i>Hypophthalmichthys molitrix</i>	mortality	72 h	A	LC50	in vivo	8.70E-02	<100	N/A	N/A	water	N/A	[95]
<i>Carassius auratus</i> (Goldfish)	mortality	72 h	A	LC50	in vivo	1.01E-01	<100	N/A	N/A	water	N/A	[95]
<i>Danio rerio</i> (zebrafish)	mortality	24 h	A	LC50	in vivo	8.40E-05	20.4	PVP	OECD 236	mineral	4.50E-05	[19]
<i>Danio rerio</i> (zebrafish)	mortality	48 h	A	LC50	in vivo	6.60E-05	20.4	PVP	OECD 236	mineral	3.20E-05	[19]
<i>Poecilia reticulata</i> (Guppy fish)	mortality	48 h	A	LC50	in vivo	3.83E-02	8.2	N/A	OECD, US EPA	water (SSF)	1.82E-02	[19]
<i>Poecilia reticulata</i> (Guppy fish)	mortality	96 h	A	LC50	in vivo	3.45E-02	8.2	N/A	OECD, US EPA	water (SSF)	1.41E-02	[19]

Species	Endpoint	Exposure Time (hours, days)	Acute/ Chronic (Based on USEtox)	Reported LC ₅₀ / EC ₅₀ / IC ₅₀	In vivo/in vitro	LC ₅₀ / EC ₅₀ / IC ₅₀ (kg Ag/m ³)	Avg Size (nm)	Coating	Method	Test Medium	LC ₅₀ / EC ₅₀ / IC ₅₀ for Ag ⁺ (kg Ag/m ³)	Ref.
<i>Oncorhynchus mykiss</i> (Rainbow trout)	mortality	96 h	A	LC50	<i>in vivo</i>	2.50E-04	16.6	N/A	OECD 215	dechlorinated tap water	N/A	[96]
<i>Oncorhynchus mykiss</i> (Rainbow trout)	mortality	96 h	A	LC50	<i>in vivo</i>	7.10E-04	16.6	N/A	OECD 215	dechlorinated tap water	N/A	[96]
<i>Oncorhynchus mykiss</i> (Rainbow trout)	mortality	96 h	A	LC50	<i>in vivo</i>	2.16E-03	16.6	N/A	OECD 215	dechlorinated tap water	N/A	[96]
<i>Oncorhynchus mykiss</i> (Rainbow trout)	mortality	24 h	A	LC50	<i>in vivo</i>	2.75E-03	16.6	N/A	OECD 215	dechlorinated tap water	N/A	[96]
<i>Oncorhynchus mykiss</i> (Rainbow trout)	mortality	24 h	A	LC50	<i>in vivo</i>	1.09E-03	16.6	N/A	OECD 215	dechlorinated tap water	N/A	[96]
<i>Oncorhynchus mykiss</i> (Rainbow trout)	mortality	24 h	A	LC50	<i>in vivo</i>	3.76E-03	16.6	N/A	OECD 215	dechlorinated tap water	N/A	[96]
<i>Oncorhynchus mykiss</i> (Rainbow trout)	mortality	48 h	A	LC50	<i>in vivo</i>	4.40E-04	16.6	N/A	OECD 215	dechlorinated tap water	N/A	[96]
<i>Oncorhynchus mykiss</i> (Rainbow trout)	mortality	48 h	A	LC50	<i>in vivo</i>	1.02E-03	16.6	N/A	OECD 215	dechlorinated tap water	N/A	[96]
<i>Oncorhynchus mykiss</i> (Rainbow trout)	mortality	48 h	A	LC50	<i>in vivo</i>	3.13E-03	16.6	N/A	OECD 215	dechlorinated tap water	N/A	[96]
<i>Oncorhynchus mykiss</i> (Rainbow trout)	mortality	72 h	A	LC50	<i>in vivo</i>	3.50E-04	16.6	N/A	OECD 215	dechlorinated tap water	N/A	[96]
<i>Oncorhynchus mykiss</i> (Rainbow trout)	mortality	72 h	A	LC50	<i>in vivo</i>	9.60E-04	16.6	N/A	OECD 215	dechlorinated tap water	N/A	[96]
<i>Oncorhynchus mykiss</i> (Rainbow trout)	mortality	72 h	A	LC50	<i>in vivo</i>	2.39E-03	16.6	N/A	OECD 215	dechlorinated tap water	N/A	[96]

Species	Endpoint	Exposure Time (hours, days)	Acute/ Chronic (Based on USEtox)	Reported LC ₅₀ / EC ₅₀ / IC ₅₀	In vivo/in vitro	LC ₅₀ / EC ₅₀ / IC ₅₀ (kg Ag/m ³)	Avg Size (nm)	Coating	Method	Test Medium	LC ₅₀ / EC ₅₀ / IC ₅₀ for Ag ⁺ (kg Ag/m ³)	Ref.
<i>Oncorhynchus mykiss</i> (Rainbow trout)	mortality	24 h	A	LC50	in vivo	3.76E-03	196.1	N/A	OECD 215	dechlorinated tap water	N/A	[97]
<i>Oncorhynchus mykiss</i> (Rainbow trout)	mortality	48 h	A	LC50	in vivo	3.13E-03	196.1	N/A	OECD 215	dechlorinated tap water	N/A	[97]
<i>Oncorhynchus mykiss</i> (Rainbow trout)	mortality	72 h	A	LC50	in vivo	2.39E-03	196.1	N/A	OECD 215	dechlorinated tap water	N/A	[97]
<i>Oncorhynchus mykiss</i> (Rainbow trout)	mortality	96 h	A	LC50	in vivo	2.16E-03	196.1	N/A	OECD 215	dechlorinated tap water	N/A	[97]
<i>Oryzias latipes</i> (Japanese medaka)	mortality	96 h	A	LC50	in vivo	1.39E-03	3.6	N/A	N/A	water	N/A	[98]
<i>Danio rerio</i> (zebrafish)	mortality	24 h	A	LC50	in vivo	2.97E-02	83.58	uncoated	OECD	mineral (OECD)	N/A	[99]
<i>Danio rerio</i> (zebrafish)	mortality	48 h	A	LC50	in vivo	2.74E-02	83.58	uncoated	OECD	mineral (OECD)	N/A	[99]
<i>Danio rerio</i> (zebrafish)	mortality	72 h	A	LC50	in vivo	2.43E-02	83.58	uncoated	OECD	mineral (OECD)	N/A	[99]
<i>Danio rerio</i> (zebrafish)	mortality	96 h	A	LC50	in vivo	1.68E-02	83.58	uncoated	OECD	mineral (OECD)	N/A	[99]
<i>Pimephales promelas</i>	mortality	48 h	A	LC50	in vivo	4.10E-05	10	N/A	US EPA 812/R-02/013	mineral (MHRW)	6.26E-06	[22]
<i>Pimephales promelas</i>	mortality	48 h	A	LC50	in vivo	6.41E-05	20	N/A	US EPA 812/R-02/013	mineral (MHRW)	6.26E-06	[22]
<i>Pimephales promelas</i>	mortality	48 h	A	LC50	in vivo	1.92E-05	29	citrate	US EPA 812/R-02/013	mineral (MHRW)	6.26E-06	[22]
<i>Pimephales promelas</i>	mortality	48 h	A	LC50	in vivo	9.00E-06	31	N/A	US EPA 812/R-02/013	mineral (MHRW)	6.26E-06	[22]
<i>Pimephales promelas</i>	mortality	48 h	A	LC50	in vivo	5.52E-05	36	N/A	US EPA 812/R-02/013	mineral (MHRW)	6.26E-06	[22]

Species	Endpoint	Exposure Time (hours, days)	Acute/ Chronic (Based on USEtox)	Reported LC ₅₀ / EC ₅₀ / IC ₅₀	In vivo/in vitro	LC ₅₀ / EC ₅₀ / IC ₅₀ (kg Ag/m ³)	Avg Size (nm)	Coating	Method	Test Medium	LC ₅₀ / EC ₅₀ / IC ₅₀ for Ag ⁺ (kg Ag/m ³)	Ref.
<i>Pimephales promelas</i>	mortality	48 h	A	LC50	in vivo	>6.99E-05	41	PVP	US EPA 812/R-02/013	mineral (MHRW)	6.26E-06	[22]
<i>Pimephales promelas</i>	mortality	48 h	A	LC50	in vivo	6.07E-05	50	N/A	US EPA 812/R-02/013	mineral (MHRW)	6.26E-06	[22]
<i>Pimephales promelas</i>	mortality	48 h	A	LC50	in vivo	1.25E-04	80	N/A	US EPA 812/R-02/013	mineral (MHRW)	6.26E-06	[22]
<i>Cyprinus carpio (common carp)</i>	mortality	96 h	A	LC50	in vivo	2.90E-04	25	N/A	OECD 203	mineral (OECD)	1.50E-04	[100]
<i>Cyprinus carpio (common carp)</i>	mortality	24 h	A	LC50	in vivo	4.30E-04	25	N/A	OECD 203	mineral (OECD)	3.80E-04	[100]
<i>Cyprinus carpio (common carp)</i>	mortality	48 h	A	LC50	in vivo	3.10E-04	25	N/A	OECD 203	mineral (OECD)	2.10E-04	[100]
<i>Cyprinus carpio (common carp)</i>	mortality	72 h	A	LC50	in vivo	2.90E-04	25	N/A	OECD 203	mineral (OECD)	1.60E-04	[100]
<i>Oryzias latipes (Japanese medaka)</i>	mortality	96 h	A	LC50	in vivo	2.80E-05	60	uncoated	OECD 203	mineral (M4)	5.00E-07	[23]
<i>Oryzias latipes (Japanese medaka)</i>	mortality	96 h	A	LC50	in vivo	6.70E-05	300	uncoated	OECD 203	mineral (M4)	5.00E-07	[23]
<i>Danio rerio (zebrafish)</i>	abnormality	48 h	A	EC50	in vivo	1.11E+00	56.6	PVP	OECD 212	mineral (ERS w/out methylene blue)	N/A	[25]
<i>Oryzias latipes (Japanese medaka)</i>	abnormality	7 d	SC	EC50	in vivo	2.89E-03	56.6	PVP	OECD 236	mineral (ERS with methylene blue)	N/A	[25]
<i>Danio rerio (zebrafish)</i>	abnormality	7 d	SC	-	in vivo	3.98E-04	56.6	PVP	OECD 236	mineral (ERS w/out methylene blue)	N/A	[25]
<i>Oryzias latipes (Japanese medaka)</i>	abnormality	16 d	SC	-	in vivo	6.08E-04	56.6	PVP	OECD 236	mineral (ERS with methylene blue)	N/A	[25]

Species	Endpoint	Exposure Time (hours, days)	Acute/ Chronic (Based on USEtox)	Reported LC ₅₀ / EC ₅₀ / IC ₅₀	In vivo/in vitro	LC ₅₀ / EC ₅₀ / IC ₅₀ (kg Ag/m ³)	Avg Size (nm)	Coating	Method	Test Medium	LC ₅₀ / EC ₅₀ / IC ₅₀ for Ag ⁺ (kg Ag/m ³)	Ref.
<i>Pimephales promelas</i>	mortality	96 h	A	LC50	in vivo	9.40E-03	35	N/A	N/A	mineral	1.50E-05	[101]
<i>Pimephales promelas</i>	mortality	96 h	A	LC50	in vivo	1.06E-02	51-60	N/A	N/A	mineral	1.50E-05	[101]
<i>Rutilus kutum</i>	mortality	96 h	A	LC50	in vivo	2.80E-05	16.6	N/A	OECD 215	mineral (OECD)	N/A	[102]
<i>Oncorhynchus mykiss</i> (Rainbow trout)	metabolic activity	24 h	A	EC50	in vitro	1.25E-03	19	citrate	N/A	complex (Leibovitz)	1.40E-04	[103]
<i>Oncorhynchus mykiss</i> (Rainbow trout)	cell membrane integrity	24 h	A	EC50	in vitro	2.11E-03	19	citrate	N/A	complex (Leibovitz)	2.27E-04	[103]
<i>Oncorhynchus mykiss</i> (Rainbow trout)	lysosome membrane integrity	24 h	A	EC50	in vitro	4.85E-04	19	citrate	N/A	complex (Leibovitz)	3.02E-04	[103]
<i>Danio rerio</i> (zebrafish)	growth inhibition	48 h	A	EC50	in vivo	1.09E-03	20	N/A	OECD 203	mineral (OECD)	7.30E-05	[104]
<i>Danio rerio</i> (zebrafish)	growth inhibition	24 h	A	EC50	in vivo	1.13E-03	20	N/A	OECD 203	mineral (OECD)	9.00E-05	[104]
<i>Danio rerio</i> (zebrafish)	mortality	24 h	A	LC50	in vivo	1.79E-03	20	N/A	OECD 203	mineral (OECD)	1.20E-04	[104]
<i>Danio rerio</i> (zebrafish)	mortality	48 h	A	LC50	in vivo	1.26E-03	20	N/A	OECD 203	mineral (OECD)	1.00E-04	[104]
<i>Danio rerio</i> (zebrafish)	mortality	48 h	A	LC50	in vivo	6.24E-03	18	coated (proprietary)	N/A	mineral	N/A	[105]
<i>Danio rerio</i> (zebrafish)	mortality	48 h	A	LC50	in vivo	9.40E-04	18	coated (proprietary)	N/A	water	1.63E-04	[105]
<i>Danio rerio</i> (zebrafish)	mortality	5 d	A	LC50	in vivo	5.00E-05	5	PVP/PEI	OECD 236	mineral (OECD)	N/A	[106]
<i>Danio rerio</i> (zebrafish)	mortality	48 h	A	LC50	in vivo	5.70E-05	5	PVP/PEI	OECD 236	mineral (OECD)	N/A	[106]
<i>Acipenser baerii</i> (Siberian sturgeon)	mortality	96 h	A	LC50	in vivo	1.50E-02	8.02	PVP	N/A	water	N/A	[107]
<i>Labeo rohita</i>	mortality	96 h	A	LC50	in vivo	3.47E-03	27	PVP	OECD 203	mineral (OECD)	N/A	[108]
<i>Labeo rohita</i>	mortality	96 h	A	LC50	in vivo	2.33E-03	103	PVP	OECD 203	mineral (OECD)	N/A	[108]

Species	Endpoint	Exposure Time (hours, days)	Acute/ Chronic (Based on USEtox)	Reported LC ₅₀ / EC ₅₀ / IC ₅₀	In vivo/in vitro	LC ₅₀ / EC ₅₀ / IC ₅₀ (kg Ag/m ³)	Avg Size (nm)	Coating	Method	Test Medium	LC ₅₀ / EC ₅₀ / IC ₅₀ for Ag ⁺ (kg Ag/m ³)	Ref.
<i>Labeo rohita</i>	mortality	7 d	SC	LC50	in vivo	1.00E-04	96	citrate	N/A	water	N/A	[109]
<i>Danio rerio</i> (zebrafish)	mortality	96 h	A	LC50	in vivo	2.52E-02	<100	lamarin	OECD 203	mineral (OECD)	N/A	[110]
<i>Danio rerio</i> (zebrafish)	mortality	96 h	A	LC50	in vivo	1.99E-02	<100	PVP	OECD 203	mineral (OECD)	N/A	[110]
<i>Danio rerio</i> (zebrafish)	mortality	24 h	A	LC50	in vivo	1.28E-04	7.5	alkane	OECD	mineral (MHW) ASTM	7.83E-05	[39]
<i>Oncorhynchus mykiss</i> (Rainbow trout)	mortality	48 h	A	LC50	N/A	3.50E-03	N/A	N/A	N/A	water	N/A	[111]
<i>Oncorhynchus mykiss</i> (Rainbow trout)	mortality	72 h	A	LC50	N/A	3.00E-03	N/A	N/A	N/A	water	N/A	[111]
<i>Oncorhynchus mykiss</i> (Rainbow trout)	mortality	96 h	A	LC50	N/A	2.30E-03	N/A	N/A	N/A	water	N/A	[111]
<i>Hypophthalmichthys molitrix</i>	mortality	24 h	A	LC50	in vivo	8.10E-04	61	N/A	OECD	dechlorinated tap water	N/A	[112]
<i>Hypophthalmichthys molitrix</i>	mortality	48 h	A	LC50	in vivo	6.48E-04	61	N/A	OECD	dechlorinated tap water	N/A	[112]
<i>Hypophthalmichthys molitrix</i>	mortality	72 h	A	LC50	in vivo	3.83E-04	61	N/A	OECD	dechlorinated tap water	N/A	[112]
<i>Hypophthalmichthys molitrix</i>	mortality	96 h	A	LC50	in vivo	2.02E-04	61	N/A	OECD	dechlorinated tap water	N/A	[112]
<i>Danio rerio</i> (zebrafish)	mortality	6 d	A	LC50	in vivo	5.86E-05	15	uncoated	OECD 210	mineral (OECD)	5.00E-06	[113]
<i>Danio rerio</i> (zebrafish)	mortality	96 h	A	LC50	in vivo	1.37E-04	15	uncoated	OECD 210	mineral (OECD)	6.05E-06	[113]
<i>Labeo rohita</i>	mortality	96 h	A	LC50	in vivo	2.50E-05	50	N/A	N/A	water	N/A	[114]
<i>Oryzias latipes</i> (Japanese medaka)	mortality	96 h	A	LC50	in vivo	1.80E-03	5	citrate	OECD 203	mineral	N/A	[46]
<i>Oreochromis niloticus</i>	mortality	24 h	A	LC50	in vivo	5.30E-02	10-20	N/A	N/A	water	N/A	[115]
<i>Gibelion catla</i> (Catla)	mortality	96 h	A	LC50	in vivo	1.27E-02	50	N/A	OECD 203	mineral (OECD)	3.60E-03	[116]

Species	Endpoint	Exposure Time (hours, days)	Acute/ Chronic (Based on USEtox)	Reported LC ₅₀ / EC ₅₀ / IC ₅₀	In vivo/in vitro	LC ₅₀ / EC ₅₀ / IC ₅₀ (kg Ag/m ³)	Avg Size (nm)	Coating	Method	Test Medium	LC ₅₀ / EC ₅₀ / IC ₅₀ for Ag ⁺ (kg Ag/m ³)	Ref.
<i>Labeo rohita</i>	mortality	96 h	A	LC50	in vivo	1.23E-02	50	N/A	OECD 203	mineral (OECD)	4.01E-03	[116]
<i>Gibelion catla (Catla)</i>	heart cell line	24 h	A	EC50	in vitro	2.08E-02	50	N/A	OECD 203	complex (Leibovitz)	3.98E-03	[116]
<i>Gibelion catla (Catla)</i>	gill cell line	24 h	A	EC50	in vitro	1.86E-02	50	N/A	OECD 203	complex (Leibovitz)	3.71E-03	[116]
<i>Labeo rohita</i>	gill cell line	24 h	A	EC50	in vitro	2.15E-02	50	N/A	OECD 203	complex (Leibovitz)	4.01E-03	[116]
<i>Chapalichthys pardalis</i>	mortality	96 h	A	LC50	in vivo	1.03E-02	11.95	PVP	OECD 203	mineral (OECD)	N/A	[117]
<i>Danio rerio (zebrafish)</i>	mortality	48 h	A	EC50	in vivo	7.80E-04	15	coated (proprietary)	OECD	mineral (OECD)	N/A	[49]
<i>Danio rerio (zebrafish)</i>	teratogenic effect	96 h	A	EC50	in vitro	8.41E-05	15	coated (proprietary)	N/A	mineral (RHFw)	7.87E-05	[51]
<i>Danio rerio (zebrafish)</i>	teratogenic effect	96 h	A	EC50	in vitro	1.74E-04	35	uncoated	N/A	mineral (RHFw)	7.87E-05	[51]
<i>Danio rerio (zebrafish)</i>	teratogenic effect	96 h	A	EC50	in vitro	1.47E-04	80	PVP	N/A	mineral (RHFw)	7.87E-05	[51]
<i>Danio rerio (zebrafish)</i>	teratogenic effect	96 h	A	EC50	in vitro	1.88E-03	200	PVP	N/A	complex	4.31E-05	[51]
<i>Oryzias latipes (Japanese medaka)</i>	mortality	72 h	A	LC50	in vivo	1.12E-03	29.9	PVP	N/A	dechlorinated tap water	N/A	[118]
<i>Oryzias latipes (Japanese medaka)</i>	mortality	96 h	A	LC50	in vivo	8.70E-04	29.9	PVP	N/A	dechlorinated tap water	N/A	[118]
<i>Oryzias latipes (Japanese medaka)</i>	mortality	48 h	A	LC50	in vivo	1.38E-03	29.9	PVP	N/A	dechlorinated tap water	N/A	[118]
<i>Oryzias latipes (Japanese medaka)</i>	mortality	48 h	A	LC50	in vivo	1.03E-03	25	PVP	N/A	water	N/A	[119]
<i>Danio rerio (zebrafish)</i>	mortality	48 h	A	LC50	in vivo	4.34E-04	70	PEG, Si, Ami-Si	N/A	mineral	N/A	[54]
<i>Cyprinus carpio (common carp)</i>	mortality	24 h	A	LC50	in vivo	1.59E-03	11.5	PVP	OECD 203	mineral (OECD)	1.30E-04	[120]
<i>Cyprinus carpio (common carp)</i>	mortality	48 h	A	LC50	in vivo	1.55E-03	11.5	PVP	OECD 203	mineral (OECD)	1.10E-04	[120]
<i>Cyprinus carpio (common carp)</i>	mortality	72 h	A	LC50	in vivo	1.53E-03	11.5	PVP	OECD 203	mineral (OECD)	1.00E-04	[120]
<i>Cyprinus carpio (common carp)</i>	mortality	96 h	A	LC50	in vivo	1.53E-03	11.5	PVP	OECD 203	mineral (OECD)	1.00E-04	[120]

Species	Endpoint	Exposure Time (hours, days)	Acute/ Chronic (Based on USEtox)	Reported LC ₅₀ / EC ₅₀ / IC ₅₀	In vivo/in vitro	LC ₅₀ / EC ₅₀ / IC ₅₀ (kg Ag/m ³)	Avg Size (nm)	Coating	Method	Test Medium	LC ₅₀ / EC ₅₀ / IC ₅₀ for Ag ⁺ (kg Ag/m ³)	Ref.
<i>Danio rerio</i> (zebrafish)	mortality	96 h	A	LC50	<i>in vivo</i>	6.10E-03	10	citrate	N/A	mineral (AFW)	N/A	[121]
<i>Barbonymus gonionotus</i> (Silver barb)	mortality	48 h	A	LC50	<i>in vivo</i>	1.76E-03	84	N/A	OECD 203	mineral (OECD)	5.70E-05	[74]
<i>Oncorhynchus mykiss</i> (Rainbow trout)	metabolic activity	24 h	A	EC50	<i>in vitro</i>	1.37E-03	19.4	citrate	N/A	complex (Leibovitz)	8.63E-05	[122]
<i>Oncorhynchus mykiss</i> (Rainbow trout)	cell membrane integrity	24 h	A	EC50	<i>in vitro</i>	1.55E-03	19.4	citrate	N/A	complex (Leibovitz)	9.71E-05	[122]
<i>Oncorhynchus mykiss</i> (Rainbow trout)	lysosome membrane integrity	24 h	A	EC50	<i>in vitro</i>	1.06E-03	19.4	citrate	N/A	complex (Leibovitz)	6.47E-05	[122]
<i>Oncorhynchus mykiss</i> (Rainbow trout)	metabolic activity	24 h	A	EC50	<i>in vitro</i>	4.15E-02	19.4	citrate	N/A	mineral	5.25E-03	[75]

Table C5. The LC₅₀/EC₅₀/IC₅₀ values collected from the literature for silver nanoparticles for freshwater protozoa (listed in alphabetical order based on references).

Species	Endpoint	Exposure Time (hours, days)	Acute/Chronic (Based on USEtox)	Reported LC ₅₀ /EC ₅₀ /IC ₅₀	LC ₅₀ /EC ₅₀ /IC ₅₀ (kg Ag/m ³)	Avg Size (nm)	Coating	Test Medium	LC ₅₀ /EC ₅₀ /IC ₅₀ for Ag ⁺ (kg Ag/m ³)	Ref.
<i>Paramecium tetraurelia</i>	mortality	20 h	A	LC50	2.34E-03	20	N/A	complex (axenic broth culture)	7.30E-04	[123]
<i>Paramecium tetraurelia</i>	inhibition	20 h	A	EC50	2.59E-03	20	N/A	complex (axenic broth culture)	7.60E-04	[123]
<i>Tetrahymena sp.</i>	mortality	1 h	A	LC50	7.96E-07	35	PVP	deionized water	N/A	[124]
<i>Tetrahymena sp.</i>	mortality	1 h	A	LC50	1.00E-09	1-3	N/A	deionized water	N/A	[124]
<i>Tetrahymena thermophila</i>	ATP concentration	2 h	A	EC50	3.20E-03	20.4	PVP	mineral	2.90E-03	[19]
<i>Tetrahymena thermophila</i>	ATP concentration	24 h	A	EC50	3.90E-03	20.4	PVP	mineral	2.90E-03	[19]
<i>Paramecium</i>	mortality	1 h	A	LC50	1.55E-02	8.2	N/A	water (SSF)	1.12E-02	[20]
<i>Tetrahymena thermophila</i>	viability (ATP content)	2 h	A	EC50	2.86E-01	<100	uncoated	MilliQ water	1.80E-03	[125]
<i>Tetrahymena thermophila</i>	viability (ATP content)	24 h	A	EC50	2.05E-01	<100	uncoated	MilliQ water	1.50E-03	[125]
<i>Tetrahymena thermophila</i>	ATP concentration	2 h	A	EC50	8.50E-02	14.6	casein	MilliQ water	2.00E-03	[126]
<i>Tetrahymena thermophila</i>	ATP concentration	24 h	A	EC50	8.95E-02	14.6	casein	MilliQ water	2.70E-03	[126]
<i>Paramecium caudatum</i>	mortality	1 h	A	LC50	3.00E-02	40	uncoated	water	N/A	[127]
<i>Paramecium caudatum</i>	mortality	1 h	A	LC50	1.60E-02	40	N/A	water	N/A	[127]
<i>Paramecium caudatum</i>	mortality	1 h	A	LC50	3.80E-02	40	PEG	water	N/A	[127]
<i>Paramecium caudatum</i>	mortality	1 h	A	LC50	3.60E-02	40	PVP	water	N/A	[127]
<i>Tetrahymena pyriformis</i>	growth inhibition	24 h	A	EC50	1.46E-03	9	ATP	complex (axenic broth culture)	N/A	[128]

References-Appendix C

1. Allen HJ, Impellitteri CA, Macke DA, Heckman JL, Poynton HC, Lazorchak JM, Govindaswamy S, Roose DL, Nadagouda MN (2010) Effects from filtration, capping agents, and presence/absence of food on the toxicity of silver nanoparticles to *Daphnia magna*. *Environmental Toxicology and Chemistry*, 29(12):2742–2750. <https://doi.org/10.1002/etc.329>
2. Asghari S, Johari SA, Lee JH, Kim YS, Jeon YB, Choi HJ, Moon MC, Yu IJ (2012) Toxicity of various silver nanoparticles compared to silver ions in *Daphnia magna*. *Journal of Nanobiotechnology*, 10(1):14. <https://doi.org/10.1186/1477-3155-10-14>
3. Banumathi B, Vaseeharan B, Suganya P, Citarasu T, Govindarajan M, Alharbi NS, Kadaikunnan S, Khaled JM, Benelli G (2017) Toxicity of Camellia sinensis-Fabricated Silver Nanoparticles on Invertebrate and Vertebrate Organisms: Morphological Abnormalities and DNA Damages. *Journal of Cluster Science*, 28(4):2027–2040. <https://doi.org/10.1007/s10876-017-1201-5>
4. Blinova I, Niskanen J, Kajankari P, Kanarbik L, Käkinen A, Tenhu H, Penttinen O-P, Kahru A (2013) Toxicity of two types of silver nanoparticles to aquatic crustaceans *Daphnia magna* and *Thamnocephalus platyurus*. *Environmental Science and Pollution Research*, 20(5):3456–3463. <https://doi.org/10.1007/s11356-012-1290-5>
5. Borase HP, Patil SV, Singhal RS (2019) *Moina macrocopa* as a non-target aquatic organism for assessment of ecotoxicity of silver nanoparticles: Effect of size. *Chemosphere*, 219:713–723. <https://doi.org/10.1016/j.chemosphere.2018.12.031>
6. Conine AL, Frost PC (2017) Variable toxicity of silver nanoparticles to *Daphnia magna*: effects of algal particles and animal nutrition. *Ecotoxicology*, 26(1):118–126. <https://doi.org/10.1007/s10646-016-1747-2>
7. Das P, Xenopoulos MA, Metcalfe CD (2013) Toxicity of Silver and Titanium Dioxide Nanoparticle Suspensions to the Aquatic Invertebrate, *Daphnia magna*. *Bulletin of Environmental Contamination and Toxicology*, 91(1):76–82. <https://doi.org/10.1007/s00128-013-1015-6>
8. Gaiser BK, Biswas A, Rosenkranz P, Jepson MA, Lead JR, Stone V, Tyler CR, Fernandes TF (2011) Effects of silver and cerium dioxide micro- and nano-sized particles on *Daphnia magna*. *Journal of Environmental Monitoring*, 13(5):1227. <https://doi.org/10.1039/c1em10060b>
9. Gao J, Youn S, Hovsepian A, Llana VL, Wang Y, Bitton G, Bonzongo J-CJ (2009) Dispersion and Toxicity of Selected Manufactured Nanomaterials in Natural River Water Samples: Effects of Water Chemical Composition. *Environmental Science & Technology*, 43(9):3322–3328. <https://doi.org/10.1021/es803315v>
10. Georgantzopoulou A, Balachandran YL, Rosenkranz P, Dusinska M, Lankoff A, Wojewodzka M, Kruszewski M, Guignard C, Audinot J-N, Giriya S, Hoffmann L, Gutleb AC (2012) Ag nanoparticles: size- and surface-dependent effects on model aquatic organisms and

uptake evaluation with NanoSIMS. *Nanotoxicology*, 7(7):1168–1178.
<https://doi.org/10.3109/17435390.2012.715312>

11. Griffitt RJ, Luo J, Gao J, Bonzongo J-C, Barber DS (2008) Effects of particle composition and species on toxicity of metallic nanomaterials in aquatic organisms. *Environmental Toxicology and Chemistry*, 27(9):1972–1978. <https://doi.org/10.1897/08-002.1>
12. Harmon AR, Kennedy AJ, Poda AR, Bednar AJ, Chappell MA, Steevens JA (2014) Determination of nanosilver dissolution kinetics and toxicity in an environmentally relevant aqueous medium: Nanosilver stability and toxicity. *Environmental Toxicology and Chemistry*, 33(8):1783–1791. <https://doi.org/10.1002/etc.2616>
13. Heinlaan M, Muna M, Knöbel M, Kistler D, Odzak N, Kühnel D, Müller J, Gupta GS, Kumar A, Shanker R, Sigg L (2016) Natural water as the test medium for Ag and CuO nanoparticle hazard evaluation: An interlaboratory case study. *Environmental Pollution*, 216:689–699. <https://doi.org/10.1016/j.envpol.2016.06.033>
14. Hoheisel SM, Diamond S, Mount D (2012) Comparison of nanosilver and ionic silver toxicity in *Daphnia magna* and *Pimephales promelas*. *Environmental Toxicology and Chemistry*, 31(11):2557–2563. <https://doi.org/10.1002/etc.1978>
15. Hou J, Zhou Y, Wang C, Li S, Wang X (2017) Toxic Effects and Molecular Mechanism of Different Types of Silver Nanoparticles to the Aquatic Crustacean *Daphnia magna*. *Environmental Science & Technology*, 51(21):12868–12878.
<https://doi.org/10.1021/acs.est.7b03918>
16. Hu Y, Chen X, Yang K, Lin D (2018) Distinct toxicity of silver nanoparticles and silver nitrate to *Daphnia magna* in M4 medium and surface water. *Science of The Total Environment*, 618:838–846. <https://doi.org/10.1016/j.scitotenv.2017.08.222>
17. Hund-Rinke K, Schlich K, Kühnel D, Hellack B, Kaminski H, Nickel C (2018) Grouping concept for metal and metal oxide nanomaterials with regard to their ecotoxicological effects on algae, daphnids and fish embryos. *NanoImpact*, 9:52–60.
<https://doi.org/10.1016/j.impact.2017.10.003>
18. Ivask A, Kurvet I, Kasemets K, Blinova I, Aruoja V, Suppi S, Vija H, Käkinen A, Titma T, Heinlaan M, Visnapuu M, Koller D, Kisand V, Kahru A (2014) Size-Dependent Toxicity of Silver Nanoparticles to Bacteria, Yeast, Algae, Crustaceans and Mammalian Cells In Vitro. *PLoS ONE*, 9(7):e102108. <https://doi.org/10.1371/journal.pone.0102108>
19. Jemec A, Kahru A, Potthoff A, Drobne D, Heinlaan M, Böhme S, Geppert M, Novak S, Schirmer K, Rekulapally R, Singh S, Aruoja V, Sihtmäe M, Juganson K, Käkinen A, Kühnel D (2016) An interlaboratory comparison of nanosilver characterisation and hazard identification: Harmonising techniques for high quality data. *Environment International*, 87:20–32.
<https://doi.org/10.1016/j.envint.2015.10.014>
20. Jenifer AA, Malaikozhundan B, Vijayakumar S, Anjugam M, Iswarya A, Vaseeharan B (2019) Green Synthesis and Characterization of Silver Nanoparticles (AgNPs) Using Leaf

Extract of *Solanum nigrum* and Assessment of Toxicity in Vertebrate and Invertebrate Aquatic Animals. *Journal of Cluster Science*, <https://doi.org/10.1007/s10876-019-01704-7>

21. Jo HJ, Choi JW, Lee SH, Hong SW (2012) Acute toxicity of Ag and CuO nanoparticle suspensions against *Daphnia magna*: The importance of their dissolved fraction varying with preparation methods. *Journal of Hazardous Materials*, 227–228:301–308. <https://doi.org/10.1016/j.jhazmat.2012.05.066>
22. Kennedy AJ, Hull MS, Bednar AJ, Goss JD, Gunter JC, Bouldin JL, Vikesland PJ, Steevens JA (2010) Fractionating Nanosilver: Importance for Determining Toxicity to Aquatic Test Organisms. *Environmental Science & Technology*, 44(24):9571–9577. <https://doi.org/10.1021/es1025382>
23. Kim J, Kim S, Lee S (2011) Differentiation of the toxicities of silver nanoparticles and silver ions to the Japanese medaka (*Oryzias latipes*) and the cladoceran *Daphnia magna*. *Nanotoxicology*, 5(2):208–214. <https://doi.org/10.3109/17435390.2010.508137>
24. Köser J, Engelke M, Hoppe M, Nogowski A, Filser J, Thöming J (2017) Predictability of silver nanoparticle speciation and toxicity in ecotoxicological media. *Environmental Science: Nano*, 4(7):1470–1483. <https://doi.org/10.1039/C7EN00026J>
25. Kwak JI, Cui R, Nam S-H, Kim SW, Chae Y, An Y-J (2016) Multispecies toxicity test for silver nanoparticles to derive hazardous concentration based on species sensitivity distribution for the protection of aquatic ecosystems. *Nanotoxicology*, 10(5):521–530. <https://doi.org/10.3109/17435390.2015.1090028>
26. Lee Y-J, Kim J, Oh J, Bae S, Lee S, Hong IS, Kim S-H (2012) Ion-release kinetics and ecotoxicity effects of silver nanoparticles: Ecotoxicity effects of silver nanoparticles. *Environmental Toxicology and Chemistry*, 31(1):155–159. <https://doi.org/10.1002/etc.717>
27. Lekamge S, Miranda AF, Ball AS, Shukla R, Nugegoda D (2019) The toxicity of coated silver nanoparticles to *Daphnia carinata* and trophic transfer from alga *Raphidocelis subcapitata*. *PLOS ONE*, 14(4):e0214398. <https://doi.org/10.1371/journal.pone.0214398>
28. Li T, Albee B, Alemayehu M, Diaz R, Ingham L, Kamal S, Rodriguez M, Bishnoi SW (2010) Comparative toxicity study of Ag, Au, and Ag-Au bimetallic nanoparticles on *Daphnia magna*. *Analytical and Bioanalytical Chemistry*, 398(2):689–700. <https://doi.org/10.1007/s00216-010-3915-1>
29. Mackevica A, Skjolding LM, Gergs A, Palmqvist A, Baun A (2015) Chronic toxicity of silver nanoparticles to *Daphnia magna* under different feeding conditions. *Aquatic Toxicology*, 161:10–16. <https://doi.org/10.1016/j.aquatox.2015.01.023>
30. McLaughlin J, Bonzongo J-CJ (2012) Effects of natural water chemistry on nanosilver behavior and toxicity to *Ceriodaphnia dubia* and *Pseudokirchneriella subcapitata*: nAg-natural water suspensions: Behavior and toxicity. *Environmental Toxicology and Chemistry*, 31(1):168–175. <https://doi.org/10.1002/etc.720>

31. Mertens J, Oorts K, Leverett D, Arijs K (2019) Effects of silver nitrate are a conservative estimate for the effects of silver nanoparticles on algae growth and *Daphnia magna* reproduction. *Environmental Toxicology and Chemistry*, :etc.4463. <https://doi.org/10.1002/etc.4463>
32. Park S-Y, Choi J-H (2010) Geno- and Ecotoxicity Evaluation of Silver Nanoparticles in Freshwater Crustacean *Daphnia magna*. *Environmental Engineering Research*, 15(1):23–27. <https://doi.org/10.4491/eer.2010.15.1.428>
33. Pham T-L (2019) Toxicity of Silver Nanoparticles to Tropical Microalgae *Scenedesmus acuminatus*, *Chaetoceros gracilis* and Crustacean *Daphnia lumholtzi*. *Turkish Journal of Fisheries and Aquatic Sciences*, 19(12):1009–1016. https://doi.org/10.4194/1303-2712-v19_12_03
34. Pokhrel LR, Dubey B, Scheuerman PR (2013) Impacts of Select Organic Ligands on the Colloidal Stability, Dissolution Dynamics, and Toxicity of Silver Nanoparticles. *Environmental Science & Technology*, 47(22):12877–12885. <https://doi.org/10.1021/es403462j>
35. Poynton HC, Lazorchak JM, Impellitteri CA, Blalock BJ, Rogers K, Allen HJ, Loguinov A, Heckman JL, Govindasmaw S (2012) Toxicogenomic Responses of Nanotoxicity in *Daphnia magna* Exposed to Silver Nitrate and Coated Silver Nanoparticles. *Environmental Science & Technology*, 46(11):6288–6296. <https://doi.org/10.1021/es3001618>
36. Rainville L-C, Carolan D, Varela AC, Doyle H, Sheehan D (2014) Proteomic evaluation of citrate-coated silver nanoparticles toxicity in *Daphnia magna*. *The Analyst*, 139(7):1678–1686. <https://doi.org/10.1039/C3AN02160B>
37. Usha Rani P, Rajasekharreddy P (2011) Green synthesis of silver-protein (core–shell) nanoparticles using Piper betle L. leaf extract and its ecotoxicological studies on *Daphnia magna*. *Colloids and Surfaces A: Physicochemical and Engineering Aspects*, 389(1–3):188–194. <https://doi.org/10.1016/j.colsurfa.2011.08.028>
38. Resano M, Lapeña AC, Belarra MA (2013) Potential of solid sampling high-resolution continuum source graphite furnace atomic absorption spectrometry to monitor the Ag body burden in individual *Daphnia magna* specimens exposed to Ag nanoparticles. *Analytical Methods*, 5(5):1130. <https://doi.org/10.1039/c2ay26456k>
39. Ribeiro F, Gallego-Urrea JA, Jurkschat K, Crossley A, Hassellöv M, Taylor C, Soares AMVM, Loureiro S (2014) Silver nanoparticles and silver nitrate induce high toxicity to *Pseudokirchneriella subcapitata*, *Daphnia magna* and *Danio rerio*. *Science of The Total Environment*, 466–467:232–241. <https://doi.org/10.1016/j.scitotenv.2013.06.101>
40. Römer I, Gavin AJ, White TA, Merrifield RC, Chipman JK, Viant MR, Lead JR (2013) The critical importance of defined media conditions in *Daphnia magna* nanotoxicity studies. *Toxicology Letters*, 223(1):103–108. <https://doi.org/10.1016/j.toxlet.2013.08.026>
41. Sakamoto M, Ha J-Y, Yoneshima S, Kataoka C, Tatsuta H, Kashiwada S (2015) Free Silver Ion as the Main Cause of Acute and Chronic Toxicity of Silver Nanoparticles to Cladocerans.

Archives of Environmental Contamination and Toxicology, 68(3):500–509.

<https://doi.org/10.1007/s00244-014-0091-x>

42. Scanlan LD, Reed RB, Loguinov AV, Antczak P, Tagmount A, Aloni S, Nowinski DT, Luong P, Tran C, Karunaratne N, Pham D, Lin XX, Falciani F, Higgins CP, Ranville JF, Vulpe CD, Gilbert B (2013) Silver Nanowire Exposure Results in Internalization and Toxicity to *Daphnia magna*. *ACS Nano*, 7(12):10681–10694. <https://doi.org/10.1021/nm4034103>

43. Seitz F, Rosenfeldt RR, Storm K, Metreveli G, Schaumann GE, Schulz R, Bundschuh M (2015) Effects of silver nanoparticle properties, media pH and dissolved organic matter on toxicity to *Daphnia magna*. *Ecotoxicology and Environmental Safety*, 111:263–270. <https://doi.org/10.1016/j.ecoenv.2014.09.031>

44. Shanthi S, David Jayaseelan B, Velusamy P, Vijayakumar S, Chih CT, Vaseeharan B (2016) Biosynthesis of silver nanoparticles using a probiotic *Bacillus licheniformis* Dabh1 and their antibiofilm activity and toxicity effects in *Ceriodaphnia cornuta*. *Microbial Pathogenesis*, 93:70–77. <https://doi.org/10.1016/j.micpath.2016.01.014>

45. Silva T, Pokhrel LR, Dubey B, Tolaymat TM, Maier KJ, Liu X (2014) Particle size, surface charge and concentration dependent ecotoxicity of three organo-coated silver nanoparticles: Comparison between general linear model-predicted and observed toxicity. *Science of The Total Environment*, 468–469:968–976. <https://doi.org/10.1016/j.scitotenv.2013.09.006>

46. Sohn EK, Johari SA, Kim TG, Kim JK, Kim E, Lee JH, Chung YS, Yu IJ (2015) Aquatic Toxicity Comparison of Silver Nanoparticles and Silver Nanowires. *BioMed Research International*, 2015:1–12. <https://doi.org/10.1155/2015/893049>

47. Ulm L, Krivohlavek A, Jurašin D, Ljubojević M, Šinko G, Crnković T, Žuntar I, Šikić S, Vinković Vrček I (2015) Response of biochemical biomarkers in the aquatic crustacean *Daphnia magna* exposed to silver nanoparticles. *Environmental Science and Pollution Research*, 22(24):19990–19999. <https://doi.org/10.1007/s11356-015-5201-4>

48. Vijayakumar S, Malaikozhundan B, Ramasamy P, Vaseeharan B (2016) Assessment of biopolymer stabilized silver nanoparticle for their ecotoxicity on *Ceriodaphnia cornuta* and antibiofilm activity. *Journal of Environmental Chemical Engineering*, 4(2):2076–2083. <https://doi.org/10.1016/j.jece.2016.03.036>

49. Voelker D, Schlich K, Hohndorf L, Koch W, Kuehnen U, Polleichtner C, Kussatz C, Hund-Rinke K (2015) Approach on environmental risk assessment of nanosilver released from textiles. *Environmental Research*, 140:661–672. <https://doi.org/10.1016/j.envres.2015.05.011>

50. Völker C, Boedicker C, Daubenthaler J, Oetken M, Oehlmann J (2013) Comparative Toxicity Assessment of Nanosilver on Three *Daphnia* Species in Acute, Chronic and Multi-Generation Experiments. *PLoS ONE*, 8(10):e75026. <https://doi.org/10.1371/journal.pone.0075026>

51. Wang Z, Chen J, Li X, Shao J, Peijnenburg WJGM (2012) Aquatic toxicity of nanosilver colloids to different trophic organisms: Contributions of particles and free silver ion. *Environmental Toxicology and Chemistry*, 31(10):2408–2413. <https://doi.org/10.1002/etc.1964>
52. Wang Z, Quik JTK, Song L, Van Den Brandhof E-J, Wouterse M, Peijnenburg WJGM (2015) Humic substances alleviate the aquatic toxicity of polyvinylpyrrolidone-coated silver nanoparticles to organisms of different trophic levels: Humic substances alleviate the aquatic toxicity of PVP-AgNPs. *Environmental Toxicology and Chemistry*, 34(6):1239–1245. <https://doi.org/10.1002/etc.2936>
53. Wang P, Ng QX, Zhang H, Zhang B, Ong CN, He Y (2018) Metabolite changes behind faster growth and less reproduction of *Daphnia similis* exposed to low-dose silver nanoparticles. *Ecotoxicology and Environmental Safety*, 163:266–273. <https://doi.org/10.1016/j.ecoenv.2018.07.080>
54. Wu F, Harper BJ, Harper SL (2017) Differential dissolution and toxicity of surface functionalized silver nanoparticles in small-scale microcosms: impacts of community complexity. *Environmental Science: Nano*, 4(2):359–372. <https://doi.org/10.1039/C6EN00324A>
55. Zhang B, Zhang H, Du C, Ng QX, Hu C, He Y, Ong CN (2017) Metabolic responses of the growing *Daphnia similis* to chronic AgNPs exposure as revealed by GC-Q-TOF/MS and LC-Q-TOF/MS. *Water Research*, 114:135–143. <https://doi.org/10.1016/j.watres.2017.02.046>
56. Zhao C-M, Wang W-X (2011) Comparison of acute and chronic toxicity of silver nanoparticles and silver nitrate to *Daphnia magna*. *Environmental Toxicology and Chemistry*, 30(4):885–892. <https://doi.org/10.1002/etc.451>
57. Zhao C-M, Wang W-X (2012) Importance of surface coatings and soluble silver in silver nanoparticles toxicity to *Daphnia magna*. *Nanotoxicology*, 6(4):361–370. <https://doi.org/10.3109/17435390.2011.579632>
58. Angel BM, Batley GE, Jarolimek CV, Rogers NJ (2013) The impact of size on the fate and toxicity of nanoparticulate silver in aquatic systems. *Chemosphere*, 93(2):359–365. <https://doi.org/10.1016/j.chemosphere.2013.04.096>
59. Duong TT, Le TS, Tran TTH, Nguyen TK, Ho CT, Dao TH, Le TPQ, Nguyen HC, Dang DK, Le TTH, Ha PT (2016) Inhibition effect of engineered silver nanoparticles to bloom forming cyanobacteria. *Advances in Natural Sciences: Nanoscience and Nanotechnology*, 7(3):035018. <https://doi.org/10.1088/2043-6262/7/3/035018>
60. González AG, Fernández-Rojo L, Leflaive J, Pokrovsky OS, Rols J-L (2016) Response of three biofilm-forming benthic microorganisms to Ag nanoparticles and Ag⁺: the diatom *Nitzschia palea*, the green alga *Uronema confervicolum* and the cyanobacteria *Leptolyngbya* sp. *Environmental Science and Pollution Research*, 23(21):22136–22150. <https://doi.org/10.1007/s11356-016-7259-z>
61. Huang T, Sui M, Yan X, Zhang X, Yuan Z (2016) Anti-algae efficacy of silver nanoparticles to *Microcystis aeruginosa*: Influence of NOM, divalent cations, and pH. *Colloids and Surfaces*

- A: *Physicochemical and Engineering Aspects*, 509:492–503.
<https://doi.org/10.1016/j.colsurfa.2016.09.009>
62. Kleiven M, Macken A, Oughton DH (2019) Growth inhibition in *Raphidocelis subcapita* – Evidence of nanospecific toxicity of silver nanoparticles. *Chemosphere*, 221:785–792.
<https://doi.org/10.1016/j.chemosphere.2019.01.055>
63. Książyk M, Asztemborska M, Stęborowski R, Bystrzejewska-Piotrowska G (2015) Toxic Effect of Silver and Platinum Nanoparticles Toward the Freshwater Microalga *Pseudokirchneriella subcapitata*. *Bulletin of Environmental Contamination and Toxicology*, 94(5):554–558. <https://doi.org/10.1007/s00128-015-1505-9>
64. Malysheva A, Voelcker N, Holm PE, Lombi E (2016) Unraveling the Complex Behavior of AgNPs Driving NP-Cell Interactions and Toxicity to Algal Cells. *Environmental Science & Technology*, 50(22):12455–12463. <https://doi.org/10.1021/acs.est.6b03470>
65. Moreno-Garrido I, Pérez S, Blasco J (2015) Toxicity of silver and gold nanoparticles on marine microalgae. *Marine Environmental Research*, 111:60–73.
<https://doi.org/10.1016/j.marenvres.2015.05.008>
66. Nam S-H, An Y-J (2019) Size- and shape-dependent toxicity of silver nanomaterials in green alga *Chlorococcum infusionum*. *Ecotoxicology and Environmental Safety*, 168:388–393.
<https://doi.org/10.1016/j.ecoenv.2018.10.082>
67. Navarro E, Piccapietra F, Wagner B, Marconi F, Kaegi R, Odzak N, Sigg L, Behra R (2008) Toxicity of Silver Nanoparticles to *Chlamydomonas reinhardtii*. *Environmental Science & Technology*, 42(23):8959–8964. <https://doi.org/10.1021/es801785m>
68. Navarro E, Wagner B, Odzak N, Sigg L, Behra R (2015) Effects of Differently Coated Silver Nanoparticles on the Photosynthesis of *Chlamydomonas reinhardtii*. *Environmental Science & Technology*, 49(13):8041–8047. <https://doi.org/10.1021/acs.est.5b01089>
69. Salas P, Odzak N, Echegoyen Y, Kägi R, Sancho MC, Navarro E (2019) The role of size and protein shells in the toxicity to algal photosynthesis induced by ionic silver delivered from silver nanoparticles. *Science of The Total Environment*, 692:233–239.
<https://doi.org/10.1016/j.scitotenv.2019.07.237>
70. Sendra M, Yeste MP, Gatica JM, Moreno-Garrido I, Blasco J (2017) Direct and indirect effects of silver nanoparticles on freshwater and marine microalgae (*Chlamydomonas reinhardtii* and *Phaeodactylum tricorutum*). *Chemosphere*, 179:279–289.
<https://doi.org/10.1016/j.chemosphere.2017.03.123>
71. Sørensen SN, Baun A (2015) Controlling silver nanoparticle exposure in algal toxicity testing – A matter of timing. *Nanotoxicology*, 9(2):201–209.
<https://doi.org/10.3109/17435390.2014.913728>
72. Taylor C, Matzke M, Kroll A, Read DS, Svendsen C, Crossley A (2016) Toxic interactions of different silver forms with freshwater green algae and cyanobacteria and their effects on

mechanistic endpoints and the production of extracellular polymeric substances. *Environmental Science: Nano*, 3(2):396–408. <https://doi.org/10.1039/C5EN00183H>

73. Xiang L, Fang J, Cheng H (2018) Toxicity of silver nanoparticles to green algae *M. aeruginosa* and alleviation by organic matter. *Environmental Monitoring and Assessment*, 190(11):667. <https://doi.org/10.1007/s10661-018-7022-7>

74. Yoo-iam M, Chaichana R, Satapanajaru T (2014) Toxicity, bioaccumulation and biomagnification of silver nanoparticles in green algae (*Chlorella* sp.), water flea (*Moina macrocopa*), blood worm (*Chironomus* spp.) and silver barb (*Barbonymus gonionotus*). *Chemical Speciation & Bioavailability*, 26(4):257–265. <https://doi.org/10.3184/095422914X14144332205573>

75. Yue Y, Li X, Sigg L, Suter MJ-F, Pillai S, Behra R, Schirmer K (2017) Interaction of silver nanoparticles with algae and fish cells: a side by side comparison. *Journal of Nanobiotechnology*, 15(1):16. <https://doi.org/10.1186/s12951-017-0254-9>

76. Zhang JL, Zhou ZP, Pei Y, Xiang QQ, Chang XX, Ling J, Shea D, Chen LQ (2018) Metabolic profiling of silver nanoparticle toxicity in *Microcystis aeruginosa*. *Environmental Science: Nano*, 5(11):2519–2530. <https://doi.org/10.1039/C8EN00738A>

77. Zhang J, Xiang Q, Shen L, Ling J, Zhou C, Hu J, Chen L (2020) Surface charge-dependent bioaccumulation dynamics of silver nanoparticles in freshwater algae. *Chemosphere*, 247:125936. <https://doi.org/10.1016/j.chemosphere.2020.125936>

78. Zhou K, Hu Y, Zhang L, Yang K, Lin D (2016) The role of exopolymeric substances in the bioaccumulation and toxicity of Ag nanoparticles to algae. *Scientific Reports*, 6(1):32998. <https://doi.org/10.1038/srep32998>

79. Zouzelka R, Cihakova P, Rihova Ambrozova J, Rathousky J (2016) Combined biocidal action of silver nanoparticles and ions against Chlorococcales (*Scenedesmus quadricauda*, *Chlorella vulgaris*) and filamentous algae (*Klebsormidium* sp.). *Environmental Science and Pollution Research*, 23(9):8317–8326. <https://doi.org/10.1007/s11356-016-6361-6>

80. Afifi M, Saddick S, Abu Zinada OA (2016) Toxicity of silver nanoparticles on the brain of *Oreochromis niloticus* and *Tilapia zillii*. *Saudi Journal of Biological Sciences*, 23(6):754–760. <https://doi.org/10.1016/j.sjbs.2016.06.008>

81. Ašmonaitė G, Boyer S, Souza KB de, Wassmur B, Sturve J (2016) Behavioural toxicity assessment of silver ions and nanoparticles on zebrafish using a locomotion profiling approach. *Aquatic Toxicology*, 173:143–153. <https://doi.org/10.1016/j.aquatox.2016.01.013>

82. Banan A, Kalbassi MR, Bahmani M, Sotoudeh E, Johari SA, Ali JM, Kolok AS (2020) Salinity modulates biochemical and histopathological changes caused by silver nanoparticles in juvenile Persian sturgeon (*Acipenser persicus*). *Environmental Science and Pollution Research*, 27(10):10658–10671. <https://doi.org/10.1007/s11356-020-07687-7>

83. Bermejo-Nogales A, Fernández M, Fernández-Cruz ML, Navas JM (2016) Effects of a silver nanomaterial on cellular organelles and time course of oxidative stress in a fish cell line (PLHC-1). *Comparative Biochemistry and Physiology Part C: Toxicology & Pharmacology*, 190:54–65. <https://doi.org/10.1016/j.cbpc.2016.08.004>
84. Bilberg K, Hovgaard MB, Besenbacher F, Baatrup E (2012) In Vivo Toxicity of Silver Nanoparticles and Silver Ions in Zebrafish (*Danio rerio*). *Journal of Toxicology*, 2012:1–9. <https://doi.org/10.1155/2012/293784>
85. Borase HP, Patil CD, Salunkhe RB, Suryawanshi RK, Salunke BK, Patil SV (2014) Catalytic and synergistic antibacterial potential of green synthesized silver nanoparticles: Their ecotoxicological evaluation on *Poecillia reticulata*: Ecotoxicological Evaluation of AgNPs on *Poecillia reticulata*. *Biotechnology and Applied Biochemistry*, 61(4):385–394. <https://doi.org/10.1002/bab.1189>
86. Caloudova H, Hodkovicova N, Sehonova P, Blahova J, Marsalek B, Panacek A, Svobodova Z (2018) The effect of silver nanoparticles and silver ions on zebrafish embryos (*Danio rerio*). *Neuroendocrinology Letters*, 39(4):299–304.
87. Chae YJ, Pham CH, Lee J, Bae E, Yi J, Gu MB (2009) Evaluation of the toxic impact of silver nanoparticles on Japanese medaka (*Oryzias latipes*). *Aquatic Toxicology (Amsterdam, Netherlands)*, 94(4):320–327. <https://doi.org/10.1016/j.aquatox.2009.07.019>
88. Cho J-G, Kim K-T, Ryu T-K, Lee J, Kim J-E, Kim J, Lee B-C, Jo E-H, Yoon J, Eom I, Choi K, Kim P (2013) Stepwise Embryonic Toxicity of Silver Nanoparticles on *Oryzias latipes*. *BioMed Research International*, 2013:1–7. <https://doi.org/10.1155/2013/494671>
89. Choi JE, Kim S, Ahn JH, Youn P, Kang JS, Park K, Yi J, Ryu D-Y (2010) Induction of oxidative stress and apoptosis by silver nanoparticles in the liver of adult zebrafish. *Aquatic Toxicology (Amsterdam, Netherlands)*, 100(2):151–159. <https://doi.org/10.1016/j.aquatox.2009.12.012>
90. Connolly M, Fernandez-Cruz M-L, Quesada-Garcia A, Alte L, Segner H, Navas J (2015) Comparative Cytotoxicity Study of Silver Nanoparticles (AgNPs) in a Variety of Rainbow Trout Cell Lines (RTL-W1, RTH-149, RTG-2) and Primary Hepatocytes. *International Journal of Environmental Research and Public Health*, 12(5):5386–5405. <https://doi.org/10.3390/ijerph120505386>
91. Cunningham S, Brennan-Fournet ME, Ledwith D, Byrnes L, Joshi L (2013) Effect of Nanoparticle Stabilization and Physicochemical Properties on Exposure Outcome: Acute Toxicity of Silver Nanoparticle Preparations in Zebrafish (*Danio rerio*). *Environmental Science & Technology*, 47(8):3883–3892. <https://doi.org/10.1021/es303695f>
92. Degger N, Tse ACK, Wu RSS (2015) Silver nanoparticles disrupt regulation of steroidogenesis in fish ovarian cells. *Aquatic Toxicology*, 169:143–151. <https://doi.org/10.1016/j.aquatox.2015.10.015>

93. Farkas J, Christian P, Urrea JAG, Roos N, Hassellöv M, Tollefsen KE, Thomas KV (2010) Effects of silver and gold nanoparticles on rainbow trout (*Oncorhynchus mykiss*) hepatocytes. *Aquatic Toxicology*, 96(1):44–52. <https://doi.org/10.1016/j.aquatox.2009.09.016>
94. Govindasamy R, Rahuman AA (2012) Histopathological studies and oxidative stress of synthesized silver nanoparticles in Mozambique tilapia (*Oreochromis mossambicus*). *Journal of Environmental Sciences*, 24(6):1091–1098. [https://doi.org/10.1016/S1001-0742\(11\)60845-0](https://doi.org/10.1016/S1001-0742(11)60845-0)
95. Jahanbakhshi A, Shalvei F, Hedayati A (2012) Detection of Silver Nanoparticles (Nanosil®) LC50 in Silver Carp (*Hypophthalmichthys molitrix*) and Goldfish (*Carassius auratus*). *World Journal of Zoology*, 7(2):126–130. <https://doi.org/10.5829/idosi.wjz.2012.7.2.62129>
96. Johari SA, Kalbassi MR, Soltani M, Yu IJ (2013) Toxicity comparison of colloidal silver nanoparticles in various life stages of rainbow trout (*Oncorhynchus mykiss*). *Iranian Journal of Fisheries Science*, 12(1):76–95.
97. Kalbassi MR, Johari SA, Soltani M, Yu IJ (2013) Particle Size and Agglomeration Affect the Toxicity Levels of Silver Nanoparticle Types in Aquatic Environment. *Ecopersia*, 1(3):273–290.
98. Kashiwada S, Ariza ME, Kawaguchi T, Nakagame Y, Jayasinghe BS, Gärtner K, Nakamura H, Kagami Y, Sabo-Attwood T, Ferguson PL, Chandler GT (2012) Silver Nanocolloids Disrupt Medaka Embryogenesis through Vital Gene Expressions. *Environmental Science & Technology*, 46(11):6278–6287. <https://doi.org/10.1021/es2045647>
99. Katuli KK, Massarsky A, Hadadi A, Pourmehran Z (2014) Silver nanoparticles inhibit the gill Na⁺/K⁺-ATPase and erythrocyte AChE activities and induce the stress response in adult zebrafish (*Danio rerio*). *Ecotoxicology and Environmental Safety*, 106:173–180. <https://doi.org/10.1016/j.ecoenv.2014.04.001>
100. Khosravi-Katuli K, Shabani A, Paknejad H, Imanpoor MR (2018) Comparative toxicity of silver nanoparticle and ionic silver in juvenile common carp (*Cyprinus carpio*): Accumulation, physiology and histopathology. *Journal of Hazardous Materials*, 359:373–381. <https://doi.org/10.1016/j.jhazmat.2018.07.064>
101. Laban G, Nies LF, Turco RF, Bickham JW, Sepúlveda MS (2010) The effects of silver nanoparticles on fathead minnow (*Pimephales promelas*) embryos. *Ecotoxicology*, 19(1):185–195. <https://doi.org/10.1007/s10646-009-0404-4>
102. Masouleh FF, Amiri BM, Mirvaghefi A, Ghafoori H, Madsen SS (2017) Silver nanoparticles cause osmoregulatory impairment and oxidative stress in Caspian kutum (*Rutilus kutum*, Kamensky 1901). *Environmental Monitoring and Assessment*, 189(9):448. <https://doi.org/10.1007/s10661-017-6156-3>
103. Minghetti M, Schirmer K (2016) Effect of media composition on bioavailability and toxicity of silver and silver nanoparticles in fish intestinal cells (RTgutGC). *Nanotoxicology*, 10(10):1526–1534. <https://doi.org/10.1080/17435390.2016.1241908>

104. Muth-Köhne E, Sonnack L, Schlich K, Hischen F, Baumgartner W, Hund-Rinke K, Schäfers C, Fenske M (2013) The toxicity of silver nanoparticles to zebrafish embryos increases through sewage treatment processes. *Ecotoxicology*, 22(8):1264–1277. <https://doi.org/10.1007/s10646-013-1114-5>
105. Olasagasti M, Gatti AM, Capitani F, Barranco A, Pardo MA, Escuredo K, Rainieri S (2014) Toxic effects of colloidal nanosilver in zebrafish embryos: Toxic effects of colloidal nanosilver in zebrafish embryos. *Journal of Applied Toxicology*, 34(5):562–575. <https://doi.org/10.1002/jat.2975>
106. Orbea A, González-Soto N, Lacave JM, Barrio I, Cajaraville MP (2017) Developmental and reproductive toxicity of PVP/PEI-coated silver nanoparticles to zebrafish. *Comparative Biochemistry and Physiology Part C: Toxicology & Pharmacology*, 199:59–68. <https://doi.org/10.1016/j.cbpc.2017.03.004>
107. Ostaszewska T, Chojnacki M, Kamaszewski M, Sawosz-Chwalibóg E (2016) Histopathological effects of silver and copper nanoparticles on the epidermis, gills, and liver of Siberian sturgeon. *Environmental Science and Pollution Research*, 23(2):1621–1633. <https://doi.org/10.1007/s11356-015-5391-9>
108. Paul M, Prasad PK, Rathore G, Kumar K, Sharma R (2016) In-vitro and in-vivo antibacterial effect of five different sizes of silver nanoparticles (Ag-NPs) in *Labeo rohita*. *The Indian journal of animal sciences*, 86(8):964–971.
109. Rajkumar KS, Kanipandian N, Thirumurugan R (2016) Toxicity assessment on haematology, biochemical and histopathological alterations of silver nanoparticles-exposed freshwater fish *Labeo rohita*. *Applied Nanoscience*, 6(1):19–29. <https://doi.org/10.1007/s13204-015-0417-7>
110. Renuka RR, Ravindranath RRS, Raguraman V, Yoganandham ST, Kasivelu G, Lakshminarayanan A (2020) In Vivo Toxicity Assessment of Laminarin Based Silver Nanoparticles from *Turbinaria ornata* in Adult Zebrafish (*Danio rerio*). *Journal of Cluster Science*, 31(1):185–195. <https://doi.org/10.1007/s10876-019-01632-6>
111. Shahbazzadeh D, Ahari H, Rahimi NM, Dastmalchi F, Soltani M, Rahmannya J, Khorasani N, Fotovat M (2009) The Effects of Nanosilver (Nanocid®) on Survival Percentage of Rainbow Trout (*Oncorhynchus mykiss*). *Pakistan Journal of Nutrition*, 8(8):1178–1179. <https://doi.org/10.3923/pjn.2009.1178.1179>
112. Shaluei F, Hedayati A, Jahanbakhshi A, Kolangi H, Fotovat M (2013) Effect of subacute exposure to silver nanoparticle on some hematological and plasma biochemical indices in silver carp (*Hypophthalmichthys molitrix*). *Human & Experimental Toxicology*, 32(12):1270–1277. <https://doi.org/10.1177/0960327113485258>
113. Shaw BJ, Liddle CC, Windeatt KM, Handy RD (2016) A critical evaluation of the fish early-life stage toxicity test for engineered nanomaterials: experimental modifications and recommendations. *Archives of Toxicology*, 90(9):2077–2107. <https://doi.org/10.1007/s00204-016-1734-7>

114. Shobana C, Rangasamy B, Poopal RK, Renuka S, Ramesh M (2018) Green synthesis of silver nanoparticles using *Piper nigrum*: tissue-specific bioaccumulation, histopathology, and oxidative stress responses in Indian major carp *Labeo rohita*. *Environmental Science and Pollution Research*, 25(12):11812–11832. <https://doi.org/10.1007/s11356-018-1454-z>
115. Anunya Srinonate, Wijit Banlunara, Pattwat Maneewattanapinyo, Chuchaat Thammacharoen, Sanong Ekgasit, Theerayuth Kaewamatawong (2015) Acute Toxicity Study of Nanosilver Particles in Tilapia (*Oreochromis niloticus*): Pathological Changes, Particle Bioaccumulation and Metallothionien Protein Expression. *Thai Journal of Veterinary Medicine*, 45(1):81–89.
116. Taju G, Abdul Majeed S, Nambi KSN, Sahul Hameed AS (2014) In vitro assay for the toxicity of silver nanoparticles using heart and gill cell lines of *Catla catla* and gill cell line of *Labeo rohita*. *Comparative Biochemistry and Physiology Part C: Toxicology & Pharmacology*, 161:41–52. <https://doi.org/10.1016/j.cbpc.2014.01.007>
117. Valerio-García RC, Carbajal-Hernández AL, Martínez-Ruíz EB, Jarquín-Díaz VH, Haro-Pérez C, Martínez-Jerónimo F (2017) Exposure to silver nanoparticles produces oxidative stress and affects macromolecular and metabolic biomarkers in the goodeid fish *Chapalichthys pardalis*. *Science of The Total Environment*, 583:308–318. <https://doi.org/10.1016/j.scitotenv.2017.01.070>
118. Wu Y, Zhou Q (2013) Silver nanoparticles cause oxidative damage and histological changes in medaka (*Oryzias latipes*) after 14 days of exposure. *Environmental Toxicology and Chemistry*, 32(1):165–173. <https://doi.org/10.1002/etc.2038>
119. Wu Y, Zhou Q, Li H, Liu W, Wang T, Jiang G (2010) Effects of silver nanoparticles on the development and histopathology biomarkers of Japanese medaka (*Oryzias latipes*) using the partial-life test. *Aquatic Toxicology (Amsterdam, Netherlands)*, 100(2):160–167. <https://doi.org/10.1016/j.aquatox.2009.11.014>
120. Xiang Q-Q, Wang D, Zhang J-L, Ding C-Z, Luo X, Tao J, Ling J, Shea D, Chen L-Q (2020) Effect of silver nanoparticles on gill membranes of common carp: Modification of fatty acid profile, lipid peroxidation and membrane fluidity. *Environmental Pollution*, 256:113504. <https://doi.org/10.1016/j.envpol.2019.113504>
121. Yen H-J, Horng J-L, Yu C-H, Fang C-Y, Yeh Y-H, Lin L-Y (2019) Toxic effects of silver and copper nanoparticles on lateral-line hair cells of zebrafish embryos. *Aquatic Toxicology*, 215:105273. <https://doi.org/10.1016/j.aquatox.2019.105273>
122. Yue Y, Behra R, Sigg L, Fernández Freire P, Pillai S, Schirmer K (2015) Toxicity of silver nanoparticles to a fish gill cell line: Role of medium composition. *Nanotoxicology*, 9(1):54–63. <https://doi.org/10.3109/17435390.2014.889236>
123. Burkart C, Tümping W von, Berendonk T, Jungmann D (2015) Nanoparticles in wastewater treatment plants: a novel acute toxicity test for ciliates and its implementation in risk assessment. *Environmental Science and Pollution Research*, 22(10):7485–7494. <https://doi.org/10.1007/s11356-014-4057-3>

124. Fuentes-Valencia MA, Fajer-Ávila EJ, Chávez-Sánchez MC, Martínez-Palacios CA, Martínez-Chávez CC, Junqueira-Machado G, Lara HH, Raggi L, Gómez-Gil B, Pestryakov AA, Bogdanchikova N (2020) Silver nanoparticles are lethal to the ciliate model *Tetrahymena* and safe to the pike silverside *Chirostoma estor*. *Experimental Parasitology*, 209:107825. <https://doi.org/10.1016/j.exppara.2019.107825>
125. Juganson K, Mortimer M, Ivask A, Kasemets K, Kahru A (2013) Extracellular conversion of silver ions into silver nanoparticles by protozoan *Tetrahymena thermophila*. *Environ. Sci.: Processes Impacts*, 15(1):244–250. <https://doi.org/10.1039/C2EM30731F>
126. Juganson K, Mortimer M, Ivask A, Pucciarelli S, Miceli C, Orupõld K, Kahru A (2017) Mechanisms of toxic action of silver nanoparticles in the protozoan *Tetrahymena thermophila* : From gene expression to phenotypic events. *Environmental Pollution*, 225:481–489. <https://doi.org/10.1016/j.envpol.2017.03.013>
127. Kvitek L, Vanickova M, Panacek A, Soukupova J, Dittrich M, Valentova E, Pucek R, Bancirova M, Milde D, Zboril R (2009) Initial Study on the Toxicity of Silver Nanoparticles (NPs) against *Paramecium caudatum*. *The Journal of Physical Chemistry C*, 113(11):4296–4300. <https://doi.org/10.1021/jp808645e>
128. Shi J-P, Ma C-Y, Xu B, Zhang H-W, Yu C-P (2012) Effect of light on toxicity of nanosilver to *Tetrahymena pyriformis*. *Environmental Toxicology and Chemistry*, 31(7):1630–1638. <https://doi.org/10.1002/etc.1864>

Appendix D

Electronic supplemental information from Chapter 5 and associated references.

Table D1. Considerations for calculating the freshwater ecotoxicity characterization factors for ENMs (listed in alphabetical order based on references).

ENM	Considered processes for fate modeling	FF (days)	XF (%)	EF (PAF.m ³ /kg)	CF (PAF.m ³ .day/kg or CTUe/kg)	Reference
CNT	Sedimentation ($k_{\text{sed}}= 6.8 \times 10^{-10} \text{ s}^{-1}$) Heteroaggregation ($k_{\text{hetero-agg}}= 6.9 \times 10^{-11} \text{ s}^{-1}$) Advection ($k_{\text{adv}}= 6.91 \times 10^{-9} \text{ s}^{-1}$)	1509	81.1	55.4	6.78+04	[1]
GO	Sedimentation ($k_{\text{sed}}= 2.5 \times 10^{-8} \text{ s}^{-1}$) Heteroaggregation ($k_{\text{hetero-agg}}= 2.3 \times 10^{-7} \text{ s}^{-1}$) Advection ($k_{\text{adv}}= 4.6 \times 10^{-8} \text{ s}^{-1}$) Photodegradation ($k_{\text{photodeg}}= 1.3 \times 10^{-7} \text{ s}^{-1}$)	27.2	93	30.7	7.78E+02	[2]
SWCNT	Calculated using substance specific partitioning coefficients	S1) 143 S2) matter of days	S1) 100 S2) 98	S1) 200 S2) 200	S1) 29000 S2) 3700	[3]
Nano-TiO ₂	Dissolution Aggregation	0.633 (free form) 44.8 (aggregated form)	<i>not mentioned</i>	26.9 (9.4–26.9)	1550 (free form)	[4]

ENM	Considered processes for fate modeling	FF (days)	XF (%)	EF (PAF.m ³ /kg)	CF (PAF.m ³ .day/kg or CTUe/kg)	Reference
nAg	Calculated using substance specific partitioning coefficients	S1) 30 S2) 130	S1) 60 S2) 80	S1) 13497 S2) 281144	S1) 2.43E+05 S2) 2.92E+07	[5]
Nano-TiO ₂	Calculated using substance specific partitioning coefficients	S1) 0.053 S2) 1	S1) 100 S2) 100	S1) 79 S2) 1180	S1) 4 S2) 1180	[5]
SWCNT	Calculated using substance specific partitioning coefficients	S1) 10 S2) 143	S1) 100 S2) 100	S1) 260 S2) 288	S1) 2600 S2) 41184	[5]
C ₆₀	Calculated using substance specific partitioning coefficients	S1) 10 S2) 143	S1) 100 S2) 100	S1) 91 S2) 161	S1) 910 S2) 23023	[5]
nAg	Assumed due to many unknowns	1	neglected	8576	8.57E+03	[6]
Nano-TiO ₂	Assumed due to many unknowns	1	neglected	26.1	2.61E+01	[6]
nCu	Sedimentation Advection Dissolution	1.15	100	5185	5.96E+03	[7]
nAg	Sedimentation Advection ($k_{adv} = 8.1 \times 10^{-9} s^{-1}$) Dissolution ($k_{diss} = 3.42 \times 10^{-6} s^{-1}$)	1.36 (3.86E-03 – 3.38E+00)	100	14502	1.98E+04	[8]
Al ₂ O ₃ -NP	Sedimentation Advection ($k_{adv} = 8.1 \times 10^{-9} s^{-1}$)	2.28 (3.87E-03 – 1.28E+03)	100	53.083	1.21E+02	[8]
Au-NP	Sedimentation Advection ($k_{adv} = 8.1 \times 10^{-9} s^{-1}$)	2.28 (3.87E-03 – 1.18E+03)	100	80.7	1.84E+02	[8]

ENM	Considered processes for fate modeling	FF (days)	XF (%)	EF (PAF.m ³ /kg)	CF (PAF.m ³ .day/kg or CTUe/kg)	Reference
C ₆₀	Sedimentation Advection (k _{adv} = 8.1×10 ⁻⁹ s ⁻¹)	2.28 (3.87E-03 – 1.33E+03)	100	544	1.24E+03	[8]
CeO ₂ -NP	Sedimentation Advection (k _{adv} = 8.1×10 ⁻⁹ s ⁻¹)	2.28 (3.87E-03 – 1.24E+03)	100	139	3.18E+02	[8]
nCu	Sedimentation Advection (k _{adv} = 8.1×10 ⁻⁹ s ⁻¹) Dissolution (k _{diss} =5.5×10 ⁻⁷ s ⁻¹)	2.06 (3.87E-03 – 2.07E+01)	100	8999	1.85E+04	[8]
nCuO	Sedimentation Advection (k _{adv} = 8.1×10 ⁻⁹ s ⁻¹) Dissolution (k _{diss} =3.87×10 ⁻⁷ s ⁻¹)	2.12 (1.37E-01 – 2.92E+01)	100	223	4.74E+02	[8]
Fe ₂ O ₃ -NP	Sedimentation Advection (k _{adv} = 8.1×10 ⁻⁹ s ⁻¹)	2.28 (3.86E-03 – 1.26E+03)	100	228	5.20E+02	[8]
Fe ₃ O ₄ -NP	Sedimentation Advection (k _{adv} = 8.1×10 ⁻⁹ s ⁻¹)	2.28 (3.87E-03 – 1.27E+03)	100	21739	4.96E+04	[8]
NiO-NP	Sedimentation Advection (k _{adv} = 8.1×10 ⁻⁹ s ⁻¹) Dissolution (k _{diss} =2.18×10 ⁻⁷ s ⁻¹)	2.19 (3.87E-03 – 5.09E+01)	100	14.2	3.10E+01	[8]
Pt-NP	Sedimentation Advection (k _{adv} = 8.1×10 ⁻⁹ s ⁻¹)	2.28 (3.86E-03 – 1.17E+03)	100	126	2.88E+02	[8]

ENM	Considered processes for fate modeling	FF (days)	XF (%)	EF (PAF.m ³ /kg)	CF (PAF.m ³ .day/kg or CTUe/kg)	Reference
SiO ₂ -NP	Sedimentation Advection ($k_{adv}= 8.1 \times 10^{-9} \text{ s}^{-1}$) Dissolution ($k_{diss}=3.79 \times 10^{-6} \text{ s}^{-1}$)	1.31 (3.86E-03 – 3.05E+00)	100	27.8	3.62E+01	[8]
Nano-TiO ₂	Sedimentation Advection ($k_{adv}= 8.1 \times 10^{-9} \text{ s}^{-1}$)	2.28 (3.87E-03 – 1.27E+03)	100	56.7	1.29E+02	[8]
ZnO-NP	Sedimentation Advection ($k_{adv}= 8.1 \times 10^{-9} \text{ s}^{-1}$) Dissolution ($k_{diss}=5.12 \times 10^{-7} \text{ s}^{-1}$)	2.07 (3.87E-03 – 2.22E+01)	100	2863	5.94E+03	[8]
SWCNT	Calculated using substance specific partitioning coefficients	29	6.5E-04	650	1.25E-01	[9]
MWCNT	Calculated using substance specific partitioning coefficients	92	100	8	7.40E+02	[9]
nCu	Calculated using substance specific partitioning coefficients	37	33	4500	5.52E+04	[9]
Nano-TiO ₂	Sedimentation Heteroaggregation Advection	0.053	100	32.1	2.81E+01	[10]

Hetero-aggregation

$$k_{het-agg} = k_{coll} * \alpha_{het-agg} * C_{SPM} \quad (D1)$$

where $\alpha_{het-agg}$ is aggregation efficiency, C_{SPM} is suspended particulate matter concentration ($1/m^3$) and k_{coll} is the collision rate (m^3/s). C_{SPM} needs to be calculated using equation (D2) as

$$C_{SPM} = \frac{C_{mass,SPM}}{\frac{4}{3} * \rho_{SPM} * \pi * \left(\frac{d_{SPM}}{2}\right)^3} \quad (D2)$$

where $C_{mass,SPM}$ is the mass concentration of suspended particulate matter in water (kg/m^3), ρ_{SPM} is the density of suspended particulate matter (kg/m^3) and d_{SPM} is the diameter of the suspended particulate matter in water (m). Another component of equation (D1), the collision rate, can be calculated using equation (D3).

$$k_{coll} = \frac{2k_B T_{water}}{3\mu_{water}} * \frac{(r_{nAg} + r_{SPM})^2}{r_{nAg} * r_{SPM}} + \frac{4}{3} G (r_{nAg} + r_{SPM})^3 + \pi (r_{nAg} + r_{SPM})^2 * |v_{set}^{nAg} - v_{set}^{SPM}| \quad (D3)$$

where k_B is Boltzmann constant (JK^{-1}), T_{water} is the temperature of the water (K), μ_{water} is the dynamic viscosity of water (Ns/m^2), r_{nAg} is the radius of nAg (m), r_{SPM} is the radius of suspended particulate matter (m), G is the shear rate of the water (1/s), v_{set}^{nAg} is the settling velocity of nAg (m/s) and v_{set}^{SPM} is the settling velocity of suspended particulate matter (m/s).

Equations (D4) and (D5) are used to calculate the settling velocities of nAg and SPM to be used in the collision rate calculation.

$$v_{set}^{nAg} = \frac{2}{9} * \frac{\rho_{nAg} - \rho_{water}}{\mu_{water}} * g * r_{nAg}^2 \quad (D4)$$

$$v_{set}^{SPM} = \frac{2}{9} * \frac{\rho_{SPM} - \rho_{water}}{\mu_{water}} * g * r_{SPM}^2 \quad (D5)$$

where ρ_{nAg} is the density of nAg (kg/m^3), ρ_{water} is the density of water (kg/m^3), μ_{water} is the dynamic viscosity of water (Ns/m^2), g is the gravitational acceleration on earth (m/s^2), r_{nAg} is the radius of nAg (m), ρ_{SPM} is the density of suspended particulate matter (kg/m^3) and r_{SPM} is the radius of suspended particulate matter (m).

Sedimentation

Scenario 2

$$k_{sed}' = k_{sed}^{nAg} + k_{agg-sed} + k_{att-sed} \quad (\text{D6})$$

where k_{sed}^{nAg} is the sedimentation rate constant (s^{-1}), $k_{agg-sed}$ is the minimum value of either pseudo-sedimentation rate constant for homo-aggregated nAg or the homo-aggregation rate constant as expressed in equation (D7) (s^{-1}) and $k_{att-sed}$ is the minimum value of either pseudo-sedimentation rate constant for hetero-aggregated (i.e. attached) nAg or the hetero-aggregation (i.e. attachment) rate constant as expressed in equation (D8) (s^{-1}).

$$k_{agg-sed} = \text{minimum} (k_{homo-agg}, k_{ps-homo-agg}) \quad (\text{D7})$$

where k_{agg} is the aggregation rate constant and k_{ps-agg} is the pseudo-sedimentation rate constant for aggregated nAg. In the current study, homo-aggregation is neglected, therefore this component is not calculated.

$$k_{att-sed} = \text{minimum} (k_{het-agg}, k_{ps-het-agg}) \quad (\text{D8})$$

where $k_{het-agg}$ is the attachment rate constant and $k_{ps-het-agg}$ is the pseudo-sedimentation rate constant for attached nAg.

$$k_{sed}^{nAg} = \frac{v_{set}^{nAg}}{h_w} \quad (\text{D9})$$

where v_{set}^{nAg} is the settling velocity of nAg as expressed in equation (D4) (m/s) and h_w is the depth of the water compartment (m).

$$k_{ps-het-agg} = \frac{v_{set}^{SPM}}{h_w} \quad (D10)$$

where v_{set}^{SPM} is the settling velocity of suspended particulate matter as expressed in equation (D5) (m/s) and h_w is the depth of the water compartment (m).

Dissolution

The second method for k_{diss} calculation is using modified version of the solubility equilibrium (i.e. Ostwald-Freundlich relation) as presented in equations (D11) and (D12), which enables calculating size-dependent dissolution rates [11–14]. It is hypothesized that the amount of dissolved nAg per unit time is proportional with the surface area of nAg [15, 16] as

$$\frac{dM}{dt} = -k_{diss} * S_{nAg} * A \quad (D11)$$

$$S_{nAg} = S_{bulk} * \exp\left(2 * \gamma * \frac{V_m}{R * T * r_{nAg}}\right) \quad (D12)$$

where M is the dissolved mass of nAg (kg), t is time (s), S_{nAg} is the solubility of nAg (kg/m³), A is the surface area of nAg (m²), S_{bulk} is the solubility of bulk silver (kg/m³), γ is the surface tension of nAg (typically 1 for nAg, J/m²), V_m is the molar volume of nAg (m³/mol), R is the gas constant (J/mol.K), T is the temperature (K) and r_{nAg} is the radius of nAg (m). Ma et al.

calculated the k_{diss} for PVP coated nAg as $5.07 \times 10^{-5} \text{ s}^{-1}$ using this method [14]. Different from the previously explained methods, Dale et al. compiled a list of model parameters for nAg transformation where they included a range for k_{diss} based on the level of dissolved oxygen in

freshwaters from $1.3 \times 10^{-8} \text{ d}^{-1}(\text{mg O}_2/\text{m}^3)^{-1}$ to $5.1 \times 10^{-4} \text{ d}^{-1}(\text{mg O}_2/\text{m}^3)^{-1}$ with a nominal value of $8.5 \times 10^{-6} \text{ d}^{-1}(\text{mg O}_2/\text{m}^3)^{-1}$ [17–19].

Table D2. Parameters for fate factor calculation extracted from a mesocosm studies by Geitner et al. and Stegemeier et al. [20–22].

Parameter	Symbol	Unit	Value (Range)
pH	pH	-	7-10
Conductivity	S	$\mu\text{S}/\text{cm}$	111 ± 20
Radius of nAg	r_{nAg}	nm	24.65 (PVP-nAg)
Diameter of nAg (DLS)	d_{nAg}	nm	49.3 (PVP-nAg)
Radius of SPM	r_{SPM}	μm	0.75
Diameter of SPM	d_{SPM}	μm	1.5 ± 12
Density of nAg	ρ_{nAg}	kg/m^3	10,500
Mass concentration of SPM	$C_{mass,SPM}$	mg/l	80 ± 12
Aggregation efficiency	$\alpha_{het-agg}$	-	0.012
Depth of water	h_w	m	1.2
Volume of water	V_w	m^3	3.56 (H/W/D 0.81/3.66/1.2)
Area of freshwater	$A_{freshwater}$	m^2	2.97
Area of soil	A_{soil}	m^2	0.732
Water temperature	T_{water}	K	295
Dynamic viscosity of water	μ_{water}	Ns/m^2	0.000958 (22°C)*
Initial concentration of nAg	C_0	ppm	10
Dissolved nAg at time t (2 days)	C_{ions}	ppm	0.53

* calculated based on the formula of $\mu_{water} = (2.414 * 10^{-5}) * 10^{247.8/(T-140)}$

Table D3. Remaining parameters for fate factor calculation that are not available in mesocosms (bold values are used in calculation).

Parameter	Symbol	Unit	Value (Range)	Reference
Density of water	ρ_{water}	kg/m ³	1000	[23]
Boltzmann constant	k_B	J/K	1.38E-23	[1, 8]
Surface water shear rate	G	s ⁻¹	10	[24]
Gravitational acceleration on earth	g	m/s ²	9.81	[23]
Precipitation rate	$k_{precipitation}$	mm/yr	710 (for US)	[25]
Density of SPM	ρ_{SPM}	kg/m ³	1570	<i>averaged value</i>
			2000 ^a	a [10]
			1230 ^b	b [8]
			1100 – 2500 ^c	c [26]
			1250 (1100 – 2000) ^d	d [27]
Water run-off fraction	φ	%	37 (for US)	[25]

Table D4. Calculated parameters based on the values presented in Tables D2-D3 (shaded values are used in FF calculation for the respective scenarios).

Parameter	Symbol	Unit	Value (Scenario 1)	Value (Scenario 2)
Dissolution rate constant	k_{diss}	s ⁻¹	3.15×10 ⁻⁷	3.15×10 ⁻⁷
Hetero aggregation rate constant	$k_{het-agg}$	s ⁻¹	3.44×10 ⁻⁵	-
Concentration of SPM	C_{SPM}	1/m ³	2.88×10 ¹³	2.88×10 ¹³
Collision rate	k_{coll}	m ³ /s	9.95×10 ⁻¹⁷	9.95×10 ⁻¹⁷
Settling velocity of nAg	v_{set}^{nAg}	m/s	1.31×10 ⁻⁸	1.31×10 ⁻⁸
Settling velocity of SPM	v_{set}^{SPM}	m/s	7.29×10 ⁻⁷	7.29×10 ⁻⁷
Sedimentation rate constant	k_{sed}	s ⁻¹	1.09×10 ⁻⁸	6.19×10 ⁻⁷
Advection rate constant	k_{adv}	s ⁻¹	2.05×10 ⁻⁸	2.05×10 ⁻⁸
Removal rate constant for freshwater	$k_{w,w}$	s ⁻¹	3.48×10 ⁻⁵	9.54×10 ⁻⁷
Fate factor	FF	days	0.33	12

Table D5. List of characterization factors calculated in the current study and the literature

values.

Reference	Scenarios	XF (%)	FF (days)	EF (PAF.m ³ /kg)	CF (PAF.m ³ .day/kg or CTUe/kg)
[5]	S1	60	30	1.35×10 ⁴	2.43×10 ⁵
	S2	80	130	2.81×10 ⁵	2.92×10 ⁷
[8]	-	100	1.36	1.45×10 ⁴	1.97×10 ⁴
[6]	-	100	1	8.58×10 ³	8.58×10 ³
This study	S1 – Optimistic (regardless of coating)	100	0.33	8.04×10 ³	2.67×10 ³
	S1 – Skeptical (regardless of coating)	100	0.33	1.47×10 ⁴	4.88×10 ³
	S2 – Optimistic (regardless of coating)	100	12.13	8.04×10 ³	9.74×10 ⁴
	S2 – Skeptical (regardless of coating)	100	12.13	1.47×10 ⁴	1.78×10 ⁵
	S1 – Optimistic (PVP coated)	100	0.33	6.58×10 ³	2.19×10 ³
	S1 – Skeptical (PVP coated)	100	0.33	1.93×10 ⁴	6.42×10 ³
	S2 – Optimistic (PVP coated)	100	12.13	6.58×10 ³	7.98×10 ⁴
	S2 – Skeptical (PVP coated)	100	12.13	1.93×10 ⁴	2.34×10 ⁵
USEtox spreadsheet	For ionic silver Ag (I)	41.2	18.1	2.60×10 ⁴	1.94×10 ⁵

Table D6. Scenario 1: sensitivity factors (SF) based on 20% change of inputs on the rate constants and fate factor. Reported numbers are SFs, where red cells indicate sensitive inputs.

	d_{nAg}	d_{SPM}	ρ_{nAg}	$\alpha_{het-agg}$	$C_{mass,SPM}$	C_0	C_{ions}	ρ_{SPM}
$k_{het-agg}$	-1.67E-01	-4.04E-01	-5.50E-05	1.67E-01	1.67E-01	0.00E+00	0.00E+00	-1.91E-01
k_{sed}	3.06E-01	0.00E+00	1.81E-01	0.00E+00	0.00E+00	0.00E+00	0.00E+00	0.00E+00
k_{diss}	0.00E+00	0.00E+00	0.00E+00	0.00E+00	0.00E+00	-2.06E-01	1.71E-01	0.00E+00
k_{adv}	0.00E+00	0.00E+00	0.00E+00	0.00E+00	0.00E+00	0.00E+00	0.00E+00	0.00E+00
$k_{w,w}$	-1.65E-01	-3.98E-01	1.51E-05	1.65E-01	1.65E-01	-1.55E-03	1.87E-03	-1.89E-01
FF	1.41E-01	2.85E-01	-1.51E-05	-1.98E-01	-1.98E-01	1.54E-03	-1.87E-03	1.59E-01

Table D7. Scenario 1: sensitivity factors (SF) based on 20% change of rate constants on fate factor. Reported numbers are SFs, where red cells indicate sensitive inputs.

	$k_{het-agg}$	k_{sed}	k_{diss}	k_{adv}
$k_{w,w}$	1.65E-01	6.29E-05	1.81E-03	-1.18E-04
FF	-1.98E-01	-6.29E-05	-1.81E-03	-1.18E-04

Table D8. Scenario 2: sensitivity factors (SF) based on 20% change of inputs on the rate constants and fate factor. Reported numbers are SFs, where red cells indicate sensitive inputs.

	d_{nAg}	d_{SPM}	ρ_{nAg}	$\alpha_{net-agg}$	$C_{mass,SPM}$	C_0	C_{ions}	ρ_{SPM}
k_{sed}	7.72E-03	3.02E-01	3.89E-03	0.00E+00	0.00E+00	0.00E+00	0.00E+00	3.51E-01
k_{diss}	0.00E+00	0.00E+00	0.00E+00	0.00E+00	0.00E+00	-2.06E-01	1.71E-01	0.00E+00
k_{adv}	0.00E+00	0.00E+00	0.00E+00	0.00E+00	0.00E+00	0.00E+00	0.00E+00	0.00E+00
$k_{w,w}$	5.02E-03	2.19E-01	2.53E-03	0.00E+00	0.00E+00	-5.96E-02	6.39E-02	2.60E-01
FF	-5.05E-03	-2.80E-01	-2.53E-03	0.00E+00	0.00E+00	5.63E-02	-6.82E-02	-3.51E-01

Table D9. Scenario 2: sensitivity factors (SF) based on 20% change of rate constants on fate factor. Reported numbers are SFs, where red cells indicate sensitive inputs.

	k_{sed}	k_{diss}	k_{adv}
$k_{w,w}$	1.15E-01	6.19E-02	4.28E-03
FF	-1.30E-01	-6.60E-02	-4.30E-03

References-Appendix D

1. Deng Y, Li J, Li T, Zhang J, Yang F, Yuan C (2017) Life cycle assessment of high capacity molybdenum disulfide lithium-ion battery for electric vehicles. *Energy*, 123:77–88. <https://doi.org/10.1016/j.energy.2017.01.096>
2. Deng Y, Li J, Qiu M, Yang F, Zhang J, Yuan C (2017) Deriving characterization factors on freshwater ecotoxicity of graphene oxide nanomaterial for life cycle impact assessment. *The International Journal of Life Cycle Assessment*, 22(2):222–236. <https://doi.org/10.1007/s11367-016-1151-4>
3. Eckelman MJ, Mauter MS, Isaacs JA, Elimelech M (2012) New Perspectives on Nanomaterial Aquatic Ecotoxicity: Production Impacts Exceed Direct Exposure Impacts for Carbon Nanotubes. *Environmental Science & Technology*, 46(5):2902–2910. <https://doi.org/10.1021/es203409a>
4. Ettrup K, Kounina A, Hansen SF, Meesters JAJ, Veia EB, Laurent A (2017) Development of Comparative Toxicity Potentials of TiO₂ Nanoparticles for Use in Life Cycle Assessment. *Environmental Science & Technology*, 51(7):4027–4037. <https://doi.org/10.1021/acs.est.6b05049>
5. Garvey T, Moore EA, Babbitt CW, Gaustad G (2019) Comparing ecotoxicity risks for nanomaterial production and release under uncertainty. *Clean Technologies and Environmental Policy*, 21(2):229–242. <https://doi.org/10.1007/s10098-018-1648-6>
6. Miseljic M, Olsen SI (2014) Life-cycle assessment of engineered nanomaterials: a literature review of assessment status. *Journal of Nanoparticle Research*, 16(6):2427. <https://doi.org/10.1007/s11051-014-2427-x>
7. Pu Y, Tang F, Adam P-M, Laratte B, Ionescu RE (2016) Fate and Characterization Factors of Nanoparticles in Seventeen Subcontinental Freshwaters: A Case Study on Copper Nanoparticles. *Environmental Science & Technology*, 50(17):9370–9379. <https://doi.org/10.1021/acs.est.5b06300>
8. Pu Y (2017) Toxicity assessment of engineered nanoparticles. <https://tel.archives-ouvertes.fr/tel-02002324>
9. Rodriguez-Garcia G, Zimmermann B, Weil M (2014) Nanotoxicity and Life Cycle Assessment: First attempt towards the determination of characterization factors for carbon nanotubes. *IOP Conference Series: Materials Science and Engineering*, 64:012029. <https://doi.org/10.1088/1757-899X/64/1/012029>
10. Salieri B, Righi S, Pasteris A, Olsen SI (2015) Freshwater ecotoxicity characterisation factor for metal oxide nanoparticles: A case study on titanium dioxide nanoparticle. *Science of The Total Environment*, 505:494–502. <https://doi.org/10.1016/j.scitotenv.2014.09.107>
11. Axson JL, Stark DI, Bondy AL, Capracotta SS, Maynard AD, Philbert MA, Bergin IL, Ault AP (2015) Rapid Kinetics of Size and pH-Dependent Dissolution and Aggregation of Silver

Nanoparticles in Simulated Gastric Fluid. *The Journal of Physical Chemistry C*, 119(35):20632–20641. <https://doi.org/10.1021/acs.jpcc.5b03634>

12. Doody MA, Wang D, Bais HP, Jin Y (2016) Differential antimicrobial activity of silver nanoparticles to bacteria *Bacillus subtilis* and *Escherichia coli*, and toxicity to crop plant *Zea mays* and beneficial *B. subtilis*-inoculated *Z. mays*. *Journal of Nanoparticle Research*, 18(10):290. <https://doi.org/10.1007/s11051-016-3602-z>

13. Johnston KA, Stabryla LM, Gilbertson LM, Millstone JE (2019) Emerging investigator series: connecting concepts of coinage metal stability across length scales. *Environmental Science: Nano*, 6(9):2674–2696. <https://doi.org/10.1039/C9EN00407F>

14. Ma R, Levard C, Marinakos SM, Cheng Y, Liu J, Michel FM, Brown GE, Lowry GV (2012) Size-Controlled Dissolution of Organic-Coated Silver Nanoparticles. *Environmental Science & Technology*, 46(2):752–759. <https://doi.org/10.1021/es201686j>

15. Molleman B, Hiemstra T (2017) Time, pH, and size dependency of silver nanoparticle dissolution: the road to equilibrium. *Environmental Science: Nano*, 4(6):1314–1327. <https://doi.org/10.1039/C6EN00564K>

16. Quik JTK, Vonk JA, Hansen SF, Baun A, Van De Meent D (2011) How to assess exposure of aquatic organisms to manufactured nanoparticles? *Environment International*, 37(6):1068–1077. <https://doi.org/10.1016/j.envint.2011.01.015>

17. Dale AL, Casman EA, Lowry GV, Lead JR, Viparelli E, Baalousha M (2015) Modeling Nanomaterial Environmental Fate in Aquatic Systems. *Environmental Science & Technology*, 49(5):2587–2593. <https://doi.org/10.1021/es505076w>

18. Levard C, Hotze EM, Lowry GV, Brown GE (2012) Environmental Transformations of Silver Nanoparticles: Impact on Stability and Toxicity. *Environmental Science & Technology*, 46(13):6900–6914. <https://doi.org/10.1021/es2037405>

19. Liu J, Sonshine DA, Shervani S, Hurt RH (2010) Controlled Release of Biologically Active Silver from Nanosilver Surfaces. *ACS Nano*, 4(11):6903–6913. <https://doi.org/10.1021/nn102272n>

20. Geitner NK, Bossa N, Wiesner MR (2019) Formulation and Validation of a Functional Assay-Driven Model of Nanoparticle Aquatic Transport. *Environmental Science & Technology*, 53(6):3104–3109. <https://doi.org/10.1021/acs.est.8b06283>

21. Geitner NK, O'Brien NJ, Turner AA, Cummins EJ, Wiesner MR (2017) Measuring Nanoparticle Attachment Efficiency in Complex Systems. *Environmental Science & Technology*, 51(22):13288–13294. <https://doi.org/10.1021/acs.est.7b04612>

22. Stegemeier JP, Colman BP, Schwab F, Wiesner MR, Lowry GV (2017) Uptake and Distribution of Silver in the Aquatic Plant *Landoltia punctata* (Duckweed) Exposed to Silver and Silver Sulfide Nanoparticles. *Environmental Science & Technology*, 51(9):4936–4943. <https://doi.org/10.1021/acs.est.6b06491>

23. Fantke P, Bijster M, Guignard C, Hauschild MZ, Huijbregts M, Jolliet O, Kounina A, Magaud V, Margni M, McKone TE, Posthuma L, Rosenbaum RK, Van De Meent D, Van Zelm R (2017) USEtox® 2.0 Documentation (Version 1.00). <https://doi.org/10.11581/DTU:00000011>
24. Meesters JAJ, Koelmans AA, Quik JTK, Hendriks AJ, Meent D van de (2014) Multimedia Modeling of Engineered Nanoparticles with SimpleBox4nano: Model Definition and Evaluation. *Environmental Science & Technology*, 48(10):5726–5736. <https://doi.org/10.1021/es500548h>
25. Kounina A, Margni M, Shaked S, Bulle C, Jolliet O (2014) Spatial analysis of toxic emissions in LCA: A sub-continental nested USEtox model with freshwater archetypes. *Environment International*, 69:67–89. <https://doi.org/10.1016/j.envint.2014.04.004>
26. Praetorius A, Scheringer M, Hungerbühler K (2012) Development of Environmental Fate Models for Engineered Nanoparticles—A Case Study of TiO₂ Nanoparticles in the Rhine River. *Environmental Science & Technology*, 46(12):6705–6713. <https://doi.org/10.1021/es204530n>
27. Quik JTK (2013) Fate of nanoparticles in the aquatic environment: removal of engineered nanomaterials from the water phase under environmental conditions.

Appendix E

Electronic supplemental information from Chapter 6 and associated references.

Table E1. Literature on Ag/nAg release from textile products during laundering (listed by the year of publication).

Product type (mass and composition <i>if available</i>)	Initial silver content (type and incorporation method <i>if available</i>)	Washing procedure and conditions	Ag release (speciation <i>if available</i>)	Ref.
Sock (29.3 g)	25.8 µg Ag/g (nano)	Socks were soaked into 500 mL ultrapure water/tap water (pH 7) and agitated for 1-14 h at 50 rpm. This step was repeated for at least 3 times.	Cumulative (four cycles): 28.53 µg/g	[1]
Sock (27.3 g)	57.8 µg Ag/g (metal)		First cycle: 2.51 µg/g (~72% Ag ⁺) Cumulative (four cycles): 67.58 µg/g (86% Ag ⁺)	
Sock (23.0 g)	1358.3 µg Ag/g (nano)		First cycle: 3.48 µg/g (~5% Ag ⁺) Cumulative (four cycles): 7.17 µg/g (69% Ag ⁺)	
Sock (21.9 g)	0.9 µg Ag/g (metal)		Cumulative (four cycles): 0.86 µg/g	
Sock (79% cotton, 14% PA, 6% fiber, 1% elastane)	21.6 mg Ag/g (metal- <i>electrolytically deposited layer on fiber</i>)	Washing procedure was implemented based on ISO standard method (ISO 105-C06). ECE 98-standard washing powder was used as a detergent with a pH 10 and the experiment was conducted at 40 °C for 30 minutes (40 ± 2 rpm) using Washtec-P Roaches washing machine. Steel balls were used to simulate physical stress.	First cycle: 314 µg/g (~7% Ag ⁺) Second cycle: 129 µg/g Bleach cycle: 172 µg/g	[2]
Sock (PES)	0.39 mg Ag/g (nano- <i>plasma coated fiber embedded in textile</i>)		First cycle: 67 µg/g (~50% Ag ⁺)	
Fabric (cotton)	0.008 mg Ag/g (AgCl- <i>bound to surface</i>)		First cycle: 2.7 µg/g (~0% Ag ⁺) Second cycle: 1.8 µg/g Bleach cycle: 3.6 µg/g	
Fabric (cotton)	0.012 mg Ag/g (AgCl- <i>incorporated in binder</i>)		First cycle: 2.4 µg/g (~0% Ag ⁺) Second cycle: 0.9 µg/g Bleach cycle: 3.2 µg/g	
Fabric (PES)	0.029 mg Ag/g (nano- <i>bound to surface</i>)		First cycle: 10.1 µg/g (~5% Ag ⁺)	

Product type (mass and composition if available)	Initial silver content (type and incorporation method if available)	Washing procedure and conditions	Ag release (speciation if available)	Ref.
Fabric (PES)	0.099 mg Ag/g (nano-incorporated into fiber)		First cycle: 1.3 µg/g (~0% Ag ⁺) Second cycle: 0.35 µg/g Bleach cycle: 2.7 µg/g	
Fabric (80% PES, 20% PA)	0.242 mg Ag/g (nano-incorporated into fiber)		First cycle: 4.3 µg/g (~0% Ag ⁺) Second cycle: 1.6 µg/g Bleach cycle: 10.2 µg/g	
Fabric (80% cotton, 20% elastic yarn)	2.66 mg Ag/g (nano-incorporated into fiber)		First cycle: 377 µg/g (~2% Ag ⁺) Second cycle: 99 µg/g Bleach cycle: 184 µg/g	
Athletic shirt (178 g)	30 ± 5.4 µg Ag/g (nano)	Samples were washed and mixed using municipal tap water (pH 7.6) for 1 hour at room temperature.	0.56 ± 0.01 µg/g	[3]
Unfinished cloth fabric	44 ± 2.4 µg Ag/g (nano)		0.8 ± 0.3 µg/g	
T-shirt (83% PES, 17% wool)	183 ± 10 mg Ag/kg (silver)	ISO standard method (ISO 105-C06) was applied in a laboratory washing machine (Washtex-P Roaches 40 ± 2 rpm), and 8.0 ± 0.2 g of fabric was washed with a detergent having pH 10.6 at 40 °C for 30 minutes. PE balls were used to simulate physical stress. The volume of wash water was 120 ± 0.15 mL and after each washing cycle, two rinsing cycles with 20 ± 0.03 mL tap water were applied for 5 minutes. Lastly, samples were dried in a room temperature.	20% of initial Ag (89% nAg, 7% Ag ₂ S-NP, 3% Ag ₂ O)	[4]
T-shirt (100% PES)	45 ± 8 mg Ag/kg (silver ions)		14.8% of initial Ag (66% nAg, 14% AgCl-NP, 9% Ag ₂ S-NP, 11% Ag ₂ O)	
Socks (80% cotton, 20% elastic yarn)	2925 ± 19 mg Ag/kg (nano-integration into fiber)		23.5% of initial Ag (8% nAg, 42% Ag ₂ S-NP, 50% Ag ₃ PO ₄)	
Trousers (93% PA, 7% elastane)	41 ± 0.4 mg Ag/kg (AgCl-NP)		17.6% of initial Ag (24% nAg, 33% AgCl-NP, 28% Ag ₂ S-NP, 15% Ag ₂ O)	
Socks (41% PP, 31% PA, 18% cotton, 10% wool)	18 ± 2 mg Ag/kg (silver-integration into fiber)		5% of initial Ag (31% AgCl-NP, 35% Ag ₂ S-NP, 14% AgNO ₃ , 20% Ag ₂ SO ₄)	
T-shirt (83% PES, 17% wool)	183 ± 10 mg Ag/kg (silver)	Machine washing was applied with a regular household cycle for 1 hour at 40 °C (1200 rpm) and Persil Megaperls powder was used as a detergent. Also, medium soiled clothes were washed	22% of initial Ag (95% nAg, 5% Ag ₂ S-NP)	[5]

Product type (mass and composition if available)	Initial silver content (type and incorporation method if available)	Washing procedure and conditions	Ag release (speciation if available)	Ref.
Socks (80% cotton, 20% elastic yarn)	2925 ± 19 mg Ag/kg (nano-integration into fiber)	with samples. Then the samples were dried in room temperature.	60% of initial Ag (59% AgCl-NP, 20% Ag ₂ S-NP, 14% Ag ₃ PO ₄ , 7% Ag ₂ SO ₄)	
Trousers (93% PA, 7% elastane)	41 ± 0.4 mg Ag/kg		80% of initial Ag (11% nAg, 42% AgCl-NP, 38% Ag ₂ S-NP, 9% Ag ₃ PO ₄)	
Textile (PES)	14.6 mg Ag/kg (AgCl-surface roll to roll)	Adapted ISO standard method (ISO 105-C06:2010) was applied with Washtex-P Roaches (40 ± 2 rpm) laboratory washing machine for 45 minutes at 40 ± 2°C. Phosphate free detergent was used with a pH of 10.5-10.8. PE balls were used to simulate physical stress.	35% total Ag (in which 3.2 % nAg)	[6]
Textile (79% cotton, 12% PA, 6% nylon, 1% lycra)	14500 mg Ag/kg (metal- surface electrolytic deposition)		0.05% total Ag	
Textile (PES)	19.5 mg Ag/kg (AgCl-TiO ₂ - surface roll to roll)		9% total Ag (in which 2% nAg)	
Laboratory prepared fabric (PES)	67.6 mg Ag/kg (Ag/zeolite- surface roll to roll)		16% total Ag (in which 3.2% nAg)	
Textile (PES)	116 ± 1 mg Ag/kg (nano Ag/SiO ₂ - bulk)		0.05% total Ag	
Textile (PES)	18.2 ± 0.3 mg Ag/kg (nano Ag/SiO ₂ - surface coated)		11% total Ag (in which 0.5 % nAg)	
Textile (PES)	15.5 ± 0.6 mg Ag/kg (nano- surface coated)		8% total Ag (in which 0.7% nAg)	
Textile	53,909 ± 14 mg Ag/kg (nano- coated via multi-target vacuum magnetron sputtering)	Artificial ageing was conducted based on AATCC (186–2006) with slight modifications. Washing experiments were conducted with vapor-bathing shaker (150 rpm) at 15-35 °C under room light to simulate natural exposure for 1 hour.	Tap water (pH 6.7): 2.1 µg/g (~70% Ag ⁺) Pond water (pH 7.1): 1.7 µg/g (~80% Ag ⁺) Rain water (pH 6.8): 7 µg/g (~25% Ag ⁺) Artificial sweat (pH 6.2): 2.5 µg/g (~100% Ag ⁺) Detergent solution (pH 5.8): 2 µg/g (~80% Ag ⁺)	[7]

Product type (mass and composition if available)	Initial silver content (type and incorporation method if available)	Washing procedure and conditions	Ag release (speciation if available)	Ref.
Fabric (100% cotton)	2.46 ± 0.77 µg Ag/g (nano-spraying on the surface)	Sequential washing (20 cycles) was conducted using Milli-Q water (neutral) and commercially available detergent (alkaline). Samples from each fabric were placed in 50 mL Milli-Q/detergent and stirred for 30 min (350 rpm) to simulate washing machine. The liquid was collected by squeezing the washed samples. All experiments were conducted at 25 °C.	30% of initial Ag with Milli-Q water	[8]
Sheet (80% cotton)	2.69 ± 0.77 µg Ag/g (nano-spraying on the surface)		52% of initial Ag with Milli-Q water	
Body suit (lycra)	2.82 ± 0.44 µg Ag/g (nano-electrolytically deposited layer on fiber)		55% of initial Ag with Milli-Q water	
Laboratory prepared fabric (cotton)	254 µg Ag/g fabric (nano-pad-dry-cure)		55% of initial Ag with Milli-Q water (10% Ag ⁺) 88% of initial Ag with detergent	
Laboratory prepared fabric (PES)	350 ± 11.33 µg Ag/g (nano-pad-dry-cure)		72% of initial Ag with Milli-Q water (3% Ag ⁺) 94% of initial Ag with detergent	
Laboratory prepared fabric (cotton with PES)	339 ± 11.00 µg Ag/g (nano-pad-dry-cure)		48% of initial Ag with Milli-Q water (2% Ag ⁺) 83% of initial Ag with detergent	
Laboratory prepared fabric (100% PES)	41.95 mg Ag/kg (100% citrate coated metallic silver)	Two scenarios were studied as direct washing and sunlight aging and washing. For sunlight aging, samples were exposed to artificial sunlight for 7 days. For washing, adapted ISO standard method (ISO 105-C06:2010) was applied with a model washing machine (Washtex-P Roaches 40 ± 2 rpm) for 0.5 g of fabric at 40 °C. PE balls were used to simulate physical stress and the washing cycle lasted 40 minutes. The volume of wash liquid was 20 mL and seven different commercial detergents were used (two liquid solutions with pH 9.3 and pH	<p>pH 3.1: 35.69 mg Ag/kg (7.27 ± 1.20 mg Ag⁺/kg)</p> <p>pH 8.9: 7.05 mg Ag/kg (0.11 ± 0.02 mg Ag⁺/kg)</p> <p>pH 9.2: 3.60 mg Ag/kg (0.10 ± 0.04 mg Ag⁺/kg)</p> <p>pH 9.3: 3.39 mg Ag/kg (0.06 ± 0.03 mg Ag⁺/kg)</p> <p>pH 10.1: 9.17 mg Ag/kg (0.01 ± 0.00 mg Ag⁺/kg)</p> <p>pH 10.9: 11.12 mg Ag/kg (0.16 ± 0.01 mg Ag⁺/kg)</p> <p>pH 11.4: 5.06 mg Ag/kg (0.05 ± 0.05 mg Ag⁺/kg)</p>	[9]
	33.59 mg Ag/kg (81% citrate coated nAg and 19% AgCl-NP)		<p>pH 3.1: 28.35 mg Ag/kg (32.86 ± 6.63 mg Ag⁺)</p> <p>pH 8.9: 19.11 mg Ag/kg (0.61 ± 0.97 mg Ag⁺)</p> <p>pH 9.2: 3.95 mg Ag/kg (1.16 ± 0.21 mg Ag⁺)</p> <p>pH 9.3: 8.40 mg Ag/kg (1.34 ± 1.38 mg Ag⁺)</p> <p>pH 10.1: 0.82 mg Ag/kg (0.12 ± 0.05 mg Ag⁺)</p> <p>pH 10.9: 2.77 mg Ag/kg (0.66 ± 0.61 mg Ag⁺)</p> <p>pH 11.4: 4.68 mg Ag/kg (0.23 ± 0.13 mg Ag⁺)</p>	

Product type (mass and composition <i>if available</i>)	Initial silver content (type and incorporation method <i>if available</i>)	Washing procedure and conditions	Ag release (speciation <i>if available</i>)	Ref.
	27.69 mg Ag/kg (73% PEG coated nAg and 24% AgCl-NP)	9.2; three powder with pH 11.4, pH 10.1 and pH 10.9; one industrial liquid with pH 8.9; and one industrial powder with pH 3.1)	<p>pH 3.1: 24.27 mg Ag/kg (22.19 ± 1.17 mg Ag⁺) pH 8.9: 21.87 mg Ag/kg (18.16 ± 3.61 mg Ag⁺) pH 9.2: 1.40 mg Ag/kg (0.78 ± 0.20 mg Ag⁺) pH 9.3: 0.78 mg Ag/kg (1.48 ± 0.95 mg Ag⁺) pH 10.1: 13.22 mg Ag/kg (0.17 ± 0.05 mg Ag⁺) pH 10.9: 21.00 mg Ag/kg (2.03 ± 0.97 mg Ag⁺) pH 11.4: 7.98 mg Ag/kg (0.46 ± 0.04 mg Ag⁺)</p>	
Sunlight aged sample-42.18 mg Ag/kg (100% citrate coated metallic silver)	<p>pH 3.1: 35.35 mg Ag/kg (5.79 ± 0.78 mg Ag⁺/kg) pH 8.9: 11.15 mg Ag/kg (1.41 ± 0.76 mg Ag⁺/kg) pH 9.2: 9.91 mg Ag/kg (0.06 ± 0.04 mg Ag⁺/kg) pH 9.3: 7.91 mg Ag/kg (0.23 ± 0.24 mg Ag⁺/kg) pH 10.1: 5.85 mg Ag/kg (0.03 ± 0.03 mg Ag⁺/kg) pH 10.9: 4.68 mg Ag/kg (0.24 ± 0.23 mg Ag⁺/kg) pH 11.4: 6.45 mg Ag/kg (0.01 ± 0.01 mg Ag⁺/kg)</p>			
Sunlight aged sample-33.59 mg Ag/kg (85% citrate coated nAg)	<p>pH 3.1: 25.30 mg Ag/kg (26.15 ± 2.00 mg Ag⁺/kg) pH 8.9: 10.68 mg Ag/kg (16.15 ± 2.00 mg Ag⁺/kg) pH 9.2: 7.05 mg Ag/kg (0.54 ± 0.21 mg Ag⁺/kg) pH 9.3: 6.28 mg Ag/kg (0.64 ± 0.21 mg Ag⁺/kg) pH 10.1: 6.02 mg Ag/kg (0.08 ± 0.02 mg Ag⁺/kg) pH 10.9: 11.49 mg Ag/kg (3.54 ± 0.81 mg Ag⁺/kg) pH 11.4: 4.92 mg Ag/kg (0.52 ± 0.20 mg Ag⁺/kg)</p>			
Sunlight aged sample-27.69 mg Ag/kg (96% PEG coated nAg)	<p>pH 3.1: 13.05 mg Ag/kg (12.36 ± 3.59 mg Ag⁺/kg) pH 8.9: 4.68 mg Ag/kg (1.35 ± 0.80 mg Ag⁺/kg) pH 9.2: 2.75 mg Ag/kg (0.38 ± 0.11 mg Ag⁺/kg) pH 9.3: 1.23 mg Ag/kg (0.26 ± 0.06 mg Ag⁺/kg) pH 10.1: 7.96 mg Ag/kg (1.07 ± 1.39 mg Ag⁺/kg) pH 10.9: 3.43 mg Ag/kg (0.80 ± 1.29 mg Ag⁺/kg)</p>			

Product type (mass and composition <i>if available</i>)	Initial silver content (type and incorporation method <i>if available</i>)	Washing procedure and conditions	Ag release (speciation <i>if available</i>)	Ref.
			pH 11.4: 2.73 mg Ag/kg (0.22 ± 0.06 mg Ag ⁺ /kg)	
Laboratory prepared fabric (100% PES)	14 mg Ag/kg (nano)	Adapted ISO standard method (ISO 105-C06:2010) was applied with Washtex-P Roaches (40 ± 2 rpm) laboratory washing machine for 45 minutes at 40 ± 2°C. Standard and bleaching detergents were used. PE balls were used to simulate physical stress.	pH 9.3 (one cycle): 10% of initial Ag pH 9.3 (ten cycles): 22% of initial Ag pH 10.2 (one cycle): 40% of initial Ag pH 10.2 (ten cycles): 82% of initial Ag	[10]
Laboratory prepared fabric (100% PES)	22.8 ± 0.1 µg Ag/g (nano- <i>covalently tethered</i>)	Adapted ISO standard method (ISO 105-C06:2010) was applied. Samples washed with AATCC 2003 detergent and water in 40 rpm mixer for 30 minutes. Glass beads were used to simulate physical stress. An additional scenario was studied to investigate the effect of light irradiation for passive release.	pH 7 (four cycles): 76% of initial Ag (18 ± 3 µg/g) pH 7 (six cycles): 90% of initial Ag (3.4 ± 0.1 µg/g more) (~92 % Ag ⁺) pH 8.5 (four cycles): 56% of initial Ag (13 ± 1 µg/g) (~31 % Ag ⁺) pH 8.5 (six cycles): 63% of initial Ag	[11]
Laboratory prepared fabric (100% PES)	1.07 ± 0.01 µg Ag/g (nano- <i>electrostatically attached</i>)		pH 7 (four cycles): 79% of initial Ag (0.79 ± 0.18 µg/g) pH 8.5 (four cycles): 58% of initial Ag (0.58 ± 0.12 µg/g)	
Shirt (PES)	16.4 ± 0.1 µg Ag/g (AgCl- <i>coated</i>)		pH 7 (four cycles): 19% of initial Ag (3.1 ± 0.7 µg/g) (~28 % Ag ⁺) pH 8.5 (four cycles): 18% of initial Ag (2.9 ± 0.1 µg/g) (~4 % Ag ⁺)	
Shirt (PES)	4,030 ± 60 µg Ag/g (metal- <i>coated</i>)		pH 7 (four cycles): 2.6% of initial Ag (106 ± 10 µg/g) (~80 % Ag ⁺) pH 8.5 (four cycles): 2.5% of initial Ag (101 ± 15 µg/g) (~22 % Ag ⁺)	
Fabric (100% cotton)	0.33% (AgCl and TiO ₂ - <i>pad-dry-cure</i>)	Washing procedure was conducted based on BS EN ISO 26330 Standard	92.27% of initial Ag	[12]

Product type (mass and composition if available)	Initial silver content (type and incorporation method if available)	Washing procedure and conditions	Ag release (speciation if available)	Ref.
Fabric (100% cotton)	0.37% (AgCl-NP- <i>pad-dry-cure</i>)	(5A) with Wascator machine and 4 g/L detergent at 40 °C for 20 cycles.	90.56% of initial Ag	
Fabric (100% cotton)	0.68% (Calcium phosphate-based silver ion-doped powder- <i>pad-dry-cure</i>)		73.43% of initial Ag	
Fabric (100% PES)	0.33% (AgCl and TiO ₂ - <i>pad-dry-cure</i>)		89.70% of initial Ag	
Fabric (100% PES)	0.37% (AgCl-NP- <i>pad-dry-cure</i>)		76.92% of initial Ag	
Fabric (100% PES)	0.68% (Calcium phosphate-based silver ion-doped powder- <i>pad-dry-cure</i>)		76.49% of initial Ag	
Sock (21 g)	4317 ± 144 mg Ag/kg (silver-electrolytically deposited layer on fiber)	Wearing and washing/rinsing procedures were applied. For wearing, two scenarios were investigated as walking for 28 hours/week (~ 8-16 km) and running for 1 hour/week (~ 15 km). For washing, adapted ISO 105-C06:2010 procedure was used. Wash water was prepared using Tide detergent and tap water (300 mL) and samples were washed for 45 minutes at 40 °C (150 rpm). As an extra scenario, PP balls were used to simulate artificial wearing. For rinsing, same procedure without the detergent was applied for three washing/rinsing cycles.	Unworn control: 16.3 mg Ag/kg sock (~ 86% nAg, 10.5% AgCl, 3.5% Ag ₂ O) Walking: First cycle: 46.6 mg Ag/kg sock Total (3 cycles): 159 mg Ag/kg sock (~91.76% nAg, 7.13% AgCl, %1.1 Ag ₂ O) Running: 38.6 mg Ag/kg sock (~98% nAg, 1% AgCl, 1% Ag ₂ O) Artificial wearing (PP balls): First cycle: 314 mg Ag/kg sock, Second cycle: 129 mg Ag/kg sock	[13]

PP: polypropylene, PA: polyamide, PEG: polyethylene glycol, PES: polyester.

Table E2. Literature on Ag/nAg release from textile products into artificial sweat (listed by the year of publication).

Product type (mass and composition <i>if available</i>)	Initial silver content (type and incorporation method <i>if available</i>)	Washing procedure and conditions	Ag release (speciation <i>if available</i>)	Ref.
Laboratory prepared fabric (100% cotton)	36.12 ± 22.42 mg Ag/kg (AgCl/TiO ₂ -coating)	Four different artificial sweat samples were used based on the following standards: ISO105-E04-2008E (pH 5.5-8.0), AATCC Test Method 15-2002 (pH 4.3), BS EN1811-1999 (pH 6.5). Fabrics were soaked in sweat samples and incubated at 37 °C for 24 hours.	pH 4.3: 21.01 ± 4.13 mg Ag/kg pH 5.5: 15.53 ± 3.62 mg Ag/kg pH 6.5: 35.83 ± 19.68 mg Ag/kg pH 8.0: 34.27 ± 2.88 mg Ag/kg	[14]
Laboratory prepared fabric (100% cotton)	56.57 ± 34.28 mg Ag/kg (AgCl/TiO ₂ -coating)		pH 4.3: 33.39 ± 15.80 mg Ag/kg pH 5.5: 28.81 ± 10.34 mg Ag/kg pH 6.5: 77.96 ± 23.80 mg Ag/kg pH 8.0: 66.54 ± 46.29 mg Ag/kg	
Laboratory prepared fabric (100% cotton)	95.12 ± 33.12 mg Ag/kg (AgCl/TiO ₂ -coating)		pH 4.3: 70.15 ± 37.29 mg Ag/kg pH 5.5: 72.69 ± 11.99 mg Ag/kg pH 6.5: 152.20 ± 36.54 mg Ag/kg pH 8.0: 82.22 ± 26.99 mg Ag/kg	
Laboratory prepared fabric (100% cotton)	425.21 ± 93.73 mg Ag/kg (AgCl/TiO ₂ -coating)		pH 4.3: 217.61 ± 81.32 mg Ag/kg pH 5.5: 177.13 ± 57.13 mg Ag/kg pH 6.5: 322.21 ± 87.00 mg Ag/kg pH 8.0: 268.31 ± 131.15 mg Ag/kg	
Shirt	15.16 ± 9.90 mg Ag/kg (nano)		pH 4.3: 0.08 ± 0.05 mg Ag/kg pH 5.5: 0.01 ± 0.01 mg Ag/kg pH 6.5: 0.36 ± 0.10 mg Ag/kg pH 8.0: 0.50 ± 0.30 mg Ag/kg	
Shirt	1.22 ± 0.87 mg Ag/kg (nano)		pH 6.5: 0.05 ± 0.00 mg Ag/kg	
Cloth (100% nylon)	16.97% (nano)		5 g of fabric was stirred with 200 rpm in simulated sweat samples. The volumes of wash liquids (artificial sweat based on ISO 105-E04) were 500 mL with pH of 3.0-8.5, and the	

Product type (mass and composition if available)	Initial silver content (type and incorporation method if available)	Washing procedure and conditions	Ag release (speciation if available)	Ref.
		washing cycle lasted for 15-250 minutes.	pH 8.5: 0.012% (15 min) – 0.018% (4 h) total Ag, consists of 85% Ag ⁺	
Shirt (89 g/male and 64 g/female; 83% PES, 17% wool)	183 ± 10 mg Ag/kg (nano)	Adapted ISO standard method (ISO 105-C06) was applied with a model washing machine (Washtex-P Roaches 40 ± 2 rpm) for 8.0 ± 0.2 g of fabric at 40 °C. The volume of wash liquid (artificial sweat based on ISO 105-E04) was 60-180 mL with a pH of 5.5-8.0. Acrylic plastic balls were used to simulate physical stress and the washing cycle lasted 30 minutes.	pH 5.5: 43 ± 1 µg/g/L Ag ⁺ ; 31 ± 5 µg/g/L nAg (< 450 nm); 30 ± 0 µg/g/L nAg (> 450 nm) pH 8.0: 31 ± 0 µg/g/L Ag ⁺ ; 34 ± 1 µg/g/L nAg (< 450 nm); 11 ± 1 µg/g/L nAg (> 450 nm)	[16]
Trousers (345 g/male and 300 g/female; 93% PA, 7% elastane)	41 ± 0 mg Ag/kg (AgCl-NP)		pH 5.5: 45 ± 5 µg/g/L Ag ⁺ pH 8.0: 25 ± 0 µg/g/L Ag ⁺ ; 23 ± 0 µg/g/L nAg (< 450 nm)	
Laboratory prepared fabric (PES, PA)	128.0 ± 12.3 mg Ag/kg (nano-integration into fiber)	Two different artificial sweat solutions were prepared based on ISO 105-E04 (pH 8 and pH 5.5). Samples were soaked in artificial sweat and incubated in 37 °C for 24-48 h.	pH 5.5 (1 d): 8.9 ± 1.4 mg/kg pH 5.5 (2 d): 2.5 mg/kg pH 8.0 (1 d): 10.5 ± 2.1 mg/kg pH 8.0 (2 d): 2.7 mg/kg	[17]
Laboratory prepared fabric (PES)	12.4 ± 0.3 mg Ag/kg (nano-coating)		pH 5.5 (1 d): 1.9 ± 0.3 mg/kg pH 8.0 (1 d): 2.1 ± 0.3 mg/kg	
Laboratory prepared fabric (PES)	26.6 ± 3.0 mg Ag/kg (AgCl-coating)		pH 5.5 (1 d): 19.9 ± 0.4 mg/kg pH 5.5 (2 d): 4.5 mg/kg pH 8.0 (1 d): 21.9 ± 5.6 mg/kg pH 8.0 (2 d): 4.6 mg/kg	
Shirt (PES)	14.2 ± 0.9 mg Ag/kg (silver-coating)		pH 5.5 (1 d): 5.5 ± 0.2 mg/kg pH 5.5 (2 d): 1.4 mg/kg pH 8.0 (1 d): 5.2 ± 0.1 mg/kg pH 8.0 (2 d): 1.6 mg/kg	
Socks (44 g/pair; cotton, spandex, nylon)	31.18-669.72 µg Ag/g (silver fiber)	Artificial sweat was prepared based on BS EN1811-1999 with a pH of 6.5, samples were soaked in 25 mL of	pH 6.5: 0.01% of initial Ag (~58% Ag ⁺) pH 10: 0.015% of initial Ag (~25% Ag ⁺)	[18]

Product type (mass and composition <i>if available</i>)	Initial silver content (type and incorporation method <i>if available</i>)	Washing procedure and conditions	Ag release (speciation <i>if available</i>)	Ref.
Socks (45.7 g/pair; cotton, PES, nylon, polyurethan)	10.84-45.83 µg Ag/g (nano)	liquid and stirred (150 rpm) at 37 °C for 1-4 h. For laundering scenario, sodium dodecyl sulfate was used as a detergent with a pH 10, samples were soaked in 25 mL of liquid and stirred (150 rpm) for 1 h. Then hydrogen peroxide was added as a bleach and stirred for 30 more minutes.	pH 6.5: 0.10% of initial Ag (~60% Ag ⁺) pH 10: 0.11% of initial Ag (~10% Ag ⁺)	
Shorts (75.3 g; cotton)	5.58-7.67 µg Ag/g (nano)		pH 6.5: 25.71% of initial Ag (~70% Ag ⁺) pH 10: 19.67% of initial Ag (~10% Ag ⁺)	
Textile (PES)	492 ± 21 µg Ag/g (silver- <i>electrolytically deposited layer on fiber</i>)	Based on AATCC Method 15, acidic (pH 3.5) and alkali (pH 8.0) artificial sweat solutions were used as a liquid. Samples were soaked in 20 mL of artificial sweat or deionized water and incubated at 37 °C for 60 minutes.	pH 3.5: 12.2 ± 0.7% of initial Ag pH 8.0: 41.0 ± 0.5% of initial Ag DI: 10.8 ± 0.5% of initial Ag	[19]
Textile (PES)	22.7 ± 1.3 µg Ag/g (AgCl)		pH 3.5: 18.9 ± 1.3% of initial Ag pH 8.0: 29.6 ± 2.1% of initial Ag DI: 10.5 ± 0.7% of initial Ag	
Laboratory prepared fabric (PES)	1.08 ± 0.19 µg Ag/g (nano- <i>electrostatic forces</i>)		pH 3.5: 40.0 ± 1.3% of initial Ag pH 8.0: 26.9 ± 4.8% of initial Ag DI: 13.8 ± 0.2% of initial Ag	
Laboratory prepared fabric (PES)	21.2 ± 1.2 µg Ag/g (nano- <i>proprietary</i>)		pH 3.5: 24.3 ± 1.7% of initial Ag pH 8.0: 16.0 ± 1.0% of initial Ag DI: 28.1 ± 3.6% of initial Ag	

PP: polypropylene, PA: polyamide, PEG: polyethylene glycol, PES: polyester

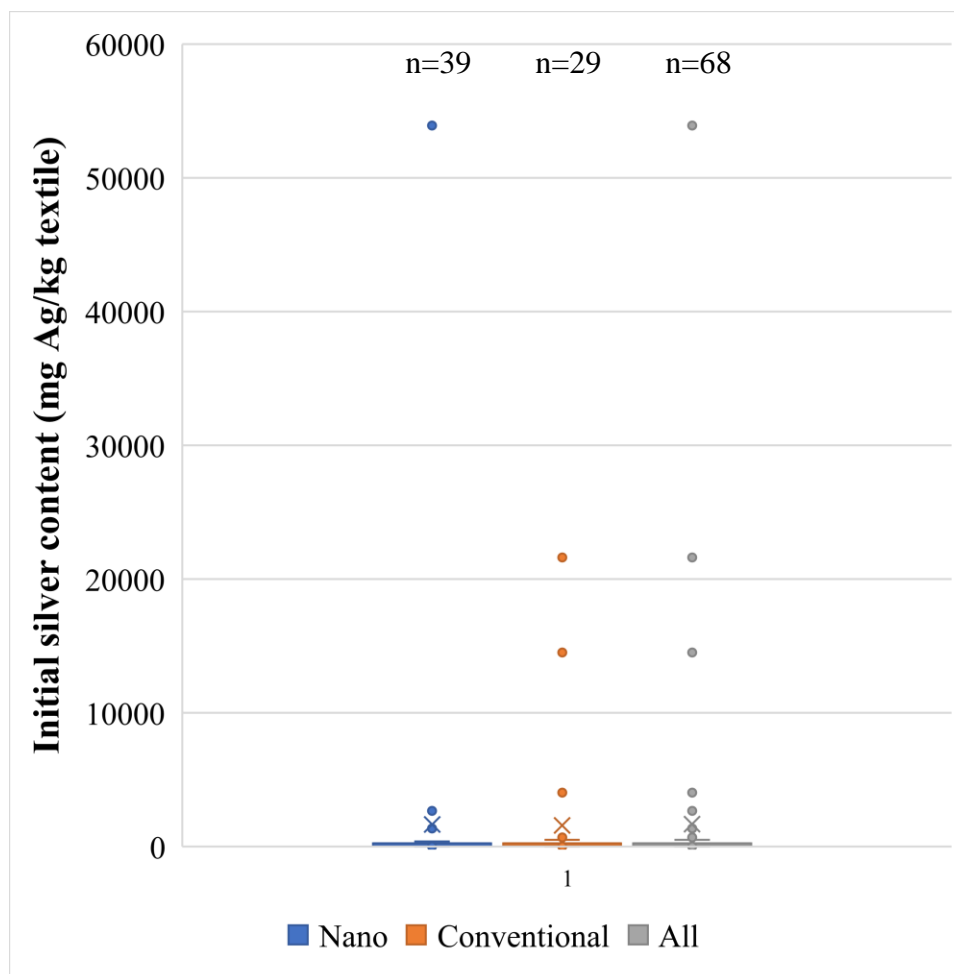


Figure E1. The range of the initial silver content in silver-enabled textiles based on the silver source (nano or conventional). n indicates the number of data points used to draw boxplots.

Table E3. Inventory data and assumptions used to model cradle-to-grave life cycle assessment.

Process	Input/flow	Unit	Value				Reference
			Product T	Product E	Product A	Product C	
nAg synthesis	nAg	µg	3,306	155.15	2,378	584,350	[20]
PES textile	PET	g	152.25	152.25	152.25	152.25	[21]
	Deionized water	kg	3.78	3.78	3.78	3.78	
	Electricity	kWh	3.01	3.01	3.01	3.01	
	Natural gas, heat	MJ	1.41	1.41	1.41	1.41	
Laundering with high efficiency washer/dryer	Electricity	kWh	0.713	0.713	0.713	0.713	[22, 23]
	Water	L	178	178	178	178	
	Detergent	mL	93	93	93	93	
Laundering with conventional efficiency washer/dryer	Electricity	kWh	7.2	7.2	7.2	7.2	[22, 23]
	Water	L	4.34	4.34	4.34	4.34	
	Detergent	mL	323	323	323	323	
Process	Output/flow	Unit	Value				Reference
			Product T	Product E	Product A	Product C	
Incineration	PES	g	7.25	7.25	7.25	7.25	[21]
Sewage	Water	m ³	0.0038	0.0038	0.0038	0.0038	[21]
Landfill	PES	g	145	145	145	145	[22]
Landfill leachate	Ag ⁺	g	N/A	N/A	N/A	327.3	This study
Wastewater treatment plant	Ag ₂ S	µg	137.20	6.44	98.69	15,194.19	This study
	Ag ⁺	µg	11.57	0.54	16.65	2,562.88	This study
	nAg	µg	11.57	0.54	N/A	N/A	This study
	Ag(0)	µg	4.96	0.23	3.57	549.19	This study
Biosolids	Ag ₂ S	µg	3,140.7	147.39	2,259.1	347,818.8	This study

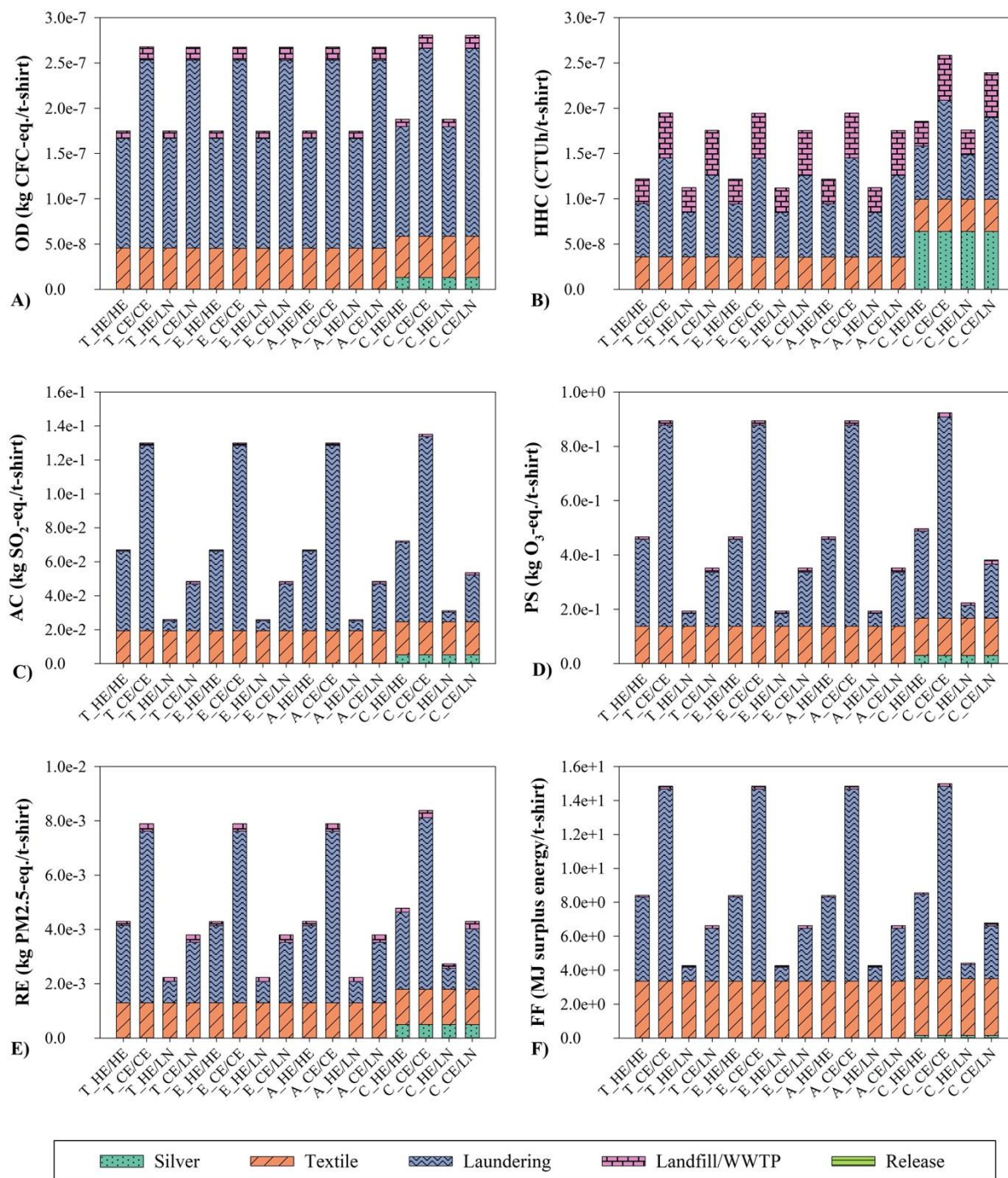


Figure E2. Environmental impacts of various silver enabled textiles under different laundering scenarios A) OD, B) HHC, C) AC, D) PS, E) RE and F) FF (x axis reads product code_type of washer/type of dryer, e.g. T_HE/LN means product T with high efficiency washer and line drying).

Table E4. (T) TRACI characterization results for 1 nAg-enabled T-shirt (145 g, covalently tethered) laundered with high efficiency washer and dryer.

T_HE_AP	Silver	Textile	Laundering	Landfill/WWTP	Release	Total
OD	7.81E-11	4.55E-08	1.21E-07	8.14E-09	-	1.75E-07
GW	1.44E-03	2.56E+00	5.58E+00	1.13E-01	-	8.26E+00
PS	1.80E-04	1.37E-01	3.20E-01	8.87E-03	-	4.67E-01
AC	3.08E-05	1.93E-02	4.69E-02	7.91E-04	-	6.70E-02
EU	2.03E-05	1.49E-03	2.17E-03	5.57E-03	-	9.25E-03
HHC	3.65E-10	3.55E-08	5.89E-08	2.74E-08	-	1.22E-07
HHNC	1.33E-08	1.85E-07	3.01E-07	3.09E-07	2.30E-07	1.04E-06
RE	2.95E-06	1.30E-03	2.84E-03	1.50E-04	-	4.30E-03
EC	1.17E-01	5.60E+00	9.21E+00	3.29E+00	3.49E-01	1.86E+01
FF	9.65E-04	3.35E+00	4.96E+00	9.11E-02	-	8.41E+00
T_HE_CR	Silver	Textile	Laundering	Landfill/WWTP	Release	Total
OD	1.20E-10	4.55E-08	1.21E-07	8.14E-09	-	1.75E-07
GW	1.70E-03	2.56E+00	5.58E+00	1.13E-01	-	8.26E+00
PS	1.92E-04	1.37E-01	3.20E-01	8.87E-03	-	4.67E-01
AC	3.14E-05	1.93E-02	4.69E-02	7.91E-04	-	6.70E-02
EU	2.04E-05	1.49E-03	2.17E-03	5.57E-03	-	9.25E-03
HHC	3.65E-10	3.55E-08	5.89E-08	2.74E-08	-	1.22E-07
HHNC	1.34E-08	1.85E-07	3.01E-07	3.09E-07	2.30E-07	1.04E-06
RE	2.92E-06	1.30E-03	2.84E-03	1.50E-04	-	4.30E-03
EC	1.17E-01	5.60E+00	9.21E+00	3.29E+00	3.49E-01	1.86E+01
FF	1.19E-03	3.35E+00	4.96E+00	9.11E-02	-	8.41E+00
T_HE_FSP	Silver	Textile	Laundering	Landfill/WWTP	Release	Total
OD	9.88E-11	4.55E-08	1.21E-07	8.14E-09	-	1.75E-07
GW	1.40E-03	2.56E+00	5.58E+00	1.13E-01	-	8.26E+00
PS	1.48E-04	1.37E-01	3.20E-01	8.87E-03	-	4.67E-01
AC	2.38E-05	1.93E-02	4.69E-02	7.91E-04	-	6.70E-02
EU	1.60E-05	1.49E-03	2.17E-03	5.57E-03	-	9.25E-03
HHC	2.84E-10	3.55E-08	5.89E-08	2.74E-08	-	1.22E-07
HHNC	1.01E-08	1.85E-07	3.01E-07	3.09E-07	2.30E-07	1.03E-06
RE	2.36E-06	1.30E-03	2.84E-03	1.50E-04	-	4.30E-03
EC	8.94E-02	5.60E+00	9.21E+00	3.29E+00	3.49E-01	1.85E+01
FF	1.25E-03	3.35E+00	4.96E+00	9.11E-02	-	8.41E+00

T_HE_Spark	Silver	Textile	Laundrying	Landfill/WWTP	Release	Total
OD	3.78E-10	4.55E-08	1.21E-07	8.14E-09	-	1.75E-07
GW	2.87E-03	2.56E+00	5.58E+00	1.13E-01	-	8.26E+00
PS	2.30E-04	1.37E-01	3.20E-01	8.87E-03	-	4.67E-01
AC	3.94E-05	1.93E-02	4.69E-02	7.91E-04	-	6.70E-02
EU	2.29E-05	1.49E-03	2.17E-03	5.57E-03	-	9.25E-03
HHC	3.92E-10	3.55E-08	5.89E-08	2.74E-08	-	1.22E-07
HHNC	1.35E-08	1.85E-07	3.01E-07	3.09E-07	2.30E-07	1.04E-06
RE	4.45E-06	1.30E-03	2.84E-03	1.50E-04	-	4.30E-03
EC	1.20E-01	5.60E+00	9.21E+00	3.29E+00	3.49E-01	1.86E+01
FF	1.96E-03	3.35E+00	4.96E+00	9.11E-02	-	8.41E+00
T_HE_AVG	Silver	Textile	Laundrying	Landfill/WWTP	Release	Total
OD	1.69E-10	4.55E-08	1.21E-07	8.14E-09	-	1.75E-07
GW	1.85E-03	2.56E+00	5.58E+00	1.13E-01	-	8.26E+00
PS	1.87E-04	1.37E-01	3.20E-01	8.87E-03	-	4.67E-01
AC	3.14E-05	1.93E-02	4.69E-02	7.91E-04	-	6.70E-02
EU	1.99E-05	1.49E-03	2.17E-03	5.57E-03	-	9.25E-03
HHC	3.51E-10	3.55E-08	5.89E-08	2.74E-08	-	1.22E-07
HHNC	1.26E-08	1.85E-07	3.01E-07	3.09E-07	2.30E-07	1.04E-06
RE	3.17E-06	1.30E-03	2.84E-03	1.50E-04	-	4.30E-03
EC	1.11E-01	5.60E+00	9.21E+00	3.29E+00	3.49E-01	1.85E+01
FF	1.34E-03	3.35E+00	4.96E+00	9.11E-02	-	8.41E+00

Table E5. (T) TRACI characterization results for 1 nAg-enabled T-shirt (145 g, covalently tethered) laundered with conventional efficiency washer and dryer.

T_CE_AP	Silver	Textile	Laundering	Landfill/WWTP	Release	Total
OD	7.81E-11	4.55E-08	2.08E-07	1.45E-08	-	2.68E-07
GW	1.44E-03	2.56E+00	1.29E+01	1.93E-01	-	1.57E+01
PS	1.80E-04	1.37E-01	7.41E-01	1.59E-02	-	8.94E-01
AC	3.08E-05	1.93E-02	1.09E-01	1.43E-03	-	1.30E-01
EU	2.03E-05	1.49E-03	4.00E-03	1.01E-02	-	1.56E-02
HHC	3.65E-10	3.55E-08	1.09E-07	4.96E-08	-	1.95E-07
HHNC	1.33E-08	1.85E-07	6.25E-07	5.59E-07	2.30E-07	1.61E-06
RE	2.95E-06	1.30E-03	6.32E-03	2.72E-04	-	7.90E-03
EC	1.17E-01	5.60E+00	1.76E+01	5.63E+00	3.49E-01	2.93E+01
FF	9.65E-04	3.35E+00	1.13E+01	1.63E-01	-	1.48E+01
T_CE_CR	Silver	Textile	Laundering	Landfill/WWTP	Release	Total
OD	1.20E-10	4.55E-08	2.08E-07	1.45E-08	-	2.68E-07
GW	1.70E-03	2.56E+00	1.29E+01	1.93E-01	-	1.57E+01
PS	1.92E-04	1.37E-01	7.41E-01	1.59E-02	-	8.94E-01
AC	3.14E-05	1.93E-02	1.09E-01	1.43E-03	-	1.30E-01
EU	2.04E-05	1.49E-03	4.00E-03	1.01E-02	-	1.56E-02
HHC	3.65E-10	3.55E-08	1.09E-07	4.96E-08	-	1.95E-07
HHNC	1.34E-08	1.85E-07	6.25E-07	5.59E-07	2.30E-07	1.61E-06
RE	2.92E-06	1.30E-03	6.32E-03	2.72E-04	-	7.90E-03
EC	1.17E-01	5.60E+00	1.76E+01	5.63E+00	3.49E-01	2.93E+01
FF	1.19E-03	3.35E+00	1.13E+01	1.63E-01	-	1.48E+01
T_CE_FSP	Silver	Textile	Laundering	Landfill/WWTP	Release	Total
OD	9.88E-11	4.55E-08	2.08E-07	1.45E-08	-	2.68E-07
GW	1.40E-03	2.56E+00	1.29E+01	1.93E-01	-	1.57E+01
PS	1.48E-04	1.37E-01	7.41E-01	1.59E-02	-	8.94E-01
AC	2.38E-05	1.93E-02	1.09E-01	1.43E-03	-	1.30E-01
EU	1.60E-05	1.49E-03	4.00E-03	1.01E-02	-	1.56E-02
HHC	2.84E-10	3.55E-08	1.09E-07	4.96E-08	-	1.95E-07
HHNC	1.01E-08	1.85E-07	6.25E-07	5.59E-07	2.30E-07	1.61E-06
RE	2.36E-06	1.30E-03	6.32E-03	2.72E-04	-	7.90E-03
EC	8.94E-02	5.60E+00	1.76E+01	5.63E+00	3.49E-01	2.93E+01
FF	1.25E-03	3.35E+00	1.13E+01	1.63E-01	-	1.48E+01

T_CE_Spark	Silver	Textile	Laundrying	Landfill/WWTP	Release	Total
OD	3.78E-10	4.55E-08	2.08E-07	1.45E-08	-	2.68E-07
GW	2.87E-03	2.56E+00	1.29E+01	1.93E-01	-	1.57E+01
PS	2.30E-04	1.37E-01	7.41E-01	1.59E-02	-	8.94E-01
AC	3.94E-05	1.93E-02	1.09E-01	1.43E-03	-	1.30E-01
EU	2.29E-05	1.49E-03	4.00E-03	1.01E-02	-	1.56E-02
HHC	3.92E-10	3.55E-08	1.09E-07	4.96E-08	-	1.95E-07
HHNC	1.35E-08	1.85E-07	6.25E-07	5.59E-07	2.30E-07	1.61E-06
RE	4.45E-06	1.30E-03	6.32E-03	2.72E-04	-	7.90E-03
EC	1.20E-01	5.60E+00	1.76E+01	5.63E+00	3.49E-01	2.93E+01
FF	1.96E-03	3.35E+00	1.13E+01	1.63E-01	-	1.48E+01
T_CE_AVG	Silver	Textile	Laundrying	Landfill/WWTP	Release	Total
OD	1.69E-10	4.55E-08	2.08E-07	1.45E-08	-	2.68E-07
GW	1.85E-03	2.56E+00	1.29E+01	1.93E-01	-	1.57E+01
PS	1.87E-04	1.37E-01	7.41E-01	1.59E-02	-	8.94E-01
AC	3.14E-05	1.93E-02	1.09E-01	1.43E-03	-	1.30E-01
EU	1.99E-05	1.49E-03	4.00E-03	1.01E-02	-	1.56E-02
HHC	3.51E-10	3.55E-08	1.09E-07	4.96E-08	-	1.95E-07
HHNC	1.26E-08	1.85E-07	6.25E-07	5.59E-07	2.30E-07	1.61E-06
RE	3.17E-06	1.30E-03	6.32E-03	2.72E-04	-	7.90E-03
EC	1.11E-01	5.60E+00	1.76E+01	5.63E+00	3.49E-01	2.93E+01
FF	1.34E-03	3.35E+00	1.13E+01	1.63E-01	-	1.48E+01

Table E6. (T) TRACI characterization results for 1 nAg-enabled T-shirt (145 g, covalently tethered) laundered with high efficiency washer and line drying.

T_HE_LN_AP	Silver	Textile	Laundering	Landfill/WWTP	Release	Total
OD	7.81E-11	4.55E-08	1.21E-07	8.14E-09	-	1.75E-07
GW	1.44E-03	2.56E+00	8.14E-01	1.13E-01	-	3.49E+00
PS	1.80E-04	1.37E-01	4.74E-02	8.87E-03	-	1.94E-01
AC	3.08E-05	1.93E-02	5.81E-03	7.91E-04	-	2.60E-02
EU	2.03E-05	1.49E-03	1.62E-03	5.57E-03	-	8.70E-03
HHC	3.65E-10	3.55E-08	4.92E-08	2.74E-08	-	1.12E-07
HHNC	1.33E-08	1.85E-07	1.39E-07	3.09E-07	2.30E-07	8.76E-07
RE	2.95E-06	1.30E-03	7.84E-04	1.50E-04	-	2.24E-03
EC	1.17E-01	5.60E+00	6.85E+00	3.29E+00	3.49E-01	1.62E+01
FF	9.65E-04	3.35E+00	8.28E-01	9.11E-02	-	4.27E+00
T_HE_LN_CR	Silver	Textile	Laundering	Landfill/WWTP	Release	Total
OD	1.20E-10	4.55E-08	1.21E-07	8.14E-09	-	1.75E-07
GW	1.70E-03	2.56E+00	8.14E-01	1.13E-01	-	3.49E+00
PS	1.92E-04	1.37E-01	4.74E-02	8.87E-03	-	1.94E-01
AC	3.14E-05	1.93E-02	5.81E-03	7.91E-04	-	2.60E-02
EU	2.04E-05	1.49E-03	1.62E-03	5.57E-03	-	8.70E-03
HHC	3.65E-10	3.55E-08	4.92E-08	2.74E-08	-	1.12E-07
HHNC	1.34E-08	1.85E-07	1.39E-07	3.09E-07	2.30E-07	8.76E-07
RE	2.92E-06	1.30E-03	7.84E-04	1.50E-04	-	2.24E-03
EC	1.17E-01	5.60E+00	6.85E+00	3.29E+00	3.49E-01	1.62E+01
FF	1.19E-03	3.35E+00	8.28E-01	9.11E-02	-	4.27E+00
T_HE_LN_FSP	Silver	Textile	Laundering	Landfill/WWTP	Release	Total
OD	9.88E-11	4.55E-08	1.21E-07	8.14E-09	-	1.75E-07
GW	1.40E-03	2.56E+00	8.14E-01	1.13E-01	-	3.49E+00
PS	1.48E-04	1.37E-01	4.74E-02	8.87E-03	-	1.94E-01
AC	2.38E-05	1.93E-02	5.81E-03	7.91E-04	-	2.60E-02
EU	1.60E-05	1.49E-03	1.62E-03	5.57E-03	-	8.69E-03
HHC	2.84E-10	3.55E-08	4.92E-08	2.74E-08	-	1.12E-07
HHNC	1.01E-08	1.85E-07	1.39E-07	3.09E-07	2.30E-07	8.73E-07
RE	2.36E-06	1.30E-03	7.84E-04	1.50E-04	-	2.24E-03
EC	8.94E-02	5.60E+00	6.85E+00	3.29E+00	3.49E-01	1.62E+01
FF	1.25E-03	3.35E+00	8.28E-01	9.11E-02	-	4.27E+00

T_HE_LN_Spark	Silver	Textile	Laundrying	Landfill/WWTP	Release	Total
OD	3.78E-10	4.55E-08	1.21E-07	8.14E-09	-	1.75E-07
GW	2.87E-03	2.56E+00	8.14E-01	1.13E-01	-	3.49E+00
PS	2.30E-04	1.37E-01	4.74E-02	8.87E-03	-	1.94E-01
AC	3.94E-05	1.93E-02	5.81E-03	7.91E-04	-	2.60E-02
EU	2.29E-05	1.49E-03	1.62E-03	5.57E-03	-	8.70E-03
HHC	3.92E-10	3.55E-08	4.92E-08	2.74E-08	-	1.13E-07
HHNC	1.35E-08	1.85E-07	1.39E-07	3.09E-07	2.30E-07	8.76E-07
RE	4.45E-06	1.30E-03	7.84E-04	1.50E-04	-	2.24E-03
EC	1.20E-01	5.60E+00	6.85E+00	3.29E+00	3.49E-01	1.62E+01
FF	1.96E-03	3.35E+00	8.28E-01	9.11E-02	-	4.27E+00
T_HE_LN_AVG	Silver	Textile	Laundrying	Landfill/WWTP	Release	Total
OD	1.69E-10	4.55E-08	1.21E-07	8.14E-09	-	1.75E-07
GW	1.85E-03	2.56E+00	8.14E-01	1.13E-01	-	3.49E+00
PS	1.87E-04	1.37E-01	4.74E-02	8.87E-03	-	1.94E-01
AC	3.14E-05	1.93E-02	5.81E-03	7.91E-04	-	2.60E-02
EU	1.99E-05	1.49E-03	1.62E-03	5.57E-03	-	8.70E-03
HHC	3.51E-10	3.55E-08	4.92E-08	2.74E-08	-	1.12E-07
HHNC	1.26E-08	1.85E-07	1.39E-07	3.09E-07	2.30E-07	8.75E-07
RE	3.17E-06	1.30E-03	7.84E-04	1.50E-04	-	2.24E-03
EC	1.11E-01	5.60E+00	6.85E+00	3.29E+00	3.49E-01	1.62E+01
FF	1.34E-03	3.35E+00	8.28E-01	9.11E-02	-	4.27E+00

Table E7. (T) TRACI characterization results for 1 nAg-enabled T-shirt (145 g, covalently tethered) laundered with conventional efficiency washer and line drying.

T_CE_LN_AP	Silver	Textile	Laundering	Landfill/WWTP	Release	Total
OD	7.81E-11	4.55E-08	2.07E-07	1.45E-08	-	2.67E-07
GW	1.44E-03	2.56E+00	3.44E+00	1.93E-01	-	6.20E+00
PS	1.80E-04	1.37E-01	1.98E-01	1.59E-02	-	3.52E-01
AC	3.08E-05	1.93E-02	2.76E-02	1.43E-03	-	4.84E-02
EU	2.03E-05	1.49E-03	2.90E-03	1.01E-02	-	1.45E-02
HHC	3.65E-10	3.55E-08	9.02E-08	4.96E-08	-	1.76E-07
HHNC	1.33E-08	1.85E-07	3.03E-07	5.59E-07	2.30E-07	1.29E-06
RE	2.95E-06	1.30E-03	2.23E-03	2.72E-04	-	3.80E-03
EC	1.17E-01	5.60E+00	1.29E+01	5.63E+00	3.49E-01	2.46E+01
FF	9.65E-04	3.35E+00	3.11E+00	1.63E-01	-	6.63E+00
T_CE_LN_CR	Silver	Textile	Laundering	Landfill/WWTP	Release	Total
OD	1.20E-10	4.55E-08	2.07E-07	1.45E-08	-	2.68E-07
GW	1.70E-03	2.56E+00	3.44E+00	1.93E-01	-	6.20E+00
PS	1.92E-04	1.37E-01	1.98E-01	1.59E-02	-	3.52E-01
AC	3.14E-05	1.93E-02	2.76E-02	1.43E-03	-	4.84E-02
EU	2.04E-05	1.49E-03	2.90E-03	1.01E-02	-	1.45E-02
HHC	3.65E-10	3.55E-08	9.02E-08	4.96E-08	-	1.76E-07
HHNC	1.34E-08	1.85E-07	3.03E-07	5.59E-07	2.30E-07	1.29E-06
RE	2.92E-06	1.30E-03	2.23E-03	2.72E-04	-	3.80E-03
EC	1.17E-01	5.60E+00	1.29E+01	5.63E+00	3.49E-01	2.46E+01
FF	1.19E-03	3.35E+00	3.11E+00	1.63E-01	-	6.63E+00
T_CE_LN_FSP	Silver	Textile	Laundering	Landfill/WWTP	Release	Total
OD	9.88E-11	4.55E-08	2.07E-07	1.45E-08	-	2.68E-07
GW	1.40E-03	2.56E+00	3.44E+00	1.93E-01	-	6.20E+00
PS	1.48E-04	1.37E-01	1.98E-01	1.59E-02	-	3.52E-01
AC	2.38E-05	1.93E-02	2.76E-02	1.43E-03	-	4.84E-02
EU	1.60E-05	1.49E-03	2.90E-03	1.01E-02	-	1.45E-02
HHC	2.84E-10	3.55E-08	9.02E-08	4.96E-08	-	1.76E-07
HHNC	1.01E-08	1.85E-07	3.03E-07	5.59E-07	2.30E-07	1.29E-06
RE	2.36E-06	1.30E-03	2.23E-03	2.72E-04	-	3.80E-03
EC	8.94E-02	5.60E+00	1.29E+01	5.63E+00	3.49E-01	2.46E+01
FF	1.25E-03	3.35E+00	3.11E+00	1.63E-01	-	6.63E+00

T_CE_LN_Spark	Silver	Textile	Laundrying	Landfill/WWTP	Release	Total
OD	3.78E-10	4.55E-08	2.07E-07	1.45E-08	-	2.68E-07
GW	2.87E-03	2.56E+00	3.44E+00	1.93E-01	-	6.20E+00
PS	2.30E-04	1.37E-01	1.98E-01	1.59E-02	-	3.52E-01
AC	3.94E-05	1.93E-02	2.76E-02	1.43E-03	-	4.84E-02
EU	2.29E-05	1.49E-03	2.90E-03	1.01E-02	-	1.45E-02
HHC	3.92E-10	3.55E-08	9.02E-08	4.96E-08	-	1.76E-07
HHNC	1.35E-08	1.85E-07	3.03E-07	5.59E-07	2.30E-07	1.29E-06
RE	4.45E-06	1.30E-03	2.23E-03	2.72E-04	-	3.80E-03
EC	1.20E-01	5.60E+00	1.29E+01	5.63E+00	3.49E-01	2.46E+01
FF	1.96E-03	3.35E+00	3.11E+00	1.63E-01	-	6.63E+00
T_CE_LN_AVG	Silver	Textile	Laundrying	Landfill/WWTP	Release	Total
OD	1.69E-10	4.55E-08	2.07E-07	1.45E-08	-	2.68E-07
GW	1.85E-03	2.56E+00	3.44E+00	1.93E-01	-	6.20E+00
PS	1.87E-04	1.37E-01	1.98E-01	1.59E-02	-	3.52E-01
AC	3.14E-05	1.93E-02	2.76E-02	1.43E-03	-	4.84E-02
EU	1.99E-05	1.49E-03	2.90E-03	1.01E-02	-	1.45E-02
HHC	3.51E-10	3.55E-08	9.02E-08	4.96E-08	-	1.76E-07
HHNC	1.26E-08	1.85E-07	3.03E-07	5.59E-07	2.30E-07	1.29E-06
RE	3.17E-06	1.30E-03	2.23E-03	2.72E-04	-	3.80E-03
EC	1.11E-01	5.60E+00	1.29E+01	5.63E+00	3.49E-01	2.46E+01
FF	1.34E-03	3.35E+00	3.11E+00	1.63E-01	-	6.63E+00

Table E8. (E) TRACI characterization results for 1 nAg-enabled T-shirt (145 g, electrostatically attached) laundered with high efficiency washer and dryer.

E_HE_AP	Silver	Textile	Laundering	Landfill/WWTP	Release	Total
OD	3.66E-12	4.55E-08	1.21E-07	8.14E-09	-	1.75E-07
GW	6.77E-05	2.56E+00	5.58E+00	1.13E-01	-	8.26E+00
PS	8.45E-06	1.37E-01	3.20E-01	8.87E-03	-	4.67E-01
AC	1.45E-06	1.93E-02	4.69E-02	7.91E-04	-	6.70E-02
EU	9.53E-07	1.49E-03	2.17E-03	5.57E-03	-	9.23E-03
HHC	1.71E-11	3.55E-08	5.89E-08	2.74E-08	-	1.22E-07
HHNC	6.26E-10	1.85E-07	3.01E-07	3.09E-07	1.08E-08	8.06E-07
RE	1.39E-07	1.30E-03	2.84E-03	1.50E-04	-	4.29E-03
EC	5.49E-03	5.60E+00	9.21E+00	3.29E+00	1.64E-02	1.81E+01
FF	4.53E-05	3.35E+00	4.96E+00	9.11E-02	-	8.41E+00
E_HE_CR	Silver	Textile	Laundering	Landfill/WWTP	Release	Total
OD	5.64E-12	4.55E-08	1.21E-07	8.14E-09	-	1.75E-07
GW	7.97E-05	2.56E+00	5.58E+00	1.13E-01	-	8.26E+00
PS	9.02E-06	1.37E-01	3.20E-01	8.87E-03	-	4.67E-01
AC	1.48E-06	1.93E-02	4.69E-02	7.91E-04	-	6.70E-02
EU	9.59E-07	1.49E-03	2.17E-03	5.57E-03	-	9.23E-03
HHC	1.71E-11	3.55E-08	5.89E-08	2.74E-08	-	1.22E-07
HHNC	6.29E-10	1.85E-07	3.01E-07	3.09E-07	1.08E-08	8.06E-07
RE	1.37E-07	1.30E-03	2.84E-03	1.50E-04	-	4.29E-03
EC	5.50E-03	5.60E+00	9.21E+00	3.29E+00	1.64E-02	1.81E+01
FF	5.60E-05	3.35E+00	4.96E+00	9.11E-02	-	8.41E+00
E_HE_FSP	Silver	Textile	Laundering	Landfill/WWTP	Release	Total
OD	4.63E-12	4.55E-08	1.21E-07	8.14E-09	-	1.75E-07
GW	6.57E-05	2.56E+00	5.58E+00	1.13E-01	-	8.26E+00
PS	6.93E-06	1.37E-01	3.20E-01	8.87E-03	-	4.67E-01
AC	1.12E-06	1.93E-02	4.69E-02	7.91E-04	-	6.70E-02
EU	7.52E-07	1.49E-03	2.17E-03	5.57E-03	-	9.23E-03
HHC	1.33E-11	3.55E-08	5.89E-08	2.74E-08	-	1.22E-07
HHNC	4.73E-10	1.85E-07	3.01E-07	3.09E-07	1.08E-08	8.06E-07
RE	1.11E-07	1.30E-03	2.84E-03	1.50E-04	-	4.29E-03
EC	4.20E-03	5.60E+00	9.21E+00	3.29E+00	1.64E-02	1.81E+01
FF	5.85E-05	3.35E+00	4.96E+00	9.11E-02	-	8.41E+00

E_HE_Spark	Silver	Textile	Laundrying	Landfill/WWTP	Release	Total
OD	1.77E-11	4.55E-08	1.21E-07	8.14E-09	-	1.75E-07
GW	1.35E-04	2.56E+00	5.58E+00	1.13E-01	-	8.26E+00
PS	1.08E-05	1.37E-01	3.20E-01	8.87E-03	-	4.67E-01
AC	1.85E-06	1.93E-02	4.69E-02	7.91E-04	-	6.70E-02
EU	1.07E-06	1.49E-03	2.17E-03	5.57E-03	-	9.23E-03
HHC	1.84E-11	3.55E-08	5.89E-08	2.74E-08	-	1.22E-07
HHNC	6.32E-10	1.85E-07	3.01E-07	3.09E-07	1.08E-08	8.06E-07
RE	2.09E-07	1.30E-03	2.84E-03	1.50E-04	-	4.29E-03
EC	5.65E-03	5.60E+00	9.21E+00	3.29E+00	1.64E-02	1.81E+01
FF	9.17E-05	3.35E+00	4.96E+00	9.11E-02	-	8.41E+00
E_HE_AVG	Silver	Textile	Laundrying	Landfill/WWTP	Release	Total
OD	7.91E-12	4.55E-08	1.21E-07	8.14E-09	-	1.75E-07
GW	8.69E-05	2.56E+00	5.58E+00	1.13E-01	-	8.26E+00
PS	8.80E-06	1.37E-01	3.20E-01	8.87E-03	-	4.67E-01
AC	1.47E-06	1.93E-02	4.69E-02	7.91E-04	-	6.70E-02
EU	9.34E-07	1.49E-03	2.17E-03	5.57E-03	-	9.23E-03
HHC	1.65E-11	3.55E-08	5.89E-08	2.74E-08	-	1.22E-07
HHNC	5.90E-10	1.85E-07	3.01E-07	3.09E-07	1.08E-08	8.06E-07
RE	1.49E-07	1.30E-03	2.84E-03	1.50E-04	-	4.29E-03
EC	5.21E-03	5.60E+00	9.21E+00	3.29E+00	1.64E-02	1.81E+01
FF	6.29E-05	3.35E+00	4.96E+00	9.11E-02	-	8.41E+00

Table E9. (E) TRACI characterization results for 1 nAg-enabled T-shirt (145 g, electrostatically attached) laundered with conventional efficiency washer and dryer.

E_CE_AP	Silver	Textile	Laundering	Landfill/WWTP	Release	Total
OD	3.66E-12	4.55E-08	2.08E-07	1.45E-08	-	2.68E-07
GW	6.77E-05	2.56E+00	1.29E+01	1.93E-01	-	1.57E+01
PS	8.45E-06	1.37E-01	7.41E-01	1.59E-02	-	8.94E-01
AC	1.45E-06	1.93E-02	1.09E-01	1.43E-03	-	1.30E-01
EU	9.53E-07	1.49E-03	4.00E-03	1.01E-02	-	1.56E-02
HHC	1.71E-11	3.55E-08	1.09E-07	4.96E-08	-	1.95E-07
HHNC	6.26E-10	1.85E-07	6.25E-07	5.59E-07	1.08E-08	1.38E-06
RE	1.39E-07	1.30E-03	6.32E-03	2.72E-04	-	7.89E-03
EC	5.49E-03	5.60E+00	1.76E+01	5.63E+00	1.64E-02	2.89E+01
FF	4.53E-05	3.35E+00	1.13E+01	1.63E-01	-	1.48E+01
E_CE_CR	Silver	Textile	Laundering	Landfill/WWTP	Release	Total
OD	5.64E-12	4.55E-08	2.08E-07	1.45E-08	-	2.68E-07
GW	7.97E-05	2.56E+00	1.29E+01	1.93E-01	-	1.57E+01
PS	9.02E-06	1.37E-01	7.41E-01	1.59E-02	-	8.94E-01
AC	1.48E-06	1.93E-02	1.09E-01	1.43E-03	-	1.30E-01
EU	9.59E-07	1.49E-03	4.00E-03	1.01E-02	-	1.56E-02
HHC	1.71E-11	3.55E-08	1.09E-07	4.96E-08	-	1.95E-07
HHNC	6.29E-10	1.85E-07	6.25E-07	5.59E-07	1.08E-08	1.38E-06
RE	1.37E-07	1.30E-03	6.32E-03	2.72E-04	-	7.89E-03
EC	5.50E-03	5.60E+00	1.76E+01	5.63E+00	1.64E-02	2.89E+01
FF	5.60E-05	3.35E+00	1.13E+01	1.63E-01	-	1.48E+01
E_CE_FSP	Silver	Textile	Laundering	Landfill/WWTP	Release	Total
OD	4.63E-12	4.55E-08	2.08E-07	1.45E-08	-	2.68E-07
GW	6.57E-05	2.56E+00	1.29E+01	1.93E-01	-	1.57E+01
PS	6.93E-06	1.37E-01	7.41E-01	1.59E-02	-	8.94E-01
AC	1.12E-06	1.93E-02	1.09E-01	1.43E-03	-	1.30E-01
EU	7.52E-07	1.49E-03	4.00E-03	1.01E-02	-	1.56E-02
HHC	1.33E-11	3.55E-08	1.09E-07	4.96E-08	-	1.95E-07
HHNC	4.73E-10	1.85E-07	6.25E-07	5.59E-07	1.08E-08	1.38E-06
RE	1.11E-07	1.30E-03	6.32E-03	2.72E-04	-	7.89E-03
EC	4.20E-03	5.60E+00	1.76E+01	5.63E+00	1.64E-02	2.89E+01
FF	5.85E-05	3.35E+00	1.13E+01	1.63E-01	-	1.48E+01

E_CE_Spark	Silver	Textile	Laundrying	Landfill/WWTP	Release	Total
OD	1.77E-11	4.55E-08	2.08E-07	1.45E-08	-	2.68E-07
GW	1.35E-04	2.56E+00	1.29E+01	1.93E-01	-	1.57E+01
PS	1.08E-05	1.37E-01	7.41E-01	1.59E-02	-	8.94E-01
AC	1.85E-06	1.93E-02	1.09E-01	1.43E-03	-	1.30E-01
EU	1.07E-06	1.49E-03	4.00E-03	1.01E-02	-	1.56E-02
HHC	1.84E-11	3.55E-08	1.09E-07	4.96E-08	-	1.95E-07
HHNC	6.32E-10	1.85E-07	6.25E-07	5.59E-07	1.08E-08	1.38E-06
RE	2.09E-07	1.30E-03	6.32E-03	2.72E-04	-	7.89E-03
EC	5.65E-03	5.60E+00	1.76E+01	5.63E+00	1.64E-02	2.89E+01
FF	9.17E-05	3.35E+00	1.13E+01	1.63E-01	-	1.48E+01
E_CE_AVG	Silver	Textile	Laundrying	Landfill/WWTP	Release	Total
OD	7.91E-12	4.55E-08	2.08E-07	1.45E-08	-	2.68E-07
GW	8.69E-05	2.56E+00	1.29E+01	1.93E-01	-	1.57E+01
PS	8.80E-06	1.37E-01	7.41E-01	1.59E-02	-	8.94E-01
AC	1.47E-06	1.93E-02	1.09E-01	1.43E-03	-	1.30E-01
EU	9.34E-07	1.49E-03	4.00E-03	1.01E-02	-	1.56E-02
HHC	1.65E-11	3.55E-08	1.09E-07	4.96E-08	-	1.95E-07
HHNC	5.90E-10	1.85E-07	6.25E-07	5.59E-07	1.08E-08	1.38E-06
RE	1.49E-07	1.30E-03	6.32E-03	2.72E-04	-	7.89E-03
EC	5.21E-03	5.60E+00	1.76E+01	5.63E+00	1.64E-02	2.89E+01
FF	6.29E-05	3.35E+00	1.13E+01	1.63E-01	-	1.48E+01

Table E10. (E) TRACI characterization results for 1 nAg-enabled T-shirt (145 g, electrostatically attached) laundered with high efficiency washer and line drying.

E_HE_LN_AP	Silver	Textile	Laundering	Landfill/WWTP	Release	Total
OD	3.66E-12	4.55E-08	1.21E-07	8.14E-09	-	1.75E-07
GW	6.77E-05	2.56E+00	8.14E-01	1.13E-01	-	3.49E+00
PS	8.45E-06	1.37E-01	4.74E-02	8.87E-03	-	1.94E-01
AC	1.45E-06	1.93E-02	5.81E-03	7.91E-04	-	2.59E-02
EU	9.53E-07	1.49E-03	1.62E-03	5.57E-03	-	8.68E-03
HHC	1.71E-11	3.55E-08	4.92E-08	2.74E-08	-	1.12E-07
HHNC	6.26E-10	1.85E-07	1.39E-07	3.09E-07	1.08E-08	6.44E-07
RE	1.39E-07	1.30E-03	7.84E-04	1.50E-04	-	2.23E-03
EC	5.49E-03	5.60E+00	6.85E+00	3.29E+00	1.64E-02	1.58E+01
FF	4.53E-05	3.35E+00	8.28E-01	9.11E-02	-	4.27E+00
E_HE_LN_CR	Silver	Textile	Laundering	Landfill/WWTP	Release	Total
OD	5.64E-12	4.55E-08	1.21E-07	8.14E-09	-	1.75E-07
GW	7.97E-05	2.56E+00	8.14E-01	1.13E-01	-	3.49E+00
PS	9.02E-06	1.37E-01	4.74E-02	8.87E-03	-	1.94E-01
AC	1.48E-06	1.93E-02	5.81E-03	7.91E-04	-	2.59E-02
EU	9.59E-07	1.49E-03	1.62E-03	5.57E-03	-	8.68E-03
HHC	1.71E-11	3.55E-08	4.92E-08	2.74E-08	-	1.12E-07
HHNC	6.29E-10	1.85E-07	1.39E-07	3.09E-07	1.08E-08	6.44E-07
RE	1.37E-07	1.30E-03	7.84E-04	1.50E-04	-	2.23E-03
EC	5.50E-03	5.60E+00	6.85E+00	3.29E+00	1.64E-02	1.58E+01
FF	5.60E-05	3.35E+00	8.28E-01	9.11E-02	-	4.27E+00
E_HE_LN_FSP	Silver	Textile	Laundering	Landfill/WWTP	Release	Total
OD	4.63E-12	4.55E-08	1.21E-07	8.14E-09	-	1.75E-07
GW	6.57E-05	2.56E+00	8.14E-01	1.13E-01	-	3.49E+00
PS	6.93E-06	1.37E-01	4.74E-02	8.87E-03	-	1.94E-01
AC	1.12E-06	1.93E-02	5.81E-03	7.91E-04	-	2.59E-02
EU	7.52E-07	1.49E-03	1.62E-03	5.57E-03	-	8.68E-03
HHC	1.33E-11	3.55E-08	4.92E-08	2.74E-08	-	1.12E-07
HHNC	4.73E-10	1.85E-07	1.39E-07	3.09E-07	1.08E-08	6.44E-07
RE	1.11E-07	1.30E-03	7.84E-04	1.50E-04	-	2.23E-03
EC	4.20E-03	5.60E+00	6.85E+00	3.29E+00	1.64E-02	1.58E+01
FF	5.85E-05	3.35E+00	8.28E-01	9.11E-02	-	4.27E+00

E_HE_LN_Spark	Silver	Textile	Laundrying	Landfill/WWTP	Release	Total
OD	1.77E-11	4.55E-08	1.21E-07	8.14E-09	-	1.75E-07
GW	1.35E-04	2.56E+00	8.14E-01	1.13E-01	-	3.49E+00
PS	1.08E-05	1.37E-01	4.74E-02	8.87E-03	-	1.94E-01
AC	1.85E-06	1.93E-02	5.81E-03	7.91E-04	-	2.59E-02
EU	1.07E-06	1.49E-03	1.62E-03	5.57E-03	-	8.68E-03
HHC	1.84E-11	3.55E-08	4.92E-08	2.74E-08	-	1.12E-07
HHNC	6.32E-10	1.85E-07	1.39E-07	3.09E-07	1.08E-08	6.44E-07
RE	2.09E-07	1.30E-03	7.84E-04	1.50E-04	-	2.23E-03
EC	5.65E-03	5.60E+00	6.85E+00	3.29E+00	1.64E-02	1.58E+01
FF	9.17E-05	3.35E+00	8.28E-01	9.11E-02	-	4.27E+00
E_HE_LN_AVG	Silver	Textile	Laundrying	Landfill/WWTP	Release	Total
OD	7.91E-12	4.55E-08	1.21E-07	8.14E-09	-	1.75E-07
GW	8.69E-05	2.56E+00	8.14E-01	1.13E-01	-	3.49E+00
PS	8.80E-06	1.37E-01	4.74E-02	8.87E-03	-	1.94E-01
AC	1.47E-06	1.93E-02	5.81E-03	7.91E-04	-	2.59E-02
EU	9.34E-07	1.49E-03	1.62E-03	5.57E-03	-	8.68E-03
HHC	1.65E-11	3.55E-08	4.92E-08	2.74E-08	-	1.12E-07
HHNC	5.90E-10	1.85E-07	1.39E-07	3.09E-07	1.08E-08	6.44E-07
RE	1.49E-07	1.30E-03	7.84E-04	1.50E-04	-	2.23E-03
EC	5.21E-03	5.60E+00	6.85E+00	3.29E+00	1.64E-02	1.58E+01
FF	6.29E-05	3.35E+00	8.28E-01	9.11E-02	-	4.27E+00

Table E11. (E) TRACI characterization results for 1 nAg-enabled T-shirt (145 g, electrostatically attached) laundered with conventional efficiency washer and line drying.

E_CE_LN_AP	Silver	Textile	Laundering	Landfill/WWTP	Release	Total
OD	3.66E-12	4.55E-08	2.07E-07	1.45E-08	-	2.67E-07
GW	6.77E-05	2.56E+00	3.44E+00	1.93E-01	-	6.20E+00
PS	8.45E-06	1.37E-01	1.98E-01	1.59E-02	-	3.52E-01
AC	1.45E-06	1.93E-02	2.76E-02	1.43E-03	-	4.84E-02
EU	9.53E-07	1.49E-03	2.90E-03	1.01E-02	-	1.45E-02
HHC	1.71E-11	3.55E-08	9.02E-08	4.96E-08	-	1.75E-07
HHNC	6.26E-10	1.85E-07	3.03E-07	5.59E-07	1.08E-08	1.06E-06
RE	1.39E-07	1.30E-03	2.23E-03	2.72E-04	-	3.80E-03
EC	5.49E-03	5.60E+00	1.29E+01	5.63E+00	1.64E-02	2.42E+01
FF	4.53E-05	3.35E+00	3.11E+00	1.63E-01	-	6.63E+00
E_CE_LN_CR	Silver	Textile	Laundering	Landfill/WWTP	Release	Total
OD	5.64E-12	4.55E-08	2.07E-07	1.45E-08	-	2.67E-07
GW	7.97E-05	2.56E+00	3.44E+00	1.93E-01	-	6.20E+00
PS	9.02E-06	1.37E-01	1.98E-01	1.59E-02	-	3.52E-01
AC	1.48E-06	1.93E-02	2.76E-02	1.43E-03	-	4.84E-02
EU	9.59E-07	1.49E-03	2.90E-03	1.01E-02	-	1.45E-02
HHC	1.71E-11	3.55E-08	9.02E-08	4.96E-08	-	1.75E-07
HHNC	6.29E-10	1.85E-07	3.03E-07	5.59E-07	1.08E-08	1.06E-06
RE	1.37E-07	1.30E-03	2.23E-03	2.72E-04	-	3.80E-03
EC	5.50E-03	5.60E+00	1.29E+01	5.63E+00	1.64E-02	2.42E+01
FF	5.60E-05	3.35E+00	3.11E+00	1.63E-01	-	6.63E+00
E_CE_LN_FSP	Silver	Textile	Laundering	Landfill/WWTP	Release	Total
OD	4.63E-12	4.55E-08	2.07E-07	1.45E-08	-	2.67E-07
GW	6.57E-05	2.56E+00	3.44E+00	1.93E-01	-	6.20E+00
PS	6.93E-06	1.37E-01	1.98E-01	1.59E-02	-	3.52E-01
AC	1.12E-06	1.93E-02	2.76E-02	1.43E-03	-	4.84E-02
EU	7.52E-07	1.49E-03	2.90E-03	1.01E-02	-	1.45E-02
HHC	1.33E-11	3.55E-08	9.02E-08	4.96E-08	-	1.75E-07
HHNC	4.73E-10	1.85E-07	3.03E-07	5.59E-07	1.08E-08	1.06E-06
RE	1.11E-07	1.30E-03	2.23E-03	2.72E-04	-	3.80E-03
EC	4.20E-03	5.60E+00	1.29E+01	5.63E+00	1.64E-02	2.42E+01
FF	5.85E-05	3.35E+00	3.11E+00	1.63E-01	-	6.63E+00

E_CE_LN_Spark	Silver	Textile	Laundrying	Landfill/WWTP	Release	Total
OD	1.77E-11	4.55E-08	2.07E-07	1.45E-08	-	2.67E-07
GW	1.35E-04	2.56E+00	3.44E+00	1.93E-01	-	6.20E+00
PS	1.08E-05	1.37E-01	1.98E-01	1.59E-02	-	3.52E-01
AC	1.85E-06	1.93E-02	2.76E-02	1.43E-03	-	4.84E-02
EU	1.07E-06	1.49E-03	2.90E-03	1.01E-02	-	1.45E-02
HHC	1.84E-11	3.55E-08	9.02E-08	4.96E-08	-	1.75E-07
HHNC	6.32E-10	1.85E-07	3.03E-07	5.59E-07	1.08E-08	1.06E-06
RE	2.09E-07	1.30E-03	2.23E-03	2.72E-04	-	3.80E-03
EC	5.65E-03	5.60E+00	1.29E+01	5.63E+00	1.64E-02	2.42E+01
FF	9.17E-05	3.35E+00	3.11E+00	1.63E-01	-	6.63E+00
E_CE_LN_AVG	Silver	Textile	Laundrying	Landfill/WWTP	Release	Total
OD	7.91E-12	4.55E-08	2.07E-07	1.45E-08	-	2.67E-07
GW	8.69E-05	2.56E+00	3.44E+00	1.93E-01	-	6.20E+00
PS	8.80E-06	1.37E-01	1.98E-01	1.59E-02	-	3.52E-01
AC	1.47E-06	1.93E-02	2.76E-02	1.43E-03	-	4.84E-02
EU	9.34E-07	1.49E-03	2.90E-03	1.01E-02	-	1.45E-02
HHC	1.65E-11	3.55E-08	9.02E-08	4.96E-08	-	1.75E-07
HHNC	5.90E-10	1.85E-07	3.03E-07	5.59E-07	1.08E-08	1.06E-06
RE	1.49E-07	1.30E-03	2.23E-03	2.72E-04	-	3.80E-03
EC	5.21E-03	5.60E+00	1.29E+01	5.63E+00	1.64E-02	2.42E+01
FF	6.29E-05	3.35E+00	3.11E+00	1.63E-01	-	6.63E+00

Table E12. (C) TRACI characterization results for 1 Ag-enabled T-shirt (145 g, coated)

laundered with high efficiency washer and dryer.

C_HE	Silver	Textile	Laundrying	Landfill/WWTP	Release	Total
OD	1.31E-08	4.55E-08	1.21E-07	8.14E-09	-	1.88E-07
GW	2.26E-01	2.56E+00	5.58E+00	1.13E-01	-	8.49E+00
PS	3.01E-02	1.37E-01	3.20E-01	8.87E-03	-	4.97E-01
AC	5.24E-03	1.93E-02	4.69E-02	7.91E-04	-	7.22E-02
EU	3.54E-03	1.49E-03	2.17E-03	5.57E-03	-	1.28E-02
HHC	6.39E-08	3.55E-08	5.89E-08	2.74E-08	-	1.86E-07
HHNC	2.36E-06	1.85E-07	3.01E-07	3.09E-07	2.55E-05	2.86E-05
RE	4.95E-04	1.30E-03	2.84E-03	1.50E-04	-	4.79E-03
EC	2.06E+01	5.60E+00	9.21E+00	3.29E+00	3.87E+01	7.74E+01
FF	1.52E-01	3.35E+00	4.96E+00	9.11E-02	-	8.56E+00

Table E13. (C) TRACI characterization results for 1 Ag-enabled T-shirt (145 g, coated)

laundered with conventional efficiency washer and dryer.

C_CE	Silver	Textile	Laundering	Landfill/WWTP	Release	Total
OD	1.31E-08	4.55E-08	2.08E-07	1.45E-08	-	2.81E-07
GW	2.26E-01	2.56E+00	1.29E+01	1.93E-01	-	1.59E+01
PS	3.01E-02	1.37E-01	7.41E-01	1.59E-02	-	9.24E-01
AC	5.24E-03	1.93E-02	1.09E-01	1.43E-03	-	1.35E-01
EU	3.54E-03	1.49E-03	4.00E-03	1.01E-02	-	1.91E-02
HHC	6.39E-08	3.55E-08	1.09E-07	4.96E-08	-	2.58E-07
HHNC	2.36E-06	1.85E-07	6.25E-07	5.59E-07	2.55E-05	2.92E-05
RE	4.95E-04	1.30E-03	6.32E-03	2.72E-04	-	8.39E-03
EC	2.06E+01	5.60E+00	1.76E+01	5.63E+00	3.87E+01	8.81E+01
FF	1.52E-01	3.35E+00	1.13E+01	1.63E-01	-	1.50E+01

Table E14. (C) TRACI characterization results for 1 Ag-enabled T-shirt (145 g, coated)

laundered with high efficiency washer and line drying.

C_HE_LN	Silver	Textile	Laundering	Landfill/WWTP	Release	Total
OD	1.31E-08	4.55E-08	1.21E-07	8.14E-09	-	1.88E-07
GW	2.26E-01	2.56E+00	8.14E-01	1.13E-01	-	3.72E+00
PS	3.01E-02	1.37E-01	4.74E-02	8.87E-03	-	2.24E-01
AC	5.24E-03	1.93E-02	5.81E-03	7.91E-04	-	3.12E-02
EU	3.54E-03	1.49E-03	1.62E-03	5.57E-03	-	1.22E-02
HHC	6.39E-08	3.55E-08	4.92E-08	2.74E-08	-	1.76E-07
HHNC	2.36E-06	1.85E-07	1.39E-07	3.09E-07	2.55E-05	2.84E-05
RE	4.95E-04	1.30E-03	7.84E-04	1.50E-04	-	2.73E-03
EC	2.06E+01	5.60E+00	6.85E+00	3.29E+00	3.87E+01	7.50E+01
FF	1.52E-01	3.35E+00	8.28E-01	9.11E-02	-	4.42E+00

Table E15. (C) TRACI characterization results for 1 Ag-enabled T-shirt (145 g, coated)

laundered with conventional efficiency washer and line drying.

C_CE_LN	Silver	Textile	Laundering	Landfill/WWTP	Release	Total
OD	1.31E-08	4.55E-08	2.07E-07	1.45E-08	-	2.81E-07
GW	2.26E-01	2.56E+00	3.44E+00	1.93E-01	-	6.42E+00
PS	3.01E-02	1.37E-01	1.98E-01	1.59E-02	-	3.82E-01
AC	5.24E-03	1.93E-02	2.76E-02	1.43E-03	-	5.36E-02
EU	3.54E-03	1.49E-03	2.90E-03	1.01E-02	-	1.80E-02
HHC	6.39E-08	3.55E-08	9.02E-08	4.96E-08	-	2.39E-07
HHNC	2.36E-06	1.85E-07	3.03E-07	5.59E-07	2.55E-05	2.89E-05
RE	4.95E-04	1.30E-03	2.23E-03	2.72E-04	-	4.30E-03
EC	2.06E+01	5.60E+00	1.29E+01	5.63E+00	3.87E+01	8.35E+01
FF	1.52E-01	3.35E+00	3.11E+00	1.63E-01	-	6.78E+00

Table E16. (A) TRACI characterization results for 1 Ag-enabled T-shirt (145 g, attached)

laundered with high efficiency washer and dryer.

A_HE	Silver	Textile	Laundering	Landfill/WWTP	Release	Total
OD	3.43E-11	4.55E-08	1.21E-07	8.14E-09	-	1.75E-07
GW	5.92E-04	2.56E+00	5.58E+00	1.13E-01	-	8.26E+00
PS	8.20E-05	1.37E-01	3.20E-01	8.87E-03	-	4.67E-01
AC	1.37E-05	1.93E-02	4.69E-02	7.91E-04	-	6.70E-02
EU	9.23E-06	1.49E-03	2.17E-03	5.57E-03	-	9.24E-03
HHC	1.67E-10	3.55E-08	5.89E-08	2.74E-08	-	1.22E-07
HHNC	6.13E-09	1.85E-07	3.01E-07	3.09E-07	1.65E-07	9.66E-07
RE	1.29E-06	1.30E-03	2.84E-03	1.50E-04	-	4.30E-03
EC	5.36E-02	5.60E+00	9.21E+00	3.29E+00	2.51E-01	1.84E+01
FF	3.98E-04	3.35E+00	4.96E+00	9.11E-02	-	8.41E+00

Table E17. (A) TRACI characterization results for 1 Ag-enabled T-shirt (145 g, attached)

laundered with conventional efficiency washer and dryer.

A_CE	Silver	Textile	Laundering	Landfill/WWTP	Release	Total
OD	3.43E-11	4.55E-08	2.08E-07	1.45E-08	-	2.68E-07
GW	5.92E-04	2.56E+00	1.29E+01	1.93E-01	-	1.57E+01
PS	8.20E-05	1.37E-01	7.41E-01	1.59E-02	-	8.94E-01
AC	1.37E-05	1.93E-02	1.09E-01	1.43E-03	-	1.30E-01
EU	9.23E-06	1.49E-03	4.00E-03	1.01E-02	-	1.56E-02
HHC	1.67E-10	3.55E-08	1.09E-07	4.96E-08	-	1.95E-07
HHNC	6.13E-09	1.85E-07	6.25E-07	5.59E-07	1.65E-07	1.54E-06
RE	1.29E-06	1.30E-03	6.32E-03	2.72E-04	-	7.90E-03
EC	5.36E-02	5.60E+00	1.76E+01	5.63E+00	2.51E-01	2.91E+01
FF	3.98E-04	3.35E+00	1.13E+01	1.63E-01	-	1.48E+01

Table E18. (A) TRACI characterization results for 1 Ag-enabled T-shirt (145 g, attached)

laundered with high efficiency washer and line drying.

A_HE_LN	Silver	Textile	Laundering	Landfill/WWTP	Release	Total
OD	3.43E-11	4.55E-08	1.21E-07	8.14E-09	-	1.75E-07
GW	5.92E-04	2.56E+00	8.14E-01	1.13E-01	-	3.49E+00
PS	8.20E-05	1.37E-01	4.74E-02	8.87E-03	-	1.94E-01
AC	1.37E-05	1.93E-02	5.81E-03	7.91E-04	-	2.59E-02
EU	9.23E-06	1.49E-03	1.62E-03	5.57E-03	-	8.68E-03
HHC	1.67E-10	3.55E-08	4.92E-08	2.74E-08	-	1.12E-07
HHNC	6.13E-09	1.85E-07	1.39E-07	3.09E-07	1.65E-07	8.04E-07
RE	1.29E-06	1.30E-03	7.84E-04	1.50E-04	-	2.23E-03
EC	5.36E-02	5.60E+00	6.85E+00	3.29E+00	2.51E-01	1.60E+01
FF	3.98E-04	3.35E+00	8.28E-01	9.11E-02	-	4.27E+00

Table E19. (A) TRACI characterization results for 1 Ag-enabled T-shirt (145 g, attached)

laundered with conventional efficiency washer and line drying.

A_CE_LN	Silver	Textile	Laundering	Landfill/WWTP	Release	Total
OD	3.43E-11	4.55E-08	2.07E-07	1.45E-08	-	2.67E-07
GW	5.92E-04	2.56E+00	3.44E+00	1.93E-01	-	6.20E+00
PS	8.20E-05	1.37E-01	1.98E-01	1.59E-02	-	3.52E-01
AC	1.37E-05	1.93E-02	2.76E-02	1.43E-03	-	4.84E-02
EU	9.23E-06	1.49E-03	2.90E-03	1.01E-02	-	1.45E-02
HHC	1.67E-10	3.55E-08	9.02E-08	4.96E-08	-	1.76E-07
HHNC	6.13E-09	1.85E-07	3.03E-07	5.59E-07	1.65E-07	1.22E-06
RE	1.29E-06	1.30E-03	2.23E-03	2.72E-04	-	3.80E-03
EC	5.36E-02	5.60E+00	1.29E+01	5.63E+00	2.51E-01	2.45E+01
FF	3.98E-04	3.35E+00	3.11E+00	1.63E-01	-	6.63E+00

Table E20. Uncertainty analysis results for product T

T_HE/HE	Median	Lower Bound	Upper Bound	T_HE/LN	Median	Lower Bound	Upper Bound
AC	6.70E-02	6.59E-02	6.84E-02	AC	2.59E-02	2.48E-02	2.73E-02
HHC	1.07E-07	6.48E-08	2.59E-07	HHC	9.76E-08	5.52E-08	2.57E-07
EC	1.79E+01	1.21E+01	3.26E+01	EC	1.50E+01	9.45E+00	2.85E+01
EU	8.94E-03	7.02E-03	1.32E-02	EU	8.39E-03	6.27E-03	1.25E-02
FF	8.39E+00	7.83E+00	9.21E+00	FF	4.21E+00	3.70E+00	5.04E+00
GW	8.25E+00	8.04E+00	8.58E+00	GW	3.47E+00	3.26E+00	3.76E+00
HHNC	9.72E-07	7.38E-07	1.75E-06	HHNC	8.04E-07	5.73E-07	1.60E-06
OD	1.67E-07	1.09E-07	2.83E-07	OD	1.68E-07	1.11E-07	2.88E-07
RE	4.28E-03	4.00E-03	4.72E-03	RE	2.21E-03	1.91E-03	2.69E-03
PS	4.66E-01	4.55E-01	4.84E-01	PS	1.93E-01	1.82E-01	2.09E-01
T_CE/CE	Median	Lower Bound	Upper Bound	T_CE/LN	Median	Lower Bound	Upper Bound
AC	1.30E-01	1.28E-01	1.32E-01	AC	4.84E-02	4.68E-02	5.06E-02
HHC	1.72E-07	1.02E-07	4.34E-07	HHC	1.51E-07	7.87E-08	4.26E-07
EC	2.74E+01	1.92E+01	5.20E+01	EC	2.33E+01	1.43E+01	4.17E+01
EU	1.51E-02	1.18E-02	2.15E-02	EU	1.42E-02	1.08E-02	2.11E-02
FF	1.48E+01	1.42E+01	1.57E+01	FF	6.60E+00	5.97E+00	7.50E+00
GW	1.57E+01	1.54E+01	1.61E+01	GW	6.19E+00	5.90E+00	6.63E+00
HHNC	1.47E-06	1.12E-06	2.67E-06	HHNC	1.16E-06	8.08E-07	2.68E-06
OD	2.51E-07	1.58E-07	4.34E-07	OD	2.56E-07	1.64E-07	4.35E-07
RE	7.85E-03	7.40E-03	8.61E-03	RE	3.78E-03	3.29E-03	4.54E-03
PS	8.93E-01	8.77E-01	9.15E-01	PS	3.51E-01	3.35E-01	3.75E-01

Table E21. Uncertainty analysis results for product E

E_HE/HE	Median	Lower Bound	Upper Bound	E_HE/LN	Median	Lower Bound	Upper Bound
AC	6.70E-02	6.59E-02	6.85E-02	AC	2.59E-02	2.48E-02	2.74E-02
HHC	1.05E-07	6.52E-08	2.54E-07	HHC	9.57E-08	5.18E-08	2.55E-07
EC	1.71E+01	1.16E+01	3.12E+01	EC	1.46E+01	9.10E+00	2.92E+01
EU	9.02E-03	7.00E-03	1.36E-02	EU	8.44E-03	6.39E-03	1.24E-02
FF	8.38E+00	7.84E+00	9.26E+00	FF	4.25E+00	3.68E+00	5.09E+00
GW	8.26E+00	8.04E+00	8.57E+00	GW	3.48E+00	3.26E+00	3.78E+00
HHNC	7.27E-07	5.02E-07	1.44E-06	HHNC	5.68E-07	3.38E-07	1.37E-06
OD	1.66E-07	1.12E-07	2.89E-07	OD	1.68E-07	1.10E-07	2.90E-07
RE	4.28E-03	3.99E-03	4.77E-03	RE	2.22E-03	1.90E-03	2.67E-03
PS	4.66E-01	4.55E-01	4.84E-01	PS	1.93E-01	1.82E-01	2.10E-01
E_CE/CE	Median	Lower Bound	Upper Bound	E_CE/LN	Median	Lower Bound	Upper Bound
AC	1.30E-01	1.28E-01	1.32E-01	AC	4.83E-02	4.69E-02	5.08E-02
HHC	1.77E-07	1.06E-07	3.77E-07	HHC	1.52E-07	8.07E-08	4.03E-07
EC	2.74E+01	1.88E+01	5.19E+01	EC	2.27E+01	1.37E+01	4.89E+01
EU	1.53E-02	1.19E-02	2.19E-02	EU	1.42E-02	1.08E-02	2.08E-02
FF	1.48E+01	1.42E+01	1.57E+01	FF	6.59E+00	5.99E+00	7.68E+00
GW	1.57E+01	1.54E+01	1.61E+01	GW	6.19E+00	5.91E+00	6.64E+00
HHNC	1.27E-06	8.74E-07	2.69E-06	HHNC	9.59E-07	5.84E-07	2.61E-06
OD	2.58E-07	1.64E-07	4.52E-07	OD	2.55E-07	1.63E-07	4.45E-07
RE	7.87E-03	7.43E-03	8.68E-03	RE	3.76E-03	3.34E-03	4.52E-03
PS	8.93E-01	8.77E-01	9.19E-01	PS	3.51E-01	3.36E-01	3.78E-01

Table E22. Uncertainty analysis results for product A

A_HE/HE	Median	Lower Bound	Upper Bound	A_HE/LN	Median	Lower Bound	Upper Bound
AC	6.69E-02	6.59E-02	6.85E-02	AC	2.59E-02	2.48E-02	2.74E-02
HHC	1.08E-07	6.23E-08	2.70E-07	HHC	9.75E-08	5.45E-08	2.69E-07
EC	1.70E+01	1.16E+01	3.16E+01	EC	1.50E+01	9.35E+00	2.95E+01
EU	8.88E-03	6.88E-03	1.35E-02	EU	8.51E-03	6.34E-03	1.25E-02
FF	8.38E+00	7.82E+00	9.15E+00	FF	4.22E+00	3.70E+00	5.05E+00
GW	8.25E+00	8.03E+00	8.56E+00	GW	3.48E+00	3.26E+00	3.75E+00
HHNC	8.73E-07	6.64E-07	1.68E-06	HHNC	7.26E-07	5.07E-07	1.56E-06
OD	1.67E-07	1.12E-07	2.76E-07	OD	1.67E-07	1.14E-07	2.87E-07
RE	4.28E-03	3.99E-03	4.72E-03	RE	2.22E-03	1.92E-03	2.64E-03
PS	4.66E-01	4.54E-01	4.84E-01	PS	1.93E-01	1.82E-01	2.08E-01
A_CE/CE	Median	Lower Bound	Upper Bound	A_CE/LN	Median	Lower Bound	Upper Bound
AC	1.30E-01	1.28E-01	1.32E-01	AC	4.83E-02	4.69E-02	5.07E-02
HHC	1.70E-07	1.04E-07	4.08E-07	HHC	1.50E-07	8.39E-08	3.82E-07
EC	2.73E+01	1.90E+01	4.80E+01	EC	2.31E+01	1.45E+01	4.98E+01
EU	1.52E-02	1.19E-02	2.10E-02	EU	1.40E-02	1.07E-02	1.99E-02
FF	1.48E+01	1.42E+01	1.57E+01	FF	6.59E+00	6.03E+00	7.55E+00
GW	1.57E+01	1.54E+01	1.61E+01	GW	6.18E+00	5.91E+00	6.64E+00
HHNC	1.41E-06	1.04E-06	2.74E-06	HHNC	1.09E-06	7.26E-07	2.48E-06
OD	2.49E-07	1.59E-07	4.56E-07	OD	2.53E-07	1.68E-07	4.35E-07
RE	7.85E-03	7.43E-03	8.54E-03	RE	3.75E-03	3.30E-03	4.55E-03
PS	8.93E-01	8.77E-01	9.17E-01	PS	3.51E-01	3.35E-01	3.75E-01

Table E23. Uncertainty analysis results for product C

C_HE/HE	Median	Lower Bound	Upper Bound	C_HE/LN	Median	Lower Bound	Upper Bound
AC	7.20E-02	7.02E-02	7.45E-02	AC	3.11E-02	2.91E-02	3.35E-02
HHC	1.60E-07	9.10E-08	4.03E-07	HHC	1.53E-07	8.44E-08	4.31E-07
EC	7.17E+01	5.72E+01	1.42E+02	EC	6.95E+01	5.46E+01	1.17E+02
EU	1.22E-02	8.91E-03	2.18E-02	EU	1.16E-02	8.42E-03	2.06E-02
FF	8.51E+00	8.00E+00	9.32E+00	FF	4.38E+00	3.81E+00	5.27E+00
GW	8.47E+00	8.26E+00	8.77E+00	GW	3.70E+00	3.46E+00	4.00E+00
HHNC	2.81E-05	2.69E-05	3.20E-05	HHNC	2.80E-05	2.68E-05	3.28E-05
OD	1.79E-07	1.20E-07	3.00E-07	OD	1.80E-07	1.25E-07	2.92E-07
RE	4.76E-03	4.43E-03	5.19E-03	RE	2.70E-03	2.39E-03	3.17E-03
PS	4.94E-01	4.75E-01	5.23E-01	PS	2.23E-01	2.03E-01	2.49E-01
C_CE/CE	Median	Lower Bound	Upper Bound	C_CE/LN	Median	Lower Bound	Upper Bound
AC	1.35E-01	1.33E-01	1.38E-01	AC	5.36E-02	5.15E-02	5.65E-02
HHC	2.28E-07	1.38E-07	5.33E-07	HHC	2.05E-07	1.19E-07	6.55E-07
EC	8.25E+01	6.60E+01	1.42E+02	EC	7.84E+01	6.09E+01	1.32E+02
EU	1.83E-02	1.40E-02	2.78E-02	EU	1.73E-02	1.30E-02	2.64E-02
FF	1.50E+01	1.44E+01	1.58E+01	FF	6.74E+00	6.14E+00	7.58E+00
GW	1.59E+01	1.56E+01	1.63E+01	GW	6.42E+00	6.11E+00	6.82E+00
HHNC	2.88E-05	2.74E-05	3.39E-05	HHNC	2.84E-05	2.71E-05	3.33E-05
OD	2.68E-07	1.70E-07	4.49E-07	OD	2.67E-07	1.70E-07	4.58E-07
RE	8.36E-03	7.89E-03	9.10E-03	RE	4.26E-03	3.76E-03	5.08E-03
PS	9.22E-01	9.00E-01	9.57E-01	PS	3.80E-01	3.58E-01	4.15E-01

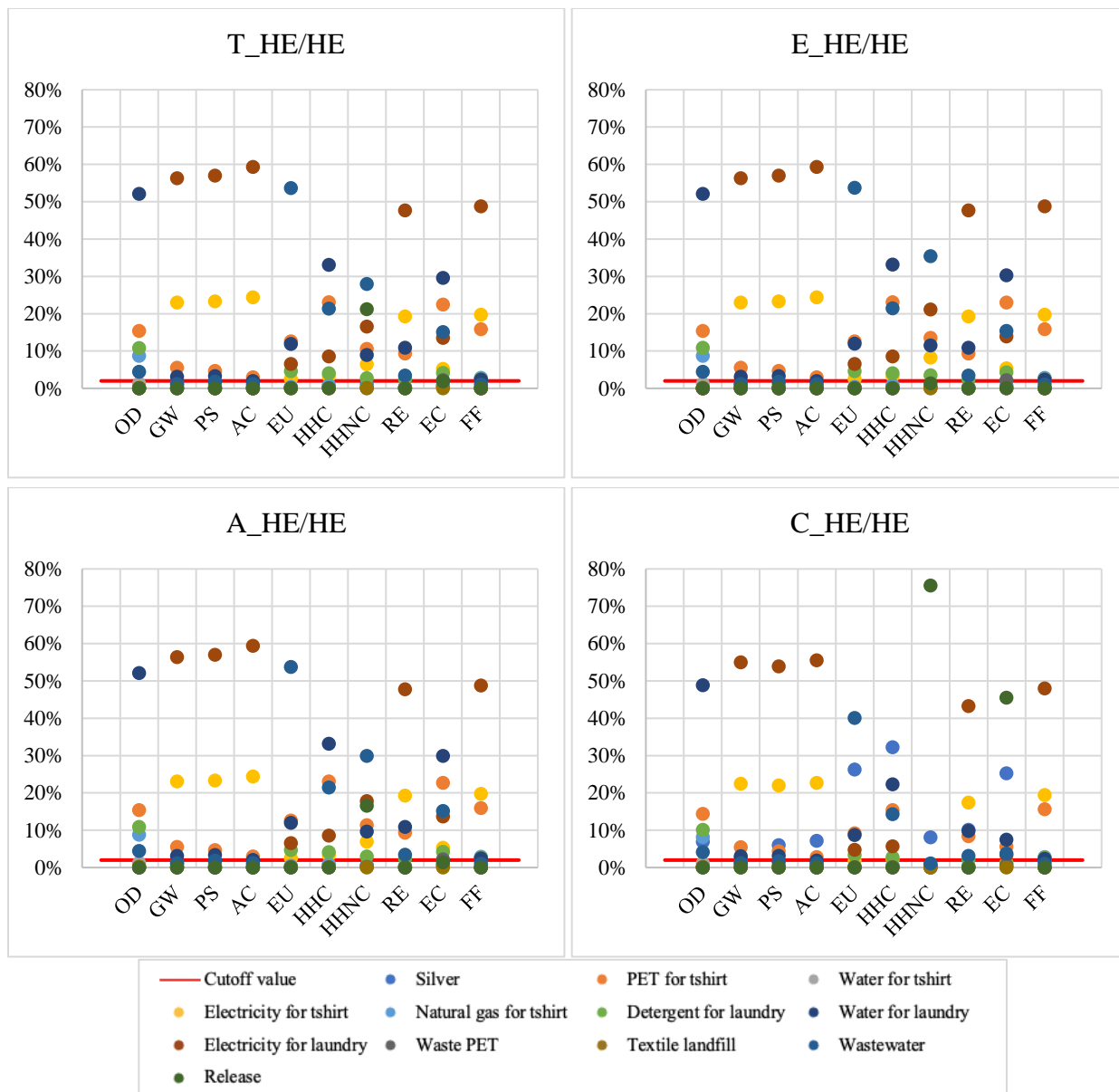


Figure E3. Sensitivity factors of each input/output parameter to environmental impact categories under HE/HE scenario.

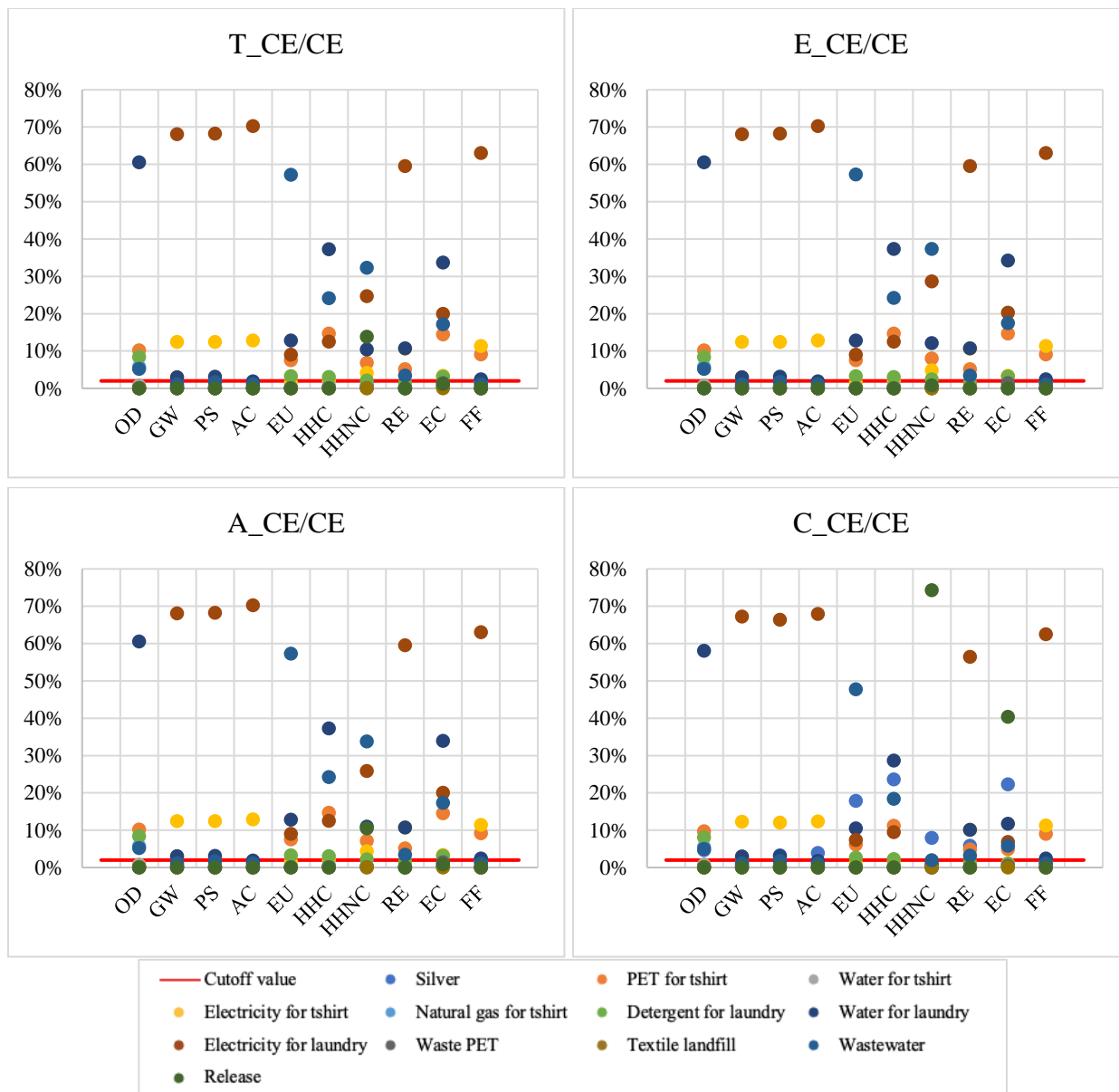


Figure E4. Sensitivity factors of each input/output parameter to environmental impact categories under CE/CE scenario.

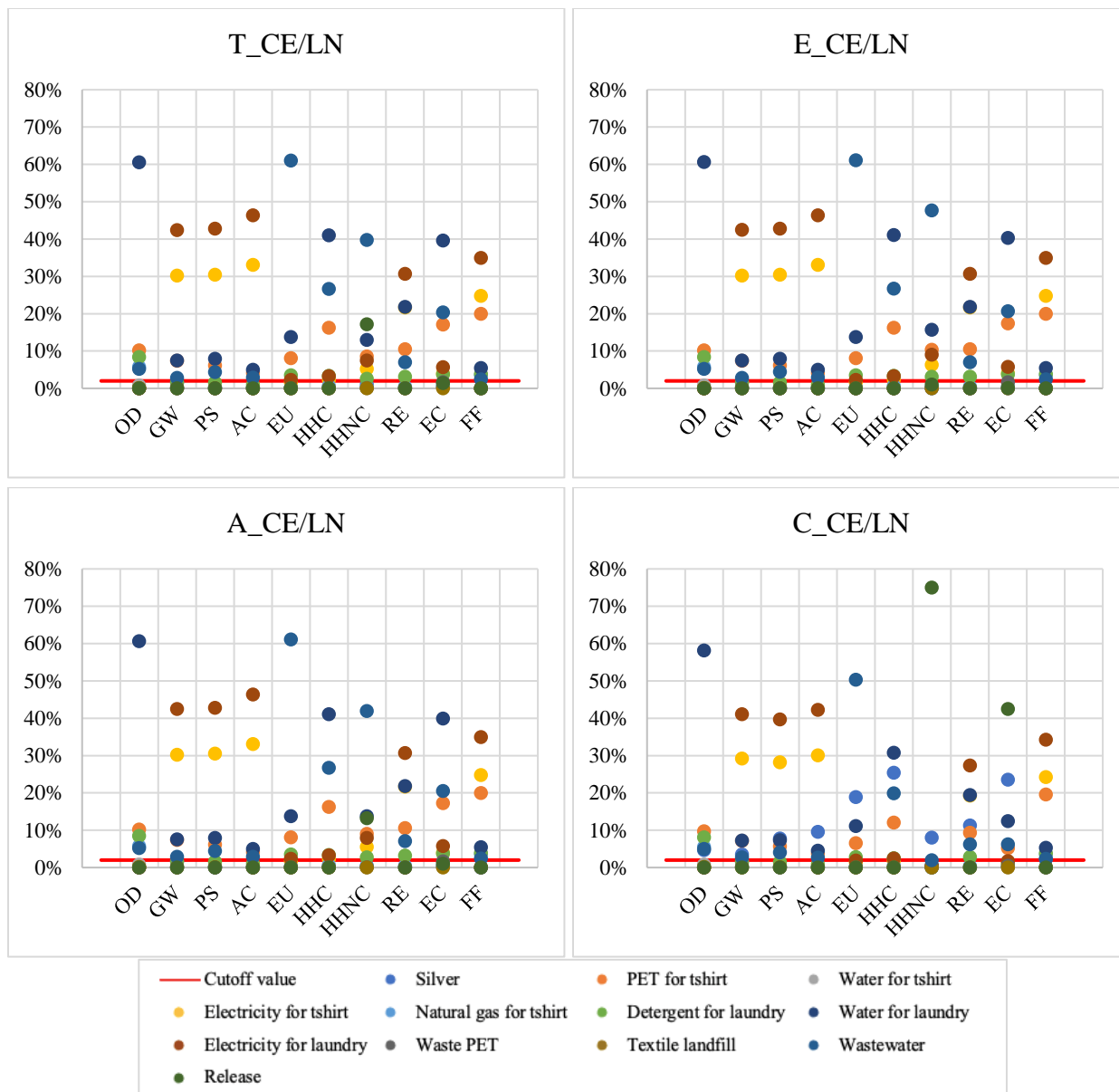


Figure E5. Sensitivity factors of each input/output parameter to environmental impact categories under CE/LN scenario.

Table E24. Sensitivity factors for product T under each scenario (red cells indicate sensitive parameters).

HE/HE	Ag/nAg	PET for t-shirt	Water for t-shirt	Electricity for t-shirt	Natural gas for t-shirt	Detergent for laundry	Water for laundry	Electricity for laundry	Waste PET	Textile landfill	WWTP	Release
OD	0.07%	15.38%	1.23%	0.02%	8.73%	10.84%	52.08%	0.05%	0.01%	0.20%	4.41%	0.00%
GW	0.02%	5.54%	0.07%	23.03%	1.20%	0.98%	3.13%	56.31%	0.18%	0.01%	1.18%	0.00%
PS	0.04%	4.66%	0.07%	23.31%	0.20%	1.01%	3.32%	56.96%	0.02%	0.03%	1.84%	0.00%
AC	0.05%	2.99%	0.04%	24.36%	0.19%	0.60%	1.99%	59.33%	0.00%	0.01%	1.16%	0.00%
EU	0.22%	12.56%	0.26%	2.49%	0.45%	4.62%	11.94%	6.50%	0.08%	0.02%	53.65%	0.00%
HHC	0.30%	23.04%	0.75%	3.28%	0.88%	4.07%	33.06%	8.54%	0.06%	0.02%	21.37%	0.00%
HHNC	1.29%	10.56%	0.19%	6.44%	0.32%	2.73%	8.97%	16.58%	0.11%	0.01%	27.95%	21.20%
RE	0.07%	9.33%	0.24%	19.28%	0.42%	2.36%	10.88%	47.69%	0.00%	0.02%	3.45%	0.00%
EC	0.63%	22.49%	0.67%	5.24%	0.65%	4.16%	29.62%	13.55%	2.18%	0.01%	15.04%	1.87%
FF	0.01%	15.88%	0.05%	19.75%	2.84%	2.58%	2.38%	48.78%	0.00%	0.04%	1.04%	0.00%
HE/LN	Ag/nAg	PET for t-shirt	Water for t-shirt	Electricity for t-shirt	Natural gas for t-shirt	Detergent for laundry	Water for laundry	Electricity for laundry	Waste PET	Textile landfill	WWTP	Release
OD	0.07%	15.39%	1.23%	0.02%	8.73%	10.85%	52.10%	0.00%	0.01%	0.20%	4.41%	0.00%
GW	0.05%	12.92%	0.16%	51.27%	2.83%	2.32%	7.34%	13.18%	0.42%	0.02%	2.78%	0.00%
PS	0.10%	11.08%	0.17%	52.70%	0.47%	2.44%	7.91%	13.58%	0.05%	0.08%	4.41%	0.00%
AC	0.12%	7.64%	0.11%	58.38%	0.49%	1.54%	5.11%	15.18%	0.01%	0.03%	2.99%	0.00%
EU	0.23%	13.34%	0.28%	2.65%	0.47%	4.91%	12.68%	0.63%	0.09%	0.02%	56.69%	0.00%
HHC	0.32%	24.92%	0.82%	3.56%	0.95%	4.42%	35.70%	0.85%	0.07%	0.02%	23.12%	0.00%
HHNC	1.53%	12.46%	0.23%	7.61%	0.38%	3.23%	10.59%	1.82%	0.13%	0.01%	32.78%	24.92%
RE	0.13%	17.64%	0.45%	35.78%	0.80%	4.53%	20.49%	8.97%	0.01%	0.04%	6.59%	0.00%
EC	0.72%	25.58%	0.76%	6.00%	0.74%	4.76%	33.63%	1.43%	2.49%	0.02%	17.15%	2.15%
FF	0.03%	30.32%	0.10%	37.43%	5.55%	5.04%	4.66%	9.40%	0.00%	0.07%	2.05%	0.00%

CE/CE	Ag/nAg	PET for t-shirt	Water for t-shirt	Electricity for t-shirt	Natural gas for t-shirt	Detergent for laundry	Water for laundry	Electricity for laundry	Waste PET	Textile landfill	WWTP	Release
OD	0.04%	10.15%	0.81%	0.01%	5.74%	8.42%	60.57%	0.07%	0.01%	0.13%	5.22%	0.00%
GW	0.01%	2.94%	0.04%	12.41%	0.63%	0.61%	2.99%	68.06%	0.09%	0.00%	1.13%	0.00%
PS	0.02%	2.44%	0.04%	12.45%	0.10%	0.63%	3.14%	68.26%	0.01%	0.02%	1.74%	0.00%
AC	0.02%	1.55%	0.02%	12.86%	0.10%	0.37%	1.87%	70.27%	0.00%	0.01%	1.09%	0.00%
EU	0.13%	7.52%	0.15%	1.48%	0.26%	3.25%	12.81%	9.04%	0.05%	0.01%	57.25%	0.00%
HHC	0.19%	14.69%	0.47%	2.06%	0.55%	3.03%	37.26%	12.51%	0.04%	0.01%	24.16%	0.00%
HHNC	0.83%	6.85%	0.12%	4.17%	0.21%	2.08%	10.44%	24.73%	0.07%	0.01%	32.35%	13.86%
RE	0.04%	5.12%	0.13%	10.68%	0.23%	1.52%	10.74%	59.53%	0.00%	0.01%	3.41%	0.00%
EC	0.40%	14.48%	0.42%	3.33%	0.41%	3.12%	33.74%	19.95%	1.38%	0.01%	17.21%	1.19%
FF	0.01%	9.12%	0.03%	11.38%	1.61%	1.73%	2.44%	63.03%	0.00%	0.02%	1.07%	0.00%
CE/LN	Ag/nAg	PET for t-shirt	Water for t-shirt	Electricity for t-shirt	Natural gas for t-shirt	Detergent for laundry	Water for laundry	Electricity for laundry	Waste PET	Textile landfill	WWTP	Release
OD	0.04%	10.16%	0.81%	0.01%	5.74%	8.43%	60.60%	0.02%	0.01%	0.13%	5.23%	0.00%
GW	0.03%	7.36%	0.09%	30.22%	1.60%	1.55%	7.50%	42.44%	0.24%	0.01%	2.84%	0.00%
PS	0.05%	6.16%	0.09%	30.46%	0.26%	1.59%	7.91%	42.77%	0.03%	0.04%	4.40%	0.00%
AC	0.06%	4.12%	0.06%	33.08%	0.26%	0.98%	4.98%	46.34%	0.01%	0.01%	2.91%	0.00%
EU	0.14%	8.09%	0.17%	1.59%	0.28%	3.49%	13.76%	2.29%	0.05%	0.01%	61.06%	0.00%
HHC	0.21%	16.24%	0.52%	2.29%	0.61%	3.36%	41.00%	3.29%	0.04%	0.02%	26.66%	0.00%
HHNC	1.04%	8.53%	0.16%	5.19%	0.26%	2.59%	12.98%	7.46%	0.09%	0.01%	39.78%	17.20%
RE	0.08%	10.52%	0.27%	21.67%	0.47%	3.15%	21.80%	30.66%	0.00%	0.02%	7.03%	0.00%
EC	0.48%	17.13%	0.50%	3.96%	0.49%	3.71%	39.63%	5.69%	1.64%	0.01%	20.34%	1.41%
FF	0.02%	19.97%	0.06%	24.78%	3.59%	3.85%	5.44%	34.96%	0.00%	0.05%	2.39%	0.00%

Table E25. Sensitivity factors for product E under each scenario (red cells indicate sensitive parameters).

HE/HE	Ag/nAg	PET for t-shirt	Water for t-shirt	Electricity for t-shirt	Natural gas for t-shirt	Detergent for laundry	Water for laundry	Electricity for laundry	Waste PET	Textile landfill	WWTP	Release
OD	0.00%	15.39%	1.23%	0.02%	8.74%	10.85%	52.11%	0.05%	0.01%	0.20%	4.42%	0.00%
GW	0.00%	5.54%	0.07%	23.03%	1.20%	0.98%	3.13%	56.32%	0.18%	0.01%	1.18%	0.00%
PS	0.00%	4.66%	0.07%	23.32%	0.20%	1.01%	3.32%	56.98%	0.02%	0.03%	1.84%	0.00%
AC	0.00%	2.99%	0.04%	24.37%	0.19%	0.60%	2.00%	59.36%	0.00%	0.01%	1.16%	0.00%
EU	0.01%	12.59%	0.26%	2.50%	0.45%	4.63%	11.96%	6.52%	0.08%	0.02%	53.76%	0.00%
HHC	0.01%	23.10%	0.75%	3.29%	0.88%	4.09%	33.15%	8.57%	0.06%	0.02%	21.43%	0.00%
HHNC	0.08%	13.51%	0.25%	8.26%	0.41%	3.50%	11.48%	21.15%	0.14%	0.01%	35.41%	1.33%
RE	0.00%	9.34%	0.24%	19.29%	0.42%	2.37%	10.88%	47.72%	0.00%	0.02%	3.46%	0.00%
EC	0.03%	23.01%	0.68%	5.37%	0.66%	4.26%	30.30%	13.88%	2.23%	0.01%	15.40%	0.09%
FF	0.00%	15.89%	0.05%	19.75%	2.84%	2.58%	2.38%	48.79%	0.00%	0.04%	1.04%	0.00%
HE/LN	Ag/nAg	PET for t-shirt	Water for t-shirt	Electricity for t-shirt	Natural gas for t-shirt	Detergent for laundry	Water for laundry	Electricity for laundry	Waste PET	Textile landfill	WWTP	Release
OD	0.00%	15.40%	1.23%	0.02%	8.74%	10.86%	52.13%	0.00%	0.01%	0.20%	4.42%	0.00%
GW	0.00%	12.93%	0.16%	51.30%	2.83%	2.32%	7.34%	13.18%	0.42%	0.02%	2.78%	0.00%
PS	0.00%	11.09%	0.17%	52.70%	0.47%	2.44%	7.92%	13.59%	0.05%	0.08%	4.41%	0.00%
AC	0.01%	7.65%	0.11%	58.40%	0.49%	1.55%	5.12%	15.20%	0.01%	0.03%	2.99%	0.00%
EU	0.01%	13.37%	0.28%	2.66%	0.47%	4.92%	12.71%	0.63%	0.09%	0.02%	56.80%	0.00%
HHC	0.02%	24.99%	0.82%	3.58%	0.96%	4.44%	35.80%	0.85%	0.07%	0.02%	23.19%	0.00%
HHNC	0.10%	16.80%	0.31%	10.30%	0.51%	4.38%	14.29%	2.48%	0.18%	0.01%	43.54%	1.67%
RE	0.01%	17.66%	0.45%	35.80%	0.80%	4.53%	20.52%	8.98%	0.01%	0.04%	6.60%	0.00%
EC	0.03%	26.27%	0.79%	6.16%	0.76%	4.89%	34.52%	1.47%	2.56%	0.02%	17.62%	0.10%
FF	0.00%	30.33%	0.10%	37.40%	5.55%	5.05%	4.66%	9.41%	0.00%	0.07%	2.05%	0.00%

CE/CE	Ag/nAg	PET for t-shirt	Water for t-shirt	Electricity for t-shirt	Natural gas for t-shirt	Detergent for laundry	Water for laundry	Electricity for laundry	Waste PET	Textile landfill	WWTP	Release
OD	0.00%	10.16%	0.81%	0.01%	5.74%	8.42%	60.59%	0.07%	0.01%	0.13%	5.22%	0.00%
GW	0.00%	2.94%	0.04%	12.41%	0.63%	0.61%	2.99%	68.07%	0.09%	0.00%	1.13%	0.00%
PS	0.00%	2.44%	0.04%	12.45%	0.10%	0.63%	3.14%	68.27%	0.01%	0.02%	1.74%	0.00%
AC	0.00%	1.55%	0.02%	12.87%	0.10%	0.37%	1.87%	70.29%	0.00%	0.01%	1.09%	0.00%
EU	0.01%	7.53%	0.15%	1.48%	0.26%	3.25%	12.83%	9.05%	0.05%	0.01%	57.31%	0.00%
HHC	0.01%	14.72%	0.47%	2.07%	0.55%	3.03%	37.32%	12.53%	0.04%	0.01%	24.20%	0.00%
HHNC	0.05%	7.98%	0.15%	4.86%	0.24%	2.43%	12.16%	28.65%	0.08%	0.01%	37.38%	0.78%
RE	0.00%	5.12%	0.13%	10.68%	0.23%	1.53%	10.74%	59.54%	0.00%	0.01%	3.41%	0.00%
EC	0.02%	14.69%	0.43%	3.38%	0.42%	3.17%	34.22%	20.25%	1.40%	0.01%	17.46%	0.06%
FF	0.00%	9.12%	0.03%	11.38%	1.61%	1.73%	2.44%	63.03%	0.00%	0.02%	1.07%	0.00%
CE/LN	Ag/nAg	PET for t-shirt	Water for t-shirt	Electricity for t-shirt	Natural gas for t-shirt	Detergent for laundry	Water for laundry	Electricity for laundry	Waste PET	Textile landfill	WWTP	Release
OD	0.00%	10.16%	0.81%	0.01%	5.74%	8.43%	60.62%	0.02%	0.01%	0.13%	5.23%	0.00%
GW	0.00%	7.36%	0.09%	30.23%	1.60%	1.55%	7.50%	42.45%	0.24%	0.01%	2.84%	0.00%
PS	0.00%	6.16%	0.09%	30.48%	0.26%	1.59%	7.91%	42.79%	0.03%	0.04%	4.41%	0.00%
AC	0.00%	4.13%	0.06%	33.10%	0.26%	0.98%	4.98%	46.37%	0.01%	0.01%	2.91%	0.00%
EU	0.01%	8.10%	0.17%	1.60%	0.28%	3.50%	13.78%	2.30%	0.05%	0.01%	61.14%	0.00%
HHC	0.01%	16.27%	0.52%	2.29%	0.61%	3.36%	41.07%	3.30%	0.04%	0.02%	26.71%	0.00%
HHNC	0.06%	10.36%	0.19%	6.32%	0.31%	3.16%	15.73%	9.06%	0.11%	0.01%	47.65%	1.02%
RE	0.00%	10.53%	0.27%	21.69%	0.47%	3.16%	21.81%	30.68%	0.00%	0.02%	7.03%	0.00%
EC	0.02%	17.43%	0.51%	4.03%	0.50%	3.78%	40.30%	5.79%	1.67%	0.01%	20.70%	0.07%
FF	0.00%	19.97%	0.06%	24.78%	3.59%	3.85%	5.44%	34.97%	0.00%	0.05%	2.39%	0.00%

Table E26. Sensitivity factors for product A under each scenario (red cells indicate sensitive parameters).

HE/HE	Ag/nAg	PET for t-shirt	Water for t-shirt	Electricity for t-shirt	Natural gas for t-shirt	Detergent for laundry	Water for laundry	Electricity for laundry	Waste PET	Textile landfill	WWTP	Release
OD	0.02%	15.39%	1.23%	0.02%	8.73%	10.85%	52.10%	0.05%	0.01%	0.20%	4.41%	0.00%
GW	0.01%	5.54%	0.07%	23.03%	1.20%	0.98%	3.13%	56.32%	0.18%	0.01%	1.18%	0.00%
PS	0.02%	4.66%	0.07%	23.32%	0.20%	1.01%	3.32%	56.97%	0.02%	0.03%	1.84%	0.00%
AC	0.02%	2.99%	0.04%	24.37%	0.19%	0.60%	1.99%	59.35%	0.00%	0.01%	1.16%	0.00%
EU	0.10%	12.58%	0.26%	2.50%	0.45%	4.62%	11.95%	6.51%	0.08%	0.02%	53.71%	0.00%
HHC	0.14%	23.07%	0.75%	3.29%	0.88%	4.08%	33.11%	8.56%	0.06%	0.02%	21.40%	0.00%
HHNC	0.63%	11.33%	0.21%	6.91%	0.34%	2.93%	9.62%	17.77%	0.12%	0.01%	29.90%	16.54%
RE	0.03%	9.34%	0.24%	19.29%	0.42%	2.37%	10.88%	47.71%	0.00%	0.02%	3.45%	0.00%
EC	0.29%	22.67%	0.67%	5.29%	0.65%	4.20%	29.87%	13.67%	2.19%	0.01%	15.17%	1.36%
FF	0.00%	15.89%	0.05%	19.75%	2.84%	2.58%	2.38%	48.78%	0.00%	0.04%	1.04%	0.00%
HE/LN	Ag/nAg	PET for t-shirt	Water for t-shirt	Electricity for t-shirt	Natural gas for t-shirt	Detergent for laundry	Water for laundry	Electricity for laundry	Waste PET	Textile landfill	WWTP	Release
OD	0.02%	15.39%	1.23%	0.02%	8.74%	10.85%	52.12%	0.00%	0.01%	0.20%	4.42%	0.00%
GW	0.02%	12.93%	0.16%	51.28%	2.83%	2.32%	7.34%	13.18%	0.42%	0.02%	2.78%	0.00%
PS	0.04%	11.08%	0.17%	52.73%	0.47%	2.44%	7.92%	13.58%	0.05%	0.08%	4.41%	0.00%
AC	0.05%	7.65%	0.11%	58.42%	0.49%	1.54%	5.12%	15.19%	0.01%	0.03%	2.99%	0.00%
EU	0.11%	13.36%	0.28%	2.66%	0.47%	4.92%	12.69%	0.63%	0.09%	0.02%	56.75%	0.00%
HHC	0.15%	24.96%	0.82%	3.57%	0.96%	4.43%	35.76%	0.85%	0.07%	0.02%	23.16%	0.00%
HHNC	0.76%	13.55%	0.25%	8.28%	0.41%	3.51%	11.51%	1.99%	0.14%	0.01%	35.49%	19.74%
RE	0.06%	17.65%	0.45%	35.81%	0.80%	4.53%	20.51%	8.97%	0.01%	0.04%	6.60%	0.00%
EC	0.33%	25.83%	0.77%	6.06%	0.75%	4.81%	33.95%	1.45%	2.51%	0.02%	17.32%	1.56%
FF	0.01%	30.33%	0.10%	37.44%	5.55%	5.04%	4.66%	9.41%	0.00%	0.07%	2.05%	0.00%

CE/CE	Ag/nAg	PET for t-shirt	Water for t-shirt	Electricity for t-shirt	Natural gas for t-shirt	Detergent for laundry	Water for laundry	Electricity for laundry	Waste PET	Textile landfill	WWTP	Release
OD	0.01%	10.16%	0.81%	0.01%	5.74%	8.42%	60.58%	0.07%	0.01%	0.13%	5.22%	0.00%
GW	0.00%	2.94%	0.04%	12.41%	0.63%	0.61%	2.99%	68.07%	0.09%	0.00%	1.13%	0.00%
PS	0.01%	2.44%	0.04%	12.45%	0.10%	0.63%	3.14%	68.27%	0.01%	0.02%	1.74%	0.00%
AC	0.01%	1.55%	0.02%	12.87%	0.10%	0.37%	1.87%	70.28%	0.00%	0.01%	1.09%	0.00%
EU	0.06%	7.53%	0.15%	1.48%	0.26%	3.25%	12.82%	9.04%	0.05%	0.01%	57.28%	0.00%
HHC	0.09%	14.71%	0.47%	2.07%	0.55%	3.03%	37.30%	12.52%	0.04%	0.01%	24.18%	0.00%
HHNC	0.40%	7.17%	0.13%	4.36%	0.22%	2.17%	10.92%	25.82%	0.08%	0.01%	33.76%	10.50%
RE	0.02%	5.12%	0.13%	10.68%	0.23%	1.52%	10.74%	59.54%	0.00%	0.01%	3.41%	0.00%
EC	0.18%	14.55%	0.43%	3.35%	0.41%	3.14%	33.91%	20.06%	1.39%	0.01%	17.30%	0.86%
FF	0.00%	9.12%	0.03%	11.38%	1.61%	1.73%	2.44%	63.03%	0.00%	0.02%	1.07%	0.00%
CE/LN	Ag/nAg	PET for t-shirt	Water for t-shirt	Electricity for t-shirt	Natural gas for t-shirt	Detergent for laundry	Water for laundry	Electricity for laundry	Waste PET	Textile landfill	WWTP	Release
OD	0.01%	10.16%	0.81%	0.01%	5.74%	8.43%	60.61%	0.02%	0.01%	0.13%	5.23%	0.00%
GW	0.01%	7.36%	0.09%	30.23%	1.60%	1.55%	7.50%	42.45%	0.24%	0.01%	2.84%	0.00%
PS	0.02%	6.16%	0.09%	30.47%	0.26%	1.59%	7.91%	42.78%	0.03%	0.04%	4.41%	0.00%
AC	0.03%	4.13%	0.06%	33.09%	0.26%	0.98%	4.98%	46.36%	0.01%	0.01%	2.91%	0.00%
EU	0.06%	8.09%	0.17%	1.59%	0.28%	3.49%	13.77%	2.30%	0.05%	0.01%	61.10%	0.00%
HHC	0.09%	16.26%	0.52%	2.29%	0.61%	3.36%	41.04%	3.30%	0.04%	0.02%	26.69%	0.00%
HHNC	0.50%	9.02%	0.17%	5.50%	0.27%	2.75%	13.72%	7.89%	0.10%	0.01%	41.92%	13.21%
RE	0.03%	10.52%	0.27%	21.68%	0.47%	3.16%	21.81%	30.67%	0.00%	0.02%	7.03%	0.00%
EC	0.22%	17.24%	0.51%	3.99%	0.49%	3.74%	39.87%	5.73%	1.65%	0.01%	20.47%	1.02%
FF	0.01%	19.97%	0.06%	24.78%	3.59%	3.85%	5.44%	34.97%	0.00%	0.05%	2.39%	0.00%

Table E27. Sensitivity factors for product C under each scenario (red cells indicate sensitive parameters).

HE/HE	Ag/nAg	PET for t-shirt	Water for t-shirt	Electricity for t-shirt	Natural gas for t-shirt	Detergent for laundry	Water for laundry	Electricity for laundry	Waste PET	Textile landfill	WWTP	Release
OD	6.89%	14.35%	1.15%	0.02%	8.14%	10.11%	48.83%	0.04%	0.01%	0.18%	4.11%	0.00%
GW	2.65%	5.40%	0.07%	22.45%	1.17%	0.96%	3.05%	54.99%	0.17%	0.01%	1.15%	0.00%
PS	5.98%	4.38%	0.07%	21.97%	0.18%	0.95%	3.12%	53.90%	0.02%	0.03%	1.73%	0.00%
AC	7.15%	2.77%	0.04%	22.69%	0.18%	0.56%	1.85%	55.53%	0.00%	0.01%	1.08%	0.00%
EU	26.26%	9.16%	0.19%	1.81%	0.32%	3.35%	8.70%	4.73%	0.06%	0.01%	40.05%	0.00%
HHC	32.21%	15.39%	0.49%	2.17%	0.58%	2.69%	22.25%	5.65%	0.04%	0.01%	14.26%	0.00%
HHNC	8.10%	0.39%	0.01%	0.24%	0.01%	0.10%	0.33%	0.62%	0.00%	0.00%	1.07%	75.54%
RE	10.13%	8.39%	0.21%	17.37%	0.37%	2.12%	9.78%	43.21%	0.00%	0.02%	3.10%	0.00%
EC	25.26%	5.58%	0.16%	1.27%	0.16%	1.00%	7.44%	3.32%	0.52%	0.00%	3.69%	45.48%
FF	1.77%	15.61%	0.05%	19.41%	2.79%	2.53%	2.34%	48.00%	0.00%	0.04%	1.02%	0.00%
HE/LN	Ag/nAg	PET for t-shirt	Water for t-shirt	Electricity for t-shirt	Natural gas for t-shirt	Detergent for laundry	Water for laundry	Electricity for laundry	Waste PET	Textile landfill	WWTP	Release
OD	6.89%	14.35%	1.15%	0.02%	8.14%	10.11%	48.85%	0.00%	0.01%	0.18%	4.11%	0.00%
GW	6.01%	12.16%	0.15%	48.47%	2.66%	2.18%	6.90%	12.40%	0.40%	0.02%	2.62%	0.00%
PS	13.10%	9.62%	0.15%	46.31%	0.41%	2.11%	6.87%	11.80%	0.04%	0.07%	3.82%	0.00%
AC	16.25%	6.38%	0.09%	49.60%	0.41%	1.29%	4.27%	12.71%	0.01%	0.02%	2.49%	0.00%
EU	27.39%	9.57%	0.20%	1.89%	0.34%	3.51%	9.09%	0.45%	0.06%	0.01%	41.72%	0.00%
HHC	33.86%	16.21%	0.52%	2.28%	0.61%	2.83%	23.41%	0.54%	0.04%	0.02%	15.02%	0.00%
HHNC	8.15%	0.39%	0.01%	0.24%	0.01%	0.10%	0.33%	0.06%	0.00%	0.00%	1.08%	75.91%
RE	17.52%	14.55%	0.37%	29.71%	0.65%	3.71%	16.92%	7.37%	0.01%	0.03%	5.42%	0.00%
EC	26.01%	5.75%	0.17%	1.31%	0.16%	1.04%	7.67%	0.31%	0.54%	0.00%	3.81%	46.77%
FF	3.42%	29.35%	0.10%	36.25%	5.36%	4.87%	4.50%	9.09%	0.00%	0.07%	1.98%	0.00%

CE/CE	Ag/nAg	PET for t-shirt	Water for t-shirt	Electricity for t-shirt	Natural gas for t-shirt	Detergent for laundry	Water for laundry	Electricity for laundry	Waste PET	Textile landfill	WWTP	Release
OD	4.63%	9.69%	0.77%	0.01%	5.48%	8.04%	58.09%	0.07%	0.01%	0.12%	4.98%	0.00%
GW	1.42%	2.90%	0.03%	12.24%	0.62%	0.60%	2.95%	67.23%	0.09%	0.00%	1.11%	0.00%
PS	3.23%	2.36%	0.04%	12.05%	0.10%	0.61%	3.04%	66.35%	0.01%	0.02%	1.69%	0.00%
AC	3.84%	1.49%	0.02%	12.38%	0.09%	0.35%	1.79%	67.94%	0.00%	0.00%	1.05%	0.00%
EU	17.85%	6.16%	0.13%	1.21%	0.22%	2.65%	10.51%	7.40%	0.04%	0.01%	47.72%	0.00%
HHC	23.57%	11.16%	0.36%	1.56%	0.42%	2.29%	28.62%	9.49%	0.03%	0.01%	18.44%	0.00%
HHNC	7.94%	0.38%	0.01%	0.23%	0.01%	0.12%	0.59%	1.43%	0.00%	0.00%	1.90%	74.28%
RE	5.83%	4.82%	0.12%	10.06%	0.21%	1.44%	10.12%	56.43%	0.00%	0.01%	3.21%	0.00%
EC	22.32%	4.91%	0.14%	1.11%	0.14%	1.04%	11.74%	6.81%	0.46%	0.00%	5.85%	40.38%
FF	1.01%	9.03%	0.03%	11.27%	1.59%	1.71%	2.42%	62.47%	0.00%	0.02%	1.06%	0.00%
CE/LN	Ag/nAg	PET for t-shirt	Water for t-shirt	Electricity for t-shirt	Natural gas for t-shirt	Detergent for laundry	Water for laundry	Electricity for laundry	Waste PET	Textile landfill	WWTP	Release
OD	4.63%	9.70%	0.77%	0.01%	5.48%	8.04%	58.12%	0.02%	0.01%	0.12%	4.99%	0.00%
GW	3.49%	7.11%	0.09%	29.23%	1.54%	1.49%	7.24%	41.08%	0.23%	0.01%	2.74%	0.00%
PS	7.76%	5.68%	0.09%	28.21%	0.24%	1.47%	7.30%	39.69%	0.03%	0.04%	4.06%	0.00%
AC	9.57%	3.73%	0.05%	30.06%	0.24%	0.88%	4.50%	42.23%	0.01%	0.01%	2.63%	0.00%
EU	18.90%	6.53%	0.13%	1.28%	0.23%	2.81%	11.13%	1.85%	0.04%	0.01%	50.34%	0.00%
HHC	25.36%	12.03%	0.38%	1.68%	0.45%	2.47%	30.78%	2.42%	0.03%	0.01%	19.86%	0.00%
HHNC	8.03%	0.39%	0.01%	0.23%	0.01%	0.12%	0.60%	0.34%	0.00%	0.00%	1.93%	74.98%
RE	11.27%	9.34%	0.24%	19.28%	0.42%	2.80%	19.40%	27.34%	0.00%	0.02%	6.23%	0.00%
EC	23.51%	5.18%	0.15%	1.18%	0.14%	1.10%	12.39%	1.69%	0.49%	0.00%	6.18%	42.44%
FF	2.23%	19.54%	0.06%	24.25%	3.51%	3.77%	5.32%	34.24%	0.00%	0.05%	2.34%	0.00%

References-Appendix E

1. Benn TM, Westerhoff P (2008) Nanoparticle Silver Released into Water from Commercially Available Sock Fabrics. *Environmental Science & Technology*, 42(11):4133–4139. <https://doi.org/10.1021/es7032718>
2. Geranio L, Heuberger M, Nowack B (2009) The Behavior of Silver Nanotextiles during Washing. *Environmental Science & Technology*, 43(21):8113–8118. <https://doi.org/10.1021/es9018332>
3. Benn T, Cavanagh B, Hristovski K, Posner JD, Westerhoff P (2010) The Release of Nanosilver from Consumer Products Used in the Home. *Journal of Environmental Quality*, 39(6):1875–1882. <https://doi.org/10.2134/jeq2009.0363>
4. Lorenz C, Windler L, Goetz N von, Lehmann RP, Schuppler M, Hungerbühler K, Heuberger M, Nowack B (2012) Characterization of silver release from commercially available functional (nano)textiles. *Chemosphere*, 89(7):817–824. <https://doi.org/10.1016/j.chemosphere.2012.04.063>
5. Lombi E, Donner E, Scheckel KG, Sekine R, Lorenz C, Goetz NV, Nowack B (2014) Silver speciation and release in commercial antimicrobial textiles as influenced by washing. *Chemosphere*, 111:352–358. <https://doi.org/10.1016/j.chemosphere.2014.03.116>
6. Mitrano DM, Rimmele E, Wichser A, Erni R, Height M, Nowack B (2014) Presence of Nanoparticles in Wash Water from Conventional Silver and Nano-silver Textiles. *ACS Nano*, 8(7):7208–7219. <https://doi.org/10.1021/nn502228w>
7. Ding D, Chen L, Dong S, Cai H, Chen J, Jiang C, Cai T (2016) Natural ageing process accelerates the release of Ag from functional textile in various exposure scenarios. *Scientific Reports*, 6(1):37314. <https://doi.org/10.1038/srep37314>
8. Limpiteprakan P, Babel S, Lohwacharin J, Takizawa S (2016) Release of silver nanoparticles from fabrics during the course of sequential washing. *Environmental Science and Pollution Research*, 23(22):22810–22818. <https://doi.org/10.1007/s11356-016-7486-3>
9. Mitrano DM, Lombi E, Dasilva YAR, Nowack B (2016) Unraveling the Complexity in the Aging of Nanoenhanced Textiles: A Comprehensive Sequential Study on the Effects of Sunlight and Washing on Silver Nanoparticles. *Environmental Science & Technology*, 50(11):5790–5799. <https://doi.org/10.1021/acs.est.6b01478>
10. Mitrano DM, Limpiteprakan P, Babel S, Nowack B (2016) Durability of nano-enhanced textiles through the life cycle: releases from landfilling after washing. *Environmental Science: Nano*, 3(2):375–387. <https://doi.org/10.1039/C6EN00023A>
11. Reed RB, Zaikova T, Barber A, Simonich M, Lankone R, Marco M, Hristovski K, Herckes P, Passantino L, Fairbrother DH, Tanguay R, Ranville JF, Hutchison JE, Westerhoff PK (2016) Potential Environmental Impacts and Antimicrobial Efficacy of Silver- and Nanosilver-

- Containing Textiles. *Environmental Science & Technology*, 50(7):4018–4026.
<https://doi.org/10.1021/acs.est.5b06043>
12. Üreyen ME, Aslan C (2016) Determination of silver release from antibacterial finished cotton and polyester fabrics into water. *The Journal of The Textile Institute*, :1–8.
<https://doi.org/10.1080/00405000.2016.1222855>
13. Gagnon V, Button M, Boparai HK, Nearing M, O’Carroll DM, Weber KP (2019) Influence of realistic wearing on the morphology and release of silver nanomaterials from textiles. *Environmental Science: Nano*, 6(2):411–424. <https://doi.org/10.1039/C8EN00803E>
14. Kulthong K, Srisung S, Boonpavanitchakul K, Kangwansupamonkon W, Maniratanachote R (2010) Determination of silver nanoparticle release from antibacterial fabrics into artificial sweat. *Particle and Fibre Toxicology*, 7(1):8. <https://doi.org/10.1186/1743-8977-7-8>
15. Yan Y, Yang H, Li J, Lu X, Wang C (2012) Release behavior of nano-silver textiles in simulated perspiration fluids. *Textile Research Journal*, 82(14):1422–1429.
<https://doi.org/10.1177/0040517512439922>
16. Goetz N von, Lorenz C, Windler L, Nowack B, Heuberger M, Hungerbühler K (2013) Migration of Ag- and TiO₂-(Nano)particles from Textiles into Artificial Sweat under Physical Stress: Experiments and Exposure Modeling. *Environmental Science & Technology*, 47(17):9979–9987. <https://doi.org/10.1021/es304329w>
17. Wagener S, Dommershausen N, Jungnickel H, Laux P, Mitrano D, Nowack B, Schneider G, Luch A (2016) Textile Functionalization and Its Effects on the Release of Silver Nanoparticles into Artificial Sweat. *Environmental Science & Technology*, 50(11):5927–5934.
<https://doi.org/10.1021/acs.est.5b06137>
18. Kim JB, Kim JY, Yoon TH (2017) Determination of silver nanoparticle species released from textiles into artificial sweat and laundry wash for a risk assessment. *Human and Ecological Risk Assessment: An International Journal*, 23(4):741–750.
<https://doi.org/10.1080/10807039.2016.1277417>
19. Spielman-Sun E, Zaikova T, Dankovich T, Yun J, Ryan M, Hutchison JE, Lowry GV (2018) Effect of silver concentration and chemical transformations on release and antibacterial efficacy in silver-containing textiles. *NanoImpact*, 11:51–57.
<https://doi.org/10.1016/j.impact.2018.02.002>
20. Temizel-Sekeryan S, Hicks AL (2020) Global environmental impacts of silver nanoparticle production methods supported by life cycle assessment. *Resources, Conservation and Recycling*, 156:104676. <https://doi.org/10.1016/j.resconrec.2019.104676>
21. Walser T, Demou E, Lang DJ, Hellweg S (2011) Prospective Environmental Life Cycle Assessment of Nanosilver T-Shirts. *Environmental Science & Technology*, 45(10):4570–4578.
<https://doi.org/10.1021/es2001248>

22. Hicks AL, Theis TL (2017) A comparative life cycle assessment of commercially available household silver-enabled polyester textiles. *The International Journal of Life Cycle Assessment*, 22(2):256–265. <https://doi.org/10.1007/s11367-016-1145-2>

23. Hicks AL, Gilbertson LM, Yamani JS, Theis TL, Zimmerman JB (2015) Life Cycle Payback Estimates of Nanosilver Enabled Textiles under Different Silver Loading, Release, And Laundering Scenarios Informed by Literature Review. *Environmental Science & Technology*, 49(13):7529–7542. <https://doi.org/10.1021/acs.est.5b01176>

Appendix F

*Published paper and associated references.

Understanding the potential environmental benefits of nanosilver enabled consumer products

The following chapter is a reproduction of an article published in the NanoImpact, with the citation:

Hicks, A.L.; Temizel-Sekeryan, S. (2019) Understanding the potential environmental benefits of nanosilver enabled consumer products, *NanoImpact*, Vol. 16, 100183.

The article appears as published, although style and formatting modifications have been made.

Authorship contribution statement

Andra L. Hicks: Designed Research, Performed Research, Analyzed Data, Wrote the Paper.

Sila Temizel-Sekeryan: Performed Research, Wrote the Paper.

Abstract

Nanoscale silver is widely utilized in consumer products due to its antimicrobial nature. This widespread application has the potential to be both environmentally beneficial and detrimental, depending on how the silver is incorporated and utilized within the products. This work reviews current life cycle assessment literature of nanosilver enabled consumer products, and ultimately divides the products into three categories of potential environmental benefits, including representative products examples. These include “human behavioral benefits”, “passive benefits”, and “replacement benefits”. In the “human behavioral benefits” category, there is an additional environmental impact due to nano-enabling the products, and any reductions in environmental impact will occur as a result of changes in human behavior which is represented by textiles. Products in the “passive benefits” category will not reduce the environmental impact of the product itself, but will have other environmental benefits, such as nanosilver food storage containers reducing food losses and thus the environmental impact of food production. In products where the silver replaces another component, “replacement benefits”, such as nanosilver replacing ointment for bandages, the potential shift in environmental impacts requires comparing the impact of the silver to what it is replacing. Through the creation of different categories of nanosilver enabled products and their potential environmental impacts, guidance is provided as to where potential environmental benefits may occur in the life cycle of these products.

1. Introduction

Silver has been utilized since antiquity due to its antimicrobial efficacy [1–3]. The antimicrobial effects present at the bulk scale have been found to be enhanced at the nanoscale, where at least one dimension of the silver is <100 nm [4]. Nanoscale silver (nAg) is commonly utilized in consumer products, and its global production is only anticipated to increase (Figure F1).

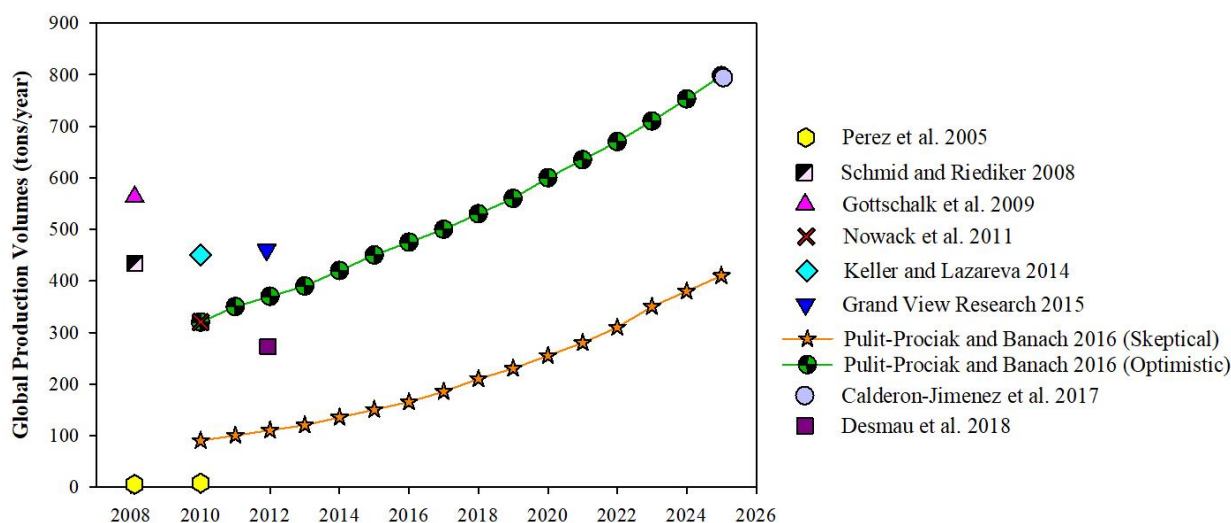


Figure F1. Estimated global nAg production forecasts [5–13]

Figure F1 presents different estimates and future forecasts of global nAg production volumes. Although the estimates have varied somewhat, and future forecasts are presented through both optimistic and skeptical lenses, nAg production is indicated to increase. In part this is due to the use of nAg in various consumer products, largely due to its antimicrobial nature [14, 15]. Figure F2 presents data from the Nanotechnology Products Database as to the current uses of nAg and relative market share [16].

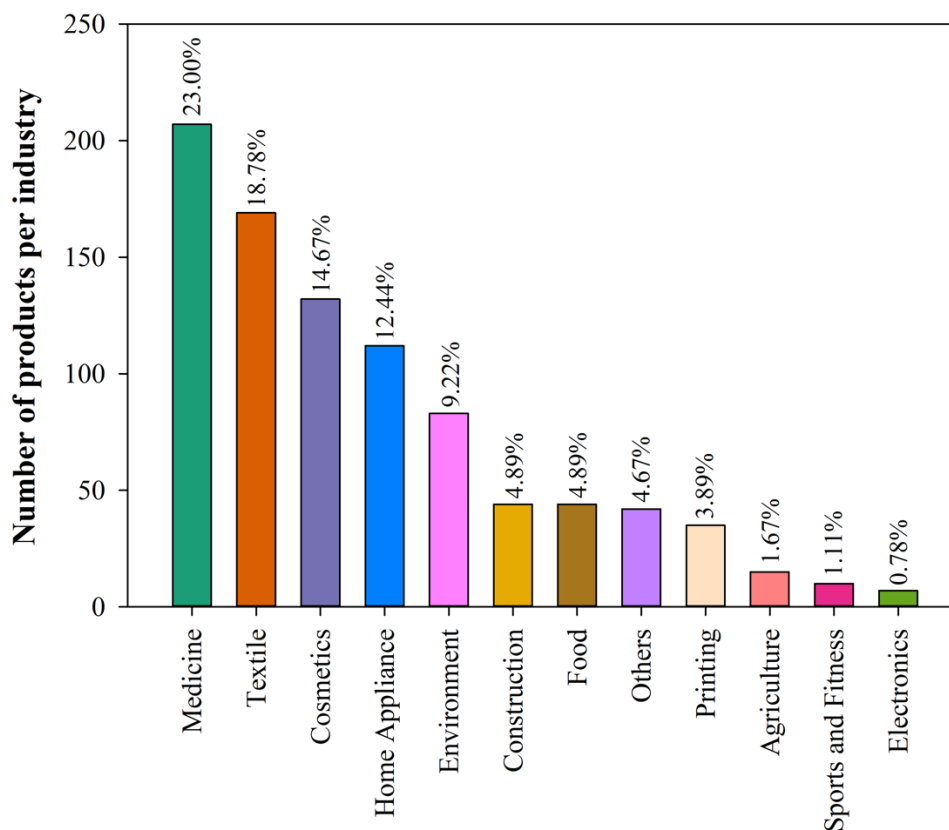


Figure F2. Number of nAg products per industry and their relative share of the market [16]

The application of nAg in products is largely attributed to its antimicrobial characteristics. Medical applications, which comprise the largest category of products in the database, include nAg enabled bandages, catheters, and creams among others [17]. Many of the medical applications have been on the market for a decade or more and their efficacy is well proven [18–23]. Textiles, comprising the second largest product group in the database, have been widely advertised as “anti-stink gear”, on the premise that sweat does not smell, but the bacteria living on the wearer's skin is what causes him or her to smell after sweating. nAg has been incorporated into wearable textiles such as socks, shirts, and underwear, and other textiles, such as baby blankets and bed sheets [14, 15, 24–30], although the efficacy of many of the textile

applications is still subject to debate [31–33]. Food storage containers, where the edible lifetime of the food is prolonged due to the addition of nAg have been studied, although their efficacy is also still subject to debate [34–48]. nAg has also been incorporated into other consumer products, such as cosmetics and home appliances, although these areas have been less well studied and environmental impact data is not widely available.

The environmental impact of nAg enabled consumer products has been analyzed previously using life cycle assessment (LCA) [14, 15, 24, 25, 34–36, 49–52]. LCA is a tool for evaluating the environmental impacts of products and processes in a systematic framework. The goal of this work is to review the previously completed nAg LCA work on consumer products, and to generate categories or groupings based on the portions of the life cycle of the products that will provide potential environmental savings as a function of nano-enabling. This will inform the discussion of nAg enabled products overall from an environmental standpoint, particularly with respect to where potential environmental benefits may be realized.

2. Methods/materials

Studies were selected from the published body of literature with respect to the LCA of nAg enabled consumer products based on multiple criteria. The criteria were based on the goal of this work to understand the potential environmental benefits of these products, compared to their conventional counterparts, across multiple life cycle stages. First, only studies using process based LCA were considered. Thus, studies that utilized Economic Input Output LCA (EIO-LCA) were excluded, due to the aggregated nature of the information provided. Meyer et al. may be given as an example study that considered EIO-LCA [50]. Although it was pioneering at its time of publication, the level of detail is fairly low due to the method utilized. Second, only studies

considering at least three stages of the entire life cycle of the product were considered. Although there are excellent studies that focus on the cradle to gate aspect of the products' lifecycles [51], a major goal of this work is to analyze the impacts across the entire lifecycle of the nAg enabled product. And finally, each study considered needed to include at least one environmental impact category in order to provide an environmental assessment.

The literature meeting the criteria are summarized in Table F1, and then expanded upon in the following sections. The products are then classified based on the commonalities within their lifecycles and environmental impacts, to inform a multiple category system. The categories are then used to suggest where the potential for environmental benefits may exist due to the usage of nAg enabled consumer products.

Table F1. Summary of cradle to grave studies considered.

Product	Impact Categories Considered	Reference
T-shirts (types: conventional, four nAg syntheses, and Triclosan, materials: polyester)	Global warming, freshwater and seawater aquatic toxicity	[24]
T-shirts (types: conventional and nAg, materials: polyester and cotton)	TRACI categories (v 2.1, nine categories)	[15]
T-shirts (types: conventional, nAg, and Triclosan, materials: bio-based man-made cellulose fibers)	ReCiPe (v 1.05), IPCC 2007, and freshwater and seawater aquatic toxicity [24]	[25]
Hospital gowns (types: conventional and nAg, materials: cotton–polyester blend)	TRACI categories (nine categories for nAg only) and CED (for hospital gowns)	[52]
T-shirts (types: conventional, and three nAg loadings, materials: polyester)	TRACI categories (v 2.1, nine categories)	[14]
Bandages (types: nAg)	TRACI (v 2., nine categories)	[49]
Food storage container (types: conventional and micron Ag, short lifetime)	TRACI categories (v 2.1, nine categories)	[34]
Food storage container (types: conventional and nAg)	TRACI categories (v 2.1, nine categories)	[35]

3. Results and discussion

LCA literature analyzing the environmental impacts of nAg enabled consumer products is summarized in Table F1. The studies were selected as described in the methods section. Textiles, and T-shirts in particular, have been the most studied consumer products, with five different LCA studies produced. For the medical category, one study investigating nAg enabled bandages was found. For the food storage containers, two studies were found that employed LCA over multiple environmental impact categories. As Eckelman and Graedel stated, with the increasing use of silver mainly in textiles, plastics and medical industries may change the environmental impacts resulting from the life cycle of silver itself, which also supports the outline of considered studies in this work [53].

3.1. Textiles

The purpose of clothing in the utilitarian sense is to protect the wearer from the elements [54], and to conceal portions of the body which society has deemed necessary [55]. Nano-enabling textiles in general does not enhance or provide new functionality to this purpose, although it may serve to shift the environmental impact of textiles and prevent textiles from transmitting infections [15, 52].

The nAg content and attachment methods of antimicrobial textiles vary significantly and influence the overall environmental impact. Many studies have sought to quantify initial nAg content along with losses during the lifetime as a function of laundering [26–30], while others have sought to determine the efficacy of nAg enabled textiles [31–33].

A comparatively smaller number of studies, as presented in Table F1, have utilized LCA to elucidate the environmental impacts of nAg enabling these textiles along with their potential

benefits. Walser et al. analyzed polyester T-shirts coated with both Triclosan and nAg in order to make them antimicrobial, utilizing environmental impacts categories of global warming potential and both fresh and saltwater eco toxicity [24]. The authors found the environmental impacts with respect to greenhouse gas emissions vary as a function of how the nAg was produced, with some of the methods producing a similar impact to both the conventional and Triclosan enabled T-shirts, while others had environmental impacts two orders of magnitude greater. When the freshwater eco toxicity was considered during the use and disposal phases, the Triclosan had a lower environmental impact, however, when seawater eco toxicity was considered the nAg had a greater environmental impact. Walser et al. also suggested that the use phase is critical to consider when looking to reduce the environmental impact of textiles, particularly with respect to frequency of launderings which may (but not necessarily) will be influenced by the penetration of nAg textiles into the market, and corresponding shifts in human laundering behaviors [24]. Manda et al. investigated nAg and Triclosan enabled T-shirts, in particular focusing on the difference in environmental impact of coating the nAg onto the fibers prior to them being incorporated into the garment [25]. Multiple environmental impact categories were considered, along with difference in the frequency of wearings prior to laundering as a function of the antimicrobial coating employed. While the conventional textile was assumed to have a lifetime of 100 wearings and 50 launderings, the antimicrobial shirts were assumed to be laundered between 30 and 46 times during their lifetime. This led to the observation of a reduction in the environmental impact of the antimicrobial shirts, in part due to reduced frequency of laundering, due to a shift in human behavior.

Hicks et al. [15] and Hicks and Theis [14] analyzed the environmental impact of nAg enabled textiles utilizing a suite of nine environmental impact categories across the life cycle.

Hicks et al. modeled both conventional cotton and polyester textiles and their nAg enabled counterparts, along with high efficiency and conventionally efficient laundering scenarios [15]. They found that for many of the impact categories the majority of the impact was due to the production of the textile itself (not the added nAg) or the laundering (when a conventionally efficient washer and dryer pairing was used). In the eco-toxicity category, the release of the nAg (modeled as ionic silver) was found to be significant with respect to environmental impact. Hicks and Theis analyzed three commercially available polyester textiles with different initial silver concentrations compared to a conventional polyester textiles [14]. One often touted benefit of nAg enabled textiles is the potential to launder them less frequently. The authors found using environmental payback period that for some of the impact categories (such as global warming) it would be possible to reduce the frequency of launderings enough to compensate for the additional environmental impact of the added silver, however, for other impact categories such as eco-toxicity it may be impossible, particularly when the silver loading of the textile is very high. Which suggests as did Walser et al. that human behavior and laundering may play the greatest role in changing the environmental impact of textiles, regardless of whether they are nAg enabled [24].

Hicks et al. compared the environmental costs of reusable nAg enabled hospital gowns to single use disposable gowns with a life cycle assessment perspective [52]. The lifetime of reusable gowns was assumed as 75 launderings, while single use gowns were assumed to be disposed immediately. They found that at wear 12, the environmental impact of nAg and disposable gowns become equal, and after this point reusable gown becomes less environmentally impactful option than its disposable alternative. It should be noted that different nAg synthesis methods may change these results significantly. In Benn et al., it is indicated that

using nAg containing products may have negative impacts on human and environmental health [56]. Also, Benn et al. suggested that consumers need to weigh the potential consequences against the benefits of using these products in order to scheme their behaviors [56], which is a similar statement as given by Walser et al. [24] and Hicks et al. [57, 58].

3.2. Medical applications

The purpose of bandages in general is to promote wound healing [59]. Nano-enabling bandages and dressings with silver provides novel functionality compared to conventional dressings in that the wounds heal more quickly and the dressings need to be changed less frequently. Beyond that, nAg enabled dressings have been found to cause less pain during dressing changes in burn victims [19]. The addition of nAg to these bandages makes them superior in performance to their conventional counterparts. The avoidance of more frequent bandage changes, a longer duration of bandage usage, and the usage of antimicrobial treatments has the potential to shift the environmental impact of treating wounds through the usage of these products.

Medical applications of nAg are arguably one of the most critical utilizations of the antimicrobial properties of nAg. This includes dental instruments, coating contact lenses, endodontic fillings, bandages and wound care, cardiovascular implants, catheters, bone cement and other implants, and for the general treatment and diagnoses of disease [17]. These are applications where infection control is critical, whereas in some of the other nAg enabled products, such as shirts, it is merely an attractive feature. Although some overlap does exist between medical applications and textiles, such as in the instances of nAg enabled hospital gowns [52] and curtains [60], the major goal of using nAg in a medical context is to reduce

infection, and it has been hailed in the popular media as a potential ‘silver bullet’ for the prevention of nosocomial infections [61, 62]. Hospital acquired infections have been associated with increases in the cost of treatment and prolonged stay durations [63, 64], making this a critical area of research.

Although there are many applications and current uses of nAg enabled products in a medical setting, there is relatively little life cycle environmental impact data available. Although there is a great deal of literature on the current or anticipated efficacy of these products [18, 65–80], to date only one study was found that fits within the literature selection criteria. Pourzahedi and Eckelman applied LCA to nAg enabled bandages, analyzing the impacts from cradle to gate and then the disposal phase (omitting the use phase) [49]. The authors found that although the nAg comprises 6% of the mass of the bandage, for the raw materials and manufacturing that the nAg is responsible for between 40% and 90% of the environmental impact. With respect to disposal, in this instance incineration, for impact categories such as eco toxicity the silver and its eventual release critically influences the environmental impact. However, for both global warming and eco toxicity impacts, the contribution of end of life stage is lower than the raw materials and manufacturing stages. As Pourzahedi and Eckelman make note in their study, it is relevant to compare the use of nAg enabled bandages to their conventional counterparts, such as a bandage coupled with an ointment, to better understand the relative tradeoffs. This is representative of the use of silver enabling a replacement of a part or a whole of a conventionally utilized product.

3.3. Food storage containers

The purpose of food storage containers is to enhance resource sustainability through the preservation of food [81]. Silver has been utilized since antiquity history to preserve liquids, in the form of silver lined storage vessels and silver coins [82]. Nano-enabling food storage containers with silver has the potential to increase the edible lifetime of food through augmented preservation due to the antimicrobial characteristic of nAg. The addition of nAg marginally changes the environmental impact of the food storage container itself, however, it has the potential to avoid food losses at the consumer level due to spoilage and thus decrease the need for replacement food and its associated environmental impact.

nAg enabled food storage containers have the potential to reduce food spoilage and losses through their antimicrobial nature. Literature has presented a fairly mixed view with respect to the efficacy of these containers, as a function of the quantity of silver used, the food type stored, and the application of the silver [37–48]. For instance, Cushen et al. compiled a detailed list of nanotechnology examples from food industry along with used nanocomponents (i.e. Ag, ZnO, Silica) and their functions (i.e. antimicrobial, anti-UV, inhibition of polymerization) [83]. Westerband and Hicks presented a review of current silver food packaging efficacy studies [36]. Despite the fact that the nAg are permanently embedded in the food containers/ packaging, many studies have found migration of silver (either nano or ionic forms) from food containers/packaging to the food and ultimately to receiving water bodies [76, 83–86] which may be a matter of concern for both the environment and public health.

Bi et al. studied both the efficacy and life cycle environmental impacts for a silver enabled (at the micro scale) food storage container compared to its conventional counterpart (a multiuse plastic food storage container) [34]. From an environmental impact perspective, the

contribution of the silver was fairly small compared to the use (washing) phase, in particular due to the low content of silver found in the container. With respect to the efficacy, based on *Escherichia coli* (E.coli) inhibition, the silver enabled container was not any better than the conventional container, suggesting that the studied container would not prolong the lifetime of food stored in it, and thus would be unable to compensate for the additional environmental impact of the silver enabling it. Westerband and Hicks found that the additional environmental impact of adding the nAg to the food storage containers was a very small percentage of the total cradle to grave environmental impact, with the use phase being the most significant [35]. Westerband and Hicks also compared the additional environmental cost of nano-enabling the food storage containers to their potential food savings benefits, finding that if the containers are effective at prolonging the lifetime of the stored food, then the additional capital environmental impact would be worth it [36]. This varies as a function of the type of food storage (i.e. meat versus vegetables) and its corresponding environmental impact, and it predicated on the effectiveness of the antimicrobial characteristics of the container. This suggests that any potential environmental benefits that will occur with the use of nAg enabled food storage containers will occur outside of the strict life cycle of the storage containers themselves, if the boundaries are drawn for only the storage container. However, if the system and boundaries were to be expanded, such as including the environmental impacts of the production of the stored food, then the benefits could be realized within the system life cycle.

3.4. Grouping potential environmental impacts and benefits

Adding nAg to consumer products to generate nano-enabled products has the potential to both increase and decrease environmental impacts, along with bestowing benefits not found in

the conventional products. For instance, due to their antibacterial properties, enabling nAg into conventional textile products helps to prevent bacterial activity on the skin thus inhibit odors [87]. Another example may be given from medical industry, where nAg enabled bandages not only eliminate the consumption of antibacterial ointment but also shorten recovery times compared to conventional bandages [51]. Further, compared to conventional food storage containers, nAg enabled containers help to extend the lifetime of the stored food which reduces food losses [35, 36]. Gilbertson et al. listed the primary life cycle impact indicators for nAg enabled consumer products and stated that the raw materials and manufacturing phases contribute significantly to global warming potential, fossil fuel depletion and mineral resource depletion, while use and end of life phases contribute on terrestrial, freshwater and marine eco toxicity and non-carcinogenics [88]. The human toxicity category is indicated as a concern for all four phases [88]. Added benefits and impacts of nano-enabled textiles, bandages and food storage containers along with break-even points are included in Table F2. There is also the potential based on the quantity of nAg added to these products for no environmental benefits to be realized. The authors also recognize the limited nature of the categories suggested here, due to existing gaps in the breadth of LCA studies on nAg enabled consumer products. And that if future nAg enabled consumer product studies become available that there is the potential to increase the number of categories.

Table F2. Added environmental benefits and impacts of nano-enabled products with break-even points.

	Added Benefits	Added Impacts	Break-even points
Textiles (Human behavioral benefits)	Potential to launder less frequently	Producing nAg and its release to environment	When the human behavioral benefits compensate the added impacts of producing and enabling nAg
Bandages (Replacement benefits)	Eliminated ointment need, better wound healing (i.e. time)	Producing nAg and its release to environment, although may be offset by avoided ointment less frequent bandage changes	When the nAg enabled bandage use compensates the life cycle of bandage coupled with an ointment
Food Storage Containers (Passive benefits)	Reduced food loss due to extended food life	Producing nAg and its release to environment, and also potential migration of nAg into stored food	When the nAg enabled food storage container production/use compensates the environmental impacts associated with food production and replacement food

Certain aspects of each of these products enable the creation of different groupings, or case studies, which illustrate if and where in the product life cycle environmental benefits will occur (Figure F3). The three presented overlapping circles acknowledge that there is also some overlap in these categories: “human behavioral benefits” which is embodied by the nAg enabled consumer textiles, “replacement benefits” which is illustrated by the nAg enabled bandages, and “passive benefits” which is displayed by the food storage containers.

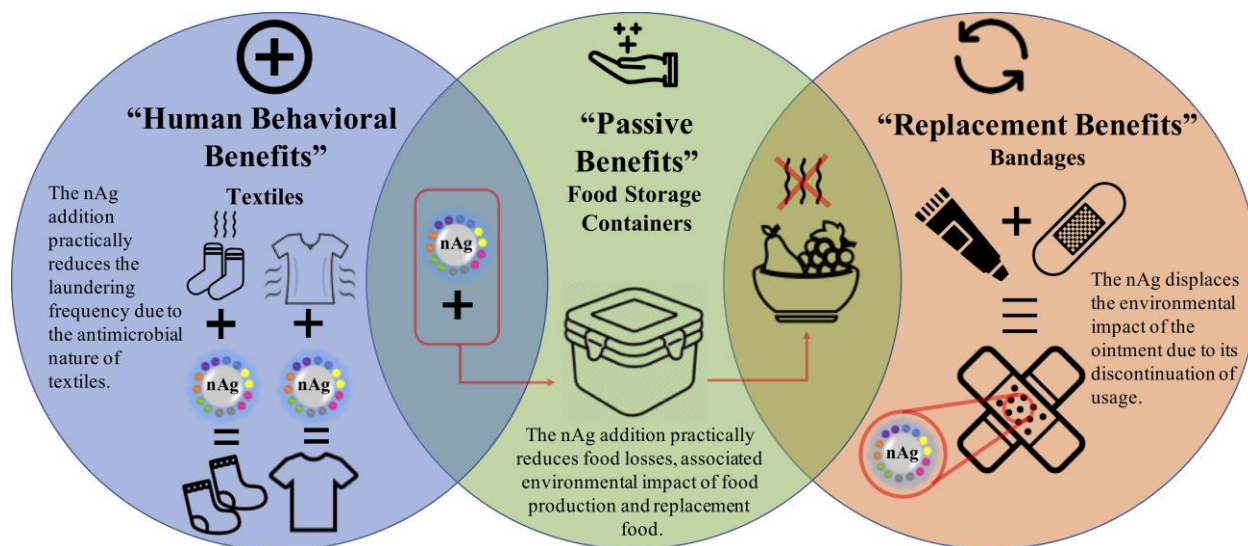


Figure F3. Bins of nAg enabled products by potential environmental benefits.

For the nAg enabled textiles, such as the T-shirts presented, the generalizable model is that from a cradle to gate perspective the environmental impact of the nAg textile will be higher, due to the environmental cost of mining, refining, nanosizing, and attaching the silver. Essentially the nAg is an “add on” component to the conventional textile. If the textile is laundered in the same manner and at the same frequency as the conventional textile, then the environmental impact of the nAg textile will be greater over the course of its lifetime. LCA research has shown that the real potential to reduce the environmental impact through the addition of nAg to textiles is a result of changes in human behavior, such as laundering frequency due to the antimicrobial nature of the textiles. If human behavior does not change, then the environmental impact of the nAg enabled textiles will actually be greater than the conventional textiles. Conversely, if human behavior does change, there will be a reduction in overall environmental impact of nAg enabled textile, i.e. due to less frequent laundering, savings in both energy and water consumption can be achieved. Human behavior, in the context of the adoption and use of new technology is challenging to both anticipate and change. Characteristics

of products that would fit within this category are as follows: 1) a significant impact due to the use phase, and 2) the potential for human behavior to greatly alter the use phase impact.

Examples of other nAg enabled consumer products within this category include common consumer textiles beyond wearables (i.e. bed linens, towels, etc.). Beyond that, if the nAg enabled product changes consumer behavior and thus environmental impact, then it would belong in this category.

The nAg enabled bandages are an example of the “replacement benefits” category, where the addition of nAg is use in the stead of another component, such as an antimicrobial ointment or more frequent bandage changes. The nAg displaces the environmental impact of the ointment (and additional bandages) due to its discontinuation of usage. Whether there is an overall reduction in the environmental impact of the nAg enabled bandage compared to the conventional bandage plus an ointment, depends on the environmental impact of the nano-enabled product compared to the two products that were utilized together previously. Characteristics of products that would belong in this category include: 1) replacement of a conventional product or component with a nAg enabled component. One example of product within this category would be a nAg enabled consumer antibacterial soap, where the nAg replaces another active antibacterial component, such as Triclosan. Another more nuanced example would involve hospital gowns. Due to growing concerns of hospital acquired infections (i.e. nosocomial infections) there has been an effort to shift to single use items. However, this is in conflict with the goal of making healthcare more sustainable [89]. In a previous study reusable nAg enabled hospital gowns were compared with single use gowns, to determine the environmental breakeven point while still maintaining antimicrobial efficacy [52]. Benefits would be seen to due to replacement of the disposal gown product with a reusable nAg enabled gown.

The “passive benefits” category is illustrated with the nAg food storage container. There is an additional environmental impact to nano-enabling the food storage container, which may range as a function of the quantity of nAg used. Like the “human behavioral benefits” category, this is in addition to essentially the environmental impact of a conventional food storage container. Unlike the textiles, however, there is the potential to extend the lifetime of the stored food. Although this does not directly affect the life cycle environmental impact of the food storage container itself, the prolonging of the time in which food is of sufficient quality to eat, has the potential to reduce food losses and waste due to spoilage. Which in turn has the potential to provide “passive benefits” overall to society through the reduction in food waste, and the associated environmental impact of food production and replacement food. Characteristics of products that would fit into this category include: 1) changing the lifetime or usage phase duration of another separate product or process. Catheters that are nAg enabled are an example for this category, where the antimicrobial efficacy does not change how the catheter is utilized, nor does it provide life cycle impact benefits, however, there is the potential for benefits to be realized outside of the product system, such as reduced infection rates which would require additional resources and environmental impacts to treat. A second example would be nAg enabled cutting boards. Cutting boards have been shown to harbor pathogens [90], which lead to illness. If the cutting board is enabled with nAg and it effectively reduces the pathogen load and thus the transmission to other foods and illness, then benefits will occur outside of the life cycle of the cutting board itself.

The three proposed categories of nAg enabled consumer products allow for the conceptualization either without or prior to conducting an LCA as to where potential environmental benefits may occur in the system. The primary benefit bestowed by nanoenabling

products with Ag is antimicrobial efficacy. This is critical in anticipating the potential environmental tradeoffs with respect to nAg enabled consumer products, and ultimately in determining which products are worth nanoenabling. This is particularly important as the number of nAg enabled products continues to grow in diversity of applications, and global nAg product continues to increase. The authors recognize that these are first attempt at categorizing the potential environmental benefits of nAg enabled consumer products and that in the future there will likely be revision and expansion of these definitions and categories.

3.5. Use phase considerations: efficacy and human behavior

As discussed previously, impacts resulting from the use phase may affect the overall environmental costs of nano-enabled products significantly. To elaborate more on the use phase considerations for each category, efficacy of nAg enabled products and human behavioral implications are included herein.

3.5.1. Textiles

In the “human behavioral benefits” category, which is illustrated by textiles, several efficacy studies have been conducted to examine the antibacterial activity of nAg enabled textiles. These studies suggested, the speciation of nAg may be modified during use phase which may limit the antibacterial efficacy [31, 91–93], therefore the efficacy is a function of transformation in the silver species as well as the attachment method [94]. Spielman-Sun et al. conducted a study where different types of silver species (i.e. Ag coated, AgCl coated, electrostatic-nAg and tethered-nAg) were tested for their efficacies by measuring the number of *E. coli* (gram-negative) recovered from polyester textiles after 24 h [94]. They found that except

the electrostatic-nAg, all speciations performed complete reduction. Further, Lee et al. studied antibacterial efficacies of nAg padded cotton and polyester textiles on *Staphylococcus aureus* (gram-positive) and *Klebsiella pneumoniae* (gram-negative), and the fabrics showed 99.9% reduction of both species [95]. Similarly, El-Rafie et al. conducted experiments to evaluate the antibacterial efficacy of nAg enabled cotton fabric on *Escherichia coli* and *Staphylococcus aureus* and a reduction of colonies by 90% was achieved [96]. Besides biocidal activities, McQueen and Ehnes mentioned that in vitro tests should also be conducted to better understand the antimicrobial efficacy of nAg enabled textiles on people [33].

Although the results of existing research on antibacterial efficacy are promising, there is still an improvement needed to balance the risks and benefits of nano-enabled products in order to assess the impact and performance together [31]. Considering that laundering phase is associated with the biggest environmental cost [15], human behavior is a prominent contributor to overall life cycle of textiles due to possible changes in laundering frequency. Hicks and Theis argued that although there are many studies on public acceptance of nanotechnology, changes in consumer behavior as a result of this new technology are not well explored [14]. Given that the premise of nAg enabled textiles from a consumer perspective is their anti-odor function [94], this may be an effective factor in changing the laundering frequency. However, as various studies discussed, besides odor reduction, there are several considerations for laundering need such as cleanliness of garment, look, shrinkage and the need to “freshen” up [97–100], as well as cultural habits, time and garment type [97, 101, 102]. Which suggests that consumers will not necessarily change their laundering behavior after adopting a nAg textile, and thus erode the potential for savings. Hicks and Theis explored the potential to pay back the initial environmental impacts invested in nAg production and loss, and found that for some environmental impact categories it

would be feasible to reduce the overall environmental impact as a function of reduced laundering, whereas for others even if no laundering occurred, it would not be possible [14].

3.5.2. Bandages

In “replacement benefits” category, which is demonstrated by bandages, there are various studies discussing the efficacy of nAg enabled bandages in wound healing. Identifying the differences between the efficacy of the nAg enabled bandages and the current protocol is one of the important considerations for the use phase. Chaloupka et al. [103] and Ge et al. [17] reviewed the efficacy studies which conducted random clinical trials and summarized that nAg enabled wound dressings could reduce the healing time by 3.35 days with an increased bacterial clearance. They also added that silver in nano form may be safer since it prevents the elevated silver concentration in blood [17, 103]. However, nAg enabled bandages may not be utilized in exactly the same manner as conventional protocols. Tredget et al. performed a randomized treatment study, to compare the nAg bandage with the institution's standard burn care procedure (0.5% silver nitrate solution) [19]. The standard protocol involved moistening the gauze soaked in the silver nitrate solution every two hours, whereas, the nAg enabled bandages were changed on a daily basis. Patients found the dressing removal significantly less painful with the nAg enabled bandage when compared to the conventional burn treatment protocol. The nursing staff reported the ease of using both dressing types to be similar to one another. This is another change in human behavior to consider when these products are utilized.

According to Fabrega et al., exposure to nAg enabled consumer products do not result in any adverse effects on humans. However, toxicity of nAg may depend on environmental conditions (i.e. organic matter, hardness, chloride levels) which may change the bioaccumulation

patterns of nAg [104, 105]. Rigo et al. demonstrated in vivo and in vitro experiments to examine the efficacy of nAg enabled wound dressings and found similar results with Fabrega et al., suggesting that these bandages lead to restoration of skin without any toxicity concerns [105, 106]. Recently, Gorka et al. published a study where they modeled human exposure scenarios for nAg wound dressings and showed that chemical and physical transformations may occur when in contact with sweat or wound fluid [107]. However, they also mentioned that these transformations do not affect the antimicrobial efficacy but may have unintended environmental consequences when disposed [107].

The body of literature on nAg enabled bandages and wound dressings has focused on the treatment of burns in a hospital setting. Different protocols and adaptations in human behavior exist compared to home treatment of small wounds. Tredget et al. discuss changes in how the nAg dressings were utilized compared to their standard treatment protocols in the case of burns treated as a hospital [19]. More recently, silver enabled bandages (both at the nano and bulk scales) have been available on the consumer market for home usage [108, 109]. In this usage scenario there is the potential for the replacement of using ointment and the conventional bandage in concert, with a silver enabled bandage, which will potentially shift the environmental impact of the product, through “replacement”.

3.5.3. Food storage containers

With respect to “passive benefits” category, which is exemplified by food storage containers, several studies suggest that nAg enabled food storage containers help increasing shelf life of solid and liquid food by inhibiting the bacterial growth in varying conditions and spans (i.e. under 2 °C for 14–25 days, 35 °C for 7 days). By utilizing nAg enabled food storage

containers Metak and Ajaal observed decreased fungi growth on carrots, An et al. reported increased shelf life of green asparagus and Emamifar et al. found reduced fungi and bacteria growth in orange juice [37, 38, 110]. Conversely, Bi et al. conducted an antimicrobial testing on food stored with nAg enabled food storage containers and found that silver inclusion did not improve eliminating the microbial activity of *E. coli* [34]. Williams et al. studied the impact of using nAg enabled food storage containers on the growth of *Salmonella typhimurium* (gram-negative) and suggested that nAg inclusion may not have significant effect to protect food from loss [111]. As the efficacy results differ dramatically, it is challenging to provide a clear statement on whether nAg enabling is promising for preventing food loss. It should be noted that the efficacy of these containers may be a function of the plastic composition, size and form of nAg embedded and manufacturing method. Bi et al. argued that polypropylene matrix effectively limits silver migration and decrease the antibacterial efficacy [34]. Overall, the efficacy tests for “passive benefits” have not been well explored. Further, impact of change in the human behavior in “passive benefits” category does not have a significant contribution on whether decreasing or increasing environmental cost because the benefit occurs outside of the product.

3.6. End of life evaluations: release and fate in the environment

Considering that nAg is the most commercialized engineered nanomaterial (ENM) accounting for >50% of the global nanomaterial consumer products [112], examining the release and fate mechanisms is critically important. Various studies have been conducted to model nAg released from consumer products and their fate in the environment. Recently, Potter et al. published a study where nAg release from 22 nAg enabled publicly available consumer products (including dietary supplements, first aid sprays and surface sanitizers) were examined by

conducting simulated use and disposal phases [113]. They argued that nAg added to consumer products do not behave same as the ones synthesized in a laboratory environment [113]. Benn et al. also studied the nAg release from consumer products used at home including textile, medical mask and cloth, toothpaste, shampoo, detergent, a towel, a toy teddy bear, and two humidifiers [56]. The initial silver concentrations were between 1.4 and 270,000 $\mu\text{g Ag/g}$ product and the amount of release was found up to 45 $\mu\text{g Ag/g}$ product [56]. Similarly, Quadros et al. assessed nAg enabled consumer products for children such as plush toy, baby blanket, sleepsuit, pair of baby scratch mitts, breast milk storage bags, sippy cups, cleaning products, humidifiers, and humidifier accessory [114]. They examined releases of nAg into different media including water, orange juice, milk formula, synthetic saliva, sweat, urine, air and dermal wipes. Initial silver content ranged between 0.6 and 109.8 $\mu\text{g Ag/g}$ product and after simulating use and aging processes, the amount of silver release ranged between 0.07 and 18.5 $\mu\text{g Ag/g}$ product [114].

Beyond simply the quantity and speciation of the released Ag, the development of adequate life cycle impact assessment characterization factors for nAg. Many of the LCA studies which exist for nAg release model the release Ag as Ag^+ [14, 15, 34–36, 52, 57, 58] due to a lack of nAg specific characterization factors. Gilbertson et al. discuss the uncertainty surrounding the release and impacts of engineered nanomaterials [88]. In particular, focusing on the existing knowledge gaps for creating LCIA factors necessary for comprehensive LCA work that adequately considers the end of life.

3.6.1. Textiles

Enabling nAg into textiles (i.e. sock, T-shirt, blanket, trousers) or fibers implies utilization of different forms of silver and application of different attachment techniques, which

affect the quantity of silver emitted from the use phase [15, 115, 116]. Review of the previous literature on silver release from nAg enabled textile products and their implications are tabulated in Table F3. It should be noted that both the mass of initial silver content and release are presented in ranges, since the particle characterization is not detailed in most of the sources. As Mitrano et al. argued, the amount of silver released may be dependent on the chemical structure of nAg, mode of binding, adhesion ability, adsorption capacity, moisture content and properties of fibers that they are incorporated in [117], and this may complicate the exposure assessment [29].

Table F3. Literature on silver (Ag) release from nAg enabled textile products.

Product Type	nAg Release Implications	Ref.
Sock (6 samples)	IC: 0.9–1,358 µg Ag/g of sock.	[27]
	P: Washing unworn and unweathered socks with ultrapure water and without detergent for 1-24 hours.	
	R: 19-1,845 µg of the Ag in sock samples were released.	
Sock (9 samples)	IC: 3–21,600 µg nAg/g of sock.	[26]
	P: Washing socks at pH 10, buffered by 0.005 M sodium carbonate with 0.1 g/L sodium dodecyl sulfate as surfactant. Bleaching cycle was examined as well.	
	R: 1.3-377 µg of the nAg in sock samples were released.	
Sock (5 samples), t-shirt (2 samples), trousers (1 sample)	IC: 1.5–2,925 µg Ag/g of textile.	[28]
	P: Washing textiles with a laboratory washing machine and a detergent having pH 10.6 (consisting of linear alkylbenzene sulfonate, (8%), sodium triphosphate (43.8%), sodium and magnesium silicate (9.4%), and sodium sulfate (21%))	
	R: 4.5–575 µg/g of Ag released into the washing solution and 1.8–113 µg/g of Ag released into the rinsing solution.	
Sock (2 samples), t- shirt (2 samples), trousers (1 sample)	IC: 18–2,925 µg Ag/g of textile.	[29]
	P: Washing textiles (1) with a laboratory washing machine (LW) using the same detergent as Lorenz et al. [28], and (2) with a commercial washing machine (CW) using Persil Megaperls for three sets.	
	R: 6.7-687 µg/g of Ag released by using LW, 0.9-1,755 µg/g of Ag released by using CW.	
Textile (5 samples)	IC: 15–14,500 µg Ag/g of textile.	[30]
	P: Washing textiles at 40°C using a phosphate-free detergent without a brightener.	
	R: 0.675-2,347 µg of the Ag in textile samples were released.	
	IC: 3.9-1,095 µg Ag/g of textile.	[118]

Product Type	nAg Release Implications	Ref.
Textile (glove and underwear)	P: Simulating a typical textile use scenario by weathering with synthetic sweat, skin surface film liquid (which consists of aqueous sweat component and a lipid sebum) and saliva and washing.	
	R: 2.12-2.46 µg of the Ag in textile samples were released.	
Textile (4 samples)	IC: 7.5-10.7 µg Ag/g of textile.	[117]
	P: Full spectrum sunlight irradiation and/or washing in seven different detergent formulas	
	R: 3.39-35.69 µg of the Ag in textile samples were released after washing only, and 4.68-35.35 µg of the Ag in textile samples were released after sunlight weathering and washing.	
T-shirt (4 samples)	IC: 1-4,076 µg Ag/g of textile.	[31]
	P: After simulated use phases, two scenarios were applied as (1) laundering with a standard American Association of Textile Colorists and Chemists (AATCC) laundry detergent, and (2) washing with deionized (DI) water.	
	R: As a result of washing with DI water, Ag ⁰ -coated textile released approximately 106 µg total Ag/g of textile, tethered-AgNP textile released 18 µg/g, electrostatic-AgNP released 0.79 µg/g and Ag salt-coated textile released 3.1 µg/g. Washing with AATCC detergent showed similar trends with the ones observed in DI water.	
Textile	IC: 35 µg Ag/g of textile.	[119]
	P: Exposure to three types of environmental weathering conditions with varying amounts of sunlight, rain and temperature during two weeks without considering wearing and washing phases.	
	R: Approximately 1.7 µg Ag/g of textile were released into the precipitation runoff sample.	
Sock (7 samples), textile (4 samples)	IC: <37 (detection limit)-6,408 µg Ag/g of textile.	[116]
	P: Two different wearing procedure was applied. First one was walking, which was carried out by three male participants in an office setting for 4 days/week (8-16 km/week). Second one was running, which was carried out by two male and two female participants for 1 hour per week (15 km/week). After wearing, standard washing procedure was applied by using Tide detergent. These wearing and washing cycles were conducted as three sets.	
	R: 46.6 µg Ag/g of sock were released after walking and washing procedure in the first cycle. 38.6 µg Ag/g of sock were released after running and washing procedure in the first cycle. The unworn control had 16.3 µg Ag/g of sock. Second and third cycles did not show a large difference between worn and unworn samples.	

IC: Initial silver content, P: Procedure and conditions, R: Silver release.

Distinct from aforementioned studies, Arvidsson et al. applied particle flow analysis in order to estimate emissions due to the usage of nAg enabled textiles [115]. Instead of mass-based indicators, they used particle number in their equations to be able to predict the variations coming from the particle properties (i.e. size) since they vary greatly because of different

synthesis methods/technologies. They modeled an ‘explorative scenario’ with extremely high adaption and calculated the amount of nAg enabled textile usage as 32 kg/capita/year in that scenario. Therefore, nAg release from textiles may be a matter of concern in the future if widespread adoption occurs.

3.6.2. Bandages

As elaborated previously, incorporating nAg into wound dressings helps decreasing the recovery time for certain degrees (i.e. level of burns or depth) of wounds. Parsons et al. investigated the release of silver from seven different commercially available wound dressings into deionized water [120]. The initial silver content was 6–13 mg/100 cm² dressing and they were put in contact with deionized water for 7 days at 37 °C. It was found that the silver release started after 48 h and varied dramatically as 17–111 µg Ag/100 cm² dressing. Authors also found no correlation between silver release and silver content, meaning that high silver content does not result in high silver release for wound dressings. In the aforementioned study by Arvidsson et al., emissions resulting from the use of wound dressings are estimated as well, by applying particle flow analysis [115]. With regard to the ‘explorative scenario’ that they modeled, the amount of nAg enabled wound dressing usage was calculated as 7 cm²/capita/year. They indicated that in wound dressings, emissions may be generated both during the use phase (i.e. when it is taped onto the wound) and the disposal phase (i.e. when it is thrown away). Although these bandages release silver during their life cycle, since their usage is relatively low comparing to the nAg enabled textiles, it might not have a major environmental importance. However, if in an effort to decrease nosocomial infections the rate of use of nAg increased, there is the potential for silver release to be of concern.

3.6.3. Food storage containers

Although the efficacy of nAg enabled food storage containers is subject to debate, many studies have demonstrated migration of silver from food storage containers to food and to environment, which should be assessed for both environmental and public health purposes. Westerband and Hicks compiled a review of the previous literature on silver migration from nAg enabled food storage containers along with initial (total) silver content and the amount of silver released [35, 36]. Products including bags (i.e. polyethylene, high density polyethylene) and rigid containers (i.e. polyolefin, low density polyethylene, polypropylene, rubber sealing container, high density polyethylene, polycarbonate) were analyzed to quantify the silver released into the food simulants. Water (ultrapure, Milli-Q, distilled), acetic acid (3%, 4%), ethanol (10%, 50%, 95%), hexane and olive oil samples were used as food simulants throughout the literature. The experimental procedure was similar in the existing research: the food containers were put in contact with the selected food simulants for certain amount of time (varied from 1 h to 15 days) under different temperature conditions (varied from 25 °C to 70 °C), and the silver released was quantified using mass spectrometry [86, 121–125]. Overall finding from these studies was that, nAg migration increases with increasing storage time and temperature and more acidic food substances result in high Ag migration. Further, Westerband and Hicks argued that nAg which migrates from the food storage containers/bags can potentially reach sewage system through ingestion and excretion of the stored food or wash water [35, 36]. In order to assess the overall environmental impact, speciation of silver that is migrated/released to food simulants need to be examined as well [85].

3.6.4. Fate in the environment

Besides release studies, examining the fate of nAg in the environment is also significant, as it influences the mobility and environmental impact of the nAg. Keller and Lazareva quantified nAg released from different industries with a cradle to grave perspective as 240 metric tons/year emissions to landfill, 45 metric tons/year emissions to soil, 95 metric tons/year emissions to water and 20 metric tons/year emissions to air, globally [8]. Donia and Carbone reviewed the fate of ENMs in environment resulting from different disposal techniques (i.e. landfill, incineration, recycling, wastewater) [126]. They suggested that the behavior of ENMs is highly dependent on their physical/chemical properties as well as characteristics of the receiving location [126]. Although most of the nAg enabled consumer products are treated as conventional wastes at end of their lives without passing through any special treatments, wastewater treatment facilities may eliminate 80% of ENMs or incinerators may capture large proportions of ENMs [126]. Another study by Wang et al. examined the effect of nAg on terrestrial environments by utilizing a 'meta-analysis' for their behavior from source through wastewater treatment plant and soil and finally to receptor [127]. They concluded that nAg loses its nano properties after passing through wastewater treatment plant and becomes less soluble and bioavailable, which reduce its risk on terrestrial plants and fauna. However, Wang et al. suggested that additional analysis is required to examine the impacts of nAg consumption on soil microbes and aquatic organisms [127]. More broadly, Cucurachi and Rocha schematized the potential release and exposure of ENMs with a cradle to grave perspective and predicted that they may have midpoint impacts on human toxicity, eco toxicity, climate change, eutrophication, ozone depletion and acidification [128]. Also, through changes in species composition and decreases in biodiversity, release and exposure of ENMs may result in endpoint impacts on human health, ecosystem damage and

natural resources [128]. However, there are still uncertainties regarding LCA studies which limit providing a general interpretation on the release and exposure impacts of nAg, in part due to the lack of consensus of LCIA factors specific to nAg.

4. Conclusions

nAg is utilized in a large variety of consumer products, chiefly due to its antimicrobial properties. As the number of products utilizing nAg continues to increase, along with a growing forecasted global production of nAg, it is critical to evaluate the consumer products currently on the market from a life cycle perspective. This allows for the grouping of products to better understand the potential environmental benefits and detriments of nAg enabled products, and where in the life cycle they have the potential to occur. As mentioned before, consumer behavior affects both use and end of life phases, which may have a significant contribution to the overall life cycle of the product. It is important to conduct a holistic LCA to distinguish the hotspots and to suggest improvements in order to increase the potential benefits and to decrease the potential drawbacks. The proposed three category system helps to provide an indication of where the potential exists for environmental benefits of nAg enabled consumer products. Also, break-even points listed for each category may help researchers to evaluate similar nano-enabled products by their respective environmental payback periods. The authors recognize that the three categories proposed are not terminal, and that future additions and modifications will occur. Besides proposing a classification framework, the current study provides a comprehensive review on existing nAg release studies. The surprising outcome from the previous literature was that, in general, the amount of silver released has been reported as a wide range which is challenging for making end of life LCA assumptions. Furthermore, identifying the speciation of silver that is

released is crucial to construct a relevant cradle to grave life cycle inventory for any nano-enabled product. Considering existing data in the literature on the use and end of life phases, potential risks of exposure of nAg enabled products are not sufficiently explored.

Acknowledgements

This work would not have been possible without the assistance of multiple sources. Both AH and STS acknowledge the financial support of the Wisconsin Alumni Research Foundation (WARF) in conducting this work. Previous LCA work on nAg, reviewed in this paper, was supported generously by the U.S. Environmental Protection Agency Assistance Agreement No. RD83558001-0. The previous work enabled the current summary work presented here. This work has not been formally reviewed by EPA or WARF. The views expressed in this document are solely those of the authors and do not necessarily reflect those of the Agency or Foundation. EPA and WARF do not endorse any products or commercial services mentioned in this publication.

References-Appendix F

1. Klasen H (2000) Historical review of the use of silver in the treatment of burns. I. Early uses. *Burns*, 26:117–130.
2. Alexander JW (2009) History of the Medical Use of Silver. *Surgical Infections*, 10(3):289–292. <https://doi.org/10.1089/sur.2008.9941>
3. Barillo DJ, Marx DE (2014) Silver in medicine: A brief history BC 335 to present. *Burns*, 40:S3–S8. <https://doi.org/10.1016/j.burns.2014.09.009>
4. National Nanotechnology Initiative (2019) What is Nanotechnology. *National Nanotechnology Initiative*, <https://www.nano.gov/nanotech-101/what/definition>
5. Calderón-Jiménez B, Johnson ME, Montoro Bustos AR, Murphy KE, Winchester MR, Vega Baudrit JR (2017) Silver Nanoparticles: Technological Advances, Societal Impacts, and Metrological Challenges. *Frontiers in Chemistry*, 5<https://doi.org/10.3389/fchem.2017.00006>
6. Desmau M, Gélabert A, Levard C, Ona-Nguema G, Vidal V, Stubbs JE, Eng PJ, Benedetti MF (2018) Dynamics of silver nanoparticles at the solution/biofilm/mineral interface. *Environmental Science: Nano*, 5(10):2394–2405. <https://doi.org/10.1039/C8EN00331A>
7. Gottschalk F, Sonderer T, Scholz RW, Nowack B (2009) Modeled Environmental Concentrations of Engineered Nanomaterials (TiO₂, ZnO, Ag, CNT, Fullerenes) for Different Regions. *Environmental Science & Technology*, 43(24):9216–9222. <https://doi.org/10.1021/es9015553>
8. Keller AA, Lazareva A (2014) Predicted Releases of Engineered Nanomaterials: From Global to Regional to Local. *Environmental Science & Technology Letters*, 1(1):65–70. <https://doi.org/10.1021/ez400106t>
9. Nowack B, Krug HF, Height M (2011) 120 Years of Nanosilver History: Implications for Policy Makers. *Environmental Science & Technology*, 45(4):1177–1183. <https://doi.org/10.1021/es103316q>
10. Perez J, Bax L, Escolano C (2005) Roadmap Report on Nanoparticles. <http://nanoparticles.org/pdf/PerezBaxEscolano.pdf>
11. Pulit-Prociak J, Banach M (2016) Silver nanoparticles – a material of the future...? *Open Chemistry*, 14(1):76–91. <https://doi.org/10.1515/chem-2016-0005>
12. Schmid K, Riediker M (2008) Use of Nanoparticles in Swiss Industry: A Targeted Survey. *Environmental Science & Technology*, 42(7):2253–2260. <https://doi.org/10.1021/es071818o>
13. Grand View Research (2015) Silver Nanoparticles Market By Application And Segment Forecasts To 2022. <https://www.grandviewresearch.com/industry-analysis/silver-nanoparticles-market>

14. Hicks AL, Theis TL (2017) A comparative life cycle assessment of commercially available household silver-enabled polyester textiles. *The International Journal of Life Cycle Assessment*, 22(2):256–265. <https://doi.org/10.1007/s11367-016-1145-2>
15. Hicks AL, Gilbertson LM, Yamani JS, Theis TL, Zimmerman JB (2015) Life Cycle Payback Estimates of Nanosilver Enabled Textiles under Different Silver Loading, Release, And Laundering Scenarios Informed by Literature Review. *Environmental Science & Technology*, 49(13):7529–7542. <https://doi.org/10.1021/acs.est.5b01176>
16. StatNano (2019) Nanotechnology Products Database (NPD). <http://product.statnano.com/>
17. Xing M, Ge L, Wang M, Li Q, Li X, Ouyang J (2014) Nanosilver particles in medical applications: synthesis, performance, and toxicity. *International Journal of Nanomedicine*, :2399. <https://doi.org/10.2147/IJN.S55015>
18. Yin HQ, Langford R, Burrell RE (1999) Comparative Evaluation of the Antimicrobial Activity of ACTICOAT Antimicrobial Barrier Dressing: *Journal of Burn Care & Rehabilitation*, 20(3):195–200. <https://doi.org/10.1097/00004630-199905000-00006>
19. Tredget EE, Shankowsky HA, Groeneveld A, Burrell R (1998) A Matched-Pair, Randomized Study Evaluating the Efficacy and Safety of Acticoat* Silver-Coated Dressing for the Treatment of Burn Wounds: *Journal of Burn Care & Rehabilitation*, 19(6):531–537. <https://doi.org/10.1097/00004630-199811000-00013>
20. Ülkür E, Öncül O, Karagöz H, Çeliköz B, Çavuşlu Ş (2005) Comparison of silver-coated dressing (Acticoat™), chlorhexidine acetate 0.5% (Bactigrass®), and silver sulfadiazine 1% (Silverdin®) for topical antibacterial effect in *Pseudomonas aeruginosa*-contaminated, full-skin thickness burn wounds in rats. *Journal of Burn Care and Rehabilitation*, 26(5):430–433.
21. Huang Y, Li X, Liao Z, Zhang G, Liu Q, Tang J, Peng Y, Liu X, Luo Q (2007) A randomized comparative trial between Acticoat and SD-Ag in the treatment of residual burn wounds, including safety analysis. *Burns*, 33(2):161–166. <https://doi.org/10.1016/j.burns.2006.06.020>
22. Rustogi R, Mill J, Fraser JF, Kimble RM (2005) The use of Acticoat™ in neonatal burns. *Burns*, 31(7):878–882. <https://doi.org/10.1016/j.burns.2005.04.030>
23. Khundkar R, Malic C, Burge T (2010) Use of Acticoat™ dressings in burns: What is the evidence? *Burns*, 36(6):751–758. <https://doi.org/10.1016/j.burns.2009.04.008>
24. Walser T, Demou E, Lang DJ, Hellweg S (2011) Prospective Environmental Life Cycle Assessment of Nanosilver T-Shirts. *Environmental Science & Technology*, 45(10):4570–4578. <https://doi.org/10.1021/es2001248>
25. Manda BMK, Worrell E, Patel MK (2015) Prospective life cycle assessment of an antibacterial T-shirt and supporting business decisions to create value. *Resources, Conservation and Recycling*, 103:47–57. <https://doi.org/10.1016/j.resconrec.2015.07.010>

26. Geranio L, Heuberger M, Nowack B (2009) The Behavior of Silver Nanotextiles during Washing. *Environmental Science & Technology*, 43(21):8113–8118. <https://doi.org/10.1021/es9018332>
27. Benn TM, Westerhoff P (2008) Nanoparticle Silver Released into Water from Commercially Available Sock Fabrics. *Environmental Science & Technology*, 42(11):4133–4139. <https://doi.org/10.1021/es7032718>
28. Lorenz C, Windler L, Goetz N von, Lehmann RP, Schuppler M, Hungerbühler K, Heuberger M, Nowack B (2012) Characterization of silver release from commercially available functional (nano)textiles. *Chemosphere*, 89(7):817–824. <https://doi.org/10.1016/j.chemosphere.2012.04.063>
29. Lombi E, Donner E, Scheckel KG, Sekine R, Lorenz C, Goetz NV, Nowack B (2014) Silver speciation and release in commercial antimicrobial textiles as influenced by washing. *Chemosphere*, 111:352–358. <https://doi.org/10.1016/j.chemosphere.2014.03.116>
30. Mitrano DM, Rimmelé E, Wichser A, Erni R, Height M, Nowack B (2014) Presence of Nanoparticles in Wash Water from Conventional Silver and Nano-silver Textiles. *ACS Nano*, 8(7):7208–7219. <https://doi.org/10.1021/nn502228w>
31. Reed RB, Zaikova T, Barber A, Simonich M, Lankone R, Marco M, Hristovski K, Herckes P, Passantino L, Fairbrother DH, Tanguay R, Ranville JF, Hutchison JE, Westerhoff PK (2016) Potential Environmental Impacts and Antimicrobial Efficacy of Silver- and Nanosilver-Containing Textiles. *Environmental Science & Technology*, 50(7):4018–4026. <https://doi.org/10.1021/acs.est.5b06043>
32. McQueen RH, Keelan M, Xu Y, Mah T (2013) In vivo assessment of odour retention in an antimicrobial silver chloride-treated polyester textile. *Journal of the Textile Institute*, 104(1):108–117. <https://doi.org/10.1080/00405000.2012.697623>
33. McQueen RH, Ehnes B (2018) Antimicrobial Textiles and Infection Prevention: Clothing and the Inanimate Environment. *Infection Prevention*, :117–126. https://doi.org/10.1007/978-3-319-60980-5_13
34. Bi Y, Westerband EI, Alum A, Brown FC, Abbaszadegan M, Hristovski KD, Hicks AL, Westerhoff PK (2018) Antimicrobial Efficacy and Life Cycle Impact of Silver-Containing Food Containers. *ACS Sustainable Chemistry & Engineering*, 6(10):13086–13095. <https://doi.org/10.1021/acssuschemeng.8b02639>
35. Westerband EI, Hicks AL (2018) Life cycle impact of nanosilver polymer-food storage containers as a case study informed by literature review. *Environmental Science: Nano*, 5(4):933–945. <https://doi.org/10.1039/C7EN01043E>
36. Westerband EI, Hicks AL (2018) Nanosilver-Enabled Food Storage Container Tradeoffs: Environmental Impacts Versus Food Savings Benefit, Informed by Literature. *Integrated Environmental Assessment and Management*, 14(6):769–776. <https://doi.org/10.1002/ieam.4093>

37. An J, Zhang M, Wang S, Tang J (2008) Physical, chemical and microbiological changes in stored green asparagus spears as affected by coating of silver nanoparticles-PVP. *LWT - Food Science and Technology*, 41(6):1100–1107. <https://doi.org/10.1016/j.lwt.2007.06.019>
38. Emamifar A, Kadivar M, Shahedi M, Soleimani-Zad S (2010) Evaluation of nanocomposite packaging containing Ag and ZnO on shelf life of fresh orange juice. *Innovative Food Science & Emerging Technologies*, 11(4):742–748. <https://doi.org/10.1016/j.ifset.2010.06.003>
39. Mihaly Cozmuta A, Peter A, Mihaly Cozmuta L, Nicula C, Crisan L, Baia L, Turila A (2015) Active Packaging System Based on Ag/TiO₂ Nanocomposite Used for Extending the Shelf Life of Bread. Chemical and Microbiological Investigations: ACTIVE PACKAGING SYSTEM BASED ON Ag/TiO₂ NANOCOMPOSITE. *Packaging Technology and Science*, 28(4):271–284. <https://doi.org/10.1002/pts.2103>
40. Li L, Zhao C, Zhang Y, Yao J, Yang W, Hu Q, Wang C, Cao C (2017) Effect of stable antimicrobial nano-silver packaging on inhibiting mildew and in storage of rice. *Food Chemistry*, 215:477–482. <https://doi.org/10.1016/j.foodchem.2016.08.013>
41. Azlin-Hasim S, Cruz-Romero MC, Morris MA, Cummins E, Kerry JP (2015) Effects of a combination of antimicrobial silver low density polyethylene nanocomposite films and modified atmosphere packaging on the shelf life of chicken breast fillets. *Food Packaging and Shelf Life*, 4:26–35. <https://doi.org/10.1016/j.fpsl.2015.03.003>
42. Dhumal S, Karale A (2017) Shelf life and overall quality of pretreated and modified atmosphere packaged ‘Ready-to-eat’ Pomegranate arils vs Bhagwa stoerd at 1 C. *Int Journal Nut Food End*, 11(11)
43. Tavakoli H, Rastegar H, Taherian M, Samadi M, Rostami H (2017) The effect of nano-silver packaging in increasing the shelf life of nuts: An in vitro model. *Italian Journal of Food Safety*, 6(4)<https://doi.org/10.4081/ijfs.2017.6874>
44. Kernberger-Fischer I, Kehrenberg C, Klein G, Schaudien D, Krischek C (2017) Influence of modified atmosphere and vacuum packaging with and without nanosilver-coated films on different quality parameters of pork. *Journal of Food Science and Technology*, 54(10):3251–3259. <https://doi.org/10.1007/s13197-017-2768-4>
45. Jiang T, Feng L, Wang Y (2013) Effect of alginate/nano-Ag coating on microbial and physicochemical characteristics of shiitake mushroom (*Lentinus edodes*) during cold storage. *Food Chemistry*, 141(2):954–960. <https://doi.org/10.1016/j.foodchem.2013.03.093>
46. Mousavi FP, Pour HH, Nasab AH, Rajabalipour AA, Barouni M (2015) Investigation Into Shelf Life of Fresh Dates and Pistachios in a Package Modified With Nano-Silver. *Global Journal of Health Science*, 8(5):134. <https://doi.org/10.5539/gjhs.v8n5p134>
47. Donglu F, Wenjian Y, Kimatu BM, Mariga AM, Liyan Z, Xinxin A, Qiuhui H (2016) Effect of nanocomposite-based packaging on storage stability of mushrooms (*Flammulina velutipes*).

Innovative Food Science & Emerging Technologies, 33:489–497.

<https://doi.org/10.1016/j.ifset.2015.11.016>

48. Costa C, Conte A, Buonocore GG, Del Nobile MA (2011) Antimicrobial silver-montmorillonite nanoparticles to prolong the shelf life of fresh fruit salad. *International Journal of Food Microbiology*, :S0168160511003011. <https://doi.org/10.1016/j.ijfoodmicro.2011.05.018>

49. Pourzahedi L, Eckelman MJ (2015) Environmental Life Cycle Assessment of Nanosilver-Enabled Bandages. *Environmental Science & Technology*, 49(1):361–368. <https://doi.org/10.1021/es504655y>

50. Meyer DE, Curran MA, Gonzalez MA (2011) An examination of silver nanoparticles in socks using screening-level life cycle assessment. *Journal of Nanoparticle Research*, 13(1):147–156. <https://doi.org/10.1007/s11051-010-0013-4>

51. Pourzahedi L, Vance M, Eckelman MJ (2017) Life Cycle Assessment and Release Studies for 15 Nanosilver-Enabled Consumer Products: Investigating Hotspots and Patterns of Contribution. *Environmental Science & Technology*, 51(12):7148–7158. <https://doi.org/10.1021/acs.est.6b05923>

52. Hicks AL, Reed RB, Theis TL, Hanigan D, Huling H, Zaikova T, Hutchison JE, Miller J (2016) Environmental impacts of reusable nanoscale silver-coated hospital gowns compared to single-use, disposable gowns. *Environmental Science: Nano*, 3(5):1124–1132. <https://doi.org/10.1039/C6EN00168H>

53. Eckelman MJ, Graedel TE (2007) Silver Emissions and their Environmental Impacts: A Multilevel Assessment. *Environmental Science & Technology*, 41(17):6283–6289. <https://doi.org/10.1021/es062970d>

54. Toups MA, Kitchen A, Light JE, Reed DL (2011) Origin of Clothing Lice Indicates Early Clothing Use by Anatomically Modern Humans in Africa. *Molecular Biology and Evolution*, 28(1):29–32. <https://doi.org/10.1093/molbev/msq234>

55. Dunlap K (1928) The Development and Function of Clothing. *The Journal of General Psychology*, 1(1):64–78. <https://doi.org/10.1080/00221309.1928.9923412>

56. Benn T, Cavanagh B, Hristovski K, Posner JD, Westerhoff P (2010) The Release of Nanosilver from Consumer Products Used in the Home. *Journal of Environmental Quality*, 39(6):1875–1882. <https://doi.org/10.2134/jeq2009.0363>

57. Hicks AL (2017) Using multi criteria decision analysis to evaluate nanotechnology: nAg enabled textiles as a case study. *Environmental Science: Nano*, 4(8):1647–1655. <https://doi.org/10.1039/C7EN00429J>

58. Hicks AL (2017) Environmental assessment of medical nanotechnologies. *Nanotechnologies in Preventive and Regenerative Medicine*, :17.

59. Queen D, Orsted H, Sanada H, Sussman G (2004) A dressing history. *International Wound Journal*, 1(1):59–77. <https://doi.org/10.1111/j.1742-4801.2004.0009.x>
60. Infection Control Today (2010) Nano Mask Launches Line of Nano Silver Technology Hospital Curtains. <https://www.infectioncontroltoday.com/personal-protective-equipment/nano-mask-launches-line-nano-silver-technology-hospital-curtains>
61. Heger M (2008) A Silver Coating in the Fight Against Microbes. *Scientific American*, <https://www.scientificamerican.com/article/silver-coating-fights-microbes>
62. Marks ED, Smith S (2016) Nanoscale Defenses. *The Scientist*, <https://www.the-scientist.com/features/nanoscale-defenses-33625>
63. Chacko B, Thomas K, David T, Paul H, Jeyaseelan L, Peter JV (2017) Attributable cost of a nosocomial infection in the intensive care unit: A prospective cohort study. *World Journal of Critical Care Medicine*, 6(1):79. <https://doi.org/10.5492/wjccm.v6.i1.79>
64. Zhang S, Palazuelos-Munoz S, Balsells EM, Nair H, Chit A, Kyaw MH (2016) Cost of hospital management of *Clostridium difficile* infection in United States—a meta-analysis and modelling study. *BMC Infectious Diseases*, 16(1):447. <https://doi.org/10.1186/s12879-016-1786-6>
65. Zhang K, Li F, Imazato S, Cheng L, Liu H, Arola DD, Bai Y, Xu HHK (2013) Dual antibacterial agents of nano-silver and 12-methacryloyloxydodecylpyridinium bromide in dental adhesive to inhibit caries: Dental Adhesive with Dual Antibacterial Agents MDPB and Nano-Silver. *Journal of Biomedical Materials Research Part B: Applied Biomaterials*, 101B(6):929–938. <https://doi.org/10.1002/jbm.b.32898>
66. Li F, Weir MD, Chen J, Xu HHK (2013) Comparison of quaternary ammonium-containing with nano-silver-containing adhesive in antibacterial properties and cytotoxicity. *Dental Materials*, 29(4):450–461. <https://doi.org/10.1016/j.dental.2013.01.012>
67. Santos VE dos, Filho AV, Ribeiro Targino AG, Pelagio Flores MA, Galembeck A, Caldas AF, Rosenblatt A (2014) A New “Silver-Bullet” to treat caries in children – Nano Silver Fluoride: A randomised clinical trial. *Journal of Dentistry*, 42(8):945–951. <https://doi.org/10.1016/j.jdent.2014.05.017>
68. Burns J, Hollands K (2015) Nano Silver Fluoride for preventing caries: Question: Is Nano Silver Fluoride (NSF) effective for preventing and arresting active caries in children? *Evidence-Based Dentistry*, 16(1):8–9. <https://doi.org/10.1038/sj.ebd.6401073>
69. Gitipour A, Al-Abed SR, Thiel SW, Scheckel KG, Tolaymat T (2017) Nanosilver as a disinfectant in dental unit waterlines: Assessment of the physicochemical transformations of the AgNPs. *Chemosphere*, 173:245–252. <https://doi.org/10.1016/j.chemosphere.2017.01.050>
70. Kalishwaralal K, BarathManiKanth S, Pandian SRK, Deepak V, Gurunathan S (2010) Silver nanoparticles impede the biofilm formation by *Pseudomonas aeruginosa* and *Staphylococcus*

epidermidis. *Colloids and Surfaces B: Biointerfaces*, 79(2):340–344.
<https://doi.org/10.1016/j.colsurfb.2010.04.014>

71. Hebeish A, El-Rafie MH, EL-Sheikh MA, Seleem AA, El-Naggar ME (2014) Antimicrobial wound dressing and anti-inflammatory efficacy of silver nanoparticles. *International Journal of Biological Macromolecules*, 65:509–515. <https://doi.org/10.1016/j.ijbiomac.2014.01.071>

72. Bowler PG, Jones SA, Walker M, Parsons D (2004) Microbicidal Properties of a Silver-Containing Hydrofiber® Dressing Against a Variety of Burn Wound Pathogens: *Journal of Burn Care & Rehabilitation*, 25(2):192–196. <https://doi.org/10.1097/01.BCR.0000112331.72232.1B>

73. Boonkaew B, Kempf M, Kimble R, Supaphol P, Cuttle L (2014) Antimicrobial efficacy of a novel silver hydrogel dressing compared to two common silver burn wound dressings: Acticoat™ and PolyMem Silver®. *Burns*, 40(1):89–96.
<https://doi.org/10.1016/j.burns.2013.05.011>

74. Totaro P, Rambaldini M (2008) Efficacy of antimicrobial activity of slow release silver nanoparticles dressing in post-cardiac surgery mediastinitis. *Interactive CardioVascular and Thoracic Surgery*, 8(1):153–154. <https://doi.org/10.1510/icvts.2008.188870>

75. Moojen DJF, Vogely HC, Fleer A, Verbout AJ, Castelein RM, Dhert WJA (2009) No efficacy of silver bone cement in the prevention of methicillin-sensitive *Staphylococcal* infections in a rabbit contaminated implant bed model. *Journal of Orthopaedic Research*, 27(8):1002–1007. <https://doi.org/10.1002/jor.20854>

76. Huang L, Dai T, Xuan Y, Tegos GP, Hamblin MR (2011) Synergistic Combination of Chitosan Acetate with Nanoparticle Silver as a Topical Antimicrobial: Efficacy against Bacterial Burn Infections. *Antimicrobial Agents and Chemotherapy*, 55(7):3432–3438.
<https://doi.org/10.1128/AAC.01803-10>

77. Moradi F, Haghgoo R (2018) Evaluation of antimicrobial efficacy of nanosilver solution, sodium hypochlorite and normal saline in root canal irrigation of primary teeth. *Contemporary Clinical Dentistry*, 9(6):227. https://doi.org/10.4103/ccd.ccd_95_18

78. Samuel U, Guggenbichler JP (2004) Prevention of catheter-related infections: the potential of a new nano-silver impregnated catheter. *International Journal of Antimicrobial Agents*, 23:75–78. <https://doi.org/10.1016/j.ijantimicag.2003.12.004>

79. Paladini F, Pollini M, Talà A, Alifano P, Sannino A (2012) Efficacy of silver treated catheters for haemodialysis in preventing bacterial adhesion. *Journal of Materials Science: Materials in Medicine*, 23(8):1983–1990. <https://doi.org/10.1007/s10856-012-4674-7>

80. Monteiro DR, Gorup LF, Takamiya AS, Camargo ER de, Filho ACR, Barbosa DB (2012) Silver Distribution and Release from an Antimicrobial Denture Base Resin Containing Silver Colloidal Nanoparticles: Silver Nanoparticle Release from Denture Base Resin. *Journal of Prosthodontics*, 21(1):7–15. <https://doi.org/10.1111/j.1532-849X.2011.00772.x>

81. Kuijt I, Finlayson B (2009) Evidence for food storage and predomestication granaries 11,000 years ago in the Jordan Valley. *Proceedings of the National Academy of Sciences*, 106(27):10966–10970. <https://doi.org/10.1073/pnas.0812764106>
82. Fromm KM (2011) Give silver a shine. *Nature Chemistry*, 3(2):178–178. <https://doi.org/10.1038/nchem.970>
83. Cushen M, Kerry J, Morris M, Cruz-Romero M, Cummins E (2012) Nanotechnologies in the food industry – Recent developments, risks and regulation. *Trends in Food Science & Technology*, 24(1):30–46. <https://doi.org/10.1016/j.tifs.2011.10.006>
84. Blaser SA, Scheringer M, MacLeod M, Hungerbühler K (2008) Estimation of cumulative aquatic exposure and risk due to silver: Contribution of nano-functionalized plastics and textiles. *Science of The Total Environment*, 390(2–3):396–409. <https://doi.org/10.1016/j.scitotenv.2007.10.010>
85. Reidy B, Haase A, Luch A, Dawson K, Lynch I (2013) Mechanisms of Silver Nanoparticle Release, Transformation and Toxicity: A Critical Review of Current Knowledge and Recommendations for Future Studies and Applications. *Materials*, 6(6):2295–2350. <https://doi.org/10.3390/ma6062295>
86. Huang Y, Chen S, Bing X, Gao C, Wang T, Yuan B (2011) Nanosilver Migrated into Food-Simulating Solutions from Commercially Available Food Fresh Containers: NANOSILVER MIGRATION FROM PLASTICS. *Packaging Technology and Science*, 24(5):291–297. <https://doi.org/10.1002/pts.938>
87. Windler L, Height M, Nowack B (2013) Comparative evaluation of antimicrobials for textile applications. *Environment International*, 53:62–73. <https://doi.org/10.1016/j.envint.2012.12.010>
88. Gilbertson LM, Wender BA, Zimmerman JB, Eckelman MJ (2015) Coordinating modeling and experimental research of engineered nanomaterials to improve life cycle assessment studies. *Environmental Science: Nano*, 2(6):669–682. <https://doi.org/10.1039/C5EN00097A>
89. Champion N, Thiel CL, Woods NC, Swanzy L, Landis AE, Bilec MM (2015) Sustainable healthcare and environmental life-cycle impacts of disposable supplies: a focus on disposable custom packs. *Journal of Cleaner Production*, 94:46–55. <https://doi.org/10.1016/j.jclepro.2015.01.076>
90. Cools I, Uyttendaele M, Cerpentier J, D’Haese E, Nelis HJ, Debevere J (2005) Persistence of *Campylobacter jejuni* on surfaces in a processing environment and on cutting boards. *Letters in Applied Microbiology*, 40(6):418–423. <https://doi.org/10.1111/j.1472-765X.2005.01694.x>
91. Mitrano DM, Motellier S, Clavaguera S, Nowack B (2015) Review of nanomaterial aging and transformations through the life cycle of nano-enhanced products. *Environment International*, 77:132–147. <https://doi.org/10.1016/j.envint.2015.01.013>
92. Levard C, Hotze EM, Colman BP, Dale AL, Truong L, Yang XY, Bone AJ, Brown GE, Tanguay RL, Di Giulio RT, Bernhardt ES, Meyer JN, Wiesner MR, Lowry GV (2013)

Sulfidation of Silver Nanoparticles: Natural Antidote to Their Toxicity. *Environmental Science & Technology*, 47(23):13440–13448. <https://doi.org/10.1021/es403527n>

93. Xu H, Shi X, Lv Y, Mao Z (2013) The preparation and antibacterial activity of polyester fabric loaded with silver nanoparticles. *Textile Research Journal*, 83(3):321–326. <https://doi.org/10.1177/0040517512454187>

94. Spielman-Sun E, Zaikova T, Dankovich T, Yun J, Ryan M, Hutchison JE, Lowry GV (2018) Effect of silver concentration and chemical transformations on release and antibacterial efficacy in silver-containing textiles. *NanoImpact*, 11:51–57. <https://doi.org/10.1016/j.impact.2018.02.002>

95. Lee HJ, Yeo SY, Jeong SH (2003) Antibacterial effect of nanosized silver colloidal solution on textile fabrics. *Journal of Materials Science*, 38(10):2199–2204.

96. El-Rafie MH, Ahmed HB, Zahran MK (2014) Characterization of nanosilver coated cotton fabrics and evaluation of its antibacterial efficacy. *Carbohydrate Polymers*, 107:174–181. <https://doi.org/10.1016/j.carbpol.2014.02.024>

97. Jack T (2013) Laundry routine and resource consumption in Australia: Laundry routines and consumption. *International Journal of Consumer Studies*, 37(6):666–674. <https://doi.org/10.1111/ijcs.12048>

98. Lindsey J (2011) Dare to Wear: An Exploration of the Attitudes and Habits of the Consumer in Regards to Garment Care and Its Relationship and Effect on the Environment.

99. Mylan J (2015) Understanding the diffusion of Sustainable Product-Service Systems: Insights from the sociology of consumption and practice theory. *Journal of Cleaner Production*, 97:13–20. <https://doi.org/10.1016/j.jclepro.2014.01.065>

100. Stawreberg L (2011) Energy Efficiency Improvements of Tumble Dryers: -Technical Development, Laundry Habits and Energy Labelling.

101. Hustvedt G (2011) Review of laundry energy efficiency studies conducted by the US Department of Energy: Review of laundry energy efficiency studies. *International Journal of Consumer Studies*, 35(2):228–236. <https://doi.org/10.1111/j.1470-6431.2010.00970.x>

102. Stamminger R (2011) Modelling resource consumption for laundry and dish treatment in individual households for various consumer segments. *Energy Efficiency*, 4(4):559–569. <https://doi.org/10.1007/s12053-011-9114-x>

103. Chaloupka K, Malam Y, Seifalian AM (2010) Nanosilver as a new generation of nanoparticle in biomedical applications. *Trends in Biotechnology*, 28(11):580–588. <https://doi.org/10.1016/j.tibtech.2010.07.006>

104. Wilkinson LJ, White RJ, Chipman JK (2011) Silver and nanoparticles of silver in wound dressings: a review of efficacy and safety. *Journal of Wound Care*, 20(11):543–549. <https://doi.org/10.12968/jowc.2011.20.11.543>

105. Fabrega J, Luoma SN, Tyler CR, Galloway TS, Lead JR (2011) Silver nanoparticles: Behaviour and effects in the aquatic environment. *Environment International*, 37(2):517–531. <https://doi.org/10.1016/j.envint.2010.10.012>
106. Rigo C, Ferroni L, Tocco I, Roman M, Munivrana I, Gardin C, Cairns W, Vindigni V, Azzena B, Barbante C, Zavan B (2013) Active Silver Nanoparticles for Wound Healing. *International Journal of Molecular Sciences*, 14(3):4817–4840. <https://doi.org/10.3390/ijms14034817>
107. Gorka DE, Lin NJ, Pettibone JM, Gorham JM (2019) Chemical and physical transformations of silver nanomaterial containing textiles after modeled human exposure. *NanoImpact*, 14:100160. <https://doi.org/10.1016/j.impact.2019.100160>
108. National Nanotechnology Infrastructure Network (2006) What is the product CURad silver bandages. <http://www.nnin.org/sites/default/files/files/NNIN-1025.pdf>
109. Elastoplast (2019) Antibacterial fabric plaster. <https://www.elastoplast.com.au/products/wound-care/antibacterial-fabric-plaster>
110. Metak AM, Ajaal TT (2013) Investigation on Polymer Based Nano-Silver as Food Packaging Materials. 7(12):7.
111. Williams K, Valencia L, Gokulan K, Trbojevich R, Khare S (2017) Assessment of antimicrobial effects of food contact materials containing silver on growth of *Salmonella Typhimurium*. *Food and Chemical Toxicology*, 100:197–206. <https://doi.org/10.1016/j.fct.2016.12.014>
112. Inshakova E, Inshakov O (2017) World market for nanomaterials: structure and trends. *MATEC Web of Conferences*, 129:02013. <https://doi.org/10.1051/mateconf/201712902013>
113. Potter PM, Navratilova J, Rogers KR, Al-Abed SR (2019) Transformation of silver nanoparticle consumer products during simulated usage and disposal. *Environmental Science: Nano*, 6(2):592–598. <https://doi.org/10.1039/C8EN00958A>
114. Quadros ME, Pierson R, Tulve NS, Willis R, Rogers K, Thomas TA, Marr LC (2013) Release of Silver from Nanotechnology-Based Consumer Products for Children. *Environmental Science & Technology*, 47(15):8894–8901. <https://doi.org/10.1021/es4015844>
115. Arvidsson R, Molander S, Sandén BA (2011) Impacts of a Silver-Coated Future: Particle Flow Analysis of Silver Nanoparticles. *Journal of Industrial Ecology*, 15(6):844–854. <https://doi.org/10.1111/j.1530-9290.2011.00400.x>
116. Gagnon V, Button M, Boparai HK, Nearing M, O’Carroll DM, Weber KP (2019) Influence of realistic wearing on the morphology and release of silver nanomaterials from textiles. *Environmental Science: Nano*, 6(2):411–424. <https://doi.org/10.1039/C8EN00803E>
117. Mitrano DM, Lombi E, Dasilva YAR, Nowack B (2016) Unraveling the Complexity in the Aging of Nanoenhanced Textiles: A Comprehensive Sequential Study on the Effects of Sunlight

and Washing on Silver Nanoparticles. *Environmental Science & Technology*, 50(11):5790–5799. <https://doi.org/10.1021/acs.est.6b01478>

118. Stefaniak AB, Duling MG, Lawrence RB, Thomas TA, LeBouf RF, Wade EE, Abbas Virji M (2014) Dermal exposure potential from textiles that contain silver nanoparticles. *International Journal of Occupational and Environmental Health*, 20(3):220–234. <https://doi.org/10.1179/2049396714Y.00000000070>

119. Lankone RS, Challis KE, Bi Y, Hanigan D, Reed RB, Zaikova T, Hutchison JE, Westerhoff P, Ranville J, Fairbrother H, Gilbertson LM (2017) Methodology for quantifying engineered nanomaterial release from diverse product matrices under outdoor weathering conditions and implications for life cycle assessment. *Environmental Science: Nano*, 4(9):1784–1797. <https://doi.org/10.1039/C7EN00410A>

120. Parsons D, Bowler PG, Myles V, Jones S (2005) Silver antimicrobial dressings in wound management: A comparison of antibacterial, physical, and chemical characteristics. *Wounds*, 17(8):222–232.

121. Echegoyen Y, Nerín C (2013) Nanoparticle release from nano-silver antimicrobial food containers. *Food and Chemical Toxicology*, 62:16–22. <https://doi.org/10.1016/j.fct.2013.08.014>

122. Goetz N von, Fabricius L, Glaus R, Weitbrecht V, Günther D, Hungerbühler K (2013) Migration of silver from commercial plastic food containers and implications for consumer exposure assessment. *Food Additives & Contaminants: Part A*, 30(3):612–620. <https://doi.org/10.1080/19440049.2012.762693>

123. Artiaga G, Ramos K, Ramos L, Cámara C, Gómez-Gómez M (2015) Migration and characterisation of nanosilver from food containers by AF4-ICP-MS. *Food Chemistry*, 166:76–85. <https://doi.org/10.1016/j.foodchem.2014.05.139>

124. Mackevica A, Olsson ME, Hansen SF (2016) Silver nanoparticle release from commercially available plastic food containers into food simulants. *Journal of Nanoparticle Research*, 18(1):5. <https://doi.org/10.1007/s11051-015-3313-x>

125. Ramos K, Gómez-Gómez MM, Cámara C, Ramos L (2016) Silver speciation and characterization of nanoparticles released from plastic food containers by single particle ICPMS. *Talanta*, 151:83–90. <https://doi.org/10.1016/j.talanta.2015.12.071>

126. Donia DT, Carbone M (2019) Fate of the nanoparticles in environmental cycles. *International Journal of Environmental Science and Technology*, 16(1):583–600. <https://doi.org/10.1007/s13762-018-1960-z>

127. Wang P, Lombi E, W. Menzies N, Zhao F-J, M. Kopittke P (2018) Engineered silver nanoparticles in terrestrial environments: a meta-analysis shows that the overall environmental risk is small. *Environmental Science: Nano*, 5(11):2531–2544. <https://doi.org/10.1039/C8EN00486B>

128. Cucurachi S, Blanco Rocha CF (2019) Life-cycle assessment of engineered nanomaterials. *Nanotechnology in Eco-efficient Construction*, :815–846. <https://doi.org/10.1016/B978-0-08-102641-0.00031-1>

Appendix G

*Published paper, electronic supplemental information associated with the paper and references.

Assessing the environmental impact and payback of carbon nanotube supported CO₂ capture technologies using LCA methodology

The following chapter is a reproduction of an article published in the Journal of Cleaner Production, with the citation:

Wu, F.; Zhou, Z.; Temizel-Sekeryan, S.; Ghamkhar, R.; Hicks, A.L. (2020) Assessing the environmental impact and payback of carbon nanotube supported CO₂ capture technologies using LCA methodology, *Journal of Cleaner Production*, Vol. 270, 122465.

The article appears as published, although style and formatting modifications have been made.

Authorship contribution statement

Fan Wu: Designed Research, Performed Research, Contributed Reagents or Analytical Tools, Analyzed Data, Wrote the Paper.

Zheng Zhou: Designed Research, Contributed Reagents or Analytical Tools, Analyzed Data.

Sila Temizel-Sekeryan: Performed Research, Wrote the Paper.

Ramin Ghamkhar: Performed Research, Wrote the Paper.

Andrea L. Hicks: Designed Research, Wrote the Paper.

Abstract

Climate change caused by excessive CO₂ emissions in the atmosphere has attracted widespread public concern in recent years. Current industrial methods generally utilize monoethanolamine for CO₂ capture; however, the CO₂ regeneration requires a high temperature and energy demand during every adsorption/desorption process, along with material losses. Many solid amines with high capture capacity and stability are developed as adsorbents to overcome the limitations. However, the environmental impacts caused by adsorbents themselves are not holistically considered and discussed; meanwhile, material syntheses and consumptions are also associated with CO₂ emission. To determine the environmental impacts and identify hotspots of novel CO₂ capture adsorbents, two carbon nanotube supported polyethyleneimine, physically adsorbed and covalently bonded, were compared with traditional monoethanolamine method using life cycle assessment. The carbon payback periods were also analyzed to gain understanding on whether the currently evaluated novel materials are suitable for industrial application. Results suggest that, material usage, especially carbon nanotubes, contributes the majority of the overall environmental impacts for both types of carbon nanotube supported polyethyleneimine. Meanwhile, their carbon payback periods are over 40 times longer than monoethanolamine during the synthesis phase. However, the energy consumption of physically adsorbed polyethyleneimine saves up to 60% compared to monoethanolamine in every adsorption/desorption cycle due to its lower heat capacity. In addition, the rate of cumulative CO₂ remission for carbon nanotube supported polyethyleneimine is twice higher than monoethanolamine, indicating the potential application for industrial CO₂ capture. Overall, our study indicates that current status of solid amine has a potential in CO₂ capture, but requires much improvements. Future research should pay attention on decreasing the initial material

synthesis and increasing the product life time due to their high environmental tradeoffs.

Meanwhile, our study highlights that unilateral emphasis of the CO₂ capture efficiency by novel materials may not be adequate, comprehensive considerations should be focused on the comparison throughout material life cycles including use and preparation phases.

1. Introduction

The use of fossil fuels, changes in land, industries, transportation and buildings have given rise to an increase in greenhouse gas (GHG) emissions [1]. The increased level of GHG emissions leads to climate change and global warming, which are unequivocal facts and cause growing concern. Carbon dioxide (CO₂) is the biggest contributor to global GHG with an approximately 80% share [2]. In addition, the result of the latest measurement for CO₂ level (in March 2020) reported by the National Aeronautics and Space Administration (NASA) [3] is 413.03 parts per million in Mauna Loa Observatory, Hawaii, which is the highest level recorded in the past 650,000 years. These realizations pave new ways to develop sustainable solutions to limit the emission and enhance the capture of CO₂. Besides moving towards energy efficient applications and fostering renewable energy usage, one option in order to minimize the environmental impacts resulting from the increased levels of CO₂ is to capture it properly [4, 5]. Carbon capture and storage is one of the climate change mitigation strategies currently under intense consideration [6, 7], which was also outlined as one of the main strategies that could limit continuous global warming [8].

CO₂ capture can be achieved by post-combustion, pre-combustion and air separation followed by oxyfuel combustion methods [9]. Due to the high efficiency, low cost, and relatively low energy demand, sorption is one of the promising CO₂ capture methods [10]. Several physical

and chemical sorption processes have been extensively investigated in previous studies for CO₂ capture [11–13]. Among those, chemical absorption using aqueous amine solutions, specifically monoethanolamine (MEA) is the most commercially used method [14–16]. Despite that MEA is efficient and economically favorable for CO₂ capture, the high energy demand, and direct and indirect CO₂ emissions at both downstream and upstream processes highlight the importance of seeking alternative CO₂ capture strategies [16]. To be more specific, research has shown the MEA solvent regeneration step can occupy about 60% of the required energy in the CO₂ capture process [17]. Additionally, the use and generation of toxic materials (e.g. ethylene oxide) during the MEA production process, increase the environmental concerns in other environmental impact considerations (e.g. eco-toxicity, human health, etc.). Since the use of MEA in CO₂ capture is a point of concern and a global application, it may not be the optimal strategy in the long run.

Many advances in solid based materials for CO₂ capture have been reviewed recently including solid sorbents and solid supports functionalized with amines [9, 18]. Polymeric amines, such as polyethyleneimine (PEI), are promising amine sources for CO₂ capture due to their higher amine group density compared to other amine-containing compounds [19, 20]. In addition, amines bonded to high surface area supports including metal oxides, zeolites, and carbon-based materials are promising adsorbents because they offer low energy solutions for regenerable, low cost, efficient and selective CO₂ capture [21]. As a support, metal oxides are cost-effective, easily modified, provide avenues for mesoporous hierarchical structure, and allow both covalent and physical grafting of amines to the surfaces, but are susceptible to thermal degradation and often undergo self-catalyzed oxidation of amines at moderate temperatures resulting in lower CO₂ sorption efficiency. Zeolites have previously been functionalized with amines [22]; however, the small pore size often limits the amount of amine that can be loaded

onto the material, and the synthesis method often impacts not only the loading of amine, but also the distribution and availability of sites. Metal organic frameworks have arguably been quite efficient at CO₂ adsorption at low temperatures and pressures; however, they are often prohibitively expensive to make and susceptible to poor gas adsorption selectivity upon exposure to water vapor [10]. With high durability, physical and chemical stability, large surface areas for adsorbate molecules, high micropore volume, and relatively low cost, carbon nanotubes (CNT) are preferable support materials for amines as adsorbents for post-combustion CO₂ capture [23].

CNT have strong electrical, chemical, thermal and mechanical properties [24, 25]. In addition, the physicochemical properties of CNT are maintained under flue gas conditions due to their hydrophobicity as well as chemical and thermal stability. Given that CNT are porous materials and have hollow structures, these properties make them favored geometric structures for both inside and outside adsorption [6]. Meanwhile, CNTs are hydrophobic therefore they are resistant to water vapor, which makes them more durable than other alternatives [26, 27]. Several studies use multi-wall (MW) CNT and amine modified MWCNTs as adsorbents for CO₂ capture [15, 28, 29]. Previous studies showed a comparable adsorption capacity of CNT-PEI compared to current MEA (30% weight) adsorption. It has been also suggested that CNT supported amine for CO₂ capturing is stable, requires much less energy for the desorption, and has a similar CO₂ capture capacity even comparable to the traditional MEA method at laboratory scale [10].

Many novel materials with high efficiency and stability are developed recently for CO₂ capture purposes. However, the material syntheses phase also involves high energy inputs, which generates CO₂ emissions. Although solid amine using CNT as novel adsorbent materials imply high capability in CO₂ capture, the impacts of material preparation, usage and disposal on the overall environment is rarely studied. Meanwhile, large quantities of electricity are used to

provide thermal and kinetic energy during the materials preparation and carbon regeneration phases, which are potential environmental burdens that could be overlooked. This study first investigates the environmental impacts of two CNT supported PEI, physisorbed (Phy-CNT-PEI) and covalently bound (Cov-CNT-PEI) synthesized at laboratory scale, using life cycle assessment (LCA). After that, the carbon payback period and economic payback are analyzed for Phy-CNT-PEI and traditional MEA methods (Figure G1). The goal of this study is to understand the life cycle impacts of CNT-PEI synthesis as novel CO₂ adsorbents, and also gain further understanding on the potential environmental benefits and tradeoffs during the use phase. Ultimately, this study aims to identify the potential limitations and applicability of novel CO₂ capture technologies.

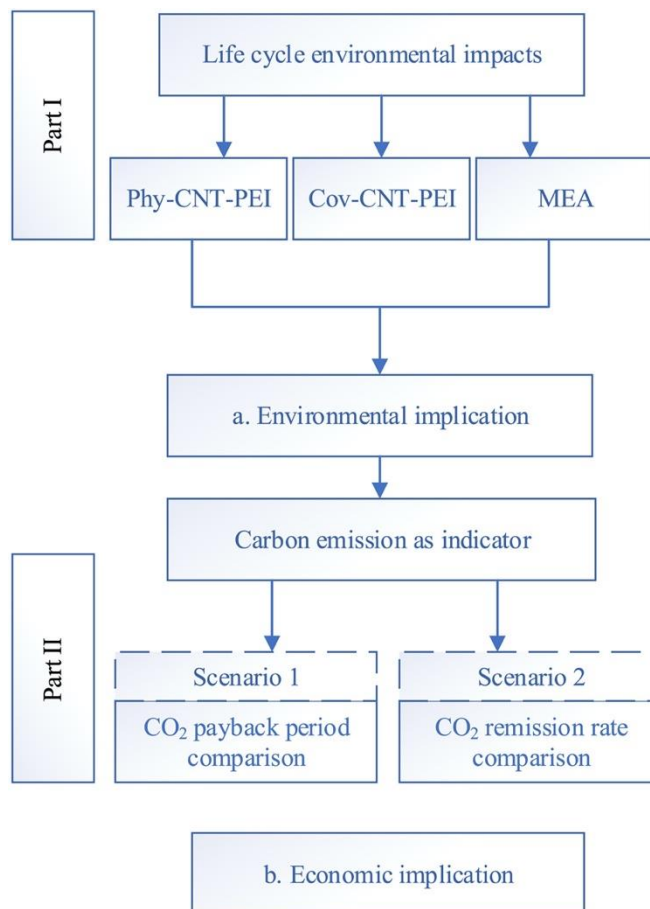


Figure G1. Flow diagram illustrates the study.

2. Methods and modeling

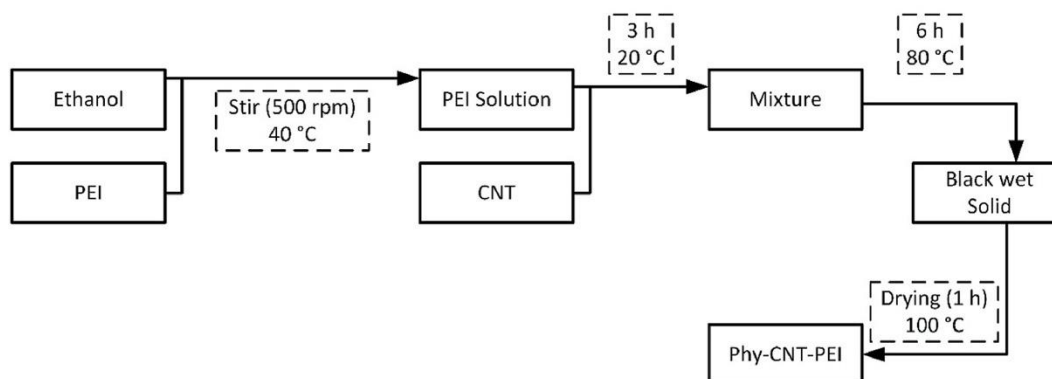
This study serves as a case study to illustrate the major challenges that solid amine as a novel CO₂ capture technology encounters in cleaner production. The methods and modeling section is divided into two parts: (I) life cycle assessment and (II) carbon payback analysis. Figure G1 illustrates the flow of current research.

2.1. Life cycle assessment

2.1.1. Goal and scope

The goals of this research are to investigate the environmental impact profiles of two laboratory synthesized CNT-PEI, identify the hotspots and gain understanding on the potential carbon payback period for different CO₂ capture methods. The environmental impacts of both types of CNT-PEI syntheses were assessed initially using LCA. LCA is a systematic tool for determining the environmental impacts (using metrics such as kilograms of carbon dioxide emitted) of a product or process across its entire life cycle or a portion of its life cycle [30, 31]. The system boundaries are depicted in Figure G2. Two functional units were used for initial direct comparison, 1 kilogram (kg) of material synthesis cost (mass-based), and materials required to adsorb 1 kg CO₂. Adsorption capacities are summarized in Table G1.

a. Phy-CNT-PEI



b. Cov-CNT-PEI

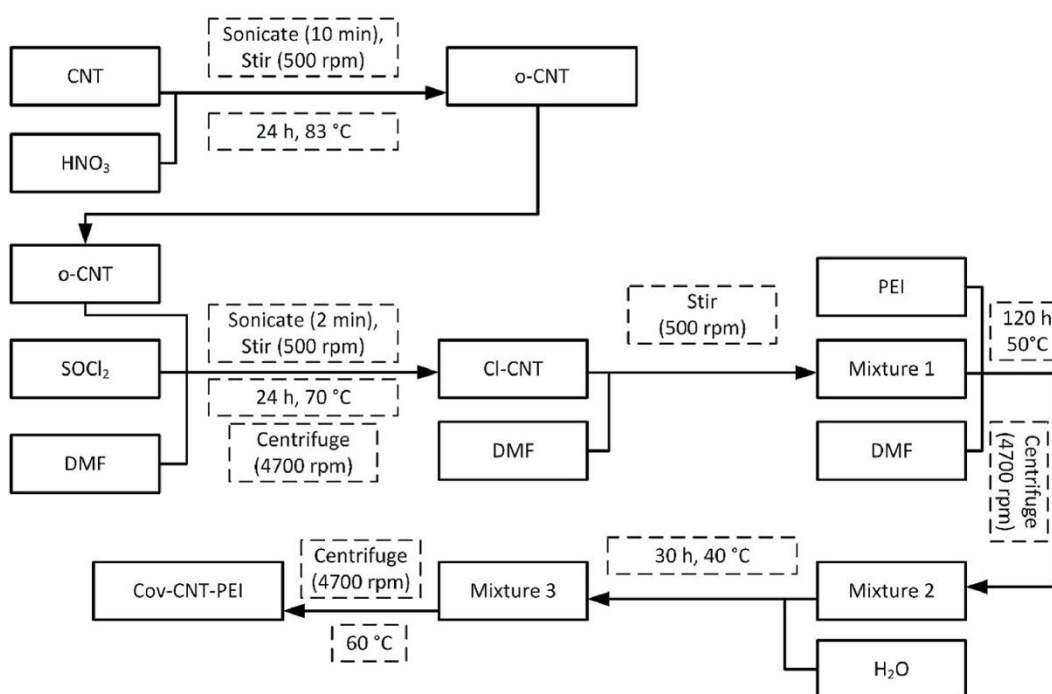


Figure G2. System boundaries and schematics of CNT-PEI (covalent&physical) syntheses (additional syntheses, including CNT, PEI, DMF, are illustrated in the SI). CNT, PEI and DMF are denoted as carbon nanotube, polyethyleneimine and dimethylformamide, respectively.

Table G1. Summary of the initial CO₂ adsorption capacity for each adsorption/desorption (A/D) cycle. Dry condition: introducing CO₂ at a flow rate of 10 mL min⁻¹ with 40 mL min⁻¹ N₂. Wet condition: 3 H₂O steam by volume was introduced in the system by bubbling 40 mL min⁻¹ N₂ into H₂O bath. CO₂ flow rate is still 10 mL min⁻¹.

Type of material	Capacity (mmol/g)		kg CO ₂ /kg material	
	Dry	Wet	Dry	Wet
Cov-CNT-PEI	0.98	1.12	0.04	0.05
Phy-CNT-PEI	6.18	0.3	0.27	0.01
MEA	6.82		0.30	

2.1.2. Life cycle inventory

Information on materials and reagents used for the laboratory syntheses was from Zhou et al. [10]. The CNT used here was synthesized through the chemical vapor deposition (CVD) method, which has also been identified as one of the most utilized methods for industrial growth of carbon nanotubes [32, 33]. In this study, materials and energy inputs were collected from a pilot scale multi-wall CNT (MWCNT) production plant (Table GS1&GS2) [34]. The life cycle impacts of the MWCNT in this study was also compared to a suite of other MWCNT synthesis studies to understand the relative impact of the production scale.

Due to the limited information from the chemical vendor, PEI synthesis procedures were obtained from multiple literature sources [35–37]. The flow chart of PEI synthesis and material inputs are presented in Figure GS1 and Table GS3&GS4, respectively. Materials and energy inputs for synthesizing both CNT-PEI are listed in Table GS5&GS6. The electricity and energy usage to produce CNT-PEI were either collected directly from the laboratory equipment, or estimated based on the first law of thermodynamics (equations GS1 and GS2) when the materials

were not synthesized on-site [38]. Detailed equations and numbers are presented in the supporting information (SI).

2.1.3. Life cycle impact assessment and interpretation

The life cycle environmental and human health impacts were modeled using the SimaPro software (version 8.5) with Ecoinvent and USLCI (U.S. Life Cycle Inventory) databases as inventories [39]. SimaPro is one of the most widely used LCA softwares, which provides a modeling environment from simple to complex products or systems. TRACI 2.1 (tool for the reduction and assessment of chemical and other environmental impacts) was used as the assessment method to represent an United States based study [40]. The midpoint categories considered include ozone depletion (OD; kg CFC-11 equivalent), global warming (GW; kg CO₂ eq), smog (PS; kg O₃ eq), acidification (AC; mol SO₂ eq), eutrophication (EU; kg N eq), carcinogenic (HHC; CTUh), non-carcinogenic (HHNC; CTUh), respiratory effects (RE; kg PM_{2.5} eq), ecotoxicity (EC; CTUe), and fossil fuel depletion (FF; MJ surplus) [38].

2.1.4. Sensitivity and uncertainty analyses

Sensitivity analysis determines the output parameter percentage change by varying an individual input parameter while all the other parameters are constant [41], which shows the influence of one parameter (the independent variable) on the value of another (the dependent variable). In this case, the purpose of the sensitivity analysis is to monitor how sensitive of each synthesis procedure is to the overall CNT-PEI production. Therefore, the sensitivities of CNT-PEI syntheses were assessed by varying a single parameter value (increased by 25%), and compare the change of the overall impact for each impact category. The uncertainties associated

with the unit processes in the life cycle database were analyzed using Monte-Carlo simulations in SimaPro for 1000 runs to the 95th confidence interval.

2.2. Carbon payback analysis

As the targeted application of the studied technology is to store CO₂, global warming potential was selected as a major indicator to analyze the environmental payback in this study. The concept of environmental payback is well established and has been used to compare the relative environmental impact of numerous conventional and emerging technologies, particularly in energy applications such as fuels and photovoltaics [42–44]. Here, the carbon payback is calculated as the number of adsorption/desorption (A/D) cycles required to obtain CO₂ saving equivalent to the initial CO₂ cost, which is generated from the material syntheses. The carbon paybacks of carbon capture technologies were compared with a commonly adapted MEA strip method to gain further understanding on the potential of application.

The summaries of CO₂ adsorption capacity under varying scenarios are presented in Table G1. From previous experiments, results suggest that Cov-CNT-PEI has a higher CO₂ adsorption capacity than Phy-CNT-PEI under wet adsorption scenario, whereas the CO₂ adsorption capacity for Phy-CNT-PEI is much higher under dry condition than Cov-CNT-PEI, and similar to MEA [10, 45, 46]. Most industrial CO₂ exhaust streams are generated in post-combustion processes, where the concentration of CO₂ in the gas mixture ranges from 3 to 20% by volume [47]. Therefore, the CO₂ concentration used in the adsorption capacity test was 20% in N₂ by volume. Phy-CNT-PEI under dry condition was investigated further for the environmental payback comparison due to the comparatively high adsorption capacity. Two scenarios were considered to evaluate the carbon payback of the targeting technology.

2.2.1. Scenario 1: CO₂ payback period comparison

In scenario 1, the number of A/D cycles required to match with the initial MEA and CNT-PEI CO₂ cost during syntheses are calculated. The net amount of CO₂ remission by 1 kg of adsorbents are expressed as eqn (G1).

$$\text{Life time CO}_2 \text{ remission} = \sum_{K=0}^n (K - D) - I \quad (G. 1)$$

In which, K represents the CO₂ adsorption after corresponding cycle (kg CO₂), and D represents the CO₂ generated from the desorption energy use (kg CO₂). $(K - D)$ represents the net gain of CO₂ remission for each corresponding cycle. I represents the initial synthesis cost (kg CO₂).

2.2.2. Scenario 2: CO₂ remission rate comparison

The rates for CO₂ remission between Phy-CNT-PEI and MEA were compared in scenario 2. More industrially relevant approach was considered by replenishing fresh MEA once the capacity decrease to a certain level. During industrial application, the CO₂ adsorption capacity should be maintained at a relatively stable level. Since liquid MEA can degrade after each A/D cycle, MEA was replenished when the adsorption capacity is decreased to 95% of the original capture capacity (which equals to every 10 cycles). No replenishing or replacement was considered for CNT-PEI due to their stability nature.

3. Results and discussion

The results are presented in the following order: life cycle impact comparison between two CNT-PEI syntheses with different functional units (Figure G3); impact contribution for two CNT-PEI synthesis (Figure G4); carbon emission for synthesizing 1 kg of each absorbent (Figure G5); carbon payback analysis: scenario 1 and scenario 2 (Figure G6 and Figure G7).

3.1. Life cycle impact of CNT-PEI production

3.1.1. Impact comparisons between two types of CNT-PEI

Figure G3 shows the relative environmental impacts comparison between Phy-CNT-PEI and Cov-CNT-PEI by using two different functional units. When the mass based functional unit was used, the environmental impacts generated from synthesizing Phy-CNT-PEI were ranged from 40 to 80% compared to Cov-CNT-PEI in all impact categories, suggesting that the Phy-CNT-PEI has low environmental burdens during synthesis phase. Only the consideration of mass may not accurately estimate the impact of CNT-PEI with respect to the utility of CO₂ remission. The functional units should specifically focus at the targeted material function, which in this case, amount of CO₂ adsorption was added as the additional functional unit for comparison. When the results were rescaled based on the CO₂ adsorption efficiency, Cov-CNT-PEI showed even higher impacts, with nearly 10 times higher impacts than Phy-CNT-PEI (Figure G3b). This is mainly due to the lower CO₂ adsorption capacity in Cov-CNT-PEI than Phy-CNT-PEI. The CO₂ adsorption capacity of Phy-CNT-PEI is nearly 6 folds higher than Cov-CNT-PEI under dry CO₂ condition (Table G1). From the previous material characterization on both types of CNT-PEI, it shows that 40% PEI was physically adsorbed on CNT (Phy-CNT-PEI), whereas only 16% PEI was covalently bound to CNT (Cov-CNT-PEI). Therefore, improve amine group that bound to CNT could potentially enhance their CO₂ capture capacity, meanwhile decrease the corresponding environmental burdens generated from material production. Overall, both functional units illustrate that the Cov-CNT-PEI has higher overall impacts than the Phy-CNT-PEI.

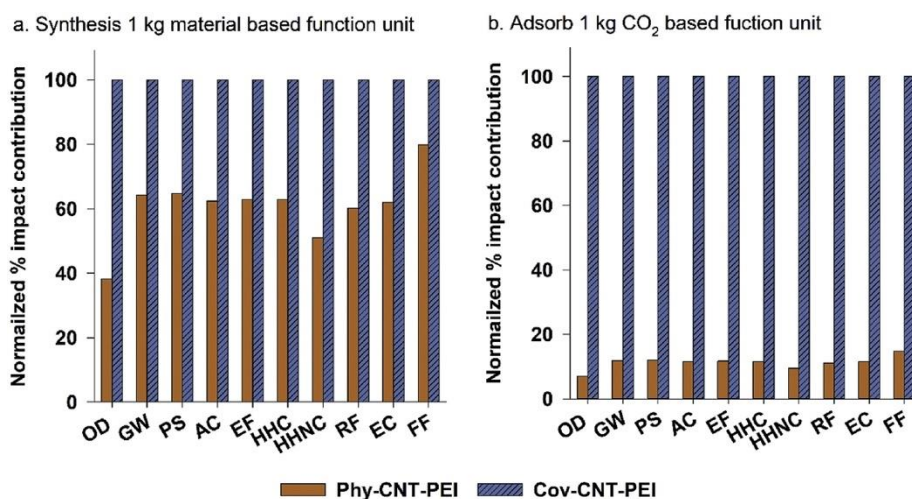


Figure G3. Normalized percent impact for all assessed categories by comparing both CNT-PEI when (a) synthesis 1 kg CNT-PEI and (b) adsorb 1 kg CO₂ as function unit, respectively. Ozone depletion (OD), global warming (GW), smog (PS), acidification (AC), eutrophication (EU), carcinogenic (HHC), noncarcinogenic (HHNC), respiratory effects (RE), ecotoxicity (EC), and fossil fuel depletion (FF).

3.1.2. Impact contributions of each procedure

Figure G4 illustrates the environmental impact contributions of each main procedure during both CNT-PEI syntheses. In Figure G4a, CNT manufacturing is the driving environmental burden in all impact categories, it contributes more than 50% of environmental burdens to all the categories due to its intense synthesis conditions such as high temperature and large amount of feedstocks (Figure GS5). PEI synthesis was identified to be the second largest contributor (~20%). Compared to the materials, the contribution by electricity consumption is negligible in Phy-CNT-PEI. For Cov-CNT-PEI, additional chemical compounds (i.e. DMF, thionyl chloride) were involved in the synthesis to form strong covalent bonds between the CNT

and PEI, which generate additional environmental burdens due to the large quantity being utilized (Figure G4b).

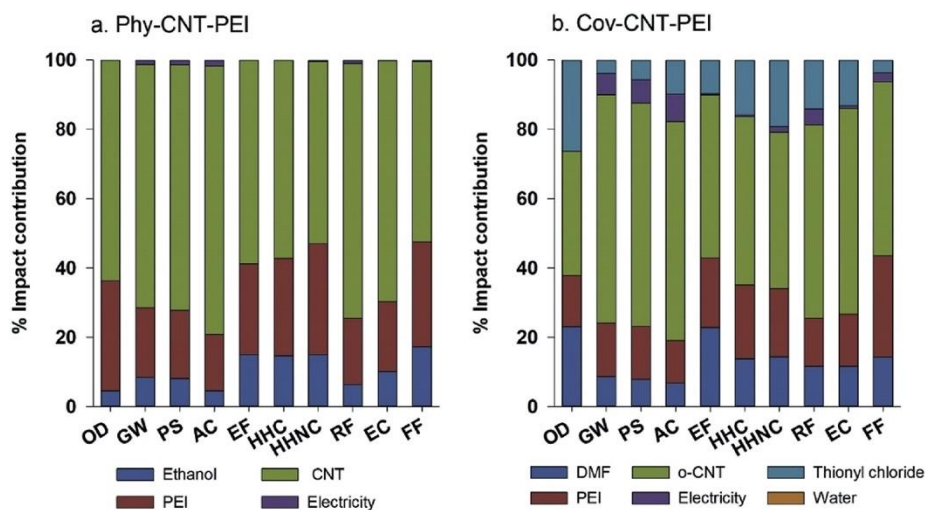


Figure G4. Impact contributions during CNT-PEI syntheses. a) impact contribution of Phy-CNT-PEI; b) Cov-CNT-PEI. (higher categories normalized as 100%). Ozone depletion (OD), globalwarming (GW), smog (PS), acidification (AC), eutrophication (EU), carcinogenic (HHC), noncarcinogenic (HHNC), respiratory effects (RE), ecotoxicity (EC), and fossil fuel depletion (FF).

Furthermore, the sensitivity analyses for both CNT-PEI syntheses are listed in Table GS15&GS16. Results show that CNT and PEI syntheses are the most sensitive parameters during material synthesis throughout life cycle, which again confirms that the CNT and PEI production dominate the environmental impacts in the both CNT-PEI syntheses. Additionally, the use of organic compounds, especially thionyl chloride (SOCl_2) and dimethylformamide (DMF) showed high sensitivity to the impacts associated with Cov-CNT-PEI. The associated uncertainties around both CNT-PEI syntheses were analyzed and revealed to be low (Figure

GS4). The environmental impacts related to all materials synthesis are tabulated in Table GS7-GS14, and the environmental impact contributions are graphically presented in Figure GS5-GS8.

By using global warming potential as an indicator, Figure G5 illustrates the CO₂ produced through the manufacturing of 1 kg of adsorbent. MEA requires much less materials and energy input than CNT-PEI due to their industrial scale manufacture. The CO₂ generation associated with CNT-PEI syntheses are 72 (Phy-CNT-PEI) and 113 (Cov-CNT-PEI) times higher than MEA. CNT contributes over 50% of GW to the overall production process in both CNT-PEI. Meanwhile, Cov-CNT-PEI generates more GHG emissions than Phy-CNT-PEI, largely attributed to the pre-treatment of CNT (for creating covalent bonds) and organic chemical compounds (e.g. DMF) used.

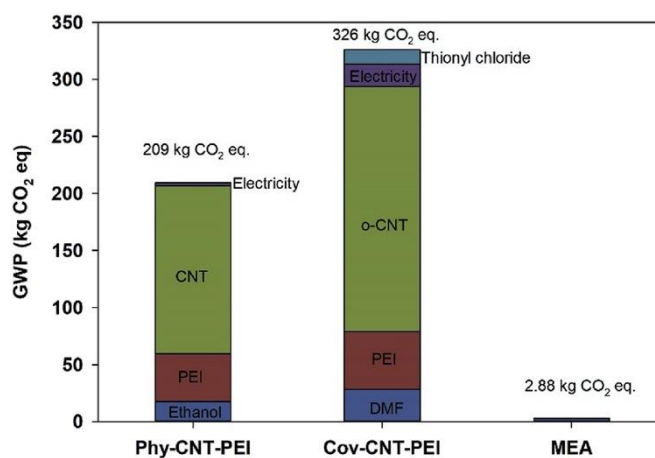


Figure G5. Quantity of CO₂ generated by synthesizing 1 kg of Phy-CNT-PEI, Cov-CNT-PEI, and MEA. Color schemes represent the materials and processes contribution in each type of product synthesis. GWP: global warming potential. (For interpretation of the references to colour in this figure legend, the reader is referred to the Web version of this article.)

3.1.3. Major GW contributor and implication

Life cycle inventory for CNT production were compiled based on a pilot scale manufacturing plant (up to 20 g MWCNT/h) [34]. LCA analysis indicates supporting gas and electricity are the two major contributors for the overall CNT production (Figure GS6). Especially for GW impact category, electricity contributed over 80% of the greenhouse gas emissions. Other LCA research also investigated the environmental impacts of CNT syntheses under laboratory conditions, and identified the largest impact was due to the energy consumption, followed by the equipment infrastructure [48]. Thus, converting to cleaner energy sources may decrease future CO₂ emissions associated with the environmental manufacturing cost. For PEI and other chemical syntheses, material usage, including organic and inorganic chemicals, and electricity dominated the environmental impacts for the production (Figure GS6-GS8).

Although environmental impact results analyzed based on laboratory scale production cannot be scaled up directly, it is helpful to identify the energy and material intensive processes, and to minimize the corresponding cost and lower the associated environmental impacts before scaling up. In addition, it provides the maximum environmental impacts possible during the material synthesis phase, which generates the most conservative comparison in CO₂ paybacks to our study.

It has to be recognized that scale up from laboratory level to pilot scale can potentially save materials and energy sources due to higher reaction yields, recycling of reagents and efficient equipment [49]. Research also suggests scaling up the process could potentially save up to 6.5 times more material and energy inputs than a typical laboratory synthesis [50]. Compared to other laboratory scale CNT syntheses, results using a pilot plant data generated up to 40 times

less CO₂ emission than the most intensive chemical vapor deposition method (Figure GS2). Since industrial scale production could further decrease the corresponding environmental impacts by improving the materials and energy efficiency, there is still a large potential for lowering the associated environmental burdens for PEI-CNT to be manufactured when scaling up.

3.2. Carbon payback comparison

Although CNT-PEI shows large CO₂ cost during synthesis, the high stability and consistency in CO₂ remission overtime provides potential for them to achieve environmental benefits in the long run. Thus, the carbon payback of Phy-CNT-PEI was analyzed and further compared with MEA.

3.2.1. Scenario 1: CO₂ payback period comparison

Table G2 summarizes the net CO₂ remission between 1 kg of Phy-CNT-PEI and MEA during one A/D cycle. Phy-CNT-PEI saves up to 60% energy demand compare to the MEA method for each A/D cycle due to its lower heat capacity. With a lower CO₂ remission capacity, Phy-CNT-PEI still shows a similar net CO₂ remission per cycle compared with MEA, due to the lower energy required per A/D cycles. This is also a benefit of utilizing solid supported amine for CO₂ capture due to the low heat capacity compared to liquid phase materials.

Table G2. Comparison of the net CO₂ remission between Phy-CNT-PEI and MEA.

Type of material	Heat capacity (KJ/kg-K)	kg CO ₂ saving/kg of Product	Energy required/cycle (KJ)	Corresponding CO ₂ produced/cycle (kg)	Net CO ₂ remission/cycle (kg)
Phy-CNT-PEI	1.40	0.27	70.20	0.02	0.26
MEA	3.46	0.30	172.85	0.04	0.26

CO₂ payback period of utilizing 1 kg MEA and Phy-CNT-PEI are calculated (based on equation (G1)) and compared in Figure G6. For MEA, the maximum CO₂ capture has been modeled to be 11.76 kg after considering the degradation (Figure G6a). Since the CO₂ cost for manufacturing 1 kg MEA equals to 2.88 kg CO₂, the net cumulative CO₂ remission is 8.88 kg CO₂/kg MEA. The CO₂ payback period is estimated to be 21 A/D cycles. There will be no CO₂ savings after 176 cycles because the amount of CO₂ generated from the desorption process is higher than the remission savings.

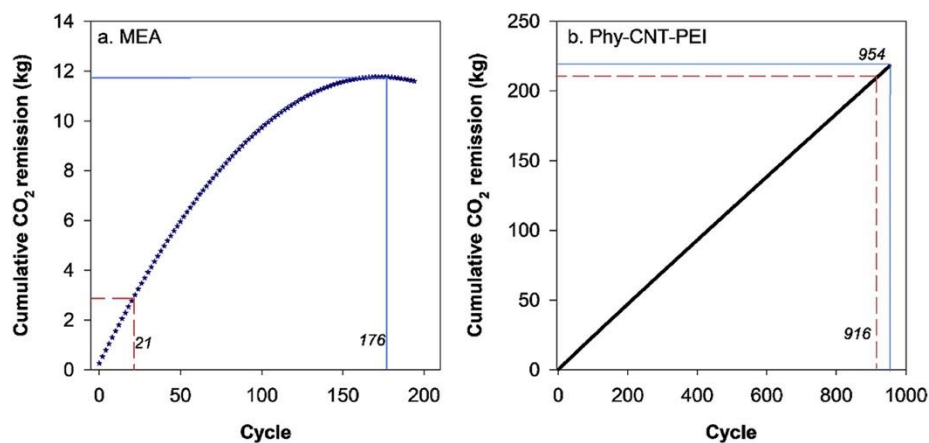


Figure G6. Lifetime cumulative CO₂ remission and payback cycles for MEA (a) and physiosorbed CNT-PEI (b) (scenario 1). Red dash line in both panels indicates the corresponding CO₂ payback after cycles of use. Blue solid line in panel a indicates the lifetime payback and cycles of use for MEA, in panel b indicates the cycles required to remediate the same quantity of

CO₂ compared to MEA. (For interpretation of the references to colour in this figure legend, the reader is referred to the Web version of this article.)

For Phy-CNT-PEI, the cumulative CO₂ remission tends to follow a linear trend because of the slow degradation rate and relative stable CO₂ recovery capacity over cycles. However, Phy-CNT-PEI has a nearly 72 times higher initial manufacturing CO₂ cost than MEA, with 209 kg CO₂ generation when synthesizing 1 kg Phy-CNT-PEI (Figure G5). The initial CO₂ cost requires an estimate of 916 A/D cycles to obtain a payback breakeven point (Figure G6b). Due to the relatively high and stable CO₂ capacity, only additional 38 A/D cycles (954 in total) reach equivalent lifetime CO₂ remission with 1 kg MEA.

3.2.2. Scenario 2: CO₂ remission rate comparison

Research indicates that MEA can be degraded to other products with much lower CO₂ adsorption capacity, such as 2-oxazolidone, N-(2-hydroxyethyl)-ethylenediamine, and 1-(2-hydroxyethyl)-2-imidazolidinone over time [46]. During this 8 weeks study, the thermal degradation of MEA has shown a reduction by 95% at 160°C [46]. Another study showed a MEA degradation by 2.5–6% every 2-week cycles [51]. In contrast, the recovery rate of CNT-PEI has been proven to be much higher and more stable than MEA. CNT-PEI has previously been proven experimentally to maintain a stable recovery rate up to 100 cycles [52]. Su et al. also showed a slow degradation for CNT-PEI, where recovery after 1, 50, and 100 A/D cycles are 100, 94.37, and 92% [52]. The CO₂ adsorption capacity for Phy-CNT-PEI and MEA through cycles were fitted with an exponential and linear decay curve, respectively. The exponential decay curve (eqn (G2)) was fitted following a recovery study conducted by Zhang et al. [53].

They showed a 10-cycle data points including the initial state and the steady state during the capture process [53]. In order to accurately estimate the material stability for CO₂ capture, the data was used to establish a prediction for material stability in a long-term CO₂ capture. For MEA, the degradation rate was fitted using eqn (G3), with a conservative estimation approximately 0.5% MEA loss per cycle [51]. The fitted models are presented in Figure GS3 and GS4.

For CNT-PEI (exponential decay):

$$y1 = -1.72 \times \ln(x) + 98.8 \quad (G. 2)$$

For MEA (linear decay):

$$y2 = -0.51x + 99.9 \quad (G. 3)$$

In eqn (G.2) and (G.3), $y1$ and $y2$ are the adsorption/absorption capacities of CNT-PEI and MEA at x cycle, respectively.

In reality, replenishing degraded and lost MEA after certain cycles could maintain a consistent and stable CO₂ capture capacity. Since approximately 5% of MEA degradation is expected with every 10 A/D cycles, to maintain a consistent capture capacity, an additional 5% of MEA was replenished after every 10 cycles for comparison in this scenario. The corresponding CO₂ generation associated with the 5% MEA replenished was included as a loss for the cumulative CO₂ remission (demonstrated in Figure G7a). The results suggest that during the 10 cycles, replenishing the first A/D cycle offsets the 5% MEA CO₂ manufacturing cost. Therefore, the remaining 9 cycles are the actual net CO₂ remission.

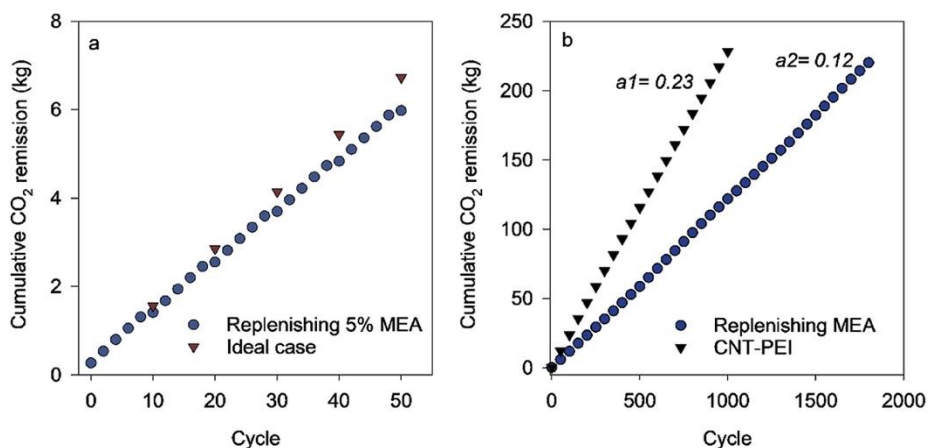


Figure G7. a) Cumulative CO₂ remission when replenishing 5% MEA back after every 10 cycles (red triangle represents an ideal condition where no degradation of MEA, blue circle represents the loss of cumulative CO₂ remission after replenishing 5% MEA every 10 cycles); b) comparative cumulative CO₂ remission between replenishing MEA scenario with Phy-CNT-PEI. (For interpretation of the references to colour in this figure legend, the reader is referred to the Web version of this article.)

The rate for CO₂ remission between Phy-CNT-PEI and replenishing MEA are compared in Figure G7b. Results show that Phy-CNT-PEI has a much higher CO₂ remission rate (0.23 kg CO₂/cycle) than the replenishing MEA scenario (0.12 kg CO₂/cycle). By simply assuming 1000 A/D cycles as a lifetime for CNT-PEI, the cumulative CO₂ remission in Phy-CNT-PEI at 1000 cycles are more than doubled compared to the MEA. Therefore, operational lifetime of CNT-PEI is the determining factor and critical for the overall environmental performance in CO₂ remission.

3.3. Environmental implications

Although many studies have conducted LCA on the capture of CO₂ under industrial post-combustion, and have found that post-combustion CO₂ capture can decrease the global warming potential [54, 55], there are other environmental impacts associated and additional fuels demanded [56]. With the limitations of current CO₂ capture technologies, novel materials are in urgently needed to improve the efficiency. Previous studies investigated the life cycle impacts of a membrane separation technology, where they found membrane separation has lower life cycle emissions compared to conventional MEA absorption process [57]. The authors indicate that the environmental impacts are strongly related to the membrane material, which is similar in our case where the materials usage are the determine factor in terms of life cycle emissions. In another study, researchers used potassium carbonate as an alternative for CO₂ capture, and the LCA results suggest potassium carbonate is better than MEA in all environmental categories [58]. Although these studies compared the life cycle impacts of different carbon capture technologies, none of these considered the environmental payback period from manufacturing and the environmental tradeoffs over the life time. Solid amine as a novel absorbent in CO₂ capture, the life cycle emissions have not been previously investigated. In addition, researchers summarize that energy penalty, functional units, scale-up issues, market effects and several other issues are the major challenges, which are overlooked in carbon capture and storage investigations [59]. Thus, the present study attempts to serve as a case study and discuss some of the current major challenges.

The results suggest that carbon payback analyzed in present study is largely dependent on the lifetime (A/D cycles) of CNT-PEI. Although many studies only showed consistent recovery rate up to 100 cycles, our results indicate that a total of 912 A/D cycles are required to be able to

obtain a breakeven CO₂ payback for Phy-CNT-PEI (Figure G6b). Currently, very limited number of studies reported the actual lifetime and the A/D cycles of CNT-PEI that can be achieved.

Begag et al. studied the capacity of a solid state amine (amine-functionalized aerogel) over 2000 A/D cycles in a fixed bed [60]. They found that the capacity was decreased by only a small amount (from 1.5 to 1.4 mmol CO₂/g sorbent) over such a large number of cycles [60]. This study provides evidence suggesting solid state amine should have a long lifetime to achieve environmental benefits. In addition, to optimize the synthesis procedures and enhance the CO₂ adsorption capacity, future research should also investigate and ensure the maximum lifetime capacity of current CNT-PEI under extreme conditions in order to receive more concise payback outcomes. Importantly, this present study simplifies the A/D process by assuming no additional adverse environmental impact caused by the degradants of MEA. In reality, MEA degradants can also dilute the MEA concentration, which decrease the CO₂ capture capacity. These technical challenges minimize the benefits of liquid phase capturing technologies, and highlight the benefits of developing solid supported amine for CO₂ remission.

Although research related to solid state amines for CO₂ capture is still in the early stage and many technical challenges needed to be overcome, solid state amines have become more attractive in CO₂ capture recently since the technology is solvent free [20], which reduces the energy penalty from regeneration compared to traditional liquid capture methods (Table G2). However, the large energy requirement for the adsorbent preparation (production and characterization) is still an issue that can almost counteract the energy requirement for regeneration. Substantial studies should be conducted to optimize the reduction of energy required in adsorbent preparation, improvement of adsorbent stability (e.g. thermal and steam) and CO₂ capture capacity under realistic flue gas conditions [9]. Moreover, reactor and process

design should be optimized for solid state amines since very few publications are involved in this field [61].

3.4. Economic implications

From a business perspective, the cost of reducing emissions should be taken into account when making economically sustainable decisions [62]. Table G3 shows the estimated price for CO₂ adsorbents and electricity used per cycle based on the material flow. For the synthesis of 1 kg Phy-CNT-PEI, 0.6 kg CNT, 0.4 kg PEI and 50 kg ethanol was used. Ethanol was recycled during syntheses and adjusts the total cost of manufacturing 1 kg Phy-CNT-PEI at \$580. CNT contributes 72% of the cost. Monoethanolamine (MEA, 98%) has been commercialized and can be directly purchased with the price of \$40/kg. Since the concentration of MEA is 30% in the industrial CO₂ capture and thus the price can be adjusted to \$12/kg. The syntheses cost of Phy-CNT-PEI is 48 times higher than MEA. However, since MEA suffers from chemical degradation and caused equipment erosion, additional material usage and maintenance are required. In addition, extra electricity will be consumed each desorption cycle, the energy cost of MEA is 2.5 times higher than Phy-CNT-PEI. Although Phy-CNT-PEI shows benefits in costs during the use phase, the high synthesis cost limits the widespread industrial application. The total cost of Phy-CNT-PEI can be reduced to be the same as MEA after 8900 cycles. By integrating economic analysis, energy stakeholders and general public would gain better interests towards environmental technologies in the future research [63].

Table G3. Summary of the CO₂ adsorbents price and electricity used per cycle. Detailed material price are presented in Table GS17.

Type of material	Market price (\$/kg)	Energy (kWh/cycle)	Mean price (\$/cycle)
Phy-CNT-PEI	580	0.02	0.0026
MEA	12	0.05	0.0064

It is relevant to note that it is an overestimation based on the assumptions such as laboratory scale and high grade of chemicals used for CNT-PEI. However, from the economic point of view, traditional MEA remains to be a better alternative for industrial application. Same as the environmental payback outcomes, decreasing the CNT and other material costs will benefit the application of solid amine adsorbents in CO₂ capture.

In general, CO₂ capture phase contributes 70%–80% of total costs during carbon capture and storage [64], therefore, developing novel CO₂ sorbents that satisfy technical and economic needs is the ultimate goal to achieve sustainability. Metal oxides, such as alumina, have low production cost, but easy to corrode over time could enhance the maintenance cost dramatically, meanwhile, high energy consumption during CO₂ desorption indicates an overall low sustainability. Zeolites, silica materials, and metal organic frameworks are known for their poor economic efficiency due to high production cost. Especially for metal organic frameworks, which typically cost several thousand dollars per kilogram, therefore limit the application at larger scales [64]. In addition, other carbon-based materials such as carbonaceous materials, are potential alternatives for CO₂ capture. They are thermal and steam stable, with reasonable production cost, and low energy consumption in the desorption process. Although the cost and the economic implication of these alternatives have not been investigated extensively. In addition to the environmental burdens generated during materials production, the economic efficiency of

alternative materials should be considered and investigated thoroughly for the future work to benefit decision making.

4. Conclusions

Many researchers develop novel CO₂ capture adsorbents generally put emphasis on improving adsorption efficiency and stability during the capture processes. However, the environmental burdens generated through material syntheses and utilization are largely overlooked. Our study serves as an example, to investigate the environmental impacts of solid amine as a carbon capture application, and performed environmental and economic trade-off comparisons with a traditional carbon capture method for the first time. The key findings of this study are:

- (1) CNT-PEI as a solid amine absorbent, showed much higher environmental costs than the traditional MEA method during their initial manufacturing phase. CNT production identified as the major contributor during the life cycle environmental impacts. There is still potential to optimize current technology, such as using more sustainable energy source, scaling up and recycle to enhance the production efficiency.
- (2) The carbon payback period for Phy-CNT-PEI is 917 cycles. With higher CO₂ remission rate, consistent capture capacity and reusability, Phy-CNT-PEI provided great potential to overcome some barriers such as offset CO₂ cost and increase the sustainability of current CO₂ capture techniques, however, high initial environmental and economic costs do not favor CNT-PEI to be used in industrial application with current performance.

Given that CO₂ emissions play a major role in global climate change, developing novel technologies that mitigate CO₂ emissions is critical. However, when implementing a novel

technology, the corresponding environmental impacts should be taken into consideration. Our study highlights that unilateral emphasis of the CO₂ capture efficiency by novel materials is not enough, comprehensive environmental and economic impact comparisons throughout material life cycles should be investigated. In this study, an understanding of hotspots in the material life cycle allows researchers and developers to work towards optimizing the production processes (CNT and PEI syntheses in the present study), and to limit negative environmental impacts that may be associated with CNT enabled adsorption technologies. In addition, future development for solid amine adsorption that enhances the CO₂ remission capacity and extends product lifetime are important in making this technology more valuable and competitive.

Acknowledgements

This work is supported by the National Science Foundation (NSF #1743891) and Wisconsin Alumni Research Foundation. This work has not been formally reviewed by the funders, and the opinions expressed are those of the authors. We thank the anonymous reviewers for their time and input.

Electronic supplemental information

Additional methods:

The electricity and energy usage to produce CNT-PEI were either collected directly from the laboratory equipment, or estimated based on the first law of thermodynamics (eqn GS1 and GS2) when the materials were not synthesized on-site.

$$Q_{heating} = m * C_p * \Delta T \quad (\text{eqn GS1})$$

where m is mass (kg), C_p is the heat capacity of the targeting compounds (KJ/(kg·°C)), and ΔT is the difference in the temperature (°C) between the system and the ambient surroundings. For evaporating and drying the liquid from the solution phase,

$$Q_{drying} = \sum m * H_v \quad (\text{eqn GS2})$$

where m is the weight of each compound in the mixture (kg) and H_v is the enthalpy of vaporization of each compound (KJ/kg). Notably, the energy calculations using the above method do not account for energy losses.

Additional discussion:

The preparation of Phy-CNT-PEI can be achieved using wet impregnation methods, which are commonly applied for grafting amines to the CNT support through Van der Waals forces between the support and the adsorbent. The method is easy to conduct for solid state amine preparation with high amine loading and CO₂ capture efficiency [65–68]. The amount of CO₂ generation resulting from the synthesis based on this method proved to conserve by 36% compared to Cov-CNT-PEI. However, a main challenge of this method is that in a prototypical tube flow reactor system for the CO₂ capture, the physically grafted amine may be separated

from the support in the presence of steam; meanwhile, the agglomeration of the residual amine on the CNT supporter has the potential to further reduce the available sites for CO₂, which lowers the sustainability and increases the cost of materials for the post-combustion CO₂ capture [69]. According to our previous study, amine loading is reduced by 33% and the CO₂ capture efficiency is reduced by 77% for Phy-CNT-PEI under steam heavy environments. To overcome the shortcoming, a more moisture resistant covalent bonded amine on CNT should be developed and investigated. In this study, although the net CO₂ removal of Cov-CNT-PEI is much less than MEA in each A/D cycle, its long-term cumulative CO₂ capture has a potential to be higher than MEA due to its high thermal and steam stability. Therefore, improving current method to covalently bond more amine to CNT may provide great potential for the improvement of CO₂ capture efficiency.

Table GS1. Input / output materials and energy required to produce Ferrocene.

	Section	Material	Amount	Unit	Corresponding LCI	Database	Comments
170 g Ferrocene	Input	Iron (III) chloride	86.2	g	Without water, in 40% solution state {CH} iron (III) chloride production, product in 40% solution state APOS, U	Ecoinvent V3	
		Iron scrap	43.1	g	Unsorted {US} container production, for collection of post-consumer waste plastic for recycling APOS, U	Ecoinvent V3	
		Water	1130	g	Deionised, from tap water, at user {RoW} production APOS, U	Ecoinvent V3	
		Sodium methoxide	121.5	g	{GLO} production APOS, U	Ecoinvent V3	
		Benzene	132	g	{RoW} production APOS, U	Ecoinvent V3	
		Methanol	472	g	{GLO} production APOS, U	Ecoinvent V3	
		Sulfuric acid	3210	g	{RoW} production APOS, U	Ecoinvent V3	
		Nitrogen	0.26	g	Liquid {RoW} air separation, cryogenic APOS, U	Ecoinvent V3	
		Electricity	0.48	kWh	At grid, US, 2010/kWh/RNA	USLCI	
		Electricity	0.02	kWh	Natural gas, at power plant/US	USLCI	
	Output	Wastewater	4.61	kg	Untreated, organic contaminated EU-27 S	ELCD	

Table GS2. Input materials and energy required to produce 1 kg of carbon nanotubes (CNT) via chemical vapor deposition (CVD) method.

	Material	Amount	Unit	Corresponding LCI	Database	Comments
1 kg Industrial CNT	Ferrocene	0.15	kg	Created		
	Benzene	13.15	kg	{RoW} production APOS, U	Ecoinvent V3	
	Hydrogen	0.00054	kg	Liquid, chlor-alkali electrolysis, at plant/RNA	USLCI	
	Argon	2.68	kg	Liquid {RoW} production APOS, U	Ecoinvent V3	
	Water	5	kg	Decarbonised, at user {RoW} water production and supply, decarbonised APOS, U	Ecoinvent V3	
	Hydrochloric acid	30.42	kg	Without water, in 30% solution state {RoW} benzene chlorination APOS, U	Ecoinvent V3	
	Electricity	482	MJ	At grid, US, 2010/kWh/RNA	USLCI	

Table GS3. Input materials and energy required to produce 1 kg PEI.

	Material	Amount	Unit	Corresponding LCI	Database	Comments
2.63 kg Monoethanolamine hydrochloride	Monoethanolamine	1.83	kg	{RoW} ethanolamine production APOS, U	Ecoinvent V3	
	Ethanol, without water	10.83	kg	In 99.7% solution state, from ethylene {RoW} ethylene hydration APOS, U	Ecoinvent V3	
	Hydrochloric acid	3.67	kg	At plant /kg/RNA	USLCI	
3 kg 2-chloroethylamine hydrochloride	Monoethanolamine hydrochloride	2.63	kg	Created		
	Thionyl chloride	3.4	kg	{RoW} production APOS, U	Ecoinvent V3	
	Toluene	3.67	kg	Liquid {RoW} production APOS, U	Ecoinvent V3	
	Electricity	0.21	kWh	At grid, US, 2010/kWh/RNA	USLCI	
1 kg Aziridine	2-chloroethylamine hydrochloride	3	kg	Created		
	Sodium hydroxide	2.58	kg	Production mix, at plant/RNA	USLCI	
	Water	17	kg	Decarbonised, at user {RoW} water production and supply, decarbonised APOS, U	Ecoinvent V3	
	Electricity	0.64	kWh	At grid, US, 2010/kWh/RNA	USLCI	Heating (3)
	Electricity	1.27	kWh	At grid, US, 2010/kWh/RNA	USLCI	Heating (4)
	Electricity	4.8	kWh	At grid, US, 2010/kWh/RNA	USLCI	
1 kg PEI	Aziridine	1	kg	Created		
	Water	12.5	kg	Decarbonised, at user {RoW} water production and supply, decarbonised APOS, U	Ecoinvent V3	
	Hydrochloric acid	0.23	kg	At plant /kg/RNA	USLCI	
	Diethyl ether	3.67	kg	without water, in 99.95% solution state {RoW} ethylene hydration APOS, U	Ecoinvent V3	
	Ethanol	0.65	kg	Without water, in 99.7% solution state, from ethylene {RoW} ethylene hydration APOS, U	Ecoinvent V3	
	Electricity	2.3	kWh	At grid, US, 2010/kWh/RNA	USLCI	Heating for 4 days
	Electricity	0.08	kWh	At grid, US, 2010/kWh/RNA	USLCI	Recycling (overall for pumping)

Table GS4. Input materials and energy required to produce Dimethylformamide (DMF) [70].

	Material	Amount	Unit	Corresponding LCI	Database	Comments
1 kg Dimethylformamide	Dimethylamine	0.62	kg	{RoW} production APOS, U	Ecoinvent V3	
	Methyl formate	0.41	kg	{RoW} production APOS, U	Ecoinvent V3	
	Electricity	3557	kJ	At grid, US, 2010/kWh/RNA	USLCI	

Table GS5. Input materials and energy required to produce physiosorbed CNT-PEI (Phy-CNT-PEI).

	Material	Amount	Unit	Corresponding LCI	Database	Comments
0.3475 kg Phy-CNT-PEI	Ethanol	5.02	g	Without water, in 99.7% solution state, from ethylene {RoW} ethylene hydration APOS, U	Ecoinvent V3	
	PEI	0.25	g	Created		
	Industrial CNT	0.375	g	Created		
	Electricity	0.0001	kWh	At grid, US, 2010/kWh/RNA	USLCI	Stirring (1)
	Electricity	0.0002	kWh	At grid, US, 2010/kWh/RNA	USLCI	Heating (1)
	Electricity	0.0011	kWh	At grid, US, 2010/kWh/RNA	USLCI	Heating (3)
	Electricity	0.000003	kWh	At grid, US, 2010/kWh/RNA	USLCI	Drying (4)
	Electricity	0.00007	kWh	At grid, US, 2010/kWh/RNA	USLCI	Recycle pump

Table GS6. Input materials and energy required to produce covalent bond CNT-PEI (Cov-CNT-PEI).

	Material	Amount	Unit	Corresponding LCI	Database	Comments
0.7321 g o-CNT	Industrial CNT	1	g	Created		
	Nitric acid	13.23	g	Without water, in 50% solution state	Ecoinvent V3	
	Electricity	0.0003	kWh	At grid, US, 2010/kWh/RNA	USLCI	Sonication (1)
	Electricity	0.0007	kWh	At grid, US, 2010/kWh/RNA	USLCI	Stirring (1)
	Electricity	0.002	kWh	At grid, US, 2010/kWh/RNA	USLCI	Heating (1)
0.4599 g Cov-CNT-PEI	Dimethylformamide (DMF)	1.90	g	Created		1 st wash
	Thionyl chloride	4.94	g	{RoW} production APOS, U	Ecoinvent V3	
	o-CNT	0.4	g	Created		
	PEI	0.4	g	Created		
	Water	9.02	g	Decarbonised water	Ecoinvent V3	
	Dimethylformamide (DMF)	1.90	g	Created		2 nd wash
	Electricity	0.00003	kWh	At grid, US, 2010/kWh/RNA	USLCI	Sonication (2)
	Electricity	0.0003	kWh	At grid, US, 2010/kWh/RNA	USLCI	Stirring (2)
	Electricity	0.0024	kWh	At grid, US, 2010/kWh/RNA	USLCI	Heating (2)
	Electricity	0.0045	kWh	At grid, US, 2010/kWh/RNA	USLCI	Centrifuging (2)
	Electricity	0.0000002	kWh	At grid, US, 2010/kWh/RNA	USLCI	Stirring (3)
	Electricity	0.0009	kWh	At grid, US, 2010/kWh/RNA	USLCI	Heating (4)
	Electricity	0.0015	kWh	At grid, US, 2010/kWh/RNA	USLCI	Centrifuging (4)
	Electricity	0.0017	kWh	At grid, US, 2010/kWh/RNA	USLCI	Stirring (4)
	Electricity	0.001	kWh	At grid, US, 2010/kWh/RNA	USLCI	Heating (5)
	Electricity	0.0015	kWh	At grid, US, 2010/kWh/RNA	USLCI	Centrifuging (6)
	Electricity	0.00006672	kWh	At grid, US, 2010/kWh/RNA	USLCI	Recycling

Table GS7. Life cycle environmental impacts of producing 1 kg carbon nanotubes (CNT) via chemical vapor deposition (CVD) used in present study (pilot scale).

Impact category	Unit	Ferrocene	Benzene	Hydrogen	Argon	Water	Hydrochloric acid	Electricity	Total
OD	kg CFC-11 eq	3.57E-07	7.34E-09	3.89E-15	4.13E-07	3.35E-12	4.30E-06	1.43E-09	5.08E-06
GW	kg CO ₂ eq	1.01E+00	2.35E+01	5.18E-03	7.21E+00	4.00E-05	1.60E+01	8.87E+01	1.36E+02
PS	kg O ₃ eq	9.10E-02	9.17E-01	3.01E-05	3.45E-01	2.34E-06	8.51E-01	5.08E+00	7.28E+00
AC	kg SO ₂ eq	2.47E-02	8.19E-02	7.71E-06	3.18E-02	1.55E-07	7.26E-02	7.63E-01	9.74E-01
EF	kg N eq	3.23E-03	3.99E-03	6.77E-08	2.86E-02	1.34E-07	1.64E-01	1.03E-02	2.11E-01
HHC	CTUh	7.73E-08	5.10E-07	7.30E-12	3.95E-07	8.55E-12	1.14E-06	1.80E-07	2.30E-06
HHNC	CTUh	5.69E-07	2.31E-07	7.84E-11	1.41E-06	1.81E-11	4.62E-06	3.01E-06	9.85E-06
RF	kg PM _{2.5} eq	1.98E-03	5.89E-03	4.41E-07	1.03E-02	4.34E-08	2.09E-02	3.83E-02	7.74E-02
EC	CTUe	1.39E+01	2.58E+01	1.53E-03	4.67E+01	6.13E-04	3.82E+02	4.37E+01	5.12E+02
FF	MJ surplus	6.74E+00	1.24E+02	1.26E-02	4.75E+00	3.90E-05	3.48E+01	7.69E+01	2.47E+02

Table GS8. Life cycle environmental impacts of producing 1 kg monoethanolamine (MEA).

1 kg MEA with water	Unit	Total
OD	kg CFC-11 eq	2.13E-07
GW	kg CO ₂ eq	2.88E+00
PS	kg O ₃ eq	1.16E-01
AC	kg SO ₂ eq	1.11E-02
EF	kg N eq	1.57E-02
HHC	CTUh	1.22E-07
HHNC	CTUh	5.78E-07
RF	kg PM _{2.5} eq	2.10E-03
EC	CTUe	1.62E+01
FF	MJ surplus	8.60E+00

Table GS9. Life cycle environmental impacts of producing 1 kg Monoethanolamine

hydrochloride for PEI synthesis.

Impact category	Unit	Total	Monoethanolamine	Ethanol	Hydrochloric acid
OD	kg CFC-11 eq	4.56E-07	1.48E-07	1.13E-07	1.95E-07
GW	kg CO ₂ eq	9.37E+00	2.00E+00	5.02E+00	2.34E+00
PS	kg O ₃ eq	4.78E-01	8.04E-02	2.57E-01	1.40E-01
AC	kg SO ₂ eq	3.55E-02	7.69E-03	1.78E-02	9.99E-03
EF	kg N eq	2.76E-02	1.09E-02	1.65E-02	1.79E-04
HHC	CTUh	2.68E-07	8.46E-08	1.81E-07	2.11E-09
HHNC	CTUh	1.33E-06	4.02E-07	8.66E-07	6.10E-08
RF	kg PM _{2.5} eq	4.08E-03	1.46E-03	2.04E-03	5.76E-04
EC	CTUe	3.45E+01	1.13E+01	2.30E+01	2.81E-01
FF	MJ surplus	3.48E+01	5.98E+00	2.52E+01	3.56E+00

Table GS10. Life cycle environmental impacts of producing 1 kg 2-chloroethylamine

hydrochloride for PEI synthesis.

Impact category	Unit	Monoethanolamine hydrochloride	Thionyl chloride	Toluene	Electricity	Total
OD	kg CFC-11 eq	1.20E-06	1.88E-06	1.55E-09	5.13E-10	3.08E-06
GW	kg CO ₂ eq	2.46E+01	3.96E+00	5.49E+00	3.18E+01	6.59E+01
PS	kg O ₃ eq	1.26E+00	3.12E-01	1.88E-01	1.82E+00	3.58E+00
AC	kg SO ₂ eq	9.33E-02	6.80E-02	1.38E-02	2.74E-01	4.49E-01
EF	kg N eq	7.26E-02	1.89E-02	8.37E-04	3.70E-03	9.61E-02
HHC	CTUh	7.04E-07	3.47E-07	9.61E-08	6.44E-08	1.21E-06
HHNC	CTUh	3.50E-06	2.41E-06	4.72E-08	1.08E-06	7.04E-06
RF	kg PM _{2.5} eq	1.07E-02	8.41E-03	1.08E-03	1.37E-02	3.40E-02
EC	CTUe	9.09E+01	5.36E+01	5.20E+00	1.57E+01	1.65E+02
FF	MJ surplus	9.15E+01	7.31E+00	3.29E+01	2.76E+01	1.59E+02

Table GS11. Life cycle environmental impacts of producing 1 kg Aziridine for PEI synthesis.

Impact category	Unit	2-chloroethylamine hydrochloride	Sodium hydroxide	Water	Electricity	Total
OD	kg CFC-11 eq	3.08E-06	3.66E-07	1.14E-11	6.36E-10	3.45E-06
GW	kg CO ₂ eq	6.59E+01	2.83E+00	1.36E-04	3.95E+01	1.08E+02
PS	kg O ₃ eq	3.58E+00	1.48E-01	7.95E-06	2.26E+00	5.98E+00
AC	kg SO ₂ eq	4.49E-01	2.44E-02	5.27E-07	3.39E-01	8.13E-01
EF	kg N eq	9.61E-02	3.72E-04	4.57E-07	4.59E-03	1.01E-01
HHC	CTUh	1.21E-06	1.04E-08	2.91E-11	7.99E-08	1.30E-06
HHNC	CTUh	7.04E-06	3.13E-07	6.15E-11	1.34E-06	8.69E-06
RF	kg PM _{2.5} eq	3.40E-02	1.34E-03	1.48E-07	1.70E-02	5.24E-02
EC	CTUe	1.65E+02	2.46E+00	2.08E-03	1.95E+01	1.87E+02
FF	MJ surplus	1.59E+02	4.48E+00	1.33E-04	3.42E+01	1.98E+02

Table GS12. Life cycle environmental impacts of producing 1 kg PEI.

Impact category	Unit	Aziridine	Water	Hydrochloric acid	Diethyl ether	Ethanol	Electricity	Total
OD	kg CFC-11 eq	3.44E-06	8.37E-12	3.21E-08	3.10E-07	1.77E-08	2.54E-11	3.80E-06
GW	kg CO ₂ eq	4.15E+01	1.00E-04	3.85E-01	1.38E+01	7.90E-01	1.58E+00	5.81E+01
PS	kg O ₃ eq	2.17E+00	5.84E-06	2.31E-02	7.08E-01	4.04E-02	9.02E-02	3.03E+00
AC	kg SO ₂ eq	2.39E-01	3.88E-07	1.64E-03	4.90E-02	2.80E-03	1.36E-02	3.06E-01
EF	kg N eq	9.33E-02	3.36E-07	2.94E-05	4.54E-02	2.59E-03	1.83E-04	1.42E-01
HHC	CTUh	1.17E-06	2.14E-11	3.48E-10	4.98E-07	2.85E-08	3.19E-09	1.70E-06
HHNC	CTUh	6.42E-06	4.52E-11	1.00E-08	2.38E-06	1.36E-07	5.36E-08	9.01E-06
RF	kg PM _{2.5} eq	2.36E-02	1.08E-07	9.47E-05	5.63E-03	3.21E-04	6.81E-04	3.03E-02
EC	CTUe	1.54E+02	1.53E-03	4.63E-02	6.33E+01	3.62E+00	7.78E-01	2.22E+02
FF	MJ surplus	1.40E+02	9.76E-05	5.86E-01	6.95E+01	3.97E+00	1.37E+00	2.16E+02

Table GS13. Life cycle environmental impacts of producing 1 kg Cov-CNT-PEI.

Impact category	Unit	Total	DMF	Thionyl chloride	o-CNT	PEI	Water	Electricity
OD	kg CFC-11 eq	2.25E-05	5.20E-06	5.93E-06	8.09E-06	3.31E-06	1.31E-11	3.22E-10
GW	kg CO ₂ eq	3.26E+02	2.83E+01	1.25E+01	2.15E+02	5.05E+01	1.57E-04	2.00E+01
PS	kg O ₃ eq	1.71E+01	1.34E+00	9.83E-01	1.10E+01	2.63E+00	9.16E-06	1.14E+00
AC	kg SO ₂ eq	2.18E+00	1.46E-01	2.15E-01	1.38E+00	2.66E-01	6.08E-07	1.72E-01
EF	kg N eq	6.15E-01	1.40E-01	5.96E-02	2.89E-01	1.23E-01	5.27E-07	2.32E-03
HHC	CTUh	6.90E-06	9.50E-07	1.09E-06	3.34E-06	1.48E-06	3.35E-11	4.04E-08
HHNC	CTUh	3.97E-05	5.69E-06	7.61E-06	1.79E-05	7.83E-06	7.09E-11	6.78E-07
RF	kg PM _{2.5} eq	1.89E-01	2.18E-02	2.66E-02	1.06E-01	2.63E-02	1.70E-07	8.63E-03
EC	CTUe	1.28E+03	1.49E+02	1.69E+02	7.60E+02	1.93E+02	2.40E-03	9.84E+00
FF	MJ surplus	6.42E+02	9.12E+01	2.31E+01	3.23E+02	1.88E+02	1.53E-04	1.73E+01

Table GS14. Life cycle environmental impacts of producing 1 kg Phy-CNT-PEI.

Impact category	Unit	Total	Ethanol	PEI	CNT	Electricity
OD	kg CFC-11 eq	8.62E-06	3.95E-07	2.74E-06	5.48E-06	4.35E-11
GW	kg CO ₂ eq	2.09E+02	1.76E+01	4.18E+01	1.47E+02	2.70E+00
PS	kg O ₃ eq	1.11E+01	9.01E-01	2.18E+00	7.86E+00	1.55E-01
AC	kg SO ₂ eq	1.36E+00	6.24E-02	2.20E-01	1.05E+00	2.32E-02
EF	kg N eq	3.87E-01	5.79E-02	1.02E-01	2.27E-01	3.14E-04
HHC	CTUh	4.34E-06	6.35E-07	1.22E-06	2.48E-06	5.47E-09
HHNC	CTUh	2.02E-05	3.03E-06	6.48E-06	1.06E-05	9.17E-08
RF	kg PM _{2.5} eq	1.14E-01	7.16E-03	2.18E-02	8.35E-02	1.17E-03
EC	CTUe	7.95E+02	8.07E+01	1.60E+02	5.53E+02	1.33E+00
FF	MJ surplus	5.13E+02	8.85E+01	1.55E+02	2.67E+02	2.34E+00

Table GS15. Sensitivity analysis of Phy-CNT-PEI production. The sensitivities of Phy-CNT-PEI production was assessed by increasing 25% of single parameter values and compare the corresponding change to the overall impact at each impact category.

Ethanol	Increase by 25%	New	<i>New:Old</i>	PEI	Increase by 25%	New	<i>New:Old</i>
OD	4.93E-07	8.71E-06	101.1%	OD	3.42E-06	9.30E-06	107.9%
GW	2.20E+01	2.14E+02	102.1%	GW	5.22E+01	2.20E+02	105.0%
PS	1.13E+00	1.13E+01	102.0%	PS	2.72E+00	1.16E+01	104.9%
AC	7.80E-02	1.37E+00	101.1%	AC	2.75E-01	1.41E+00	104.1%
EF	7.23E-02	4.02E-01	103.7%	EF	1.27E-01	4.13E-01	106.6%
HHC	7.93E-07	4.50E-06	103.7%	HHC	1.53E-06	4.65E-06	107.0%
HHNC	3.79E-06	2.10E-05	103.8%	HHNC	8.10E-06	2.19E-05	108.0%
RF	8.95E-03	1.15E-01	101.6%	RF	2.72E-02	1.19E-01	104.8%
EC	1.01E+02	8.15E+02	102.5%	EC	2.00E+02	8.35E+02	105.0%
FF	1.11E+02	5.35E+02	104.3%	FF	1.94E+02	5.52E+02	107.6%

CNT	Increase by 25%	New	<i>New:Old</i>	Electricity	Increase by 25%	New	<i>New:Old</i>
OD	6.85E-06	9.99E-06	115.9%	OD	5.44E-11	8.62E-06	100.0%
GW	1.84E+02	2.46E+02	117.6%	GW	3.38E+00	2.10E+02	100.3%
PS	9.82E+00	1.31E+01	117.7%	PS	1.93E-01	1.11E+01	100.3%
AC	1.31E+00	1.62E+00	119.4%	AC	2.90E-02	1.36E+00	100.4%
EF	2.84E-01	4.44E-01	114.7%	EF	3.93E-04	3.87E-01	100.0%
HHC	3.10E-06	4.96E-06	114.3%	HHC	6.84E-09	4.34E-06	100.0%
HHNC	1.33E-05	2.29E-05	113.1%	HHNC	1.15E-07	2.03E-05	100.1%
RF	1.04E-01	1.35E-01	118.4%	RF	1.46E-03	1.14E-01	100.3%
EC	6.91E+02	9.33E+02	117.4%	EC	1.66E+00	7.95E+02	100.0%
FF	3.33E+02	5.79E+02	113.0%	FF	2.93E+00	5.13E+02	100.1%

Table GS16. Sensitivity analysis of Cov-CNT-PEI production. The sensitivities of Phy-CNT-PEI production was assessed by increasing 25% of single parameter values and compare the corresponding change to the overall impact at each impact category.

DMF	Increase by 25%	New	<i>New:Old</i>	Thionyl chloride	Increase by 25%	New	<i>New:Old</i>
OD	6.49E-06	2.38E-05	105.8%	OD	7.41E-06	2.40E-05	106.6%
GW	3.53E+01	3.33E+02	102.2%	GW	1.56E+01	3.29E+02	101.0%
PS	1.68E+00	1.75E+01	102.0%	PS	1.23E+00	1.74E+01	101.4%
AC	1.83E-01	2.21E+00	101.7%	AC	2.68E-01	2.23E+00	102.5%
EF	1.75E-01	6.50E-01	105.7%	EF	7.46E-02	6.30E-01	102.4%
HHC	1.19E-06	7.14E-06	103.4%	HHC	1.37E-06	7.17E-06	104.0%
HHNC	7.11E-06	4.11E-05	103.6%	HHNC	9.52E-06	4.16E-05	104.8%
RF	2.72E-02	1.94E-01	102.9%	RF	3.32E-02	1.96E-01	103.5%
EC	1.86E+02	1.32E+03	102.9%	EC	2.11E+02	1.32E+03	103.3%
FF	1.14E+02	6.64E+02	103.6%	FF	2.88E+01	6.47E+02	100.9%

o-CNT	Increase by 25%	New	<i>New:Old</i>	PEI	Increase by 25%	New	<i>New:Old</i>
OD	1.01E-05	2.45E-05	109.0%	OD	4.14E-06	2.33E-05	103.7%
GW	2.69E+02	3.80E+02	116.5%	GW	6.32E+01	3.39E+02	103.9%
PS	1.38E+01	1.99E+01	116.1%	PS	3.29E+00	1.78E+01	103.8%
AC	1.72E+00	2.52E+00	115.8%	AC	3.33E-01	2.24E+00	103.1%
EF	3.62E-01	6.87E-01	111.8%	EF	1.54E-01	6.45E-01	105.0%
HHC	4.17E-06	7.74E-06	112.1%	HHC	1.85E-06	7.27E-06	105.3%
HHNC	2.24E-05	4.42E-05	111.3%	HHNC	9.79E-06	4.17E-05	104.9%
RF	1.32E-01	2.15E-01	114.0%	RF	3.29E-02	1.96E-01	103.5%
EC	9.50E+02	1.47E+03	114.8%	EC	2.41E+02	1.33E+03	103.8%
FF	4.03E+02	7.22E+02	112.6%	FF	2.34E+02	6.89E+02	107.3%

Water	Increase by 25%	New	<i>New:Old</i>	Electricity	Increase by 25%	New	<i>New:Old</i>
OD	1.64E-11	2.25E-05	100.0%	OD	4.02E-10	2.25E-05	100.0%
GW	1.96E-04	3.26E+02	100.0%	GW	2.50E+01	3.31E+02	101.5%
PS	1.15E-05	1.71E+01	100.0%	PS	1.43E+00	1.74E+01	101.7%
AC	7.60E-07	2.18E+00	100.0%	AC	2.15E-01	2.22E+00	102.0%
EF	6.59E-07	6.15E-01	100.0%	EF	2.90E-03	6.15E-01	100.1%
HHC	4.19E-11	6.90E-06	100.0%	HHC	5.05E-08	6.91E-06	100.1%
HHNC	8.86E-11	3.97E-05	100.0%	HHNC	8.48E-07	3.99E-05	100.4%
RF	2.13E-07	1.89E-01	100.0%	RF	1.08E-02	1.91E-01	101.1%
EC	3.00E-03	1.28E+03	100.0%	EC	1.23E+01	1.28E+03	100.2%
FF	1.91E-04	6.42E+02	100.0%	FF	2.16E+01	6.46E+02	100.7%

Table GS17. Costs of feedstocks for CO₂ adsorbents

Materials	Vendor	Price (\$/kg)	Reference
EtOH	Decon Laboratories, 200 proof	20	www.laballey.com/products/ethanol-200-proof-100-usp-decon-labs
PEI	Sigma-Aldrich	400	www.sigmaaldrich.com/catalog/search?term=25987-06-8&interface=CAS%20No.&N=0+&mode=partialmax&lang=en&region=US&focus=product
CNT	Cheaptubes, >95%	700	www.cheaptubes.com/product/multi-walled-carbon-nanotubes-20-30nm/
MEA	Sigma-Aldrich, >98%	40	www.sigmaaldrich.com/catalog/product/sial/e9508?lang=en&region=US
MEA	Sigma-Aldrich, 30%	12	According to the calculation 40 kg * 30% =12 kg

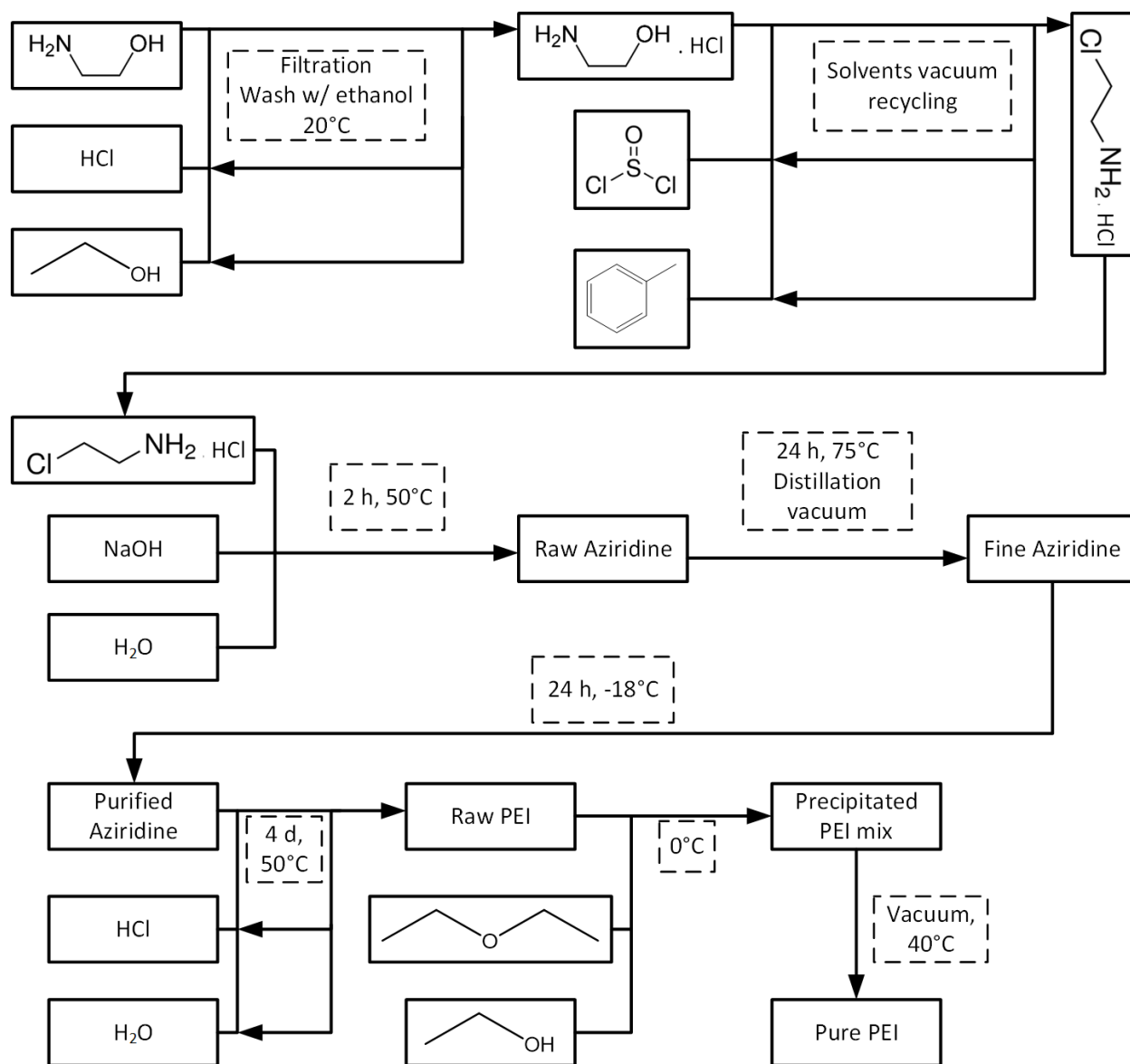


Figure GS1. Scheme for the production of PEI [71–73].

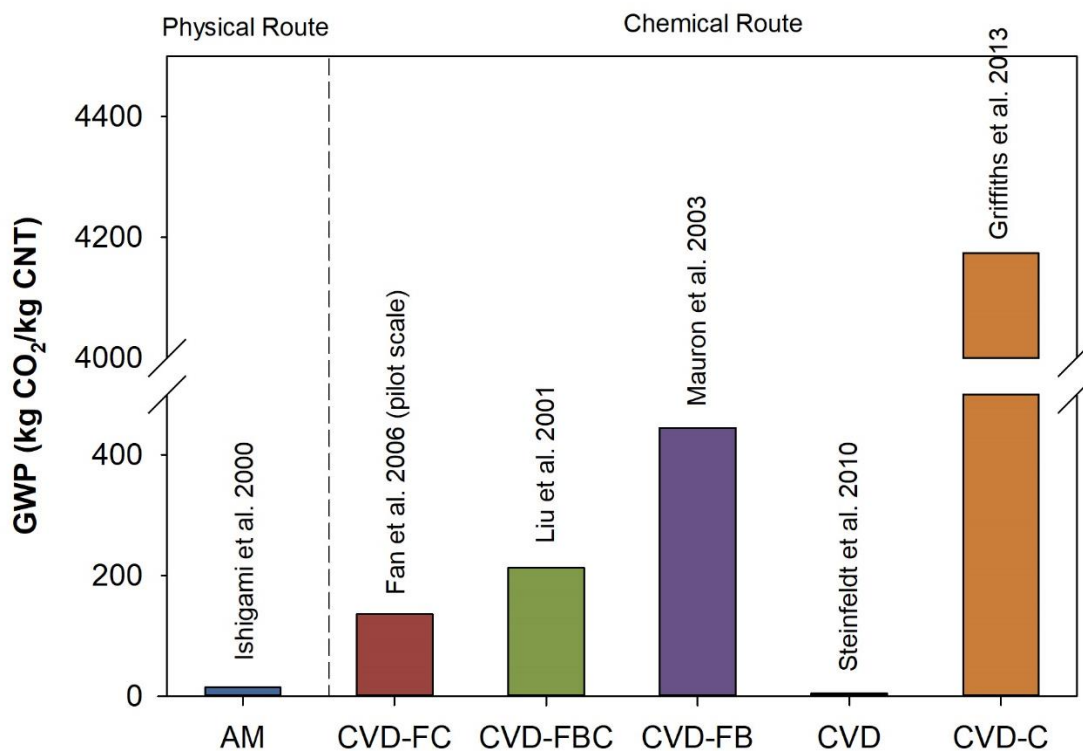


Figure GS2. The GWP comparison between the laboratory and pilot scale CNT production methods (AM: arc-method [74]; CVD-FC: chemical vapor deposition with horizontal tubular reactor made of quartz tube [75]; CVD- FBC: chemical vapor deposition with fluidized bed catalytic reactor [76]; CVD-FB: chemical vapor deposition with quartz glass tube and vertical furnace [77]; CVD: chemical vapor deposition (Steinfeldt, 2010); CVD-C: chemical vapor deposition with horizontal three zone tube furnace [79]).

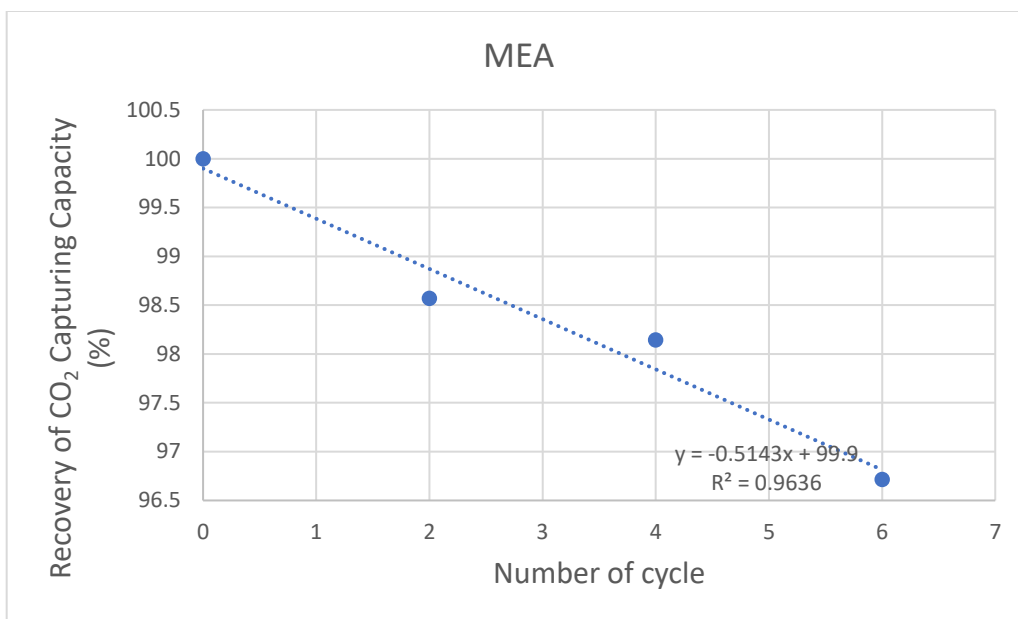


Figure GS3. The fitted linear degradation of MEA over the adsorption/desorption (A/D) cycles.

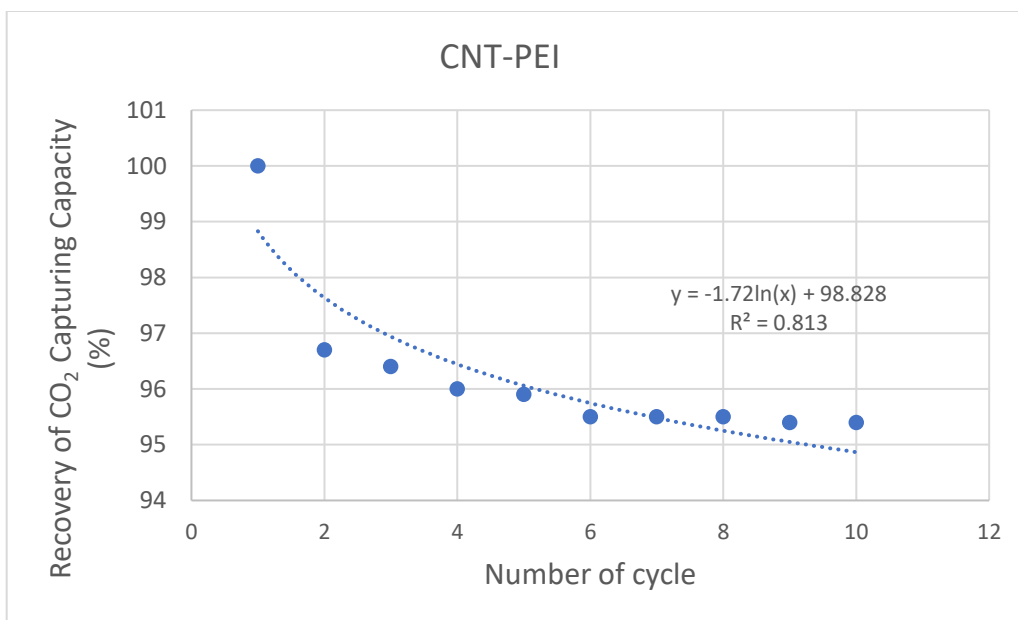


Figure GS4. The fitted degradation of CNT-PEI over the A/D cycles.

Logarithmic	100	1000 cycles	10000 cycles
1.72	7.92	11.88	15.84
98.828	90.91	86.95	82.99

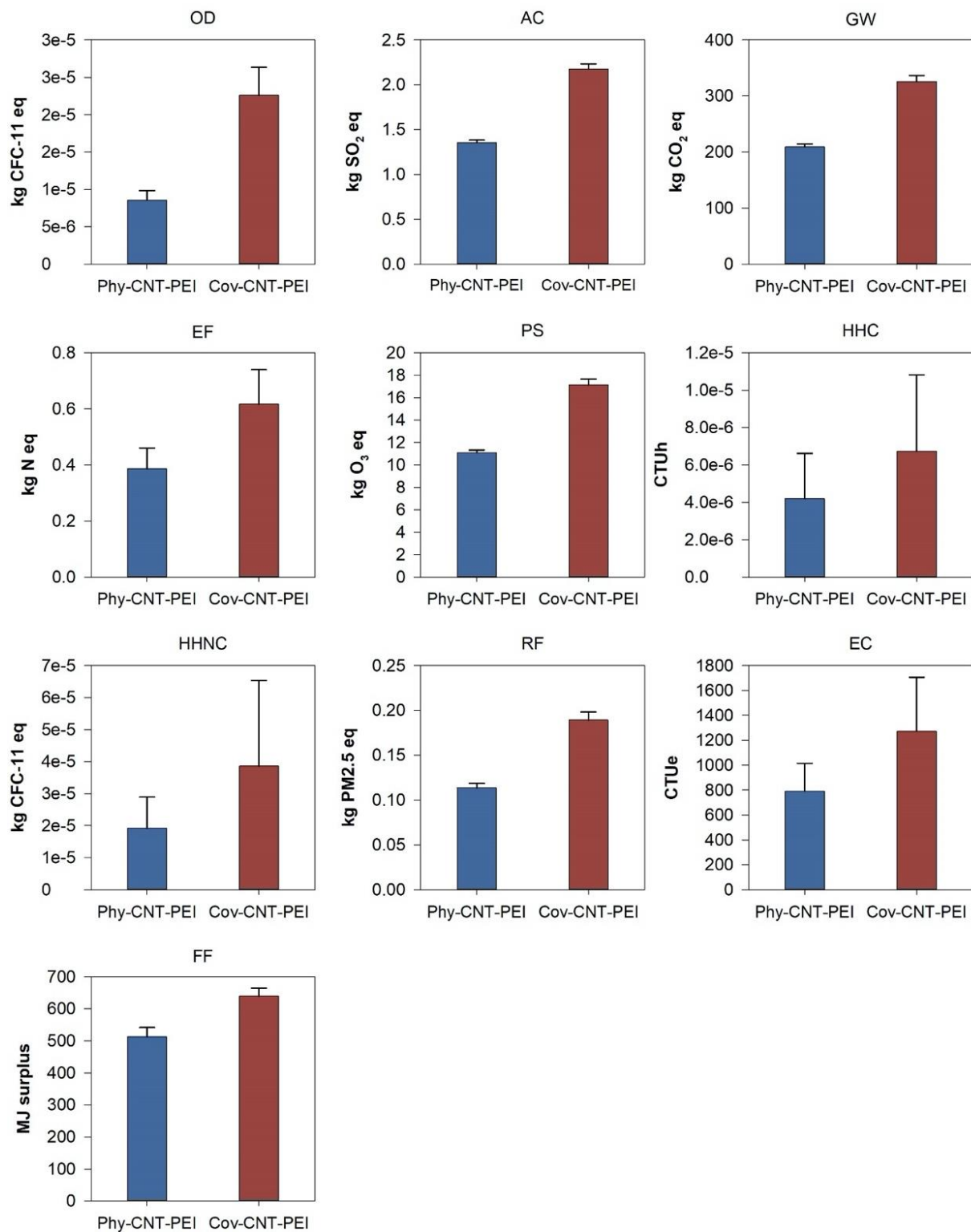


Figure GS5. TRACI impact and the associated uncertainty for both physiosorbed and covalently bond CNT-PEI.

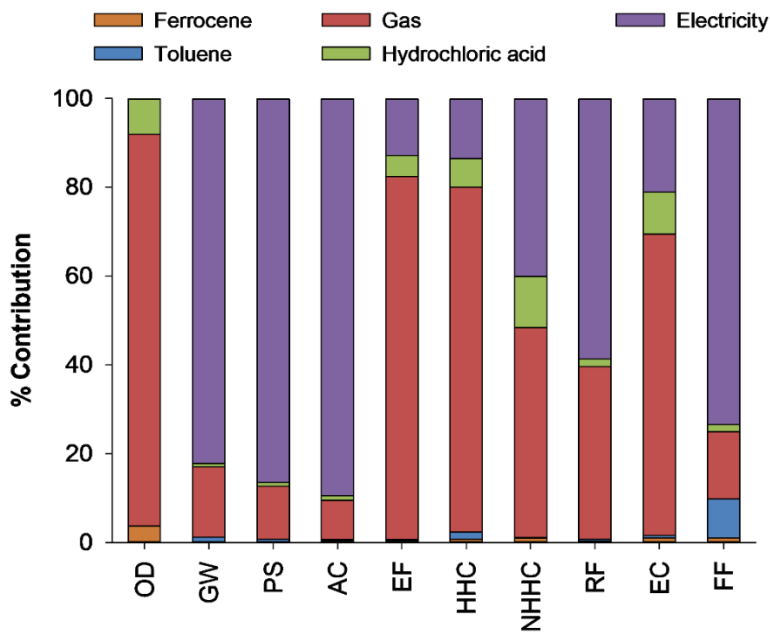


Figure GS6. Percent of environmental impact contribution of synthesizing CNT using chemical vapor deposition in a pilot plant.

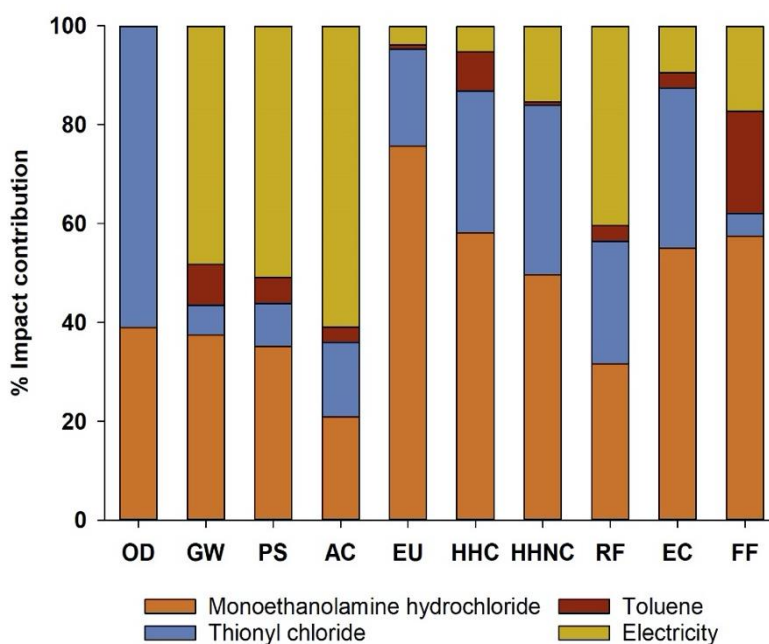


Figure GS7. Percent of environmental impact contribution of synthesizing 3-chloroethylamine hydrochloride to be used in producing PEI.

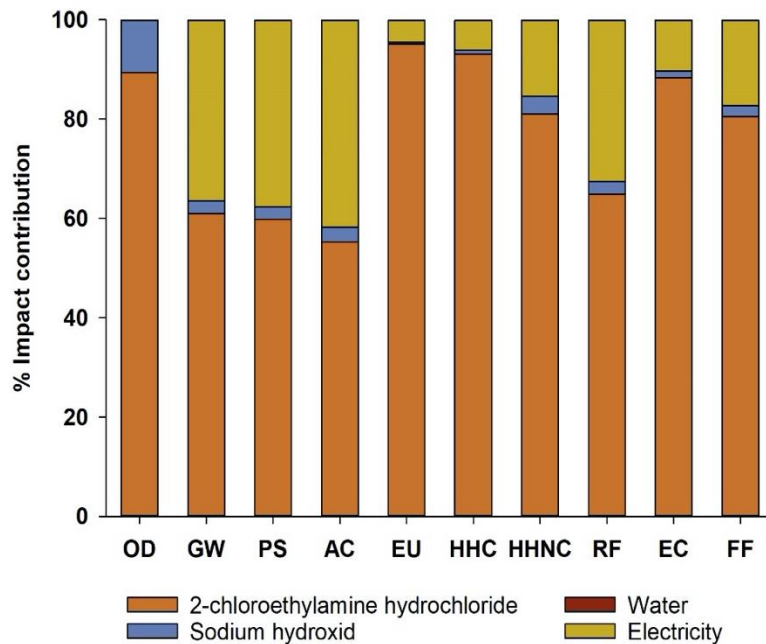


Figure GS8. Percent of environmental impact contribution of synthesizing Aziridine to be used in producing PEI.

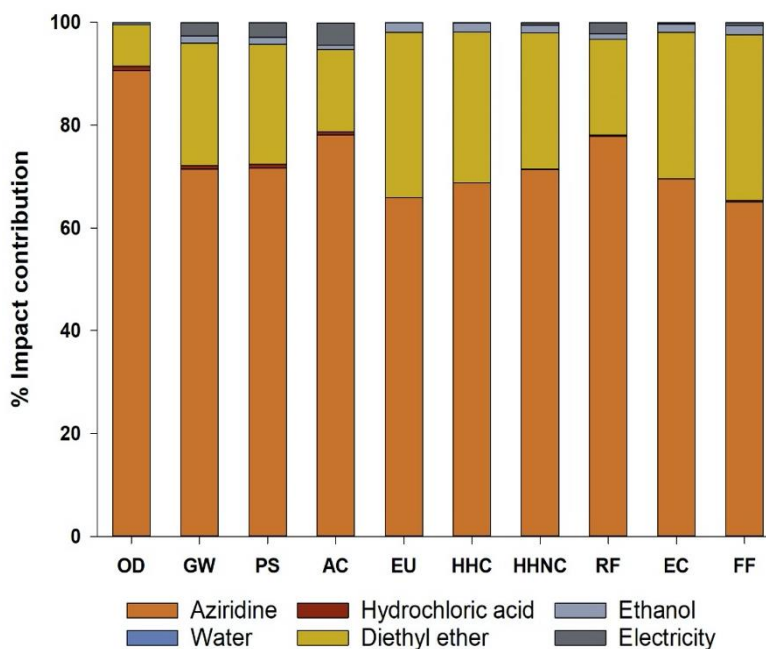


Figure GS9. Percent of environmental impact contribution of synthesizing PEI.

References-Appendix G

1. US EPA (2015) Sources of Greenhouse Gas Emissions. <https://www.epa.gov/ghgemissions/sources-greenhouse-gas-emissions>
2. IPCC (2014) Climate Change 2014 - Synthesis Report Summary for Policymakers. :32. https://www.ipcc.ch/site/assets/uploads/2018/02/AR5_SYR_FINAL_SPM.pdf
3. NASA (2019) Global Climate Change: Vital Signs of the Planet. *National Aeronautics and Space Administration*, <https://climate.nasa.gov/>
4. Kätelhön A, Meys R, Deutz S, Suh S, Bardow A (2019) Climate change mitigation potential of carbon capture and utilization in the chemical industry. *Proceedings of the National Academy of Sciences*, 116(23):11187–11194. <https://doi.org/10.1073/pnas.1821029116>
5. Kocs EA (2017) The global carbon nation: Status of CO₂ capture, storage and utilization. *EPJ Web of Conferences*, 148:00002. <https://doi.org/10.1051/epjconf/201714800002>
6. Boot-Handford ME, Abanades JC, Anthony EJ, Blunt MJ, Brandani S, Mac Dowell N, Fernández JR, Ferrari M-C, Gross R, Hallett JP, Haszeldine RS, Heptonstall P, Lyngfelt A, Makuch Z, Mangano E, Porter RTJ, Pourkashanian M, Rochelle GT, Shah N, Yao JG, Fennell PS (2014) Carbon capture and storage update. *Energy Environ. Sci.*, 7(1):130–189. <https://doi.org/10.1039/C3EE42350F>
7. Haszeldine RS (2009) Carbon Capture and Storage: How Green Can Black Be? *Science*, 325(5948):1647–1652. <https://doi.org/10.1126/science.1172246>
8. Withey P, Johnston C, Guo J (2019) Quantifying the global warming potential of carbon dioxide emissions from bioenergy with carbon capture and storage. *Renewable and Sustainable Energy Reviews*, 115:109408. <https://doi.org/10.1016/j.rser.2019.109408>
9. D’Alessandro DM, Smit B, Long JR (2010) Carbon Dioxide Capture: Prospects for New Materials. *Angewandte Chemie International Edition*, 49(35):6058–6082. <https://doi.org/10.1002/anie.201000431>
10. Zhou Z, Anderson CM, Butler SK, Thompson SK, Whitty KJ, Shen T-C, Stowers KJ (2017) Stability and efficiency of CO₂ capture using linear amine polymer modified carbon nanotubes. *Journal of Materials Chemistry A*, 5(21):10486–10494. <https://doi.org/10.1039/C7TA02576A>
11. Palomar J, Gonzalez-Miquel M, Polo A, Rodriguez F (2011) Understanding the Physical Absorption of CO₂ in Ionic Liquids Using the COSMO-RS Method. *Industrial & Engineering Chemistry Research*, 50(6):3452–3463. <https://doi.org/10.1021/ie101572m>
12. Sistla YS, Khanna A (2015) CO₂ absorption studies in amino acid-anion based ionic liquids. *Chemical Engineering Journal*, 273:268–276. <https://doi.org/10.1016/j.cej.2014.09.043>

13. Xie N, Chen B, Tan C, Liu Z (2017) Energy Consumption and Exergy Analysis of MEA-Based and Hydrate-Based CO₂ Separation. *Industrial & Engineering Chemistry Research*, 56(51):15094–15101. <https://doi.org/10.1021/acs.iecr.7b03729>
14. Jung J, Jeong YS, Lim Y, Lee CS, Han C (2013) Advanced CO₂ Capture Process Using MEA Scrubbing: Configuration of a Split Flow and Phase Separation Heat Exchanger. *Energy Procedia*, 37:1778–1784. <https://doi.org/10.1016/j.egypro.2013.06.054>
15. Lee M-S, Lee S-Y, Park S-J (2015) Preparation and characterization of multi-walled carbon nanotubes impregnated with polyethyleneimine for carbon dioxide capture. *International Journal of Hydrogen Energy*, 40(8):3415–3421. <https://doi.org/10.1016/j.ijhydene.2014.12.104>
16. Luis P (2016) Use of monoethanolamine (MEA) for CO₂ capture in a global scenario: Consequences and alternatives. *Desalination*, 380:93–99. <https://doi.org/10.1016/j.desal.2015.08.004>
17. Kuramochi T, Ramírez A, Turkenburg W, Faaij A (2012) Comparative assessment of CO₂ capture technologies for carbon-intensive industrial processes. *Progress in Energy and Combustion Science*, 38(1):87–112. <https://doi.org/10.1016/j.peccs.2011.05.001>
18. Wang J, Huang L, Yang R, Zhang Z, Wu J, Gao Y, Wang Q, O'Hare D, Zhong Z (2014) Recent advances in solid sorbents for CO₂ capture and new development trends. *Energy Environ. Sci.*, 7(11):3478–3518. <https://doi.org/10.1039/C4EE01647E>
19. Choi MK, Choi WS (2018) Polymeric Amine Based Carbon Dioxide Adsorbents.
20. Min K, Choi W, Kim C, Choi M (2018) Oxidation-stable amine-containing adsorbents for carbon dioxide capture. *Nature Communications*, 9(1):726. <https://doi.org/10.1038/s41467-018-03123-0>
21. Liu Y, Ye Q, Shen M, Shi J, Chen J, Pan H, Shi Y (2011) Carbon Dioxide Capture by Functionalized Solid Amine Sorbents with Simulated Flue Gas Conditions. *Environmental Science & Technology*, 45(13):5710–5716. <https://doi.org/10.1021/es200619j>
22. Cavenati S, Grande CA, Rodrigues AE (2004) Adsorption Equilibrium of Methane, Carbon Dioxide, and Nitrogen on Zeolite 13X at High Pressures. *Journal of Chemical & Engineering Data*, 49(4):1095–1101. <https://doi.org/10.1021/je0498917>
23. Min K, Choi W, Kim C, Choi M (2018) Rational Design of the Polymeric Amines in Solid Adsorbents for Postcombustion Carbon Dioxide Capture. *ACS Applied Materials & Interfaces*, 10(28):23825–23833. <https://doi.org/10.1021/acsami.8b05988>
24. Abdalla S, Al-Marzouki F, Al-Ghamdi AA, Abdel-Daiem A (2015) Different Technical Applications of Carbon Nanotubes. *Nanoscale Research Letters*, 10(1):358. <https://doi.org/10.1186/s11671-015-1056-3>

25. Zhang Q, Huang J-Q, Qian W-Z, Zhang Y-Y, Wei F (2013) The Road for Nanomaterials Industry: A Review of Carbon Nanotube Production, Post-Treatment, and Bulk Applications for Composites and Energy Storage. *Small*, 9(8):1237–1265. <https://doi.org/10.1002/sml.201203252>
26. Ganesh EN (2013) Single Walled and Multi Walled Carbon Nanotube Structure, Synthesis and Applications. 2(4):10.
27. Osler K, Dheda D, Ngoy J, Wagner N, Daramola MO (2017) Synthesis and evaluation of carbon nanotubes composite adsorbent for CO₂ capture: a comparative study of CO₂ adsorption capacity of single-walled and multi-walled carbon nanotubes. *International Journal of Coal Science & Technology*, 4(1):41–49. <https://doi.org/10.1007/s40789-017-0157-2>
28. Jin Y, Hawkins SC, Huynh CP, Su S (2013) Carbon nanotube modified carbon composite monoliths as superior adsorbents for carbon dioxide capture. *Energy & Environmental Science*, 6(9):2591. <https://doi.org/10.1039/c3ee24441e>
29. Keller L, Ohs B, Abduly L, Wessling M (2019) Carbon nanotube silica composite hollow fibers impregnated with polyethylenimine for CO₂ capture. *Chemical Engineering Journal*, 359:476–484. <https://doi.org/10.1016/j.cej.2018.11.100>
30. Finnveden G, Hauschild MZ, Ekvall T, Guinée J, Heijungs R, Hellweg S, Koehler A, Pennington D, Suh S (2009) Recent developments in Life Cycle Assessment. *Journal of Environmental Management*, 91(1):1–21. <https://doi.org/10.1016/j.jenvman.2009.06.018>
31. Klöpffer W (1997) Life cycle assessment: From the beginning to the current state. *Environmental Science and Pollution Research*, 4(4):223–228. <https://doi.org/10.1007/BF02986351>
32. Kushnir D, Sandén BA (2008) Energy Requirements of Carbon Nanoparticle Production. *Journal of Industrial Ecology*, 12(3):360–375. <https://doi.org/10.1111/j.1530-9290.2008.00057.x>
33. Zhang Q, Huang J-Q, Zhao M-Q, Qian W-Z, Wei F (2011) Carbon Nanotube Mass Production: Principles and Processes. *ChemSusChem*, 4(7):864–889. <https://doi.org/10.1002/cssc.201100177>
34. Fan Y-Y, Kaufmann A, Mukasyan A, Varma A (2006) Single- and multi-wall carbon nanotubes produced using the floating catalyst method: Synthesis, purification and hydrogen uptake. *Carbon*, 44(11):2160–2170. <https://doi.org/10.1016/j.carbon.2006.03.009>
35. Bieber T, Elsässer H-P (2001) Preparation of a Low Molecular Weight Polyethylenimine for Efficient Cell Transfection. *BioTechniques*, 30(1):74–81. <https://doi.org/10.2144/01301st03>
36. Chaikittisilp W, Didas SA, Kim H-J, Jones CW (2013) Vapor-Phase Transport as A Novel Route to Hyperbranched Polyamine-Oxide Hybrid Materials. *Chemistry of Materials*, 25(4):613–622. <https://doi.org/10.1021/cm303931q>
37. Tauhardt L, Kempe K, Knop K, Altuntaş E, Jäger M, Schubert S, Fischer D, Schubert US (2011) Linear Polyethyleneimine: Optimized Synthesis and Characterization - On the Way to

“Pharmagrade” Batches. *Macromolecular Chemistry and Physics*, :n/a-n/a.
<https://doi.org/10.1002/macp.201100190>

38. Wu F, Zhou Z, Hicks AL (2019) Life Cycle Impact of Titanium Dioxide Nanoparticle Synthesis through Physical, Chemical, and Biological Routes. *Environmental Science & Technology*, 53(8):4078–4087. <https://doi.org/10.1021/acs.est.8b06800>

39. Wernet G, Bauer C, Steubing B, Reinhard J, Moreno-Ruiz E, Weidema B (2016) The ecoinvent database version 3 (part I): overview and methodology. *The International Journal of Life Cycle Assessment*, 21(9):1218–1230. <https://doi.org/10.1007/s11367-016-1087-8>

40. US EPA (2014) Tool for Reduction and Assessment of Chemicals and Other Environmental Impacts (TRACI). https://www.epa.gov/sites/production/files/2015-12/traci_2_1_2014_dec_10_0.xlsx

41. Stoykova E (2010) Low resource consumption buildings and constructions by use of lca in design and decision making the project LoRe-LCA. 2:985–992.

42. Gibbs HK, Johnston M, Foley JA, Holloway T, Monfreda C, Ramankutty N, Zaks D (2008) Carbon payback times for crop-based biofuel expansion in the tropics: the effects of changing yield and technology. *Environmental Research Letters*, 3(3):034001.
<https://doi.org/10.1088/1748-9326/3/3/034001>

43. Jonker JGG, Junginger M, Faaij A (2014) Carbon payback period and carbon offset parity point of wood pellet production in the South-eastern United States. *GCB Bioenergy*, 6(4):371–389. <https://doi.org/10.1111/gcbb.12056>

44. Rankine RK, Chick JP, Harrison GP (2006) Energy and carbon audit of a rooftop wind turbine. *Proceedings of the Institution of Mechanical Engineers, Part A: Journal of Power and Energy*, 220(7):643–654. <https://doi.org/10.1243/09576509JPE306>

45. Zhou Z, Balijepalli SK, Nguyen-Sorenson AHT, Anderson CM, Park JL, Stowers KJ (2018) Steam-Stable Covalently Bonded Polyethylenimine Modified Multiwall Carbon Nanotubes for Carbon Dioxide Capture. *Energy & Fuels*, 32(11):11701–11709.
<https://doi.org/10.1021/acs.energyfuels.8b02864>

46. Zoannou K-S, Sapsford DJ, Griffiths AJ (2013) Thermal degradation of monoethanolamine and its effect on CO₂ capture capacity. *International Journal of Greenhouse Gas Control*, 17:423–430. <https://doi.org/10.1016/j.ijggc.2013.05.026>

47. Markewitz P, Kuckshinrichs W, Leitner W, Linssen J, Zapp P, Bongartz R, Schreiber A, Müller TE (2012) Worldwide innovations in the development of carbon capture technologies and the utilization of CO₂. *Energy & Environmental Science*, 5(6):7281.
<https://doi.org/10.1039/c2ee03403d>

48. Griffiths OG, O’Byrne JP, Torrente-Murciano L, Jones MD, Mattia D, McManus MC (2013) Identifying the largest environmental life cycle impacts during carbon nanotube synthesis via

chemical vapour deposition. *Journal of Cleaner Production*, 42:180–189.
<https://doi.org/10.1016/j.jclepro.2012.10.040>

49. Gao T, Jelle BP, Sandberg LIC, Gustavsen A (2013) Monodisperse Hollow Silica Nanospheres for Nano Insulation Materials: Synthesis, Characterization, and Life Cycle Assessment. *ACS Applied Materials & Interfaces*, 5(3):761–767.
<https://doi.org/10.1021/am302303b>

50. Piccinno F, Hischier R, Seeger S, Som C (2018) Predicting the environmental impact of a future nanocellulose production at industrial scale: Application of the life cycle assessment scale-up framework. *Journal of Cleaner Production*, 174:283–295.
<https://doi.org/10.1016/j.jclepro.2017.10.226>

51. Davis J, Rochelle G (2009) Thermal degradation of monoethanolamine at stripper conditions. *Energy Procedia*, 1(1):327–333. <https://doi.org/10.1016/j.egypro.2009.01.045>

52. Su F, Lu C, Chung A-J, Liao C-H (2014) CO₂ capture with amine-loaded carbon nanotubes via a dual-column temperature/vacuum swing adsorption. *Applied Energy*, 113:706–712.
<https://doi.org/10.1016/j.apenergy.2013.08.001>

53. Zhang Z, Ma X, Wang D, Song C, Wang Y (2012) Development of silica-gel-supported polyethylenimine sorbents for CO₂ capture from flue gas. *AIChE Journal*, 58(8):2495–2502.
<https://doi.org/10.1002/aic.12771>

54. Castelo Branco DA, Moura MCP, Szklo A, Schaeffer R (2013) Emissions reduction potential from CO₂ capture: A life-cycle assessment of a Brazilian coal-fired power plant. *Energy Policy*, 61:1221–1235. <https://doi.org/10.1016/j.enpol.2013.06.043>

55. Young B, Krynock M, Carlson D, Hawkins TR, Marriott J, Morelli B, Jamieson M, Cooney G, Skone TJ (2019) Comparative environmental life cycle assessment of carbon capture for petroleum refining, ammonia production, and thermoelectric power generation in the United States. *International Journal of Greenhouse Gas Control*, 91:102821.
<https://doi.org/10.1016/j.ijggc.2019.102821>

56. Chisalita D-A, Petrescu L, Cobden P, Dijk HAJ (Eric) van, Cormos A-M, Cormos C-C (2019) Assessing the environmental impact of an integrated steel mill with post-combustion CO₂ capture and storage using the LCA methodology. *Journal of Cleaner Production*, 211:1015–1025. <https://doi.org/10.1016/j.jclepro.2018.11.256>

57. Giordano L, Roizard D, Favre E (2018) Life cycle assessment of post-combustion CO₂ capture: A comparison between membrane separation and chemical absorption processes. *International Journal of Greenhouse Gas Control*, 68:146–163.
<https://doi.org/10.1016/j.ijggc.2017.11.008>

58. Grant T, Anderson C, Hooper B (2014) Comparative life cycle assessment of potassium carbonate and monoethanolamine solvents for CO₂ capture from post combustion flue gases. *International Journal of Greenhouse Gas Control*, 28:35–44.
<https://doi.org/10.1016/j.ijggc.2014.06.020>

59. Sathre R, Chester M, Cain J, Masanet E (2012) A framework for environmental assessment of CO₂ capture and storage systems. *Energy*, 37(1):540–548. <https://doi.org/10.1016/j.energy.2011.10.050>
60. Begag R, Krutka H, Dong W, Mihalcik D, Rhine W, Gould G, Baldic J, Nahass P (2013) Superhydrophobic amine functionalized aerogels as sorbents for CO₂ capture. *Greenhouse Gases: Science and Technology*, 3(1):30–39. <https://doi.org/10.1002/ghg.1321>
61. Dutcher B, Fan M, Russell AG (2015) Amine-Based CO₂ Capture Technology Development from the Beginning of 2013—A Review. *ACS Applied Materials & Interfaces*, 7(4):2137–2148. <https://doi.org/10.1021/am507465f>
62. Schwartz H, Gustafsson M, Spohr J (2020) Emission abatement in shipping – is it possible to reduce carbon dioxide emissions profitably? *Journal of Cleaner Production*, 254:120069. <https://doi.org/10.1016/j.jclepro.2020.120069>
63. Sun Y, Li Y, Cai B, Li Q (2020) Comparing the explicit and implicit attitudes of energy stakeholders and the public towards carbon capture and storage. *Journal of Cleaner Production*, 254:120051. <https://doi.org/10.1016/j.jclepro.2020.120051>
64. Lee S-Y, Park S-J (2015) A review on solid adsorbents for carbon dioxide capture. *Journal of Industrial and Engineering Chemistry*, 23:1–11. <https://doi.org/10.1016/j.jiec.2014.09.001>
65. Wang J, Chen H, Zhou H, Liu X, Qiao W, Long D, Ling L (2013) Carbon dioxide capture using polyethylenimine-loaded mesoporous carbons. *Journal of Environmental Sciences*, 25(1):124–132. [https://doi.org/10.1016/S1001-0742\(12\)60011-4](https://doi.org/10.1016/S1001-0742(12)60011-4)
66. Liu Q, Shi J, Wang Q, Tao M, He Y, Shi Y (2014) Carbon Dioxide Capture with Polyethylenimine-Functionalized Industrial-Grade Multiwalled Carbon Nanotubes. *Industrial & Engineering Chemistry Research*, 53(44):17468–17475. <https://doi.org/10.1021/ie503118j>
67. Ye Q, Jiang J, Wang C, Liu Y, Pan H, Shi Y (2012) Adsorption of Low-Concentration Carbon Dioxide on Amine-Modified Carbon Nanotubes at Ambient Temperature. *Energy & Fuels*, 26(4):2497–2504. <https://doi.org/10.1021/ef201699w>
68. Irani M, Jacobson AT, Gasem KAM, Fan M (2017) Modified carbon nanotubes/tetraethylenepentamine for CO₂ capture. *Fuel*, 206:10–18. <https://doi.org/10.1016/j.fuel.2017.05.087>
69. Zhou Z, Anderson CM, Butler SK, Thompson SK, Whitty KJ, Shen T-C, Stowers KJ (2017) Stability and efficiency of CO₂ capture using linear amine polymer modified carbon nanotubes. *Journal of Materials Chemistry A*, 5(21):10486–10494. <https://doi.org/10.1039/C7TA02576A>
70. Maliszewskyj RJ, Turcotte MG, Mitchell JW (2004) Dimethylformamide synthesis via reactive distillation of methyl formate and dimethylamine. <https://patents.google.com/patent/US6723877B1/en>

71. Wystrach VP, Kaiser DW, Schaefer FC (1955) Preparation of Ethylenimine and Triethylenemelamine. *Journal of the American Chemical Society*, 77(22):5915–5918. <https://doi.org/10.1021/ja01627a040>
72. Chaikittisilp W, Didas SA, Kim H-J, Jones CW (2013) Vapor-Phase Transport as A Novel Route to Hyperbranched Polyamine-Oxide Hybrid Materials. *Chemistry of Materials*, 25(4):613–622. <https://doi.org/10.1021/cm303931q>
73. Tauhardt L, Kempe K, Knop K, Altuntaş E, Jäger M, Schubert S, Fischer D, Schubert US (2011) Linear Polyethyleneimine: Optimized Synthesis and Characterization – On the Way to “Pharmagrade” Batches. *Macromolecular Chemistry and Physics*, 212(17):1918–1924. <https://doi.org/10.1002/macp.201100190>
74. Ishigami M, Cumings J, Zettl A, Chen S (2000) A simple method for the continuous production of carbon nanotubes. *Chemical Physics Letters*, 319(5):457–459. [https://doi.org/10.1016/S0009-2614\(00\)00151-2](https://doi.org/10.1016/S0009-2614(00)00151-2)
75. Fan Y-Y, Kaufmann A, Mukasyan A, Varma A (2006) Single- and multi-wall carbon nanotubes produced using the floating catalyst method: Synthesis, purification and hydrogen uptake. *Carbon*, 44(11):2160–2170. <https://doi.org/10.1016/j.carbon.2006.03.009>
76. Liu B-C, Tang S-H, Liang Q, Gao L-Z, Zhang B-L, Qu M-Z, Yu Z-L (2001) Production of Carbon Nanotubes over Pre-reduced LaCoO₃ by Using Fluidized-bed Catalytic Reactor. *Chinese Journal of Chemistry*, 19(10):983–986. <https://doi.org/10.1002/cjoc.20010191013>
77. Mauron Ph, Emmenegger Ch, Sudan P, Wenger P, Rentsch S, Züttel A (2003) Fluidised-bed CVD synthesis of carbon nanotubes on Fe₂O₃/MgO. *Diamond and Related Materials*, 12(3):780–785. [https://doi.org/10.1016/S0925-9635\(02\)00337-0](https://doi.org/10.1016/S0925-9635(02)00337-0)
78. Steinfeldt M Development of sustainable solutions for nanotechnology-based products based on hazard characterization and LCA | NANOSUSTAIN Project | FP7 | CORDIS | European Commission. <https://cordis.europa.eu/project/rcn/94362/factsheet/de>
79. Griffiths OG, O’Byrne JP, Torrente-Murciano L, Jones MD, Mattia D, McManus MC (2013) Identifying the largest environmental life cycle impacts during carbon nanotube synthesis via chemical vapour deposition. *Journal of Cleaner Production*, 42:180–189. <https://doi.org/10.1016/j.jclepro.2012.10.040>

Appendix H

*Published paper, electronic supplemental information associated with the paper and references.

Life Cycle Assessment of Struvite Precipitation from Anaerobically Digested Dairy Manure: A Wisconsin Perspective

The following chapter is a reproduction of an article published in the Integrated Environmental Assessment and Management, with the citation:

Temizel-Sekeryan, S.; Wu, F.; Hicks, A.L. (2020) Life Cycle Assessment of Struvite Precipitation from Anaerobically Digested Dairy Manure: A Wisconsin Perspective, *Integrated Environmental Assessment and Management*.

The article appears as published, although style and formatting modifications have been made.

Authorship contribution statement

Sila Temizel-Sekeryan: Designed Research, Performed Research, Analyzed Data, Wrote the Paper.

Fan Wu: Designed Research, Contributed Reagents or Analytical Tools.

Andrea L. Hicks: Designed Research, Wrote the Paper.

Abstract

Recovering valuable nutrients (e.g., P and N) from waste materials has been extensively investigated at the laboratory scale. Although it has been shown that struvite precipitation from several manure sources contributes to nutrient management practices by recovering valuable nutrients and preventing them from reaching water bodies, it has not been widely applied in commercial (i.e., farm) scales. The purpose of this study is to evaluate the potential environmental impacts of the struvite recovery process from the liquid portion of the anaerobically digested dairy cow manure generated in Wisconsin, USA, dairy farms using life cycle assessment methodology for both bench- and farm-scale scenarios. The struvite precipitation process involves the use of additional chemicals and energy; therefore, investigating upstream impacts is crucial to evaluate the environmental costs and benefits of this additional treatment process. Results indicate that up to a 78% impact decrease in eutrophication potential can be achieved when P and N are recovered in the form of struvite and are applied in lieu of conventional fertilizers, rather than using the liquid portion of the anaerobically digested dairy manure as a fertilizer. Additionally, significant differences are identified in the majority of environmental impact categories when the struvite precipitation process is modeled and evaluated in a farm-scale setting. Future work should expand to evaluate the overall environmental impacts and trade-offs of struvite recovery application, including the anaerobic digestion system itself at the farm scale.

Introduction

Phosphorus (P) and nitrogen (N) are key nutrients for both plants and animals, and play a central role in agricultural applications. Worldwide phosphate fertilizer demand is expected to reach a total of 46 million tons, and N fertilizer need is forecasted to exceed 118 million tons by 2020 [1]. Phosphorus used in fertilizers is typically produced by mining of phosphate rock (in the form of P_2O_5), and the consumption of phosphate rock is estimated to increase to 50.5 million tons in 2022 [2]. There is a growing concern regarding the sustainability of global phosphate rock deposits; being a finite resource, they are expected to be exhausted in 100 to 250 y [3–5]. Meanwhile, given that 78% of the atmosphere is comprised of N, the Haber–Bosch process is typically used to fixate N in the form of ammonia [4]. However, the Haber–Bosch process relies heavily on natural gas, which also raises concerns as to its environmental consequences [6]. For reference, 1% of the global energy is consumed for fixing atmospheric N using the Haber–Bosch process [7]. These 2 nutrients are grouped under the process named “biogeochemical flows,” which is one of the 9 processes that are listed as planetary boundaries [8–10]. In addition to concern about the increased demand for P and N, their excessive release to water bodies is the reason for their inclusion in the planetary boundaries [11, 12]. Research suggests that recovering valuable nutrients (such as P and N) from waste materials contributes to decreasing the burdens that contribute to planetary boundaries and is part of a circular economy approach [13–16].

Twenty-three percent of the dairy farms in the United States are located in Wisconsin, accounting for 1.3 million dairy cows [17]. Given that each dairy cow generates 20 tons of manure annually [18], more than 25 million tons of manure is expected to be generated per year from Wisconsin. Spreading animal manure as fertilizer is the most applied manure management strategy for small-scale farms [19]. For larger farms (i.e., farms that have more than 200 head of

cattle), anaerobic digestion is a common manure management method [20]. As of March 2020, there are 41 dairy farms with anaerobic digesters in Wisconsin [21]. These farms are feeding a total of 109,685 dairy cows, which corresponds to 8.7% of cows in Wisconsin [21]. There are several benefits to anaerobic digestion, including biogas recovery and energy generation (e.g., electricity, fuel, compressed natural gas), methane emissions reduction, pathogen elimination, and odor reduction [22]. While the solid fraction of anaerobically digested dairy manure can be used as a flowerpot or livestock bedding material, the liquid fraction (AD-L-dairy manure) can be applied as a fertilizer or further processed and sold. However, the nutrients (P and N) that make manure and/or digestate a valuable fertilizer also cause eutrophication of ground and surface water due to agricultural runoff [23]. For instance, if the fertilizer (i.e., manure/digestate) need is calculated to meet the N demand of the soil, P (that is already present in the manure/digestate together with N) may be over applied and reach to water bodies due to runoff [24].

One method to recover P and N from manure is through struvite precipitation. Struvite (i.e., magnesium ammonium phosphate or $\text{MgNH}_4\text{PO}_4 \cdot 6\text{H}_2\text{O}$) is a slow-release fertilizer that has a high nutrient density and can be used directly without any postprocessing [25]. Being an odorless, nonsludgy, light and insoluble crystal, struvite is a good alternative for conventional fertilizers [26]. There have been numerous studies on struvite precipitation from different types of manure sources as well as various pretreatment approaches, as detailed in Supplemental Data Table HS1. The characteristics (i.e., physicochemical composition) of the same type (animal source) of manure may vary depending on both internal and external factors such as seasons, animal diet, feeding operations, manure collection and handling practices, location, and climate conditions, which are constraints for developing a standardized experimental setting for struvite

precipitation [27]. Therefore, studies that are presented in Supplemental Data Table HS1 used individualized procedures based on the treated manure characteristics. An additional table is included in the Supplemental Data to summarize the literature on struvite precipitation from anaerobically digested dairy manure (Supplemental Data Table HS2), which is the primary input of the present study.

Research on recovering economically and environmentally valuable nutrients from waste materials is gaining momentum; however, the environmental implications of these processes have not historically been well studied. One way to analyze the environmental impacts of a struvite recovery system is through life cycle assessment (LCA). Life cycle assessment is a tool to evaluate the potential environmental impacts of any product or process by quantifying the inputs and outputs throughout their life cycles, from raw materials acquisition to end of life, including manufacturing, use, and disposal phases [28]. Previous LCAs mostly examined the struvite precipitation (i.e., nutrient recovery) from wastewater treatment plants (WWTPs). Sena and Hicks compiled a review of the previous LCA literature on struvite recovery from WWTPs and separated urine streams along with details on data collection, methodology, and functional units considered [4]. They suggested that inclusion of a conventional fertilizer offset should be a component of all LCA studies, and the amount of struvite that is equivalent to P and N fertilizers should be stated explicitly. This suggestion is applicable for all struvite precipitation and nutrient recovery research in the sense that the struvite replaces the conventional fertilizer. Furthermore, LCA literature on struvite recovery from all types of manure is very limited. A summary is presented in Supplemental Data Table HS3 along with the details of the LCA components considered.

Environmental impact assessments based on bench-scale inventories help identify hotspots of the system. However, given that bench-scale studies are not optimized in terms of resource efficiency because processes are not in a continuous flow setting [29], scaling bench-scale results to project farm-scale impacts would not be accurate. As Li et al. identified this gap in their review, most studies on struvite crystallization were performed in laboratory scale and few of them conducted analyses on an industrial scale [5]. For instance, Bowers and Westerman applied a field-scale (10.6 m³/d) continuous crystallizer [30], and Suzuki et al. used a pilot-scale reactor (0.58 m³/d) to recover struvite from swine waste [31]. However, they have not incorporated the environmental implications of crystallizing struvite, which prevents evaluating the process feasibility at different scales.

The objective of the present study is to evaluate the environmental impacts of struvite precipitation from the AD-L-dairy manure generated in Wisconsin farms using LCA methodology. Additionally, environmental impacts as a result of farm-scale struvite precipitation process are also predicted by using simplified literature-based data in order to address the potential savings in the materials and energy consumption per unit mass of product. Results will provide an understanding of the performance of the particular nutrient recovery technology in the context of dairy waste management.

Materials And Methods

System description

Struvite formation can be achieved when the 3 ions magnesium (Mg²⁺), ammonium (NH₄⁺), and phosphate (PO₄³⁻) are in the solution with a 1:1:1 molar ratio to reach supersaturation [32]. There are several considerations that need to be taken into account while

designing the struvite precipitation process. A detailed overview is included in the Supplemental Data, where various literature on struvite precipitation from dairy manure are summarized. The struvite precipitation procedure in the present work is based on the reviewed literature.

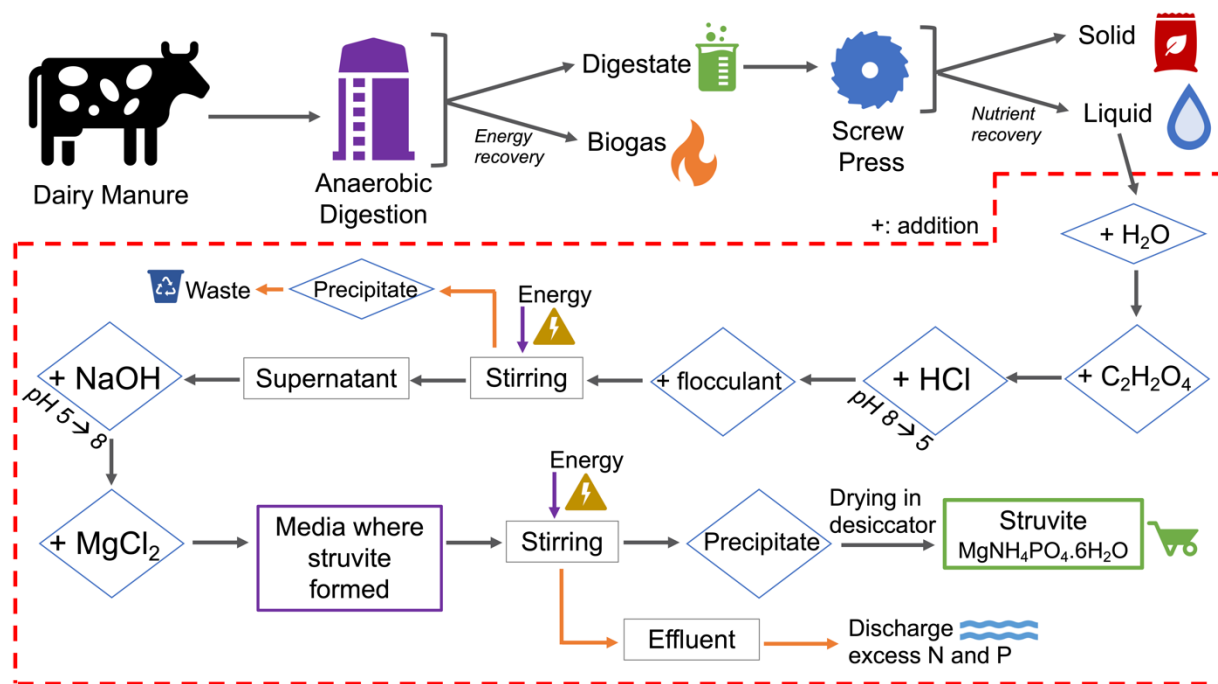


Figure H1. System description for struvite precipitation from AD-L-dairy manure (bench scale), where dashed outline indicates system boundaries for life cycle assessment. AD-L = liquid fraction of anaerobically digested dairy cow manure; $C_2H_2O_4$ = oxalic acid; H_2O = water; HCl = hydrochloric acid; $MgCl_2$ = magnesium chloride; N = nitrogen; $NaOH$ = sodium hydroxide; P = phosphorus

Figure H1 shows the framework of the present study. It includes the details of struvite crystallization procedure from anaerobically digested dairy cow manure in a laboratory setting. Firstly, the AD-L-dairy manure is diluted using deionized water. Following this step, oxalic acid

is added into the solution to remove the Ca impurities [33], because they may interfere with P compounds that prevent Mg from forming struvite [34]. This reaction should take place in an acidic environment; therefore, by using hydrochloric acid (HCl, 1M), pH is decreased to 5 [32]. In order to further remove the suspended solids formed in the solution, an anionic flocculant, polyacrylamide, is used (Krishnapuram Karthikeyan, University of Wisconsin-Madison Biological Systems Engineering, USA, personal communication), and the solution is stirred using a jar tester [35]. After the precipitates are removed, pH of the solution is increased to 8 using sodium hydroxide (NaOH, 1M) because higher pH is favorable for struvite formation [36]. Next, magnesium chloride ($MgCl_2$) is added to the system until the majority of P precipitates as struvite[3]. Following the stirring and decanting the solids, the precipitate (i.e., struvite) is dried in a desiccator, and the effluent is discharged to surface waters.

Life cycle assessment

Goal and scope definition

The goal of the present study is to evaluate the environmental impacts of a struvite precipitation process from anaerobically digested dairy cow manure generated by Wisconsin farms. As mentioned in the Introduction section, struvite can be applied instead of conventional fertilizers, which helps avoid production of N and P fertilizers. Therefore, these offsets are also included in the assessment in order to highlight the potential benefits to the environment. The dashed outline in Figure H1 indicates the system boundaries considered in the present study. Anaerobic digestion and screw press (i.e., solid–liquid separation) processes are excluded from the system boundaries because the primary objective of these processes is not struvite precipitation. Wisconsin has the highest number of farm-based anaerobic digestion systems

compared to other states in the United States, regardless of having the additional process of struvite recovery [21]. Currently a large number of farms have already implemented anaerobic digestion and solid–liquid separation systems as a manure management strategy and take advantage of their benefits. These benefits include on-site energy generation (e.g., electricity cogeneration or compressed natural gas), emission and odor control, as well as producing fertilizers and/or soil amendments from digestate. The present work represents a new scope of further processing the digestate; for this reason, producing digestate is excluded from the system boundaries.

Functional unit is a quantified performance that helps evaluate the environmental impacts of a product or system based on a reference [28]. There are different functional units used in the published body of literature for projecting the impacts of struvite recovery from different sources of manure. These include mass of manure produced per day [37], mass of treated manure [38], and volume of treated manure per day [39, 40]. In the present study, 2 different functional units are selected in order to account for properties of the produced struvite for fertilization purposes and the necessity of manure management. Both are mass-based units that represent different functions: 1 kg of AD-L-dairy manure treated, and 1 kg of struvite produced from the anaerobically digested dairy cow manure input.

Inventory analysis

Before quantifying inputs and outputs of the system, characteristics of the AD-L-dairy manure are listed in order to calculate the quantity of chemicals required to precipitate struvite. Data from Wang et al. [41], Aguirre-Villegas et al. [42, 43], and Sampat et al. [44] are used to calculate total nitrogen (TN), total phosphorus (TP), calcium (Ca^{2+}), and magnesium (Mg^{2+})

parameters for the AD-L-dairy manure input, as these studies are based on Wisconsin farms. Other microminerals are listed as a miscellaneous category. Supplemental Data Table HS4 shows the basis for calculation of struvite recovery from raw dairy manure and wash water. Using this information, AD-L-dairy manure (with wash water) characteristics are developed and summarized in Table H1.

Table H1. Liquid fraction of anaerobically digested (AD-L-) dairy cow manure characteristics (for 1 kg) considered in the current study.

Parameter	Value	Values are derived by making assumptions from:
Density ^a (for anaerobically digested dairy manure)	1023 kg/m ³	[41]
Dry matter ^b (for raw dairy manure)	78.5 g	[43]
Water	0.965 kg	[41–43]
Calcium (Ca ²⁺) ^c	1.74 g	[42]
Magnesium (Mg ²⁺) ^d	0.846 g	[42]
Total nitrogen (TN)	1.59 g	[41–44]
Total phosphorus (TP)	0.680 g	[41–44]
Miscellaneous	30.24 g	[41–44]

^a Density of anaerobically digested dairy cow manure ranges from 990-1056 kg/m³; ^b Total solids content of raw manure = 7%; ^c Calcium = 2.19% of dry mass; ^d Magnesium = 1.06% of dry mass.

As mentioned in the System description section, the struvite precipitation procedure in the present work is designed using information from the literature. Therefore, using values listed in Table H1, the required quantities of oxalic acid (C₂H₂O₄) and magnesium chloride (MgCl₂) were calculated. Inventory of a bench-scale experiment for struvite precipitation is presented in Table H2, where the efficiency of P recovery as struvite is calculated as 66%. Given that struvite can be used as a replacement for conventional fertilizers, the avoided impacts resulting from the

production of N and P fertilizers are also presented in Table H2. Specific inventory choices (Supplemental Data Table HS5) and further calculations are included in the Supplemental Data.

Table H2. Life cycle inventory for bench-scale struvite precipitation per 1 kg of AD-L-dairy cow manure treated.

Input Parameter	Value	Notes
HCl (1M)	1.61 g	to decrease pH from 8 to pH 5
NaOH (1M)	1.76 g	to increase pH from 5 to pH 8
Water	3.28 L	to dilute the liquid portion of the digestate
Oxalic acid	3.92 g	to bind calcium and precipitate it as calcium oxalate (desired calcium to oxalic acid ratio=1:1)
Polyacrylamide	2.19 mL	anionic flocculant suspension, polymer
Magnesium chloride (10%)	8.74 g	to ensure there is enough magnesium for struvite precipitation (desired magnesium to phosphate ratio=2:1)
Electricity	0.789 kWh	stirring jar tester
Output Parameter	Value	Notes
Struvite	4.77 g	66% phosphorus recovery as struvite
Calcium oxalate precipitate	5.66 g	waste management
Nitrogen, total	1.36 g	excess nutrient, discharged to surface water
Phosphate, total	0.114 g	excess nutrient, discharged to surface water
Water	3.50 kg	effluent
Avoided Impacts	Value	Notes
Nitrogen fertilizer	0.744 g	1 kg struvite \equiv 0.156 kg nitrogen fertilizer as N
Phosphate fertilizer	2.78 g	1 kg struvite \equiv 0.583 kg phosphate fertilizer as P ₂ O ₅

In the present study, efficiency of recovery indicates the ratio of P in the struvite to the TP in the raw dairy manure. Given that the efficiency of P recovery in the form of struvite ranges from 60% to 80% [27], different efficiencies were assumed and back calculations were performed considering 60%, 70%, 75%, and 78% recovery yields. On the basis of the manure characteristics presented in Table H1, 78% is the maximum efficiency that could be achieved,

that is, where the majority of P present in the AD-L-dairy manure was precipitated in the form of struvite. It is assumed that the excess nutrients in the effluent were discharged to surface waters [37, 38].

Inventory analysis for farm-scale struvite precipitation

Potential environmental impacts per functional unit for a farm-scale struvite precipitation are expected to be lower due to the interconnections of industrial production line [45]. According to De Vrieze et al., the electricity consumption per ton of manure for struvite crystallization is 0.5 kWh for a farm that has a treatment capacity of 160 to 200 m³/d [46]. Assuming 0.5 kWh/ton electricity requirement and the same stoichiometry for struvite precipitation (Table H2), farm-scale struvite precipitation from AD-L-dairy manure was modeled. In a farm setting, there will be an anaerobic digestion step prior to struvite precipitation. Given that energy can be produced by anaerobic digestion, for farm-scale LCA inventory, biogas is assumed as an energy source. Furthermore, in order to dilute the AD-L-dairy manure in a farm, using deionized water in farm settings would not be realistic. In order to imitate farm-scale process, 2 different water sources, well and gray water, are considered as water inputs. Similar to the bench-scale process, impact assessments for 60%, 70%, 75%, and 78% recovery yields were also conducted. The authors recognize that projecting farm scale impacts using these data is a simplified approach. However, given that there is a lack of primary data collected from dairy farms, this approach can help to project preliminary environmental impacts of farm-scale struvite precipitation process.

Impact assessment

Environmental impacts of the current system are modeled using the SimaPro 8.5.2 software [47] with Ecoinvent 3 [48] and United States Life Cycle Inventory (USLCI) [49] databases. Tool for the Reduction and Assessment of Chemical and Other Environmental Impacts (TRACI 2.1) [50] and Building for Environmental and Economic Sustainability (BEES) [51] impact assessment methodologies are used to quantify the impacts of the considered system. The midpoint environmental impact categories, along with their units and abbreviations based on TRACI 2.1 are ozone depletion (ODP in kg CFC11-eq), global warming (GWP in kg CO₂-eq), smog (SP in kg O₃-eq), acidification (AP in kg SO₂-eq), eutrophication (EP in kg N-eq.), carcinogenics (CP in comparative toxic unit for human [CTUh]), noncarcinogenics (NCP in CTUh), respiratory effects (RP in kg PM_{2.5}-eq), ecotoxicity (ETP in comparative toxic unit for ecotoxicity), and fossil fuel depletion (FFP in megajoules [MJ] surplus energy) potentials. Additionally, in order to assess the direct and indirect water consumption of the system, BEES provides water intake impact category in liters (WP in L). The TRACI 2.1 impact assessment was selected because it considers the best applicable methodologies within each category for the United States [50], and BEES methodology is included because it provides the overall water footprint for the considered processes.

Sensitivity and uncertainty analyses

A sensitivity analysis was performed in order to highlight the parameters to which the LCA results of the struvite precipitation system are sensitive. The value for each of the input parameters was modified by 20%. Following this step, the potential environmental impacts of the system were recalculated to determine how the change in the inputs affected the overall LCA

results. Sensitivity factor (SFs; i.e., the relative change of the output over relative change of the input) for each parameter was calculated, and the parameters with an SF of $\leq 2\%$ were considered as not sensitive to the system [52]. Additionally, uncertainty analysis was conducted using Monte Carlo simulations in SimaPro 8.5.2 in order to estimate the highest and the lowest bounds of environmental impacts for each scenario. For the present evaluation, 95% confidence interval was selected, and analysis was run 1000 times. Results are provided in the Supplemental Data Table HS6 for the bench-scale scenario, Table HS7 for the farm-scale scenario using well water, and Table HS8 for the farm-scale scenario using gray water.

Results and Discussion

Life cycle impact assessment for bench-scale process

Evaluation of the struvite precipitation from AD-L-dairy manure (i.e., digestate from anaerobically digested cow manure) was performed, and characterization results are presented in Figure H2 by involving the impact categories from TRACI 2.1 and BEES. Impact assessment results of each input and output parameter are tabulated in Supplemental Data Tables HS9 and HS10.

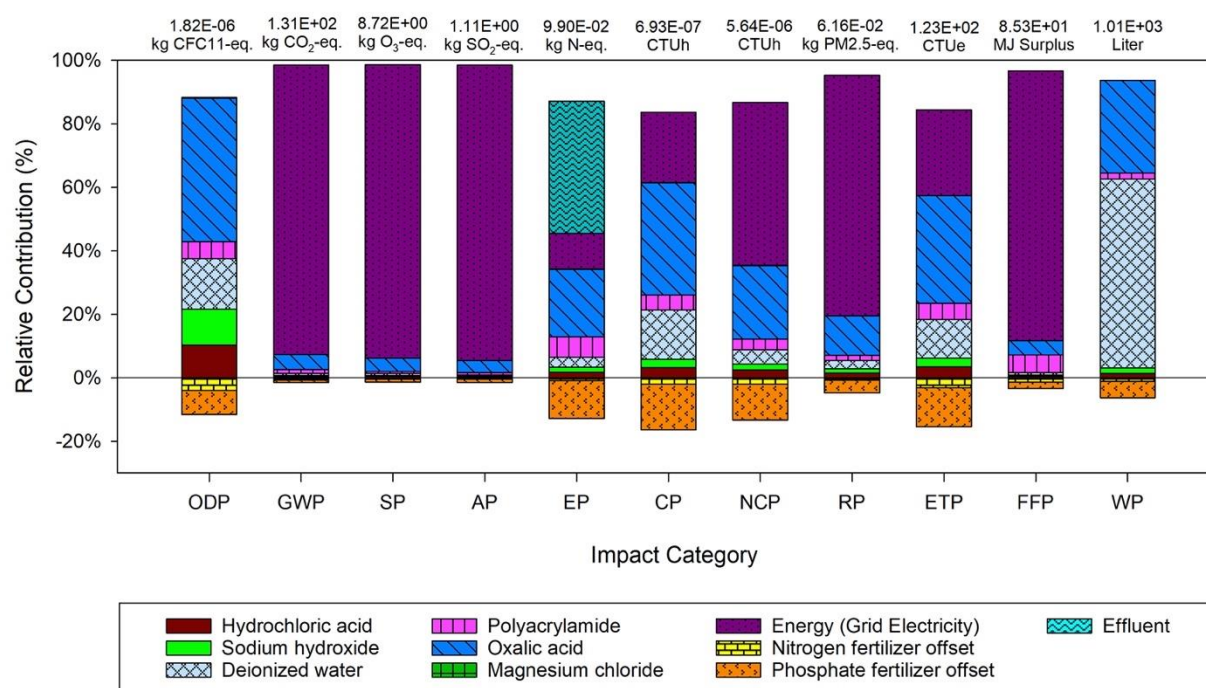


Figure H2. Total life cycle environmental impacts and relative contributions of all input and output parameters for a bench-scale study, where the functional unit is 1 kg struvite precipitation. AP = acidification; CFC = chlorofluorocarbon; CP = carcinogenic; CTU = comparative toxic unit; EP = eutrophication, ETP = ecotoxicity; FFP = fossil fuel depletion; GWP= global warming; MJ = megajoule; NCP = noncarcinogenic; ODP = ozone depletion; PM= particulate matter; RP = respiratory effects; SP = smog; WP = water intake.

The analysis shows that the MgCl₂ input has a negligible impact in all categories. In the majority of the environmental impact categories considered (GWP, SP, AP, NCP, RP, and FFP), electricity is found to be the main contributor, accounting for more than 51% impact share. Grid electricity (US average grid) input is used for stirring purposes throughout the bench-scale struvite precipitation process. Additionally, results indicated that oxalic acid is the major contributor among other chemicals. It contributes more than 45% of ODP, 35% of CP, 34% of

ETP, 29% of WP, 23% of NCP, and 21% of EP. These findings are compatible with those of Ishii and Boyer, who found that the upstream impacts of manufacturing chemicals as well as the grid electricity are the main reasons for high environmental cost of the system [53]. As expected, in the WP category, deionized water input is the most impactful contributor (>60%). Lastly, for EP, the effluent discharge (42%) is found as the most impactful parameter. As mentioned in the Methods section and depicted in Figure H1, the effluent is considered as being directly discharged to surface waters. Given that the effluent discharge contains the excess N and P that are not recovered as struvite, its contribution to EP is reasonable.

There are several promising aspects of struvite precipitation. These include converting waste materials (e.g., dairy manure in the present study) into valuable resources (i.e., slow-release fertilizer), avoiding production of conventional mineral fertilizers and nutrient management [54]. In the present study, N and phosphate fertilizer offsets due to the utilization of struvite are calculated and incorporated into the overall life cycle impact assessment results. Avoided N fertilizer manufacturing shows the most offset in the ODP impact category with a -4% share. Offset in ETP follows ODP with a -3% impact ratio. The rest of the categories show 0.3% to 2% decrease in environmental impacts. In terms of avoided phosphate fertilizer production, the largest offsets are observed in CP, EP, ETP, NCP, and ODP categories with ratios of -14%, -12%, -12%, -11%, and -8%, respectively. Offsets in WP (-5%) and RP (-4%) follow the trend. Similar to the case of N fertilizer, the rest of the categories show 1% to 2% decrease in environmental impacts resulting from the decreased manufacturing of conventional phosphate fertilizer. It should be highlighted that these results are representative for 1 kg of struvite precipitation on a bench-scale study. Results for struvite precipitation from 1 kg of AD-L-dairy manure treated are presented in Supplemental Data Figure HS1.

Life cycle impact assessment for farm-scale process

Considering farm-scale inventory for struvite precipitation, characterization results are presented in Figure H3 by involving the impact categories from TRACI 2.1 and BEES. Impact assessment results of each input and output parameter are tabulated in Supplemental Data Tables HS11 and HS12.

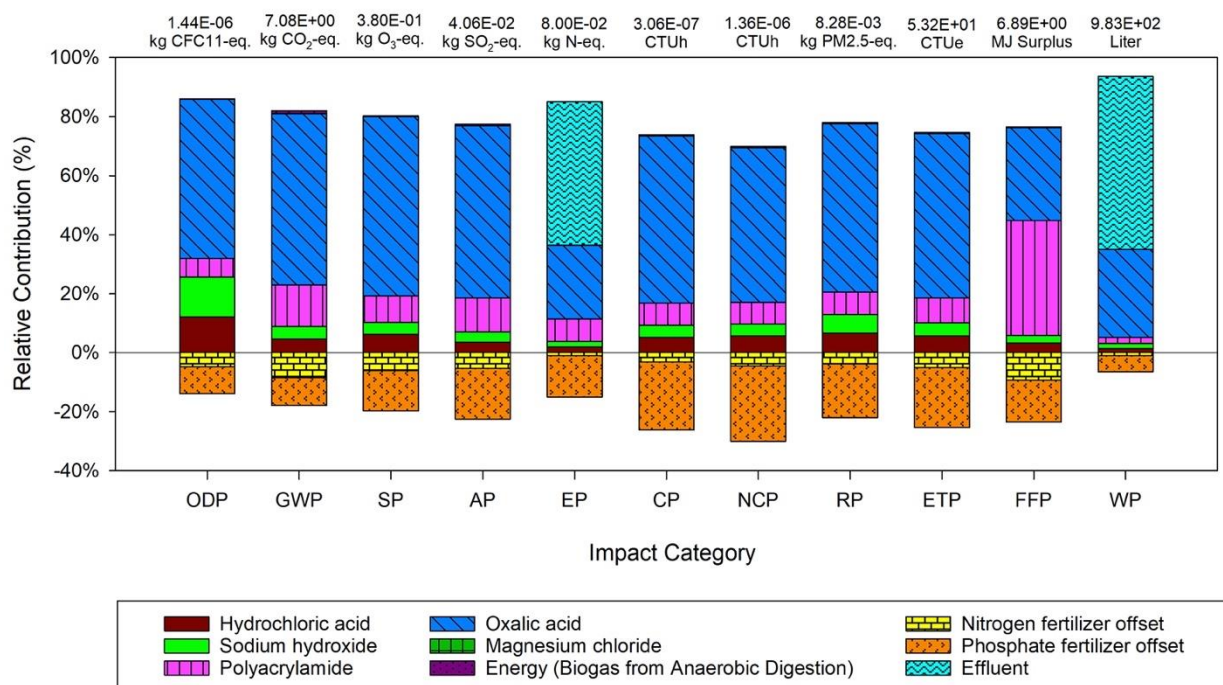


Figure H3. Total life cycle environmental impacts and relative contributions of all input and output parameters for a farm-scale study, where the functional unit is 1 kg struvite precipitation. AP = acidification; CFC = chlorofluorocarbon; CP = carcinogenic; CTU = comparative toxic unit; EP = eutrophication, ETP = ecotoxicity; FFP = fossil fuel depletion; GWP= global warming; MJ = megajoule; NCP = noncarcinogenic; ODP = ozone depletion; PM= particulate matter; RP = respiratory effects; SP = smog; WP = water intake.

The farm-scale LCA results show that MgCl_2 and energy (biogas) inputs have negligible impact contributions in all impact categories. In the majority of the environmental impact categories considered (ODP, GWP, SP, AP, CP, NCP, RP, and ETP), oxalic acid is found to be the main contributor, accounting for more than 52% impact share. Given that a significant amount of nitric acid is needed to produce oxalic acid itself [55], oxalic acid input has the greatest contribution in the majority of impact categories. Scaling the process for farm scale showed a negligible change in the total WP. However, the impact contribution resulting from the effluent discharge on WP increased significantly (>58%). The effluent is modeled by considering that the excess nutrients contaminate the water that was initially obtained from natural origins (e.g., well water). Lastly, for EP, the effluent discharge (49%) is found as the most impactful parameter due to containing excess N and P that cannot be recovered as struvite.

In terms of the negative impacts (i.e., environmental benefits) resulting from avoided N fertilizer manufacturing, the largest offset is identified in the FFP impact category with a -9% share. Offsets in GWP, SP, ODP, AP, and ETP follow FFP with -8%, -6%, -5%, -5%, and -5% impact ratios, respectively. The rest of the categories show less than 3% decrease in environmental impacts. Considering associated environmental benefits resulting from avoided phosphate fertilizer manufacturing, more than 17% offset is observed in the NCP, CP, ETP, RP, and AP impact categories. Fossil fuel depletion, EP, and SP follow the trend with equal amounts of offsets as 14%. The rest of the impact categories show less than 5% to 9% decrease in environmental impacts resulting from the avoided manufacturing of conventional phosphate fertilizer. Results for farm-scale struvite precipitation from 1 kg of AD-L-dairy manure are presented in Supplemental Data Figure HS2.

As expected, farm-scale environmental impact assessment results showed lower impacts in all of the 11 potential environmental impact categories. With the farm-scale struvite precipitation from AD-L-dairy manure, life cycle impacts per unit mass of AD-L-dairy manure treated (or unit mass of struvite precipitated) showed a significant decrease (>55%) in 8 of the 11 potential environmental impact categories (GWP, SP, AP, CP, NCP, RP, ETP, and FFP). The main reason for this decrease in the majority of environmental impacts is the utilization of biogas as an energy source instead of grid electricity. Research suggested that up to 49% decrease in greenhouse gas emissions (and therefore potential environmental impacts) can be achieved by substituting grid electricity with biogas [56], which is comparable to the results obtained in the present study. Due to the excess nutrient discharge to surface waters, EP did not show as much as reduction as other impact categories (19%). Lastly, 21% decrease in ODP and 3% decrease in WP were observed as a result of farm-scale struvite precipitation model.

Environmental impacts using different functional units

Depending of the purpose of the project, results can be presented using different functional units. For instance, if the primary objective is to treat dairy manure, the mass of treated manure can be used as a reference unit [38]. Moreover, if the main objective is to precipitate the struvite, the mass of struvite generation may be selected. Analyzing LCA results using multiple units enables incorporation of multifunctionality and increases the accuracy [52]. Figure H4 shows four of the potential environmental impacts of struvite precipitation process for 2 different functional units under bench and farm scales. Global warming potential is included in Figure H4, as it has been historically used to report single category results as climate change [57]. Ecotoxicity potential is presented because it showed a significant offset compared to other

potential environmental impact categories due to the avoided fertilizer production. Water intake potential is selected because struvite precipitation is a water-intensive process and evaluating this category is essential. Lastly, EP is included in Figure H4 because eutrophication is the primary consequence of excess nutrient runoff to water streams. Error bars represent the standard deviations of impacts resulting from the inclusion of different efficiencies, and the rest of the characterization graphs are presented in Supplemental Data Figures HS3 and HS4.

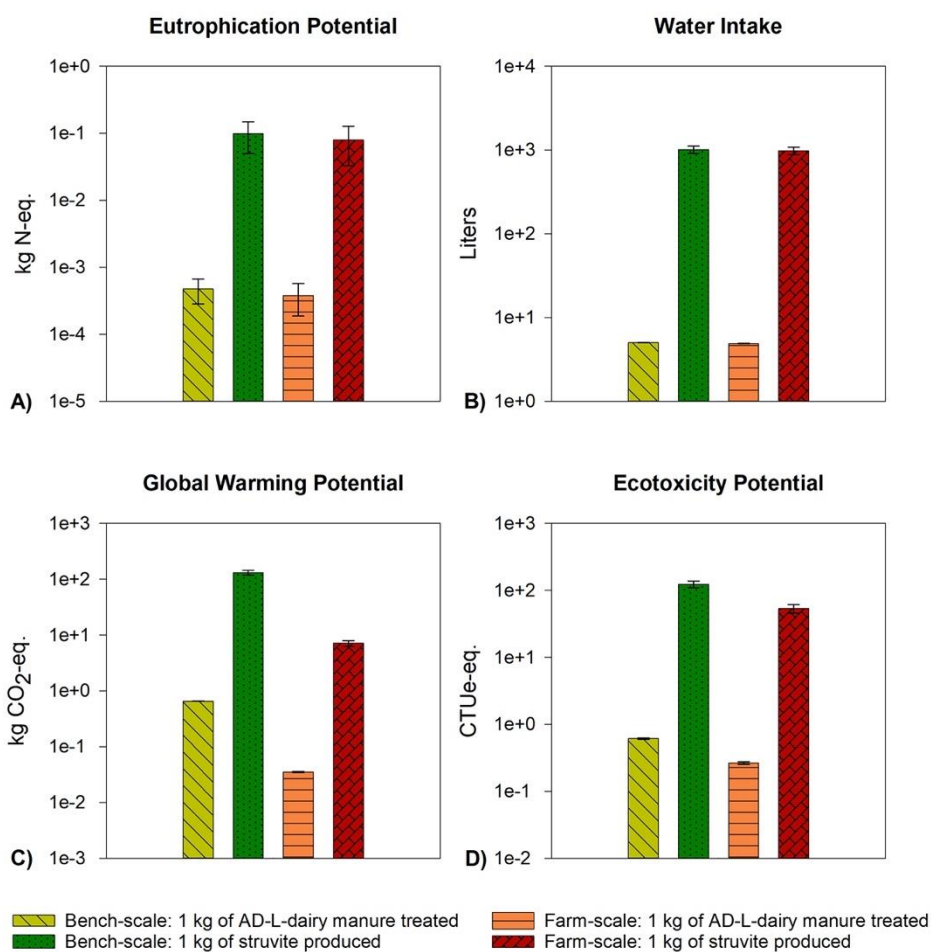


Figure H4. Potential environmental impacts based on different functional units represented in logarithmic scale: EP (A), WP (B), GWP (C), and ETP (D). (Error bars represent the standard deviations of impacts resulting from the inclusion of different efficiencies.) AD-L = liquid

fraction of anaerobically digested dairy cow manure; EP = eutrophication; ETP = ecotoxicity; GWP = global warming; WP = water intake potential.

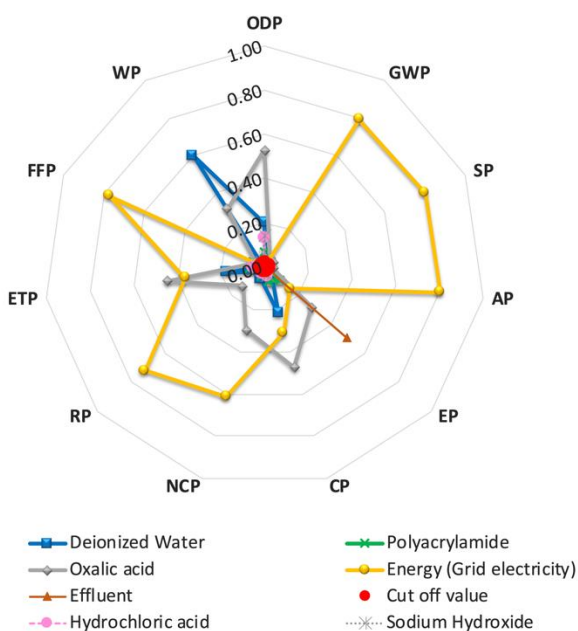
As demonstrated, LCA results based on the unit mass of struvite precipitation resulted in more than 200 times higher impacts in all impact categories. This is due to a relatively larger amount of dairy manure need to precipitate 1 kg of struvite. For reference, to obtain 1 kg of struvite, 200 to 260 kg of raw dairy manure is needed, considering manure characteristics from Wisconsin farms [41–44], which corresponds to collecting manure from 4 to 5 cows per day. Therefore, potentially, larger farms (≥ 200 head) that have anaerobic digesters may produce a minimum of 40 to 50 kg of struvite per day. Although a significant quantity of dairy manure is needed, it is an inescapable byproduct of farming, inexpensive, and abundantly available, which make it an appropriate source for struvite recovery [54]. From struvite production point of view, given that it serves as an alternative fertilizer to decrease the amount of excess nutrients from reaching water sources, it helps to reduce the risk of eutrophication. In both ways, struvite recovery technology is promising in terms of its contributions to managing dairy manure.

Sensitivity analysis

For all of the 11 potential environmental impact categories, sensitivity analysis was conducted and SFs were calculated. Figure H5 shows the SFs for each input parameter with respective impact categories for bench-scale (Figure H5A) and farm-scale (Figure H5B) struvite precipitation process. The red circle in the center indicates the cutoff value (2%). Sensitivity factors that are located outside of the red circle (i.e., cutoff value) are considered sensitive parameters, whereas SFs that are inside the circle are considered not sensitive. Because the

impact assessment results for both bench and farm scale processes are not sensitive to magnesium chloride, it is excluded from Figure H5.

A) SFs for bench-scale struvite precipitation process



B) SFs for farm-scale struvite precipitation process

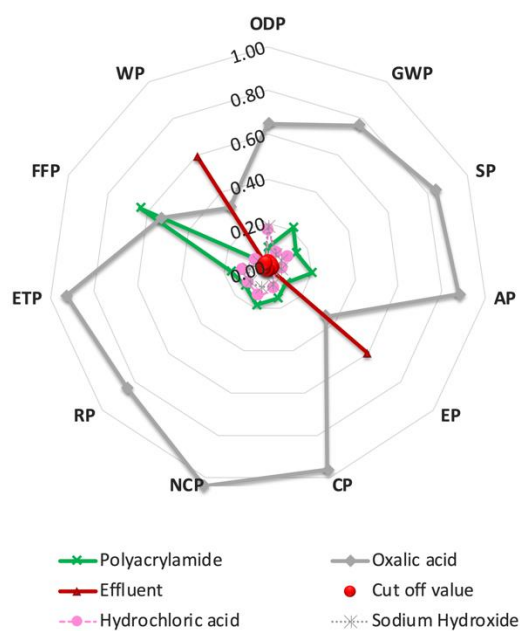


Figure H5. Sensitivity factors (SFs) of all inputs associated with the investigated potential environmental impact categories for bench scale (A) and farmscale (B). AP = acidification; CP = carcinogenic; EP= eutrophication, ETP= ecotoxicity; FFP = fossil fuel depletion; GWP = global warming; NCP= noncarcinogenic; ODP = ozone depletion; RP= respiratory effect; SP = smog; WP = water intake potential.

In terms of bench-scale process, as depicted in Figure H5A, the SFs for 6 inputs are sensitive for more than 5 of the 11 impact categories considered. These can be listed as HCl, NaOH, energy produced from grid electricity, oxalic acid, polyacrylamide, and deionized water inputs. With respect to ODP, HCl, NaOH, oxalic acid, deionized water, and polyacrylamide are

found to be the sensitive parameters. This means that any changes in other inputs (e.g., grid electricity and MgCl_2) will not have any significant impact on the overall ODP of the system. Considering CP, NCP, and ETP categories, grid electricity is identified as an additional sensitive parameter besides the aforementioned ones. Considering EP, in addition to these parameters, effluent is identified as a sensitive parameter. For GWP, SP, and AP categories, only two of the inputs, oxalic acid and grid electricity, are identified as sensitive inputs. For RP, sensitive inputs are found to be deionized water, oxalic acid, and electricity grid. Finally, in FFP, polyacrylamide, oxalic acid, and electricity grid inputs showed sensitivity.

Among all inputs, grid electricity has the highest SFs ($0.8 > \text{SF} > 0.15$) for 9 of the 11 impact categories (i.e., all except ODP and WP), meaning that any small change in electricity input will significantly change the overall environmental impact of the struvite precipitation from the AD-L-dairy manure process. As expected, the deionized water input is the most sensitive parameter for WP ($\text{SF} \approx 0.6$), followed by oxalic acid ($\text{SF} \approx 0.31$). The trend for SFs is found to be very different for the ODP impact category, where oxalic acid was the most sensitive parameter ($\text{SF} \approx 0.53$), followed by deionized water ($\text{SF} \approx 0.20$), NaOH ($\text{SF} \approx 0.14$), HCl ($\text{SF} \approx 0.13$), and polyacrylamide, respectively. All of the SFs for the bench-scale struvite precipitation process are tabulated and can be found in Supplemental Data Table HS13.

Regarding the farm-scale struvite precipitation process, the trends for SFs changed drastically. Four inputs of the system, HCl, NaOH, oxalic acid, and polyacrylamide, are found to be sensitive parameters for all the 11 impact categories considered. As presented in Figure H5B, for the farm-scale process, oxalic acid showed the highest sensitivity in all impact categories ($\text{SF} > 0.65$) except FFP ($\text{SF} \approx 0.53$), EP ($\text{SF} \approx 0.35$), and WP ($\text{SF} \approx 0.32$). This means any small change in oxalic acid input would change the overall environmental impact of the struvite

precipitation process. For EP and WP, the effluent was identified as the most sensitive parameter. This is due to the high consumption of flush water to dilute the AD-L-dairy manure and the excess N and P contained in the discharged stream. All of the SFs for the farm-scale struvite precipitation process are tabulated and can be found in Supplemental Data Table HS14.

Discussion and implications

Struvite precipitation process contributes to both manure management and nutrient management practices. Given that N and P recovery can be achieved in the form of struvite, it may replace the conventional fertilizers. This decreases the utilization of Haber–Bosch process [58, 59] as well as reduces the need of phosphate mining [60, 61] to manufacture synthetic fertilizers. Additionally, the nutrients (P and N) that are present in dairy manure can cause eutrophication [62]. Because P and N from AD-L-dairy manure can be recovered in the form of struvite, there is a lower risk of eutrophication due to agricultural runoff. For reference, 7.29 kg N-eq/kg of P and 0.986 kg N-eq/kg of N of impact (i.e., eutrophication potential) is omitted as a result of nutrient recovery [63].

Munasinghe-Arachchige and Nirmalakhandan ranked 5 different technologies for nutrient recovery from the liquid portion of anaerobically digested sludge, including air stripping, ion exchange, struvite precipitation, reverse osmosis, and gas permeable membrane separation, using multicriteria decision analysis [59]. Based on 10 performance criteria, they concluded that struvite precipitation performs as the second best (after gas permeable membrane technology) in terms of recovery performance, operating conditions, and the amount of chemical and energy requirements [59]. Several other researchers recommended the implementation of struvite

precipitation technology for both nutrient recovery and waste management practices due to its relatively low cost and high performance [61, 64–66].

Considering the AD-L-dairy manure characteristics (i.e., TP, TN, and other parameters as presented in Table 1), a simple LCA for a direct discharge scenario is modeled in SimaPro. It is found that, if the AD-L-dairy manure would be discharged directly to the water streams (e.g., surface water, river) without further treatment process, the eutrophication potential would be 1.69×10^{-3} kg N-eq per 1 kg AD-L-dairy manure treated. However, the EP of farm-scale struvite precipitation from AD-L-dairy manure process is found as 3.80×10^{-4} kg N-eq per 1 kg AD-L-dairy manure treated, even though it also contains upstream impacts (e.g., energy, acquisition of chemicals). In Wisconsin, there are 41 farms with 109,685 cows, which have anaerobic digesters [21]. This is equivalent to 2.194 million tons of dairy manure generation per year. Taking into account that all of this would be converted to struvite, more than 2.87×10^6 kg of N-eq emissions could be saved annually. This amount of N-eq emissions is equivalent to releasing more than 23,900 tons of ammonia to air or dumping 395 tons of P to water. For reference, the EP of releasing 1 kg of ammonia to air is 0.12 kg N-eq, and discharging 1 kg of P to water is 7.3 kg N-eq [50, 63]. This highlights the importance of further treatment approaches in nutrient management and environmental impact mitigation.

Another benefit of struvite crystallization is the reduced transportation costs for hauling the waste stream. Farmers with limited available land spaces may want to transport the manure generated from their farms to off-site management facilities, rather than managing them on-site. However, the waste stream generated from dairy farms is expected to be very dilute, which results in high environmental and economic costs associated with hauling. Struvite is a light crystal [26]; therefore, its transportation would be easier and economical [18]. Besides all these

direct and indirect benefits of this technology, chemicals and energy consumed to recover the struvite may have additional environmental implications, which are presented throughout the present study. Results are intended to inform future research in this area, particularly evaluating potential costs and benefits of further processing the dairy manure in order to decrease environmental impacts associated with managing this inescapable material.

Conclusions

Struvite crystallization, which is recovering valuable nutrients from waste materials (e.g., wastewater or manure), is one of the promising approaches for nutrient management practices. The present study investigated the environmental implications as well as impact hotspots of bench-scale and farm-scale struvite precipitation from AD-L-dairy manure (i.e., digestate from anaerobically digested cow manure) process using LCA methodology. The midpoint LCA results highlight that incorporating the struvite recovery process may help reduce EP up to 78% while managing the amount of nutrients that reach water bodies as a result of agricultural runoff. Oxalic acid, polyacrylamide, HCl, and NaOH were found as sensitive parameters for the majority of impact categories of both bench-scale and farm-scale processes. In addition to those, deionized water and grid electricity were identified as sensitive parameters for the bench-scale struvite recovery process. In other words, a minor reduction in any of those inputs can result in a major reduction in overall environmental impacts. Moreover, with the farm-scale scenario, due to the utilization of biogas instead of grid electricity, more than 55% impact reduction was observed in the majority of environmental impacts associated with the struvite precipitation process. Future work should combine both economic (e.g., operational and capital expenditure) and environmental cost and benefit implications of these processes for strong and sustainable

decision making. Finally, incorporating all respective processes (e.g., anaerobic digestion, screw press, struvite reactor) in the form of a continuous flow should be considered for more thorough evaluation.

Acknowledgment

This work is supported by the National Institute for Food and Agriculture (NIFA, 2017-67003-26055). Authors would like to thank the project team for the insightful discussions. This work has not been formally reviewed by the NIFA; any opinions, conclusions or recommendations shared in this publication belong to the authors.

Electronic supplemental information

Table HS1. Previously published studies for struvite precipitation from different types of manure sources with various pretreatment options

Manure Source	Pretreatment	Reference
Dairy manure	Anaerobic digestion	[32, 67–71]
Swine waste	Anaerobic digestion	[72–77]
Poultry manure	Anaerobic digestion	[78–82]
Livestock waste	Anaerobic digestion	[83–85]
Dairy manure	Acidification	[86]
Dairy manure	Microwave	[87–89]
Swine manure	ultrasound/H ₂ O ₂ digestion	[90]

Table HS2. Review of literature on struvite precipitation from anaerobically digested dairy manure

Source	Location	Equipment	Mg source and amount added	pH and adjustment method	Temp.	%P removal or recovery	%N removal or recovery
[67]	Japan	semi-continuous stirred tank reactor	MgCl ₂ Desired ratio of Mg ²⁺ : PO ₄ ³⁻ is 1-10:1	pH: 10 by CO ₂ removal	38°C	N/A (in experimental phase)	N/A (in experimental phase)
[68]	USA (WA)	struvite reactor	MgCl ₂ (10%) Desired ratio of Mg ²⁺ : PO ₄ ³⁻ is 1.5:1	pH: 8.2 by NaOH addition	N/A	62% TP removal as struvite, and total of 80% TP removal	N/A
[69]	Spain	high load anaerobic reactor	MgCl ₂ .6H ₂ O Desired ratio of Mg ²⁺ : PO ₄ ³⁻ is 0.75-1.2:1 and of Mg ²⁺ : NH ₃ is 1.2:1	pH: 8.3-9.8 by NaOH addition	N/A	N/A	70.8-92.7%
[71]	USA (WA)	continuously stirred batch reactor	MgCl ₂ .6H ₂ O, Mg(OH) ₂ Mg ²⁺ : 0.016-0.137 M	pH: 8.5-9.2 by NaOH addition	21-22°C	N/A	95%
[70]	USA (WA)	same anaerobic digestion reactor	MgCl ₂ .6H ₂ O: 7-78 mL Mg(OH) ₂ : 7.2-28.8 mL	pH: 8.53-9.6 not adjusted	N/A	N/A	objective was ammonia removal (11% extra NH ₃ removed)
[32]	USA (WA)	cone-shaped fluidized bed struvite crystallizer	MgCl ₂ : 0-155.4 mmol/L	pH: 7.8 by NaOH addition	N/A	65-82% as struvite	N/A

°C: Celsius; CO₂: Carbon dioxide; L: liter; M: molar; mL: milliliter; mmol: millimole; Mg²⁺: Magnesium; MgCl₂: Magnesium chloride; MgCl₂.6H₂O:

Magnesium chloride hexahydrate; Mg(OH)₂: Magnesium hydroxide; NaOH: Sodium hydroxide; NH₃: Ammonia; N/A: no such information available; PO₄³⁻:

Phosphate; TP: Total Phosphorus; WA: Washington

Table HS3. Summary of LCA studies on struvite precipitation from different types of manure

Source	Location (L) and Manure (M)	Data Collection	Methodology (M) and Software (S)	System Boundary	Functional Unit (FU) and Scale (S)	System Description
[39, 40]	L: United States (FL) M: Swine	literature, laboratory experiments, surveys and interviews with industry professionals	M: TRACI (version not specified) S: SimaPro v7.2	cradle to use	FUn: 50.82 m ³ /day of swine waste treated for 20 years S: medium (7000 pigs) and large (33600 pigs)	anaerobic digestion, dewatering, struvite precipitation and recovery of N/K by ion exchange
[37]	L: Spain M: Livestock (pig and cow)	literature, laboratory experiments and Ecoinvent database (v3.2)	M: ReCiPe Midpoint (H) v1.12 S: N/A	cradle to gate	FUn: 274 tons/day S: medium/pilot (100,000-ton feeding mixture per year)	anaerobic digestion, acidification, centrifugation, membrane ultrafiltration, struvite precipitation, nitrification, denitrification, high rate activated sludge and partial nitrification anammox
[38]	L: Cyprus M: Livestock	laboratory experiments of LiveWaste project and Ecoinvent database	M: ReCiPe Midpoint (H) (version not specified) S: N/A	only the treatment processes	FUn: 1 ton of livestock waste treated S: full scale treatment plant	LiveWaste treatment plant: anaerobic digestion, solid/liquid separation, digestate treatment, struvite application, biotrickling filter, biofilter, cogeneration heat and power and composting

FL: Florida; **m³/day:** cubic meters per day; **Midpoint (H):** midpoint hierarchist method; **N:** nitrogen; **N/A:** no such information available; **TRACI:** the tool for

the reduction and assessment of chemical and other environmental impacts.

Overview of Struvite Precipitation

Struvite formation can be achieved when the three ions, magnesium (Mg^{2+}), ammonium (NH_4^+) and phosphate (PO_4^{3-}) are in the solution with a 1:1:1 molar ratio to reach supersaturation [32, 67]. However, this process may be affected by the pH of the solution or the differing physicochemical characteristics of the manure itself (e.g. having calcium as an impurity). Besides being a widely implemented farm-scale energy recovery method, anaerobic digestion is one of the pretreatment options applied to dairy manure in order to stabilize the waste, to break down organic materials and convert organic phosphates into inorganic phosphorus for increasing the available phosphate/phosphorus ratio [68, 69, 81]. However, the calcium (Ca^{2+}) that is present in the digested manure and the neutral to alkali conditions of the media [32, 72] result in formation of $\text{Ca}_3(\text{PO}_4)_2$, $\text{Ca}(\text{H}_2\text{PO}_4)_2$, CaHPO_4 and other compounds before Mg forms struvite [34]. In order to dissolve the Ca- PO_4 compounds, acidification is the most applied option [32]. Examples include the addition of oxalic acid, which decreases the pH of the solution and break the Ca- PO_4 bonds as well as binds the Ca and make it insoluble in the form of calcium oxalate. Since higher pH is favorable for struvite formation, Ca should be captured before the pH adjustment stage. Additionally, in most of the cases addition of Mg source is required to increase the amount of struvite produced [69]. Yilmazel and Demirer suggested that in order to supplement Mg, compounds such as MgO , $\text{Mg}(\text{OH})_2$ and $\text{MgCl}_2 \cdot 6\text{H}_2\text{O}$ are the popular alternatives; however, depending on the objective (e.g. either P or N removal/recovery) the preference may be different, although $\text{MgCl}_2 \cdot 6\text{H}_2\text{O}$ is the most favored option for all cases [3]. The quantity of Mg source added may not be the same due to the different characteristics of manure.

Table HS4. Basis for calculation of struvite recovery from dairy manure and wash water (100 kg)

[41–44]	Amount	Unit	Output Flow
100 kg raw dairy manure + wash water	93.03	kg	water
	0.08	kg	P
	0.19	kg	N
	6.7	kg	miscellaneous
Process: Anaerobic Digestion	98.79	kg	digestate
	92.98	kg	water
	0.08	kg	P
	0.19	kg	N
	5.54	kg	miscellaneous
	1.21	kg	biogas
	0.49	kg	methane
	0.67	kg	carbon dioxide
	0.05	kg	water
Process: Screw Press	10.87	kg	solid digestate
	8.15	kg	water
	0.01	kg	P
	0.05	kg	N
	2.66	kg	miscellaneous
	87.92	kg	liquid digestate
	84.83	kg	water
	0.06	kg	P
	0.14	kg	N
2.88	kg	miscellaneous	
Process: Granulation	2.61	kg	pellet
	0.261	kg	water
	0.0017	kg	P
	0.05	kg	N
	2.30	kg	miscellaneous
	8.26	kg	liquid
	7.89	kg	water
	0.01	kg	P
	0.00	kg	N
0.36	kg	miscellaneous	
Process: Struvite Precipitation <i>(final waste: 66% P recovery, 13% N recovery, 0.5% moisture content)</i>	0.42	kg	struvite precipitation
	0.00211	kg	water
	0.053	kg	P
	0.024	kg	N
	0.34	kg	miscellaneous
	87.50	kg	liquid
	84.83	kg	water
	0.01	kg	P
	0.12	kg	N
2.54	kg	miscellaneous	

Assumptions and calculations for creating life cycle inventory

- **Oxalic Acid**

Desired calcium to oxalic acid ratio is 1:1 [68]:

$$\frac{1.741 \text{ g calcium}}{1 \text{ kg AD - L - dairy manure}} * \frac{1 \text{ mol}}{40 \text{ g calcium}} = \frac{0.044 \text{ mol}}{1 \text{ kg AD - L - dairy manure}}$$

$$\frac{90.03 \text{ g oxalic acid}}{\text{mol}} * \frac{0.044 \text{ mol}}{1 \text{ kg AD - L - dairy manure}} = \frac{3.92 \text{ g oxalic acid}}{1 \text{ kg AD - L - dairy manure}}$$

- **Magnesium Chloride (10%)**

Desired magnesium to phosphate ratio is 2:1 [37, 68]

[$TPO_4 = TP * 3.065$ [91]]

$$\frac{2.0842 \text{ g phosphate}}{1 \text{ kg AD - L - dairy manure}} * \frac{1 \text{ mol}}{94.97 \text{ g phosphate}} = \frac{0.022 \text{ mol}}{1 \text{ kg AD - L - dairy manure}}$$

$$\frac{24.3 \text{ g magnesium}}{\text{mol}} * \frac{2 * 0.022 \text{ mol}}{1 \text{ kg AD - L - dairy manure}} = \frac{1.067 \text{ g magnesium}}{1 \text{ kg AD - L - dairy manure}}$$

0.846 g magnesium is already present $\rightarrow 1.067 - 0.846 = 0.223 \text{ g Mg is needed}$

MgCl₂ (10%) addition is assumed = in 100 g solution, 10 g is MgCl₂ = 0.105 mol = 2.55 g Mg

$$\frac{0.223 \text{ g Mg} * 100 \text{ g solution}}{2.55 \text{ g Mg}} = 8.74 \text{ g MgCl}_2 \text{ (10\%)} \text{ is needed}$$

- **Sodium Hydroxide**

0.044 mole Mg²⁺ is present in the system and the ratio should be Mg²⁺:Na⁺ = 1:1 [92]

$$0.044 \text{ mol} * 40 \frac{\text{g}}{\text{mol}} = 1.76 \text{ g NaOH}$$

- **Electricity requirement**

Stirring for 30 minutes with Phipps and bird PB-900 jar tester [35].

Power 24 volts \rightarrow 360 Watt (with a current of 15 amps) = 0.18 kWh/0.228 kg AD-L-dairy

For 1 kg AD-L-dairy manure = 0.789 kWh

- **Avoided Phosphorus fertilizer**

From the corresponding SimaPro processes it was assumed that 48% of P is available as P_2O_5 in triple superphosphate. Given that struvite fertilizer contains 28% available P as P_2O_5 , avoided phosphorus fertilizer resulting from using 1 kg of struvite is 0.583 kg [39, 93, 94]. In other words, 0.583 kg phosphate fertilizer is equivalent to 1 kg of struvite in terms of P content based on the aforementioned assumptions.

- **Avoided Nitrogen fertilizer**

From the corresponding SimaPro processes it was assumed that 32% N is available in urea ammonium nitrate. Given that struvite fertilizer contains 5% total N, avoided nitrogen fertilizer resulting from using 1 kg of struvite is 0.156 kg [39, 93, 94]. In other words, 0.156 kg nitrogen fertilizer is equivalent to 1 kg of struvite in terms of N content based on the aforementioned assumptions.

- **Electricity from biogas generation in farm scale scenario**

According to Sampat et al., 1.24 m³ biogas (obtained as a result of anaerobic digestion of manure) can generate 2.18 kWh electricity [44]. De Vrieze et al. mentioned that the electricity consumption per ton of manure for struvite crystallization is 0.5 kWh [46]. Therefore, in order to have 0.005 kWh of electricity for 1 kg AD-L-dairy manure, 284.4 cm³ biogas is required.

Table HS5. Life cycle inventory data and unit process details for bench-scale struvite precipitation per 1 kg of AD-L-dairy manure treated

Input Parameter	Value	Notes	Unit Process Selected in SimaPro 8.5.2
HCl (1M)	1.61 g	to decrease pH from 8 to pH 5	Hydrochloric acid, without water, in 30% solution state {RoW} hydrochloric acid production, from the reaction of hydrogen with chlorine Alloc Def, U
NaOH (1M)	1.76 g	to increase pH from 5 to pH 8	Sodium hydroxide, without water, in 50% solution state {RoW} chlor-alkali electrolysis, diaphragm cell Alloc Def, U
Water	3.29 L	to dilute the liquid portion of the digestate	Water, deionised, from tap water, at user {RoW} production Alloc Def, U
Oxalic acid	3.92 g	to have a 1:1 molar ratio with Ca ²⁺	Citric acid {RoW} production Alloc Def, U [95]
Polyacrylamide	2.19 mL	anionic flocculant suspension, polymer	Polyacrylamide {GLO} production Alloc Def, U
Magnesium chloride (10%)	8.74 g	desired magnesium to phosphate ratio=2:1	new process was created based on the inventory data from [96]
Electricity	0.789 kWh	stirring jar tester	Electricity, at grid, US/US
Output Parameter	Value	Notes	Unit Process Selected in SimaPro 8.5.2
Struvite	4.77 g	66% phosphorus recovery as struvite	<i>product</i>
Calcium oxalate precipitate	5.66 g	waste management	Calcium compounds, unspecified
Nitrogen, total	1.36 g	excess nutrient	Nitrogen, total, discharged to surface water
Phosphate, total	0.114 g	excess nutrient	Phosphate, total, discharged to surface water
Water	3.5 kg	effluent	Waste water, unspecified, discharged to surface water
Avoided Impacts	Value	Notes	Unit Process Selected in SimaPro 8.5.2
Nitrogen fertilizer	0.744 g	1 kg struvite \equiv 0.156 kg nitrogen fertilizer	Nitrogen fertiliser, as N {RoW} urea ammonium nitrate production Alloc Def, U
Phosphate fertilizer	2.78 g	1 kg struvite \equiv 0.583 kg phosphate fertilizer	Phosphate fertiliser, as P2O5 {RoW} triple superphosphate production Alloc Def, U

Table HS6. Uncertainties around each efficiency (phosphorus recovery) simulated by Monte Carlo Analysis for bench-scale LCA

BENCH-SCALE		Functional unit: 1 kg of AD-L-dairy manure treated					Functional unit: 1 kg of struvite produced				
C1	C2	60%	66%	70%	75%	78%	60%	66%	70%	75%	78%
AP	LB	5.50E-03	5.49E-03	5.48E-03	5.48E-03	5.47E-03	1.27E+00	1.15E+00	1.09E+00	1.01E+00	9.75E-01
	M	5.54E-03	5.53E-03	5.53E-03	5.52E-03	5.52E-03	1.28E+00	1.16E+00	1.10E+00	1.02E+00	9.83E-01
	UB	5.57E-03	5.57E-03	5.56E-03	5.56E-03	5.55E-03	1.29E+00	1.17E+00	1.10E+00	1.03E+00	9.89E-01
CP	LB	2.44E-09	2.33E-09	2.15E-09	2.02E-09	2.00E-09	5.52E-07	4.76E-07	4.22E-07	3.78E-07	3.38E-07
	M	3.42E-09	3.36E-09	3.32E-09	3.29E-09	3.27E-09	7.89E-07	7.02E-07	6.59E-07	6.07E-07	5.81E-07
	UB	5.43E-09	5.37E-09	5.23E-09	5.36E-09	5.25E-09	1.28E-06	1.13E-06	1.07E-06	1.02E-06	9.61E-07
ETP	LB	5.17E-01	4.96E-01	4.78E-01	4.68E-01	4.61E-01	1.19E+02	9.55E+01	9.26E+01	8.55E+01	8.14E+01
	M	6.24E-01	6.08E-01	6.05E-01	5.98E-01	5.88E-01	1.44E+02	1.27E+02	1.21E+02	1.10E+02	1.06E+02
	UB	8.15E-01	7.67E-01	7.99E-01	7.64E-01	7.74E-01	1.88E+02	1.63E+02	1.56E+02	1.42E+02	1.36E+02
EP	LB	7.31E-04	5.41E-04	4.25E-04	2.72E-04	1.78E-04	1.69E-01	1.14E-01	8.48E-02	4.96E-02	3.23E-02
	M	7.73E-04	5.84E-04	4.70E-04	3.17E-04	2.26E-04	1.79E-01	1.22E-01	9.33E-02	5.87E-02	4.06E-02
	UB	8.31E-04	6.50E-04	5.25E-04	3.75E-04	2.84E-04	1.93E-01	1.35E-01	1.04E-01	6.97E-02	4.97E-02
FFP	LB	4.19E-01	4.17E-01	4.16E-01	4.15E-01	4.14E-01	9.70E+01	8.73E+01	8.26E+01	7.69E+01	7.37E+01
	M	4.27E-01	4.25E-01	4.25E-01	4.24E-01	4.23E-01	9.88E+01	8.92E+01	8.43E+01	7.85E+01	7.54E+01
	UB	4.36E-01	4.35E-01	4.34E-01	4.33E-01	4.32E-01	1.01E+02	9.14E+01	8.60E+01	8.03E+01	7.71E+01
GWP	LB	6.51E-01	6.51E-01	6.50E-01	6.49E-01	6.48E-01	1.51E+02	1.36E+02	1.29E+02	1.20E+02	1.16E+02
	M	6.55E-01	6.54E-01	6.54E-01	6.53E-01	6.53E-01	1.52E+02	1.37E+02	1.30E+02	1.21E+02	1.16E+02
	UB	6.60E-01	6.59E-01	6.59E-01	6.58E-01	6.58E-01	1.53E+02	1.38E+02	1.31E+02	1.22E+02	1.17E+02
NCP	LB	2.49E-08	2.36E-08	2.34E-08	2.31E-08	2.23E-08	5.85E-06	4.68E-06	4.44E-06	4.17E-06	3.98E-06
	M	2.89E-08	2.85E-08	2.84E-08	2.80E-08	2.80E-08	6.70E-06	5.97E-06	5.62E-06	5.21E-06	4.98E-06
	UB	3.24E-08	3.14E-08	3.17E-08	3.15E-08	3.12E-08	7.65E-06	6.82E-06	6.32E-06	5.73E-06	5.64E-06
ODP	LB	7.49E-09	7.34E-09	7.20E-09	7.00E-09	7.02E-09	1.74E-06	1.52E-06	1.42E-06	1.30E-06	1.24E-06
	M	9.09E-09	9.03E-09	8.83E-09	8.79E-09	8.78E-09	2.11E-06	1.87E-06	1.77E-06	1.63E-06	1.56E-06
	UB	1.19E-08	1.16E-08	1.17E-08	1.18E-08	1.15E-08	2.72E-06	2.48E-06	2.30E-06	2.19E-06	2.07E-06
RP	LB	3.02E-04	3.00E-04	2.99E-04	2.98E-04	2.97E-04	6.99E-02	6.29E-02	5.94E-02	5.51E-02	5.30E-02
	M	3.09E-04	3.07E-04	3.06E-04	3.06E-04	3.05E-04	7.15E-02	6.44E-02	6.08E-02	5.66E-02	5.43E-02
	UB	3.19E-04	3.16E-04	3.16E-04	3.15E-04	3.14E-04	7.36E-02	6.62E-02	6.26E-02	5.84E-02	5.59E-02
SP	LB	4.33E-02	4.32E-02	4.32E-02	4.32E-02	4.31E-02	1.00E+01	9.07E+00	8.58E+00	7.99E+00	7.68E+00
	M	4.36E-02	4.35E-02	4.35E-02	4.34E-02	4.34E-02	1.01E+01	9.12E+00	8.63E+00	8.05E+00	7.73E+00
	UB	4.39E-02	4.38E-02	4.37E-02	4.37E-02	4.37E-02	1.02E+01	9.18E+00	8.68E+00	8.10E+00	7.78E+00
WP	LB	-1.01E+00	-8.97E-01	-9.47E-01	-7.91E-01	-5.23E-01	-4.58E+02	-2.56E+02	-2.65E+02	-6.71E+01	-8.03E+01
	M	5.07E+00	5.12E+00	4.77E+00	4.68E+00	4.81E+00	1.11E+03	1.03E+03	9.94E+02	8.85E+02	8.72E+02
	UB	1.24E+01	1.24E+01	1.23E+01	1.11E+01	1.16E+01	2.87E+03	2.51E+03	2.44E+03	2.13E+03	1.97E+03

C1: Potential environmental impact categories considered in the current study. C2: Lower bound (LB), median (M) and upper bound (UB) of emissions based on 95% confidence intervals for the uncertainties. ODP in kg CFC11-eq., GWP in kg CO₂-eq., SP in kg O₃-eq., AP in kg SO₂-eq., EP in kg N-eq., HHCP in CTUh, HHNCP in CTUh, RP in kg PM_{2.5}-eq., ETP in CTUe, FFP in MJ surplus energy, WP in Liters

Table HS7. Uncertainties around each efficiency (i.e. phosphorus recovery) simulated by Monte Carlo Analysis for farm-scale LCA using well water for dilution.

LARGE & WELL		Functional unit: 1 kg of AD-L-dairy manure treated					Functional unit: 1 kg of struvite produced				
C1	C2	60%	66%	70%	75%	78%	60%	66%	70%	75%	78%
AP	LB	1.81E-04	1.70E-04	1.64E-04	1.55E-04	1.50E-04	4.24E-02	3.49E-02	3.25E-02	2.90E-02	2.65E-02
	M	2.14E-04	2.08E-04	2.03E-04	1.98E-04	1.94E-04	4.96E-02	4.36E-02	3.99E-02	3.64E-02	3.46E-02
	UB	2.42E-04	2.34E-04	2.32E-04	2.26E-04	2.23E-04	5.55E-02	4.93E-02	4.58E-02	4.18E-02	3.98E-02
CP	LB	7.00E-10	6.04E-10	6.03E-10	4.49E-10	2.58E-10	1.58E-07	8.26E-08	1.33E-07	6.82E-08	5.36E-08
	M	1.66E-09	1.61E-09	1.58E-09	1.54E-09	1.53E-09	3.91E-07	3.40E-07	3.18E-07	2.85E-07	2.70E-07
	UB	2.39E-09	2.16E-09	2.10E-09	2.05E-09	2.05E-09	5.37E-07	4.82E-07	4.38E-07	4.01E-07	3.47E-07
ETP	LB	1.74E-01	1.53E-01	1.23E-01	9.20E-02	9.85E-02	4.43E+01	3.12E+01	2.60E+01	2.04E+01	1.88E+01
	M	2.90E-01	2.83E-01	2.72E-01	2.66E-01	2.62E-01	6.73E+01	5.89E+01	5.41E+01	4.94E+01	4.67E+01
	UB	3.59E-01	3.39E-01	3.31E-01	3.21E-01	3.26E-01	8.17E+01	7.31E+01	6.70E+01	6.10E+01	5.58E+01
EP	LB	6.41E-04	4.53E-04	3.33E-04	1.75E-04	8.94E-05	1.49E-01	9.50E-02	6.73E-02	3.36E-02	1.59E-02
	M	6.80E-04	4.90E-04	3.77E-04	2.25E-04	1.34E-04	1.57E-01	1.03E-01	7.50E-02	4.16E-02	2.42E-02
	UB	7.14E-04	5.25E-04	4.14E-04	2.63E-04	1.72E-04	1.65E-01	1.11E-01	8.14E-02	4.83E-02	3.06E-02
FFP	LB	2.82E-02	2.68E-02	2.53E-02	2.49E-02	2.27E-02	6.71E+00	5.59E+00	5.17E+00	4.63E+00	4.24E+00
	M	3.60E-02	3.51E-02	3.43E-02	3.30E-02	3.24E-02	8.34E+00	7.33E+00	6.79E+00	6.14E+00	5.76E+00
	UB	4.43E-02	4.43E-02	4.32E-02	4.22E-02	4.23E-02	1.04E+01	9.38E+00	8.70E+00	7.73E+00	7.43E+00
GWP	LB	3.34E-02	3.23E-02	3.17E-02	3.11E-02	3.02E-02	7.76E+00	6.82E+00	6.31E+00	5.75E+00	5.45E+00
	M	3.66E-02	3.57E-02	3.52E-02	3.46E-02	3.41E-02	8.47E+00	7.51E+00	6.99E+00	6.39E+00	6.10E+00
	UB	3.98E-02	3.89E-02	3.84E-02	3.77E-02	3.75E-02	9.26E+00	8.12E+00	7.63E+00	6.97E+00	6.70E+00
NCP	LB	3.26E-09	2.10E-09	-1.85E-10	6.10E-12	3.55E-10	6.65E-07	4.36E-07	1.61E-07	5.36E-08	-1.23E-07
	M	7.83E-09	7.55E-09	7.26E-09	6.96E-09	6.87E-09	1.82E-06	1.58E-06	1.44E-06	1.29E-06	1.22E-06
	UB	9.92E-09	9.34E-09	9.17E-09	8.94E-09	8.91E-09	2.22E-06	1.96E-06	1.83E-06	1.66E-06	1.56E-06
ODP	LB	6.15E-09	5.88E-09	5.78E-09	5.69E-09	5.64E-09	1.42E-06	1.26E-06	1.15E-06	1.04E-06	9.66E-07
	M	7.29E-09	7.17E-09	7.06E-09	6.97E-09	6.92E-09	1.69E-06	1.51E-06	1.41E-06	1.29E-06	1.24E-06
	UB	8.96E-09	8.98E-09	8.71E-09	8.66E-09	8.78E-09	2.09E-06	1.86E-06	1.76E-06	1.61E-06	1.57E-06
RP	LB	3.84E-05	3.67E-05	3.52E-05	3.33E-05	3.28E-05	8.80E-03	7.64E-03	6.96E-03	6.14E-03	5.88E-03
	M	4.32E-05	4.20E-05	4.10E-05	4.00E-05	3.93E-05	1.00E-02	8.83E-03	8.12E-03	7.39E-03	7.03E-03
	UB	4.92E-05	4.75E-05	4.64E-05	4.56E-05	4.54E-05	1.14E-02	9.91E-03	9.18E-03	8.46E-03	8.08E-03
SP	LB	1.75E-03	1.69E-03	1.65E-03	1.61E-03	1.56E-03	4.12E-01	3.56E-01	3.27E-01	2.98E-01	2.81E-01
	M	1.97E-03	1.93E-03	1.89E-03	1.85E-03	1.83E-03	4.57E-01	4.04E-01	3.74E-01	3.43E-01	3.25E-01
	UB	2.17E-03	2.10E-03	2.09E-03	2.03E-03	2.02E-03	4.99E-01	4.42E-01	4.11E-01	3.78E-01	3.60E-01
WP	LB	2.62E+00	2.54E+00	2.62E+00	2.58E+00	2.82E+00	5.83E+02	5.66E+02	5.16E+02	5.04E+02	4.80E+02
	M	4.95E+00	4.95E+00	4.88E+00	4.94E+00	4.83E+00	1.16E+03	1.05E+03	9.63E+02	9.03E+02	8.63E+02
	UB	7.24E+00	7.04E+00	6.95E+00	7.31E+00	7.22E+00	1.68E+03	1.45E+03	1.42E+03	1.29E+03	1.28E+03

Table HS8. Uncertainties around each efficiency (i.e. phosphorus recovery) simulated by Monte Carlo Analysis for farm-scale LCA using gray water for dilution.

LARGE & GRAY		Functional unit: 1 kg of AD-L-dairy manure treated					Functional unit: 1 kg of struvite produced				
C1	C2	60%	66%	70%	75%	78%	60%	66%	70%	75%	78%
AP	LB	1.79E-04	1.69E-04	1.65E-04	1.52E-04	1.50E-04	4.17E-02	3.56E-02	3.23E-02	2.96E-02	2.63E-02
	M	2.14E-04	2.07E-04	2.03E-04	1.98E-04	1.93E-04	4.97E-02	4.35E-02	4.04E-02	3.66E-02	3.43E-02
	UB	2.40E-04	2.37E-04	2.30E-04	2.28E-04	2.24E-04	5.61E-02	4.93E-02	4.58E-02	4.23E-02	4.01E-02
CP	LB	7.98E-10	5.63E-10	4.28E-10	3.69E-10	2.08E-10	1.18E-07	1.22E-07	9.50E-08	5.18E-08	4.28E-08
	M	1.68E-09	1.62E-09	1.60E-09	1.52E-09	1.49E-09	3.91E-07	3.39E-07	3.14E-07	2.84E-07	2.64E-07
	UB	2.28E-09	2.20E-09	2.07E-09	2.08E-09	1.97E-09	5.29E-07	4.54E-07	4.21E-07	4.07E-07	3.57E-07
ETP	LB	1.69E-01	1.37E-01	1.41E-01	1.03E-01	1.01E-01	4.24E+01	3.15E+01	2.49E+01	2.19E+01	2.04E+01
	M	2.90E-01	2.81E-01	2.74E-01	2.66E-01	2.61E-01	6.71E+01	5.90E+01	5.44E+01	4.98E+01	4.65E+01
	UB	3.55E-01	3.41E-01	3.31E-01	3.25E-01	3.21E-01	8.21E+01	7.04E+01	6.65E+01	6.11E+01	5.88E+01
EP	LB	6.40E-04	4.47E-04	3.35E-04	1.82E-04	8.83E-05	1.48E-01	9.50E-02	6.64E-02	3.41E-02	1.57E-02
	M	6.79E-04	4.90E-04	3.77E-04	2.24E-04	1.33E-04	1.57E-01	1.03E-01	7.49E-02	4.19E-02	2.41E-02
	UB	7.15E-04	5.28E-04	4.11E-04	2.62E-04	1.76E-04	1.66E-01	1.10E-01	8.14E-02	4.85E-02	3.07E-02
FFP	LB	2.85E-02	2.71E-02	2.48E-02	2.50E-02	2.35E-02	6.64E+00	5.53E+00	5.13E+00	4.69E+00	4.10E+00
	M	3.62E-02	3.51E-02	3.38E-02	3.29E-02	3.21E-02	8.43E+00	7.37E+00	6.76E+00	6.12E+00	5.77E+00
	UB	4.51E-02	4.34E-02	4.38E-02	4.20E-02	4.08E-02	1.05E+01	9.30E+00	8.62E+00	7.99E+00	7.37E+00
GWP	LB	3.36E-02	3.24E-02	3.18E-02	3.09E-02	3.05E-02	7.83E+00	6.82E+00	6.32E+00	5.69E+00	5.41E+00
	M	3.65E-02	3.58E-02	3.52E-02	3.46E-02	3.41E-02	8.48E+00	7.51E+00	6.98E+00	6.39E+00	6.06E+00
	UB	3.96E-02	3.90E-02	3.84E-02	3.78E-02	3.77E-02	9.18E+00	8.13E+00	7.67E+00	6.99E+00	6.64E+00
NCP	LB	2.55E-09	2.06E-09	1.53E-09	1.52E-10	2.97E-10	9.26E-07	1.89E-07	3.66E-07	1.23E-07	-6.86E-08
	M	7.85E-09	7.46E-09	7.29E-09	7.03E-09	6.86E-09	1.82E-06	1.58E-06	1.45E-06	1.31E-06	1.20E-06
	UB	9.54E-09	9.49E-09	9.07E-09	8.88E-09	8.63E-09	2.22E-06	1.93E-06	1.82E-06	1.68E-06	1.60E-06
ODP	LB	6.11E-09	6.00E-09	5.82E-09	5.71E-09	5.60E-09	1.43E-06	1.25E-06	1.14E-06	1.04E-06	9.69E-07
	M	7.28E-09	7.20E-09	7.09E-09	7.00E-09	6.94E-09	1.69E-06	1.51E-06	1.40E-06	1.30E-06	1.24E-06
	UB	8.93E-09	8.95E-09	8.93E-09	8.81E-09	8.52E-09	2.08E-06	1.83E-06	1.76E-06	1.60E-06	1.55E-06
RP	LB	3.80E-05	3.67E-05	3.50E-05	3.38E-05	3.29E-05	8.75E-03	7.61E-03	6.98E-03	6.19E-03	5.86E-03
	M	4.35E-05	4.21E-05	4.10E-05	4.01E-05	3.92E-05	1.00E-02	8.80E-03	8.18E-03	7.42E-03	6.98E-03
	UB	4.83E-05	4.78E-05	4.67E-05	4.57E-05	4.47E-05	1.13E-02	9.95E-03	9.29E-03	8.47E-03	8.01E-03
SP	LB	1.76E-03	1.71E-03	1.65E-03	1.61E-03	1.55E-03	4.14E-01	3.59E-01	3.27E-01	2.97E-01	2.76E-01
	M	1.98E-03	1.93E-03	1.89E-03	1.85E-03	1.82E-03	4.60E-01	4.04E-01	3.76E-01	3.43E-01	3.24E-01
	UB	2.14E-03	2.12E-03	2.07E-03	2.05E-03	2.02E-03	5.03E-01	4.42E-01	4.12E-01	3.80E-01	3.59E-01
WP	LB	2.74E+00	2.46E+00	2.74E+00	2.78E+00	2.75E+00	5.62E+02	4.60E+02	5.45E+02	4.88E+02	4.75E+02
	M	4.91E+00	4.94E+00	4.89E+00	4.78E+00	4.85E+00	1.15E+03	1.03E+03	9.68E+02	8.98E+02	8.53E+02
	UB	7.23E+00	7.40E+00	7.19E+00	6.97E+00	7.14E+00	1.69E+03	1.53E+03	1.43E+03	1.31E+03	1.25E+03

Table HS9. Midpoint impact assessment results for treating 1 kg AD-L-dairy manure for struvite production with process contributions (bench-scale)

	HCl	NaOH	DI-Water	Polyacrylamide	Oxalic acid	MgCl ₂	Electricity (Grid)	Nitrogen fertilizer offset	Phosphate fertilizer offset	Effluent	TOTAL
ODP	1.21E-09	1.34E-09	1.88E-09	6.20E-10	5.34E-09	9.45E-12	1.11E-11	-4.72E-10	-9.09E-10	0.00E+00	9.03E-09
GWP	2.53E-03	2.35E-03	4.81E-03	7.83E-03	3.18E-02	4.74E-05	6.14E-01	-4.68E-03	-5.27E-03	0.00E+00	6.54E-01
SP	1.94E-04	1.27E-04	2.88E-04	2.79E-04	1.90E-03	1.71E-06	4.13E-02	-1.91E-04	-4.32E-04	0.00E+00	4.35E-02
AP	1.33E-05	1.24E-05	2.48E-05	4.29E-05	2.15E-04	2.24E-07	5.30E-03	-1.97E-05	-6.41E-05	0.00E+00	5.52E-03
EP	1.16E-05	1.05E-05	2.09E-05	4.31E-05	1.42E-04	1.04E-07	7.50E-05	-5.67E-06	-8.08E-05	2.59E-04	4.75E-04
CP	1.64E-10	1.36E-10	7.99E-10	2.38E-10	1.81E-09	3.86E-12	1.14E-09	-1.03E-10	-7.43E-10	0.00E+00	3.45E-09
NCP	9.75E-10	6.67E-10	1.75E-09	1.26E-09	8.88E-09	2.01E-11	1.97E-08	-7.57E-10	-4.38E-09	0.00E+00	2.81E-08
RP	4.90E-06	4.65E-06	8.83E-06	5.65E-06	4.20E-05	4.13E-08	2.57E-04	-2.82E-06	-1.35E-05	0.00E+00	3.07E-04
ETP	3.10E-02	2.36E-02	1.08E-01	4.55E-02	3.00E-01	4.62E-04	2.40E-01	-2.74E-02	-1.11E-01	0.00E+00	6.10E-01
FFP	2.15E-03	1.64E-03	3.71E-03	2.51E-02	2.04E-02	9.07E-05	3.87E-01	-6.06E-03	-9.27E-03	0.00E+00	4.25E-01
WP	7.46E-02	1.06E-01	3.43E+00	1.12E-01	1.68E+00	3.82E-03	0.00E+00	-6.15E-02	-3.04E-01	0.00E+00	5.04E+00

ODP in kg CFC11-eq., GWP in kg CO₂-eq., SP in kg O₃-eq., AP in kg SO₂-eq., EP in kg N-eq., HHCP in CTUh, HHNCP in CTUh, RP in kg PM_{2.5}-eq., ETP in CTUe, FFP in MJ surplus energy, WP in Liters

Table HS10. Midpoint impact assessment results for 1 kg struvite production from AD-L-manure with process contributions (bench-scale)

	HCl	NaOH	DI-Water	Polyacryl amide	Oxalic acid	MgCl ₂	Electricity (Grid)	Nitrogen fertilizer offset	Phosphate fertilizer offset	Effluent	TOTAL
ODP	2.43E-07	2.69E-07	3.77E-07	1.24E-07	1.07E-06	1.90E-09	2.24E-09	-9.39E-08	-1.81E-07	0.00E+00	1.82E-06
GWP	5.07E-01	4.71E-01	9.65E-01	1.57E+00	6.39E+00	9.52E-03	1.23E+02	-9.31E-01	-1.05E+00	0.00E+00	1.31E+02
SP	3.90E-02	2.54E-02	5.78E-02	5.60E-02	3.82E-01	3.43E-04	8.29E+00	-3.79E-02	-8.60E-02	0.00E+00	8.72E+00
AP	2.68E-03	2.49E-03	4.98E-03	8.60E-03	4.31E-02	4.49E-05	1.06E+00	-3.91E-03	-1.28E-02	0.00E+00	1.11E+00
EP	2.32E-03	2.11E-03	4.20E-03	8.65E-03	2.84E-02	2.09E-05	1.50E-02	-1.13E-03	-1.61E-02	5.55E-02	9.90E-02
CP	3.30E-08	2.74E-08	1.60E-07	4.79E-08	3.63E-07	7.75E-10	2.29E-07	-2.06E-08	-1.48E-07	0.00E+00	6.93E-07
NCP	1.96E-07	1.34E-07	3.52E-07	2.54E-07	1.78E-06	4.04E-09	3.94E-06	-1.51E-07	-8.72E-07	0.00E+00	5.64E-06
RP	9.84E-04	9.34E-04	1.77E-03	1.13E-03	8.42E-03	8.28E-06	5.16E-02	-5.60E-04	-2.69E-03	0.00E+00	6.16E-02
ETP	6.22E+00	4.73E+00	2.17E+01	9.13E+00	6.03E+01	9.26E-02	4.81E+01	-5.45E+00	-2.21E+01	0.00E+00	1.23E+02
FFP	4.32E-01	3.28E-01	7.45E-01	5.05E+00	4.09E+00	1.82E-02	7.76E+01	-1.21E+00	-1.84E+00	0.00E+00	8.53E+01
WP	1.50E+01	2.12E+01	6.88E+02	2.24E+01	3.36E+02	7.67E-01	0.00E+00	-1.22E+01	-6.06E+01	0.00E+00	1.01E+03

ODP in kg CFC11-eq., GWP in kg CO₂-eq., SP in kg O₃-eq., AP in kg SO₂-eq., EP in kg N-eq., HHCP in CTUh, HHNCP in CTUh, RP in kg PM_{2.5}-eq., ETP in CTUe, FFP in MJ surplus energy, WP in Liters

Table HS11. Midpoint impact assessment results for treating 1 kg AD-L-dairy manure for struvite production with process contributions (farm-scale)

	HCl	NaOH	Polyacrylamide	Oxalic acid	MgCl ₂	Energy (Biogas)	Nitrogen fertilizer offset	Phosphate fertilizer offset	Effluent	TOTAL
ODP	1.21E-09	1.34E-09	6.20E-10	5.34E-09	9.45E-12	1.17E-11	-4.72E-10	-9.09E-10	0.00E+00	7.16E-09
GWP	2.53E-03	2.35E-03	7.83E-03	3.18E-02	4.74E-05	5.63E-04	-4.68E-03	-5.27E-03	0.00E+00	3.52E-02
SP	1.94E-04	1.27E-04	2.79E-04	1.90E-03	1.71E-06	6.95E-06	-1.91E-04	-4.32E-04	0.00E+00	1.89E-03
AP	1.33E-05	1.24E-05	4.29E-05	2.15E-04	2.24E-07	1.95E-06	-1.97E-05	-6.41E-05	0.00E+00	2.02E-04
EP	1.16E-05	1.05E-05	4.31E-05	1.42E-04	1.04E-07	8.76E-07	-5.67E-06	-8.08E-05	2.59E-04	3.80E-04
CP	1.64E-10	1.36E-10	2.38E-10	1.81E-09	3.86E-12	9.27E-12	-1.03E-10	-7.43E-10	0.00E+00	1.52E-09
NCP	9.75E-10	6.67E-10	1.26E-09	8.88E-09	2.01E-11	6.26E-11	-7.57E-10	-4.38E-09	0.00E+00	6.73E-09
RP	4.90E-06	4.65E-06	5.65E-06	4.20E-05	4.13E-08	2.24E-07	-2.82E-06	-1.35E-05	0.00E+00	4.11E-05
ETP	3.10E-02	2.36E-02	4.55E-02	3.00E-01	4.62E-04	1.56E-03	-2.74E-02	-1.11E-01	0.00E+00	2.64E-01
FFP	2.15E-03	1.64E-03	2.51E-02	2.04E-02	9.07E-05	1.05E-04	-6.06E-03	-9.27E-03	0.00E+00	3.42E-02
WP	7.46E-02	1.06E-01	1.12E-01	1.68E+00	3.82E-03	1.29E-03	-6.15E-02	-3.04E-01	3.29E+00	4.90E+00

ODP in kg CFC11-eq., GWP in kg CO₂-eq., SP in kg O₃-eq., AP in kg SO₂-eq., EP in kg N-eq., HHCP in CTUh, HHNCP in CTUh, RP in kg PM2.5-eq., ETP in CTUe, FFP in MJ surplus energy, WP in Liters

Table HS12. Midpoint impact assessment results for 1 kg struvite production from AD-L-manure with process contributions (farm-scale)

	HCl	NaOH	Polyacrylamide	Oxalic acid	MgCl ₂	Energy (Biogas)	Nitrogen fertilizer offset	Phosphate fertilizer offset	Effluent	TOTAL
ODP	2.43E-07	2.69E-07	1.24E-07	1.07E-06	1.90E-09	2.35E-09	-9.39E-08	-1.81E-07	0.00E+00	1.44E-06
GWP	5.07E-01	4.71E-01	1.57E+00	6.39E+00	9.52E-03	1.13E-01	-9.31E-01	-1.05E+00	0.00E+00	7.08E+00
SP	3.90E-02	2.54E-02	5.60E-02	3.82E-01	3.43E-04	1.40E-03	-3.79E-02	-8.60E-02	0.00E+00	3.80E-01
AP	2.68E-03	2.49E-03	8.60E-03	4.31E-02	4.49E-05	3.92E-04	-3.91E-03	-1.28E-02	0.00E+00	4.06E-02
EP	2.32E-03	2.11E-03	8.65E-03	2.84E-02	2.09E-05	1.76E-04	-1.13E-03	-1.61E-02	5.55E-02	8.00E-02
CP	3.30E-08	2.74E-08	4.79E-08	3.63E-07	7.75E-10	1.86E-09	-2.06E-08	-1.48E-07	0.00E+00	3.06E-07
NCP	1.96E-07	1.34E-07	2.54E-07	1.78E-06	4.04E-09	1.26E-08	-1.51E-07	-8.72E-07	0.00E+00	1.36E-06
RP	9.84E-04	9.34E-04	1.13E-03	8.42E-03	8.28E-06	4.49E-05	-5.60E-04	-2.69E-03	0.00E+00	8.28E-03
ETP	6.22E+00	4.73E+00	9.13E+00	6.03E+01	9.26E-02	3.13E-01	-5.45E+00	-2.21E+01	0.00E+00	5.32E+01
FFP	4.32E-01	3.28E-01	5.05E+00	4.09E+00	1.82E-02	2.11E-02	-1.21E+00	-1.84E+00	0.00E+00	6.89E+00
WP	1.50E+01	2.12E+01	2.24E+01	3.36E+02	7.67E-01	2.59E-01	-1.22E+01	-6.06E+01	6.60E+02	9.83E+02

ODP in kg CFC11-eq., GWP in kg CO₂-eq., SP in kg O₃-eq., AP in kg SO₂-eq., EP in kg N-eq., HHCP in CTUh, HHNCP in CTUh, RP in kg PM_{2.5}-eq., ETP in CTUe, FFP in MJ surplus energy, WP in Liters

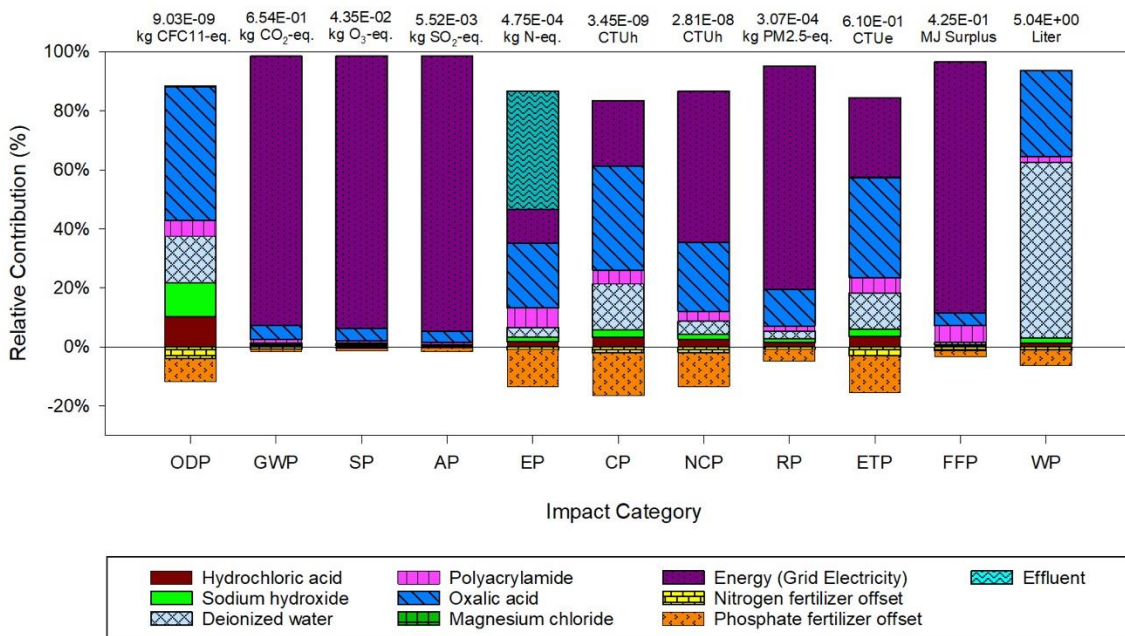


Figure HS1. Total life cycle environmental impacts and relative contributions of all input and output parameters (functional unit: 1 kg of AD-L-dairy manure treated).

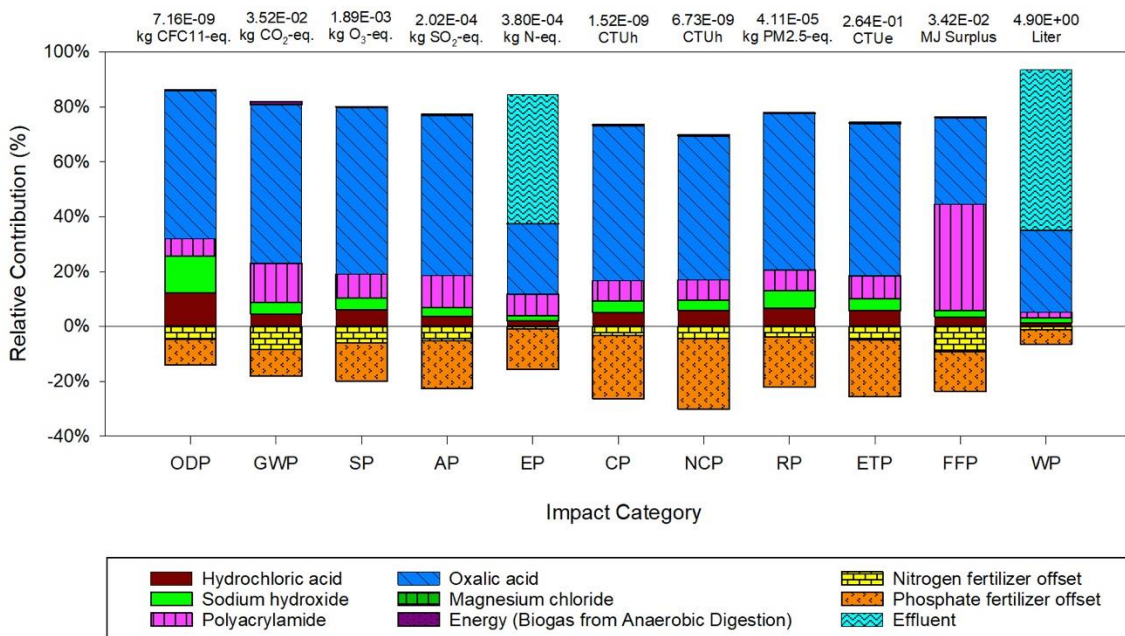


Figure HS2. Total life cycle environmental impacts and relative contributions of all input and output parameters for a farm-scale study (functional unit: 1 kg of AD-L-dairy manure treated).

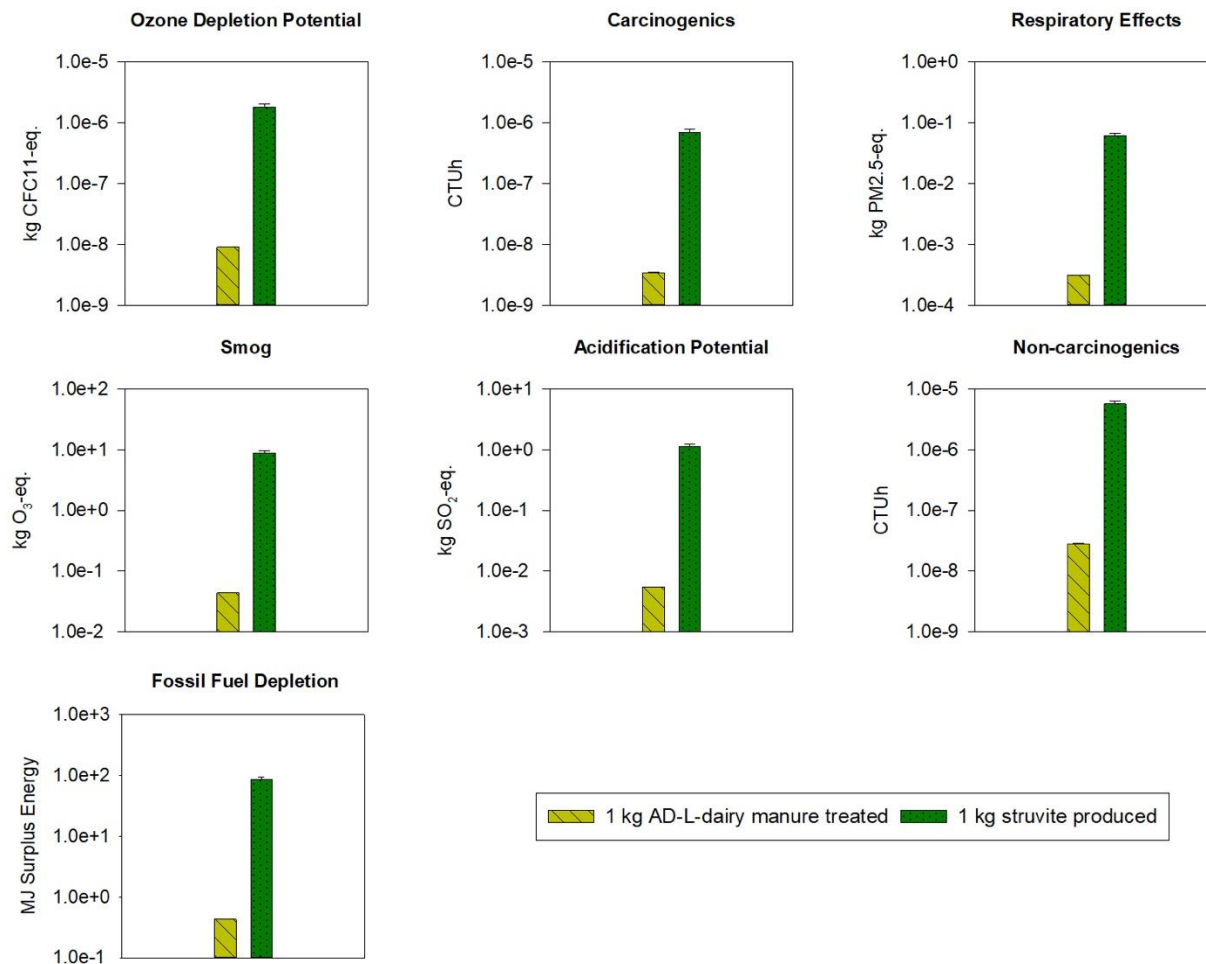


Figure HS3. Potential environmental impacts based on different functional units represented in logarithmic scale for bench-scale. Error bars represent the standard deviations of impacts resulting from the inclusion of different efficiencies.

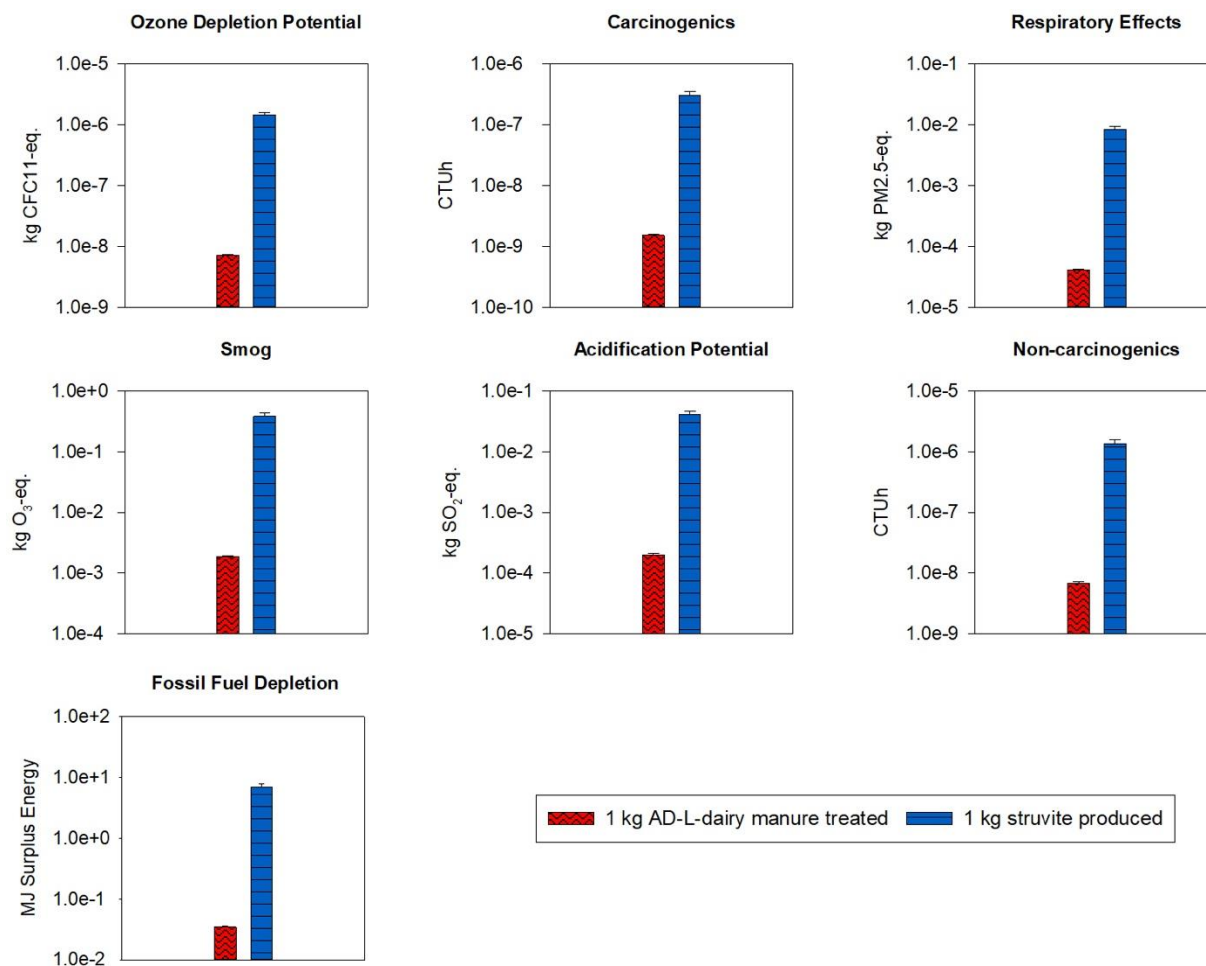


Figure HS4. Potential environmental impacts based on different functional units represented in logarithmic scale for farm-scale. Error bars represent the standard deviations of impacts resulting from the inclusion of different efficiencies.

Table HS13. Bench-scale: Sensitivity factors (SF) based on 20% inputs change for different impact contributors of the assessed process. Reported numbers are SFs, where red cells indicate sensitive inputs.

	HCl	NaOH	DI-Water	Polyacryl amide	Oxalic acid	MgCl ₂	Electricity (from grid)	Effluent
ODP	1.31E-01	1.44E-01	2.00E-01	6.77E-02	5.29E-01	1.05E-03	1.23E-03	-
GWP	3.86E-03	3.59E-03	7.34E-03	1.19E-02	4.82E-02	7.25E-05	7.91E-01	-
SP	4.46E-03	2.92E-03	6.62E-03	6.41E-03	4.34E-02	3.93E-05	7.98E-01	-
AP	2.41E-03	2.24E-03	4.48E-03	7.75E-03	3.86E-02	4.05E-05	8.05E-01	-
EP	2.42E-02	2.20E-02	4.36E-02	8.90E-02	2.81E-01	2.19E-04	1.53E-01	4.91E-01
CP	4.72E-02	3.93E-02	2.22E-01	6.82E-02	4.75E-01	1.12E-03	3.10E-01	-
NCP	3.45E-02	2.37E-02	6.16E-02	4.46E-02	2.98E-01	7.16E-04	6.14E-01	-
RP	1.59E-02	1.51E-02	2.86E-02	1.84E-02	1.33E-01	1.35E-04	7.18E-01	-
ETP	5.03E-02	3.83E-02	1.71E-01	7.35E-02	4.48E-01	7.57E-04	3.64E-01	-
FFP	5.06E-03	3.85E-03	8.73E-03	5.85E-02	4.76E-02	2.13E-04	7.71E-01	-
WP	1.48E-02	2.09E-02	5.99E-01	2.21E-02	3.12E-01	7.59E-04	-	-

Table HS14. Farm-scale: Sensitivity factors (SF) based on 20% inputs change for different impact contributors of the assessed process. Reported numbers are SFs, where red cells indicate sensitive inputs.

	HCl	NaOH	Polyacrylamide	Oxalic acid	MgCl ₂	Energy (from biogas)	Effluent
ODP	1.64E-01	1.81E-01	8.52E-02	6.50E-01	1.32E-03	1.64E-03	-
GWP	7.08E-02	6.58E-02	2.13E-01	7.66E-01	1.35E-03	1.59E-02	-
SP	1.01E-01	6.63E-02	1.44E-01	8.39E-01	9.05E-04	3.68E-03	-
AP	6.52E-02	6.06E-02	2.04E-01	8.78E-01	1.11E-03	9.66E-03	-
EP	3.02E-02	2.75E-02	1.11E-01	3.47E-01	2.73E-04	2.30E-03	5.99E-01
CP	1.06E-01	8.83E-02	1.52E-01	9.64E-01	2.54E-03	6.10E-03	-
NCP	1.41E-01	9.72E-02	1.81E-01	1.04E+00	2.99E-03	9.28E-03	-
RP	1.16E-01	1.11E-01	1.34E-01	8.48E-01	1.00E-03	5.44E-03	-
ETP	1.15E-01	8.76E-02	1.67E-01	9.27E-01	1.75E-03	5.91E-03	-
FFP	6.21E-02	4.74E-02	6.41E-01	5.33E-01	2.65E-03	3.07E-03	-
WP	1.52E-02	2.15E-02	2.27E-02	3.20E-01	7.81E-04	2.64E-04	5.92E-01

References-Appendix H

1. FAO (2017) World fertilizer trends and outlook to 2020. <http://www.fao.org/3/a-i6895e.pdf>
2. USGS (2019) Phosphate rock. <https://prd-wret.s3-us-west-2.amazonaws.com/assets/palladium/production/atoms/files/mcs-2019-phosp.pdf>
3. Yilmazel YD, Demirer GN (2013) Nitrogen and phosphorus recovery from anaerobic co-digestion residues of poultry manure and maize silage via struvite precipitation. *Waste Management & Research*, 31(8):792–804. <https://doi.org/10.1177/0734242X13492005>
4. Sena M, Hicks A (2018) Life cycle assessment review of struvite precipitation in wastewater treatment. *Resources, Conservation and Recycling*, 139:194–204. <https://doi.org/10.1016/j.resconrec.2018.08.009>
5. Li B, Boiarkina I, Yu W, Huang HM, Munir T, Wang GQ, Young BR (2019) Phosphorous recovery through struvite crystallization: Challenges for future design. *Science of The Total Environment*, 648:1244–1256. <https://doi.org/10.1016/j.scitotenv.2018.07.166>
6. Cheema II, Krewer U (2018) Operating envelope of Haber–Bosch process design for power-to-ammonia. *RSC Advances*, 8(61):34926–34936. <https://doi.org/10.1039/C8RA06821F>
7. Mayer BK, Baker LA, Boyer TH, Drechsel P, Gifford M, Hanjra MA, Parameswaran P, Stoltzfus J, Westerhoff P, Rittmann BE (2016) Total Value of Phosphorus Recovery. *Environmental Science & Technology*, 50(13):6606–6620. <https://doi.org/10.1021/acs.est.6b01239>
8. Steffen W, Richardson K, Rockstrom J, Cornell SE, Fetzer I, Bennett EM, Biggs R, Carpenter SR, Vries W de, Wit CA de, Folke C, Gerten D, Heinke J, Mace GM, Persson LM, Ramanathan V, Reyers B, Sorlin S (2015) Planetary boundaries: Guiding human development on a changing planet. *Science*, 347(6223):1259855–1259855. <https://doi.org/10.1126/science.1259855>
9. Vanham D, Leip A, Galli A, Kastner T, Bruckner M, Uwizeye A, Dijk K van, Ercin E, Dalin C, Brandão M, Bastianoni S, Fang K, Leach A, Chapagain A, Van der Velde M, Sala S, Pant R, Mancini L, Monforti-Ferrario F, Carmona-Garcia G, Marques A, Weiss F, Hoekstra AY (2019) Environmental footprint family to address local to planetary sustainability and deliver on the SDGs. *Science of The Total Environment*, 693:133642. <https://doi.org/10.1016/j.scitotenv.2019.133642>
10. Lade SJ, Steffen W, Vries W de, Carpenter SR, Donges JF, Gerten D, Hoff H, Newbold T, Richardson K, Rockström J (2020) Human impacts on planetary boundaries amplified by Earth system interactions. *Nature Sustainability*, 3(2):119–128. <https://doi.org/10.1038/s41893-019-0454-4>
11. Meyer K, Newman P (2020) The Phosphorus Quota. *Planetary Accounting: Quantifying How to Live Within Planetary Limits at Different Scales of Human Activity*, :207–219. https://doi.org/10.1007/978-981-15-1443-2_15

12. Rockström J, Edenhofer O, Gaertner J, DeClerck F (2020) Planet-proofing the global food system. *Nature Food*, 1(1):3–5. <https://doi.org/10.1038/s43016-019-0010-4>
13. Suárez-Eiroa B, Fernández E, Méndez-Martínez G, Soto-Oñate D (2019) Operational principles of circular economy for sustainable development: Linking theory and practice. *Journal of Cleaner Production*, 214:952–961. <https://doi.org/10.1016/j.jclepro.2018.12.271>
14. Chojnacka K, Moustakas K, Witek-Krowiak A (2020) Bio-based fertilizers: A practical approach towards circular economy. *Bioresource Technology*, 295:122223. <https://doi.org/10.1016/j.biortech.2019.122223>
15. Desing H, Brunner D, Takacs F, Nahrath S, Frankenberger K, Hirsch R (2020) A circular economy within the planetary boundaries: Towards a resource-based, systemic approach. *Resources, Conservation and Recycling*, 155:104673. <https://doi.org/10.1016/j.resconrec.2019.104673>
16. Robles Á, Aguado D, Barat R, Borrás L, Bouzas A, Giménez JB, Martí N, Ribes J, Ruano MV, Serralta J, Ferrer J, Seco A (2020) New frontiers from removal to recycling of nitrogen and phosphorus from wastewater in the Circular Economy. *Bioresource Technology*, 300:122673. <https://doi.org/10.1016/j.biortech.2019.122673>
17. USDA NASS (2019) Wisconsin Statistics. *USDA's National Agricultural Statistics Service Wisconsin Field Office*, https://www.nass.usda.gov/Statistics_by_State/Wisconsin/index.php
18. Sampat AM, Martín-Hernández E, Martín M, Zavala VM (2018) Technologies and logistics for phosphorus recovery from livestock waste. *Clean Technologies and Environmental Policy*, 20(7):1563–1579. <https://doi.org/10.1007/s10098-018-1546-y>
19. Porter S, Rushmann R (2020) Wisconsin Nutrient Management Basics. <https://datcp.wi.gov/Documents/NMBrochure.pdf>
20. US EPA (2020) AgSTAR: Biogas Recovery in the Agriculture Sector. <https://www.epa.gov/agstar>
21. US EPA (2020) Livestock Anaerobic Digester Database. <https://www.epa.gov/agstar/livestock-anaerobic-digester-database>
22. US EPA (2014) The Benefits of Anaerobic Digestion. <https://www.epa.gov/agstar/benefits-anaerobic-digestion>
23. USDA (1998) Manure Management Choices for Wisconsin Dairy and Beef Cattle Operations. <http://runoffinfo.uwex.edu/pdf/farm.lomanure.pdf>
24. Çelen I, Buchanan JR, Burns RT, Bruce Robinson R, Raj Raman D (2007) Using a chemical equilibrium model to predict amendments required to precipitate phosphorus as struvite in liquid swine manure. *Water Research*, 41(8):1689–1696. <https://doi.org/10.1016/j.watres.2007.01.018>

25. Martín-Hernández E, Sampat AM, Zavala VM, Martín M (2018) Optimal integrated facility for waste processing. *Chemical Engineering Research and Design*, 131:160–182. <https://doi.org/10.1016/j.cherd.2017.11.042>
26. Kataki S, West H, Clarke M, Baruah DC (2016) Phosphorus recovery as struvite from farm, municipal and industrial waste: Feedstock suitability, methods and pre-treatments. *Waste Management*, 49:437–454. <https://doi.org/10.1016/j.wasman.2016.01.003>
27. Tao W, Fattah KP, Huchzermeier MP (2016) Struvite recovery from anaerobically digested dairy manure: A review of application potential and hindrances. *Journal of Environmental Management*, 169:46–57. <https://doi.org/10.1016/j.jenvman.2015.12.006>
28. ISO (2006) ISO 14040:2006 - Environmental management -- Life cycle assessment -- Principles and framework. <https://www.iso.org/standard/37456.html>
29. Piccinno F, Hischier R, Seeger S, Som C (2016) From laboratory to industrial scale: a scale-up framework for chemical processes in life cycle assessment studies. *Journal of Cleaner Production*, 135:1085–1097. <https://doi.org/10.1016/j.jclepro.2016.06.164>
30. Bowers KE, Westerman PW (2005) Performance of Cone-Shaped Fluidized Bed Struvite Crystallizers in Removing Phosphorus from Wastewater. *Transactions of the ASAE*, 48(3):1227–1234. <https://doi.org/10.13031/2013.18523>
31. Suzuki K, Tanaka Y, Kuroda K, Hanajima D, Fukumoto Y (2005) Recovery of phosphorus from swine wastewater through crystallization. *Bioresource Technology*, 96(14):1544–1550. <https://doi.org/10.1016/j.biortech.2004.12.017>
32. Zhang T, Bowers KE, Harrison JH, Chen S (2010) Releasing Phosphorus from Calcium for Struvite Fertilizer Production from Anaerobically Digested Dairy Effluent. *Water Environment Research*, 82(1):34–42. <https://doi.org/10.2175/106143009X425924>
33. Brown K, Harrison J, Bowers K (2018) Struvite Precipitation from Anaerobically Digested Dairy Manure. *Water, Air, & Soil Pollution*, 229(7):217. <https://doi.org/10.1007/s11270-018-3855-5>
34. Ackerman JN, Cicek N (2011) Phosphorus Removal and Recovery from Hog Lagoon Supernatant Using a Gravity-Settled Batch Reactor and Increased pH. *Biological Engineering Transactions*, 4(4):207–218. <https://doi.org/10.13031/2013.40406>
35. Fisher Scientific (2020) Phipps & Bird PB-900 Series Programmable Jar Testers. <https://www.fishersci.com/shop/products/hipps-bird-pb-900-series-programmable-jar-testers-5/p-4643499>
36. Andriamanohiarisoamanana FJ, Saikawa A, Kan T, Qi G, Pan Z, Yamashiro T, Iwasaki M, Ihara I, Nishida T, Umetsu K (2018) Semi-continuous anaerobic co-digestion of dairy manure, meat and bone meal and crude glycerol: Process performance and digestate valorization. *Renewable Energy*, 128:1–8. <https://doi.org/10.1016/j.renene.2018.05.056>

37. Pedizzi C, Noya I, Sarli J, González-García S, Lema JM, Moreira MT, Carballa M (2018) Environmental assessment of alternative treatment schemes for energy and nutrient recovery from livestock manure. *Waste Management*, 77:276–286. <https://doi.org/10.1016/j.wasman.2018.04.007>
38. Lijó L, Frison N, Fatone F, González-García S, Feijoo G, Moreira MT (2018) Environmental and sustainability evaluation of livestock waste management practices in Cyprus. *Science of The Total Environment*, 634:127–140. <https://doi.org/10.1016/j.scitotenv.2018.03.299>
39. Amini A (2014) Sustainable Energy and Nutrient Recovery from Swine Waste. <https://scholarcommons.usf.edu/cgi/viewcontent.cgi?article=6173&context=etd>
40. Amini A, Aponte-Morales V, Wang M, Dilbeck M, Lahav O, Zhang Q, Cunningham JA, Ergas SJ (2017) Cost-effective treatment of swine wastes through recovery of energy and nutrients. *Waste Management*, 69:508–517. <https://doi.org/10.1016/j.wasman.2017.08.041>
41. Wang H, Aguirre-Villegas HA, Larson RA, Alkan-Ozkaynak A (2019) Physical Properties of Dairy Manure Pre- and Post-Anaerobic Digestion. *Applied Sciences*, 9(13):2703. <https://doi.org/10.3390/app9132703>
42. Aguirre-Villegas HA, Sharara MA, Larson RA (2018) Nutrient Variability Following Dairy Manure Storage Agitation. *Applied Engineering in Agriculture*, 34(6):908–917. <https://doi.org/10.13031/aea.12796>
43. Aguirre-Villegas HA, Larson RA, Sharara MA (2019) Anaerobic digestion, solid-liquid separation, and drying of dairy manure: Measuring constituents and modeling emission. *Science of The Total Environment*, 696:134059. <https://doi.org/10.1016/j.scitotenv.2019.134059>
44. Sampat AM, Ruiz-Mercado GJ, Zavala VM (2018) Economic and Environmental Analysis for Advancing Sustainable Management of Livestock Waste: A Wisconsin Case Study. *ACS Sustainable Chemistry & Engineering*, 6(5):6018–6031. <https://doi.org/10.1021/acssuschemeng.7b04657>
45. Maranghi S, Parisi ML, Basosi R, Sinicropi A (2020) LCA as a Support Tool for the Evaluation of Industrial Scale-Up. *Life Cycle Assessment in the Chemical Product Chain*, :125–143. https://doi.org/10.1007/978-3-030-34424-5_6
46. De Vrieze J, Colica G, Pintucci C, Sarli J, Pedizzi C, Willeghems G, Bral A, Varga S, Prat D, Peng L, Spiller M, Buysse J, Colsen J, Benito O, Carballa M, Vlaeminck SE (2019) Resource recovery from pig manure via an integrated approach: A technical and economic assessment for full-scale applications. *Bioresour Technol*, 272:582–593. <https://doi.org/10.1016/j.biortech.2018.10.024>
47. PRé Sustainability (2020) SimaPro LCA software. *Sustainability software for fact-based decisions*, <https://pre-sustainability.com/solutions/tools/simapro/>
48. ecoinvent (2020) Ecoinvent 3. *ecoinvent - the world's most consistent & transparent life cycle inventory database*, <https://www.ecoinvent.org/>

49. NREL (2020) U.S. Life Cycle Inventory Database. *U.S. Life Cycle Inventory (USLCI) Database*, <https://www.nrel.gov/lci/>
50. Bare J (2012) Tool for the Reduction and Assessment of Chemical and Other Environmental Impacts (TRACI) version 2.1. <https://nepis.epa.gov/Adobe/PDF/P100HN53.pdf>
51. Lippiatt BC (2002) BEES 3.0 Building for Environmental and Economic Sustainability Technical Manual and User Guide. :207. https://www.usgbc.org/drupal/legacy/usgbc/docs/LEED_tsac/VSI_BEES.pdf
52. Ghamkhar R, Hartleb C, Wu F, Hicks A (2020) Life cycle assessment of a cold weather aquaponic food production system. *Journal of Cleaner Production*, 244:118767. <https://doi.org/10.1016/j.jclepro.2019.118767>
53. Ishii SKL, Boyer TH (2015) Life cycle comparison of centralized wastewater treatment and urine source separation with struvite precipitation: Focus on urine nutrient management. *Water Research*, 79:88–103. <https://doi.org/10.1016/j.watres.2015.04.010>
54. Kataki S, Baruah DC (2018) Prospects and Issues of Phosphorus Recovery as Struvite from Waste Streams. *Handbook of Environmental Materials Management*, :1–50. https://doi.org/10.1007/978-3-319-58538-3_19-1
55. Gürü M, Bilgesü AY, Pamuk V (2001) Production of oxalic acid from sugar beet molasses by formed nitrogen oxides. *Bioresource Technology*, 77(1):81–86. [https://doi.org/10.1016/S0960-8524\(00\)00122-X](https://doi.org/10.1016/S0960-8524(00)00122-X)
56. Natividad Pérez-Camacho M, Curry R, Cromie T (2019) Life cycle environmental impacts of biogas production and utilisation substituting for grid electricity, natural gas grid and transport fuels. *Waste Management*, 95:90–101. <https://doi.org/10.1016/j.wasman.2019.05.045>
57. Heijungs R (2014) Ten easy lessons for good communication of LCA. *The International Journal of Life Cycle Assessment*, 19(3):473–476. <https://doi.org/10.1007/s11367-013-0662-5>
58. Erisman JW, Sutton MA, Galloway J, Klimont Z, Winiwarter W (2008) How a century of ammonia synthesis changed the world. *Nature Geoscience*, 1(10):636–639. <https://doi.org/10.1038/ngeo325>
59. Munasinghe-Arachchige SP, Nirmalakhandan N (2020) Nitrogen-Fertilizer Recovery from the Centrate of Anaerobically Digested Sludge. *Environmental Science & Technology Letters*, :acs.estlett.0c00355. <https://doi.org/10.1021/acs.estlett.0c00355>
60. Chowdhury RB, Moore GA, Weatherley AJ, Arora M (2017) Key sustainability challenges for the global phosphorus resource, their implications for global food security, and options for mitigation. *Journal of Cleaner Production*, 140:945–963. <https://doi.org/10.1016/j.jclepro.2016.07.012>
61. Zangarini S, Pepè Sciarria T, Tambone F, Adani F (2020) Phosphorus removal from livestock effluents: recent technologies and new perspectives on low-cost strategies.

Environmental Science and Pollution Research, 27(6):5730–5743.

<https://doi.org/10.1007/s11356-019-07542-4>

62. Lötjönen S, Temmes E, Ollikainen M (2020) Dairy Farm Management when Nutrient Runoff and Climate Emissions Count. *American Journal of Agricultural Economics*, 102(3):960–981.

<https://doi.org/10.1002/ajae.12003>

63. US EPA (2014) Tool for Reduction and Assessment of Chemicals and Other Environmental Impacts (TRACI). [https://www.epa.gov/sites/production/files/2015-](https://www.epa.gov/sites/production/files/2015-12/traci_2_1_2014_dec_10_0.xlsx)

[12/traci_2_1_2014_dec_10_0.xlsx](https://www.epa.gov/sites/production/files/2015-12/traci_2_1_2014_dec_10_0.xlsx)

64. Vaneckhaute C, Lebuf V, Michels E, Belia E, Vanrolleghem PA, Tack FMG, Meers E (2017) Nutrient Recovery from Digestate: Systematic Technology Review and Product Classification. *Waste and Biomass Valorization*, 8(1):21–40. <https://doi.org/10.1007/s12649-016-9642-x>

65. Macura B, Johannesdottir SL, Piniewski M, Haddaway NR, Kvarnström E (2019) Effectiveness of ecotechnologies for recovery of nitrogen and phosphorus from anaerobic digestate and effectiveness of the recovery products as fertilisers: a systematic review protocol. *Environmental Evidence*, 8(1):29. <https://doi.org/10.1186/s13750-019-0173-3>

66. Sigurnjak I, Van Poucke R, Vaneckhaute C, Michels E, Meers E (2020) Manure as a Resource for Energy and Nutrients. *Biorefinery of Inorganics*, :65–82.

<https://doi.org/10.1002/9781118921487.ch3-1>

67. Andriamanohiarisoamanana FJ, Saikawa A, Kan T, Qi G, Pan Z, Yamashiro T, Iwasaki M, Ihara I, Nishida T, Umetsu K (2018) Semi-continuous anaerobic co-digestion of dairy manure, meat and bone meal and crude glycerol: Process performance and digestate valorization. *Renewable Energy*, 128:1–8. <https://doi.org/10.1016/j.renene.2018.05.056>

68. Brown K, Harrison J, Bowers K (2018) Struvite Precipitation from Anaerobically Digested Dairy Manure. *Water, Air, & Soil Pollution*, 229(7):217. <https://doi.org/10.1007/s11270-018-3855-5>

69. Rico C, García H, Rico JL (2011) Physical–anaerobic–chemical process for treatment of dairy cattle manure. *Bioresource Technology*, 102(3):2143–2150.

<https://doi.org/10.1016/j.biortech.2010.10.068>

70. Uludag-Demirer S, Demirer GN, Frear C, Chen S (2008) Anaerobic digestion of dairy manure with enhanced ammonia removal. *Journal of Environmental Management*, 86(1):193–200. <https://doi.org/10.1016/j.jenvman.2006.12.002>

71. Uludag-Demirer S, Demirer GN, Chen S (2005) Ammonia removal from anaerobically digested dairy manure by struvite precipitation. *Process Biochemistry*, 40(12):3667–3674.

<https://doi.org/10.1016/j.procbio.2005.02.028>

72. Cerrillo M, Palatsi J, Comas J, Vicens J, Bonmatí A (2015) Struvite precipitation as a technology to be integrated in a manure anaerobic digestion treatment plant - removal efficiency,

- crystal characterization and agricultural assessment. *Journal of Chemical Technology & Biotechnology*, 90(6):1135–1143. <https://doi.org/10.1002/jctb.4459>
73. Hidalgo D, Martín-Marroquín JM, Corona F (2019) A multi-waste management concept as a basis towards a circular economy model. *Renewable and Sustainable Energy Reviews*, 111:481–489. <https://doi.org/10.1016/j.rser.2019.05.048>
74. Karakashev D, Schmidt JE, Angelidaki I (2008) Innovative process scheme for removal of organic matter, phosphorus and nitrogen from pig manure. *Water Research*, 42(15):4083–4090. <https://doi.org/10.1016/j.watres.2008.06.021>
75. L. B. Moody, R. T. Burns, K. J. Stalder (2009) Effect of Anaerobic Digestion on Manure Characteristics for Phosphorus Precipitation from Swine Waste. *Applied Engineering in Agriculture*, 25(1):97–102. <https://doi.org/10.13031/2013.25430>
76. Perera PWA, Wu W-X, Chen Y-X, Han Z-Y (2009) Struvite Recovery from Swine Waste Biogas Digester Effluent through a Stainless Steel Device under Constant pH Conditions. *Biomedical and Environmental Sciences*, 22(3):201–209. [https://doi.org/10.1016/S0895-3988\(09\)60046-5](https://doi.org/10.1016/S0895-3988(09)60046-5)
77. Romero-Güiza MS, Astals S, Mata-Alvarez J, Chimenos JM (2015) Feasibility of coupling anaerobic digestion and struvite precipitation in the same reactor: Evaluation of different magnesium sources. *Chemical Engineering Journal*, 270:542–548. <https://doi.org/10.1016/j.cej.2015.02.057>
78. Hidalgo D, Corona F, Martín-Marroquín JM, Álamo J del, Aguado A (2016) Resource recovery from anaerobic digestate: struvite crystallisation versus ammonia stripping. *Desalination and Water Treatment*, 57(6):2626–2632. <https://doi.org/10.1080/19443994.2014.1001794>
79. Huchzermeier MP, Tao W (2012) Overcoming Challenges to Struvite Recovery from Anaerobically Digested Dairy Manure. *Water Environment Research*, 84(1):34–41. <https://doi.org/10.2175/106143011X13183708018887>
80. Yetilmezsoy K, Sapci-Zengin Z (2009) Recovery of ammonium nitrogen from the effluent of UASB treating poultry manure wastewater by MAP precipitation as a slow release fertilizer. *Journal of Hazardous Materials*, 166(1):260–269. <https://doi.org/10.1016/j.jhazmat.2008.11.025>
81. Yilmazel YD, Demirer GN (2013) Nitrogen and phosphorus recovery from anaerobic co-digestion residues of poultry manure and maize silage via struvite precipitation. *Waste Management & Research*, 31(8):792–804. <https://doi.org/10.1177/0734242X13492005>
82. Yilmazel YD, Demirer GN (2011) Removal and recovery of nutrients as struvite from anaerobic digestion residues of poultry manure. *Environmental Technology*, 32(7):783–794. <https://doi.org/10.1080/09593330.2010.512925>
83. Pintucci C, Carballa M, Varga S, Sarli J, Peng L, Bousek J, Pedizzi C, Rusalleda M, Tarragó E, Prat D, Colica G, Picavet M, Colsen J, Benito O, Balaguer M, Puig S, Lema JM,

- Colprim J, Fuchs W, Vlaeminck SE (2017) The ManureEcoMine pilot installation: advanced integration of technologies for the management of organics and nutrients in livestock waste. *Water Science and Technology*, 75(6):1281–1293. <https://doi.org/10.2166/wst.2016.559>
84. Tarragó E, Rusalleda M, Colprim J, Balaguer MD, Puig S (2018) Towards a methodology for recovering K-struvite from manure: Towards a methodology for recovering K-struvite from manure. *Journal of Chemical Technology & Biotechnology*, 93(6):1558–1562. <https://doi.org/10.1002/jctb.5518>
85. Zeng L, Li X (2006) Nutrient removal from anaerobically digested cattle manure by struvite precipitation. *Journal of Environmental Engineering and Science*, 5(4):285–294. <https://doi.org/10.1139/s05-027>
86. Y. Shen, J. A. Ogejo, K. E. Bowers (2011) Abating the Effects of Calcium on Struvite Precipitation in Liquid Dairy Manure. *Transactions of the ASABE*, 54(1):325–336. <https://doi.org/10.13031/2013.36260>
87. Jin Y, Hu Z, Wen Z (2009) Enhancing anaerobic digestibility and phosphorus recovery of dairy manure through microwave-based thermochemical pretreatment. *Water Research*, 43(14):3493–3502. <https://doi.org/10.1016/j.watres.2009.05.017>
88. Qureshi A, Lo KV, Liao PH (2008) Microwave treatment and struvite recovery potential of dairy manure. *Journal of Environmental Science and Health, Part B*, 43(4):350–357. <https://doi.org/10.1080/03601230801941709>
89. Srinivasan A, Nkansah-Boadu F, Liao PH, Lo KV (2014) Effects of acidifying reagents on microwave treatment of dairy manure. *Journal of Environmental Science and Health, Part B*, 49(7):532–539. <https://doi.org/10.1080/03601234.2014.896681>
90. Zhang T, Wang Q, Deng Y, Jiang R (2018) Recovery of Phosphorus From Swine Manure by Ultrasound/H₂O₂ Digestion, Struvite Crystallization, and Ferric Oxide Hydrate/Biochar Adsorption. *Frontiers in Chemistry*, 6:464. <https://doi.org/10.3389/fchem.2018.00464>
91. Oram B (2019) Conversion Factors for Water Quality. *Water Research Watershed Center*, <https://water-research.net/index.php/conversion-factors-for-water-quality>
92. Yu R, Ren H, Wang Y, Ding L, Geng J, Xu K, Zhang Y (2013) A kinetic study of struvite precipitation recycling technology with NaOH/Mg(OH)₂ addition. *Bioresource Technology*, 143:519–524. <https://doi.org/10.1016/j.biortech.2013.06.042>
93. Sena M (2019) Environmental Impacts and Economic Implications of Phosphorus Recovery.
94. Ostara Nutrient Recovery Technologies Inc. (2019) Analysis. <https://crystalgreen.com/nutrient-recovery/analysis-msds/>
95. Vahidi E, Navarro J, Zhao F (2016) An initial life cycle assessment of rare earth oxides production from ion-adsorption clays. *Resources, Conservation and Recycling*, 113:1–11. <https://doi.org/10.1016/j.resconrec.2016.05.006>

96. Igos E, Besson M, Navarrete Gutiérrez T, Bisinella de Faria AB, Benetto E, Barna L, Ahmadi A, Spérandio M (2017) Assessment of environmental impacts and operational costs of the implementation of an innovative source-separated urine treatment. *Water Research*, 126:50–59. <https://doi.org/10.1016/j.watres.2017.09.016>

Curriculum Vitae (CV)

Sila Temizel Sekeryan

silatemizel@gmail.com; temizelseker@wisc.edu

708 Eagle Heights Apt A, 53705, Madison, WI

(201)-877-3824

EDUCATION

- PhD Environmental Engineering, *Expected December 2020*, University of Wisconsin-Madison, Department of Civil and Environmental Engineering, Madison, Wisconsin (GPA: 4.00/4.00)
- DE Environmental Engineering, *Transferred to UW-Madison in 2018*, Lamar University, Department of Civil and Environmental Engineering, Beaumont, Texas (GPA: 4.00/4.00)
- MS Environmental Technology, January 2017, Boğaziçi University, Institute of Environmental Sciences, Istanbul, Turkey (GPA: 3.78/4.00)
- BS Environmental Engineering (double major), August 2013, Yıldız Technical University, Faculty of Civil Engineering, Istanbul, Turkey (GPA: 3.34/4.00, honored student)
- BS Chemistry, May 2012, Yıldız Technical University, Faculty of Arts and Sciences, Istanbul, Turkey (GPA: 3.33/4.00, honored student)
- LLP-Erasmus, August 2010, Universidade Do Minho, School of Sciences, Braga, Portugal

PROFESSIONAL HISTORY

University of Wisconsin-Madison, Madison, Wisconsin

Graduate Research Assistant and Graduate Student September 2018 – Present

Lamar University, Beaumont, Texas

Teaching and Research Assistant and Graduate Student January 2017 – September 2018

United Nations Sustainable Development Solutions Network, Istanbul, Turkey

National Network Coordinator for Turkey April 2015 – February 2017

Boğaziçi University, Sustainable Development and Cleaner Production Center, Istanbul, Turkey

Senior Researcher September 2014 – January 2017

GlaxoSmithKline (GSK) Pharmaceuticals Limited, Istanbul, Turkey

Medical Departmental Assistant April 2013 – September 2014

Scientific and Technological Research Council of Turkey, Marmara Research Center

Environmental Institute (TUBITAK-MAM), Istanbul, Turkey

Environmental Engineering Intern August-September 2011

TEACHING AND MENTORING EXPERIENCE

- Mentored an undergraduate student from the Department of Civil and Environmental Engineering at the University of Wisconsin-Madison, September 2019-February 2020
- Teaching Assistant (35 students) – Statics, CVEN 2301, Lamar University, 2017 (Spring)

PUBLICATIONS

Journal Articles

- Hicks, A.L.; **Temizel-Sekeryan, S.**; Kontar, W.; Ghamkhar, R.; Rodriguez Morris, M. (2020) Personal respiratory protection and resiliency in a pandemic, the evolving disposable versus reusable debate and its effect on waste generation, *Resources, Conservation and Recycling*, 105262. <https://doi.org/10.1016/j.resconrec.2020.105262>
- **Temizel-Sekeryan, S.**; Hicks, A.L. (2020) Emerging investigator series: Calculating size- and coating- dependent effect factors for silver nanoparticles to inform characterization factor development for usage in life cycle assessment, *Environmental Science: Nano*, Vol. 7, Issue. 9, pp. 2436-2453. <https://doi.org/10.1039/DOEN00675K>
- **Temizel-Sekeryan, S.**; Wu, F.; Hicks, A.L. (2020) Life Cycle Assessment of Struvite Precipitation from Anaerobically Digested Dairy Manure: A Wisconsin Perspective, *Integrated Environmental Assessment and Management*. <https://doi.org/10.1002/ieam.4318>
- Wu, F.; Zhou, Z.; **Temizel-Sekeryan, S.**; Ghamkhar, R.; Hicks, A.L. (2020) Assessing the environmental impact and payback of carbon nanotube supported CO₂ capture technologies using LCA methodology, *Journal of Cleaner Production*, Vol. 270, 122465. <https://doi.org/10.1016/j.jclepro.2020.122465>
- **Temizel-Sekeryan, S.**; Hicks, A.L. (2020) Global Environmental Impacts of Silver Nanoparticle Production Methods Supported by Life Cycle Assessment, *Resources, Conservation and Recycling*, Vol. 156, 104676. <https://doi.org/10.1016/j.resconrec.2019.104676>
- Hicks, A.L.; **Temizel-Sekeryan, S.** (2019). Understanding the potential environmental benefits of nanosilver enabled consumer products, *Nanoimpact*, Vol. 16, 100183. <https://doi.org/10.1016/j.impact.2019.100183>
- Haselbach, L. and **Temizel-Sekeryan, S.** (2019). Feedstock Energy Reporting Compilation for the Paving and Other Related Industries, *Sustainability: The Journal of Record*, Vol. 12, Issue.1, pp. 18–27. <http://doi.org/10.1089/sus.2018.0022>
- Bafana, A.; Kumar, S.V.; **Temizel-Sekeryan, S.**; Dahoumane, S.A.; Haselbach, L.; Jeffryes, C.S. (2018). Evaluating microwave-synthesized silver nanoparticles from silver nitrate with life cycle assessment techniques, *Science of the Total Environment*, Vol. 636, pp. 936–943.

<https://doi.org/10.1016/j.scitotenv.2018.04.345>

- Haselbach, L. and **Temizel-Sekeryan, S.** (2018). Inclusive Reporting of Feedstock Energy and Stored Carbon: Asphalt Case Study, *International Journal of Global Warming*, Vol. 16, No. 3, pp. 281–298. <https://doi.org/10.1504/IJGW.2018.095389>

Journal articles that are currently under review

- **Temizel-Sekeryan, S.**; Hicks, A.L. (*under review*) Cradle-to-grave environmental impact assessment of silver enabled t-shirts: Do direct impacts exceed the indirect emissions?, *ACS Sustainable Chemistry & Engineering*.
- **Temizel-Sekeryan, S.**; Hicks, A.L. (*under review*) Developing physicochemical property-based ecotoxicity characterization factors for silver nanoparticles under mesocosm conditions for use in life cycle assessment, submitted to *Environmental Science: Nano*.
- **Temizel-Sekeryan, S.**; Wu, F.; Hicks, A.L. (*under review*) Global Scale Life Cycle Environmental Impacts of Single- and Multi-Walled Carbon Nanotube Synthesis Methods, submitted to the *International Journal of Life Cycle Assessment*.

Book Chapters

- Ciliz, N.; Yildirim, H.; **Temizel, S.** (2016). Structure Development for Effective Medical Waste and Hazardous Waste Management System, *Handbook of Research on Waste Management Techniques for Sustainability*. Hershey, PA, USA. (ISBN13: 978-1-4666-9723-2)

Technical Reports

- Haselbach, L.; **Temizel-Sekeryan, S.**; Ross, M.; Almeida, N. (2018). Evaluation of Deicer Impacts on Pervious Concrete Specimens (Phase II), *Center for Environmentally Sustainable Transportation in Cold Climates (CESTiCC)*. Fairbanks, AK, USA. (INE/AUTC 18.10)
- Haselbach, L.; **Temizel-Sekeryan, S.** (2018). Transportation Life Cycle Assessment (LCA) Synthesis (Phase II), *Center for Environmentally Sustainable Transportation in Cold Climates (CESTiCC)*. Fairbanks, AK, USA. (INE/AUTC 2018.07)

SELECTED PRESENTATIONS

Platform Presentations

- **Temizel-Sekeryan, S.**; Hicks, A.L. (2020). “Developing Characterization Factors for Silver Nanoparticles: Case Studies for Mesocosms”, *9th Nano Conference (SNO/NanOEH)*, Virtual.
- **Temizel-Sekeryan, S.**; Wu, F.; Hicks, A.L. (2020). “Environmental Impact Assessment of Struvite

Precipitation from Anaerobically Digested Dairy Manure”, *SETAC North America 41st Annual Meeting & SciCon2 Virtual Meeting*.

- **Temizel-Sekeryan, S.;** Hicks, A.L. (2020). “Global Environmental Footprints of Silver Nanoparticle Synthesis Methods and Industry Based Impact Projections Using Life Cycle Assessment”, *ACLCA 2020 Conference*, Virtual.
- **Temizel-Sekeryan, S.;** Wu, F.; Hicks, A.L. (2020). “Environmental Impacts of Single- and Multi-Walled Carbon Nanotube Synthesis Methods and Industry Based Large-Scale Impact Projections Using Life Cycle Assessment”, *ACLCA 2020 Conference*, Virtual.
- **Temizel-Sekeryan, S.;** Hicks, A.L. (2019). “Global Environmental Impacts of Single-Walled and Multi-Walled Carbon Nanotube Synthesis Methods and Implications of Scaling Up”, *SETAC North America 40th Annual Meeting*, Toronto, Canada.
- **Temizel-Sekeryan, S.;** Hicks, A.L. (2019). “Evaluating the Global Environmental Impacts of Different Silver Nanoparticle Synthesis Methods Using Life Cycle Assessment” (presented by Fan Wu), *10th International Conference on Industrial Ecology*, Beijing, China.
- **Temizel-Sekeryan, S.;** Hicks, A.L. (2019). “Comparative Global Environmental Impacts of Silver Nanoparticle Synthesis Techniques Using Life Cycle Assessment”, *27th Annual Meeting of the Midwest SETAC*, La Crosse, WI, USA.
- **Temizel, S.;** Ciliz, N. (2016). “Decision Making Tools in the Production Systems of Personal Care Products”, *Green & Sustainable Chemistry Conference*, Berlin, Germany.
- **Temizel, S.** (2015). “Proposed Structure of SDSN Youth and institutional integration with SDSN”, *2nd SDSN Mediterranean Conference, Solutions for Agri-food Sustainability in the Mediterranean, Policies, Technologies and Business Models*, Siena, Italy.

Poster Presentations

- **Temizel-Sekeryan, S.;** Wu, F.; Hicks, A.L. (2020). “Global life cycle impacts of manufacturing the selected engineered nanomaterials: case studies on nano-silver, nano-titanium dioxide and carbon nanotubes”, *Industrial Ecology Gordon Research Seminar and Conference (GRS/GRC)*, Newry, ME, USA. [Conference is withdrawn by the organizers due to COVID-19]
- **Temizel-Sekeryan, S.;** Wu, F.; Hicks, A.L. (2019). “Environmental Impacts of Single- and Multi-Walled Carbon Nanotube Synthesis Methods and Industry Based Large-Scale Impact Projections Using Life Cycle Assessment”, *Sigma Xi Annual Meeting & Student Research Conference*, Madison, WI, USA.
- Hicks, A.L.; **Temizel-Sekeryan, S.** (2019). “Insight from the life cycle assessment of nanosilver enabled consumer products”, *SETAC North America 40th Annual Meeting*, Toronto, Canada.

- **Temizel-Sekeryan, S.**; Hicks, A.L. (2019). “Global Environmental Footprints of Silver Nanoparticle Synthesis Methods and Industry Based Impact Projections Using Life Cycle Assessment”, *SETAC North America 40th Annual Meeting*, Toronto, Canada.
- Garcia, J.L.; Hicks, A.L.; Grant, C.A.; Ghamkhar, R.; **Temizel-Sekeryan, S.** (2019). “Life Cycle Assessment and Environmental Payback Periods of Monocrystalline-Silicon Photovoltaic Systems”, presented at the *Summer Undergraduate Research Experience (SURE) Closing Ceremony at University of Wisconsin-Madison*, Madison, WI, USA.
- **Temizel-Sekeryan, S.**; Hicks, A.L. (2019). “Comparative Global Environmental Impacts of Silver Nanoparticle Synthesis Techniques Using Life Cycle Assessment”, *2019 American Institute of Professional Geologists (AIPG) WI Workshop PFAS: Life Cycle, Regulations and Solutions*, Pewaukee, WI, USA.
- Bafana, A.; Kumar, S.; Pawar, P.; **Temizel-Sekeryan, S.**; Dahoumane, S.A.; Haselbach, L.; Jeffries, C. (2018). “Environmental Impact Assessment for High Conversion Synthesis of <10 Nm Silver Nanoparticles Using Microwave Assisted Heating by Life Cycle Techniques”, *2018 AIChE Annual Meeting*, Pittsburgh, PA, USA.
- Haselbach, L. and **Temizel-Sekeryan, S.** (2018). “Capturing Comprehensive Environmental Considerations in Environmental Product Declarations for Asphalt Pavements”, *ASCE International Conference on Transportation & Development (ICTD)*, Pittsburgh, PA, USA.
- Haselbach, L. and **Temizel-Sekeryan, S.** (2018). “Synthesis of Feedstock Energy Reporting in the Paving and Other Related Industries”, *97th Transportation Research Board (TRB) Annual Meeting*, Washington, DC, USA.

AWARDS AND HONORS

- Planetary Health Graduate Scholarship (Global Health Institute and the Nelson Institute for Environmental Studies, University of Wisconsin Madison, 2020-2021)
- Sustainable Nanotechnology Organization, 9th Nano Conference Student Award (Fall 2020)
- SETAC North America 41st Annual Meeting (Virtual) Student Attendance Grant (Fall 2020)
- Becker Travel Supplements - Travel Award (Spring 2020)
- Student Research Grants Competition Travel Award (University of Wisconsin Madison Graduate School, Spring 2020)
- Becker Travel Supplements - Travel Award (Fall 2019)
- Midwest SETAC Student Travel Award (Spring 2019)

MEMBERSHIP IN PROFESSIONAL ASSOCIATIONS



- International Society for Industrial Ecology (IS4IE)
- Sustainable Nanotechnology Organization (SNO)
- Association of Environmental Engineering and Science Professors (AEESP)
- Society of Environmental Toxicology and Chemistry (SETAC)
- American Society of Civil Engineers (ASCE)
- American Academy of Environmental Engineers and Scientists (AAEES)


COMPUTER SKILLS

SimaPro, GaBi, SigmaPlot, AutoCad, ArcGIS, PostgreSQL, Microsoft Office

Permissions

Temizel-Sekeryan, S.; Hicks, A.L. (2020) Global Environmental Impacts of Silver Nanoparticle Production Methods Supported by Life Cycle Assessment, *Resources, Conservation and Recycling*, Vol. 156, 104676. <https://doi.org/10.1016/j.resconrec.2019.104676>

Home Help Email Support Sign in Create Account



Global environmental impacts of silver nanoparticle production methods supported by life cycle assessment

Author: Sila Temizel-Sekeryan, Andrea L. Hicks

Publication: Resources, Conservation and Recycling

Publisher: Elsevier

Date: May 2020

© 2020 Elsevier B.V. All rights reserved.

Please note that, as the author of this Elsevier article, you retain the right to include it in a thesis or dissertation, provided it is not published commercially. Permission is not required, but please ensure that you reference the journal as the original source. For more information on this and on your other retained rights, please visit: <https://www.elsevier.com/about/our-business/policies/copyright#Author-rights>

BACK

CLOSE WINDOW

© 2020 Copyright - All Rights Reserved | Copyright Clearance Center, Inc. | Privacy statement | Terms and Conditions
Comments? We would like to hear from you. E-mail us at customer-care@copyright.com

Temizel-Sekeryan, S.; Hicks, A.L. (2020) Emerging investigator series: Calculating size- and coating- dependent effect factors for silver nanoparticles to inform characterization factor development for usage in life cycle assessment, *Environmental Science: Nano*, Vol. 7, Issue. 9, pp. 2436-2453. <https://doi.org/10.1039/D0EN00675K>

Emerging investigator series: calculating size- and coating-dependent effect factors for silver nanoparticles to inform characterization factor development for usage in life cycle assessment

S. Temizel-Sekeryan and A. L. Hicks, *Environ. Sci.: Nano*, 2020, **7**, 2436

DOI: 10.1039/D0EN00675K

If you are not the author of this article and you wish to reproduce material from it in a third party non-RSC publication you must [formally request permission](#) using Copyright Clearance Center. Go to our [Instructions for using Copyright Clearance Center page](#) for details.

Authors contributing to RSC publications (journal articles, books or book chapters) do not need to formally request permission to reproduce material contained in this article provided that the correct acknowledgement is given with the reproduced material.

Reproduced material should be attributed as follows:

- For reproduction of material from NJC:
Reproduced from Ref. XX with permission from the Centre National de la Recherche Scientifique (CNRS) and The Royal Society of Chemistry.
- For reproduction of material from PCCP:
Reproduced from Ref. XX with permission from the PCCP Owner Societies.
- For reproduction of material from PPS:
Reproduced from Ref. XX with permission from the European Society for Photobiology, the European Photochemistry Association, and The Royal Society of Chemistry.
- For reproduction of material from all other RSC journals and books:
Reproduced from Ref. XX with permission from The Royal Society of Chemistry.

If the material has been adapted instead of reproduced from the original RSC publication "Reproduced from" can be substituted with "Adapted from".

In all cases the Ref. XX is the XXth reference in the list of references.

If you are the author of this article you do not need to formally request permission to reproduce figures, diagrams

etc. contained in this article in third party publications or in a thesis or dissertation provided that the correct acknowledgement is given with the reproduced material.

Reproduced material should be attributed as follows:

- For reproduction of material from NJC:
[Original citation] - Reproduced by permission of The Royal Society of Chemistry (RSC) on behalf of the Centre National de la Recherche Scientifique (CNRS) and the RSC
- For reproduction of material from PCCP:
[Original citation] - Reproduced by permission of the PCCP Owner Societies
- For reproduction of material from PPS:
[Original citation] - Reproduced by permission of The Royal Society of Chemistry (RSC) on behalf of the European Society for Photobiology, the European Photochemistry Association, and RSC
- For reproduction of material from all other RSC journals:
[Original citation] - Reproduced by permission of The Royal Society of Chemistry



If you are the author of this article you still need to obtain permission to reproduce the whole article in a third party publication with the exception of reproduction of the whole article in a thesis or dissertation.

Information about reproducing material from RSC articles with different licences is available on our [Permission Requests page](#).

Deposition and sharing rights

The following details apply only to authors accepting the standard licence to publish. Authors who have accepted one of the open access licences to publish, or are thinking of doing so, should refer to the [details for open access deposition rights](#).

When the author accepts the licence to publish for a journal article, he/she retains certain rights concerning the deposition of the whole article. This table summarises how you may distribute the accepted manuscript and version of record of your article.



Sharing rights	Accepted manuscript	Version of record
Share with individuals on request, for personal use	✓	✓
Use for teaching or training materials	✓	✓
Use in submissions of grant applications, or academic requirements such as theses or dissertations*	✓	✓
Share with a closed group of research collaborators, for example via an intranet or privately via a scholarly communication network	✓	✓
Share publicly via a scholarly communication network that has signed up to STM sharing principles		×
Share publicly via a personal website, institutional repository or other not-for-profit repository		×
Share publicly via a scholarly communication network that has not signed up to STM sharing principles	×	×


*You may include your article in the electronic version of your thesis or dissertation as long as it is not made available as a separate document.

 Accepted manuscripts may be distributed via repositories after an embargo period of 12 months

Hicks, A.L.; Temizel-Sekeryan, S. (2019) Understanding the potential environmental benefits of nanosilver enabled consumer products, *NanoImpact*, Vol. 16, 100183.

<https://doi.org/10.1016/j.impact.2019.100183>

Home ? Help Email Support Sign in Create Account



Understanding the potential environmental benefits of nanosilver enabled consumer products
Author: Andrea L. Hicks, Sila Temizel-Sekeryan
Publication: NanoImpact
Publisher: Elsevier
Date: April 2019
© 2019 Elsevier B.V. All rights reserved.

Please note that, as the author of this Elsevier article, you retain the right to include it in a thesis or dissertation, provided it is not published commercially. Permission is not required, but please ensure that you reference the journal as the original source. For more information on this and on your other retained rights, please visit: <https://www.elsevier.com/about/our-business/policies/copyright#Author-rights>

[BACK](#) [CLOSE WINDOW](#)

© 2020 Copyright - All Rights Reserved | [Copyright Clearance Center, Inc.](#) | [Privacy statement](#) | [Terms and Conditions](#)
Comments? We would like to hear from you. E-mail us at customer-care@copyright.com

Wu, F.; Zhou, Z.; Temizel-Sekeryan, S.; Ghamkhar, R.; Hicks, A.L. (2020) Assessing the environmental impact and payback of carbon nanotube supported CO₂ capture technologies using LCA methodology, *Journal of Cleaner Production*, Vol. 270, 122465.

<https://doi.org/10.1016/j.jclepro.2020.122465>



RightsLink®



Home



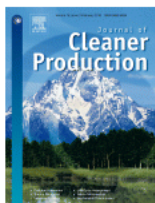
Help



Email Support



Sila Temizel Sekeryan ▾



Assessing the environmental impact and payback of carbon nanotube supported CO₂ capture technologies using LCA methodology

Author: Fan Wu,Zheng Zhou,Sila Temizel-Sekeryan,Ramin Ghamkhar,Andrea L. Hicks

Publication: Journal of Cleaner Production

Publisher: Elsevier

Date: 10 October 2020

© 2020 Elsevier Ltd. All rights reserved.

Please note that, as the author of this Elsevier article, you retain the right to include it in a thesis or dissertation, provided it is not published commercially. Permission is not required, but please ensure that you reference the journal as the original source. For more information on this and on your other retained rights, please visit: <https://www.elsevier.com/about/our-business/policies/copyright#Author-rights>

BACK

CLOSE WINDOW



Home > About > Policies > Copyright

Copyright

Describes the rights related to the publication and distribution of research. It governs how authors (as well as their employers or funders), publishers and the wider general public can use, publish and distribute articles or books.

[Journal author rights](#) [Government employees](#) [Elsevier's rights](#) [Protecting author rights](#) [Open access](#)

Journal author rights


In order for Elsevier to publish and disseminate research articles, we need publishing rights. This is determined by a publishing agreement between the author and Elsevier. This agreement deals with the transfer or license of the copyright to Elsevier and authors retain significant rights to use and share their own published articles. Elsevier supports the need for authors to share, disseminate and maximize the impact of their research and these rights, in Elsevier proprietary journals* are defined below:

For subscription articles	For open access articles
<p>Authors transfer copyright to the publisher as part of a journal publishing agreement, but have the right to:</p> <ul style="list-style-type: none"> Share their article for Personal Use, Internal Institutional Use and Scholarly Sharing purposes, with a DOI link to the version of record on ScienceDirect (and with the Creative Commons CC-BY-NC-ND license for author manuscript versions) Retain patent, trademark and other intellectual property rights (including research data). Proper attribution and credit for the published work. 	<p>Authors sign an exclusive license agreement, where authors have copyright but license exclusive rights in their article to the publisher**. In this case authors have the right to:</p> <ul style="list-style-type: none"> Share their article in the same ways permitted to third parties under the relevant user license (together with Personal Use rights) so long as it contains a CrossMark logo, the end user license, and a DOI link to the version of record on ScienceDirect. Retain patent, trademark and other intellectual property rights (including research data). Proper attribution and credit for the published work.

*Please note that society or third party owned journals may have different publishing agreements. Please see the journal's guide for authors for journal specific copyright information.

**This includes the right for the publisher to make and authorize [commercial use](#), please see "[Rights granted to Elsevier](#)" for more details.

Help and Support

- Download a sample publishing agreement for subscription articles in [English](#) and [French](#).
- Download a sample publishing agreement for open access articles for authors choosing a [commercial user license](#) and [non-commercial user license](#).
- For authors who wish to self-archive see our [sharing guidelines](#)
- See our [author pages](#) for further details about how to promote your article.
- For use of Elsevier material not defined below please see our [permissions page](#) or visit the [Permissions Support Center](#) 

Government employees

Elsevier has specific publishing agreements with certain government and inter-governmental organizations for their employee authors. These agreements enable authors to retain substantially the same rights as detailed in the "[Author Rights section](#)" but are specifically tailored for employees from the relevant organizations, including:

- World Bank
- World Health Organization
- For US government employees, works created within the scope of their employment are considered to be public domain and Elsevier's publishing agreements do not require a transfer or license of rights for such works.

- In the UK and certain commonwealth countries, a work created by a government employee is copyrightable but the government may own the copyright (Crown copyright). [Click here](#) for information about UK government employees publishing open access

Rights granted to Elsevier

For both subscription and open access articles, published in proprietary titles, Elsevier is granted the following rights:

- The exclusive right to publish and distribute an article, and to grant rights to others, including for commercial purposes.
- For open access articles, Elsevier will apply the relevant third party [user license](#) where Elsevier publishes the article on its online platforms.
- The right to provide the article in all forms and media so the article can be used on the latest technology even after publication.
- The authority to enforce the rights in the article, on behalf of an author, against third parties, for example in the case of plagiarism or copyright infringement.

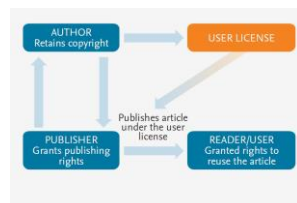
Protecting author rights

Copyright aims to protect the specific way the article has been written to describe an experiment and the results. Elsevier is committed to its authors to protect and defend their work and their reputation and takes allegations of infringement, plagiarism, ethic disputes and fraud very seriously.

If an author becomes aware of a possible plagiarism, fraud or infringement we recommend contacting their Elsevier publishing contact who can then liaise with our in-house legal department. Note that certain open access user licenses may permit quite [broad re-use](#) that might otherwise be counted as copyright infringement. For details about how to seek permission to use an article see our [permission page](#).

Open access

How copyright works with open access licenses



For Elsevier proprietary journals the following steps apply:

- 1 Authors sign a publishing agreement where they will have copyright but grant broad publishing and distribution rights to the publisher, including the right to publish the article on Elsevier's online platforms.
- 2 The author chooses an [end user license](#) under which readers can use and share the article.
- 3 The publisher makes the article available online with the author's choice of end user license.

Quick definitions

Personal use

Authors can use their articles, in full or in part, for a wide range of scholarly, non-commercial purposes as outlined below:

- Use by an author in the author's classroom teaching (including distribution of copies, paper or electronic)
- Distribution of copies (including through e-mail) to known research colleagues for their personal use (but not for Commercial Use)
- Inclusion in a thesis or dissertation (provided that this is not to be published commercially)
- Use in a subsequent compilation of the author's works
- Extending the Article to book-length form

- Preparation of other derivative works (but not for Commercial Use)
- Otherwise using or re-using portions or excerpts in other works

These rights apply for all Elsevier authors who publish their article as either a subscription article or an open access article. In all cases we require that all Elsevier authors always include a full acknowledgement and, if appropriate, a link to the final published version hosted on Science Direct.

Commercial use

This is defined as the use or posting of articles:

- **For commercial gain without a formal agreement with the publisher.**
 - For example by associating advertising with the full-text of the article, by providing hosting services to other repositories or to other organizations (including where an otherwise non-commercial site or repository provides a service to other organizations or agencies), or charging fees for document delivery or access
- **To substitute for the services provided directly by the journal.**
 - For example article aggregation, systematic distribution of articles via e-mail lists or share buttons, posting, indexing, or linking for promotional/marketing activities, by commercial companies for use by customers and intended target audiences of such companies (e.g. pharmaceutical companies and healthcare professionals/physician-prescribers).

If you would like information on how to obtain permission for such uses [click here](#) or if you would like to make commercial use of the article please visit the [Permissions Support Center](#) 

Internal institutional use

- Use by the author's institution for classroom teaching at the institution and for internal training purposes (including distribution of copies, paper or electronic, and use in coursepacks and courseware programs, but not in Massive Open Online Courses)
- Inclusion of the Article in applications for grant funding
- For authors employed by companies, the use by that company for internal training purposes

Solutions

[Scopus](#)
[ScienceDirect](#)
[Mendeley](#)
[Evolve](#)
[Knovel](#)
[Reaxys](#)
[ClinicalKey](#)

Researchers

[Submit your paper](#)
[Find books & journals](#)
[Visit Author Hub](#)
[Visit Editor Hub](#)
[Visit Librarian Hub](#)
[Visit Reviewer Hub](#)

About Elsevier

[About](#)
[Careers](#)
[Newsroom](#)
[Events](#)
[Publisher relations](#)
[Advertising, reprints and supplements](#)

How can we help?

[Support and Contact](#)

Follow Elsevier



Select location/language

 Global - English



Copyright © 2020 Elsevier, except certain content provided by third parties

Cookies are used by this site. [Cookie Settings](#)

[Terms and Conditions](#) [Privacy Policy](#) [Cookie Notice](#) [Sitemap](#)



Temizel-Sekeryan, S.; Wu, F.; Hicks, A.L. (2020) Life Cycle Assessment of Struvite Precipitation from Anaerobically Digested Dairy Manure: A Wisconsin Perspective, *Integrated Environmental Assessment and Management*. <https://doi.org/10.1002/ieam.4318>

RightsLink Printable License

10/19/20, 3:53 PM

JOHN WILEY AND SONS LICENSE
TERMS AND CONDITIONS

Oct 19, 2020

This Agreement between University of Wisconsin Madison -- Sila Temizel Sekeryan ("You") and John Wiley and Sons ("John Wiley and Sons") consists of your license details and the terms and conditions provided by John Wiley and Sons and Copyright Clearance Center.

License Number 4932681070031

License date Oct 19, 2020

Licensed Content Publisher John Wiley and Sons

Licensed Content Publication Integrated Environmental Assessment and Management

Licensed Content Title Life Cycle Assessment of Struvite Precipitation from Anaerobically Digested Dairy Manure: A Wisconsin Perspective

Licensed Content Author Andrea L Hicks, Fan Wu, Sila Temizel-Sekeryan

Licensed Content Date Sep 17, 2020

Licensed Content Volume 0

Licensed
Content Issue 0

Licensed
Content Pages 13

Type of use Dissertation/Thesis

Requestor type Author of this Wiley article

Format Print and electronic

Portion Full article

Will you be
translating? No

Title Global Environmental Impact Assessment of the Selected Engineered
Nanomaterials and Development of Characterization Factors

Institution name Univeristy of Wisconsin Madison

Expected
presentation
date Dec 2020

Requestor
Location University of Wisconsin Madison
708 Eagle Heights Apt A
MADISON, WI 53705
United States
Attn: University of Wisconsin Madison

Publisher Tax EU826007151

ID

Total 0.00 USD

Terms and Conditions

TERMS AND CONDITIONS

This copyrighted material is owned by or exclusively licensed to John Wiley & Sons, Inc. or one of its group companies (each a "Wiley Company") or handled on behalf of a society with which a Wiley Company has exclusive publishing rights in relation to a particular work (collectively "WILEY"). By clicking "accept" in connection with completing this licensing transaction, you agree that the following terms and conditions apply to this transaction (along with the billing and payment terms and conditions established by the Copyright Clearance Center Inc., ("CCC's Billing and Payment terms and conditions"), at the time that you opened your RightsLink account (these are available at any time at <http://myaccount.copyright.com>).

Terms and Conditions

- The materials you have requested permission to reproduce or reuse (the "Wiley Materials") are protected by copyright.
- You are hereby granted a personal, non-exclusive, non-sub licensable (on a stand-alone basis), non-transferable, worldwide, limited license to reproduce the Wiley Materials for the purpose specified in the licensing process. This license, **and any CONTENT (PDF or image file) purchased as part of your order**, is for a one-time use only and limited to any maximum distribution number specified in the license. The first instance of republication or reuse granted by this license must be completed within two years of the date of the grant of this license (although copies prepared before the end date may be distributed thereafter). The Wiley Materials shall not be used in any other manner or for any other purpose, beyond what is granted in the license. Permission is granted subject to an appropriate acknowledgement given to the author, title of the material/book/journal and the publisher. You shall also duplicate the copyright notice that appears in the Wiley publication in your use of the Wiley Material. Permission is also granted on the understanding that nowhere in the text is a previously published source acknowledged for all or part of this Wiley Material. Any third party content is expressly excluded from this permission.
- With respect to the Wiley Materials, all rights are reserved. Except as expressly granted by the terms of the license, no part of the Wiley Materials may be copied, modified, adapted (except for minor reformatting required by the new Publication), translated, reproduced, transferred or distributed, in any form or by any means, and no

derivative works may be made based on the Wiley Materials without the prior permission of the respective copyright owner. **For STM Signatory Publishers clearing permission under the terms of the [STM Permissions Guidelines](#) only, the terms of the license are extended to include subsequent editions and for editions in other languages, provided such editions are for the work as a whole in situ and does not involve the separate exploitation of the permitted figures or extracts,** You may not alter, remove or suppress in any manner any copyright, trademark or other notices displayed by the Wiley Materials. You may not license, rent, sell, loan, lease, pledge, offer as security, transfer or assign the Wiley Materials on a stand-alone basis, or any of the rights granted to you hereunder to any other person.

- The Wiley Materials and all of the intellectual property rights therein shall at all times remain the exclusive property of John Wiley & Sons Inc, the Wiley Companies, or their respective licensors, and your interest therein is only that of having possession of and the right to reproduce the Wiley Materials pursuant to Section 2 herein during the continuance of this Agreement. You agree that you own no right, title or interest in or to the Wiley Materials or any of the intellectual property rights therein. You shall have no rights hereunder other than the license as provided for above in Section 2. No right, license or interest to any trademark, trade name, service mark or other branding ("Marks") of WILEY or its licensors is granted hereunder, and you agree that you shall not assert any such right, license or interest with respect thereto
- NEITHER WILEY NOR ITS LICENSORS MAKES ANY WARRANTY OR REPRESENTATION OF ANY KIND TO YOU OR ANY THIRD PARTY, EXPRESS, IMPLIED OR STATUTORY, WITH RESPECT TO THE MATERIALS OR THE ACCURACY OF ANY INFORMATION CONTAINED IN THE MATERIALS, INCLUDING, WITHOUT LIMITATION, ANY IMPLIED WARRANTY OF MERCHANTABILITY, ACCURACY, SATISFACTORY QUALITY, FITNESS FOR A PARTICULAR PURPOSE, USABILITY, INTEGRATION OR NON-INFRINGEMENT AND ALL SUCH WARRANTIES ARE HEREBY EXCLUDED BY WILEY AND ITS LICENSORS AND WAIVED BY YOU.
- WILEY shall have the right to terminate this Agreement immediately upon breach of this Agreement by you.
- You shall indemnify, defend and hold harmless WILEY, its Licensors and their respective directors, officers, agents and employees, from and against any actual or threatened claims, demands, causes of action or proceedings arising from any breach of this Agreement by you.
- IN NO EVENT SHALL WILEY OR ITS LICENSORS BE LIABLE TO YOU OR ANY OTHER PARTY OR ANY OTHER PERSON OR ENTITY FOR ANY SPECIAL, CONSEQUENTIAL, INCIDENTAL, INDIRECT, EXEMPLARY OR PUNITIVE DAMAGES, HOWEVER CAUSED, ARISING OUT OF OR IN CONNECTION WITH THE DOWNLOADING, PROVISIONING, VIEWING OR USE OF THE MATERIALS REGARDLESS OF THE FORM OF ACTION,

WHETHER FOR BREACH OF CONTRACT, BREACH OF WARRANTY, TORT, NEGLIGENCE, INFRINGEMENT OR OTHERWISE (INCLUDING, WITHOUT LIMITATION, DAMAGES BASED ON LOSS OF PROFITS, DATA, FILES, USE, BUSINESS OPPORTUNITY OR CLAIMS OF THIRD PARTIES), AND WHETHER OR NOT THE PARTY HAS BEEN ADVISED OF THE POSSIBILITY OF SUCH DAMAGES. THIS LIMITATION SHALL APPLY NOTWITHSTANDING ANY FAILURE OF ESSENTIAL PURPOSE OF ANY LIMITED REMEDY PROVIDED HEREIN.

- Should any provision of this Agreement be held by a court of competent jurisdiction to be illegal, invalid, or unenforceable, that provision shall be deemed amended to achieve as nearly as possible the same economic effect as the original provision, and the legality, validity and enforceability of the remaining provisions of this Agreement shall not be affected or impaired thereby.
- The failure of either party to enforce any term or condition of this Agreement shall not constitute a waiver of either party's right to enforce each and every term and condition of this Agreement. No breach under this agreement shall be deemed waived or excused by either party unless such waiver or consent is in writing signed by the party granting such waiver or consent. The waiver by or consent of a party to a breach of any provision of this Agreement shall not operate or be construed as a waiver of or consent to any other or subsequent breach by such other party.
- This Agreement may not be assigned (including by operation of law or otherwise) by you without WILEY's prior written consent.
- Any fee required for this permission shall be non-refundable after thirty (30) days from receipt by the CCC.
- These terms and conditions together with CCC's Billing and Payment terms and conditions (which are incorporated herein) form the entire agreement between you and WILEY concerning this licensing transaction and (in the absence of fraud) supersedes all prior agreements and representations of the parties, oral or written. This Agreement may not be amended except in writing signed by both parties. This Agreement shall be binding upon and inure to the benefit of the parties' successors, legal representatives, and authorized assigns.
- In the event of any conflict between your obligations established by these terms and conditions and those established by CCC's Billing and Payment terms and conditions, these terms and conditions shall prevail.
- WILEY expressly reserves all rights not specifically granted in the combination of (i) the license details provided by you and accepted in the course of this licensing transaction, (ii) these terms and conditions and (iii) CCC's Billing and Payment terms and conditions.
- This Agreement will be void if the Type of Use, Format, Circulation, or Requestor

Type was misrepresented during the licensing process.

- This Agreement shall be governed by and construed in accordance with the laws of the State of New York, USA, without regards to such state's conflict of law rules. Any legal action, suit or proceeding arising out of or relating to these Terms and Conditions or the breach thereof shall be instituted in a court of competent jurisdiction in New York County in the State of New York in the United States of America and each party hereby consents and submits to the personal jurisdiction of such court, waives any objection to venue in such court and consents to service of process by registered or certified mail, return receipt requested, at the last known address of such party.

WILEY OPEN ACCESS TERMS AND CONDITIONS

Wiley Publishes Open Access Articles in fully Open Access Journals and in Subscription journals offering Online Open. Although most of the fully Open Access journals publish open access articles under the terms of the Creative Commons Attribution (CC BY) License only, the subscription journals and a few of the Open Access Journals offer a choice of Creative Commons Licenses. The license type is clearly identified on the article.

The Creative Commons Attribution License

The [Creative Commons Attribution License \(CC-BY\)](#) allows users to copy, distribute and transmit an article, adapt the article and make commercial use of the article. The CC-BY license permits commercial and non-

Creative Commons Attribution Non-Commercial License

The [Creative Commons Attribution Non-Commercial \(CC-BY-NC\) License](#) permits use, distribution and reproduction in any medium, provided the original work is properly cited and is not used for commercial purposes.(see below)

Creative Commons Attribution-Non-Commercial-NoDerivs License

The [Creative Commons Attribution Non-Commercial-NoDerivs License \(CC-BY-NC-ND\)](#) permits use, distribution and reproduction in any medium, provided the original work is properly cited, is not used for commercial purposes and no modifications or adaptations are made. (see below)

Use by commercial "for-profit" organizations

Use of Wiley Open Access articles for commercial, promotional, or marketing purposes requires further explicit permission from Wiley and will be subject to a fee.

Further details can be found on Wiley Online Library
<http://olabout.wiley.com/WileyCDA/Section/id-410895.html>

Other Terms and Conditions:**v1.10 Last updated September 2015****Questions? customercare@copyright.com or +1-855-239-3415 (toll free in the US) or +1-978-646-2777.**
